LINKING ECOSYSTEM FUNCTION TO MICROBIAL DIVERSITY

EDITED BY: Anne E. Bernhard and John J. Kelly

PUBLISHED IN: Frontiers in Microbiology and Frontiers in Marine Science

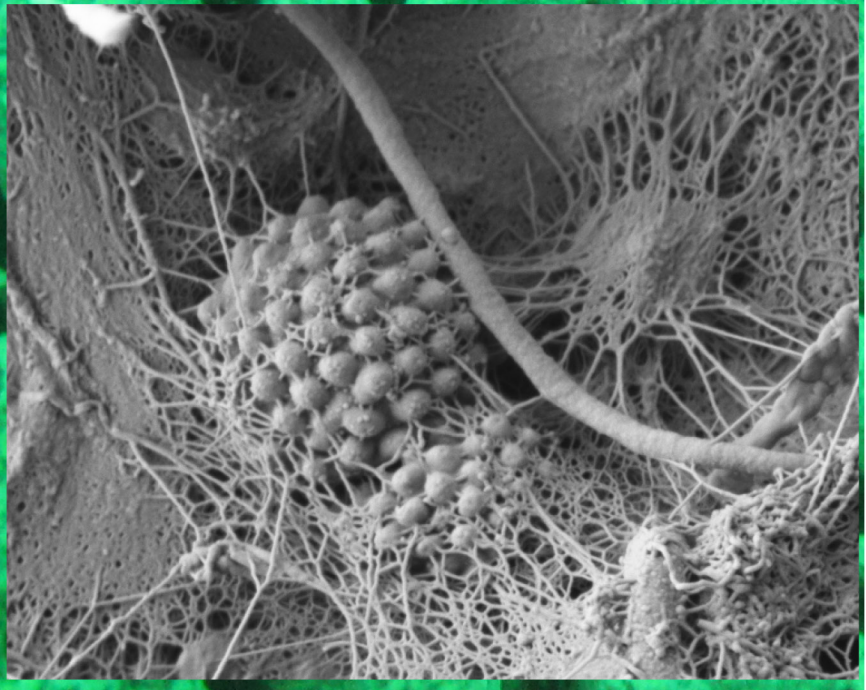

frontiers Research Topics

frontiers

ISSN 1664-8714
ISBN 978-2-88919-985-3
DOI 10.3389/978-2-88919-985-3

About Frontiers

Frontiers is more than just an open-access publisher of scholarly articles: it is a pioneering approach to the world of academia, radically improving the way scholarly research is managed. The grand vision of Frontiers is a world where all people have an equal opportunity to seek, share and generate knowledge. Frontiers provides immediate and permanent online open access to all its publications, but this alone is not enough to realize our grand goals.

Frontiers Journal Series

The Frontiers Journal Series is a multi-tier and interdisciplinary set of open-access, online journals, promising a paradigm shift from the current review, selection and dissemination processes in academic publishing. All Frontiers journals are driven by researchers for researchers; therefore, they constitute a service to the scholarly community. At the same time, the Frontiers Journal Series operates on a revolutionary invention, the tiered publishing system, initially addressing specific communities of scholars, and gradually climbing up to broader public understanding, thus serving the interests of the lay society, too.

Dedication to Quality

Each Frontiers article is a landmark of the highest quality, thanks to genuinely collaborative interactions between authors and review editors, who include some of the world's best academicians. Research must be certified by peers before entering a stream of knowledge that may eventually reach the public - and shape society; therefore, Frontiers only applies the most rigorous and unbiased reviews.
Frontiers revolutionizes research publishing by freely delivering the most outstanding research, evaluated with no bias from both the academic and social point of view.
By applying the most advanced information technologies, Frontiers is catapulting scholarly publishing into a new generation.

What are Frontiers Research Topics?

Frontiers Research Topics are very popular trademarks of the Frontiers Journals Series: they are collections of at least ten articles, all centered on a particular subject. With their unique mix of varied contributions from Original Research to Review Articles, Frontiers Research Topics unify the most influential researchers, the latest key findings and historical advances in a hot research area! Find out more on how to host your own Frontiers Research Topic or contribute to one as an author by contacting the Frontiers Editorial Office: **researchtopics@frontiersin.org**

LINKING ECOSYSTEM FUNCTION TO MICROBIAL DIVERSITY

Topic Editors:
Anne E. Bernhard, Connecticut College, USA
John J. Kelly, Loyola University Chicago, USA

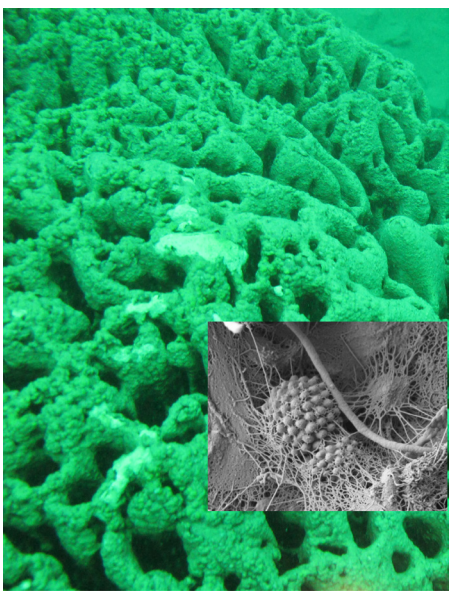

Pavilion Lake microbialite (Marble Canyon, British Columbia, Canada) at 20 m, filamentous cyanobacterial mat (inset). Photo by Donnie Reid and Tyler McKay and SEM by Ian Power.

Understanding the link between microbial diversity and ecosystem processes is a fundamental goal of microbial ecologists, yet we still have a rudimentary knowledge of how changes in diversity affect nutrient cycling and energy transfer in ecosystems. Due to the complexity of the problem, many published studies on this topic have been conducted in artificial or manipulated systems. Although researchers have begun to expose some possible mechanisms using these approaches, most have not yet been able to produce conclusive results that relate directly to natural systems. The few studies that have explored the link between diversity and activity in natural systems have typically focused on specific nutrient cycles or processes, such as nitrification, denitrification, and organic carbon degradation pathways, and the microbes that mediate them. What we have learned from these studies is that there are often strong associations between the physical and chemical features of the environment, the composition of the microbial communities, and their activities, but the rules that govern these associations have not been fully elucidated. These earlier studies of microbial diversity and processes in natural systems provide a framework for additional studies to broaden our understanding of the role of microbial diversity in ecosystem function. The problem is complex, but with recent advances in sequencing technology, -omics, and in-situ measurements of ecosystem processes and their applications to microbial communities, making direct connections between ecosystem function and microbial diversity seems more tractable than ever.

Citation: Bernhard, A. E., Kelly, J. J., eds. (2016). Linking Ecosystem Function to Microbial Diversity. Lausanne: Frontiers Media. doi: 10.3389/978-2-88919-985-3

Table of Contents

05 ***Editorial: Linking Ecosystem Function to Microbial Diversity***
Anne E. Bernhard and John J. Kelly

07 ***Addendum: Editorial: Linking Ecosystem Function to Microbial Diversity***
Anne E. Bernhard and John J. Kelly

Section 1: Using artificial and manipulated systems to elucidate mechanisms governing diversity-function relationships

08 ***Metacommunity dynamics of bacteria in an arctic lake: the impact of species sorting and mass effects on bacterial production and biogeography***
Heather E. Adams, Byron C. Crump and George W. Kling

18 ***Phytoplankton communities from San Francisco Bay Delta respond differently to oxidized and reduced nitrogen substrates—even under conditions that would otherwise suggest nitrogen sufficiency***
Patricia M. Glibert, Frances P. Wilkerson, Richard C. Dugdale, Alexander E. Parker, Jeffrey Alexander, Sarah Blaser and Susan Murasko

34 ***Connecting the dots: linking nitrogen cycle gene expression to nitrogen fluxes in marine sediment mesocosms***
Jennifer L. Bowen, Andrew R. Babbin, Patrick J. Kearns and Bess B. Ward

Section 2: Linking elemental cycling processes to microbial diversity in natural systems

44 ***Linking DNRA community structure and activity in a shallow lagoonal estuarine system***
Bongkeun Song, Jessica A. Lisa and Craig R. Tobias

54 ***Microbial abundance and diversity patterns associated with sediments and carbonates from the methane seep environments of Hydrate Ridge, OR***
Jeffrey J. Marlow, Joshua A. Steele, David H. Case, Stephanie A. Connon, Lisa A. Levin and Victoria J. Orphan

70 ***Benthic ammonia oxidizers differ in community structure and biogeochemical potential across a riverine delta***
Julian Damashek, Jason M. Smith, Annika C. Mosier and Christopher A. Francis

Section 3: Defining impacts of microbial diversity on decomposition processes

88 ***Loss of diversity in wood-inhabiting fungal communities affects decomposition activity in Norway spruce wood***
Lara Valentín, Tiina Rajala, Mikko Peltoniemi, Jussi Heinonsalo, Taina Pennanen and Raisa Mäkipää

99 ***Lignocellulose-responsive bacteria in a southern California salt marsh identified by stable isotope probing***
Lindsay E. Darjany, Christine R. Whitcraft and Jesse G. Dillon

Section 4: Using "-omics" approaches to identify diversity-function relationships

108 ***The transcriptional response of microbial communities in thawing Alaskan permafrost soils***
Marco J. L. Coolen and William D. Orsi

122 ***Metagenomic analysis reveals that modern microbialites and polar microbial mats have similar taxonomic and functional potential***
Richard Allen White III, Ian M. Power, Gregory M. Dipple, Gordon Southam and Curtis A. Suttle

136 ***Metagenomic analysis suggests modern freshwater microbialites harbor a distinct core microbial community***
Richard Allen White III, Amy M. Chan, Gregory S. Gavelis, Brian S. Leander, Allyson L. Brady, Gregory F. Slater, Darlene S. S. Lim and Curtis A. Suttle

Section 5: Combining ecophysiology and molecular tools to build trait-based frameworks

150 ***Trait-based approaches for understanding microbial biodiversity and ecosystem functioning***
Sascha Krause, Xavier Le Roux, Pascal A. Niklaus, Peter M. Van Bodegom, Jay T. Lennon, Stefan Bertilsson, Hans-Peter Grossart, Laurent Philippot and Paul L. E. Bodelier

frontiers in Microbiology

EDITORIAL
published: 30 June 2016
doi: 10.3389/fmicb.2016.01041

Editorial: Linking Ecosystem Function to Microbial Diversity

Anne E. Bernhard[1]* *and John J. Kelly*[2]

[1] Biology Department, Connecticut College, New London, CT, USA, [2] Biology Department, Loyola University Chicago, Chicago, IL, USA

Keywords: nitrogen, nitrification, DNRA, microbialites, metagenomics, methane seeps, stable isotope probing, metacommunity

The Editorial on the Research Topic

Linking Ecosystem Function to Microbial Diversity

Understanding the link between microbial diversity and ecosystem processes is a fundamental goal of microbial ecologists, yet we still have a rudimentary knowledge of how changes in diversity affect nutrient cycling and energy transfer in ecosystems. Due to the complexity of the problem, many published studies on this topic have been conducted in artificial or manipulated systems. Studies of artificial assemblages of microbial species have shown direct links between species evenness and ecosystem stability (Wittebolle et al., 2009), and the importance of complementarity for resource use among taxa (Salles et al.). Others have taken a microcosm approach. Webster et al. (2005) added nitrogen to soil microcosms and showed a link between ammonia-oxidizing bacterial diversity and nitrification rates, while Philippot et al. (2013) used a dilution approach to elucidate impacts of the loss of diversity of denitrifying communities on denitrification rates. One commonality of these studies is the focus on specific functional traits and functional gene sequences, which may serve as better proxies of the relationship between diversity and function, compared to more general phylogenetic markers of diversity. In this Research Topic, researchers expand on this theme by conducting transplantation experiments to study metacommunity dynamics in arctic lakes (Adams et al.), using mesocosms to quantify the relationship between nitrifiers and nitrification rates (Bowen et al.), and challenging long-held paradigms about the impacts of nutrient supply and phytoplankton community composition (Glibert et al.).

Although these approaches have allowed researchers to begin to elucidate some possible mechanisms governing ecosystem function and diversity, it is still a challenge to produce conclusive results that relate directly to natural systems. The few studies that have explored the link between diversity and activity in natural systems have typically focused on specific nutrient cycles or processes, such as nitrification, denitrification, and organic carbon degradation pathways, and the microbes that mediate them. For example, Cavigelli and Robertson (2000) found that soil denitrifying communities from tilled agricultural soils respond differently to environmental changes compared to native soils, and Kelly et al. (2011) reported that communities of ammonia-oxidizing archaea and ammonia-oxidizing bacteria respond differently to soil amendments, with ammonia-oxidizing archaea most strongly linked to nitrification rates. These studies emphasize the importance of native microbial communities in responding to environmental changes and modulating critical biochemical processes. Similarly, Bernhard et al. (2007) found functionally distinct ammonia-oxidizing bacterial communities along an estuarine salinity gradient, providing another direct, and quantitative link between microbial biodiversity and ecosystem function. Not surprisingly, many of the studies in this Research Topic focus again on nitrogen-cycling processes in natural systems and how the diversity of functional genes relates to the dominance of specific processes under different environmental conditions. Song et al. provide one of the first studies to

OPEN ACCESS

Edited and reviewed by:
Lisa Y. Stein,
University of Alberta, Canada

***Correspondence:**
Anne E. Bernhard
aeber@conncoll.edu

Specialty section:
This article was submitted to Terrestrial Microbiology, a section of the journal Frontiers in Microbiology

Received: *02 June 2016*
Accepted: *21 June 2016*
Published: *30 June 2016*

Citation:
Bernhard AE and Kelly JJ (2016) Editorial: Linking Ecosystem Function to Microbial Diversity. Front. Microbiol. 7:1041. doi: 10.3389/fmicb.2016.01041

show that diversity of bacteria that carry out dissimilatory nitrate reduction to ammonium (DNRA) may have significant impacts on DNRA rates, ultimately controlling the fate of nitrogen in estuaries. Damashek et al. report data from the nutrient-rich regions of San Francisco Bay suggesting that community structure of nitrifiers and biogeochemical function respond to differences in nutrient loading. And in a departure from the N cycle, Marlow et al. help to elucidate drivers of community structure and function at deep-sea methane seeps, and provide insight into differences in elemental cycling between archaeal and bacterial communities.

Earlier studies of microbial diversity and processes in natural systems provide a framework for additional studies to broaden our understanding of the role of microbial diversity in ecosystem function. The problem is complex, but with recent advances in sequencing technology, -omics, and *in-situ* measurements of ecosystem processes, and their applications to microbial communities, making direct connections between ecosystem function and microbial diversity seems more tractable than ever. In this Research Topic, metagenomic analysis of microbialites reveals novel functional guilds distinct from surrounding water and sediment (White et al.). In a companion study of an anthropogenic microbialite-forming ecosystem, White et al. again use metagenomic approaches to identify metabolic drivers of microbialite formation in the subarctic. Using stable isotope probing (SIP), Darjany et al. identify specific bacteria capable of using lignocellulose from salt marsh plants, representing one of the first studies to show a direct link between the source and fate of salt marsh macrophyte carbon.

What we have learned from these studies is that there are often strong associations between the physical and chemical features of the environment, the composition of the microbial communities, and their activities, but the rules that govern these associations have not been fully elucidated. Krause et al. argue in this Research Topic that using a combination of ecophysiology approaches and contemporary molecular tools to develop a trait-based framework, microbial ecologists have an opportunity to forge new understandings of biodiversity and ecosystem function relationships and to generate systematic principles that apply to both micro- and macro-ecology. This Research Topic focuses on studies that address the role of microbial diversity in ecosystem processes, with emphasis on direct and quantitative links between biodiversity and processes in natural systems.

AUTHOR CONTRIBUTIONS

All authors listed, have made substantial, direct and intellectual contribution to the work, and approved it for publication.

REFERENCES

Bernhard, A. E., Tucker, J., Giblin, A. E., and Stahl, D. A. (2007). Functionally distinct communities of ammonia-oxidizing bacteria along an estuarine salinity gradient. *Environ. Microbiol.* 9, 1439–1447. doi: 10.1111/j.1462-2920.2007.01260.x

Cavigelli, M. A., and Robertson, G. P. (2000). The functional significance of denitrifier community composition in a terrestrial ecosystem. *Ecology* 81, 1402–1414. doi: 10.1890/0012-9658(2000)081[1402:TFSODC]2.0.CO;2

Kelly, J. J., Policht, K., Grancharova, T., and Hundal, L. S. (2011). Distinct responses in ammonia-oxidizing archaea and bacteria after addition of biosolids to an agricultural soil. *Appl. Environ. Microbiol.* 77, 6551–6558. doi: 10.1128/AEM.02608-10

Philippot, L., Spor, A., Henault, C., Bru, D., Bizouard, F., Jones, C. M., et al. (2013). Loss in microbial diversity affects nitrogen cycling in soil. *ISME J.* 7, 1609–1619. doi: 10.1038/ismej.2013.34

Webster, G., Embley, T. M., Freitag, T. E., Smith, Z., and Prosser, J. I. (2005). Links between ammonia oxidizer species composition, functional diversity and nitrification kinetics in grassland soils. *Environ. Microbiol.* 7, 676–684. doi: 10.1111/j.1462-2920.2005.00740.x

Wittebolle, L., Marzorati, M., Clement, L., Balloi, A., Daffonchio, D., Heylen, K., et al. (2009). Initial community evenness favours functionality under selective stress. *Nature* 458, 623–626. doi: 10.1038/nature 07840

Conflict of Interest Statement: The authors declare that the research was conducted in the absence of any commercial or financial relationships that could be construed as a potential conflict of interest.

frontiers in Microbiology

CORRECTION
published: 22 August 2016
doi: 10.3389/fmicb.2016.01299

Addendum: Editorial: Linking Ecosystem Function to Microbial Diversity

Anne E. Bernhard[1]* *and John J. Kelly*[2]

[1] Biology Department, Connecticut College, New London, CT, USA, [2] Biology Department, Loyola University Chicago, Chicago, IL, USA

Keywords: metatranscirptomics, permafrost, fungi, decomposition, diversity

An addendum on

Editorial: Linking Ecosystem Function to Microbial Diversity
by Bernhard, A. E., and Kelly, J. J. (2016). Front. Microbiol. 7:1041. doi: 10.3389/fmicb.2016.01041

Two additional papers that are featured in this Research Topic are published in Frontiers in Terrestrial Microbiology. Valentin et al. (2014) explore relationships of fungal diversity and respiration rates of decomposing wood. And, using metatranscriptomics to investigate microbial activities in thawing permafrost, Coolen and Orsi (2015) demonstrate a potential link between bacteria carrying out acetogenesis and methanogenesis.

AUTHOR CONTRIBUTIONS

Both authors consulted on and drafted the commentary.

REFERENCES

Coolen, M. J. L., and Orsi, W. D. (2015). The transcriptional response of microbial communities in thawing Alaskan permafrost soils. *Front. Microbiol.* 6:197. doi: 10.3389/fmicb.2015.00197

Valentin, L., Rajala, T., Peltoniemi, M., Pannanen, T., Heinonsalo, J., and Mäkipää, R. (2014). Loss of diversity in wood-inhabiting fungal communities affects decomposition activity in Norway spruce wood. *Front. Microbiol.* 5:230. doi: 10.3389/fmicb.2014.00230

Conflict of Interest Statement: The authors declare that the research was conducted in the absence of any commercial or financial relationships that could be construed as a potential conflict of interest.

OPEN ACCESS

Edited and reviewed by:
Lisa Y. Stein,
University of Alberta, Canada

***Correspondence:**
Anne E. Bernhard
anne.bernhard@conncoll.edu

Specialty section:
This article was submitted to Terrestrial Microbiology, a section of the journal Frontiers in Microbiology

Received: *05 August 2016*
Accepted: *08 August 2016*
Published: *22 August 2016*

Citation:
Bernhard AE and Kelly JJ (2016) Addendum: Editorial: Linking Ecosystem Function to Microbial Diversity. Front. Microbiol. 7:1299. doi: 10.3389/fmicb.2016.01299

frontiers in MICROBIOLOGY

ORIGINAL RESEARCH ARTICLE
published: 04 March 2014
doi: 10.3389/fmicb.2014.00082

Metacommunity dynamics of bacteria in an arctic lake: the impact of species sorting and mass effects on bacterial production and biogeography

***Heather E. Adams*[1], *Byron C. Crump*[2]* *and George W. Kling*[1]**

[1] *Department of Ecology and Evolutionary Biology, University of Michigan, Ann Arbor, MI, USA*
[2] *College of Earth, Ocean and Atmospheric Science, Oregon State University, Corvallis, OR, USA*

Edited by:
Anne Bernhard, Connecticut College, USA

Reviewed by:
Hans Paerl, University of North Carolina-Chapel Hill, USA
Warwick F. Vincent, Laval University, Canada

***Correspondence:**
Byron C. Crump, College of Earth, Ocean and Atmospheric Science, Oregon State University, 104 CEOAS Admin Bldg., Corvallis, OR 97331, USA
e-mail: bcrump@coas.oregonstate.edu

To understand mechanisms linking ecosystem processes and microbial diversity in freshwater ecosystems, bacterial productivity and the metacommunity dynamics of species sorting and mass effects were investigated in an 18 ha headwater lake in northern Alaska. On most sampling dates, the phylogenetic composition of bacterial communities in inflowing streams (inlets) was strikingly different than that in the lake and the outflowing stream (outlet) (16S DGGE fingerprinting), demonstrating the shift in composition that occurs as these communities transit the lake. Outlet and downstream communities were also more productive than inlet and upstream communities (^{14}C-leucine incorporation). Inlet bacteria transplanted to the outlet stream in dialysis bags were equally or less productive than control bacteria, suggesting that the inlet bacteria are capable of growing under lake conditions, but do not remain abundant because of species sorting in the lake. Outlet bacteria (representative of epilimnetic bacteria) transplanted to the inlet stream were less productive than control bacteria, suggesting that lake bacteria are not as well adapted to growing under inlet conditions. Based on water density, inlet stream water and bacteria generally entered the lake at the base of the epilimnion. However, during low to medium flow in the inlet stream the residence time of the epilimnion was too long relative to bacterial doubling times for these allochthonous bacteria to have a mass effect on the composition of outlet bacteria. The highest community similarity between inlet and outlet bacteria was detected after a large rain event in 2003, with over 61% similarity (average non-storm similarities were 39 ± 8%). While mass effects may be important during large storm events, species sorting appears to be the predominant mechanism structuring bacterial communities within the lake, leading to the assembly of a lake community that has lost some ability to function in stream habitats.

Keywords: aquatic microbiology, arctic, bacterial production, species sorting, mass effects, metacommunity theory, transplant experiments

INTRODUCTION

Dispersal and competition are two fundamental mechanisms that influence the presence and dominance of populations within biological communities including plants, animals, and microorganisms. In aquatic systems, a primary dispersal mechanism for bacterial communities is water flow from terrestrial soils into lakes and streams, resulting in a mixture of communities and resources that may favor certain populations or alter overall community growth (e.g., Crump et al., 2012). Dormant and slow-growing bacterial cells can become active when their preferred carbon and nutrient resources appear (Judd et al., 2006; Jones and Lennon, 2010; Lennon and Jones, 2011; Gibbons et al., 2013), and previously active cells may be at a competitive disadvantage given the new mix of substrates input from upstream. Over relatively short time scales (minutes to months), dispersal via advection and selective competition among organisms (i.e., species sorting) generate microbial biogeographic patterns across aquatic ecosystems and landscapes (Hanson et al., 2012; Logue et al., 2012), but little is known about the relative importance of the processes generating these biogeographic patterns (e.g., Logue and Lindstrom, 2010) or about how these patterns in diversity affect bacterial function in ecosystems.

Metacommunity theory incorporates the mechanisms of dispersal and competition into four main perspectives that act alone or interact within a habitat: species sorting, mass effects, patch dynamics, and neutral processes (Leibold et al., 2004). Species sorting emphasizes spatial niche separation where relatively low levels of dispersal allow communities to respond to local conditions (Leibold and Wilbur, 1992). In contrast, mass effects allow inferior competitors to persist in the community due to high levels of dispersal from other habitats (Urban, 2004). Patch dynamics defines habitat patches as identical with local species diversity determined by dispersal or species interactions, and requires trade-offs in species traits for regional co-existence to occur (Mouquet et al., 2005). Neutral theory assumes functional equivalency among species such that patterns in diversity

are non-deterministic and driven by immigration and chance (Sloan et al., 2006; Lindström and Langenheder, 2012). Mass effects and species sorting are thought to be most applicable to aquatic bacterial communities for several reasons: bacteria are easily dispersed by water flow and have potentially high rates of immigration and emigration (Lindström and Bergström, 2004), environment patches are heterogeneous, especially at the microbial scale (Scheffer et al., 2003), bacterial community composition can shift on very short time scales (e.g., days to weeks; Judd et al., 2006; Van der Gucht et al., 2007; Hornak and Corno, 2012), and bacterial populations differ in growth rates and metabolic capabilities (Amon and Benner, 1996; Lapara et al., 2002; Bertoni et al., 2008; Adams et al., 2010). The relative importance of these mechanisms in controlling bacterial community assembly depends on traits of bacterial populations such as resource specialization and dispersal ability (Lindström and Langenheder, 2012). The persistence of bacterial populations that immigrate via water to a new habitat will depend on the number of cells dispersed to that habitat, and their ability to outcompete pre-existing populations through growth and avoidance of grazing or viral lysis.

Time scales of bacterial growth and dispersal also influence whether mass effects or species sorting are most important in structuring a bacterial community (Logue, 2010; Lindström and Langenheder, 2012). In lake catchments, the main mode of bacterial dispersal is likely unidirectional as water flows downhill from upstream soils, groundwater, hyporheic zones, streams, and lakes, although atmospheric deposition can also disperse bacteria (Jones and McMahon, 2009). Bacterial cells entrained in flowing water rely on the water pathways and mixing to reach suitable resources within new habitats. In order for bacteria to establish in a new habitat, they must have a sufficient growth rate to compete with other populations for resources, and population growth must exceed the rate of emigration due to water flow out of a habitat (i.e., mass effect). The physiological response of bacteria to new environmental conditions can be quite fast; e.g., productivity can respond to changes in temperature within 1–2 h (Kirchman et al., 2005; Bertoni et al., 2008; Adams et al., 2010). However, community shifts due to species sorting may take longer than the time that bacterial populations can remain in a habitat, particularly during a storm event with high water flow.

The mechanisms of community assembly at work in these habitats have consequences for processing of DOM and other resources across the landscape. Bacterial response to temperature and substrate- or nutrient-limiting conditions may be specific to the physiological capabilities of the community assemblage present at a given time. For example, soil bacteria transported into aquatic systems along with terrestrial dissolved organic matter (DOM) mix with stream communities that likely contain bacteria accustomed to processing terrestrial DOM. But when this community enters a lake, it encounters lake populations that may be limited in their ability to process terrestrial DOM. For example, Judd et al. (2006) showed experimentally that shifts in community composition along a landscape gradient (upland terrestrial to lowland aquatic ecosystems) occur in response to changes in the available dissolved organic substrates, and in turn the community productivity changes; Crump et al. (2007, 2012) observed these shifts in natural communities along the same landscape gradients. In addition, the community composition originally present may constrain the microbial physiological adjustment to a change in environment or resources (e.g., Comte and Del Giorgio, 2009), but dispersal may alter this original community composition independent of any metabolic response (Crump et al., 2007). Thus, the metacommunity processes have a direct effect on ecosystem function by replacing species and altering the resultant community's ability to process available nutrients and carbon. Here we investigate the role of mass effects and species sorting in structuring bacterial communities by examining the natural variability of habitat conditions and bacterial communities upstream and downstream of a small arctic headwater lake. We also measured the impact of dispersal on both community structure and growth rates of bacterial communities in different habitats. We address three main questions: (1) How do lakes alter habitat characteristics and bacterial community activity and diversity along landscape flowpaths? This is addressed by comparing habitats and bacterial communities upstream and downstream of a headwater lake. (2) Do stream communities remain active in a lake habitat when competition with lake communities is removed? (3) Do lake communities retain the ability to process upstream DOM, or do community shifts in the lake result in the loss of most bacterial populations with this ability? These latter two questions are addressed using transplantation of natural communities in dialysis bags between habitats.

MATERIALS AND METHODS

STUDY SITE

Sites are located on the north slope of the Brooks Range, Alaska, at the Arctic Long Term Ecological Research site. Samples were collected from upstream of, downstream of, and within Lake I-8, which is located two kilometers upstream of Toolik Lake. Lake I-8 is 18.2 ha in area with a volume of 642,500 m^3 and drains a catchment of 2910 ha. It is oligotrophic, with mean epilimnetic primary productivity of 17.4 μg C/L/d (range = 2.1–38.8) and mean chlorophyll *a* of 0.92 μg/L during the ice-free season (Kling et al., 2000). Lake I-8 has a main inflowing (inlet) stream, sampled ∼5 km upstream of the lake at the site I-8 HW, as well as where the stream flows into the lake at site I-8 inlet. There are three smaller inlet streams, (I-8 NE inlet, I-8 SE inlet, and I-8 S inlet) that also flow into the lake, and a single outflowing stream (I-8 outlet). Site I8-I9 is one km downstream of the lake outlet (**Figure 1**). Water temperatures for summers 2003–2007 (June–August) ranged from 3.3 to 18°C (mean = 10.5°C) at I-8 inlet, and ranged from 5.8 to 18.4°C (mean = 12.9°C) at I-8 outlet. There are usually 2–3 storm events during the summer season, post snow-melt.

FIELD MEASUREMENTS

Bacterial production, bacterial community composition, temperature, and DOM concentration were measured weekly at Lake I-8 inlet, I-8 outlet, and at site I8-I9 in the summers of 2003–2007 (**Figure 1**). The smaller inlets to the lake were also sampled weekly during the summer of 2007. I-8 HW stream and the lake itself were sampled three times every summer, with weekly sampling of the lake occurring during the summer of 2003 and a more

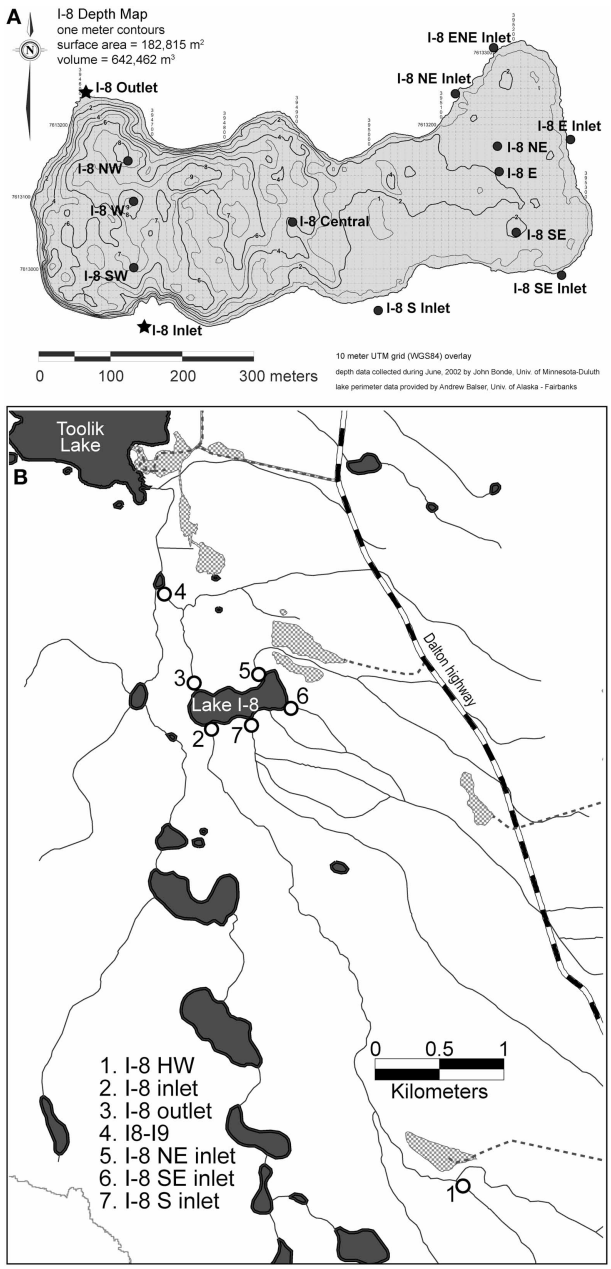

FIGURE 1 | (A) Lake spatial sampling sites at Lake I-8, Northern Alaska. I-8 outlet is located at 394605.858 Easting 7613243.017 Northing on the UTM Zone 6 North, WGS84 coordinate system (149.59°W, 68.61°N). **(B)** Sampling locations in the I-series catchment to Toolik Lake, Alaska.

intense spatial sampling at eight sites across the lake on 4 July 2007 (**Figure 1**). Stream water samples were collected from midstream while avoiding disturbance of streambed surfaces. Lake samples were collected using a Van Dorn bottle sampler, typically at the depths of 1 m (epilimnion) and 6 m (hypolimnion). Temperature was measured with a digital thermometer, conductivity with a model 122 Orion meter, and pH with a model 210A Orion meter. Stream discharge and temperature were monitored at the sites using dataloggers (Onset StowAways and Hobos) and a Marsh-McBirney Flowmate discharge meter. Water residence time (WRT) of the lake was calculated by dividing the lake volume by the mean outlet stream discharge. Epilimnetic WRT was calculated using the lake volume from surface to 3 m, which is the mean thermocline depth during the summer season. Time series temperature measurements in 2003 were obtained from the I-8 W station with seven Brancker TR 1050 self-contained temperature loggers (thermistors) at depths 0.05, 0.53, 1.03, 3.03, 4.03, 5.03, and 6.03 m (installed by MacIntyre). Isotherm depths were determined by linear interpolation of readings taken every 15 min. Thermistors had an accuracy of 0.002°C and a time constant of <3 s (MacIntyre, pers. comm.).

Bacterial production (BP) was measured using ^{14}C labeled-leucine uptake following Kirchman (1992), and assuming an intracellular isotopic dilution of 1. Each measure was calculated from incubation of three unfiltered 10 mL subsamples and one 10 mL trichloroacetic acid (TCA) killed control for ∼3 h before ending by adding TCA to a final concentration of 5%. Samples were filtered onto 0.2 μm nitro-cellulose filters and extracted using 5 mL of ice-cold 5% TCA. Filters were then dissolved in scintillation vials using ethylene glycol monoethyl ether, flooded with Scintisafe scintillation cocktail and counted on a liquid scintillation counter (Packard Tri-Carb 2100TR).

DOM samples were filtered in the field through ashed Whatman GF/F filters and stored at 4°C until analysis. Protein concentrations were determined within 48 h using the Bradford reagent assay (modified from Bradford, 1976) and phenolic concentrations were determined within 48 h using the Folin-Ciocalteu assay (Waterman and Mole, 1994). DOC and chlorophyll *a* concentrations were determined as in Kling et al. (2000).

Samples for cell counts were preserved with 2.5% final concentration of gluteraldehyde and stored at 4°C until analysis. Samples from 2005 were counted on a FACSCalibur (BD Biosciences) flow cytometer following del Delgiorgio et al. (1996). Sub-samples were stained with SYBR green nucleic acid stain in the dark for a minimum of 15 min (Marie et al., 1997; Lebaron et al., 1998). The concentration of the standard 1 μm bead solution and multiple confirmatory cell count samples were measured by epifluorescence microscopy. Samples from 2006 to 2007 were counted on a LSR II flow cytometer (BD Biosciences) as described by Ewart et al. (2008) with data acquired in log mode for at least 60 s and until 20,000 events were recorded, with the minimum green fluorescence (channel 200) set as the threshold. Cell doubling times were calculated using BP, average cell counts from environmental samples, and a conversion factor of 20 fg C/cell (Lee and Fuhrman, 1987).

Bacterial community composition was measured with denaturing gradient gel electrophoresis (DGGE) of PCR-amplified 16S rRNA genes applied to DNA samples. DNA was collected by filtering ∼500 mL of sample through a Sterivex 0.2 μm filter, stored at −80°C, and processed as described fully in Crump et al. (2003) and Adams et al. (2010). Imaging of DGGE gels was performed with Quantity One software on a Chemi-Doc gel documentation system (Bio-Rad) and gel bands were identified using GelCompar software to create a presence-absence matrix as described by Crump and Hobbie (2005). Each band represents an operational taxonomic unit (OTU) of bacteria. Dice transformation

(SPSS 14.0 through 17.0) was used to condense presence-absence of OTUs into percent community similarities between samples. PROXCAL (SPSS Categories, versions 14.0 through 17.0) was used to create non-metric multi-dimensional scaling (NMDS) graphs of sample similarities. Two-tailed paired *t*-tests (Excel 2003) were used to compare the number of populations (bands) between sites.

TRANSPLANT EXPERIMENTS

Transplantation of bacterial communities was performed to test activity in different habitats. Dialysis bags (Sigma dialysis tubing cellulose membrane, 76 mm flat width, typical molecular weight cut-off ~14,000 Da) were used to isolate bacterial communities from inputs of new bacteria (Gasol et al., 2002). Substrates smaller than 12,000 Da diffuse across the tubing membrane in less than 18 h, as confirmed with a diffusion test of ^{14}C-labeled leucine (Supplemental Figure 1), allowing exposure of the contained bacteria to ambient temperature and nutrient conditions. Bags were washed and soaked in DI water to remove excess glycerin for a minimum of 12 h before use, no sections of tubing were used more than once, and nitrile gloves were worn when handling the bags. At each site, three (two in 2005) replicate samples of whole water were collected in acid-washed 1L opaque Nalgene bottles and either transported to another site within 15 min or immediately transferred to 45.7 cm sections of tubing and closed (final volume 640 mL). Grazers were not removed for these experiments due to co-occurrence with particle-attached bacteria. Filled bags were then secured to dowels with plastic ties within open-topped plastic covered metal cages of dimensions 70 × 55 × 55 cm and secured in streams using rebar. Each of three replicate bags for each treatment was allowed to incubate *in situ* for 2–4 days. Upon collection, the contents of each bag were transferred to an acid-washed 1 L opaque Nalgene bottle from which 40 mL was used to measure bacterial production, 180 mL was filtered to measure chl *a*, proteins, phenolics, and DOC, 10–15 mL was preserved for cell counts, and the remainder was filtered to collect DNA.

Several transplant experiments were conducted at I-8 inlet and outlet. The first set of experiments presented here was performed on 18–21 July 2006 and consisted of incubating the I-8 inlet community at both the inlet and outlet sites to test if the community flowing into the lake would be active downstream. The second set of experiments conducted on 5–9 July 2005 and 2–4 July 2007 included the incubation of the outlet community at inlet and outlet sites to test if the downstream community retained the ability to process DOM from upstream. The third set of experiments conducted on 26–28 July 2005 and 1–3 August 2006 consisted of transplantation of both inlet and outlet communities between sites in addition to controls incubated at their original habitat.

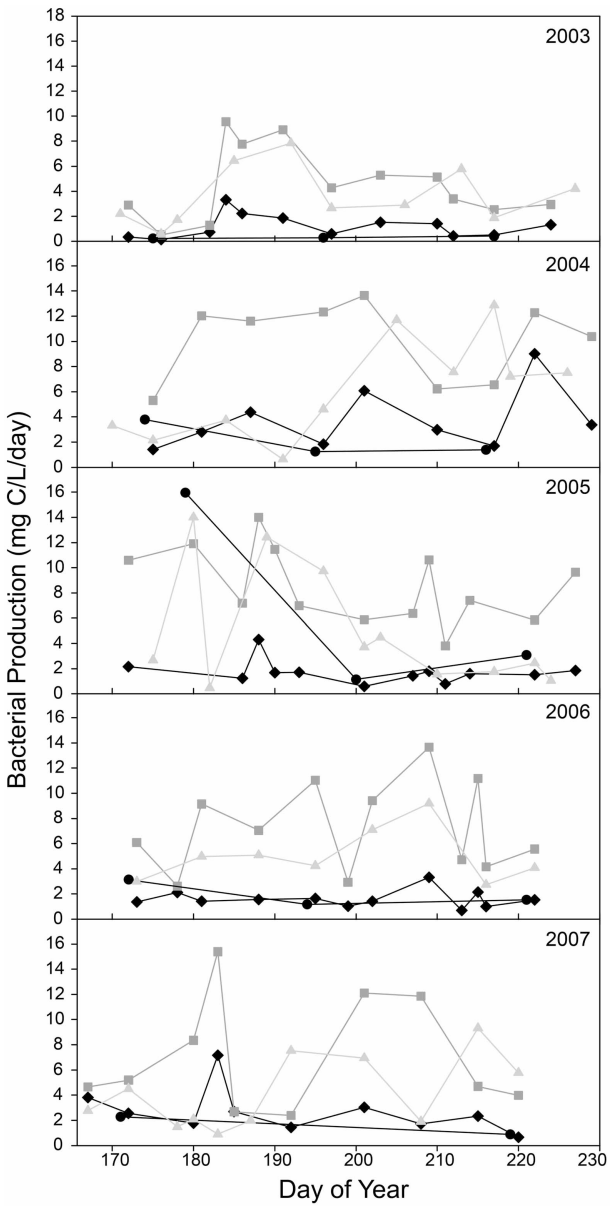

FIGURE 2 | Bacterial Production at sites upstream and downstream of Lake I-8 for sites I-8 headwaters (black circles), I-8 inlet (black diamonds), I-8 outlet (gray squares), and I-8 to I-9 (gray triangles).

RESULTS

DIFFERENCES IN ACTIVITY AND COMMUNITY COMPOSITION BETWEEN SITES

During the ice-free summer season, bacterial productivity (BP) was usually greater downstream of Lake I-8 than upstream (**Figure 2**). At upstream sites from 2003 to 2007, BP averaged 4.3 μg C/L/d ($SD = 7.6$, $n = 15$) at I-8 HW and 2.1 μg C/L/d ($SD = 1.6$, $n = 56$) at I-8 inlet. At downstream sites, BP averaged 7.5 μg C/L/d ($SD = 3.8$, $n = 57$) at I-8 outlet and 4.8 μg C/L/d ($SD = 3.4$, $n = 50$) ~1 km downstream at site I8-I9.

Community composition was also consistently different between sites upstream and downstream of the lake. In 2003, the bacterial community composition at I-8 inlet was variable over time with a low average similarity of 45% between inlet samples (inlet vs. inlet in **Figure 3**, Supplemental Table 1). Mid-lake and outlet communities were generally more stable during the summer and had average similarities of 74 and 63%, respectively. On each sampling date, the lake and outlet communities ("lake vs. out" in **Figure 3**) had a very high mean similarity of 79%;

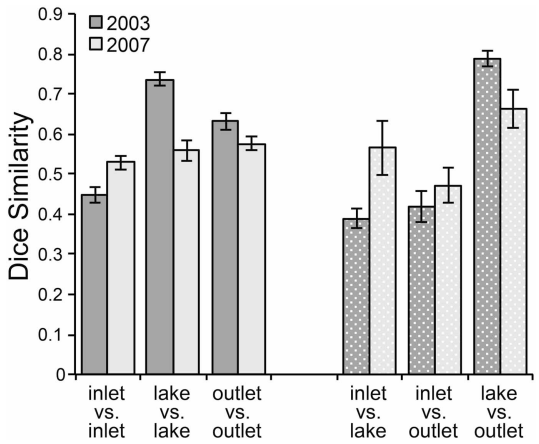

FIGURE 3 | Dice similarity of DGGE banding patterns at sites at Lake I-8 in summer 2003–2007. Error bars are standard error of the mean. Solid columns show average pair-wise similarity among communities at each site (inlet, lake, outlet) across sampling dates. Stippled columns show average pair-wise similarities between communities at different sites sampled on the same day. "Inlet" designates the I-8 inlet stream, "outlet" designates the outlet stream, and "lake" designates samples collected from the lake water column at the I-8 West station.

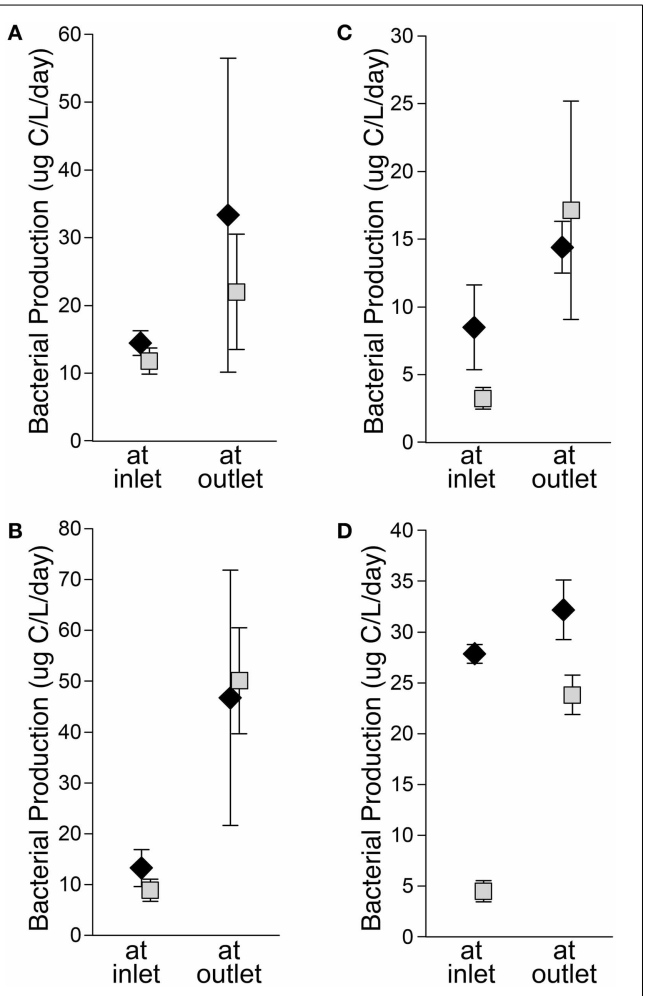

FIGURE 4 | Left: Early summer transplants at I-8 inlet and outlet from 5 to 9 July 2005 (A) and 2–4 July 2007 (B). Right: Late summer transplants at I-8 inlet and outlet from 26 to 28 July 2005 **(C)** and 1–3 Aug. 2006 **(D)**. For all graphs, diamonds are inlet communities and squares are outlet communities. Error bars are standard error of the mean.

this was expected because the outlet is essentially an integrated sample of the lake epilimnion. The inlet communities were less similar to the other two sites (average similarity of ∼40%). In 2007, community similarity between sites had a similar pattern but absolute differences were muted. The number of OTUs also differed between sites, with 20 ± 2 bands on average at the inlet and 26 ± 3 at the outlet in 2003 (p-value $= 0.003$). The inlet also had significantly fewer OTUs than the outlet in 2007 with 12 ± 3 bands found at the inlet and 18 ± 4 at the outlet (p-value $= 0.01$).

TRANSPLANT EXPERIMENTS

Bacteria transplanted between sites showed patterns in activity similar to those observed *in situ*. To test if bacteria flowing into the lake have the potential to be active in lake habitats, bacteria from the inlet were held in place or moved to the outlet, which represented lake conditions (Kling et al., 2000). Bacteria from the inlet (diamonds on **Figure 4**) incubated at the outlet always had greater bacterial production than control incubations at the inlet, although the difference was not always statistically significant. Bacteria were also moved from the outlet to the inlet to test if the communities that developed across the lake could process stream inlet DOM. Bacteria from the outlet (squares on **Figure 4**) incubated at the inlet always had depressed activity relative to control incubations at the outlet. In the early season transplants, rates of bacterial production were similar for inlet and outlet communities regardless of incubation location, but in the late season the transplants of inlet communities often had higher bacterial production rates than outlet communities suggesting community-specific responses to treatments. For all transplant experiments, the outlet habitat had more chl *a* and generally more protein and DOC than the inlet habitat (Supplemental Table 2). Temperatures tended to be warmer at the outlet, but transplants were conducted under a range of conditions including nearly equal temperatures and warmer at the inlet. The effect of temperature on bacterial productivity and community composition at these sites was previously found to be complicated due to multiple temperature optima within the communities (Adams, 2010; Adams et al., 2010).

LAKE INPUTS

The main I-8 inlet is the largest contributor of water to the lake, and in 2007 it had the greatest contribution to inflow when total inflow was highest (**Table 1**). The other inlets to the lake were either ephemeral (I-8 SE inlet and I-8 E inlet) or had much lower flow compared to the main inlet. I-8 NE inlet accounted for over 36% of water inputs on 4 July 2007, possibly due to rainstorms only in that part of the catchment, but its flow was only 10.2 L/s, which would have been 2% of the total inflow a month later on 3 August 2007 (**Table 2**). During wetter years, it is anticipated that I-8 inlet accounts for the majority of the water inputs due to its large

Table 1 | Water contribution to Lake I-8 for summer 2007.

Date	% contribution to lake inflow				Inflow (L/s)	Outflow (L/s)
	I-8 NE inlet	I-8 S inlet	I-8 SE inlet	I-8 inlet		
16 June 2007					10.2	32.7
18 June 2007	6.4	5.1	1.0	87.4	24.4	34.4
21 June 2007					8.5	32.1
29 June 2007					42.9	41.9
4 July 2007	36.1	6.4	n/a	57.5	28.3	27.1
11 July 2007					11.2	17.9
16 July 2007	14.0	8.7	0.8	76.4	320	47.6
20 July 2007	10.0	8.2	1.2	80.6	134	162
28 July 2007	8.3	8.9	0.9	81.9	48.3	50.7
3 Aug. 2007	5.2	5.8	0.4	88.7	503	619

Outflow is stream discharge measured at the I-8 outlet. Inflow is the sum of discharge rates for all lake inlets; inflows for dates 16, 21, and 29 June, and 11 July are based only on discharge measured at I-8 inlet.

Table 2 | Water residence time (WRT) for Lake I-8 and doubling times (DT) for I-8 inlet and outlet bacteria, based on data from 2003 to 2007.

Year	Lake WRT (days)			Epilimnetic WRT (days)		
	Baseflow	Mean	Storms	Baseflow	Mean	Storms
2003	120	3.9	1.0	89	2.9	0.8
2004	122	5.8	1.3	90	4.3	1.0
2005	811	20	1.5	600	15	1.1
2006	39	9.4	2.1	29	6.9	1.5
2007	328	23	2.7	243	17	2.0
Average	284	12.5	1.7	210	9.3	1.3

Site	Longest DT (days)	Mean DT (days)	Shortest DT (days)
I-8 inlet	30	1.9	0.4
I-8 outlet	12	0.9	0.4

Average WRT is provided for baseflow conditions, all conditions (Mean), and during storm events.

catchment size of 1281 ha, which is 44% of the total catchment for Lake I-8.

In order to determine the depth at which I-8 inlet water and bacteria enter the lake, a thermistor chain was deployed at the deep sampling site of the western basin (Lake I-8 W, Supplemental Figure 2). The summer of 2003 was relatively cold and wet with several large storm events (**Figure 5**; Adams et al., 2010). During the summer, the lake had periods of stratification until the last week of July, and had isothermal conditions for most of August and for brief periods earlier in the summer. The depth of inflow (dark columns on Supplemental Figure 2) varied throughout the summer, with base flow and early season run-off events intruding at the base of the epilimnion. Inflowing water occasionally entered a well-mixed water column or formed surface overflows. Deep intrusions to the very bottom of the hypolimnion were typically found in August when inlet water temperatures were colder (e.g., 6 August).

The spatial extent of inflowing water also affects bacterial dispersal into the lake, and the degree of mixing between inflow and lake impacts the strength of mass effects on community composition. Conductivity and pH profiles from the western sampling stations of the lake indicate that after the first small rain event of the season in 2007, the inflow signal intruded at the base of the epilimnion around 3 m, but was only detectable at the southwest station closest to I-8 inlet (Supplemental Figure 3). Presumably, this stream water mixed into the epilimnion and lost its distinct conductivity and pH signature before reaching the next sampling station.

The amount of time that inflowing water persists in a habitat directly affects community dynamics by setting the amount of time available for bacterial populations to grow and overcome dilution and dispersal. Epilimnion water retention time averaged ∼9 days but varied from <1 to 600 days, depending on stream discharge (**Table 2**). Previous estimates of WRT at this site were based on the lake-area relationship between Lake I-8 and Toolik Lake (Kling et al., 2000; Crump et al., 2007) instead of the direct measurements of discharge presented here. Bacteria cell doubling times were highly variable (**Table 2**). The shortest doubling time (0.4 days) was shorter than the shortest WRT (0.8 days), but the wide range of doubling times indicates that WRT

was occasionally shorter than doubling time, creating a condition in which species sorting has little effect. The balance between doubling time and WRT affects the persistence of populations within the habitat. A large but variable fraction of populations in the outlet community were concurrently detected in the inlet community, ranging from 32 to 63% (mean of 48%) in 2003 and from 50 to 71% (mean of 59%) in 2007. The degree of overlap between the inlet and outlet community was related to the amount of stream flow, and thus the WRT of the lake (**Figure 6**), in July and August. Overall community similarity between the inlet and outlet calculated for each sampling date ranged from 29 to 62% (mean 42%) and was greatest after the largest storm event of 2003 (**Figures 3**, **5**).

Bacterial communities collected from three inlet streams, the outlet stream, and several locations in the lake on 4 July 2007 clustered based on lotic or lentic habitat (**Figure 7**). Lake communities collected at several locations and depths within the lake, including I-8 outlet, had a high mean similarity to each other of 76% (± 9% *SD*), while inlet communities had a lower mean similarity to each other of 32% (± 30% *SD*) and had only 28% average similarity to the lake communities (*SD* of 9%). The two inlet streams draining catchments south of the lake (I-8 inlet and I-8 S inlet) had two-thirds of their bacterial community members in common, while the I-8 NE inlet had very low similarity to the other two inlet sites (13 and 17%, respectively).

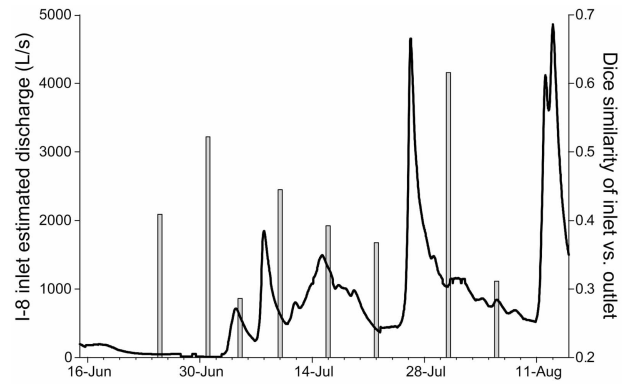

FIGURE 5 | Modeled discharge at I-8 inlet (black line) and % similarity of bacterial communities at I-8 inlet and I-8 outlet in the summer of 2003 (gray bars). Discharge was modeled using the relationship of discharge between Toolik Lake inlet and I-8 inlet in 2005–2007. Highest DNA similarity between I-8 inlet and outlet was detected after a large rain event near the end of July.

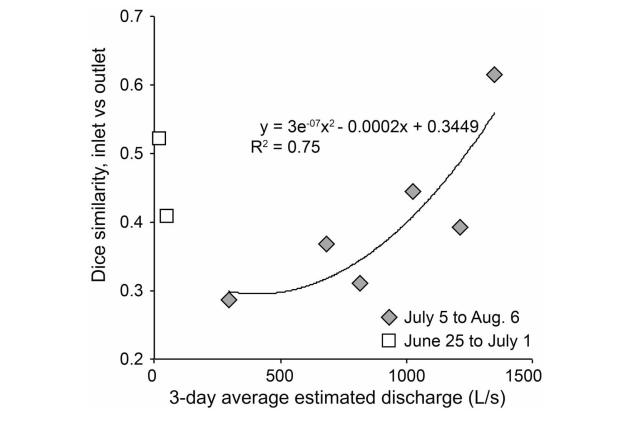

FIGURE 6 | Dice similarity between inlet and outlet bacterial community composition against the average estimated discharge for 3 days prior to community composition comparisons. A polynomial line is fit to samples collected after July 1.

DISCUSSION

Bacterial populations that are best adapted to local environmental conditions should dominate in habitats with those conditions provided that species sorting is the primary mechanism structuring the community. Thus, when dispersal is relatively low and species sorting dominates, community composition in habitats with different environmental conditions should be dissimilar. However, if dispersal is high and different habitats are linked hydrologically, then mass effects can produce greater similarity in community composition between habitats. Based on our hydrologic assessment, the inlets and outlet of lake I-8 are not highly linked except during large storm events when the communities in these two environments became more similar, demonstrating the impact of mass effects on patterns in microbial diversity over time scales of days.

The main outlet of Lake I-8 supported both greater bacterial productivity and a more stable community composition than the main inlet to the lake (**Figures 2**, **3**). This elevated BP is likely supported by relatively labile DOM sources from autochthonous production in the lake, as indicated by higher levels of chl *a* and proteins at the outlet than the inlet (Supplemental Table 2). Community BP is not strongly correlated with temperature in these habitats (Adams, 2010; Adams et al., 2010), and a multiple regression analysis of field data showed that temperature was only one of several parameters required to explain patterns in BP including dissolved organic carbon, chlorophyll *a*, and total

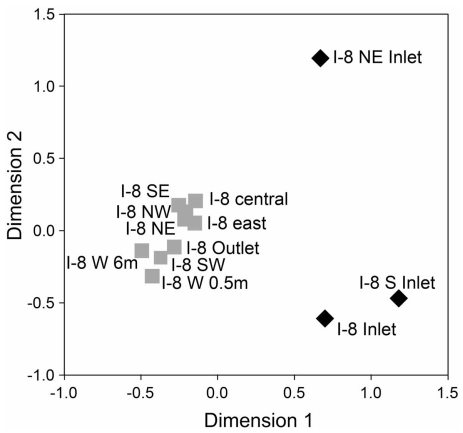

FIGURE 7 | NMDS of bacterial communities at Lake I-8 on 4 July 2007 determined from Dice similarities of 16S rRNA DGGE banding patterns for Inlet samples (black diamonds) and outlet and lake samples (gray squares). All samples were collected from surface water (0.01 m for streams, 0.5 m for lake) unless otherwise noted. Normalized raw stress = 0.009.

dissolved nitrogen and phosphorous concentrations. This work also identified multiple temperature optima within these bacterial communities (Adams et al., 2010), suggesting that rates of bacterial production are influenced by the composition of bacterial communities. The stability of the outlet community appears to be related to the retention of water in the lake. Lakes slow the transport of bacteria through catchments, and given sufficient time allow species sorting processes to control community dynamics and to result in downstream communities that are best adapted to local environmental conditions (Van der Gucht et al., 2007). However, we found that mass effects periodically disrupt the relatively stable community composition in the lake when large storm events occur, resulting in more similar communities at the inlet and outlet (**Figures 5**, **6**). During these periods, the communities at both locations are likely to be able to process the allochthonous DOM also being transported downstream, changing the function of the ecosystem.

When transplanted, bacteria from the inlet remain active at the outlet and have equal, if not greater, activity in this new habitat (**Figure 4**). However, less than half of inlet bacterial populations detected as OTUs on DGGE gels persist during transport across the lake to the outlet (**Figure 3**, Supplemental Table 1). This suggests that the inlet bacteria brought into the lake are being out-competed by bacteria better adapted to process lake DOM and grow under lake conditions (e.g., lower nitrate concentration, higher temperature; Supplemental Table 3) (e.g., Lindström and Langenheder, 2012). Kritzberg et al. (2005) determined that lake bacterial production is correlated with autochthonous primary production, even in habitats with high levels of allochthonous (terrestrial) DOM, suggesting that lake bacteria are better adapted to grow on autochthonous organic matter than allochthonous organic matter. When communities from the Lake I-8 outlet were transplanted to the inlet habitat, in general their productivity dropped, and in the late season they were less productive than the inlet communities incubated at the same time (**Figure 4**). This suggests that outlet communities no longer include (in large numbers) populations of bacteria that are able to rapidly process upstream DOM and grow under inlet conditions, possibly due to species sorting in the lake during which inlet bacteria were either outcompeted or diluted to low numbers within the new lake community. These inlet bacteria, though still present in the lake, appear to be either poor competitors or potentially limited in their dispersal to the outlet habitat during low-flow periods.

The dispersal of inlet communities into the lake is limited by the depth, spatial extent, and volume of stream inflow. Although the main inlet provides the majority of water to the lake (**Table 1**), this water may not extend far into the lake due to mixing or insufficient volume of inflow, as observed on 4 Jul 2007 (Supplemental Figure 3), or it may flow directly to the hypolimnion where it becomes isolated until the lake mixes deeply (Supplemental Figure 2). However, during large storm events the inflow is very high and concurrent cold air and water temperatures can result in deep mixing. Large storm events also decrease the WRT, and in other systems short WRTs have been found to increase community similarity (Lindström and Bergström, 2004). Both sufficient water volume and inflow penetration into the epilimnion would be required for mass effects to have a large impact on the outlet community, such as occurred around 30 Jul 2003 (**Figure 5**, Supplemental Figure 2). During this large storm event (∼4500 L/s discharge), the community similarity of I-8 inlet and I-8 outlet was 62% compared to 37% similarity before the storm. However, storms of such magnitude are relatively rare; only 13% of summer storm events from 1991 to 2008 had a similar or greater magnitude (Arctic LTER data).

The inlets to the lake drain sub-catchments that differ in vegetation and surface geomorphology, both of which impact bacterial communities and therefore the types of populations that can move downstream (Judd and Kling, 2002). The fact that the I-8 NE inlet had very low similarity to the other two inlet sites (13 and 17%, respectively; **Figure 7**) highlights that catchment-related differences in source communities can play a role in the metacommunity dynamics in a lake. However, most populations from the smaller inlets do not appear to persist in the lake, with very low similarities between inlet and lake communities. This is likely due to the small number of inlet bacterial cells becoming diluted within the lake, as seen in other studies (Lindström and Bergström, 2004), or due to unfavorable conditions during and after dispersal (Lindström and Langenheder, 2012). Lower population sizes can result in stochastic extinctions and can decrease the ability of new populations to compete with existing lake populations, although for biofilm communities assembly appears to be robust to such stochastic processes (Besemer et al., 2012). Samples collected at several locations within the lake indicated a laterally well-mixed epilimnetic bacterial community with high similarity between communities at distant sites within the lake (**Figure 7**). Chemical measures of lake water support this being a well-mixed habitat (Supplemental Table 3, Supplemental Figure 2) and there was no evidence for a gradient of community composition along a gradient of allochthonous inputs across the lake such as that found in a much larger reservoir by Simek et al. (2001).

In Lake I-8, there is evidence that both species sorting and mass effects structure bacterial community composition, with the impact of mass effects being limited to large stream-inflow events. Transplant experiments showed that although inlet communities have the potential for successful establishment as defined by Hanson et al. (2012) through metabolic activity in the lake and outlet habitat, outlet communities consist of many bacteria that are more limited in their ability to remain active in the inlet habitat and process allochthonous DOM (at least to the level of our detection), particularly later in the summer season. The analysis of depth, spatial extent, and volume of water inflow determined the potential dispersal of inlet bacteria to the lake. The relative magnitude of bacterial growth rates that drive species sorting, compared to physical flows and WRT which controls water-borne dispersal, determines the persistence of inlet bacteria in the lake and outlet habitat. When WRT is short and mass effects dominate, inlet stream bacteria mix farther into the lake and result in more similar community composition between inlet and outlet. WRT, along with environmental conditions, has been found to control the persistence of bacterial groups in other systems as well (Lindström et al., 2005; Crump et al., 2007), although a threshold for the importance of mass effects across habitats remains undetermined (Logue and Lindstrom, 2010). It appears that when WRT is relatively long, competition and predation

structure the community in the lake, and many inlet populations do not persist or persist in very low numbers. Van der Gucht et al. (2007) suggest that high growth rates and regular dispersal allows bacterial communities to track environmental conditions but that oligotrophic systems should be more prone to mass effects than eutrophic systems with similar hydrology. In our oligotrophic study system, bacteria have a faster average doubling time than the average WRT, suggesting that species sorting dominates while mass effects may be important only during aperiodic, summer storm events. These metacommunity dynamics appear to directly influence the ecosystem function of microbial communities, by changing the species composition of communities through dispersal, and altering the ability of microbial communities to process different DOM substrates and their rates of activity under different conditions.

ACKNOWLEDGMENTS

Field measurements and laboratory experiments were performed at the University of Alaska Fairbanks Toolik Field Station. Jessica Spence, Maria Dzul, Alex Mettler, Christina Maki, Lauren Yelen, Christopher Wallace, and Scott Houghton assisted with field sampling. Jen Kostrzewski assisted with tracking the influence of inflow and quantifying the hydrologic effects of storm events. Ashley Larsen's work on the spatial sampling was part of an NSF-REU project. MacIntyre provided Lake I-8 thermistor data from 2003. John Bonde and Andrew Balser provided bathymetric data and lake volume. Jude Apple and Erica Kiss assisted with molecular analyses. Craig Nelson performed cell counts for 2006 and 2007 samples. Funding was provided by NSF-DEB 0639805, 0423385, 981022, NSF-OPP 9911278, and to Heather E. Adams by the University of Michigan (Rackham, Department of EEB, Whittaker Mentoring Fellowship, and Helen Olsen Brower Endowed Fellowship) and the EPA Science to Achieve Results (STAR) Graduate Fellowship Program (the EPA has not officially endorsed this publication and the views expressed herein may not reflect the views of the EPA).

SUPPLEMENTARY MATERIAL

The Supplementary Material for this article can be found online at: http://www.frontiersin.org/journal/10.3389/fmicb.2014.00082/abstract

REFERENCES

Adams, H. E. (2010). *Controls on Bacterial Productivity in Arctic Lakes and Streams*. Ph.D., University of Michigan, Michigan.

Adams, H. E., Crump, B. C., and Kling, G. W. (2010). Temperature controls on aquatic bacterial production and community dynamics in arctic lakes and streams. *Environ. Microbiol.* 12, 1319–1333. doi: 10.1111/j.1462-2920.2010.02176.x

Amon, R. M. W., and Benner, R. (1996). Bacterial utilization of different size classes of dissolved organic matter. *Limnol. Oceanogr.* 41, 41–51. doi: 10.4319/lo.1996.41.1.0041

Bertoni, R., Callieri, C., Balseiro, E., and Modenutti, B. (2008). Susceptibility of bacterioplankton to nutrient enrichment of oligotrophic and ultraoligotrophic lake waters. *J. Limnol.* 67, 120–127. doi: 10.4081/jlimnol.2008.120

Besemer, K., Peter, H., Logue, J. B., Langenheder, S., Lindstrom, E. S., Tranvik, L. J., et al. (2012). Unraveling assembly of stream biofilm communities. *Isme J.* 6, 1459–1468. doi: 10.1038/ismej.2011.205

Bradford, M. M. (1976). Rapid and sensitive method for quantitation of microgram quantities of protein utilizing principle of protein-dye binding. *Anal. Biochem.* 72, 248–254. doi: 10.1016/0003-2697(76)90527-3

Comte, J., and Del Giorgio, P. A. (2009). Links between resources, C metabolism and the major components of bacterioplankton community structure across a range of freshwater ecosystems. *Environ. Microbiol.* 11, 1704–1716. doi: 10.1111/j.1462-2920.2009.01897.x

Crump, B. C., Adams, H. E., Hobbie, J. E., and Kling, G. W. (2007). Biogeography of bacterioplankton in lakes and streams of an arctic tundra catchment. *Ecology* 88, 1365–1378. doi: 10.1890/06-0387

Crump, B. C., Amaral-Zettler, L. A., and Kling, G. W. (2012). Microbial diversity in arctic freshwaters is structured by inoculation of microbes from soils. *Isme J.* 6, 1629–1639. doi: 10.1038/ismej.2012.9

Crump, B. C., and Hobbie, J. E. (2005). Synchrony and seasonality in bacterioplankton communities of two temperate rivers. *Limnol. Oceanogr.* 50, 1718–1729. doi: 10.4319/lo.2005.50.6.1718

Crump, B. C., Kling, G. W., Bahr, M., and Hobbie, J. E. (2003). Bacterioplankton community shifts in an arctic lake correlate with seasonal changes in organic matter source. *Appl. Environ. Microbiol.* 69, 2253–2268. doi: 10.1128/AEM.69.4.2253-2268.2003

Delgiorgio, P., Bird, D. F., Prairie, Y. T., and Planas, D. (1996). Flow cytometric determination of bacterial abundance in lake plankton with the green nucleic acid stain SYTO 13. *Limnol. Oceanogr.* 41, 783–789. doi: 10.4319/lo.1996.41.4.0783

Ewart, C. S., Meyers, M. K., Wallner, E. R., McGillicuddy, D. J., and Carlson, C. A. (2008). Microbial dynamics in cyclonic and anticyclonic mode-water eddies in the northwestern Sargasso Sea. *Deep-Sea Res. Part II-Top. Stud. Oceanogr.* 55, 1334–1347. doi: 10.1016/j.dsr2.2008.02.013

Gasol, J. M., Comerma, M., Garcia, J. C., Armengol, J., Casamayor, E. O., Kojecka, P., et al. (2002). A transplant experiment to identify the factors controlling bacterial abundance, activity, production, and community composition in a eutrophic canyon-shaped reservoir. *Limnol. Oceanogr.* 47, 62–77. doi: 10.4319/lo.2002.47.1.0062

Gibbons, S. M., Caporaso, J. G., Pirrung, M., Field, D., Knight, R., and Gilbert, J. A. (2013). Evidence for a persistent microbial seed bank throughout the global ocean. *Proc. Natl. Acad. Sci. U.S.A.* 110, 4651–4655. doi: 10.1073/pnas.1217767110

Hanson, C. A., Fuhrman, J. A., Horner-Devine, M. C., and Martiny, J. B. H. (2012). Beyond biogeographic patterns: processes shaping the microbial landscape. *Nat. Rev. Microbiol.* 10, 497–506. doi: 10.1038/nrmicro2795

Hornak, K., and Corno, G. (2012). Every coin has a back side: invasion by limnohabitans planktonicus promotes the maintenance of species diversity in bacterial communities. *PLoS ONE* 7:e51576. doi: 10.1371/journal.pone.0051576

Jones, S. E., and Lennon, J. T. (2010). Dormancy contributes to the maintenance of microbial diversity. *Proc. Natl. Acad. Sci. U.S.A.* 107, 5881–5886. doi: 10.1073/pnas.0912765107

Jones, S. E., and McMahon, K. D. (2009). Species-sorting may explain an apparent minimal effect of immigration on freshwater bacterial community dynamics. *Environ. Microbiol.* 11, 905–913. doi: 10.1111/j.1462-2920.2008.01814.x

Judd, K. E., Crump, B. C., and Kling, G. W. (2006). Variation in dissolved organic matter controls bacterial production and community composition. *Ecology* 87, 2068–2079. doi: 10.1890/0012-9658(2006)87[2068:VIDOMC]2.0.CO;2

Judd, K. E., and Kling, G. W. (2002). Production and export of dissolved C in arctic tundra mesocosms: the roles of vegetation and water flow. *Biogeochemistry* 60, 213–234. doi: 10.1023/A:1020371412061

Kirchman, D. L. (1992). Incorporation of thymidine and leucine in the sub-arctic Pacific - application to estimating bacterial production. *Mar. Ecol. Prog. Ser.* 82, 301–309. doi: 10.3354/meps082301

Kirchman, D. L., Malmstrom, R. R., and Cottrell, M. T. (2005). Control of bacterial growth by temperature and organic matter in the Western Arctic. *Deep-Sea Res. Part II-Top. Stud. Oceanogr.* 52, 3386–3395. doi: 10.1016/j.dsr2.2005.09.005

Kling, G. W., Kipphut, G. W., Miller, M. M., and O'Brien, W. J. (2000). Integration of lakes and streams in a landscape perspective: the importance of material processing on spatial patterns and temporal coherence. *Freshw. Biol.* 43, 477–497. doi: 10.1046/j.1365-2427.2000.00515.x

Kritzberg, E. S., Cole, J. J., Pace, M. M., and Graneli, W. (2005). Does autochthonous primary production drive variability in bacterial metabolism and growth efficiency in lakes dominated by terrestrial C inputs? *Aquat. Microb. Ecol.* 38, 103–111. doi: 10.3354/ame038103

Lapara, T. M., Zakharova, T., Nakatsu, C. H., and Konopka, A. (2002). Functional and structural adaptations of bacterial communities growing on particulate

substrates under stringent nutrient limitation. *Microb. Ecol.* 44, 317–326. doi: 10.1007/s00248-002-1046-8

Lebaron, P., Parthuisot, N., and Catala, P. (1998). Comparison of blue nucleic acid dyes for flow cytometric enumeration of bacteria in aquatic systems. *Appl. Environ. Microb.* 64, 1725–1730.

Lee, S., and Fuhrman, J. A. (1987). Relationships between biovolume and biomass of naturally derived marine bacterioplankton. *Appl. Environ. Microbiol.* 53, 1298–1303.

Leibold, M. A., Holyoak, M., Mouquet, N., Amarasekare, P., Chase, J. M., Hoopes, M. F., et al. (2004). The metacommunity concept: a framework for multi-scale community ecology. *Ecol. Lett.* 7, 601–613. doi: 10.1111/j.1461-0248.2004.00608.x

Leibold, M. A., and Wilbur, H. M. (1992). Interactions between food-web structure and nutrients on pond organisms. *Nature* 360, 341–343. doi: 10.1038/360341a0

Lennon, J. T., and Jones, S. E. (2011). Microbial seed banks: the ecological and evolutionary implications of dormancy. *Nat. Rev. Microbiol.* 9, 119–130. doi: 10.1038/nrmicro2504

Lindström, E. S., and Bergström, A. K. (2004). Influence of inlet bacteria on bacterioplankton assemblage composition in lakes of different hydraulic retention time. *Limnol. Oceanogr.* 49, 125–136. doi: 10.4319/lo.2004.49.1.0125

Lindström, E. S., Kamst-Van Agterveld, M. P., and Zwart, G. (2005). Distribution of typical freshwater bacterial groups is associated with pH, temperature, and lake water retention time. *Appl. Environ. Microbiol.* 71, 8201–8206. doi: 10.1128/AEM.71.12.8201-8206.2005

Lindström, E. S., and Langenheder, S. (2012). Local and regional factors influencing bacterial community assembly. *Environ. Microbiol. Rep.* 4, 1–9. doi: 10.1111/j.1758-2229.2011.00257.x

Logue, J. B. (2010). *Factors Influencing the Biogeography of Bacteria in Fresh Waters - A Metacommunity Approach*. Ph.D. thesis, Uppsala University, Uppsala.

Logue, J. B., Langenheder, S., Andersson, A. F., Bertilsson, S., Drakare, S., Lanzen, A., et al. (2012). Freshwater bacterioplankton richness in oligotrophic lakes depends on nutrient availability rather than on species-area relationships. *Isme J.* 6, 1127–1136. doi: 10.1038/ismej.2011.184

Logue, J. B., and Lindstrom, E. S. (2010). Species sorting affects bacterioplankton community composition as determined by 16S rDNA and 16S rRNA fingerprints. *Isme J.* 4, 729–738. doi: 10.1038/ismej.2009.156

Marie, D., Partensky, F., Jacquet, S., and Vaulot, D. (1997). Enumeration and cell cycle analysis of natural populations of marine picoplankton by flow cytometry using the nucleic acid stain SYBR Green I. *Appl. Environ. Microbiol.* 63, 186–193.

Mouquet, N., Belrose, V., Thomas, J. A., Elmes, G. W., Clarke, R. T., and Hochberg, M. E. (2005). Conserving community modules: a case study of the endangered lycaenid butterfly Maculinea alcon. *Ecology* 86, 3160–3173. doi: 10.1890/04-1664

Scheffer, M., Rinaldi, S., Huisman, J., and Weissing, F. J. (2003). Why plankton communities have no equilibrium: solutions to the paradox. *Hydrobiologia* 491, 9–18. doi: 10.1023/A:1024404804748

Simek, K., Armengol, J., Comerma, M., Garcia, J. C., Kojecka, P., Nedoma, J., et al. (2001). Changes in the epilimnetic bacterial community composition, production, and protist-induced mortality along the longitudinal axis of a highly eutrophic reservoir. *Microb. Ecol.* 42, 359–371. doi: 10.1007/s00248-001-0014-z

Sloan, W. T., Lunn, M., Woodcock, S., Head, I. M., Nee, S., and Curtis, T. P. (2006). Quantifying the roles of immigration and chance in shaping prokaryote community structure. *Environ. Microb.* 8, 732–740. doi: 10.1111/j.1462-2920.2005.00956.x

Urban, M. C. (2004). Disturbance heterogeneity determines freshwater metacommunity structure. *Ecology* 85, 2971–2978. doi: 10.1890/03-0631

Van der Gucht, K., Cottenie, K., Muylaert, K., Vloemans, N., Cousin, S., Declerck, S., et al. (2007). The power of species sorting: Local factors drive bacterial community composition over a wide range of spatial scales. *Proc. Natl. Acad. Sci. U.S.A.* 104, 20404–20409. doi: 10.1073/pnas.0707200104

Waterman, P. G., and Mole, S. (1994). *Analysis of Phenolic Plant Metabolites.* Boston, MASS: Blackwell Scientific Publications.

Conflict of Interest Statement: The authors declare that the research was conducted in the absence of any commercial or financial relationships that could be construed as a potential conflict of interest.

Received: 01 January 2014; paper pending published: 24 January 2014; accepted: 14 February 2014; published online: 04 March 2014.

*Citation: Adams HE, Crump BC and Kling GW (2014) Metacommunity dynamics of bacteria in an arctic lake: the impact of species sorting and mass effects on bacterial production and biogeography. Front. Microbiol. **5**:82. doi: 10.3389/fmicb.2014.00082*

This article was submitted to Aquatic Microbiology, a section of the journal Frontiers in Microbiology.

frontiers in
MARINE SCIENCE

ORIGINAL RESEARCH ARTICLE
published: 07 July 2014
doi: 10.3389/fmars.2014.00017

Phytoplankton communities from San Francisco Bay Delta respond differently to oxidized and reduced nitrogen substrates—even under conditions that would otherwise suggest nitrogen sufficiency

Patricia M. Glibert[1]*, Frances P. Wilkerson[2], Richard C. Dugdale[2], Alexander E. Parker[2,3], Jeffrey Alexander[1], Sarah Blaser[2] and Susan Murasko[1,4]

[1] *Horn Point Laboratory, University of Maryland Center for Environmental Science, Cambridge, MD, USA*
[2] *Romberg Tiburon Center, San Francisco State University, Tiburon, CA, USA*
[3] *The California Maritime Academy, Vallejo, CA, USA*
[4] *Florida Fish and Wildlife Conservation Commission, Fish and Wildlife Research Institute, St. Petersburg, FL, USA*

Edited by:
Anne Bernhard, Connecticut College, USA

Reviewed by:
Kathleen Scott, University of South Florida, USA
Michael A. Mallin, University of North Carolina Wilmington, USA

****Correspondence:***
Patricia M. Glibert, Horn Point Laboratory, University of Maryland Center for Environmental Science, PO Box 775, 2020 Horns Point Rd., Cambridge, MD 21613, USA
e-mail: glibert@umces.edu

The effect of equivalent additions of nitrogen (N, 30–40 μM-N) in different forms (ammonium, NH_4^+, and nitrate, NO_3^-) under conditions of different light exposure on phytoplankton community composition was studied in a series of four, 5-day enclosure experiments on water collected from the nutrient-rich San Francisco Bay Delta over 2 years. Overall, proportionately more chlorophyll *a* and fucoxanthin (generally indicative of diatoms) was produced per unit N taken up in enclosures enriched with NO_3^- and incubated at reduced (~15% of ambient) light intensity than in treatments with NO_3^- with high (~60% of ambient) light exposure or with NH_4^+ under either light condition. In contrast, proportionately more chlorophyll *b* (generally indicative of chlorophytes) and zeaxanthin (generally indicative of cyanobacteria) was produced in enclosures enriched with NH_4^+ and incubated under high light intensity than in treatments with low light or with added NO_3^- at either light level. Rates of maximal velocities (V_{max}) of uptake of N substrates, measured using ^{15}N tracer techniques, in all enclosures enriched with NO_3^- were higher than those enriched with NH_4^+. Directionality of trends in enclosures were similar to phytoplankton community shifts observed in transects of the Sacramento River to Suisun Bay, a region in which large changes in total N quantity and form occur. These data substantiate the growing body of experimental evidence that dichotomous microbial communities develop when enriched with the same absolute concentration of oxidized vs. reduced N forms, even when sufficient N nutrient was available to the community prior to the N inoculations.

Keywords: nitrate, ammonium, phytoplankton pigments, food webs, new and regenerated production

INTRODUCTION

Two classic tenets in oceanographic phytoplankton ecology are that ammonium (NH_4^+) is used preferentially to nitrate (NO_3^-) and that the fate of production on NH_4^+ and NO_3^- differs in terms of the microbial community composition supported. The assimilation of NH_4^+ is considered to be less energy expensive for the cell, and NH_4^+ is more easily transported across the cell membrane than NO_3^- under both balanced growth or N limited conditions (Raven, 1984). Field efforts have provided considerable evidence of preferential uptake of NH_4^+ over NO_3^- at concentrations of NH_4^+ exceeding a few μM. McCarthy et al. (1975) illustrated, for the Chesapeake Bay, the relationship between the fraction of total N utilized by natural assemblages and the concentration of ambient NH_4^+; the uptake of oxidized forms of N never exceeded more than a few percent of the total N ration when NH_4^+ concentrations exceeded 1–2 μM. Berman et al. (1984) illustrated the same pattern for Lake Kinneret and, more recently, Dugdale et al. (2007) reported a comparable relationship for San Francisco Bay estuarine phytoplankton.

In an oceanographic context, based on the concept of "new" and "regenerated" production it is generally assumed that NH_4^+ leads to production that is cycled within the microbial loop, whereas NO_3^- —based production more often leads to production that supports a food web leading to secondary production as well as export out of the euphotic zone (Dugdale and Goering, 1967; Eppley and Peterson, 1979). Shifts in nitrogen (N) form from NO_3^- to NH_4^+ have been shown in numerous systems to lead to community shifts away from plankton communities dominated by diatoms to those dominated by flagellates, cyanobacteria, and bacteria, in turn, resulting in a shift in composition of higher food webs (e.g., Legendre and Rassoulzadegan, 1995; Glibert, 1998; Mousseau et al., 2001; Berg et al., 2003; Heil et al., 2007). In

coastal and estuarine environments, both forms of N can be supplied as "new" nutrients, and therefore the question emerges as to whether N form plays a similar regulatory role in shaping food webs as it does in the oceanic realm. In fact, dichotomous production of different phytoplankton communities with N form under N sufficiency is at odds with another paradigm of phytoplankton ecology; that nutrients cannot be controlling of phytoplankton composition when they are at levels sufficient to saturate the phytoplankton demand. As stated by Reynolds (1999, p. 31), "... there should be no selective effect, consequential upon different affinities of storage capabilities for a nutrient resource, that might distinguish between the potential performances of any pair of planktonic algae, so long as the resource concentrations are able to saturate the growth demand. If that is true, then the ratio between the (saturating) concentration of any of the resources also fails to exert any regulatory significance." It is thus classically assumed, based on invariant kinetic relationships and cell quotas (e.g., Droop, 1983), that when cells are growing at maximal growth rates (set by culture or environmental conditions of light, temperature, etc.), the total N taken up will be the same whether the cells are provided NO_3^- or NH_4^+ (or urea or other forms of N), and therefore it has also been assumed in field studies and models that growth and phytoplankton biomass should respond similarly regardless of the form of N (e.g., Gowen et al., 1992).

In recent years, the idea that regulation occurs across the entire spectrum of nutrient gradients has begun to take hold, replacing the notion that regulation of phytoplankton growth occurs only at the limiting end of the nutrient spectrum (Glibert et al., 2013 and references therein). Recognition of the complexity and variability in uptake kinetics has contributed to our evolving ideas of regulation by nutrients (Glibert et al., 2013 and references therein). However, because of the persistent focus on the role of "limiting substrates," the effects of high nutrient concentrations on phytoplankton processes and composition has been significantly understudied. An important question in this context is whether the physiological and ecological consequences of dependence on NO_3^- vs. NH_4^+ remain the same under nutrient sufficiency as under nutrient deficiency.

Moreover, growth in and of itself is not the only ecologically relevant parameter. A clear example of this is many mixotrophic, toxic dinoflagellates have inherently slower growth rates than their non-mixotrophic counterparts, namely diatoms, yet play key roles in ecological functioning (e.g., Flynn et al., 2013). Related important ecological concepts are how the nutrient signal propagates through the food web, whether variance in nutrient constituents can be related to that of primary producers and whether variances in each step of the food chain can be related to each other. While individual nutrients, light availability, and cellular nutrient ratios regulate the growth rate of phytoplankton, the wide plasticity of cell composition in algae under both nutrient limited and nutrient- saturated conditions alters the elemental quality of the algal food available to grazers. What is unclear is whether changes in nutrient quality under conditions of nutrient sufficiency alter the composition of the primary producers that, in turn, have an effect on the composition of the food web.

These questions have a high degree of relevance for the San Francisco Bay Delta ecosystem (**Figure 1**). This system is one in which the regulatory role of nutrients has been historically dismissed because most nutrients have been assumed to be at levels that saturate (maximize) phytoplankton growth; instead phytoplankton growth has been considered to be regulated primarily by light limitation (Cole and Cloern, 1984; Alpine and Cloern, 1992; Cloern and Dufford, 2005) and biomass is thought to be limited by grazing (Kimmerer, 2004). However, over the past decades there have been large changes in phytoplankton community composition and the role of nutrients in these changes has received increasing scrutiny because nutrient loads are high and increasing (e.g., Wilkerson et al., 2006; Dugdale et al., 2007, 2013; Van Nieuwenhuyse, 2007; Glibert, 2010; Glibert et al., 2011, 2013). One of the major sources of nutrients to the Bay Delta is sewage effluent (Van Nieuwenhuyse, 2007; Jassby, 2008), with one of the largest wastewater treatment plants (WWTP) discharging N primarily as NH_4^+ at the rate of 14–15 tons day^{-1}, and at concentrations that have increased from ~10 mg L^{-1} when the plant came on line in the early 1980s to > 20 mg L^{-1} in the 2000s (Glibert, 2010; Glibert et al., 2011). Approximately 90% of the total N in northern San Francisco Estuary originates from this single point source (Jassby, 2008).

Although nutrient effects have been dismissed as controlling factors in San Francisco Estuary in favor of factors such as light and grazing, the more subtle ecological impacts of NH_4^+ loading and the importance of changes in NO_3^-:NH_4^+ in phytoplankton succession are beginning to be considered as important factors that may have contributed to historical changes seen in the food web (e.g., Dugdale et al., 2007, 2012; Glibert, 2010, 2012; Glibert et al., 2011; Parker et al., 2012a,b). Not only have dominant species changed in this system, but rates of primary production

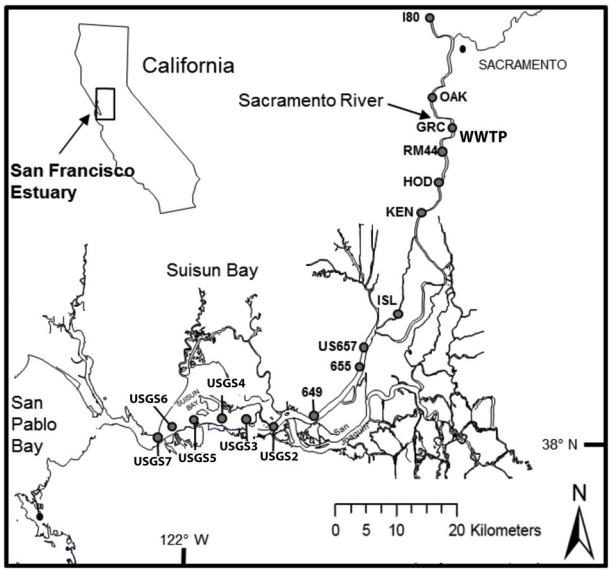

FIGURE 1 | Locations of sampling sites for transects conducted along the Sacramento River to Suisun Bay (San Francisco Bay Delta) in September 2011, 2012 and in March 2012, 2013. At sites Garcia Bend and USGS4, additional samples were collected for experimental manipulations, as described in text.

have also declined over the course of the past few decades (e.g., Jassby et al., 2002; Kimmerer et al., 2012). In particular, increased NH_4^+ loading relative to NO_3^- in conjunction with changes in nitrogen (N) and phosphorus (P) stoichiometry are now thought to be related to the long-term changes in the food web because of their effects on the dominant primary producers (Dugdale et al., 2007, 2012; Glibert, 2010; Glibert et al., 2011). While phytoplankton productivity throughout most of the year is, in fact, supported by NH_4^+, productivity on NH_4^+ is reduced relative to that of NO_3^- due to differences in cellular metabolism of NH_4^+ vs. NO_3^- and the resulting phytoplankton community that differentially develops under these different substrates (Dugdale et al., 2007; Parker et al., 2012a,b; Glibert et al., 2014). The reduction in N productivity with increasing NH_4^+ availability is a function of NH_4^+ repression of NO_3^- uptake on the short time scale (minutes to hours), followed by differential growth of different phytoplankton taxa on a longer time scale (days to weeks). Much has been written about the inhibition or repression of NO_3^- uptake by NH_4^+ (Dortch, 1990); in general, with increasing concentrations of NH_4^+, the cell down-regulates its ability to take up or assimilate NO_3^-. The typical response of NO_3^- uptake in the presence of increasing NH_4^+ concentrations is a near complete suppression and examples of this relationship in the literature abound (e.g., Caperon and Ziemann, 1976; Collos et al., 1989; Dortch et al., 1991; Flynn, 1999; Lomas and Glibert, 1999a,b; Maguer et al., 2007; L'Helguen et al., 2008). While the relationship between NH_4^+ availability and NO_3^- uptake and transport suppression is robust, it is now recognized that down-stream metabolites, not NH_4^+ *per se*, are responsible for this down-regulation (e.g., Flynn et al., 1997). In most algae, the regulation is via the size of the glutamine pool, and such regulation has been incorporated into biochemical models that simulate the interactions of NH_4^+ and NO_3^- in "generic" algae based on a cell quota approach (e.g., Flynn and Fasham, 1997; Flynn et al., 1997).

Here we directly tested the effects of alterations of nutrient form on phytoplankton composition and rates of N-based productivity for samples collected from the freshwater and low salinity reaches of San Francisco Estuary. Understanding the factors changing this ecosystem is crucial to water management, but understanding how aquatic trophic cascades are modified by nutrients and other factors is a key scientific question and a major challenge more broadly (e.g., Carpenter and Kitchell, 1993; Polis and Strong, 1996). As part of a broader study of the effects of nutrient forms and light on phytoplankton, we report on a series of enclosure experiments in which samples were collected from different locations along a river to bay transect during different seasons, enriched with NH_4^+ or NO_3^- and tracked over a period of several days when incubated under different light treatments. We focus only on the effects of additions of the inorganic nutrient forms of NH_4^+ and NO_3^- because of the direct relevance of these forms to the potential effect on the composition and productivity of primary producers that might be expected as a result of management actions to increase nitrification in WWTP processing of effluent in the coming years. We specifically hypothesized that a greater proportion of diatoms would be produced when samples were enriched with NO_3^- and that a greater proportion of cyanobacteria and other NH_4^+-tolerant flagellates would be produced when enriched with NH_4^+; and that if samples were indeed light limited, a lower rate of production overall would be evident at reduced light levels of incubation. We expected these changes even against a background of elevated nutrient concentrations in the ambient environment. These experiments supplement and extend previous "enclosure" experiments conducted in Bay Delta waters (Dugdale et al., 2007; Parker et al., 2012a) in which N depletion trends and N uptake rates were measured on samples that did not receive supplement nutrient enrichments.

MATERIALS AND METHODS

SITE DESCRIPTION AND SAMPLE COLLECTION

The San Francisco Estuary consists of South San Francisco Bay, Central Bay, San Pablo Bay, Suisun Bay, and the Sacramento-San Joaquin Bay Delta, a complex of rivers, channels, wetlands, and floodplains (Atwater et al., 1979; Nichols et al., 1986; Muller-Solger et al., 2002). The upper estuary is an inverse delta and receives the majority of its flow from the Sacramento and San Joaquin Rivers (**Figure 1**, Atwater et al., 1979; Nichols et al., 1986). The Sacramento River is the larger river, contributing ∼80% of the freshwater to the system (Jassby, 2008); the upper reaches of the Sacramento River drain 61,721 km^2, while the upper San Joaquin River drains 19,030 km^2 (Sobota et al., 2009). With exception of the deeper Central Bay, the mean depths of the various sub-embayments in the estuary range from 3.3 to 5.7 m (Kimmerer, 2004).

Samples were collected from the R/V *Questuary* during 4 seasons over 2 years, September 2011, March 2012, September 2012, and March 2013. During each period of sampling, a transect from the upper Sacramento River to Suisun Bay was conducted, with sites beginning above the Sacramento WWTP and ending at Suisun Bay (**Figure 1**). Each survey was conducted during outgoing tide, although the absolute phase of the tide was not the same for each sampling period. At each station, a Seabird Electronics SB-32 rosette mounted with 6, 3-L Niskin bottles and fitted with a Seabird SBE-19 plus CTD was deployed to collect vertical profiles of temperature and salinity and to collect near-surface water samples.

At each site, samples were immediately filtered on board (precombusted, 2 h 450°C, Whatman GF/F filters) for the collection of chlorophyll *a* (chl *a*), and accessory pigments (accessory pigments were not collected in September 2011). Filters were immediately frozen and returned to the laboratory for analysis. The filtrate was also stored on ice, returned to the laboratory and immediately analyzed for NH_4^+ and NO_3^- (within 3 h). Aliquots of sample were also frozen for subsequent analysis of PO_4^{3-} as well as silicate ($Si(OH)_4$) and organic nutrient forms of N and P; ($Si(OH)_4$ and organic nutrient data not shown).

During September 2011 and March 2012, over 400 L of water were also collected from the site identified as Garcia Bend (GRC), which is located just above the Sacramento WWTP, and during September 2012 and March 2013 similar bulk collections of water were undertaken at Garcia Bend as well as in Suisun Bay at site USGS4. This water was pre-screened through 150 μm mesh to remove large grazers, held in large carboys, shaded and returned to the shore-based laboratory at the end of the day.

EXPERIMENTAL TREATMENTS

All large-volume samples collected from Garcia Bend and USGS4 were held overnight at ambient temperatures at the Romberg Tiburon Laboratory and were enriched with different N substrates by midmorning the following day. In "cubitainers" of 20 L volume, samples were enriched with either 40 μM (September 2011, March 2012) or 30 μM (September 2012, March 2013) NO_3^- or NH_4^+, with cubitainers from each site being enriched with each N form in parallel. The level of N enrichment was targeted to raise the total available N to a value >40 μM, representing a change that was >2-fold larger than that observed in NH_4^+ along the riverine transects. The cubitainers were then placed in large (1000 L), water-filled enclosures to maintain ambient temperatures. They were covered with either a single layer of neutral density screening to simulate 60% neutral irradiance (high light) or with 3 layers of neutral density screening to simulate 15% of natural irradiance (low light). The overall experiment was thus a 2 × 2 factorial, with 2 N sources and 2 light treatments. Cubitainers were incubated under these conditions for up to 5 days.

On a daily basis at midmorning, subsamples were collected from each cubitainer and immediately filtered as described above for chl *a*, accessory pigments and ambient nutrient concentrations. Samples for chl *a* were subsequently extracted as described below, while samples for accessory pigments (collected only on selected days) were flash frozen in liquid N_2 until subsequently analyzed. The filtrates were also frozen for nutrient analysis.

At the same time subsamples were collected for nutrient and pigment analysis, subsamples from the cubitainers were also collected on days 1–2 (September 2011, March 2012) and on days 1–5 (September 2012, March 2013) for determination of the rates of uptake of NH_4^+ and NO_3^-. Sufficient sample was removed from each cubitainer to prepare 3, 200 mL incubation bottles to which an additional 30 μM-N were added to each, but each bottle was enriched with a different form of ^{15}N- labeled substrate: NH_4^+, NO_3^- or urea. These ^{15}N enrichments were at levels that were assumed to be more than sufficient to saturate the N uptake system (these enrichments supplemented the initial NH_4^+ or NO_3^- enrichment of the cubitainers). These enrichments were designed to be large, pulsed additions and were not representative of "trace" uptake. The goal was to characterize how the phytoplankton responded to a pulsed addition, analogous to the interception of a plume of effluent in a river. Each bottle was immediately returned to the enclosures under screening that was the same as the cubitainers from which the respective samples were taken. Incubations for ^{15}N uptake were ∼1 h, after which time the bottles were removed from the enclosure, immediately filtered onto Whatman precombusted GF/F filters and frozen. Samples were later analyzed by mass spectrometry as described below.

ANALYTICAL PROTOCOLS

Ambient nutrients were analyzed using manual colorimetric assays (NH_4^+) and autoanalysis techiques (NO_3^-, PO_4^{3-}, $Si(OH)_4$). Concentration of NH_4^+ was analyzed according to Solórzano (1969). Samples from the transects were never frozen, while daily samples from the cubitainers were frozen. Concentration of NO_3^- was analyzed on samples from the transects that were also never frozen, using a Bran and Luebbe Autoanalyzer II according to Whitledge et al. (1981) and Bran and Luebbe (1999c) Method G-172-96, while cubitainer samplings for NO_3^- as well as PO_4^{3-} and silicate ($Si(OH)_4$) were analyzed on the same instrument after a period of frozen storage, although there was a 24 h thawing period before analysis (MacDonald et al., 1986). Methods for these latter analytes were Bran and Luebbe (1999b) Method G-175-96 and for $Si(OH)_4$, Bran and Luebbe (1999a) Method G-177-96. Samples for chl *a* were analyzed using a Turner Designs Model 10-AU fluorometer following a 24 h 90% acetone extraction at 4°C (Arar and Collins, 1992), and a 10% hydrochloric acid addition to correct for phaeophytin. The fluorometer was calibrated with commercially available chl *a* (Turner Designs).

Accessory pigment samples were frozen at −80°C until analysis, approximately 6 weeks after sampling. They were processed by High Performance Liquid Chromatograph (Agilent) following the protocols of Van Heukelem and Thomas (2001). All ^{15}N analyses were done on a Sercon mass spectrometer following drying of the filters and encapsulation into tin capsules.

CALCULATIONS AND STATISTICAL ANALYSES

For each cubitainer for each day of incubation, the daily change in inorganic N (typically removal) and the daily change in chl *a* or accessory pigments (typically increase) were calculated and compared, thus giving a daily chl *a* or pigment yield per unit N consumed. In sum, accounting for all sites and seasons, for each light level, there were 22 pairs of N treatments for which such calculations were possible for chl *a*. Given that accessory pigments were only collected on selected days, there were 14 such paired treatments.

For each incubation irradiance condition and each N form, all data from all dates of sampling and stations were combined. Pearson correlation analysis was used to compare the strength of the response in each pigment in relation to the change in total DIN. The strength of the correlation (Pearson correlation coefficient, *r*) and the rates of change (slopes or regression coefficients) for all treatments (high vs. low irradiance with NH_4^+ or NO_3^- enrichment) were calculated. Significance of the regressions is reported for both $p < 0.05$ and $p < 0.01$ levels.

For the ^{15}N analyses conducted on each day for each cubitainer, rates were calculated as biomass-specific uptake rates, V (h^{-1}), using the following formula (Dugdale and Wilkerson, 1986; Glibert and Capone, 1993):

$$V = \frac{V\ =\ (^{15}\text{N atom \% sample}\ -\ ^{15}\text{N atom \% normal})}{(^{15}\text{N atom\% enrichment}\ \times\ \text{incubation duration})}$$

where atom % sample is the ^{15}N enrichment in the sample, atom % normal is the natural ^{15}N background enrichment, and ^{15}N atom % enrichment is the initial isotope enrichment based on added plus ambient substrates (Glibert and Capone, 1993). Given the elevated concentration of ^{15}N made to these experiments, these rates are assumed to be representative of V_{max} and no isotope dilution correction was necessary (Glibert et al., 1982; Glibert and Capone, 1993). The individual rates for NH_4^+, NO_3^- and urea were calculated and these rates were summed. The summation is provided as a physiological index; it does not represent

the actual uptake by the cells but rather the potential for $\sum$N uptake should all forms of N be provided at or near saturating conditions. These summed rates were compared across N and light treatments for each day of incubation of the cubitainers. When summed, the values are referred to as N-based productivity rates (Wilkerson et al., 2006); here they represent maximal N-based productivity rates. Data were analyzed using a 2-Way ANOVA.

RESULTS

AMBIENT ENVIRONMENTAL CONDITIONS AND RIVERINE TRANSECTS

Changes in nutrient concentration and form were apparent in all transects (**Figures 2A–D**). In all but March 2012, a large (20–30 μM-N) increase in NH_4^+ was noted just south of the Garcia Bend site, which is also just south of the WWTP discharge site. A smaller peak (~7 μM-N) in NH_4^+ was noted during March 2012 in the same river region. While increased concentrations of NH_4^+ were detected in all cases below the Garcia Bend site, it is recognized that our surface sampling does not capture the peak of the effluent plume. While it is not known why the March 2012 peak was smaller than that observed during the other seasons, the WWTP does alter its discharge, even holding it for several days without discharge, depending on conditions at the plant at the time. As water moved from the Sacramento River toward Suisun Bay, the NH_4^+ peaks in September 2011, 2012, and March 2013 dissipated, but near equivalent increases in NO_3^- were noted, suggestive of nitrification. Increases in PO_4^{3-} downstream were also noted. In March 2012, concentrations of NH_4^+ did not decrease downstream, but nevertheless concentrations of NO_3^- increased significantly.

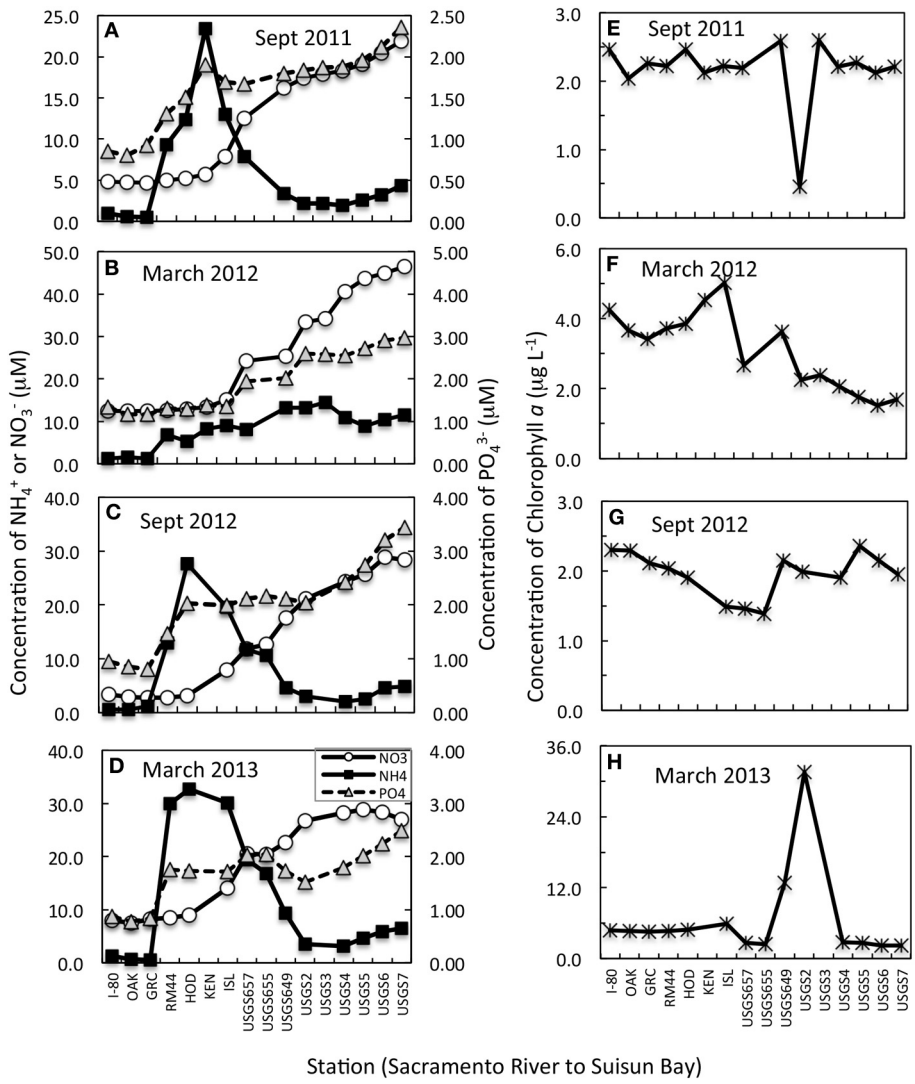

FIGURE 2 | (A–D) Concentration changes in NH_4^+, NO_3^- (primary Y axis) and PO_4^{3-} (secondary Y axis) from the upper Sacramento River to Suisun Bay for transects conducted on dates indicated. All data shown are from near surface samples. Note that the scales change from panel to panel but the relationship to the primary to secondary axis remains the same for all panels. **(E–H)** Concentration changes in chlorophyll *a* from the upper Sacramento River to Suisun Bay for transects conducted on dates indicated.

The trends in chl *a* along the river to bay transects were highly variable from sampling period to sampling period (**Figures 2E–H**). In general, concentrations of chl *a* were $< 3\,\mu g\ L^{-1}$ regardless of sampling site or time period, but there was one important exception to this trend. In March 2013, all chl *a*-values were higher by a few $\mu g\ L^{-1}$ than observed in previous time periods and at site USGS2, a spatially limited phytoplankton bloom was found, with chl *a*-values reaching $30\,\mu g\ L^{-1}$ (**Figure 2H**). Interestingly, in September 2011, the same USGS2 site had a depression in chl *a*-values (from ∼2.5 to 0.5 mg L^{-1}) compared to the other sites along the transect (**Figure 2E**).

Large changes were observed in accessory pigments along the riverine to bay transect, indicative of changes in species composition (**Figure 3**; note that no accessory pigment data are available for September 2011). Whether the accessory pigment data are expressed in relation to concentrations of chl *a* (**Figures 3A,C,E**), or in relation to concentrations measured at Garcia Bend (located above the WWTP; **Figures 3B,D,F**), the pattern is fundamentally the same: decreased concentrations of fucoxanthin, suggestive of fewer diatoms, and increased concentrations of alloxanthin, suggestive of more cryptophytes. In all cases, fucoxanthin declined from the upper Sacramento River to Suisun Bay, although secondary peaks in fucoxanthin:chl *a* were noted in Suisun Bay in both March 2012 and September 2012 (**Figures 3A,C**). Alloxanthin increased toward Suisun Bay relative to both chl *a* and relative to values at Garcia Bend in all transects. In September 2012, an increase in zeaxanthin (generally indicative of cyanobacteria) toward Suisun Bay was also noted. Chl *b* had a pronounced increase toward Suisun Bay in March 2013 when viewed both in relation to chl *a* and relative to values determined at Garcia Bend (**Figures 3E,F**).

Samples used in the N enrichment experiments were collected during periods in which temperatures ranged over a gradient from 11 to 19.6°C (**Table 1**) and salinities were fresh (all salinities <5.9, and most ≤1.0). Secchi depths reflected the turbid conditions of river and bay, with values ranging from 0.3 to 1.3 m, but consistently the upper Sacramento River had higher light penetration than did Suisun Bay (**Table 1**). Ambient chl *a*-values did not vary by much more than a factor of 2 (1.91–4.60 $\mu g\ L^{-1}$) across the variable spatial and temporal sampling. Nutrient concentrations for all inorganic N and P forms were never at levels reflective of depletion; NH_4^+ concentrations ranged from 0.50 to 3.2 μM-N, NO_3^- concentrations ranged from 2.70 to 28.2 μM-N, and PO_4^{3-} values ranged from 0.80 to 2.42 μM-P (**Table 1**). Molar

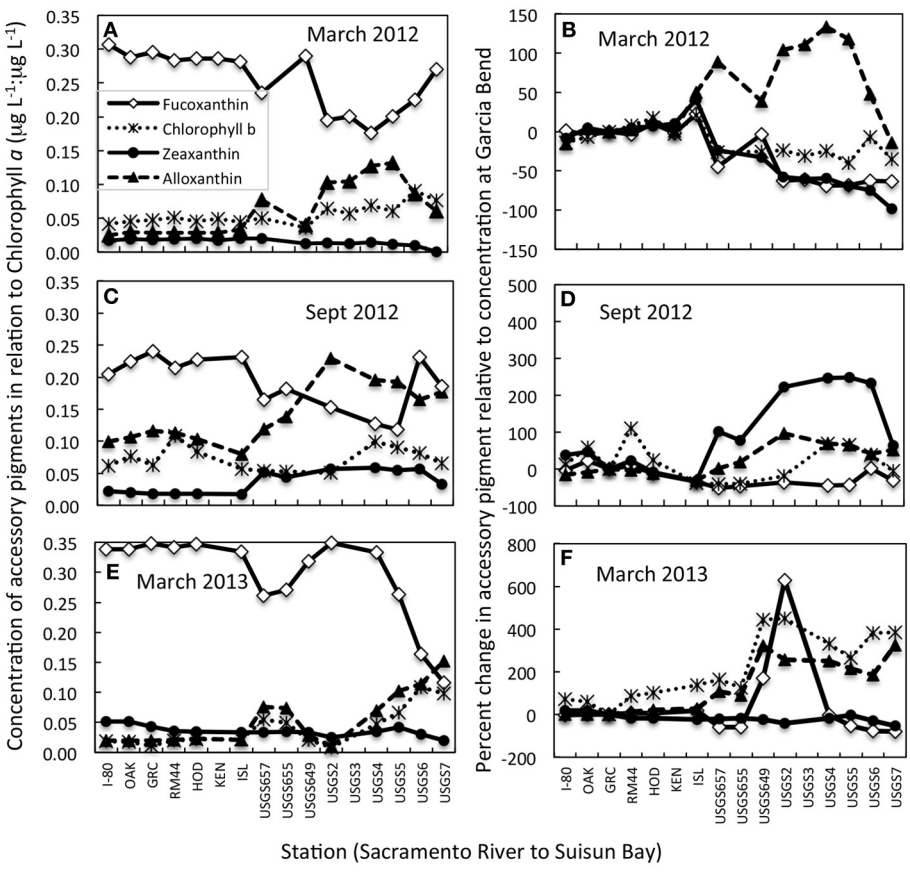

FIGURE 3 | Changes in concentrations of accessory pigments from the upper Sacramento River to Suisun Bay for transects conducted on dates indicated. (A,C,E) Data are expressed as concentrations of accessory pigment relative to concentrations of chlorophyll *a*. **(B,D,F)** Data are expressed as the percent change in the accessory pigment relative to concentrations of the same pigments at the Garcia Bend station. All data shown are from near surface samples. Note that the scales change from panel to panel.

Table 1 | Ambient environmental conditions of sites sampled in the San Francisco Bay Delta from which samples were subsequently incubated under varying N and light conditions.

Date of sample collection	Site	Temperature (°C)	Salinity	Secchi depth (m)	Chlorophyll *a* ($\mu g\ L^{-1}$)	Ammonium (μM)	Nitrate (μM)	Phosphate (μM)	DIN:PO_4^{3-} (molar)
September 2011	Garcia Bend	20.1	<1.0	1.0	2.26	0.50	4.70	0.90	5.78
March 2012	Garcia Bend	11.0	<1.0	0.3	3.42	1.24	12.50	1.20	11.45
September 2012	Garcia Bend	19.6	<1.0	1.1	2.11	1.14	2.70	0.80	4.80
	Suisun Bay (USGS4)	19.3	5.91	0.6	1.91	2.02	24.3	2.42	10.88
March 2013	Garcia Bend	13.2	<1.0	1.3	4.60	0.51	8.30	0.83	10.61
	Suisun Bay (USGS4)	14.9	1.01	0.3	2.72	3.20	28.20	1.79	17.54

ratios of DIN (sum of NO_3^- and NH_4^+) to PO_4^{3-} were less than the canonical Redfield ratio for all sampling sites except for Suisun Bay in March 2013 when the value was 17.5. Values of $Si(OH)_4$ for all samples (not shown) were in the several 100 μM-Si range for all samples collected.

RESPONSES IN PHYTOPLANKTON PIGMENTS TO DIFFERENT FORMS OF N AND IRRADIANCE LEVELS

In the enrichment experiments, when all data from all sites and seasons were compiled, a linear relationship emerged when the daily rate of change in chl *a* was compared to the daily change in N (**Figures 4A,D**; $r > 0.66$ in all cases; **Table 2**). However, the rate of change in chl *a* differed significantly for those samples enriched with NH_4^+ compared to those enriched with NO_3^- when these samples were incubated under low light conditions. Those that were enriched with NH_4^+ under low light yielded ~1 μg chl *a*:1 μM N consumed; for those that were enriched with NO_3^-, the chl *a* yield was ~2 μg chl *a*:1 μM N consumed (**Figures 4A,C**; **Table 2**; significance of t-statistic for regression comparison <0.01). The chl *a* yield for all high light treatments was ~1 μg chl *a*:1 μM N.

When the daily yields in individual pigments are compared in the analogous way, the responses were quite varied (Note that the responses for fucoxanthin are illustrated in **Figures 4E–H**; the slopes of the regression lines for all pigment changes in relation to changes in N are compared in **Figure 5**; **Table 2** compares all regression statistics for all pigments). For fucoxanthin, as with chl *a*, there was approximately a doubling of the yield per unit N consumed for samples that were enriched with NO_3^- and incubated under low light compared with the parallel samples incubated with NH_4^+ under low light (**Figures 4E,G, 5**, **Table 2**; significance of t-statistic for regression comparison <0.05). Interestingly, the relationship between the daily yield of fucoxanthin and daily change in NH_4^+ for samples held under high light was not significant ($r = 0.52$; **Table 2**, **Figures 4**, **5**). When changes in fucoxanthin were compared to changes in chl *a*, all treatments were significantly related and not different from each other ($r =$ 0.72–0.89; not shown).

The response of alloxanthin to change in N form differed somewhat from those of the aforementioned pigments. In this case, significant increases in relation to changes in N were observed for samples enriched with NH_4^+ and incubated under both high or low light as well as for samples enriched with NO_3^- and incubated under reduced irradiance, but the relationship was not significant for samples enriched with NO_3^- and incubated under high light ($r = 0.61$–0.82 vs. 0.50; **Figure 5**, **Table 2**). Highest yields in alloxanthin were found for samples incubated with NO_3^- at low light (**Figure 5**). All alloxanthin responses were significant when compared to changes in chl *a* ($r > 0.64$; not shown).

The responses of chl *b* and zeaxanthin were quite different from those of fucoxanthin and alloxanthin. For these pigments, the most significant relationships in terms of the change in pigment in relation to change in N were observed in the treatments that were enriched with NH_4^+ and incubated at high light ($r =$ 0.67 and 0.70, respectively; **Figure 5**, **Table 2**; significance of t-statistic for regression comparisons of both pigments at high vs. low light <0.01). In the case of chl *b*, but not zeaxanthin, samples incubated with NO_3^- and also held under high light were significantly related to the change in N (**Table 2**). Additionally, whereas there was a relationship between change in N and change in zeaxanthin for the NH_4^+ and high light treatment, no such relationship was observed for the change in zeaxanthin in relation to the change in chl *a* ($r < 0.5$, $p > 0.05$, not shown) suggestive that under these conditions the proportional change in zeaxanthin was greater.

BIOMASS-SPECIFIC N PRODUCTIVITY RATES

In contrast to the classic assumption that when provided nutrients in sufficiency, rates of uptake should not vary by N form, here it was found, based on ^{15}N uptake measurements, that maximal N-based biomass-specific productivity rates ($V_{max}\ h^{-1}$) were consistently higher for those samples taken from experimental cubitainers that were initially enriched with NO_3^- compared to those initially enriched with NH_4^+ (**Figure 6**; see SI for fractional uptake of each N form). [Note that the same pattern emerges if instead of summed rates, the average uptake rates are reported]. The directionality of the different rates between samples initially enriched with NO_3^- and those with NH_4^+ was similar to the differences in total chl *a* and fucoxanthin, which also trended higher under NO_3^- enrichment than with NH_4^+ enrichment. These differences were due overwhelmingly to the depression in rates of V_{max} NO_3^- in those treatments originally enriched with NH_4^+. Rates of V_{max} NO_3^- were depressed by 88–96% in September 2011, 54–73% in March 2012, 69–95% in September 2012 and 58–93% in March 2013 in treatments enriched with NH_4^+ relative to treatments enriched with NO_3^- initially. Rates of V_{max} NH_4^+, or V_{max} urea, however, were not proportionately higher to

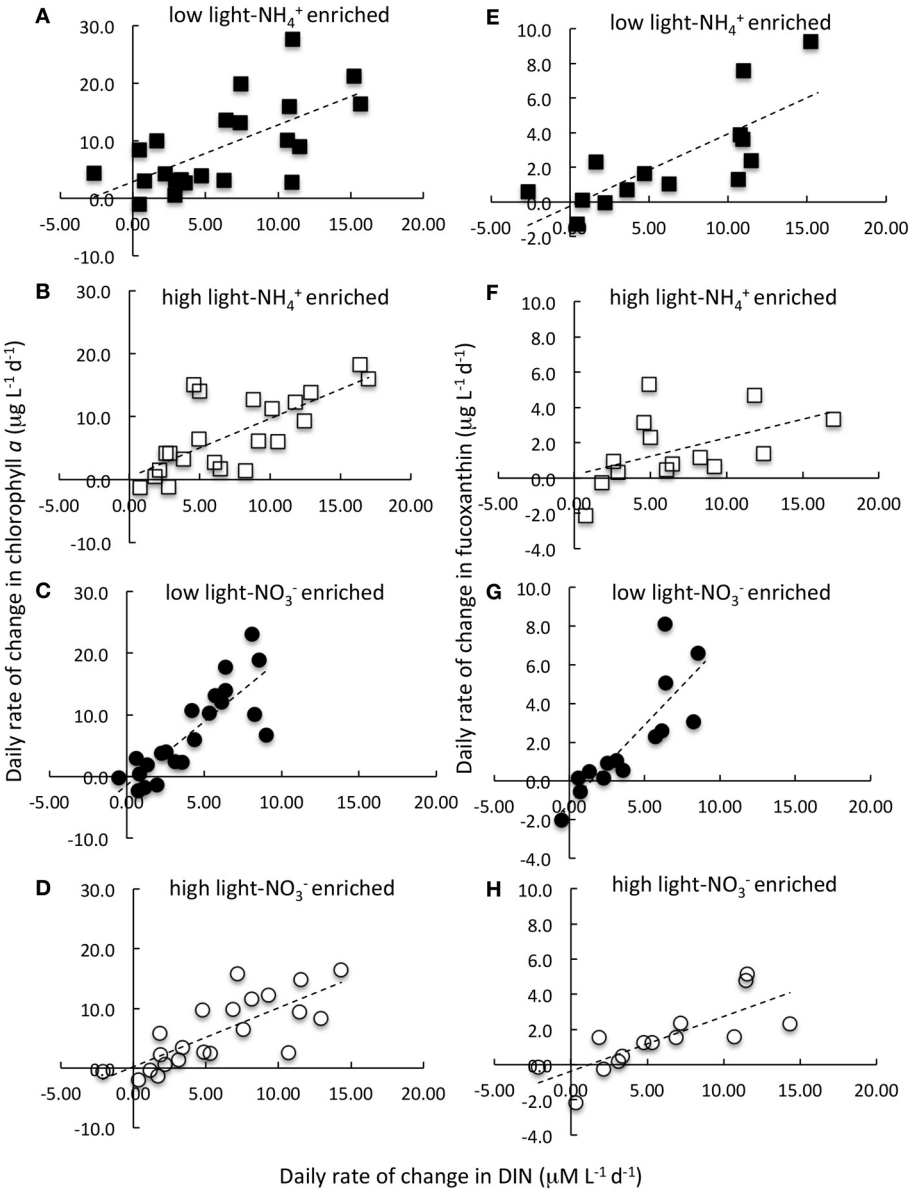

FIGURE 4 | Daily rate of change in chlorophyll *a* (A–D) and in fucoxanthin (E–H) in relation to daily rate of change in the dissolved inorganic nitrogen (DIN) concentration. Data are the composite of all N-enrichment experiments conducted on samples collected from the Sacramento River (Garcia Bend) and Suisun Bay (USGS4) in September 2011, 2012, and in March 2012 and 2013. Samples were enriched with NH_4^+ (**A,B,E,F**; squares) or NO_3^- (**C,D,G,H**; circles) and incubated at 15% of ambient irradiance (**A,E,C,G**; filled symbols) or 60% of surface irradiance (**B,F,D,H**; open symbols). Nitrogen enrichment levels and other experimental details are described in text. Lines represent linear regressions. Note that of all the pigments measured, only fucoxanthin is illustrated here. Regression statistics and comparisons for these data as well as for other pigments are given in **Table 2** and **Figure 5**.

compensate, and therefore total rates were lower. Thus, every one of the 14 experiments had rates of summed uptake for the NO_3^- enrichments that were higher than for the NH_4^+ enrichments-even though in each case the pairs of treatments had exactly the same amounts of added N. Averaging all data from all dates, the rates of summed V_{max} (and the same is the case for average V_{max}) for the NO_3^- enrichment treatments were 65% higher than those of the NH_4^+ enrichment treatments. A Two-Way ANOVA confirmed that there were significant effects with regard to substrate form ($p < 0.0001$) but not with light for either substrate.

DISCUSSION

The range of nutrient values from the riverine transects described here (**Figure 2**) are consistent with previously reported nutrient values in the Sacramento River in 2005 (Parker et al., 2012a,b). Previous studies have also observed a large step increase in NH_4^+ downstream of the WWTP, leading to peak values in the central region of river for the stage of tide on which these transects were made. The values reported herein are also similar to those previously reported for Suisun Bay (site USGS6) in 2002, where throughout the year NO_3^- concentrations values

Table 2 | Comparison of correlation statistics for trends in the daily rate of change in major phytoplankton pigments (μg L^{-1} d^{-1}) in relation to the daily rate of change in total dissolved inorganic N (DIN, μM d^{-1}) for samples from San Francisco Bay Delta enriched with NH_4^+ or NO_3^- and incubated at high or low light levels.

Response variable and incubation condition (daily change); statistical parameter	Chlorophyll *a*	Fucoxanthin	Alloxanthin	Chlorophyll *b*	Zeaxanthin
LOW LIGHT—NH_4^+ ENRICHED					
Regression coefficient (slope)	1.07	0.48	0.017	0.006	0.001
Correlation coefficient (r)	***0.66*** **	***0.79*** **	***0.82*** **	0.16	0.22
Significance (p) of r	<0.01	<0.01	<0.01	0.74	0.46
N	22	14	14	14	14
HIGH LIGHT—NH_4^+ ENRICHED					
Regression coefficient (slope)	0.93	0.21	0.013	0.129	0.007
Correlation coefficient (r)	***0.73*** **	0.52	***0.61*** *	***0.67*** **	***0.70*** **
Significance (p) of r	<0.01	0.07	0.02	<0.01	<0.01
N	22	14	14	14	14
LOW LIGHT—NO_3^- ENRICHED					
Regression coefficient (slope)	2.06	0.81	0.025	0.018	0.0005
Correlation coefficient (r)	***0.83*** **	***0.84*** **	***0.67*** *	0.22	−0.03
Significance (p) of r	<0.01	<0.01	0.013	0.45	0.86
N	22	14	14	14	14
HIGH LIGHT—NO_3^- ENRICHED					
Regression coefficient (slope)	0.99	0.31	0.013	0.037	0.0013
Correlation coefficient (r)	***0.77*** **	***0.78*** **	0.50	***0.58*** *	0.25
Significance (p) of r	<0.01	<0.01	0.07	0.04	0.39
N	22	14	14	14	14

*Sampling periods, locations, substrate enrichment and incubation details are given in text. Correlation coefficients (r) that were significant at $p < 0.01$ are indicated by **; those that are significant at $p < 0.05$ are indicated by *; all significant values are also shown in bold italic font.*

were >30 μM-N, NH_4^+ values ranged from 1.3 to 16 μM-N, PO_4^{3-} values were >2 μM-P, and $Si(OH)_4$ values were >200 μM-Si (Wilkerson et al., 2006). Values of chl *a* along the transects (**Figure 3**) were also consistent with previously reported ranges for this region of the estuary for most years (Wilkerson et al., 2006; Kimmerer et al., 2012; Parker et al., 2012a). Both previous studies reported ambient chl *a* in Suisun Bay to be in the 1–2 μg L^{-1} range for most of the year (occasional blooms excepted), and long-term data covering the period from 1975 to 2005 also show that Suisun Bay chl *a*-values tend to be <5 μg L^{-1} on average. Because of the seeming abundance of ambient nutrients in contrast to the chl *a* levels accumulated, this system is typically characterized as a High Nutrient Low Growth or Low Chlorophyll (HNLG or HNLC) region (Cloern, 2001; Yoshiyama and Sharp, 2006; Dugdale et al., 2007). Suppression of productivity by elevated NH_4^+ levels is thought to be a major factor contributing to the low growth/low biomass in this system.

The values of chl *a* yield found here ranged from ∼1 μg chl *a*:1 μM N for both nutrient enrichment conditions at high irradiance levels as well as for reduced irradiance with NH_4^+ enrichment, but about twice that value, ∼2 μg chl *a*:1 μM N, for samples enriched with NO_3^- and held under reduced irradiance. These values are comparable to previous values of chl *a* yield reported from a range of environments (Gowen et al., 1992; Edwards et al., 2005). Gowen et al. (1992) reported a range from 0.25 to 4.4 μg chl *a*:1 μM N, with a median of 1.1 μg chl *a*:1 μM N for Scottish coastal waters, and a similar range was found by Edwards et al. (2005) in studies of a coastal lagoon and of the coast of Portugal. Although both investigators compared various environment or seasonality in their assessments of chl *a* yields, and recognized that different phytoplankton communities likely contributed to the differences in such yields, neither reported the effects of changing forms of N nor related their findings to variable N forms.

Phytoplankton ecologists have long known that NH_4^+ is energetically favored over NO_3^- (Raven, 1984) and thus it is thought to be universally preferred as an N substrate. The evidence for NH_4^+ preference is several-fold, much of this understanding grounded in the classical physiological literature, and, importantly, in studies where N was the limiting nutrient. In culture experiments where both NH_4^+ and NO_3^- are supplied together, as well in experimental mesocosm experiments in which both substrates are available, the typical pattern is for NH_4^+ to be drawn down first, and only then is NO_3^- used in any substantial way, as evidenced by disappearance from the water or media provided. However, except in culture studies, rarely are natural phytoplankton in an environment in which only one form of N is available, and this condition is particularly rare in nutrient-enriched or eutrophic environments. More typically in such conditions, a cell is balancing the uptake of both oxidized and reduced forms of N. Importantly, different phytoplankton functional groups differ in their ability to take up and assimilate different forms of N, and molecular genetics on NO_3^- transporters confirm that there are clear

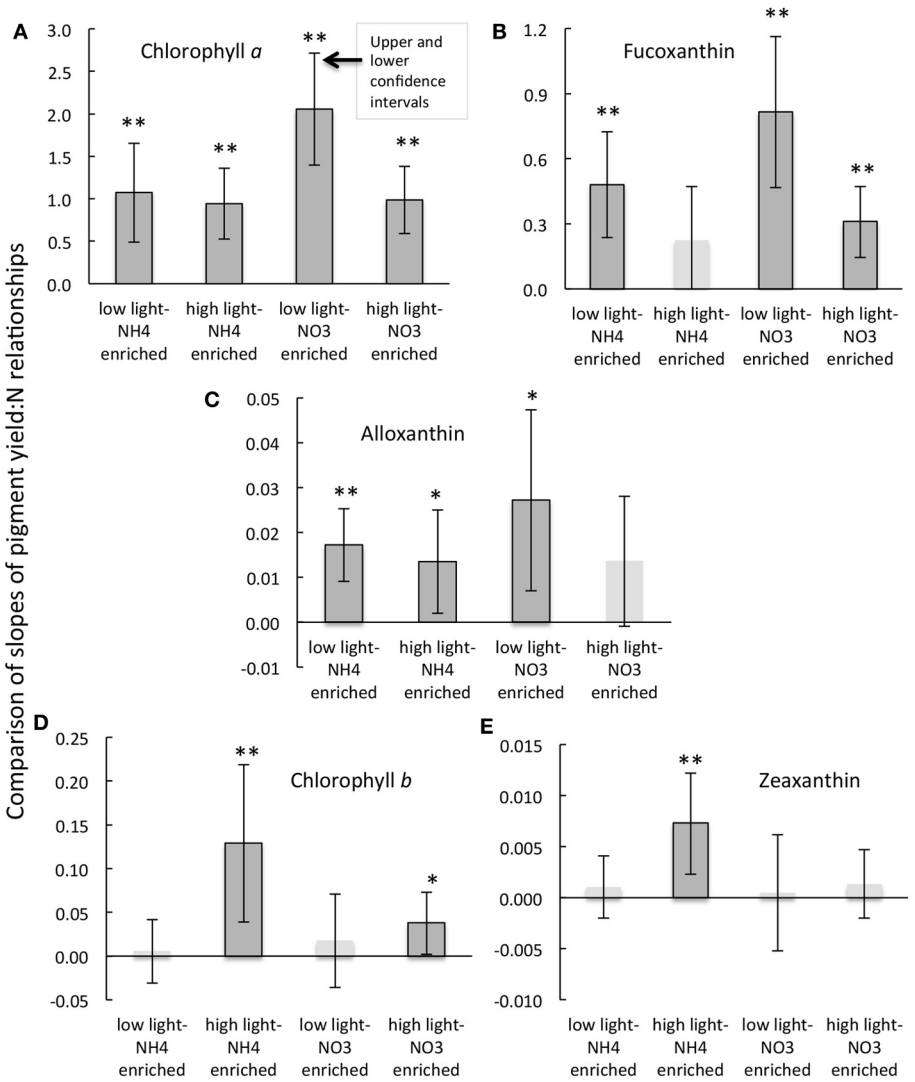

FIGURE 5 | Comparisons of the slopes and the upper and lower confidence intervals (at the 5% significance level) for the regressions of the daily rate of change in pigment as a function of the daily rate of change in dissolved inorganic N (A–E) for the experimental treatments indicated and as described in text. Regressions that were significant at the $p < 0.01$ level are indicated by **; those that are significant at the $p < 0.05$ levels are indicted by *. Note that slopes for regression that were not significant are shown as pale bars without outlines and their confidence intervals are given for reference purposes only. Further details of the correlation statistics are given in **Table 2**.

differences between the major algal groups (Song and Ward, 2007). Diatoms tend to have more copies of high affinity transporters for NO_3^-, while some picoplankton and cyanobacteria may not have any (Lindell and Post, 2001; Moore et al., 2002; Song and Ward, 2007). Moreover, for many cyanobacteria, the high affinity transporter for NH_4^+ is not regulated at all, being constitutively expressed (Lindell and Post, 2001). Similarly, NO_3^- reductase shows a great deal of genetic diversity across species groups. The net effect of these metabolic differences is that, as a generality, diatoms appear to be NO_3^- specialists, while many cyanobacteria are NH_4^+ specialists (Lomas and Glibert, 1999a,b, 2000).

The concept of differential rates of production under NH_4^+ vs. NO_3^- enrichment, even when the total load remains the same, is not necessarily intuitive and therefore has not traditionally been appreciated in nutrient-enriched systems, even though it is well accepted in oceanic environments. In order to have effects on higher trophic levels, it is often assumed that the levels of NH_4^+ must be in the range that causes direct toxicity, and typically that is considered only relevant when NH_3, rather than NH_4^+ is the dominant form. However, any environmental factor that affects the availability of substrates, the nutritional state of the cell, the regulation of photosynthesis, or the rate of enzyme activity will affect the rates by which NH_4^+ or NO_3^- are transported and/or assimilated. Ultimately these differences play a regulatory role in the community composition. The more subtle ecological impacts of NH_4^+ and the importance of changes in NO_3^-:NH_4^+ in phytoplankton metabolism and succession have been more difficult

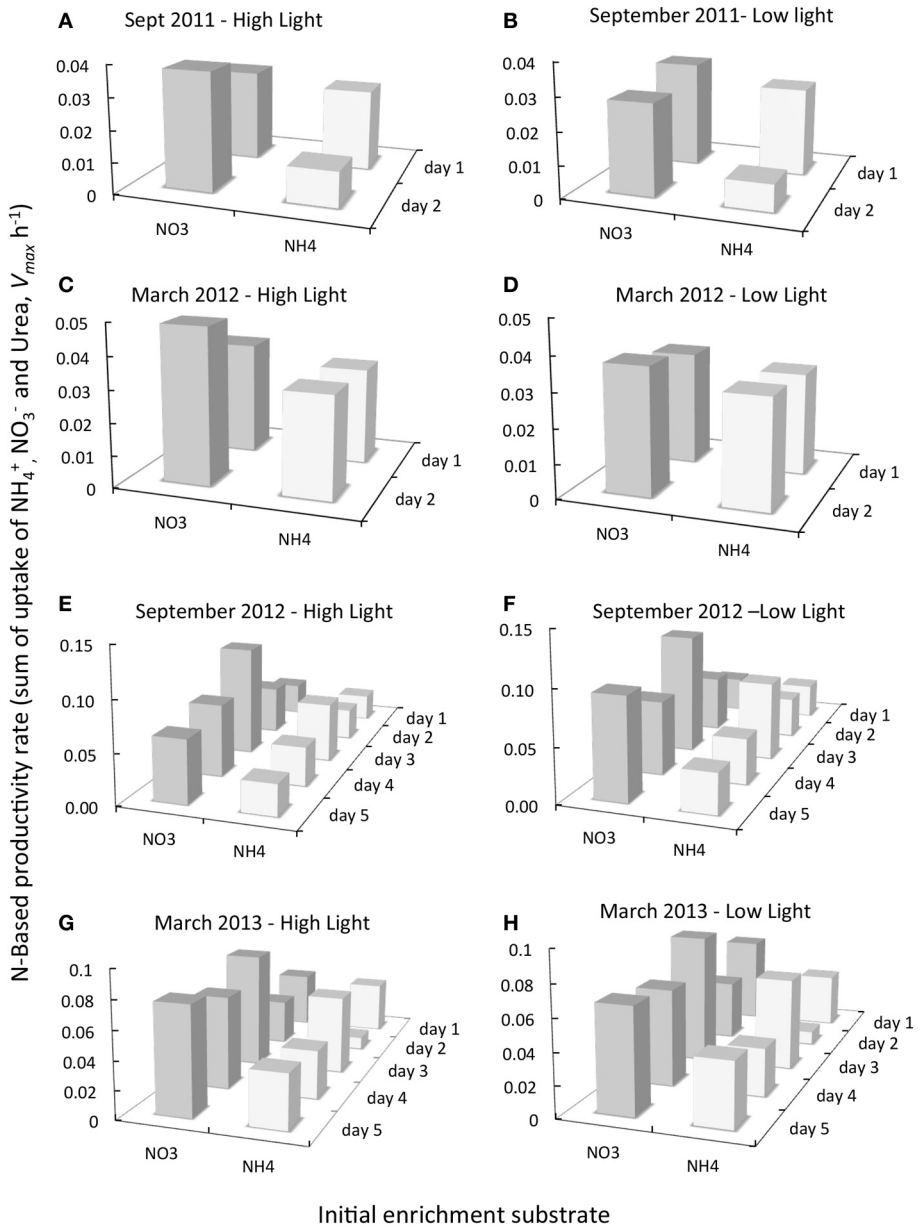

FIGURE 6 | Comparison of the daily change in N-based productivity rate (V_{max} h^{-1}) for samples removed from experiments initially enriched with NO_3^- (dark gray bars) or NH_4^+ (pale gray bars) and subsequently incubated with saturating levels of ^{15}N- NO_3^-, NH_4^+ and urea as described in text for dates indicted. All experiments shown are for samples originally collected from Garcia Bend. ^{15}N uptake rates for all substrates were summed for each day of experimentation and for each treatment from which the samples were obtained [only 2 days of these ^{15}N experiments were conducted in September 2011 and March 2012 **(A–D)**, but 5 days of ^{15}N experimentation were conducted in September 2012 and March 2013 **(E–H)**]. The initial enrichment substrate (NO_3^- or NH_4^+) is given along the X axis. The day of sampling of the experiments is also indicted.

to appreciate. While NH_4^+ can be characterized as a paradoxical nutrient—preferentially used at one end of the concentration spectrum when N is limiting and toxic to the cell when supplied at super-saturating levels (Britto and Kronzucker, 2002), its regulatory effects span the entire spectrum of its availability.

The responses shown here by individual components of the phytoplankton communities were as hypothesized based on the oceanographic paradigms of response to oxidized (classically termed "new") vs. reduced (classically termed "regenerated") N forms. These data provide direct experimental evidence that dichotomous phytoplankton communities developed when enriched with the same absolute concentration of oxidized vs. reduced N forms, even when seemingly sufficient N nutrient was available to the community prior to the N inoculations (**Figures 4**, **5**). These observations are contradictory to the notion of Reynolds (1999) that at or near saturation of the growth demand, different types of algae should not have differential success when nutrients change but remain

at saturated levels. The Reynolds idea has heretofore been used to argue that if nutrients are not limiting for growth in the San Francisco Bay Delta then some other factor, namely light must be limiting for phytoplankton growth (Cole and Cloern, 1984; Jassby et al., 2002).

Overall, greater response by fucoxanthin-containing organisms (diatoms) was observed in those samples enriched with NO_3^- and incubated under reduced irradiance, and greater responses by zeaxanthin and Chl *b*-containing organisms (predominantly cyanobacteria and chlorophytes) were observed in samples enriched with NH_4^+ and incubated under higher irradiance. Where pigment changes were significantly correlated to changes in N on a daily basis, the relationships were not a function of seasonal or site differences: data from different seasons and sites fell on the same trend line. The experimental results shown here also are supportive of reduced rates of N-based productivity for samples incubated with NH_4^+ enrichment compared to those incubated with NO_3^- enrichment (**Figure 6**). These data add to the emerging body of evidence that such responses are not solely observed in oligotrophic systems. The pattern of low rates of productivity in the presence of elevated NH_4^+ conditions in the Sacramento River and Suisun Bay is comparable to observations in other river, estuarine and coastal ecosystems impacted by wastewater effluent (MacIsaac et al., 1979; Yoshiyama and Sharp, 2006; Waiser et al., 2011). The inhibitory effect of NH_4^+ on diatoms seen here has, for example, been observed in other estuaries, such as the Delaware Estuary and the inner bay of Hong Kong Harbor (Yoshiyama and Sharp, 2006; Xu et al., 2012). In the Delaware Estuary, inhibition by NH_4^+ was greatest when diatoms dominated (Yoshiyama and Sharp, 2006). A series of 3-week nutrient-rich mesocosm experiments conducted in Wascana Lake, Saskatchewan, Canada, yielded largely similar findings: total cyanobacterial biomass was associated with NH_4^+ additions, but diatom biomass was associated with NO_3^- additions (Donald et al., 2013). And, earlier mesocosm experiments conducted in eutrophic Delaware Bay revealed higher primary production with NO_3^- than with NH_4^+ (Parker, 2004).

The responses reported here were also related to the exposure irradiance level, but not necessarily in a manner originally anticipated. Whereas light has previously been thought to be limiting in this system (e.g., Cole and Cloern, 1984), low light enhanced the N-based yields of chl *a*, fucoxanthin and alloxanthin, while high light enhanced the response of chl *b* and zeaxanthin. However, pigment yields are a product of both cell growth as well as photoacclimation. The light responses here suggest that rather than being light limited, cells were low-light adapted and, in fact, may have experienced some degree of photoinhibition in the treatments with higher irradiance. It is interesting to compare these responses in the experimental manipulations to light responses along the riverine transects. In all of the transects reported here, Secchi depths were never greater than 1.6 m, and the greatest light penetration was always observed in the Sacramento River, above site USGS655. Reductions in light penetration were noted in Suisun Bay compared to the upper reaches of the river (**Table 1**), as also previously observed by Parker et al. (2012b). In all transects, fucoxanthin declined downriver (with the exception of two single sites around USGS2 in March 2013). Shifts away from diatoms in the transects in the region of Suisun Bay occurred despite the decrease in light penetration, the opposite direction of our experimental findings in which more fucoxanthin was produced in treatments with lower light. These shifts in community composition were, however, consistent with a lesser production of fucoxanthin in waters influenced by the NH_4^+—enriched conditions. In the transects reported herein, Secchi depths varied by factors of 2.5 to 5, with the largest range measured in March 2013, but, by contrast, NH_4^+ concentrations varied along the transects by a minimum of 11-fold (in March 2012) to 65-fold (in March 2013), and the ratio of NH_4^+: NO_3^- varied along the same spatial gradient by 4-fold (in September 2011) to >100-fold (in September 2012). If light were the dominant regulatory factor, we would have expected to see shifts in community composition along the transects that compared at least in directionality with those of the experimental high vs. low light manipulations. The difference in the experimental enclosures when incubated with differing nutrient forms were indeed consistent with trends in changes in pigments, and we thus suggest that the large nutrient changes, delivered over a short section of the river, were the dominant factors contributing to changes in phytoplankton community composition, observed along the riverine to bay transects (**Figure 3**).

During September 2012 (the only September for which pigment transect data are available), a large increase down-river in zeaxanthin was also noted. Cyanobacteria not only are preferential users of NH_4^+ compared to NO_3^- (Berg et al., 2003; Glibert and Berg, 2009), but they also are favored under the warmer temperatures of that season compared to temperatures observed in March (Paerl and Huisman, 2008). All transects had a >100% increase in alloxanthin (relative to values at Garcia Bend) beginning at the riverine site where the pulse of NH_4^+ became pronounced- a trend also consistent with reductions in water column transparency from the upper river to the bay (not shown).

There are a number of important implications of these data in the context of management implications of nutrient loads in the San Francisco Bay Delta region. These results bear substantially on the ongoing management debate in the Bay Delta region concerning the importance of reducing total N loads from sewage effluent and/or adding nitrification with or without N reductions. Water management in California is challenging and contentious, and a significant fraction of the water supply for state needs is extracted from the Delta. The Bay Delta is also the subject of considerable national public awareness due to the sociopolitical and socioeconomic tension surrounding the plight of the endemic delta smelt (*Hypomesus transpacificus*), a small (length ca. 6 cm) fish whose decline has been taken as a sign of adverse environmental conditions in the region. The delta smelt was put on the Threatened Species list in 1993 (Wanger, 2007a,b) and it underwent further population decline along with longfin smelt (*Spirinchus thaleichthys*), threadfin shad (*Dorosoma petenense)* and young-of-the-year striped bass (*Morone saxatilis)* in the early 2000s (Sommer et al., 2007). Accelerated losses during the last decade have been termed the "Pelagic Organism Decline" (POD) period (Sommer et al., 2007). An important

question is whether fish declines are related to changes in both abundance and species composition of the primary producers, and if so, are the changes in primary producers a result of shifts in nutrient quantity and quality? Before 1982, chl *a* concentrations in Suisun Bay were relatively high, averaging 9 μg L^{-1}, with numerous values exceeding 30 μg L^{-1}, and diatoms and delta smelt were abundant. The decline in diatoms, which began in 1982, has been shown to be highly correlated with the increase in NH_4^+ loading that occurred with the start of the operations of the WWTP on the Sacramento River (Dugdale et al., 2007; Glibert, 2010; Glibert et al., 2011). Beginning around 1999, when sharp declines in fish species began to be noted, NH_4^+ loading from wastewater discharge increased >25%, from ∼9 tons day^{-1} to 12–14 metric tons day^{-1}, and flagellates and cyanobacteria emerged as the dominant phytoplankton class (Lehman, 1996; Muller-Solger et al., 2002; Lehman et al., 2005, 2008; Brown, 2010; Glibert, 2010; Glibert et al., 2011).

The data herein lend support to a growing experimental body of evidence that an important management strategy for the San Francisco Bay Delta is the planned improvement in effluent N discharge through nitrification and denitrification; such a strategy is projected to increase the proportional production of diatoms and should lead to an increase in food quality (and amount) for fish and other higher trophic level consumers (Wilkerson et al., 2006; Dugdale et al., 2007, 2012; Glibert, 2010; Glibert et al., 2011; Parker et al., 2012a,b). Based on the data here, it can be inferred that by increasing the fractional availability of NO_3^- relative to NH_4^+, N-based production should increase, as will the yield per unit N of both chl *a* and fucoxanthin in this low-light environment. This growing consensus is further supported by recent modeling efforts of Dugdale et al. (2012; 2013). Dugdale et al. (2012) developed a conceptual model that correctly predicted the development of two unusual spring phytoplankton blooms in Suisun Bay based on only three criteria: the rate of NH_4^+ loading (based on present day sewage effluent loads), the water column concentration of NH_4^+, and river flow (analogous in steady-state chemostat growth to "washout"). This conceptual model was further advanced in a one-dimensional, N-based model (Dugdale et al., 2013) that included terms for the time-varying rates of maximum NO_3^- uptake as a function of NO_3^- concentration and for inhibition of NO_3^- uptake by NH_4^+ and that predicted either a high-biomass state that occurred under low flow and variable NH_4^+ levels, or a low-biomass state that occurred under high flow conditions but high NH_4^+ conditions. The modeled high-biomass, NO_3^--based, high-productivity state is analogous to the pre-1982, diatom era during which delta smelt were plentiful (Glibert, 2010; Glibert et al., 2011). Interestingly, in 2014, a major spring bloom was observed in Suisun Bay that also conformed to the low-flow, high NO_3^-, high biomass state. This bloom is thought to have been a response to the long-term drought that not only resulted in longer residence time for phytoplankton growth and accumulation, but also allowed a longer period of time for nitrification to occur, reducing sewage-derived NH_4^+ to a level where the NO_3^- could be accessed for uptake and growth (Glibert et al., 2014). The modeled low-biomass, low-productivity state based on NH_4^+ is analogous to the post-1982 cryptophyte/flagellate era that is related to the decline of smelt, threadfin shad, and young-of-the-year striped bass (Glibert, 2010; Glibert et al., 2011).

Placing these findings in the context of other observations of physiological changes in phytoplankton metabolism along the entire spectrum of nutrient availability suggests that the form of N plays a regulatory role in physiology and community composition at all concentration levels, not just at the limiting end of the spectrum (Glibert et al., 2013). Finally, the findings herein also point to an important consideration in the development of numeric criteria for nutrients in estuaries, a challenge that many states are now facing (U.S. EPA, 2010). Many such criteria, or integrated indices of water quality status and trends, are based on total N or P, rather than specific forms of N or P (U.S. EPA, 2010). The more subtle ecological impacts of NH_4^+ loading and the importance of changes in NO_3^-:NH_4^+ in phytoplankton succession have not been appreciated in nutrient criteria development to date. These findings show that N form is related to the "quality" of phytoplankton and that has previously been related to the trajectory of higher trophic levels in this N-rich ecosystem.

AUTHOR CONTRIBUTIONS

All authors contributed to the experimental design, acquisition and analysis of the data; Patricia M. Glibert, Frances P. Wilkerson, Richard C. Dugdale and Alexander E. Parker drafted the manuscript; Jeffrey Alexander, Sarah Blaser, and Susan Murasko contributed intellectual content and manuscript critiques; all authors approved the final manuscript version.

ACKNOWLEDGMENTS

This study was co-funded by the Delta Stewardship Council (Grant Number 2038) and the State and Federal Contractors Water Agency (Grant Number 12-20). We thank E. Kiss and M. Maddox from the Horn Point Laboratory, and A. Pimenta, C. Buck, A. Johnson, J. Lee, E. Kress, N. Travis, S. Strong, J. Fuller, D. Bell, and D. Morgan from the Romberg Tiburon Center, for assistance with sampling and analysis. HPL Analytical Services Laboratory provided analysis of the accessory pigments. The authors thank the reviewers for helpful comments on an earlier version of this paper. This is contribution number 4879 from the University of Maryland Center for Environmental Science.

SUPPLEMENTARY MATERIAL

The Supplementary Material for this article can be found online at: http://www.frontiersin.org/journal/10.3389/fmars.2014.00017/abstract

REFERENCES

Arar, E. J., and Collins, G. B. (1992). "*In vivo* determination of chlorophyll *a* and phaeophytin *a* in marine and freshwater phytoplankton by fluorescence," in *Methods for the Determination of Chemical Substances in Marine and Estuarine Samples* (Cincinnati, OH: Environmental Monitoring and Support Laboratory, Office of Research an Development, U.S. EPA, OH EPA/600/R-92/121), 22.

Alpine, A. E., and Cloern, J. E. (1992). Trophic interactions and direct physical effects control phytoplankton biomass and production in an estuary. *Limnol. Oceanogr.* 37, 946–955. doi: 10.4319/lo.1992.37.5.0946

Atwater, B. F., Conard, S. G., Dowden, J. N., Hedel, C. W., MacDonald, R. L., and Savage, W. (1979). "History, landforms, and vegetation of the estuary's tidal marshes," in *San Francisco Bay: The Ecosystem*, ed J. T. Hollibaugh (San Francisco, CA: Pacific Division of the American Association for the Advancement of Science), 347–385

Berg, G. M., Balode, M., Purina, I., Bekere, S., Béchemin, C., and Maestrini, S. (2003). Plankton community composition in relation to availability and uptake of oxidized and reduced nitrogen. *Aquatic. Microb. Ecol.* 30, 263–274. doi: 10.3354/ame030263

Berman, T., Sherr, B. F., Sherr, E., Wynne, D., and McCarthy, J. J. (1984). The characteristics of ammonium and nitrate uptake by phytoplankton in Lake Kinneret. *Limnol. Oceanogr.* 29, 287–297. doi: 10.4319/lo.1984.29.2.0287

Bran and Luebbe, Inc. (1999a). *Bran Luebbe Autoanalyzer Applications: AutoAnalyzer Method No. G-177-96 Silicate in Water and Seawater*. Buffalo Grove, IL: Bran Luebbe, Inc.

Bran and Luebbe, Inc. (1999b). *Bran Luebbe AutoAnalyzer Applications: AutoAnalyzer Method No. G-175-96 Phosphate in Water and Seawater*. Buffalo Grove, IL: Bran Luebbe, Inc.

Bran and Luebbe, Inc. (1999c). *Bran Luebbe AutoAnalyzer Applications: AutoAnalyzer Method No. G-172-96 Nitrate and Nitrite in Water and Seawater*. Buffalo Grove, IL: Bran Luebbe, Inc.

Britto, D. T., and Kronzucker, H. J. (2002). NH_4^+ toxicity in higher plants: a critical review. *J. Plant Physiol.* 159, 567–584. doi: 10.1078/0176-1617-0774

Brown, T. (2010). Phytoplankton community composition: the rise of the flagellates. *IEP Newslett.* 22, 20–28.

Caperon, J., and Ziemann, D. A. (1976). Synergistic effects of nitrate and ammonium ion on the growth and uptake kinetics of *Monochrysis lutheri* in continuous culture. *Mar. Biol.* 36, 73–84. doi: 10.1007/BF00388430

Carpenter, S. R., and Kitchell, J. F. (eds.). (1993). *The Trophic Cascade in Lakes*. New York, NY: Cambridge University Press.

Cloern, J. E. (2001). Our evolving conceptual model of the coastal eutrophication problem. *Mar. Ecol. Prog. Ser.* 210, 223–253. doi: 10.3354/meps210223

Cloern, J. E., and Dufford, R. (2005). Phytoplankton community ecology: principles applied in San Francisco Bay. *Mar. Ecol. Prog. Ser.* 285, 1–28. doi: 10.3354/meps285011

Cole, B. E., and Cloern, J. E. (1984). Significance of biomass and light availability to phytoplankton productivity in San Francisco Bay. *Mar. Ecol. Prog. Ser.* 17, 15–24. doi: 10.3354/meps017015

Collos, Y., Maestrini, S. Y., and Robert, M. (1989). High long-term nitrate uptake by oyster-pond microalgae in the presence of high ammonium concentrations. *Limnol. Oceanogr.* 34, 957–964. doi: 10.4319/lo.1989.34.5.0957

Donald, D. B., Bogard, M. J., Finlay, K., Bunting, L., and Leavitt, P. R. (2013). Phytoplankton-specific response to enrichment of phosphorus-rich surface waters with ammonium, nitrate, and urea. *PLoS ONE* 8:e53277. doi: 10.1371/journal.pone.0053277

Dortch, Q. (1990). The interaction between ammonium and nitrate uptake in phytoplankton. *Mar. Ecol. Prog. Ser.* 61, 183–201. doi: 10.3354/meps061183

Dortch, Q., Thompson, P. A., and Harrison, P. J. (1991). Short-term interaction between nitrate and ammonium uptake in *Thalassiosira pseudonana*: effect of preconditioning nitrogen source and growth rate. *Mar. Biol.* 110, 183–193. doi: 10.1007/BF01313703

Droop, M. R. (1983). 25 years of algal growth kinetics. *Bot. Mar.* 26, 99–112. doi: 10.1515/botm.1983.26.3.99

Dugdale, R. C., and Goering, J. J. (1967). Uptake of new and regenerated forms of nitrogen in primary productivity. *Limnol. Oceanogr.* 12, 196–206. doi: 10.4319/lo.1967.12.2.0196

Dugdale, R. C., and Wilkerson, F. P. (1986). The use of ^{15}N to measure nitrogen uptake in eutrophic oceans; experimental considerations. *Limnol. Oceanogr.* 31, 673–689. doi: 10.4319/lo.1986.31.4.0673

Dugdale, R. C., Wilkerson, F. P., Hogue, V. E., and Marchi, A. (2007). The role of ammonium and nitrate in spring bloom development in San Francisco Bay. *Est. Coast. Shelf Sci.* 73, 17–29. doi: 10.1016/j.ecss.2006.12.008

Dugdale, R. C., Wilkerson, F. P., and Parker, A. E. (2013). A biogeochemical model of phytoplankton productivity in an urban estuary: the importance of ammonium and freshwater flow. *Ecol. Model.* 263, 291–307. doi: 10.1016/j.ecolmodel.2013.05.015

Dugdale, R. C., Wilkerson, F. P., Parker, A. E., Marchi, A., and Taberski, K. (2012). River flow and ammonium discharge determine spring phytoplankton blooms in an urbanized estuary. *Est. Coast. Shelf Sci.* 115, 187–199. doi: 10.1016/j.ecss.2012.08.025

Edwards, V., Icely, J., Newton, A., and Webster, R. (2005). The yield of chlorophyll from nitrogen: a comparison between the shallow Ria Formosa lagoon and the deep oceanic conditions at Sagres along the southern coast of Portugal. *Est. Coast. Shelf Sci.* 62, 391–405. doi: 10.1016/j.ecss.2004.09.004

Eppley, R. W., and Peterson, B. J. (1979). Particulate organic matter flux and planktonic new production in the deep ocean. *Nature* 282, 677–680. doi: 10.1038/282677a0

Flynn, K. J. (1999). Nitrate transport and ammonium-nitrate interactions at high nitrate concentrations and low temperatures. *Mar. Ecol. Prog. Ser.* 187, 283–287. doi: 10.3354/meps187283

Flynn, K. J., and Fasham, M. J. R. (1997). A short version of the ammonium-nitrate interaction model. *J. Plankt. Res.* 19, 1881–1897. doi: 10.1093/plankt/19.12.1881

Flynn, K. J., Fasham, M. J. R., and Hipkin, C. R. (1997). Modelling the interactions between ammonium and nitrate uptake in marine phytoplankton. *Phil. Trans. R. Soc.* 352, 1625–1645.

Flynn, K. J., Stoecker, D. K., Mitra, A., Raven, J. A., Glibert, P. M., Hansen, P. J., et al. (2013). Misuse of the phytoplankton-zooplankton dichotomy: the need to assign organisms as mixotrophs within plankton functional types. *J. Plank. Res.* 35, 3–11. doi: 10.1093/plankt/fbs062

Glibert, P. M. (1998). Interactions of top-down and bottom-up control in planktonic nitrogen cycling. *Hydrobiology* 363, 1–12. doi: 10.1023/A:1003125805822

Glibert, P. M. (2010). Long-term changes in nutrient loading and stoichiometry and their relationships with changes in the food web and dominant pelagic fish species in the San Francisco Estuary, California. *Rev. Fish. Sci.* 18, 211–232. doi: 10.1080/10641262.2010.492059

Glibert, P. M. (2012). Ecological stoichiometry and its implications for aquatic ecosystem sustainability. *Curr. Opin. Envir. Sustainabil.* 4, 272–277. doi: 10.1016/j.cosust.2012.05.009

Glibert, P. M., and Berg, G. M. (2009). "Nitrogen form, fate and phytoplankton composition," in *Experimental Ecosystems and Scale: Tools for Understanding and Managing Coastal Ecosystems*, eds V. S. Kennedy, W. M. Kemp, J. E. Peterson, and W. C. Dennison (New York, NY: Springer), 183–189.

Glibert, P. M., and Capone, D. G. (1993). "Mineralization and assimilation in aquatic, sediment, and wetland systems," in *Nitrogen Isotope Techniques*, eds R. Knowles and T. H. Blackburn (San Diego, CA: Academic), 243–271.

Glibert, P. M., Dugdale, R. C., Wilkerson, F., Parker, A. E., Alexander, J., Antell, E., et al. (2014). Major- but rare- spring blooms in 2014 in San Francisco Bay Delta, California, a result of the long-term drought, increased residence time, and altered nutrient loads and forms. *J. Exp. Mar. Biol. Ecol.* 460, 8–18. doi: 10.1016/j.jembe.2014.06.001

Glibert, P. M., Fullerton, D., Burkholder, J. M., Cornwell, J., and Kana, T. M. (2011). Ecological stoichiometry, biogeochemical cycling, invasive species, and aquatic food webs: San Francisco Estuary and comparative systems. *Rev. Fish. Sci.* 19, 358–417. doi: 10.1080/10641262.2011.611916

Glibert, P. M., Kana, T. M., and Brown, K. (2013). From limitation to excess: consequences of substrate excess and stoichiometry for phytoplankton physiology, trophodynamics and biogeochemistry, and implications for modeling. *J. Mar. Syst.* 125, 14–28. doi: 10.1016/j.jmarsys.2012.10.004

Glibert, P. M., Lipschultz, F., McCarthy, J. J., and Altabet, M. A. (1982). Isotope dilution models of uptake and remineralization of ammonium by marine plankton. *Limnol. Oceanogr.* 27, 639–650. doi: 10.4319/lo.1982.27.4.0639

Gowen, R. J., Tett, P., and Jones, K. J. (1992). Predicting marine eutrophication: the yield of chlorophyll from nitrogen in Scottish coastal waters. *Mar. Ecol. Prog. Ser.* 85, 153–161. doi: 10.3354/meps085153

Heil, C. A., Revilla, M., Glibert, P. M., and Murasko, S. (2007). Nutrient quality drives phytoplankton community composition on the West Florida Shelf. *Limnol. Oceanogr.* 52, 1067–1078. doi: 10.4319/lo.2007.52.3.1067

Jassby, A. (2008). Phytoplankton in the upper San Francisco Estuary: re- cent biomass trends, their causes and their trophic significance. *San Francisco Estuar. Watershed Sci.* 6, 1–26.

Jassby, A. D., Cloern, J. E., and Cole, B. B. (2002). Annual primary production: patterns and mechanisms of change in a nutrient-rich tidal ecosystem. *Limnol. Oceanogr.* 47, 698–712. doi: 10.4319/lo.2002.47.3.0698

Kimmerer, W. J. (2004). Open water processes of the San Francisco Estuary: from physical forcing to biological responses. *San Francisco Estuar. Watershed Sci.* 2, 1–140.

Kimmerer, W. J., Parker, A. E., Lidstrom, U., and Carpenter, E. J. (2012). Short-term and interannual variability in primary productivity in the low-salinity zone of the San Francisco Estuary. *Estuar. Coast*. 35, 913–920. doi: 10.1007/s12237-012-9482-2

Legendre, L., and Rassoulzadegan, F. (1995). Plankton and nutrient dynamics in marine waters. *Ophelia* 41, 153–172.

Lehman, P. W. (1996). "Changes in chlorophyll-a concentration and phytoplankton community composition with water-year type in the upper San Francisco Estuary," in *San Francisco Bay: The Ecosystem*, ed J. T. Hollibaugh (San Francisco, CA: Pacific Division of the American Association for the Advancement of Science), 351–374.

Lehman, P. W., Boyer, G., Hall, C., Walker, S., and Gehrts, K. (2005). Distribution and toxicity of a new colonial *Microcystis aeruginosa* bloom in the San Francisco Bay Estuary, California. *Hydrobiology* 541, 87–99. doi: 10.1007/s10750-004-4670-0

Lehman, P. W., Boyer, G., Stachwell, M., and Walker, S. (2008). The influence of environmental conditions on seasonal variation of *Microcystis* abundance and microcystins concentration in San Francisco Estuary. *Hydrobiology* 600, 187–204. doi: 10.1007/s10750-007-9231-x

L'Helguen, S., Maguer, J.-F., and Caradec. J. (2008). Inhibition kinetics of nitrate uptake by ammonium in sze-fractionated oceanic phytoplankton communities: implications for new production and *f*-ratio estimates. *J. Plankt. Res*. 10, 1179–1188. doi: 10.1093/plankt/fbn072

Lindell, D., and Post, A. F. (2001). Ecological aspects of *ntcA* gene expression and its use as an indicator of the nitrogen status of marine *Synechococcus* spp. *Appl. Envir. Microbiol.* 67, 3340–3349. doi: 10.1128/AEM.67.8.3340-3349.2001

Lomas, M. W., and Glibert, P. M. (1999a). Temperature regulation of nitrate uptake: a novel hypothesis about nitrate uptake and reduction in cool-water diatoms. *Limnol. Oceanogr.* 44, 556–572. doi: 10.4319/lo.1999.44.3.0556

Lomas, M. W., and Glibert, P. M. (1999b). Interactions between NH_4^+ and NO_{3--} uptake and assimilation: comparison of diatoms and dinoflagellates at several growth temperatures. *Mar. Biol.* 133, 541–551. doi: 10.1007/s002270050494

Lomas, M. W., and Glibert, P. M. (2000). Comparisons of nitrate uptake, storage and reduction in marine diatoms and flagellates. *J. Phycol*. 36, 903–913. doi: 10.1046/j.1529-8817.2000.99029.x

MacDonald, R. W., McLaughlin, F. A., and Wong, C. S. (1986). The storage of reactive silicate samples by freezing. *Limnol. Oceanogr*. 31, 1139–1142. doi: 10.4319/lo.1986.31.5.1139

MacIsaac, J. J., Dugdale, R. C., Huntsman, S., and Conway, H. L. (1979). The effect of sewage on uptake of inorganic nitrogen and carbon by natural populations of marine phytoplankton. *J. Mar. Sci.* 37, 51–66.

Maguer, J.-F., L'Helguen, S., Madec, C., Labry, C., and Le Corre, P. (2007). Nitrogen uptake and assimilation kinetics in *Alexandrium minutum* (Dinophyceae): effect of N-limited growth rate on nitrate and ammonium interactions. *J. Phycol.* 43, 295–303. doi: 10.1111/j.1529-8817.2007.00334.x

McCarthy, J. J., Taylor, W. R., and Taft, J. L. (1975). "The dynamics of nitrogen and phosphorus cycling in the open waters of Chesapeake Bay," in *Marine Chemistry in the Coastal Environment*, ed T. M. Church (Washington, DC: American Chemical Society), 664–681.

Moore, L. R., Post, A. F., Rocap, G., and Chisholm, S. W. (2002). Utilization of different nitrogen sources by the marine cyanobacteria *Prochlorochoccus* and *Synechococcus*. *Limnol. Oceanogr*. 47, 989–996. doi: 10.4319/lo.2002.47.4.0989

Mousseau, L., Klein, B., Legendre, L., Dauchez, S., Tamigneaux, E., Tremblay, J.-E., et al. (2001). Assessing the trophic pathways that dominate food webs: an approach based on simple ecological ratios. *J. Plank. Res.* 23, 765–777. doi: 10.1093/plankt/23.8.765

Muller-Solger, A. B., Jassby, A. D., and Muller-Navarra, D. (2002). Nutritional quality of food resources for zooplankton (Daphnia) in a tidal freshwater system (Sacramento-San Joaquin River Delta). *Limnol. Oceanogr.* 47, 1468–1476. doi: 10.4319/lo.2002.47.5.1468

Nichols, F. H., Cloern, J. E., Luoma, S. N., and Peterson, D. H. (1986). The modification of an estuary. *Science* 231, 567–573. doi: 10.1126/science.231.4738.567

Paerl, H. W., and Huisman, J. (2008). Blooms like it hot. *Science* 320, 57–58. doi: 10.1126/science.1155398

Parker, A. E. (2004). *Assessing the Phytoplankton-Heterotrophic Bacterial Link in the Eutrophic Delaware Estuary,* Ph.D. dissertation, University of Delaware.

Parker, A. E., Hogue, V. E., Wilkerson, F. P., and Dugdale, R. C. (2012a). The effect of inorganic nitrogen speciation on primary production in San Francisco Estuary. *Est. Coast. Shelf Sci.* 104–105, 91–101. doi: 10.1016/j.ecss.2012.04.001

Parker, A. E., Wilkerson, F. P., and Dugdale, R. C. (2012b). Elevated ammonium concentrations from wastewater discharge depress primary productivity in the Sacramento River and the northern San Francisco Estuary. *Mar. Poll. Bull*. 64, 574–586. doi: 10.1016/j.marpolbul.2011.12.016

Polis, G. A., and Strong, D. R. (1996). Food web complexity and community dynamics. *Am. Nat.* 147, 813–846. doi: 10.1086/285880

Raven, J. A. (1984). *Energetics and Transport in Aquatic Plants*. New York, NY: Alan R. Liss, Inc, 587.

Reynolds, C. S. (1999). Non-determinism to probability, or N:P in the community ecology of phytoplankton. *Arch. Hydrobiol.* 146, 23–35.

Sobota, D. J., Harrison, J. A., and Dahlgren, R. A. (2009). Influences of climate, hydrology, and land use on input and export of nitrogen in California watersheds. *Biogeochemistry* 94, 1–20. doi: 10.1007/s10533-009-9307-y

Solórzano, L. (1969). Determination of ammonia in natural waters by the phenolhypochlorite method. *Limnol. Oceanogr.* 14, 799–801. doi: 10.4319/lo.1969.14.5.0799

Sommer, T. R., Armor, C., Baxter, R., Breuer, R., Brown, L., Chotkowski, M., et al. (2007). The collapse of pelagic fishes in the upper San Francisco Estuary. *Fisheries* 32, 270–277. doi: 10.1577/1548-8446(2007)32[270:TCOPFI]2.0.CO;2

Song, B., and Ward, B. B. (2007). Molecular cloning and characterization of high-affinity nitrate transporters in marine phytoplankton. *J. Phycol.* 43, 542–552. doi: 10.1111/j.1529-8817.2007.00352.x

U.S., Environmental Protection Agency (EPA). (2010). *Nutrients in Estuaries and Relation to Water Quality Criteria Derivation State of the Science*, eds P. Glibert, C. Madden, W. Boynton, D. Flemer, C. Heil, and J. Sharp (EPA Office of Water), 190.

Van Heukelem, L., and Thomas, C. S. (2001). Computer-assisted high-performance liquid chromatography method development with applications to the isolation and analysis of phytoplankton pigments. *J. Chromatogr. A* 910, 31–49. doi: 10.1016/S0378-4347(00)00603-4

Van Nieuwenhuyse, E. (2007). Response of summer chlorophyll concentration to reduced total phosphorus concentration in the Rhine River (Netherlands) and the Sacramento-San Joaquin Delta (California, USA). *Can. J. Fish. Aquat. Sci.* 64, 1529–1542. doi: 10.1139/f07-121

Waiser, M. J., Tumber, V., and Holm, J. (2011). Effluent-dominated streams. Part I. Presence and effects of excess nitrogen and phosphorus in Wascana Creek, Saskatchewan, Canada. *Environ. Toxicol. Chem*. 30, 496–507. doi: 10.1002/etc.399

Wanger, O. W. (2007a). *Findings of Fact and Conclusions of Law re Interim Remedies re: Delta Smelt ESA Remand and Reconsultation*. Case 1:05-cv- 01207-OWW-GSA, Document 01561. Fresno, CA: United States District Court, Eastern District of California.

Wanger, O. W. (2007b). *Interim Remedial Order Following Summary Judgment and Evidentiary Hearing*. Case 1:05-cv-01207-OWW-GSA, Document 01560. Fresno, CA: United States District Court, Eastern District of California.

Whitledge, T. E., Malloy, S. C., Patton, C. J., and Wirick, C. D. (1981). *Automated Nutrient Analyses in Seawater*. Report 51398. Upton, NY: Brookhaven National Laboratory.

Wilkerson, F. P., Dugdale, R. C., Hogue, V. E., and Marchi, A. (2006). Phytoplankton blooms and nitrogen productivity in the San Francisco Bay. *Estuar. Coast.* 29, 401–416.

Xu, J., Yin, K., Lee, J. H. W., Liu, H., Ho, A. Y. T., Yuan, X. et al. (2012). Long-term and seasonal changes in nutrients, phytoplankton biomass, and

dissolved oxygen in Deep Bay, Hong Kong. *Estuar. Coast.* 33, 399–416. doi: 10.1007/s12237-009-9213-5

Yoshiyama, K., and Sharp, J. H. (2006). Phytoplankton response to nutrient enrichment in an urbanized estuary: apparent inhibition of primary production by over-eutrophication. *Limnol. Oceanogr.* 51, 424–434. doi: 10.4319/lo.2006.51.1_part_2.0424

Conflict of Interest Statement: P. Glibert and R. Dugdale have previously consulted for the State and Federal Contractors Water Agency (SFCWA); that work terminated 22 months ago. SFWCA in recent years has been developing a rigorous science program. They co-funded the work herein with the Delta Stewardship Council in an open competition. SFWCA has no knowledge of the data described here or their interpretations. The authors declare that the research was conducted in the absence of any commercial or financial relationships that could be construed as a potential conflict of interest.

Received: 23 January 2014; accepted: 13 June 2014; published online: 07 July 2014.
Citation: Glibert PM, Wilkerson FP, Dugdale RC, Parker AE, Alexander J, Blaser S and Murasko S (2014) Phytoplankton communities from San Francisco Bay Delta respond differently to oxidized and reduced nitrogen substrates—even under conditions that would otherwise suggest nitrogen sufficiency. Front. Mar. Sci. ***1****:17. doi: 10.3389/fmars.2014.00017*
This article was submitted to Aquatic Microbiology, a section of the journal Frontiers in Marine Science.

frontiers in MICROBIOLOGY

ORIGINAL RESEARCH ARTICLE
published: 21 August 2014
doi: 10.3389/fmicb.2014.00429

Connecting the dots: linking nitrogen cycle gene expression to nitrogen fluxes in marine sediment mesocosms

Jennifer L. Bowen[1]*, Andrew R. Babbin[2], Patrick J. Kearns[1] and Bess B. Ward[2]

[1] *Department of Biology, University of Massachusetts Boston, Boston, MA, USA*
[2] *Department of Geosciences, Princeton University, Princeton, NJ, USA*

Edited by:
John J. Kelly, Loyola University Chicago, USA

Reviewed by:
Guang Gao, Chinese Academy of Sciences, China
Andreas Schramm, Aarhus University, Denmark
Iris C. Anderson, College of William and Mary, USA

****Correspondence:***
Jennifer L. Bowen, Department of Biology, University of Massachusetts Boston, 100 Morrissey Blvd., Boston, MA 02125, USA
e-mail: jennifer.bowen@umb.edu

Connecting molecular information directly to microbial transformation rates remains a challenge, despite the availability of molecular methods to investigate microbial biogeochemistry. By combining information on gene abundance and expression for key genes with quantitative modeling of nitrogen fluxes, we can begin to understand the scales on which genetic signals vary and how they relate to key functions. We used quantitative PCR of DNA and cDNA, along with biogeochemical modeling to assess how the abundance and expression of microbes responsible for two steps in the nitrogen cycle changed over time in estuarine sediment mesocosms. Sediments and water were collected from coastal Massachusetts and maintained in replicated 20 L mesocosms for 45 days. Concentrations of all major inorganic nitrogen species were measured daily and used to derive rates of nitrification and denitrification from a Monte Carlo-based non-negative least-squares analysis of finite difference equations. The mesocosms followed a classic regeneration sequence in which ammonium released from the decomposition of organic matter was subsequently oxidized to nitrite and then further to nitrate, some portion of which was ultimately denitrified. Normalized abundances of ammonia oxidizing archaeal ammonia monoxoygenase (*amoA*) transcripts closely tracked rates of ammonia oxidation throughout the experiment. No such relationship, however, was evident between denitrification rates and the normalized abundance of nitrite reductase (*nirS* and *nirK*) transcripts. These findings underscore the complexity of directly linking the structure of the microbial community to rates of biogeochemical processes.

Keywords: ammonia oxidizing archaea, denitrification, nitrification, *nirS*, *amoA*, estuarine sediments, nitrogen cycle, quantitative PCR

INTRODUCTION

In shallow estuarine ecosystems the biogeochemistry of sediments and the overlying water column are tightly coupled (Howarth et al., 2011). Human perturbation, however, has resulted in a substantial increase in nutrient loading to coastal waters (Bowen and Valiela, 2001; Galloway et al., 2003) resulting in a host of deleterious effects, including increases in the frequency of anoxic events (Diaz and Rosenberg, 2008) and other associated symptoms of eutrophication (Valiela et al., 1992; Cloern, 2001; Smith, 2003). Increased anthropogenic nutrient additions can alter the biogeochemical coupling between estuarine sediments and waters (Burgin and Hamilton, 2007), which can further exacerbate eutrophic conditions (Howarth et al., 2011). The microbial communities within estuarine sediments are responsible for numerous geochemical processes that can remove anthropogenic nitrogen, including canonical denitrification, coupled nitrification and denitrification, and anaerobic ammonium oxidation (anammox). As a result of these nitrogen removal pathways, microbes help to ameliorate the threat of coastal eutrophication.

The capacity of estuarine sediments to remove fixed nitrogen depends on a suite of factors. Remineralization of organic matter in estuarine sediments typically results in reducing conditions and high porewater ammonium (NH_4^+) concentrations. When estuarine bottom waters are oxic, some portion of NH_4^+ formed in the sediment is oxidized at the sediment water interface to form nitrite (NO_2^-) and then nitrate (NO_3^-) through the microbially mediated nitrification pathway. This oxidized NO_3^- is then lost as nitrogen gas from the adjoining suboxic sediments through a coupling of the nitrification and denitrification pathways (Jenkins and Kemp, 1984; An and Joye, 2001; Risgaard-Petersen, 2003). In estuaries that have frequent summertime bottom water hypoxia or anoxia, the coupling of nitrification and denitrification can be interrupted as nitrification becomes inhibited by a lack of oxygen and by the accumulation of sulfide (Joye and Hollibaugh, 1995).

Canonical denitrification has typically been considered the dominant nitrogen loss process in estuarine sediments (Burdige, 2012). Rates of denitrification are controlled primarily by the absence of oxygen and the availability of both organic matter and oxidized nitrogen (Zumft, 1997). Anaerobic ammonia oxidation

(anammox) can also be an important nitrogen loss process in some environments (Dalsgaard et al., 2005) but tends to account for a smaller proportion of fixed nitrogen loss in organic rich systems such as those found in the coastal zone (Dalsgaard et al., 2005; Rich et al., 2008; Nicholls and Trimmer, 2009). A third process, dissimilatory reduction of NO_3^- to NH_4^+ (DNRA) can also occur in estuarine sediments (Giblin et al., 2013). This process does not remove nitrogen from the system, rather, it results in a change in the oxidation state of the nitrogen such that it remains bioavailable. Fixed nitrogen loss (both from anammox and denitrification) can be limited by a lack of oxidized nitrogen substrates, competition for substrate by DNRA, and sulfide inhibition (An and Gardner, 2002; Burgin and Hamilton, 2007). Although these pathways have been fairly well documented in estuarine sediments, how these important biogeochemical cycles are regulated at the microbial genetic level has received considerably less attention.

The exact nature of the coupling between geochemical rates and microbial gene expression is complex (van de Leemput et al., 2011) and appears to vary in space and time (Nogales et al., 2002; Smith et al., 2007; Abell et al., 2010; Laverock et al., 2013). Directly linking these biogeochemical processes to the genetic structure and activity of the microbial community responsible for facilitating these processes has remained a challenge. A series of reciprocal transplant experiments in estuarine sediments demonstrated that changes in microbial community composition had a direct effect on ecosystem function (Reed and Martiny, 2012), though it was not possible to directly tie these ecosystem scale effects to changes in relevant functional genes. Numerous correlational studies in coastal systems have linked functional gene abundance or expression to environmental drivers (Bernhard et al., 2007; Mosier and Francis, 2008; Abell et al., 2010), though far fewer studies include examination of these patterns over time (Laverock et al., 2013) or as a result of experimental manipulation. More quantitative data directly linking microbial genetics to geochemical fluxes are needed to improve the predictive capacity of geochemical models (Treseder et al., 2011).

Defining the relationship between microbial genetic diversity and ecosystem function is a central goal of microbial ecology (Morales and Holben, 2010). Advances in molecular methods have rapidly accelerated our understanding of microbial community structure and gene expression, yet translating shifts in microbial community structure into changes in ecosystem function remains a challenge (Knight et al., 2012; Ottesen et al., 2013). Metatranscriptomics approaches currently offer glimpses of how transcription profiles of the dominant microbial taxa respond to environmental changes (Ottesen et al., 2013) but do not allow insight into the activity of low abundance phylotypes that may also be active contributors to ecosystem function (Campbell et al., 2011; Campbell and Kirchman, 2012). Metatranscriptomic analyses are an even greater challenge in complex systems with high taxonomic richness such as those that exist in estuarine sediments.

In this study we examined the relationships among gene abundance and expression, nutrient fluxes, and modeled rates of nitrification and denitrification in a coastal sediment mesocosm experiment. The intention of this experiment was not to mimic processes as they occur in coastal sediments. Rather, it was to set in motion a chain reaction of geochemical fluxes that also occur in coastal systems, and to monitor changes in gene abundance and expression that occur coincident with changes in the mesocosm geochemistry. We hypothesized that because ammonia oxidation is largely the only metabolic option for this phylogenetically constrained group of organisms, the abundance of the ammonia monooxygenase (*amoA*) gene (and thus the ammonia oxidizing bacteria and archaea) would closely track rates of ammonia oxidation. If a tight coupling between *amoA* gene expression and ammonia oxidation rates is observed, it suggests that other ammonia loss processes (those that do not require ammonia monooxygenase or, like anammox, that occur under strictly anoxic conditions; Kartal et al., 2011), might not be important contributors to nutrient cycling in the mesocosms.

Further, we hypothesized that the correlation between the abundance of genes that encode nitrite reductase, a key enzyme in the denitrification pathway, and associated rates of denitrification would be more difficult to disentangle. Denitrifying bacteria are capable of utilizing numerous electron acceptors, including NO_3^-, and therefore the presence of the *nirS* gene does not necessarily indicate that active denitrification is occurring. However, we predicted that gene expression, when normalized to the total amount of the gene present in the samples, would roughly predict modeled rates, as it is only those bacteria actively expressing the genes and synthesizing proteins that are responsible for the biogeochemical process *in situ*. Establishing quantitative relationships between biogeochemical process rates of nitrification and denitrification and the underlying genetic controls on these processes could help increase the predictive power of biogeochemical models and our understanding of the marine microbial environment.

MATERIALS AND METHODS

EXPERIMENTAL DESIGN AND SAMPLE COLLECTION

We used a benthic grab deployed from a small boat to collect surface sediment from five locations within Eel Pond in Woods Hole Massachusetts (41° 31′33 N, 70° 40′12 W) on 28 September 2008. Sediments were collected from 3 to 4 meters of water with a salinity of 28 ppt and a temperature of 19°C. None of the sediments collected exhibited signs of sulfide accumulation. Surface sediments (1–2 cm) from each grab were sectioned off with a knife, pooled together, and stored on ice until arrival at Princeton University, where they were then stored in a 12°C cold room until processing. Additionally, we collected 120 L of site water from Eel Pond, filtered it through a Whatman® GF/F filter and stored it in the dark until the mesocosms were constructed.

Four replicate mesocosms were established on 1 October 2008, each containing 3 kg of sediments overlain with 20 liters of filtered site water. Sediments from the initial grabs were thoroughly homogenized and visible macrofauna were removed. The 3 kg of sediment was then distributed evenly over the 0.1 m^2 area of the mesocosm to a depth of approximately 2 cm. 20 L of filtered site water was then added to the mesocosm and sediments were allowed to settle for 24 h prior to sampling. Each mesocosm was fitted with a tightly sealed lid containing a two-port valve. One port of the valve was fitted with an air stone to gently circulate

air through the overlying waters. The other port contained a sampling tube for removal of water for nutrient analyses. The overlying waters of the mesocosm remained oxic throughout the experiment and there was no evidence of sulfide accumulation.

The mesocosms were maintained in a darkened room for 45 days. Initial duplicate samples of sediment from the homogenized pool were collected with a 5 cc syringe corer and stored at −80°C. Two 15 mL aliquots of initial water were also collected for later nutrient analyses as described below. Every day or every other day water was withdrawn for nutrient analysis using a syringe to draw water through the sampling valve. pH and dissolved oxygen were measured on 20 mL of the withdrawn water using a YSI handheld meter. Two 15 mL aliquots were also removed and were filtered through a Whatman® GF/F filter and stored frozen for later nutrient analysis. Approximately once per week each mesocosm was opened and a sterile 5 cc syringe corer was used to remove an entire sediment column from the mesocosm. Sediment cores (3–4 cores taken through the entire depth of the sediment column) were collected, homogenized, and split between duplicate cryovials for immediate storage at −80°C.

NUTRIENT ANALYSES AND MODELED GEOCHEMICAL RATES

At each time point we measured duplicate water column concentrations of NH_4^+, NO_2^-, and NO_3^-. Colorimetric analyses were used to measure NO_2^- (Strickland and Parsons, 1972) and NH_4^+ (Koroleff, 1983). NO_3^- concentrations were measured by chemiluminescence after vanadium reduction (Garside, 1982; Braman and Hendrix, 1989). The measured nutrient concentration data were used to derive modeled rates of ammonification, ammonia oxidation, nitrite oxidation, and denitrification (Babbin and Ward, 2013). Briefly, a simple box model linking the three measured DIN species via these four biological processes was implemented.

To calculate rates of sediment biological N transformation from DIN measurements in the overlying water, we generated, in a Monte Carlo fashion ($n = 5000$), random sets of DIN measurements derived from the means and standard deviations of our concentration measurements. We then smoothed the concentrations with time using a Savitzky-Golay filter to minimize sampling noise. Time derivatives were numerically calculated for each of the three DIN species, and a least squares non-negative fit of rates was determined using the algorithm of Lawson and Hanson (1974) in Matlab. The Monte Carlo simulation accounted for the replicate variability in DIN concentration measurements, and the means and standard deviations of the trials are reported.

DNA AND RNA EXTRACTIONS

DNA was extracted in duplicate from approximately 0.5 g (wet weight) of sediment using the MoBio PowerSoil® DNA Isolation Kit (MoBio Laboratories, Carlsbad, CA) following manufacturer's instructions. Extracted DNA was purified via isopropanol precipitation and quantified using Quant-iT™ PicoGreen® dsDNA Assay (Life Technologies, Grand Island, NY). RNA was extracted from ∼1 g of sediment using the MoBio RNA Powersoil® Total RNA isolation kit (MoBio Laboratories, Carlsbad CA), also following manufacturer's instructions. mRNA was quantified using a NanoDrop ND-1000 UV-Vis spectrophotmeter (Thermo Fisher Scientific, Pittsburgh, PA), and immediately reverse transcribed to cDNA using SuperScript® III First Strand Synthesis System (Invitrogen™, now Life Technologies, Grand Island, NY). Residual DNA was digested using DNase1 (New England Biolabs, Ipswich, MA) and removal of all DNA contamination was verified via PCR amplification and gel electrophoresis following manufacturer's instructions.

QUANTITATIVE PCR

Denitrifier nirS qPCR

We performed qPCR of the *nirS* gene in bacterial DNA and cDNA using primers from Braker et al. (1998). The 25 μL reaction comprised 12.5 μL of SYBR®Green Brilliant III Ultra-Fast master mix (Agilent Technologies, Santa Clara, CA), 2.5 μL each of 20 μM nirS1F and nirS3R primer stocks (Braker et al., 1998), 1 μL of 1 ng/μL template DNA or cDNA, and 6.5 μL H_2O. The qPCR reaction was carried out on a Stratagene MX-3000 (Stratagene, La Jolla, CA) with an initial denaturation step at 95°C for 15 min, followed by 40 cycles of 94°C for 15 s, 62°C for 30 s, and 72°C for 30 s. A melt curve was then performed to test the stringency of the reaction, and resulting PCR products were examined via gel electrophoresis to confirm specificity of product formation.

Denitrifier nirK qPCR

We performed qPCR of the *nirK* gene in bacterial DNA using the nirK1F and nirK5R primers from Braker et al. (1998). Each 25 μL reaction contained 12.5 μL SYBR®Green Brilliant III Ultra-Fast master mix (Agilent Technologies, Santa Clara, CA), 8.7 μL MilliQ water 1.25 μL each of the forward and reverse primers (0.5 μM final concentration), 0.3 μL ROX dye, and 1 μL of 10 ng μL^{-1} DNA. The qPCR reaction was performed on an Agilent MX3005p qPCR system, with an initial denaturing step at 94°C for 5 min, followed by 35 cycles of 95°C for 30 s, 58°C for 40 s and 72°C for 40 s. Melt curves were performed to test the stringency of the reaction and the PCR product size was confirmed via gel electrophoresis. Repeated attempts to quantify *nirK* in the cDNA were unsuccessful.

Ammonia oxidizer amoA qPCR

We performed qPCR on the *amoA* gene in DNA and cDNA from ammonia oxidizing bacteria (AOB) using previously published AOB *amoA* primers (Rotthauwe et al., 1997). Briefly, in a 20 μL reaction we added 1 μL of 12 ng/μL template DNA or cDNA, 10 μL SYBR®Green Brilliant III Ultra-Fast master mix (Agilent Technologies, Santa Clara, CA), 0.3 μL ROX dye, 1 μL each of 10 μM forward and reverse primers, 0.6 μL BSA (300 μg/mL) and 6.1 μL water. To amplify the *amoA* gene from ammonia oxidizing archaea (AOA) we also used previously published primers (Francis et al., 2005) in 20 μL reactions containing 1 μL of 12 ng/μL DNA or cDNA template, 10 μL SYBR®Green Brilliant III Ultra-Fast master mix (Agilent Technologies, Santa Clara, CA), 0.3 μL ROX, 0.2 μL each of 0.2 μM forward and reverse primers, 0.6 μL BSA (300 μg/mL), 0.5 μL $MgCl_2$(3 mM final concentration) and 7.2 μL water. Both AOA and AOB qPCR reactions were performed on an Agilent MX3005p qPCR system with an initial 5 min denaturing step at 94°C, followed by 42 cycles of 94°C for 1 min, 50°C for 1.5 min, and 72°C for 1.5 min. Melt

curves were again derived to test for amplification stringency, and resulting PCR products checked for specificity of product via gel electrophoresis.

Standards for all four genes (*nirS*, *nirK*, AOA, and AOB *amoA*) were prepared from cloned gene fragments and were serially diluted over six orders of magnitude to generate a standard curve. Gene copy numbers were calculated from Quant-iT™ PicoGreen® dsDNA Assay (Life Technologies, Grand Island, NY) quantification of the most concentrated standard. All samples from each mesocosm and for all dates for a specific gene were analyzed in triplicate on a single 96-well plate to avoid plate-to-plate variability in quantification. All plates included triplicate standard curves as well as triplicate no template controls. The Agilent software automatically generated cycle threshold values (C_T) and, if present in the no template controls, the C_T values were at least five cycles higher than the C_T values for the lowest standard. Amplification efficiencies ranged from 80 to 94% for *nirS* and *nirK* DNA and cDNA qPCR reactions and 75–84% for AOA and AOB *amoA* qPCR reactions.

RESULTS

NUTRIENT CONCENTRATIONS

Each of the mesocosms followed a classic remineralization sequence, with an initial rapid flux of NH_4^+ resulting from decomposition of the ambient organic matter present in these rich coastal sediments at the time of sampling (**Figure 1**, blue diamonds). This flux of NH_4^+ was followed by a large flux of NO_2^- (**Figure 1**, green triangles), and a lower and more gradual increase in NO_3^- (**Figure 1**, red circles). The magnitude of the NH_4^+ concentration maximum varied from 20 to 37 μM and occurred within the first 9 days of the experiment. In all tanks NH_4^+ concentrations increased from approximately 3 μM in the initial water to over 10 μM within the first 2 days and remained above 10 μM for up to 2 weeks. Subsequently, typically after 9–12 days, the concentration of NO_2^- began to increase to peak concentrations ranging from 31 to 62 μM. The increase in NO_2^- concentration coincided with a relatively rapid decrease in NH_4^+. The NO_2^- peaks persisted in the mesocosms until NH_4^+ concentrations were depleted and then NO_2^- concentrations decreased to low levels (below 3 μM) for the remainder of the experiment. The concentrations of NO_3^- did not show the same sharp peak as was observed with the concentrations of NH_4^+ or NO_2^-. Rather, the concentrations of NO_3^- generally increased at a gradual rate throughout the duration of the experiment, with the highest concentrations of NO_3^- evident at day 40 or later. All four mesocosm experiments demonstrated the same general patterns, though the timing and magnitude of peak nutrient concentrations varied slightly from tank to tank.

RATES OF NITROGEN CYCLING

Calculated rates of both stepwise components of nitrification (ammonia oxidation and nitrite oxidation) and denitrification also exhibited patterns that varied with regard to the magnitude and timing of their peaks (**Figure 2**), but that generally showed the same basic pattern among the four replicates. Rates were integrated over the entire sediment column and were calculated based on the changes of each nutrient in the overlying water.

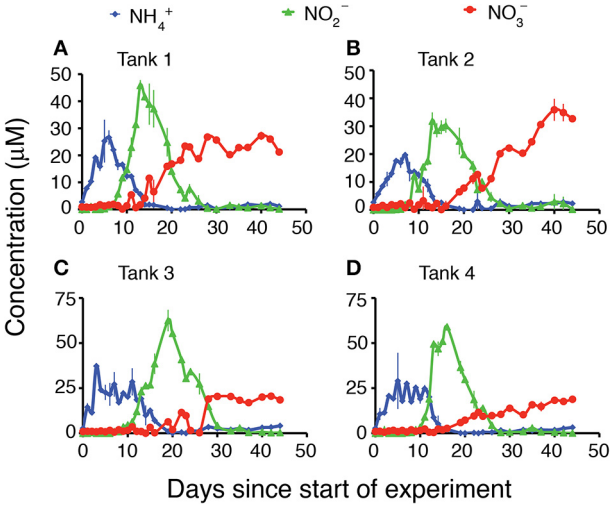

FIGURE 1 | Water column concentrations (μM) of NH_4, NO_2, and NO_3 during the 45 days of the experiment. (A) Tank 1, **(B)** Tank 2, **(C)** Tank 3, **(D)** Tank 4.

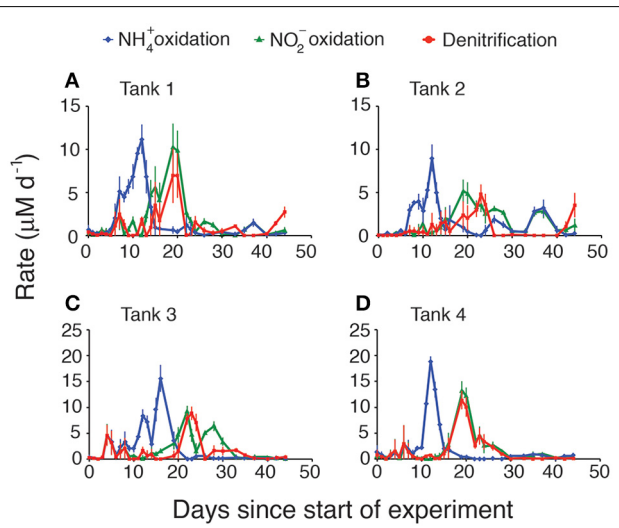

FIGURE 2 | Modeled rates of ammonia oxidation, nitrite oxidation, and denitrification in each mesocosm. (A) Tank 1, **(B)** Tank 2, **(C)** Tank 3, **(D)** Tank 4.

As expected, ammonia oxidation rates peaked first (**Figure 2**, blue diamonds), typically around day 10–12. The highest rates of ammonia oxidation were observed in tank 4, where they peaked at 19 μM d^{-1}. In all cases there was a lag of approximately 5 days between peak ammonia oxidation rates and peak nitrite oxidation rates (**Figure 2**, green triangles). The magnitude of the peaks in nitrite oxidation rates was also consistently lower than the peaks in ammonia oxidation rates. Nitrite oxidation either immediately preceded or exactly co-occurred with peak rates of denitrification (**Figure 2**, red circles) though denitrification rates were typically slightly lower than nitrite oxidation rates. When each of the rates was integrated over time, consistent patterns emerged across

all mesocosms (**Figure 3**). The total amount of ammonification (**Figure 3**, yellow bars) established the absolute amount of reactive nitrogen in the system and amounts of ammonia (**Figure 3**, blue bars) and nitrite oxidation (**Figure 3**, green bars) did not surpass the amount set by ammonification. In each case, however, the integrated amount of denitrification (**Figure 3**, red bars) never achieved parity with other processes. Denitrification attained only 52–76% of the maximum possible, as estimated from the amount of nitrate produced.

GENE ABUNDANCE AND EXPRESSION

We used qPCR to quantify the gene abundance (via DNA) and gene expression (via cDNA) for key genes in the nitrification and denitrification pathways. In all mesocosms the abundance of AOA *amoA* in microbial DNA was around three orders of magnitude higher than the abundance of AOB *amoA* (**Figure 4A** vs. **Figure 4C**). For both AOA and AOB the abundance of *amoA* was relatively uniform throughout the experiment, displaying no temporal changes in the genetic capacity for ammonia oxidation for either domain of ammonia oxidizers (**Figures 4A,C**). By contrast, *amoA* gene expression for both AOA (**Figure 4B**) and AOB (**Figure 4D**) varied much more dramatically than in the DNA, with AOA peaking on day 14, and AOB peaking on day 22. Rates of AOB *amoA* gene expression were below the limits of detection, except on Days 14 and 22. Both the *nirS* (**Figure 4E**) and *nirK* (Figure S1) genes, which encode the two functionally redundant dissimilatory nitrite reductases in the denitrification pathway, when quantified in the DNA, were also relatively uniform. All mesocosms contained roughly similar numbers of copies of the *nirS* gene (10^8–10^9 copies per gram of sediment) and abundances did not change systematically through the experiment (**Figure 4E**). Similarly, there were no differences among the mesocosms with regard to the abundance of the *nirK* gene (Figure S1), though it was present only in $\sim 10^5$ copies per gram of sediment, 3–4 orders of magnitude less abundant than the *nirS* gene. There were, however, widely different degrees of *nirS* gene expression (**Figure 4F**) among the different mesocosms with a low of 1.9×10^6 copies per gram sediment in the cDNA of mesocosm #2 to a high of 1.4×10^9 copies per gram of sediment in mesocosm #3. We were unable to amplify *nirK* from the cDNA, suggesting minimal expression of the *nirK* gene during this experiment.

Normalizing gene expression to the total gene abundance present in DNA yielded trends that closely tracked rates of ammonia oxidation (**Figure 5**, left panels) and that occasionally, though not typically, tracked rates of denitrification (**Figure 5**, right panels). In all of the mesocosms, NH_4^+ concentrations peaked within the first 10 days of the experiment. After a lag of approximately a week, there was a simultaneous peak in both ammonia oxidation rate and in the ratio of AOA *amoA* cDNA:DNA. NH_4^+ concentrations were essentially depleted by the time both rates and normalized gene expression values peaked. AOB *amoA* expression (and thus the cDNA:DNA ratio) was high only on day 22, well after the decline of the peak in ammonium concentration. The trend in normalized *nirS* gene expression occasionally mirrored denitrification rates (e.g., **Figure 5A**), but was considerably offset from maximal rates in most mesocosms.

We assessed whether the normalized gene expression of ammonia oxidizers and denitrifiers, calculated as the ratio of cDNA to DNA for AOA *amoA* and *nirS*, was predictive of the modeled rates of these processes by linear regression analysis (**Figure 6**). Rates of ammonia oxidation did increase linearly as a function of normalized gene expression (**Figure 6A**) with a moderate coefficient of determination. There was no statistically significant relationship between normalized gene expression and rates of denitrification.

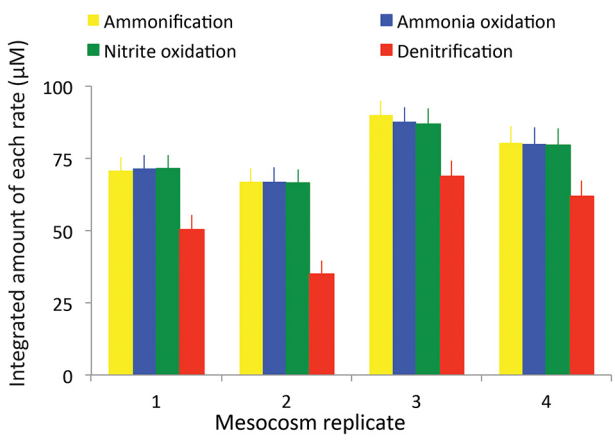

FIGURE 3 | Total integrated rates of ammonification, ammonia oxidation, nitrite oxidation, and denitrification in each mesocosm.

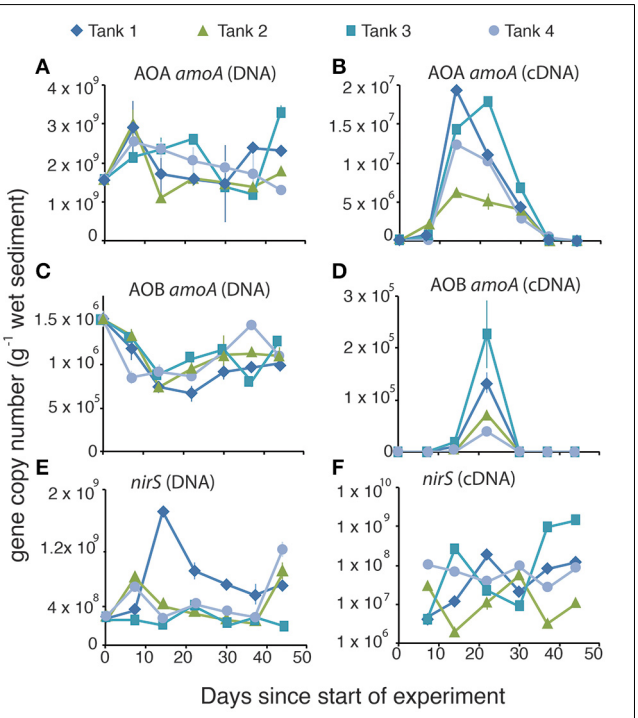

FIGURE 4 | Gene abundance (A,C,E) and gene expression (B,D,F) for ammonia oxidizing archaeal *amoA* (A,B), ammonia oxidizing bacterial *amoA* (C,D), and *nirS* denitrifiers (E,F) during the time course of the experiment.

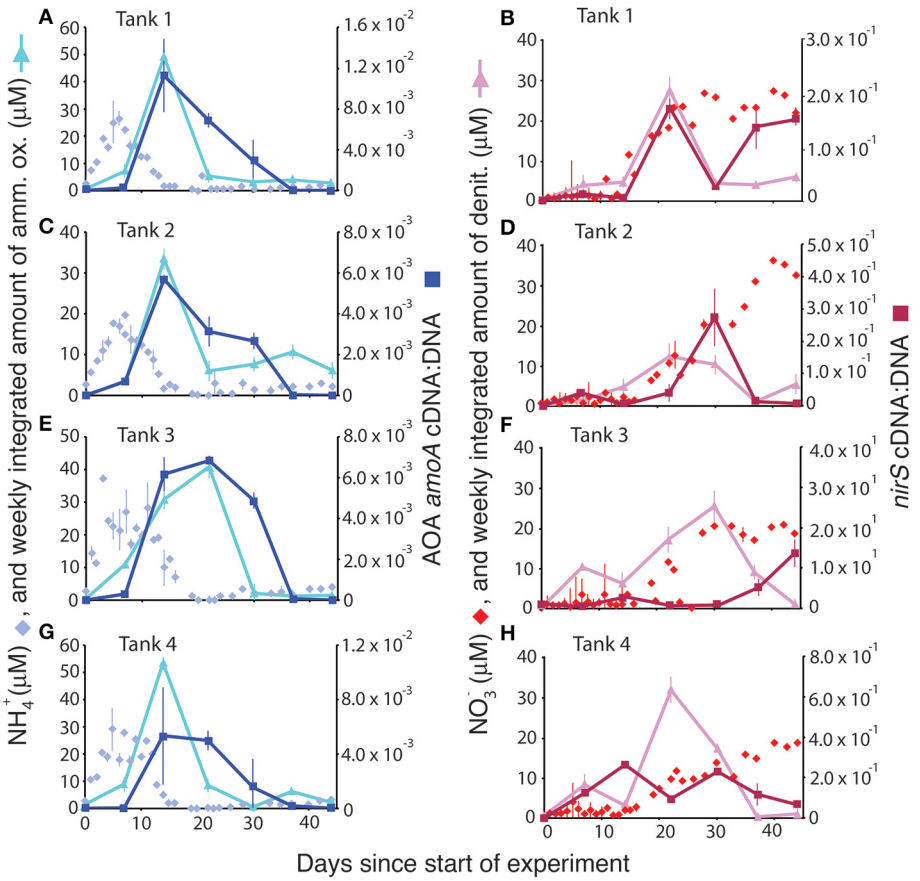

FIGURE 5 | Comparison of ammonium concentrations (μM) and ammonia oxidation rates (A,C,E,G) and nitrate concentrations (μM) and denitrification rates (B,D,F,H) with the normalized gene expression for ammonia oxidation (via AOA *amoA* cDNA:DNA) and denitrification (*nirS* cDNA:DNA).

DISCUSSION

Our objective was to induce a series of biogeochemical reactions that mimic the nitrogen remineralization sequence and to determine whether changes in geochemistry would be mirrored by changes in the expression of associated genes. The ultimate goal was to determine quantifiable relationships between functional gene abundance and geochemical change to help inform geochemical models (Reed et al., 2014). The nitrogen cycle, however, is particularly complicated to model because of the numerous functional genes involved and because different taxonomic groups can dominate in different environments. For example, research in the Gulf of California showed that ammonia oxidizing archaeal (AOA) but not bacterial (AOB) gene copy number tracked ammonia oxidation rates quite closely, suggesting that the relationship between gene expression and ecosystem function is quantifiable, and dominated by AOA (Beman et al., 2008). However, in agricultural soils Jia and Conrad (2009) show that changes in ammonia oxidation rates, upon addition of NH_4^+, co-occurred with changes in abundance of AOB gene copy number but not AOA copy number, despite the fact that AOA were numerically much more abundant. More data on what functional genes are abundant and active under what environmental conditions are needed to better constrain geochemical models.

We hypothesized that rates of nitrification, which is assumed to be largely an obligate metabolism, would roughly track with changes in total abundance of the *amoA* gene. In general, the data confirmed this hypothesis. There was a significant linear relationship between modeled rates of ammonia oxidation and the normalized expression of the AOA *amoA* gene (**Figure 6A**). Interestingly, despite the largely obligate nature of the pathway, the abundance of *amoA* in the DNA of our samples, while variable, did not systematically change throughout the experiment. It is possible that some AOA in the sediments use alternative metabolisms that do not depend on *amoA* gene expression (Mußmann et al., 2011), which would further obscure the relationship between the quantity of *amoA* in DNA and the rates of ammonia oxidation. There was, however, a distinct pattern in the expression of the AOA *amoA* gene, with peaks in expression occurring about 2 weeks into the experiment. Gene expression of AOB *amoA* showed a similar sharp peak shortly after the peak in abundance of AOA *amoA* gene expression but the AOB transcripts were at least three orders of magnitude less abundant than the AOA transcripts. These results indicate that more emphasis needs to be placed on analysis of gene expression, rather than abundance, as inactive cells in the environment could obscure the linkage between gene abundance and ecosystem function.

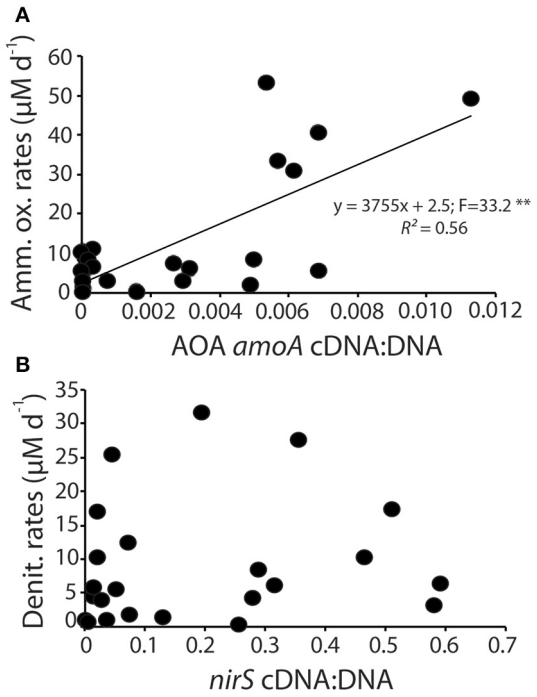

FIGURE 6 | Linear regression analysis of the normalized gene expression for AOA *amoA* compared to ammonia oxidation rates (A) and normalized *nirS* gene expression and denitrification rates (B). (** $p < 0.01$).

These results highlight the importance of AOA in the nitrogen cycling of estuarine sediments, as has been previously demonstrated (Beman and Francis, 2006; Caffrey et al., 2007; Bernhard et al., 2010). Although mesocosm experiments such as these cannot be considered analogs for *in situ* processes, the results do suggest that it is primarily the AOA that are carrying out ammonia oxidation in these experiments. AOA in the initial (T0) sediments were three orders of magnitude more abundant than AOB (**Figures 4A,C**), indicating that the estuarine conditions at the time of collection strongly favored AOA. The numbers of AOA and AOB stayed consistent throughout the experiment, but the AOA gene expression peaked at much higher numbers and more quickly, than AOB gene expression when a source of mineralized NH_4^+ became available. AOB, by contrast, appear to only increase expression of their *amoA* gene after the AOA *amoA* expression decreased. It is worth noting, however, that although AOB *amoA* gene expression was much lower than AOA *amoA* gene expression, the normalized gene expression (cDNA:DNA) of AOB was approximately 0.1, compared to 0.01 for AOA, suggesting that AOB may play a disproportionately large role, relative to their total abundance, in the observed ammonia oxidation rates.

In contrast to the ammonia oxidizers, we hypothesized that the facultative denitrification pathway would be more difficult to disentangle. Since denitrifying bacteria are capable of utilizing a number of different electron acceptors, we expected that the absolute abundance of *nirS* in sediments would not track rates of denitrification, though we did expect to see a greater correlation between denitrification rates and the number or *nirS* mRNA transcripts in the sediments. In general the half-life of mRNA is relatively short (Selinger et al., 2003; Frias-Lopez et al., 2008; Steglich et al., 2010; Moran et al., 2013), and in experimental studies of the denitrifier *Pseudomonas stutzeri* the half life of *nirS* was approximately 13 min (Härtig and Zumft, 1999). The operon, however, was shown to operate nearly continuously through the 3 h experiment until resources were depleted and nitrite reduction ceased (Härtig and Zumft, 1999). Based on these experimental results we expected to see a stronger correlation between *nirS* gene expression and rates of denitrification. Our data, however, indicate that there was no consistent relationship between the normalized gene expression of the *nirS* gene and modeled rates of denitrification (**Figure 6B**).

Since *nirS* is one of two functionally redundant nitrite reductases encoded by prokaryotes, we hypothesized that the relationship between *nirS* and denitrification rates could be obscured by nitrogen loss by organisms containing the other nitrite reductase, *nirK*. We quantified *nirK* gene abundance in the mesocosm sediments and determined that the abundance was at least three orders of magnitude lower than the abundance of *nirS* (Figure S1). Further, we were unable to amplify *nirK* from the cDNA. We thus concluded that the abundance and activity of *nirK* denitrifiers is not likely sufficient to obscure the relationship between gene expression and modeled rates of denitrification. Nitrogen loss through the anammox reaction is another possible mechanism that could obscure the relationship between denitrification rates and *nirS* and *nirK* gene abundance. In general anammox rates are low in carbon rich environments such as are found in coastal sediments (Rich et al., 2008; Koop Jakobsen and Giblin, 2009). Furthermore, if anammox were an important process in the mesocosms it would also obscure the relationship between NH_4^+ oxidation rates and *amoA* gene expression because there would be an additional unaccounted for loss of NH_4^+. That we see a relatively tight relationship between NH_4^+ and *amoA* gene expression (**Figure 6A**), we can conclude that anammox rates are not sufficiently high to account for the lack of a relationship between *nirS* gene expression and denitrification rates. Instead we can only conclude that the facultative nature of denitrifying bacteria makes it challenging to directly link *nirS* gene expression with rates of denitrification.

Measureable accumulation of NO_2^- in coastal waters is rare, although this may in part be a methodological artifact, as data are most often recorded as NO_3^-+NO_2^-. Differences in the reaction rates between ammonia oxidation and nitrite oxidation, however, can lead to transitory accumulation of NO_2^-. Culture experiments with *Nitrobacter*, a key nitrite oxidizer, demonstrated that high concentrations of NH_4^+ in the culture inhibited nitrite oxidation and resulted in the accumulation of NO_2^- (Anthonisen et al., 1976). Additional modeling work indicated that the threshold concentrations for the inhibition of nitrite oxidation by free ammonia and free nitrous acid were much lower than for ammonia oxidation (Park and Bae, 2009). In our study, all four mesocosm tanks demonstrated a sharp increase in NO_2^- concentrations (**Figure 1**), and accumulation of NO_2^- in the overlying water began during times of high NH_4^+ concentrations. NO_2^- continued to accumulate in the mesocosms

until ammonia oxidizers were able to reduce available NH_4^+ concentrations sufficiently that inhibition of nitrite oxidizers was released.

The inhibition of nitrite oxidation by initially high NH_4^+ concentrations provides one plausible explanation for the overall reduced NO_3^- removal capacity that was evident in the mesocosms (**Figure 3**). Although nearly 100% of the ammonia generated from ammonification was oxidized to NO_2^- and then to NO_3^-, only between 52 and 76% of the oxidized NO_3^- was ultimately denitrified (**Figure 7**) and, unlike NH_4^+ and NO_2^-, NO_3^- concentrations remained high at the end of the experiment. Rates of NO_3^- removal via denitrification can be limited by, among other things, the supply of NO_3^- or labile organic carbon. As there was no initial NO_3^- in the overlying water, the only sources of NO_3^- to promote denitrification are from oxidation of accumulated NO_2^- that then diffuses into the anoxic sediments, or from direct coupling of nitrification and denitrification. The accumulation of NH_4^+ in the overlying water and the inhibition of nitrite oxidation suggests that, initially, denitrification was limited by NO_3^- supply. Further evidence for this limitation comes from the close coupling in time between rates of nitrite oxidation and rates of denitrification in the first weeks of the experiment (**Figure 2**).

Ultimately, however, it is likely carbon limitation that prevents complete denitrification in the mesocosms, as eventually complete oxidation of NO_2^- to NO_3^- did occur and NO_3^- concentrations persisted in the overlying waters through the end of the experiment (**Figure 1**). Carbon limitation has been shown to limit denitrification in coastal sediments both in mesocosms (Babbin and Ward, 2013) and in biogeochemical models (Algar and Vallino, 2014), and is likely to be the ultimate factor limiting complete denitrification in this system. Regardless of whether it is carbon or NO_3^- limitation, the limitation was ultimately observed at the genetic level. Although there was no direct relationship between denitrification rate and *nirS* gene abundance (**Figure 6**), when *nirS* gene expression was averaged over the time course of the experiment (**Figure 7**), the mean abundance of transcripts mirrored the differences in total NO_3^- removal capacity, such that the mesocosm with the lowest NO_3^- removal capacity also had the lowest average expression of the *nirS* gene.

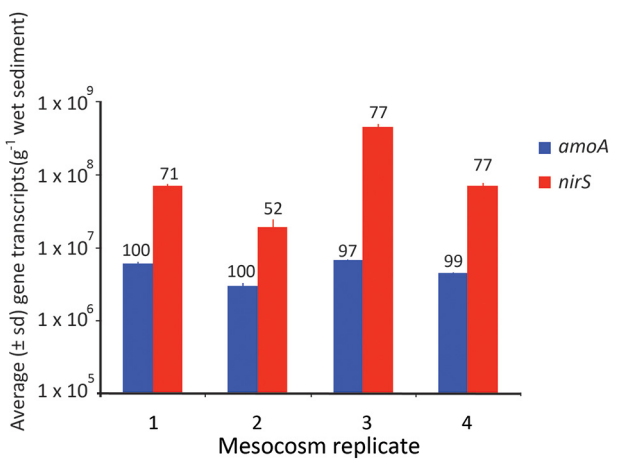

FIGURE 7 | Average (± SD) number of gene transcripts found in each mesocosm for the *amoA* and *nirS* gene. The numbers above each bar refer to the % completion of the process facilitated by that gene.

Although it is difficult to extrapolate from mesocosm experiments to rates and processes in coastal sediments more broadly, these experiments bring us one step closer to understanding environmental microbial processes than experiments done solely with cultured organisms. The four mesocosms examined here replicated fairly well, with each tank demonstrating a classic regeneration sequence. The variations in the timing and magnitude of fluxes in each of the mesocosms, however, illustrate the small-scale heterogeneity that exists in coastal marine sediments. These experiments allowed us to establish a quantitative relationship between microbial community structure and ecosystem function for ammonia oxidizing archaea, but not for the much more genetically diverse denitrifiers (Bowen et al., 2013). Additional work is needed to see if the AOA/nitrification relationship is generalizable to different systems, but it is a first step in providing quantitative data on the role that these microbes play in coastal sediments and can form a basis for incorporating microbial ecology into geochemical models.

AUTHOR CONTRIBUTIONS

Jennifer L. Bowen and Bess B. Ward designed the research, Jennifer L. Bowen collected samples, set up and monitored the mesocosms, and performed all nutrient analyses, Jennifer L. Bowen and Patrick J. Kearns did the DNA/mRNA extraction and qPCR, and analyzed the data. Andrew R. Babbin designed and implemented the model. Jennifer L. Bowen, Bess B. Ward, Andrew R. Babbin, and Patrick J. Kearns wrote the paper.

ACKNOWLEDGMENTS

Salary support for Jennifer L. Bowen was provided by a fellowship from Princeton University's Council on Science and Technology and from startup funds from the University of Massachusetts Boston. Andrew R. Babbin was funded by a National Defense Science and Engineering Graduate Fellowship (32 CFR 168a). Additional support for this work came from multiple NSF grants to Bess B. Ward, including DEB-1019624 to Bess B. Ward and Jennifer L. Bowen. Joe Degiorgis assisted with sample collection, Nicholas Bouskill and Punyasloke Bhadury assisted with daily sampling of the mesocosms. Three reviewers greatly improved the quality of this manuscript.

SUPPLEMENTARY MATERIAL

The Supplementary Material for this article can be found online at: http://www.frontiersin.org/journal/10.3389/fmicb.2014.00429/abstract

REFERENCES

Abell, G. C. J., Revill, A. T., Smith, C., Bissett, A. P., Volkman, J. K., and Robert, S. S. (2010). Archaeal ammonia oxidizers and *nirS*-type denitrifiers dominate sediment nitrifying and denitrifying populations in a subtropical macrotidal estuary. *ISME J.* 4, 286–300. doi: 10.1038/ismej.2009.105

Algar, C. K., and Vallino, J. J. (2014). Predicting microbial nitrate reduction pathways in coastal sediments. *Aquat. Microb. Ecol.* 71, 223–238. doi: 10.3354/ame01678

An, S., and Gardner, W. S. (2002). Dissimilatory nitrate reduction to ammonium (DNRA) as a nitrogen link, versus denitrification as a sink in a shallow estuary (Laguna Madre/Baffin Bay, Texas). *Mar. Ecol. Prog. Ser.* 237, 41–50. doi: 10.3354/meps237041

An, S., and Joye, S. B. (2001). Enhancement of coupled nitrification-denitrification by benthic photosynthesis in shallow estuarine sediments. *Limnol. Oceanogr.* 46, 62–74. doi: 10.4319/lo.2001.46.1.0062

Anthonisen, A. C., Loehr, R. C., Prakasam, T. B. S., and Srinath, E. G. (1976). inhibition of nitrification by ammonia and nitrous-acid. *J. Water Pollut. Control Fed.* 5, 835–852.

Babbin, A. R., and Ward, B. B. (2013). Controls on nitrogen loss processes in chesapeake bay sediments. *Environ. Sci. Technol.* 47, 4189–4196. doi: 10.1021/es304842r

Beman, J. M., and Francis, C. A. (2006). Diversity of ammonia-oxidizing archaea and bacteria in the sediments of a hypernutrified subtropical estuary: bahía del Tóbari, Mexico. *Appl. Environ. Microbiol.* 72, 7767–7777. doi: 10.1128/AEM.00946-06

Beman, J. M., Popp, B. N., and Francis, C. A. (2008). Molecular and biogeochemical evidence for ammonia oxidation by marine Crenarchaeota in the Gulf of California. *ISME J.* 2, 429–441. doi: 10.1038/ismej.2007.118

Bernhard, A. E., Landry, Z. C., Blevins, A., la Torre de, J. R., Giblin, A. E., and Stahl, D. A. (2010). Abundance of ammonia-oxidizing archaea and bacteria along an estuarine salinity gradient in relation to potential nitrification rates. *Appl. Environ. Microbiol.* 76, 1285–1289. doi: 10.1128/AEM.02018-09

Bernhard, A. E., Tucker, J., Giblin, A. E., and Stahl, D. A. (2007). Functionally distinct communities of ammonia-oxidizing bacteria along an estuarine salinity gradient. *Environ. Microbiol.* 9, 1439–1447. doi: 10.1111/j.1462-2920.2007.01260.x

Bowen, J. L., Byrnes, J. E. K., Weisman, D., and Colaneri, C. (2013). Functional gene pyrosequencing and network analysis: an approach to examine the response of denitrifying bacteria to increased nitrogen supply in salt marsh sediments. *Front. Microbiol.* 4:342. doi: 10.3389/fmicb.2013.00342

Bowen, J. L., and Valiela, I. (2001). The ecological effects of urbanization of coastal watersheds: historical increases in nitrogen loads and eutrophication of Waquoit Bay estuaries. *Can. J. Fish. Aquat. Sci.* 58, 1489–1500. doi: 10.1139/f01-094

Braker, G., Fesefeldt, A., and Witzel, K.-P. (1998). Development of PCR primer systems for amplification of nitrite reductase genes (*nirK* and *nirS*) to detect denitrifying bacteria in environmental samples. *Appl. Environ. Microbiol.* 64, 3769–3775.

Braman, R. S., and Hendrix, S. A. (1989). Nanogram nitrite and nitrate determination in environmental and biological-materials by vanadium- (III) reduction with chemi-luminescence detection. *Anal. Chem.* 61, 2715-2718. doi: 10.1021/ac00199a007

Burdige, D. J. (2012). "Estuarine and coastal sediments – coupled biogeochemical cycling," in *Treatise on Estuarine and Coastal Science*, eds E. Wolanski and D. McLusky (Waltham, MA: Academic Press), 279–316.

Burgin, A. J., and Hamilton, S. K. (2007). Have we overemphasized the role of denitrification in aquatic ecosystems? A review of nitrate removal pathways. *Front. Ecol. Environ.* 5:89–96. doi: 10.1890/1540-9295(2007)5[89:HWOTRO]2.0.CO;2

Caffrey, J. M., Bano, N., Kalanetra, K., and Hollibaugh, J. T. (2007). Ammonia oxidation and ammonia-oxidizing bacteria and archaea from estuaries with differing histories of hypoxia. *ISME J.* 1, 660–662. doi: 10.1038/ismej.2007.79

Campbell, B. J., and Kirchman, D. L. (2012). Bacterial diversity, community structure and potential growth rates along an estuarine salinity gradient. *ISME J.* 7, 210–220. doi: 10.1038/ismej.2012.93

Campbell, B. J., Yu, L., Heidelberg, J. F., and Kirchman, D. L. (2011). Activity of abundant and rare bacteria in a coastal ocean. *Proc. Natl. Acad. Sci. U.S.A.* 108, 12776–12781. doi: 10.1073/pnas.1101405108

Cloern, J. E. (2001). Our evolving conceptual model of the coastal eutrophication problem. *Mar. Ecol. Prog. Ser.* 210, 223–253. doi: 10.3354/meps210223

Dalsgaard, T., Thamdrup, B., and Canfield, D. E. (2005). Anaerobic ammonium oxidation (anammox) in the marine environment. *Res. Microbiol.* 156, 457–464. doi: 10.1016/j.resmic.2005.01.011

Diaz, R. J., and Rosenberg, R. (2008). Spreading dead zones and consequences for marine ecosystems. *Science* 321, 926–929. doi: 10.1126/science.1156401

Francis, C. A., Roberts, K. J., Beman, J. M., Santoro, A. E., and Oakley, B. B. (2005). Ubiquity and diversity of ammonia-oxidizing archaea in water columns and sediments of the ocean. *Proc. Natl. Acad. Sci. U.S.A.* 102, 14683–14688. doi: 10.1073/pnas.0506625102

Frias-Lopez, J., Shi, Y., Tyson, G. W., Coleman, M. L., Schuster, S. C., Chisholm, S. W., et al. (2008). Microbial community gene expression in ocean surface waters. *Proc. Natl. Acad. Sci. U.S.A.* 105, 3805–3810. doi: 10.1073/pnas.0708897105

Galloway, J. N., Aber, J. D., Erisman, J. W., Seitzinger, S. P., Howarth, R. W., Cowling, E. B., et al. (2003). The nitrogen cascade. *Bioscience* 53, 341–356. doi: 10.1641/0006-3568(2003)053[0341:TNC]2.0.CO;2

Garside, C. (1982). A chemi-luminescent technique for the determination of nanomolar concentrations of nitrate and nitrite in seawater. *Mar. Chem.* 11, 159-167. doi: 10.1016/0304-4203(82)90039-1

Giblin, A. E., Tobias, C. R., Song, B., Weston, N., Banta, G. T., and Rivera-Monroy, V. H. (2013). The importance of dissimilatory nitrate reduction to ammonium (DNRA) in the nitrogen cycle of coastal ecosystems. *Oceanography* 26, 124–131. doi: 10.5670/oceanog.2013.54

Härtig, E., and Zumft, W. G. (1999). Kinetics of *nirS* expression (cytochrome cd_1 nitrite reductase)in *Pseudomonas stutzeri* during the transition from aerobic respiration to denitrification: evidence for a denitrification-specific nitrate-and nitrite-responsive regulatory system. *J. Bacteriol.* 181, 161–166.

Howarth, R., Chan, F., Conley, D. J., Garnier, J., Doney, S. C., Marino, R., et al. (2011). Coupled biogeochemical cycles: eutrophication and hypoxia in temperate estuaries and coastal marine ecosystems. *Front. Ecol. Environ.* 9:8. doi: 10.1890/100008

Jenkins, M. C., and Kemp, W. M. (1984). The coupling of nitrification and denitrification in two estuarine sediments. *Limnol. Oceanogr.* 29, 609–619. doi: 10.4319/lo.1984.29.3.0609

Jia, Z., and Conrad, R. (2009). *Bacteria* rather than *Archaea* dominate microbial ammonia oxidation in an agricultural soil. *Environ. Microbiol.* 11, 1658–1671. doi: 10.1111/j.1462-2920.2009.01891.x

Joye, S. B., and Hollibaugh, J. T. (1995). Influence of sulfide inhibtion of nitrification on nitrogen regeneration in sediments. *Science* 270, 623–625. doi: 10.1126/science.270.5236.623

Kartal, B., Maalcke, W. J., de Almeida, N. M., Cirpus, I., Gloerich, J., Geerts, W., et al. (2011). Molecular mechanism of anaerobic ammonium oxidation. *Nature* 479, 127–132. doi: 10.1038/nature10453

Knight, R., Jansson, J., Field, D., Fierer, N., Desai, N., Fuhrman, J. A., et al. (2012). Unlocking the potential of metagenomics through replicated experimental design. *Nat. Biotechnol.* 30, 513–520. doi: 10.1038/nbt.2235

Koop Jakobsen, K., and Giblin, A. E. (2009). Anammox in tidal marsh sediments: the role of salinity, nitrogen loading, and marsh vegetation. *Estuar. Coasts* 32, 238–245. doi: 10.1007/s12237-008-9131-y

Koroleff, F. (1983). "Determination of nutrients," in *Methods of Seawater Analysis*, eds K. Grasshoff, M. Ehrhardt, and K. Kremling (Weinheim: Verlag Chemie), 162–173.

Laverock, B., Tait, K., Gilbert, J. A., Osborn, A. M., and Widdicombe, S. (2013). Impacts of bioturbation on temporal variation in bacterial and archaeal nitrogen-cycling gene abundance in coastal sediments. *Environ. Microbiol. Rep.* 6, 113–121. doi: 10.1111/1758-2229.12115

Lawson, C. L., and Hanson, R. J. (1974). *Solving Least Squares Problems*. Englewood Cliffs, NJ: Prentice Hall.

Morales, S. E., and Holben, W. E. (2010). Linking bacterial identities and ecosystem processes: can "omic" analyses be more than the sum of their parts? *FEMS Microbiol. Ecol.* 75, 2–16. doi: 10.1111/j.1574-6941.2010.00938.x

Moran, M. A., Satinksy, B., Gifford, S. M., Luo, H., Rivers, A., Chan, L.-K., et al. (2013). Sizing up metatranscriptomics. *ISME J.* 7, 237–243. doi: 10.1038/ismej.2012.94

Mosier, A., and Francis, C. (2008). Relative abundance and diversity of ammonia-oxidizing archaea and bacteria in the San Francisco Bay estuary. *Environ. Microbiol.* 10, 3002–3016. doi: 10.1111/j.1462-2920.2008.01764.x

Mußmann, M., Brito, I., Pitcher, A., Sinninghe Damasté, J. S., Hatzenpichler, R., Richter, A., et al. (2011). Thaumarchaeotes abundant in refinery nitrifying sludges express *amoA* but are not obligate autotrophic ammonia oxidizers. *Proc. Natl. Acad. Sci. U.S.A.* 108, 16771–16776. doi: 10.1073/pnas.1106427108

Nicholls, J. C., and Trimmer, M. (2009). Widespread occurrence of the anammox reaction in estuarine sediments. *Aquat. Microb. Ecol.* 55, 105–113. doi: 10.3354/ame01285

Nogales, B., Timmis, K. N., and Nedwell, D. B. (2002). Detection and diversity of expressed denitrification genes in estuarine sediments after reverse transcription-PCR amplification from mRNA. *Appl. Environ. Microbiol.* 35, 275–298. doi: 10.1128/AEM.68.10.5017-5025.2002

Ottesen, E. A., Young, C. R., Eppley, J. M., Ryan, J. P., Chavez, F. P., Scholin, C. A., et al. (2013). Pattern and synchrony of gene expression among sympatric

marine microbial populations. *Proc. Natl. Acad. Sci.U.S.A.* 110, E488–E497. doi: 10.1073/pnas.1222099110

Park, S., and Bae, W. (2009). Modeling kinetics of ammonia oxidation under simultaneious inhibition by free ammonia and free nitrous acid. *Process Biochem.* 6, 631–640. doi: 10.1016/j.procbio.2009.02.002

Reed, D. C., Algar, C. K., Huber, J. A., and Dick, G. J. (2014). Gene-centric approach to integrating environmental genomics and biogeochemical models. *Proc. Natl. Acad. Sci. U.S.A.* 111, 1879–1884. doi: 10.1073/pnas.1313713111

Reed, H. E., and Martiny, J. B. (2012). Microbial composition affects the functioning of estuarine sediments. *ISME J.* 7, 868–879. doi: 10.1038/ismej.2012.154

Rich, J. J., Dale, O. R., Song, B., and Ward, B. B. (2008). Anaerobic ammonium oxidation (Anammox) in Chesapeake Bay sediments. *Microb. Ecol.* 55, 311–320. doi: 10.1007/s00248-007-9277-3

Risgaard-Petersen, N. (2003). Coupled nitrification-denitrification in autotrophic and heterotrophic estuarine sediments: on the influence of benthic microalgae. *Limnol. Oceanogr.* 48, 93–105. doi: 10.4319/lo.2003.48.1.0093

Rotthauwe, J. H., Witzel, K.-P., and Liesack, W. (1997). The ammonia monooxygenase structural gene *amoA* as a functional marker: molecular fine-scale analysis of natural ammonia-oxidizing populations. *Appl. Environ. Microbiol.* 63, 4704–4712.

Selinger, D. W., Saxena, R. M., Cheung, K. J., Church, G. M., and Rosenow, C. (2003). Global RNA half-life analysis in *Escherichia coli* reveals positional patters of transcript degradation. *Genome Res.* 13, 216–223. doi: 10.1101/gr.912603

Smith, C. J., Nedwell, D. B., Dong, L. F., and Osborne, A. M. (2007). Diversity and abundance of nitrate reductase genes (*narG* and *napA*), nitrite reductase genes (*nirS* and *nrfA*), and their transcripts in estuarine sediments. *Appl. Environ. Microbiol.* 73, 3612–3622. doi: 10.1128/AEM.02894-06

Smith, V. H. (2003). Eutrophication of freshwater and coastal marine ecosystems a global problem. *Environ. Sci. Pollut. Res.* 10, 126–139. doi: 10.1065/espr2002.12.142

Steglich, C., Lindell, D., Futschik, M., Rector, T., Steen, R., and Chisholm, S. W. (2010). Short RNA half-lives in the slow-growing marine cyanobacterium *Prochlorococcus*. *Genome Biol.* 11, R54. doi: 10.1186/gb-2010-11-5-r54

Strickland, J. D. H., and Parsons, T. R. (1972). *A Practical Handbook of Seawater Analysis, 2nd Edn*, Ottawa: Fisheries Research Board of Canada.

Treseder, K. K., Balser, T. C., Bradford, M. A., Brodie, E. L., Dubinsky, E. A., Eviner, V. T., et al. (2011). Integrating microbial ecology into ecosystem models: challenges and priorities. *Biogeochemistry* 109, 7–18. doi: 10.1007/s10533-011-9636-5

Valiela, I., Foreman, K., LaMontagne, M., Hersh, D., Costa, J., Peckol, P., et al. (1992). Couplings of watersheds nad coastal waters -sources and consequecnes of nutrient enrichment in Waquoit Bay, Massachusetts. *Estuaries* 15, 443–457. doi: 10.2307/1352389

van de Leemput, I. A., Veraart, A. J., Dakos, V., de Klein, J. J. M., Strous, M., and Scheffer, M. (2011). Predicting microbial nitrogen pathways from basic principles. *Environ. Microbiol.* 13, 1477–1487. doi: 10.1111/j.1462-2920.2011.02450.x

Zumft, W. (1997). Cell biology and molecular basis of denitrification. *Microbiol. Mol. Biol. Res.* 61, 533–615.

Conflict of Interest Statement: The authors declare that the research was conducted in the absence of any commercial or financial relationships that could be construed as a potential conflict of interest.

Received: 30 April 2014; accepted: 29 July 2014; published online: 21 August 2014.
*Citation: Bowen JL, Babbin AR, Kearns PJ and Ward BB (2014) Connecting the dots: linking nitrogen cycle gene expression to nitrogen fluxes in marine sediment mesocosms. Front. Microbiol. **5**:429. doi: 10.3389/fmicb.2014.00429*
This article was submitted to Aquatic Microbiology, a section of the journal Frontiers in Microbiology.

frontiers in MICROBIOLOGY

ORIGINAL RESEARCH ARTICLE
published: 03 September 2014
doi: 10.3389/fmicb.2014.00460

Linking DNRA community structure and activity in a shallow lagoonal estuarine system

Bongkeun Song[1]*, Jessica A. Lisa[1] and Craig R. Tobias[2]

[1] Department of Biological Sciences, Virginia Institute of Marine Science, College of William & Mary, Gloucester Point, VA, USA
[2] Department of Marine Science, University of Connecticut, Groton, CT, USA

Edited by:
Anne Bernhard, Connecticut College, USA

Reviewed by:
Barbara J. Campbell, Clemson University, USA
Alyson E. Santoro, University of Maryland Center for Environmental Science, USA

***Correspondence:**
Bongkeun Song, Department of Biological Sciences, Virginia Institute of Marine Science, College of William & Mary, PO Box 1346, Gloucester Point, VA 23062, USA
e-mail: songb@vims.edu

Dissimilatory nitrate reduction to ammonium (DNRA) and denitrification are two nitrate respiration pathways in the microbial nitrogen cycle. Diversity and abundance of denitrifying bacteria have been extensively examined in various ecosystems. However, studies on DNRA bacterial diversity are limited, and the linkage between the structure and activity of DNRA communities has yet to be discovered. We examined the composition, diversity, abundance, and activities of DNRA communities at five sites along a salinity gradient in the New River Estuary, North Carolina, USA, a shallow temporal/lagoonal estuarine system. Sediment slurry incubation experiments with ^{15}N-nitrate were conducted to measure potential DNRA rates, while the abundance of DNRA communities was calculated using quantitative PCR of *nrfA* genes encoding cytochrome C nitrite reductase, commonly found in DNRA bacteria. A pyrosequencing method targeting *nrfA* genes was developed using an Ion Torrent sequencer to examine the diversity and composition of DNRA communities within the estuarine sediment community. We found higher levels of *nrfA* gene abundance and DNRA activities in sediments with higher percent organic content. Pyrosequencing analysis of *nrfA* genes revealed spatial variation of DNRA communities along the salinity gradient of the New River Estuary. Percent abundance of dominant populations was found to have significant influence on overall activities of DNRA communities. Abundance of dominant DNRA bacteria and organic carbon availability are important regulators of DNRA activities in the eutrophic New River Estuary.

Keywords: DNRA, *nrfA*, qPCR, pyrosequencing, diversity

INTRODUCTION

Sedimentary nitrogen (N) cycling in rivers and estuaries is highly dependent on microbial processes. Nitrate can be dissimilated by denitrification, dissimilatory nitrate reduction to ammonium (DNRA) and anaerobic ammonium oxidation (anammox), depending on prevailing environmental conditions. Denitrification and anammox remove fixed nitrogen by producing dinitrogen (N_2) gas. In comparison, DNRA retains nitrogen within an ecosystem by recycling nitrate (NO_3^-) to ammonium (NH_4^+). Denitrification and DNRA both compete for NO_3^- as an electron acceptor and both processes generally rely on organic carbon and sulfide as the source of electrons in anoxic sediments.

DNRA has been found to be an important nitrogen cycling pathway in various aquatic ecosystems including estuaries (Kelly-Gerreyn et al., 2001; An and Gardner, 2002) and salt marshes (Tobias et al., 2001a; Koop-Jakobsen and Giblin, 2010). Geochemical and physical features such as high carbon to NO_3^- ratios, high levels of sulfide, elevated temperature and salinity provide favorable conditions to support DNRA over denitrification in estuarine and coastal sediments (An and Gardner, 2002; Giblin et al., 2010; Dong et al., 2011). However, abundance, composition, and diversity of DNRA communities have not been evaluated as microbial controls of DNRA in an ecosystem.

A diverse group of microorganisms has been shown to use DNRA as an anaerobic respiratory pathway (Simon and Klotz, 2013). DNRA is carried out by fermentative bacteria or by chemolithotrophic bacteria, which oxidize sulfide or other reduced inorganic substrates. The genes and enzymes involved in the DNRA pathway by fermentative bacteria are well characterized (Simon, 2002). However, little is known about chemolithotrophic bacterial DNRA (Giblin et al., 2013).

A pentaheme cytochrome C nitrite reductase (NrfA) is the central enzyme which catalyzes the reduction of nitrite (NO_2^-) to NH_4^+ (Einsle et al., 1999). The functional gene *nrfA* is present in diverse groups of bacteria including *Proteobacteria*, *Planctomycetes*, *Bacteroides*, and *Firmicutes* (Mohan et al., 2004). Some members of the *Epsilonproteobacteria*, such as *Campylobacter* spp. and *Nautilia profundicola*, are capable of DNRA in the absence of *nrfA* genes through the use of a putative reverse hydroxylamine:ubiquione reductase module pathway (Hanson et al., 2013). In addition, respiratory metabolism pathways in DNRA bacteria are diverse, including fermentation, denitrification, anammox, and sulfate reduction (Simon, 2002; Kartal et al., 2007). Due to this metabolic versatility, the diversity and abundance of DNRA bacteria might be greater than other N transforming organisms in sediments. However, DNRA

community composition in sediments has only been examined in two previous studies of the Colne River Estuary, based on *nrfA* gene analysis (Takeuchi, 2006; Smith et al., 2007). The limitation of studies examining the diversity and composition of DNRA bacteria is due to the lack of proper molecular methods capable of *nrfA* gene detection in environmental samples.

In order to gain a better understanding of the microbial and geochemical factors affecting DNRA processes, we examined sediment communities along the estuarine gradient of the New River Estuary, North Carolina, USA. The New River Estuary is a shallow and microtidal estuary with high anthropogenic N loading. The mesohaline regions of the estuary were found to have organic and sulfidic sediments, which may support DNRA (Anderson et al., 2013). In addition, Lisa et al. (2014) suggested a linkage between DNRA and anammox in sulfidogenic sediment communities of the estuary. These characteristics make the New River Estuary an ideal place to examine the importance of DNRA in the estuarine N cycle. Sediment slurry incubation experiments with $^{15}NO_3^-$ were conducted to measure potential DNRA rates, while abundance of DNRA communities was quantified using quantitative PCR (qPCR) of *nrfA* genes. A new method utilizing next generation sequencing techniques was developed to examine diversity and composition of *nrfA* genes in the sediment communities of the New River Estuary.

MATERIALS AND METHODS

SITE DESCRIPTION

The New River Estuary is located in southeastern North Carolina, USA. It is a shallow estuary (<5 m deep) with broad lagoons connected by narrow channels. The New River watershed encompasses a 1436 km^2 area and receives drainage from mostly forested and agricultural lands in the upper regions of the watershed, while the lower estuary is bordered by extensive intertidal wetlands (Burkholder et al., 1997; Mallin et al., 2005). Barrier islands located at the mouth of the estuary prevent tidal exchange, contributing to the 64 day mean flushing time in the estuary (Ensign et al., 2004). Within the watershed are large numbers of industrialized livestock facilities, the City of Jacksonville and the United States Marine Corps Base at Camp Lejeune. The estuary has been classified as "a nutrient sensitive" estuary since 1998, with nitrogen being the limiting nutrient (Mallin et al., 2000). It is a vulnerable ecosystem with various anthropogenic disturbances.

SEDIMENT SAMPLING

Sampling along nutrient and salinity gradients from the headwaters to the mouth of the estuary was conducted in April of 2010 (**Figure 1**). Five sites were examined and included an upstream site AA2 (34°76′N, 77°45′W), two mid-estuary sites JAX (34°73′N, 77°43′W), M47 (34°68′N, 77°39′W), and two lower estuary sites M31 (34°59′N, 77°40′W), M15 (34°55′N, 77°35′W). All samples and measurements were collected in the channel west of the indicated channel markers. Environmental parameters including sediment characteristics and geochemical features of porewater and bottom waters were previously reported by Lisa et al. (2014).

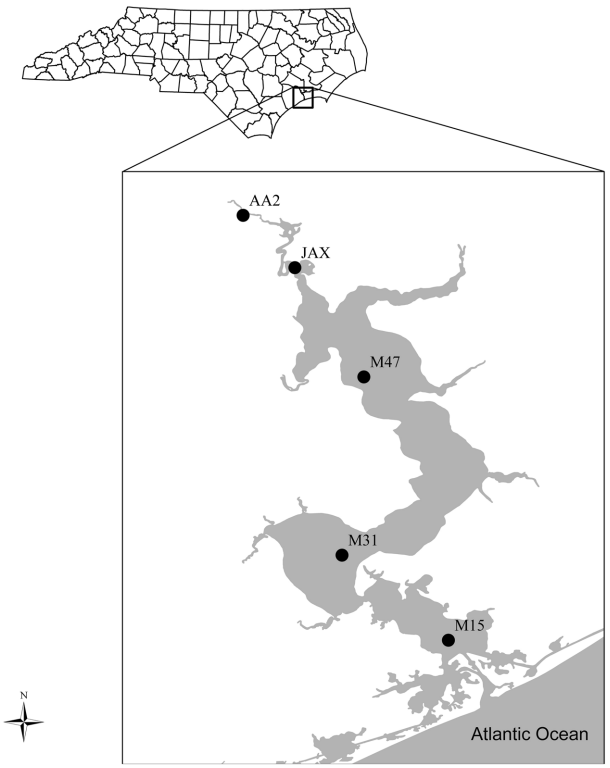

FIGURE 1 | Sampling Sites in the New River Estuary, NC, USA. Five sites include an upper estuary site (AA2), two mid-estuary sites (JAX and M47), and two lower estuary sites (M31 and M15).

^{15}N TRACER INCUBATIONS

Sediment slurry incubation experiments with ^{15}N tracer, using a modified method of Tobias et al. (2001b), were conducted to measure potential DNRA rates. Sediment slurries containing two grams of homogenized surface sediment (upper 3 cm) were incubated anaerobically in helium-purged Exetainer tubes, following the addition of $^{15}NO_3^-$ tracer (99at%, 200 nmoles). Time series samples were sacrificed by adding saturated $ZnCl_2$. DNRA was calculated from the amount of ^{15}N tracer measured in the extractable NH_4^+ pool. NH_4^+ was isolated from the slurry by alkaline acid trap diffusion (Holmes et al., 1998) following the addition of 7 ml of 40 ppt NaCl solution, 0.15 g MgO, and 3 μmoles of unlabeled NH_4^+ carrier. The mole fraction excess $^{15}NH_4^+$ (MF) was measured via continuous flow isotope ratio spectrometry using an elemental analyzer interface. The DNRA rate was calculated from:

$$DNRA = \frac{MF_{\,15NH4} \bullet [NH4]}{MF_{\,15NO3} \bullet t}$$

where *MF* is the ^{15}N mole fraction excess of either the extractable ammonium or the added nitrate tracer. The MF_{15NH4} is corrected for the mass of the carrier ammonium. The extractable ammonium concentration $[NH_4]$ was measured spectrophotometrically using the phenol-hypochlorite method on split sediment slurries, and "*t*" represents the incubation time.

DNA EXTRACTION AND QUANTITATIVE PCR OF *nrfA* GENES

Sediment DNA was extracted from homogenized sediments using PowerSoil DNA Kit (Mo-Bio Laboratories, Inc., Carlsbad, CA) following the manufacturer's protocol with the following modifications: wet sediment (0.6 g) was used for the extraction and Thermo Savant Fast Prep FP 120 Cell Disrupter (Qbiogene Inc. Carlsbad, CA) was used for cell disruption. qPCR assays of *nrfA* genes were carried out to quantify the abundance of DNRA bacteria in the sediment communities. qPCR reactions were carried out in a volume of 20 uL containing SYBR green using Go-Taq qPCR Master Mix (Promega Corporation, Madison, WI) with 10 ng of DNA and the primers nrfAF2aw (CARTGYCAYGTBGARTA) and nrfAR1 (TWNGGCATRTGRCARTC) (Mohan et al., 2004; Welsh et al., 2014). The primers target heme-binding motifs, which are conserved and diagnostic for the *nrfA* gene. Welsh et al. (2014) tested specificity of the primers with proteobacterial isolates and a soil sample. The expected size of the PCR product is 235–250 bp. PCR conditions were as follows: an initial cycle of 94°C for 10 min; 50 cycles of 94°C for 15 s, 52°C for 45 s, 72°C for 20 s, 80°C for 35 s (data acquisition step); and a dissociation step of 95°C for 15 s, 52°C for 1 min, 95°C for 15 s. Thermal cycling, fluorescent data collection, and data analysis was carried out using ABI Prism 7500 Real Time PCR System Sequence Detection System (Applied Biosystems, Carlsbad, CA).

In order to generate qPCR standards the *nrfA* gene fragment in *Escherichia coli* K-12 was amplified using the primers and PCR conditions described above. The PCR product was cloned using the pGEM-T Easy cloning kit (Promega, Madison, WI) following the manufacturer's instruction. Plasmid DNA was extracted from a culture of recombinant *E. coli* JM109 using the FastPlasmid Mini kit (5 PRIME, Gaithersburg, MD). The plasmid was linearized using the *EcoRI* restriction enzyme and purified using the Wizard SV Gel and PCR Clean-Up System (Promega, Madison, WI). The purified products were quantified using Qubit DNA quantitation assay (Life Technologies, Grand Island, NY) following the manufacturer's instructions. A ten-fold serial dilution of a known copy number of the purified plasmid was prepared for qPCR standards. The qPCR standard has 92.5% identity of DNA sequences with the *nrfA* gene of *Escherichia albertii* in **Figure 3**. qPCR efficiency and the detection limit were evaluated by treating qPCR standards as unknown samples. The qPCR efficiency was 98.9%, although the detection limit was 9×10^4 copies of *nrfA* genes. qPCR inhibition was not apparent based on an additional test using a mixture of qPCR standards and sediment DNA.

ION TORRENT PGM SEQUENCING OF *nrfA* GENES

Composition and diversity of *nrfA* genes in sediment samples were examined with a barcode pyrosequencing method using the Ion Torrent PGM sequencer. PCR was conducted in duplicate with each 20 μL sample reaction containing the nrfA2Faw and nrfAR1 primers modified to include 8-bp barcode (forward primers) (Hamady et al., 2008) and adapter sequences for the Ion Torrent PGM sequencer (Life Technologies, Grand Island, NY). The primer sequences used for pyrosequencing are listed in Supplementary Table 1. PCR reactions were carried out using Platinum PCR Supermix (Life Technologies, Grand Island, NY) with the following PCR cycle: an initial 5 min at 94°C, 40 cycles of 94°C for 30 s, 52°C for 45 s, and 72°C for 20 s, followed by 5 min at 72°C. PCR results, generating 290 base pair fragments, were checked by running an aliquot on a 2% agarose gel. Duplicate reactions were combined, and amplicons were purified using UltraClean GelSpin DNA Purification Kit (Mo-Bio, Carlsbad, CA). The concentration of purified PCR products was measured using a 2200 TapeStation instrument and D1K reagents (Agilent Technologies, Santa Clara, CA) following the manufacturer's instruction. Pyrosequencing was conducted using an Ion Torrent PGM sequencer with barcode samples pooled on 316 chips, following the Ion Torrent 400 bp sequencing kit protocol (Life Technologies, Grand Island, NY).

BIOINFORMATIC ANALYSIS OF *nrfA* SEQUENCES

The bioinformatic pipeline of *nrfA* gene pyrosequences is outlined in Supplementary Figure 1. The pipeline contains easy-to-use web based programs and computer based programs. The FastQ file was downloaded from the Torrent Server after primary base calling was conducted using Torrent Suite v3.0 software (Life Technologies). The RDP Pipeline Initial Process (https://pyro.cme.msu.edu/init/form.spr) was used to sort the *nrfA* sequences in 5 libraries based on the barcode sequences. Primer sequences were trimmed, and sequences shorter than 200 bp and lower than 25 quality score were removed. Acacia (Bragg et al., 2012) was used to de-noise the trimmed sequences, and a chimera check was performed using UCHIME in the FunGene Pipeline (http://fungene.cme.msu.edu/FunGenePipeline/chimera_check/form.spr) (Fish et al., 2013). The selected sequences were translated and compared to NrfA reference sequences using the FunGene Pipeline Frambot tool (http://fungene.cme.msu.edu/FunGenePipeline). A total of 383 sequences was used as reference NrfA sequences after trimming and dereplicating 1690 sequences available in the FunGene repository (http://fungene.cme.msu.edu). The Frambot translated sequences were visually inspected to detect and to remove frame-shift errors. PRINSEQ (http://edwards.sdsu.edu/cgi-bin/prinseq/prinseq.cgi) (Schmieder and Edwards, 2011) was used to rename each sequence ID corresponding to the sampling sites. Sequences with renamed IDs (valid sequences) were used to examine diversity of NrfA sequences and compare the composition of DNRA communities.

In order to reduce sequence redundancy in diversity computation, identical NrfA sequences were dereplicated using PRINSEQ (Schmieder and Edwards, 2011). Unique NrfA sequences in each sediment community were aligned by MUSCLE (Edgar, 2004) in MEGA 5.2 (Tamura et al., 2011). The Protdist program in Phylogeny Inference Package (PHYLIP) (Felsenstein, 1989) was used to generate a distance matrix of aligned NrfA sequences with Kimura's method. Rarefaction, richness estimates, and diversity indices were computed based on a distance matrix using DOTUR (Schloss and Handelsman, 2005). Pielou's evenness was calculated by dividing the Shannon diversity index (H) by the natural log (Ln) of total number of operational taxonomic units (OTUs) (Pielou, 1966). In order to select protein distance for OTU determination, a total of

123 NrfA reference sequences from 123 species and 82 genera were analyzed using DOTUR. A protein distance of 0.1 was found to be the sub-genus level cutoff, while a distance of 0.2 was at the genus level. The OTUs were determined based on 0.1 protein distance cutoff, which is approximately 90% amino acid sequence identity. OTUs, determined with 90% amino acid sequence identity, were used in other pyrosequencing analyses of functional genes involved in nitrogen cycling pathways (Mao et al., 2013, 2011; Pereira E Silva et al., 2013).

The composition of sedimentary DNRA communities at the five sites was compared using CD-HIT (Li and Godzik, 2006) by clustering valid NrfA sequences that shared more than 90% identities. For phylogenetic analysis, a representative OTU sequence from each cluster was aligned through MEGA 5.2 (Tamura et al., 2011) using MUSCLE (Edgar, 2004). Normalized weighted UniFrac (Lozupone et al., 2006) was conducted for PCoA analysis to compare differences among the five DNRA communities. The NrfA sequences, found in only one community, were used to compute percent abundance of endemic sequences and OTUs in each community. In addition, the OTUs containing more than 1% of total NrfA sequences in each community were defined as dominant OTUs (or sequences), and percent abundance of the dominant sequences were calculated. The representative sequences of dominant OTUs, along with the reference NrfA sequences, were also used for phylogenetic analysis. Bootstrap analysis of 1000 repetitions was used to estimate reliability of phylogenetic reconstruction with 50% support threshold. In addition, a heat map was constructed with the percent abundance of dominant OTUs using Microsoft Excel.

STATISTICAL ANALYSIS

Pearson's correlation and analysis of variance (ANOVA) were conducted to identify relationships among DNRA rates, *nrfA* gene abundance, diversity, composition, and environmental parameters using the StatPlus program (AnalystSoft Inc.). Canonical correspondence analysis (CCA) was also performed to examine covariance among environmental variables and the dominant OTUs.

NUCLEOTIDE SEQUENCE ACCESSION NUMBERS

The pyrosequences of *nrfA* genes were deposited in the ENA Short Read Archive under submission number PRJEB6248.

RESULTS

PHYSICAL AND GEOCHEMICAL CHARACTERISTICS OF THE NEW RIVER ESTUARY

Geochemical and physical characteristics of bottom water and sediment samples at the five sites are reported in **Table 1**. The data were obtained from the seasonal study of anammox communities (Lisa et al., 2014). Bottom water salinity ranged from 9.1 to 33.6 ppt along the estuary. AA2 was designated as an oligiohaline site, JAX and M47 were both mesohaline, and M31 and M15 were situated in the polyhaline reaches of the estuary. Bottom water NH_4^+ concentration was higher than NO_3^- concentration at all the sampling sites. Higher concentrations of H_2S in porewater were measured in the mesohaline sites JAX and M47 compared to other sites. Sediment % organic content and extractable NH_4^+ were also higher in these mesohaline sediments (**Table 1**).

ABUNDANCE AND ACTIVITIES OF DNRA COMMUNITIES

Potential rates of DNRA at the five sites ranged from 2.15 to 25.09 nmoles N g^{-1} h^{-1} (**Table 2**). Higher DNRA rates (>20 nmoles N $g^{-1}h^{-1}$) were measured in the sediments from JAX, M47, and M31, while the lowest rate was found at M15. Abundance of DNRA communities based on *nrfA* gene detection agreed with rate measurements as higher abundance of *nrfA* was also measured in the sediments of JAX, M47, and M31. Among geochemical characteristics measured at each site, % organic content and extractable NH_4^+ in sediments positively correlated with *nrfA* gene abundance and DNRA rates with no significant statistical support (Supplementary Table 2).

Table 2 | Potential rates of DNRA and *nrfA* gene abundance in the five sediment communities of the New River Estuary.

Sampling site	DNRA rates nmoles N g^{-1} h^{-1}	*nrfA* gene copies g^{-1}
AA2	13.8 ± 1.8	$7.72 \times 10^8 \pm 4.76 \times 10^7$
JAX	20.7 ± 0.02	$2.58 \times 10^9 \pm 6.27 \times 10^7$
M47	22.6 ± 1.0	$1.56 \times 10^9 \pm 2.68 \times 10^8$
M31	25.1 ± 3.4	$2.18 \times 10^9 \pm 3.16 \times 10^8$
M15	2.2 ± 0.8	$2.31 \times 10^8 \pm 2.50 \times 10^7$

Table 1 | Physical and geochemical characteristics measured at 5 sampling sites in the New River Estuary.

Sampling site	Bottom water			Sediment			
	Salinity ppt	NO_3^- μM	NH_4^+ μM	% organic	H_2S μM	NO_x^- μM	Extractable NH_4^+ μmol g^{-1}
AA2	9.1	0.44	7.8	15.57	0.90	0.26	0.06
JAX	17.8	0.25	0.75	17.98	486.90	0.23	0.21
M47	16.4	0.37	1.18	18.95	249.87	0.54	0.28
M31	27.0	0.47	1.45	10.19	3.21	0.33	0.20
M15	33.6	0.62	1.32	0.33	0.20	0.72	0.04

DIVERSITY OF DNRA COMMUNITIES BASED ON *nrfA* GENE PYROSEQUENCING

A total of 50,882 sequences was obtained following the initial process of filtering the sequences. Total numbers of sequences per site are listed in **Table 3**. Denoising and chimera check yielded 47,591 sequences, which were translated to amino acid sequences using Frambot. After manually removing frame shift errors, 46,165 valid NrfA sequences were used to compare composition and diversity of DNRA communities (**Table 3**). After dereplicating identical NrfA sequences, approximately 2000 sequences were classified as unique to each site.

Richness and diversity of each DNRA community were evaluated based on the unique NrfA sequences (**Table 4**). Chao1 and ACE estimates showed highest richness of NrfA in AA2 sediment, while the lowest was in M47 community. Shannon index showed the highest diversity of NrfA in AA2 and the lowest in M47. The highest sequence evenness was found at M15, where the lowest DNRA rate was measured (**Table 2**). The M31 community, with the highest DNRA rate, was found to have the lowest evenness. Among the environmental variables, extractable NH_4^+ had a significant and negative correlation with NrfA sequence diversity ($r = -0.94$ and $p = 0.016$, Supplementary Table 2). There was no clear trend between salinity gradients and NrfA diversity, although highest richness and diversity of NrfA sequences were observed at AA2, the oligohaline site (**Table 4**).

COMPARISON OF DNRA COMMUNITY COMPOSITION BASED ON *nrfA* GENE PYROSEQUENCING

Based on 90% identity as a cutoff of sub-genus level, the valid sequences were clustered into OTUs, and a representative sequence from each OTU was used for normalized weighted Unifrac analysis. **Figure 2** shows the spatial variation of the DNRA communities with 75.41% percent variation explained (sum of the first and second PCoA principal coordinates). The AA2 community was the most distinct of the DNRA communities. The composition of JAX and M47 communities were more similar to each other than to other communities, while M31 and M15 communities also clustered together. Salinity was a significant environmental factor ($p < 0.05$) segregating these communities along the P1 coordinate, while bottom water NO_3^- concentrations, porewater H_2S and extractable NH_4^+ became significant variables ($P < 0.05$) along the variation of the P2 coordinate.

Cluster analysis revealed that endemic sequences comprised less than 17% of total NrfA sequences in JAX, M47, and M31 communities and more than 30% in AA2 and M15 (**Table 3**). Relative percent of endemic sequences (sequences found in only one community) was higher in AA2 and M15 communities, where rates were lowest, than in the mid estuarine communities. The highest relative percent of endemic sequences was found in the M15 community with 39.8%, while the JAX community had the lowest with 11.7% (**Table 3**). The numbers of endemic OTUs in each community significantly and positively correlated with diversity of NrfA sequences ($r = 0.95$, $p < 0.05$). Most of the OTUs with endemic sequences were rare OTUs ($\leq$0.1% of total sequence) or low abundant OTUs (between 0.1 and 1% of total sequences) in each community. Percent abundance of endemic sequences was significantly and negatively correlated with the DNRA rates and *nrfA* gene abundance ($r = -0.93$ and $r = -0.93$, respectively). In contrast, the

Table 3 | Number of *nrfA* sequences filtered during different steps of bioinformatic analysis.

Sampling site	Number of sequences					
	Initial RDP process	Denoise/Chimea Check	Frambot[a]	Valid[b]	Dominant[c](%)	Endemic[d](%)
AA2	7,918	7,557	7,483	7,346	42.3	30.9
JAX	8,821	7,940	7,910	7,852	50.7	11.7
M47	13,870	13,464	13,130	12,952	46.8	13.6
M31	11,197	10,243	10,218	10,000	50.2	16.7
M15	9,076	8,387	8,330	8,015	38.6	39.8

[a] *Frambot converted DNA sequences into amino acid sequences and identified nrfA genes based on the reference sequences.*

[b] *Valid sequences were defined as amino acid sequences without frame-shift errors.*

[c] *Dominant sequences were defined as an OTU comprising of more than 1% of total NrfA sequences in each community.*

[d] *Endemic sequences were detected at only one site.*

Table 4 | Estimates of sedimentary NrfA sequence richness and diversity in the New River Estuary.

Sampling site	Unique	OTUs[a]	Chao1[a]	ACE[a]	Shannon[a]	Evenness[b]
AA2	2,052	1,012	1,958.6	2,162.3	6.507	0.940
JAX	1,714	827	1,569.5	1,638.0	6.298	0.938
M47	2,022	799	1,237.8	1,381.5	6.188	0.926
M31	2,210	1,005	1,897.8	2,106.9	6.360	0.920
M15	2,157	933	1,489.9	1,603.5	6.446	0.943

[a] *Richness and diversity were determined based on 0.1 protein distance.*

[b] *Evenness was calculated by dividing Shannon index by Ln (OTUs).*

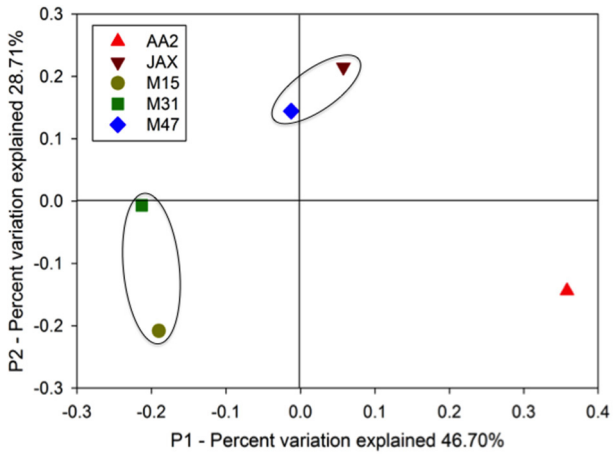

FIGURE 2 | Weighted and normalized PcoA plot of the DNRA communities in the New River Estuary. Unifrac analysis was conducted with representative NrfA OTUs in the five sediment communities. The black circles indicate the communities sharing higher composition similarities.

dominant OTUs were more abundant in the mid estuarine communities than the AA2 and M15 communities. More than 50% of total NrfA sequences in JAX and M31 sites were clustered with the dominant OTUs (**Table 3**). Percent abundance of dominant sequences had significant and positive correlations with activities and abundance of DNRA communities ($r = 0.92$ and $r = 0.99$, respectively).

COMPARISON OF DOMINANT NrfA OTUS IN SEDIMENT COMMUNITIES

A total of 69 dominant OTUs was found in five sediment communities. The sequences associated with the dominant OTUs in each community were included in the heat map analysis, although this accounted for less than 1% of sequence abundance (**Figure 3**). A representative sequence of each OTU was phylogenetically compared with NrfA sequences found in bacterial isolates (**Figure 3**). The AA2, JAX, and M15 communities had higher numbers of dominant OTUs (18, 20, and 19, respectively) than the M47 and M31 communities, which had 16 and 13 dominant OTUs, respectively (Supplementary Table 3). Most of dominant OTUs were found in more than one community, with the exception of 10 OTUs. OTU1 and OTU2 were endemic at AA2, while OTU27, OTU36, OTU37, OTU46, and OTU47 were only found in the M15 community. OTU60 and OTU65 were endemic at M47, and OTU54 was only present at M31. In contrast, OTU11, OTU23, OTU31, and OTU 55 were cosmopolitan OTUs commonly present in all five sediment communities, although none of them were predominant in any of the five sediment communities. OTU11 and OTU23 were dominant in the AA2 and JAX communities, but not in other communities. OTU31 and OTU55 were only dominant in M15.

Among 69 OTUs, OTU53 was the most abundant member of M31 (28.2%) and M15 (9.1%), but accounted for less than 1% at M47 and was not detectable at AA2 and JAX (**Figure 3**). Phylogenetic analysis showed that OTU53 was closely related to NrfA found in *Escherichia albertii, Shewanella oneidensis*, and *Aggregatibacter actinomycetemcomitans* (**Figure 3**). The most abundant member in M47 community was OTU21 (6.1%), while OTU35 accounted for 5.6 and 14.6% at JAX and M47, respectively. NrfA sequences found in bacterial isolates did not cluster with these OTUs (**Figure 3**). OTU19, which is closely related to *Holophaga foetida* NrfA, was most abundant, composing 8.1% in the AA2 community, but contributed less than 1% in JAX, and not detected in other sites (**Figure 3**). Phylogenetic analysis showed that OTU9, dominant in M47, was closely associated with *Sulfurospirillum deleyianum* and OTU32, the dominant member of JAX and M47 communities, was related to *Thioalkalivibrio nitratireducens* (**Figure 3**).

CCA with dominant OTUs showed that the first two CCA axes (CCA1 and CCA2) explained 67.5% of the cumulative variance of the DNRA communities in the New River Estuary (**Figure 4**). Different environmental variables affected relative abundance of dominant OTUs in sediment communities. Group A was composed of 24 OTUs that were dominant members of M31 or M15 communities. Salinity significantly and positively influenced the abundance of OTU49, OTU50, and OTU55 within Group A. OTU49 and OTU50 were closely related to *Planctomyces* spp. (**Figure 3**). Group B was made up of three OTUs (25, 31, and 56) found in three to five communities. Porewater NO_x^- concentrations had a positive significant correlation with this group. The OTUs in Group C were dominant members of JAX or M47 communities. Sulfide concentration was shown to have significant and positive influences on 10 OTUs (17, 20, 24, 29, 30, 32, 35, 63, and 67) within this group. None was closely related to NrfA sequences found in bacterial isolates. Group D was composed of 12 OTUs (1, 2, 10, 13, 15, 16, 18, 19, 22, 26, 45, and 62) found primarily in the AA2 community (**Figure 3**). They had a significant and positive correlation with bottom water NH_4^+ concentration. Among these dominant OTUs, OTU1, OTU16, and OTU19 were closely associated with *H. foetida*, while OTU2 showed high similarity to *Pelobacter carbinolicus*. Together, the CCA and phylogenetic analyses revealed that different environmental variables contributed to the presence of the different dominant members in DNRA communities at oligohaline, mesohaline, and polyhaline reaches of the New River Estuary.

DISCUSSION

Two dissimilatory NO_3^- reduction pathways, DNRA and denitrification, influence the recycling and removal of fixed N in an aquatic ecosystem. We found that sedimentary DNRA activities were higher than the reported denitrification activities collected from AA2, M47, M31, and M15 during the same time (Supplementary Figure 2; Lisa et al., 2014). DNRA was responsible for 44–74% of sedimentary dissimilatory NO_3^- reduction. This demonstrates that DNRA was the major dissimilatory NO_3^- reduction process in the New River Estuary, as shown in other estuarine ecosystems (Kelly-Gerreyn et al., 2001; Tobias et al., 2001a,b; An and Gardner, 2002). DNRA rates measured in the New River Estuary are comparable to those reported in shallow coastal systems and salt marshes (Sørensen, 1978; Gardner and McCarthy, 2009; Koop-Jakobsen and Giblin, 2010).

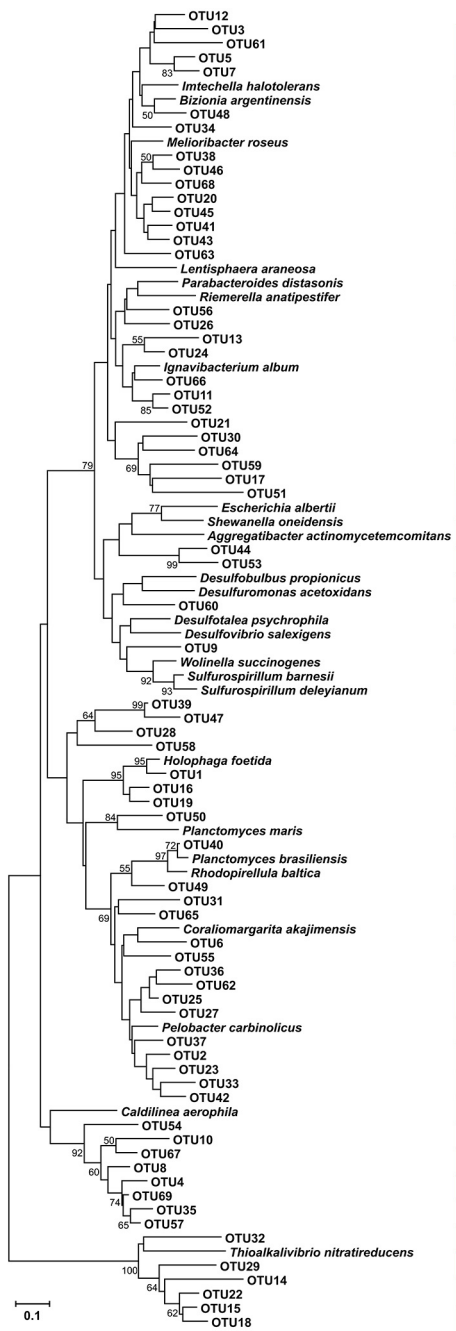

	AA2	JAX	M47	M31	M15
OTU12	0.29	1.04	2.12	0.05	0.00
OTU3	0.48	4.60	0.00	0.00	0.00
OTU61	0.00	0.61	2.54	0.00	0.02
OTU5	0.65	1.21	0.03	0.00	0.00
OTU7	1.10	2.18	0.91	0.00	0.00
OTU48	0.00	0.00	0.00	0.37	1.70
OTU34	0.00	0.01	0.00	3.84	0.32
OTU38	0.00	0.00	0.00	0.03	1.24
OTU46	0.00	0.00	0.00	0.00	1.20
OTU68	0.00	0.03	0.18	1.04	0.04
OTU20	0.37	1.39	0.32	0.03	0.00
OTU45	1.46	0.04	0.03	0.00	0.01
OTU41	0.00	0.00	0.00	1.58	0.20
OTU43	0.00	0.00	0.00	1.02	0.12
OTU63	0.00	2.98	2.04	0.05	1.07
OTU56	0.00	0.00	0.94	0.72	1.27
OTU26	3.06	0.01	0.00	0.00	0.00
OTU13	1.62	0.15	0.06	0.00	0.00
OTU24	0.04	1.25	0.07	0.02	0.00
OTU66	0.00	0.03	0.12	1.01	0.21
OTU11	3.78	4.02	0.97	0.09	0.05
OTU52	0.00	0.00	0.00	0.06	1.05
OTU21	0.01	0.59	6.10	0.00	0.00
OTU30	0.12	1.24	0.57	0.02	0.00
OTU64	0.00	0.11	1.18	0.01	0.00
OTU59	0.00	0.00	1.16	0.03	0.00
OTU17	0.01	1.02	0.84	0.11	0.00
OTU51	0.00	0.00	0.00	2.63	0.04
OTU44	0.00	0.00	0.00	1.28	0.46
OTU53	0.00	0.00	0.12	28.21	9.10
OTU60	0.00	0.00	2.32	0.00	0.00
OTU9	0.27	0.09	3.39	0.00	0.00
OTU39	0.03	0.08	1.37	0.00	0.00
OTU47	0.00	0.00	0.00	0.00	1.15
OTU28	1.20	1.27	0.26	0.00	0.00
OTU58	0.00	0.00	3.09	0.24	0.00
OTU1	1.32	0.00	0.00	0.00	0.00
OTU16	1.46	0.01	0.00	0.00	0.00
OTU19	8.11	0.03	0.00	0.00	0.00
OTU50	0.00	0.00	0.00	0.62	1.12
OTU40	0.00	0.00	0.00	0.09	1.50
OTU49	0.00	0.00	0.00	1.05	1.16
OTU31	0.01	0.20	0.39	0.35	1.38
OTU65	0.00	0.00	1.84	0.00	0.00
OTU6	1.40	0.60	0.59	0.00	0.00
OTU55	0.01	0.01	0.02	0.93	1.62
OTU36	0.00	0.00	0.00	0.00	1.71
OTU62	1.63	0.00	0.02	0.00	0.00
OTU25	0.00	0.01	3.34	2.40	6.99
OTU27	0.00	0.00	0.00	0.00	2.31

FIGURE 3 | Phylogenetic tree and heat map of dominant NrfA OTUs in the New River Estuary. Dominant OTUs were defined as the OTUs containing more than 1% of total number of NrfA sequences in each community. Neighbor-joining tree was constructed from amino acid sequences and bootstrap analysis with 1000 replicates used to estimate confidence. Bootstrap values of >50% were listed in the tree. The heat map was constructed in Microsoft Excel based on the percent relative of each OTU in each sediment community.

Positive correlation between DNRA rates and extractable NH_4^+ in sediments indicates that DNRA is an important process for sediment NH_4^+ flux, as well as mineralization. Higher DNRA rates were measured in the mid estuarine sites where H_2S concentration and % organic contents in sediments were elevated. High H_2S may inhibit nitrification and denitrification, which results in a greater contribution of DNRA to dissimilatory NO_3^- reduction processes. This was also shown in a shallow estuary in southern Texas (An and Gardner, 2002). In addition, H_2S can be utilized as an electron donor by DNRA bacteria. Two dominant OTUs in JAX and M47 were closely related with *S. deleyianum* and *T. nitratireducens*. *S. deleyianum*

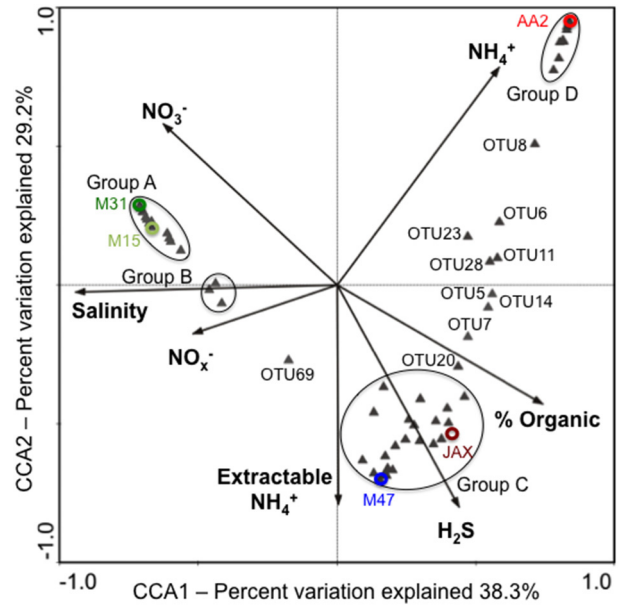

FIGURE 4 | CCA ordination plot deciphering the relationship between dominant NrfA OTUs and environmental variables in the New River Estuary. Color circles represent the ordinates of each community based on dominant OTUs. Some of dominant OTUs were clustered in groups as indicated with black circles. Group A contains OTUs 27, 31, 34, 36, 37, 38, 40, 41, 42, 43, 44, 46, 47, 48, 49, 50, 51, 52, 53, 54, 55, 56, 57, 66, and 68. Group B has OTUs25, 31, and 56. Group C carries OTUs 3, 4, 9, 12, 17, 21, 24, 29, 30, 32, 33, 35, 39, 58, 59, 60, 61, 63, 64, 65, and 67. Group D includes OTUs 1, 2, 10, 13, 15, 16, 18, 19, 22, 26, 45, and 62.

is a mixotrophic bacterium that can utilize organic carbon and H_2S as electron sources (Eisenmann et al., 1995), while the obligate chemolithoautotrophic bacterium, *T. nitratireducens,* reduces NO_3^- coupled to sulfur oxidation (Tikhonova et al., 2006). The presence of *Sulfurosprillum* spp. and *Thioalkalivibrio* spp. suggests the use of sulfur compounds as reducing power for dissimilatory NO_3^- reduction in these sediment communities.

The abundance of bacteria capable of DNRA can be an important microbial regulator for the respiratory process in aquatic ecosystems. However, quantification of DNRA bacteria based on *nrfA* gene detection has had limited success. To our knowledge Dong et al. (2009) is the only other study that measured three subsets of *nrfA* gene abundance in the Colne River Estuary. The new primer combination used in this study was able to amplify *nrfA* genes in all five of the sediment samples, even though more than $9x10^4$ copies of *nrfA* genes were required for proper detection. This high detection limit might be due to degeneracy of PCR primers. qPCR success allowed quantification of total abundance of *nrfA* carrying bacteria in estuarine sediments communities, which were then compared with DNRA activities. This is the first study reporting a co-occurrence of higher DNRA rates in the sediment communities with higher *nrfA* gene abundance, and suggests the abundance of DNRA bacteria can act as an important microbial control in estuarine sediments. In addition, *nrfA* gene abundance may have the potential to be used as a genetic proxy of DNRA potential in sediments.

Composition and diversity of DNRA bacteria can be another microbial regulator of DNRA in aquatic sediments. Differences in DNRA community composition were found along the salinity gradient of the New River Estuary. Takeuchi (2006) reported a similar trend in the Colne River Estuary. Endemic populations accounted for 10–40% of the sediment communities in the New River Estuary. The increased numbers of an endemic population supported higher diversity of NrfA sequences, but negatively influenced the DNRA activities. This finding leads us to hypothesize that selected members of DNRA communities become predominant and responsible for overall community activities. We found that relative abundance of dominant populations had a significant positive correlation with the rates and abundance of DNRA communities in the New River Estuary. Bulow et al. (2008) and Francis et al. (2013) demonstrated the presence of a few dominant OTUs in denitrifying communities along the salinity gradient of the Chesapeake Bay, based on the *nirS* gene analysis. The dominant *nirS* OTUs were also highly expressed in the mesohaline and polyhaline sediment communities (Bulow et al., 2008), which supports the importance of dominant populations in *in situ* community activities. These findings readdress the importance of dominant population and their roles in overall community activities.

Dominant DNRA populations were influenced by different geochemical and physical parameters in the New River Estuary. The dominant members in JAX and M47 communities, positively influenced by H_2S, might be able to oxidize both organic carbon and sulfide as observed in *S. deleyianum* (Eisenmann et al., 1995). Alternatively, DNRA communities in JAX and M47 were more tolerable and adaptive to high sulfidogenic conditions. The dominant members in the oligohaline AA2 community were positively correlated with bottom water NH_4^+ concentration, while the members in M31 and M15 were influenced by salinity. This suggests that the dominant populations of each community are well adapted to different environmental conditions present in their unique environments. Sun et al. (2013) reported 13 dominant OTUs were mainly responsible for changes in metal and hydrocarbon contaminants in estuarine sediments based on 16S rRNA gene pyrosequencing analysis. Abundance of different dominant populations in each community strongly influences overall community activities, while geochemical and physical conditions affect the composition of DNRA communities in the New River Estuary. This study reveals that the relative abundances of dominant populations serves as an important microbial control for community activities, while the abundance of endemic populations is an important factor for DNRA bacterial diversity in estuarine sediments.

ACKNOWLEDGMENTS

This study was supported through grants provided by the US National Science Foundation (DEB1020944, EAR1024662, and OCE0851435). We acknowledge Ashley Smyth and Ann Arfken for providing comments and feedback on this manuscript. This paper is Contribution No. 3393 of the Virginia Institute of Marine Science, College of William & Mary.

SUPPLEMENTARY MATERIAL

The Supplementary Material for this article can be found online at: http://www.frontiersin.org/journal/10.3389/fmicb.2014.00460/abstract

REFERENCES

An, S., and Gardner, W. (2002). Dissimilatory nitrate reduction to ammonium (DNRA) as a nitrogen link, versus denitrification as a sink in a shallow estuary (Laguna Madre/Baffin Bay, Texas). *Mar. Ecol. Prog. Ser.* 237, 41–50. doi: 10.3354/meps237041

Anderson, I. C., Brush, M. J., Piehler, M. F., Currin, C. A., Stanhope, J. W., Smyth, A. R., et al. (2013). Impacts of climate-related drivers on the benthic nutrient filter in a shallow photic estuary. *Estuar. Coasts* 37, 46–62. doi: 10.1007/s12237-013-9665-5

Bragg, L., Stone, G., Imelfort, M., Hugenholtz, P., and Tyson, G. W. (2012). Fast, accurate error-correction of amplicon pyrosequences using Acacia. *Nat. Methods* 9, 425–426. doi: 10.1038/nmeth.1990

Bulow, S. E., Francis, C. A., Jackson, G. A., and Ward, B. B. (2008). Sediment denitrifier community composition and *nirS* gene expression investigated with functional gene microarrays. *Environ. Microbiol.* 10, 3057–3069. doi: 10.1111/j.1462-2920.2008.01765.x

Burkholder, J. M., Mallin, M. A., Glasgow, H. B. Jr., Larsen, L. M., McIver, M. R., Shank, G. C., et al. (1997). Impacts to a coastal river and estuary from rupture of a swine waste holding lagoon. *J. Environ. Qual.* 26, 1451–1466. doi: 10.2134/jeq1997.00472425002600060003x

Dong, L. F., Naqasima Sobey, M., Smith, C. J., Rusmana, I., Phillips, W., Stott, A., et al. (2011). Dissimilatory reduction of nitrate to ammonium, not denitrification or anammox, dominates benthic nitrate reduction in tropical estuaries. *Limnol. Oceanogr.* 56, 279–291. doi: 10.4319/lo.2011.56.1.0279

Dong, L. F., Smith, C. J., Papaspyrou, S., Stott, A., Osborn, A. M., and Nedwell, D. B. (2009). Changes in benthic denitrification, nitrate ammonification, and anammox process rates and nitrate and nitrite reductase gene abundances along an estuarine nutrient gradient (the Colne estuary, United Kingdom). *Appl. Environ. Microbiol.* 75, 3171–3179. doi: 10.1128/AEM.02511-08

Edgar, R. C. (2004). MUSCLE: multiple sequence alignment with high accuracy and high throughput. *Nucleic Acids Res.* 32, 1792–1797. doi: 10.1093/nar/gkh340

Einsle, O., Messerschmidt, A., Stach, P., Bourenkov, G. P., Bartunik, H. D., Huber, R., et al. (1999). Structure of cytochrome c nitrite reductase. *Nature* 400, 476–480. doi: 10.1038/22802

Eisenmann, E., Beuerie, J., Sulger, K., Kroneck, P. M. H., and Schumacher, W. (1995). Lithotrophic growth of *Sulforosprillum delianum* with sulfide as electron donor coupled to respiratory reduction of nitrate to ammonia. *Arch. Microbiol.* 164, 180–185. doi: 10.1007/BF02529969

Ensign, S. H., Halls, J. N., and Mallin, M. A. (2004). Application of digital bathymetry data in an analysis of flushing times of two large estuaries. *Comput. Geosci.* 30, 501–511. doi: 10.1016/j.cageo.2004.03.015

Felsenstein, J. (1989). PHYLIP – Phylogeny Inference Package (Version 3.2). *Cladistics* 5, 164–166

Fish, J. A., Chai, B., Wang, Q., Sun, Y., Brown, C. T., Tiedje, J. M., et al. (2013). FunGene: the functional gene pipeline and repository. *Front. Microbiol.* 4:291. doi: 10.3389/fmicb.2013.00291

Francis, C. A., O'Mullan, G. D., Cornwell, J. C., and Ward, B. B. (2013). Transitions in *nirS*-type denitrifier diversity, community composition, and biogeochemical activity along the Chesapeake Bay estuary. *Front. Microbiol.* 4:237. doi: 10.3389/fmicb.2013.00237

Gardner, W. S., and McCarthy, M. J. (2009). Nitrogen dynamics at the sediment-water interface in shallow, sub-tropical Florida Bay: why denitrification efficiency may decrease with increased eutrophication. *Biogeochemistry* 95, 185–198. doi: 10.1007/s10533-009-9329-5

Giblin, A. E., Tobias, C. R., Song, B., Weston, N., and Banta, G. T. (2013). The importance of dissimilatory nitrate reduction to ammonium (DNRA) in the nitrogen cycle of coastal ecosystems. *Oceanography* 26, 124–131. doi: 10.5670/oceanog.2013.54

Giblin, A. E., Weston, N. B., Banta, G. T., Tucker, J., and Hopkinson, C. S. (2010). The effects of salinity on nitrogen losses from an oligohaline estuarine sediment. *Estuar. Coasts* 33, 1054–1068. doi: 10.1007/s12237-010-9280-7

Hamady, M., Walker, J. J., Harris, J. K., Gold, N. J., and Knight, R. (2008). Error-correcting barcoded primers for pyrosequencing hundreds of samples in multiplex. *Nat. Methods* 5, 235–237. doi: 10.1038/nmeth.1184

Hanson, T. E., Campbell, B. J., Kalis, K. M., Campbell, M. A., and Klotz, M. G. (2013). Nitrate ammonification by *Nautilia profundicola* AmH: experimental evidence consistent with a free hyroxylamine intermediate. *Front. Microbiol.* 4:180. doi: 10.3389/fmicb.2013.00180

Holmes, R., McClelland, J., Sigman, D., Fry, B., and Peterson, B. (1998). Measuring $-NH_4^+$ in marine, estuarine and fresh waters: an adaptation of the ammonia diffusion method for samples with low ammonium concentrations. *Mar. Chem.* 60, 235–243. doi: 10.1016/S0304-4203(97)00099-6

Kartal, B., Kuypers, M. M. M., Lavik, G., Schalk, J., Op den Camp, H. J. M., Jetten, M. S. M., et al. (2007). Anammox bacteria disguised as denitrifiers: nitrate reduction to dinitrogen gas via nitrite and ammonium. *Environ. Microbiol.* 9, 635–642. doi: 10.1111/j.1462-2920.2006.01183.x

Kelly-Gerreyn, B. A., Trimmer, M., and Hydes, D. J. (2001). A diagenetic model discriminating denitrification and dissimilatory nitrate reduction to ammonium in a temperate estuarine sediment. *Mar. Ecol. Prog. Ser.* 220, 33–46.

Koop-Jakobsen, K., and Giblin, A. E. (2010). The effect of increased nitrate loading on nitrate reduction via denitrification and DNRA in salt marsh sediments. *Limnol. Oceanogr.* 55, 789–802. doi: 10.4319/lo.2009.55.2.0789

Li, W., and Godzik, A. (2006). Cd-hit: a fast program for clustering and comparing large sets of protein or nucleotide sequences. *Bioinformatics* 22, 1658–1659. doi: 10.1093/bioinformatics/btl158

Lisa, J., Song, B., Tobias, C., and Duernberger, K. (2014). Impacts of freshwater flushing on anammox community structure and activities in the New River Estuary, USA. *Aquat. Microb. Ecol.* 72, 17–31. doi: 10.3354/ame01682

Lozupone, C., Hamady, M., and Knight, R. (2006). UniFrac–an online tool for comparing microbial community diversity in a phylogenetic context. *BMC Bioinformatics* 7:371. doi: 10.1186/1471-2105-7-371

Mallin, M. A., Burkholder, J. M., Cahoon, L. B., and Posey, M. H. (2000). North and South Carolina Coasts. *Mar. Pollut. Bull.* 41, 56–75. doi: 10.1016/S0025-326X(00)00102-8

Mallin, M. A., McIver, M. R., Wells, H. A., Parsons, D. C., and Johnson, V. L. (2005). Reversal of eutrophication following sewage treatment upgrades in the New River Estuary, North Carolina. *Estuaries* 28, 750–760. doi: 10.1007/BF02732912

Mao, Y., Yannarell, A. C., Davis, S. C., and Mackie, R. I. (2013). Impact of different bioenergy crops on N-cycling bacterial and archaeal communities in soil. *Environ. Microbiol.* 15, 928–942. doi: 10.1111/j.1462-2920.2012.02844.x

Mao, Y., Yannarell, A. C., and Mackie, R. I. (2011). Changes in N-transforming archaea and bacteria in soil during the establishment of bioenergy crops. *PLoS ONE* 6:e24750. doi: 10.1371/journal.pone.0024750

Mohan, S. B., Schmid, M., Jetten, M., and Cole, J. (2004). Detection and widespread distribution of the *nrfA* gene encoding nitrite reduction to ammonia, a short circuit in the biological nitrogen cycle that competes with denitrification. *FEMS Microbiol. Ecol.* 49, 433–443. doi: 10.1016/j.femsec.2004.04.012

Pereira E Silva, M. C., Schloter-Hai, B., Schloter, M., van Elsas, J. D., and Salles, J. F. (2013). Temporal dynamics of abundance and composition of nitrogen-fixing communities across agricultural soils. *PLoS ONE* 8:e74500. doi: 10.1371/journal.pone.0074500

Pielou, E. (1966). The measurement of diversity in different types of biological collections. *J. Theor. Biol.* 13, 131–144. doi: 10.1016/0022-5193(66)90013-0

Schloss, P. D., and Handelsman, J. (2005). Introducing DOTUR, a computer program for defining operational taxonomic units and estimating species richness. *Appl. Environ. Microbiol.* 71, 1501–1506. doi: 10.1128/AEM.71.3.1501-1506.2005

Schmieder, R., and Edwards, R. (2011). Quality control and preprocessing of metagenomic datasets. *Bioinformatics* 27, 863–864. doi: 10.1093/bioinformatics/btr026

Simon, J. (2002). Enzymology and bioenergetics of respiratory nitrite ammonification. *FEMS Microbiol. Rev.* 26, 285–309. doi: 10.1111/j.1574-6976.2002.tb00616.x

Simon, J., and Klotz, M. G. (2013). Diversity and evolution of bioenergetic systems involved in microbial nitrogen coupound transformations. *Biochim. Biosphy. Acta* 1827, 114–135. doi: 10.1016/j.bbabio.2012.07.005

Smith, C. J., Nedwell, D. B., Dong, L. F., Osborn, A. M., Park, W., Sciences, P., et al. (2007). Diversity and abundance of nitrate reductase (*narG* and *napA*), and nitrite reductase (*nirS* and *nrfA*) genes and transcripts in estuarine sediments. *Appl. Environ. Microbiol*. 73, 3612–3622. doi: 10.1128/AEM.02894-06

Sørensen, J. (1978). Capacity for denitrification and reduction of nitrate to ammonia in a coastal marine sediment. *Appl. Environ. Microbiol*. 35, 301–305.

Sun, M. Y., Dafforn, K. A., Johnston, E. L., and Brown, M. V. (2013). Core sediment bacteria drive community response to anthropogenic contamination over multiple environmental gradients. *Environ. Microbiol.* 15, 2517–2531. doi: 10.1111/1462-2920.12133

Takeuchi, J. (2006). Habitat segregation of a functional gene encoding nitrate ammonification in estuarine sediments. *Geomicrobiol. J*. 23, 75–87. doi: 10.1080/01490450500533866

Tamura, K., Peterson, D., Peterson, N., Stecher, G., Nei, M., and Kumar, S. (2011). MEGA5: molecular evolutionary genetics analysis using maximum likelihood, evolutionary distance, and maximum parsimony methods. *Mol. Biol. Evol*. 28, 2731–2739. doi: 10.1093/molbev/msr121

Tikhonova, T. V., Slutsky, A., Antipov, A. N., Boyko, K. M., Polyakov, K. M., Sorokin, D. Y., et al. (2006). Molecular and catalytic properties of a novel cytochrome c nitrite reductase from nitrate-reducing haloalkaliphilic sulfur-oxidizing bacterium Thioalkalivibrio nitratireducens. *Biochim. Biophys. Acta* 1764, 715–723. doi: 10.1016/j.bbapap.2005.12.021

Tobias, C. R., Anderson, I. C., Canuel, E. A., and Macko, S. A. (2001b). Nitrogen cycling through a fringing marsh-aquifer ecotone. *Mar. Ecol. Prog. Ser*. 210, 25–39. doi: 10.3354/meps210025

Tobias, C. R., Macko, S. A., Anderson, I. C., Canuel, E. A., and Harvey, J. W. (2001a). Tracking the fate of a high concentration groundwater nitrate plume through a fringing marsh: a combined groundwater tracer and *in situ* isotope enrichment study. *Limnol. Oceanogr*. 46, 1977–1989. doi: 10.4319/lo.2001.46.8.1977

Welsh, A., Chee-Sanford, J. C., Connor, L. M., Löffler, F. E., and Sanford, R. A. (2014). Refined NrfA phylogeny improves PCR-based *nrfA* gene detection. *Appl. Environ. Microbiol*. 80, 2110–2119. doi: 10.1128/AEM.03443-13

Conflict of Interest Statement: The authors declare that the research was conducted in the absence of any commercial or financial relationships that could be construed as a potential conflict of interest.

Received: 30 April 2014; accepted: 13 August 2014; published online: 03 September 2014.

*Citation: Song B, Lisa JA and Tobias CR (2014) Linking DNRA community structure and activity in a shallow lagoonal estuarine system. Front. Microbiol. **5**:460. doi: 10.3389/fmicb.2014.00460*

This article was submitted to Aquatic Microbiology, a section of the journal Frontiers in Microbiology.

frontiers in
MARINE SCIENCE

ORIGINAL RESEARCH ARTICLE
published: 28 October 2014
doi: 10.3389/fmars.2014.00044

Microbial abundance and diversity patterns associated with sediments and carbonates from the methane seep environments of Hydrate Ridge, OR

Jeffrey J. Marlow[1]*, Joshua A. Steele[1], David H. Case[1], Stephanie A. Connon[1], Lisa A. Levin[2] and Victoria J. Orphan[1]*

[1] *Division of Geological and Planetary Sciences, California Institute of Technology, Pasadena, CA, USA*
[2] *Integrative Oceanography Division, Scripps Institution of Oceanography, University of California, San Diego, La Jolla, CA, USA*

Edited by:
Anne Bernhard, Connecticut College, USA

Reviewed by:
Lisa Moore, University of Southern Maine, USA
Florence Schubotz, Massachusetts Institute of Technology, USA

****Correspondence:***
Jeffrey J. Marlow and Victoria J. Orphan, Division of Geological and Planetary Sciences, California Institute of Technology, MC 100-23, Pasadena, CA 91101, USA
e-mail: jjmarlow@caltech.edu; vorphan@gps.caltech.edu

Methane seeps are among the most productive habitats along continental margins, as anaerobic methane-oxidizing euryarchaeaota and sulfur-metabolizing deltaproteobacteria form the biological base of a dynamic deep-sea ecosystem. The degree of methane seepage therefore represents one important variable in ecosystem dynamics, and the recent discovery of carbonate-hosted endolithic methanotrophy exposes another potentially discriminating factor: physical substrate type. Methanotrophic microbial communities have been detected within diverse seep-associated habitats, including unlithified sediments, protolithic carbonate nodules, and lithified carbonate slabs and chemoherms of distinct mineralogies. However, a systematic assessment of the diversity and community structure associated with these different habitats has been lacking. In this study, microbial aggregate analysis, microbial abundance quantification, mineralogical identification, and archaeal and bacterial 16S rRNA gene clone libraries were used to deconvolve the relationships between seepage activity, substrate type, and microbial community structure. We report prevalent methane-oxidizing archaeal lineages in both active and low-activity seep settings, and a strong community dependence on both seepage activity and substrate type. Statistical treatments of relative taxa abundances indicate that archaeal community structure is more dependent on the degree of methane seepage than physical substrate type; bacterial assemblages appear to be more strongly influenced by the type of colonization substrate than seepage activity. These findings provide a window into the determinants of community structure and function, improving our understanding of potential elemental cycling at seep sites.

Keywords: methane seeps, anaerobic methane oxidation, microbial diversity, 16S rRNA gene, microbe-mineral interaction

INTRODUCTION

The seafloor is a dynamic and varied environment whose biological communities are dependent upon organic detritus from surface waters and/or chemically reduced fluids emitted from the subseafloor. Benthic habitats cover a range of productivities; in all cases, microorganisms play critical roles in mobilizing chemical or organic energy sources and mediating elemental fluxes (Orcutt et al., 2011 and references therein). Many studies of seafloor microbial ecology have focused on near-surface sediment, examining, for example, methane generation (Claypool and Kvenvolden, 1983), dinitrogen production (Thamdrup and Dalsgaard, 2002), or organic matter remineralization with a range of electron acceptors (Reeburgh, 1983). As the full extent of benthic microbial activity comes into focus, clarifying the identities, distribution, and metabolic roles of constituent organisms in not only sediments, but also endolithic and deeper-seated habitats across a spectrum of energetic regimes, has emerged as a priority.

Methane seeps are among the most productive habitats on the sub-photic zone seafloor. In these regions, reduced, methane-rich fluids come into contact with oxidized seawater, fueling chemosynthetic communities such as anaerobic methanotrophic archaea (ANME)/Deltaproteobacteria consortia that mediate the sulfate-coupled anaerobic oxidation of methane (AOM). AOM is a globally significant process which consumes an estimated 80–90% of methane at the seafloor (Reeburgh, 2007). The cultivation-independent investigation of the microorganisms responsible for AOM has revealed two primary constituents: methane-oxidizing archaea and sulfur-metabolizing bacteria. ANME are believed to activate methane and transfer reducing equivalents to their syntrophic partners, sulfate-reducing or sulfur disproportionating bacteria (SRB; Hoehler et al., 1994; Nauhaus et al., 2002; Milucka et al., 2012). The metabolic byproducts of methanotrophy support micro- and macrofaunal communities in the seep food web, including sulfide-oxidizing bacteria (*Beggiatoa*, *Thioploca*), chemosynthetic clams (*Vesicomya*), mussels (*Bathymodiolus*), tube worms (Siboglinidae), and ampharetid polychaetes that serve as visual manifestations of CH_4 seepage on the seafloor

(Van Dover et al., 2003; Levin, 2005; Niemann et al., 2013).

Detailed examination of microbial communities within methane seep sediments has further revealed the community composition and exposed relationships between constituent members. The archaeal group ANME-1 is currently divided into two subgroups (ANME-1a and ANME-1b) and represents a novel order within the Euryarchaeota (Hinrichs et al., 1999; Hallam et al., 2004; Meyerdierks et al., 2005). These anaerobic methane-oxidizing microorganisms have been observed as single cells, as monospecific aggregates, and in association with bacteria (Orphan et al., 2002; Treude et al., 2007; Holler et al., 2011). The Methanosarcinales-affiliated ANME-2 (divisible into three phylogenetic subgroups, ANME-2a, -2b, and -2c; Orphan et al., 2001a) frequently form aggregates with members of the Desulfobacteraceae family (e.g., the Seep-SRB1 group; Boetius et al., 2000; Knittel et al., 2005; Schreiber et al., 2010) or Desulfobulbaceae (Pernthaler et al., 2008; Green-Saxena et al., 2014). Members of the ANME-3 clade have been shown to associate with Bacteria most closely related to another lineage within the Desulfobulbaceae (Lösekann et al., 2007; Green-Saxena et al., 2014).

Sulfate-coupled methane oxidation produces two units of alkalinity per unit of dissolved inorganic carbon, thereby promoting the precipitation of authigenic carbonate minerals (Aloisi et al., 2002). These precipitates form loosely consolidated protoliths, hereafter referred to as "nodules," found below the sediment-water interface within methane-perfused sediments (Orphan et al., 2004; Watanabe et al., 2008). Larger, fully lithified carbonate rocks also form, likely within methane-perfused sediment (Stadnitskaia et al., 2008; Bian et al., 2013), and can be exposed at the seabed following episodes of uplift and winnowing (Greinert et al., 2001; Naehr et al., 2007; Ussler and Paull, 2008). AOM activity associated with methane seepage at the seabed results in a heterogeneous landscape of reduced sediments and carbonate pavements, chemoherms, and large mounds, covered by patches of chemosynthetic communities. Carbonate structures can be hundreds of meters tall and likely represent the time-integrated accretion of AOM-linked authigenic carbonate precipitation (Greinert et al., 2001). Subsurface advective methane flow can shift with time, turning "active" habitats, which exhibit gas bubbling and/or seafloor chemosynthetic communities, into "low-activity" sites with minimal or no apparent methane flux to the seabed (Treude et al., 2003; Boetius and Suess, 2004). These low-activity areas often contain carbonates with negative $\delta^{13}C$ values that are presumed to reflect previous AOM activity, yet it remains unclear how sediment and carbonate-hosted microbial communities differ between active and low-activity sites.

The recent quantification of active metabolic rates of methanotrophic microbial biomass living within the pore spaces of authigenic carbonates in active and low-activity areas further motivates the study of endolithic microbial communities (Marlow et al., 2014). Previous literature has characterized the common taxa associated with carbonates in methane-rich regimes such as cold seeps and mud volcanoes by examining lipid biomarkers (Blumenberg et al., 2004; Stadnitskaia et al., 2005, 2008; Gontharet et al., 2009) and 16S rRNA gene signatures (Reitner et al., 2005; Stadnitskaia et al., 2005, 2008; Heijs et al., 2006). These published findings have been used to discuss the paleo seepage record (Gontharet et al., 2009), as well as stages of carbonate formation (Reitner et al., 2005; Stadnitskaia et al., 2005, 2008; Bahr et al., 2009). Microbial communities associated with carbonate crusts and sediments have been broadly compared in the euxinic Black Sea (Stadnitskaia et al., 2005) and the eastern Mediterranean Sea (Heijs et al., 2006), but the extent to which methanotrophic communities within partially and fully lithified habitats differ from adjacent sediment-hosted communities at continental margin seeps remains largely unconstrained. Given the influence of AOM in methane processing, the community structure of carbonate-based habitats may exert a significant influence on methane and sulfur biogeochemical processes in the deep sea.

This study examines microbial abundance and community diversity in six structural classes of methane seep habitats (active sediments, active nodules, active carbonates, low-activity sediments, low-activity carbonates, and off-seep background sediments), which integrate two key environmental variables: seepage activity and physical substrate type. We analyze mineralogy, 16S rRNA gene archaeal and bacterial sequence diversity, and cell abundances of 12 samples, from six different deep-sea habitats associated with methane seepage at Hydrate Ridge, OR, USA (**Table 1**; **Figure 1**). With this dataset, we characterize the microbial diversity and the potential importance of seepage activity and substrate as determinants of microbial community structure in and around methane seeps.

METHODS

SITE DESCRIPTION

Microbial DNA samples were collected from active and low-activity sites around Hydrate Ridge, Oregon, a convergent tectonic margin well established as a site of methane seepage and sediment-based AOM (e.g., Suess et al., 1999; Tryon et al., 2002; Treude et al., 2003). Samples were collected in consecutive years, with the *DSV Alvin* during R/V *Atlantis* leg AT-15-68 (September 2010), and with the *ROV Jason* during *Atlantis* leg AT-18-10 (September 2011). Two samples representative of each substrate-activity pairing were used in this study—one from Hydrate Ridge North (44°40.25′N, 125°06.30′W, ∼600 m water depth), and one from Hydrate Ridge South (44°34.09′N, 125°09.14′W, ∼780 m water depth), a separation distance of approximately 11.2 km. Sampling at two distinct seep-influenced locations at Hydrate Ridge confers interpretive power across a relatively broad spatial scale (km rather than meters). Active nodules were recovered from a corresponding active sediment push core (i.e., AN-3730N refers to a carbonate nodule found within the AS-3730 sediment core). Background sediment was collected from an off-seep site approximately 15 km east of Hydrate Ridge (**Table 1**, **Figure 1**). The sulfate-methane transition zone (SMTZ) at Hydrate Ridge active seep sites has been reported to occur within the top several cm of seafloor sediment, corresponding to peak values of microbial aggregate abundance, methane oxidation, and sulfate reduction (Boetius et al., 2000; Boetius and Suess, 2004). Methane concentrations within the most active seep sediments reach several mM, and have been measured and modeled at values up to

Table 1 | Identification numbers, site location details, and mineralogical identifications of carbonate, sediment, and nodule samples used in this study from the Oregon margin, USA.

Identification number	Seep activity level	Sample depth horizon	Physical substrate type	Site	Location (latitude, longitude)	Water depth (m)	Mineralogy
AS-3730	Active	0–6 cm	Sediment	HR South	44°34.20′,125°8.87′	775	Quartz
AS-5119	Active	6–9 cm	Sediment	HR North, site 7	44°40.02′, 125°5.99′	600	Quartz
AN-3730N	Active	0–6 cm	Nodule	HR South	44°34.20′, 125°8.87′	775	Q/C/A Mix
AN-5119N	Active	6–9 cm	Nodule	HR North, site 7	44°40.02′, 125°5.99′	600	Q/C/A Mix
AC-3439	Active	Seafloor*	Carbonate	HR South	44°34.11′, 125°9.17′	774	Aragonite
AC-5120	Active	Seafloor*	Carbonate	HR North, site 7	44°40.02′, 125°6.00′	601	Dolomite
LS-3433	Low activity	0–6 cm	Sediment	HR South	44°34.23′, 125°8.80′	774	Quartz
LS-5164	Low activity	6–9 cm	Sediment	HR North, site 8	44°40.05′,125°6.03′	601	Quartz
LC-3662	Low activity	Seafloor*	Carbonate	HR South	44°34.09′, 125°9.18′	788	Aragonite
LC-5189	Low activity	Seafloor*	Carbonate	HR North, site 8	44°40.06′, 125°6.04′	604	Q/C/A Mix
OS-3487	Off-seep	0–5 cm	Sediment	Off-seep	44°35.27′, 124°53.50′	600	Quartz
OS-3582	Off-seep	10–15 cm	Sediment	Off-seep	44°35.28′, 124°53.56′	589	Quartz

Identification numbers are encoded with information regarding the seepage activity of the sample site (A, active; L, low-activity; O, off-seep) and the physical substrate type (S, sediment; N, nodule; C, carbonate rock). Q/C/A Mix, refers to a mineralogical mixture of quartz, calcite, and aragonite.

**All carbonate rocks were collected from the seafloor; samples used for mineralogical, cell count, and phylogenetic analysis were manually isolated from endolithic fractions >5 cm from the exposed surface.*

70 mM (Boetius and Suess, 2004) and 50 mM (Tryon et al., 2002), respectively.

SAMPLE COLLECTION AND PROCESSING

On the seafloor, sediment was collected in push cores (35 cm long) deployed by the *ROV Jason* or *DSV Alvin*. Individual carbonate rocks were collected with the manipulator arm and placed inside Plexiglas compartments in a subdivided, insulated biobox with a lid to minimize water column or cross-sample contamination during recovery. During ascent to the surface, supersaturated methane may have degassed during depressurization, as was apparent from gas pockets in core tubes. Shipboard, push cores and carbonates within their respective plexiglass containers were immediately transferred to a 4°C walk-in cold room and processed within several hours. Samples intended for DAPI (4′,6-diamidino-2-phenylindole) counts and fluorescence *in situ* hybridization (FISH) were fixed in 2% paraformaldehyde and stored at 4°C overnight, while samples intended for DNA extraction were frozen at −80°C. The next day, the formaldehyde was washed from the sample with sterile 1× PBS buffer and then replaced with 100% ethanol and transferred to a −80°C freezer. In the case of carbonate rocks, interior portions (≥5 cm from an exposed surface) were isolated to ensure the analysis of endolithic communities; this was done by breaking the sample with an autoclaved ceramic mortar and pestle and removing the outer surface with a sterile razor blade. Similar mortar and pestle treatment of sediment and subsequent DAPI visualization confirmed that aggregate morphology is not an artifact of carbonate sample preparation.

X-RAY DIFFRACTION

Samples for X-ray diffraction analysis (XRD) were powdered with an autoclaved ceramic mortar and pestle. The diffraction profiles were measured with a Phillips X'Pert Multi Purpose X-Ray Diffractometer housed in the Division of Materials Science at Caltech. SiO_2 was used as an internal standard, and best-fit analyses (with peak-shifting permitted) were conducted with the X'Pert HighScore software and its library of diffractograms.

The analysis of XRD data focused on four components: quartz (SiO_2), calcite ($CaCO_3$), dolomite [$CaMg(CO_3)_2$], and aragonite ($CaCO_3$). These minerals are the primary constituents of seep-associated carbonates (Greinert et al., 2001). The following peaks were used as diagnostic markers following peak-shifting: calcite (104) $2\theta = 30.0°$, dolomite (104) $2\theta = 31.2°$, aragonite (221) $2\theta = 46.0°$, and quartz (011) $2\theta = 27.0°$ (Kontoyannis and Vagenas, 2000; Zhang et al., 2010). Each of these peaks is the most prominent for its respective mineral type, allowing for qualitative compositional characterization by relative peak heights (Tennant and Berger, 1957; Bergmann, 2013). Minor constituents not accounted for by the four components described above cannot be ruled out, but these four peaks, as well as the additional peaks associated with each mineral, account for the majority of XRD features in all spectra.

MICROSCOPY DETERMINATION OF RELATIVE MICROBIAL BIOMASS

Formaldehyde/ethanol fixed samples of carbonate and sediments were prepared for microbial aggregate characterization and FISH as follows. Nodules and interior carbonate pieces were pulverized with an autoclaved porcelain mortar and pestle. To concentrate biomass away from mineral and sediment particles, a percoll density separation was performed on all samples following a modified protocol outlined in Orphan et al. (2001b). Specifically, 60 µl sample was mixed with 1290 µl TE (pH = 9.0) and heated for 3 min at 60°C to permeabilize cells. The sample tubes were placed on ice for 5 min; 4.5 µl of 30% H_2O_2 was then added (to deactivate native peroxidase for CARD-FISH) and incubated at room temperature for 10 min. Tubes were placed back on ice, and 150 µl 0.1 M sodium pyrophosphate was introduced. Sample

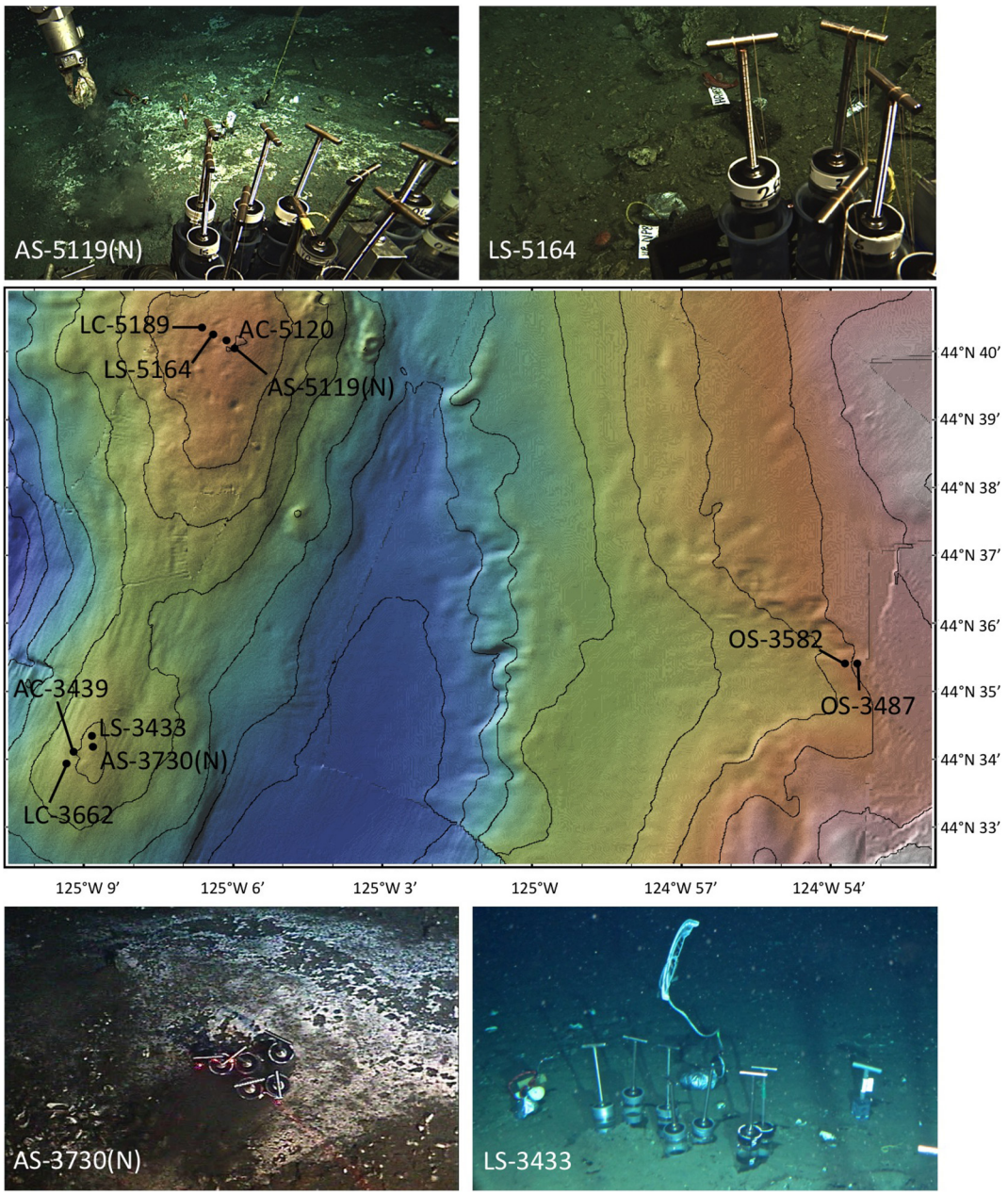

FIGURE 1 | A map of Hydrate Ridge, OR, showing the locations of origin of the samples used in this study, accompanied by images showing the general locations of sample collection. Samples LC-5189, LC-5164, AC-5120, AS-5119, and AS-5119N were collected from Hydrate Ridge north (mound summit ~600 m depth); samples AC-3439, LS-3433, LC-3662, AS-3730, and AS-3730N were collected from Hydrate Ridge south (mound top ~780 m depth); samples OS-3582 and OS-3487 were collected off-seep from a water depth of ~600 m. Hydrate Ridge north and south sampling sites were located approximately 12 km apart. Base map is derived from Global Multi-Resolution Topography (GMRT, Ryan et al., 2009; GeoMapApp); contour lines represent 100 m of depth, and each minute of latitude represents 1.85 km. In the images, push cores are 10 cm in diameter for scale.

mixtures were sonicated (Branson sonifier 150) on ice 3 times at 8 W (10 s each time) and overlaid on a percoll density gradient. The gradient tubes were then centrifuged at 4800 rpm for 15 min at 4°C (Allegra X-15R, Beckman Coulter, Indianapolis, IN). The percoll supernatant overlaying the sediment/carbonate pellet was removed and concentrated by vacuum filtration through both a 3 μm and a 0.22 μm white polycarbonate filter (Millipore). Filtered samples were immediately rinsed with 2 ml sterile 1× PBS and dehydrated with 2 ml of a 1:1 ethanol:PBS solution while on the filter tower. Dried filters were removed and stored in the dark at 4°C prior to analysis. Cell counts were performed on an epifluorescence microscope (Olympus BX51) under 60× magnification (Plan Apo N objective) using the general DNA stain DAPI (4′,6-diamidino-2-phenylindole). 25 fields

Table 2 | Cell abundance parameters from all seep-associated samples.

Sample	Number of aggregates/cm^3	Mean aggregate diameter, μm (*SD*)	Aggregate biovolume factor (*SD*)	Proportion of single cells	Cell abundance (per cm^3)	Relative cell abundance
AS-3730	9.59E+07	6.2 (1.3)	1* (0.19)	0.15	1.99E+10	0.77
AS-5119	8.67E+07	5.7 (1.1)	1* (0.19)	0.18	1.45E+10	0.56
AN-3730N	1.04E+08	6.8 (1.7)	0.46* (0.03)	0.12	1.26E+10	0.49
AN-5119N	1.07E+08	6.4 (1.9)	0.46* (0.03)	0.16	1.14E+10	0.44
AC-3439	1.35E+08	10.2* (2.2)	0.215* (0.07)	0.11	2.57E+10	1.00
AC-5120	1.37E+08	9.7 (2.3)	0.215* (0.07)	0.16	2.36E+10	0.92
LS-3433	4.08E+07	6.2 (0.9)	0.88 (0.16)	0.29	8.92E+09	0.35
LS-5164	5.16E+07	5.8 (1.4)	0.88 (0.16)	0.31	9.50E+09	0.37
LC-3662	6.49E+07	5.6 (1.7)	0.35 (0.05)	0.28	4.10E+09	0.16
LC-5189	6.23E+07	5.9 (1.6)	0.35 (0.05)	0.23	4.30E+09	0.17
OS-3487	NA	NA	NA	> 0.99	1.93E+08	7.50E-03
OS-3582	NA	NA	NA	> 0.99	1.50E+08	5.85E-03

*Values marked with * indicate data from Marlow et al. (2014). SD = standard deviation.*

of view were counted for each of the 10 seep-linked samples (**Table 2**).

The architecture of DAPI-stained aggregates was examined by acquiring a z-stack of epifluorescence images with a DeltaVision RT microscope and the associated Softworx program (Applied Precision, Inc., Issaquah, WA). Subsequent image processing was conducted with the DAIME image analysis and 3D visualization program (Daims et al., 2006). By recognizing fluorescently stained cells within manually delineated aggregate boundaries throughout a z-stack of images, DAIME is able to calculate biovolume and the pair correlation function. Biovolume is determined by dividing the 3D integrated volume of cells by the overall aggregate volume, and the peak pair correlation value corresponds to the most favored cell-cell distance (Daims et al., 2006). Biovolume and pair correlation values were obtained from five representative aggregates from each habitat; individual cell sizes were broadly consistent for all samples.

Relative microbial abundance within the 12 distinct samples was determined by calculating the cumulative aggregate volume per unit volume sample, dividing by a typical cell (1 μm diameter) volume, multiplying by the maximum possible spherical packing density (0.7405; Steinhaus, 1999), and scaling by the DAIME-determined biovolume aggregate factor. The abundance of single cells (recovered on the 0.22 μm filter) was then added to the aggregate value, and the sum of both aggregate-associated cells and single cells was divided by the largest cell abundance calculated for the dataset (sample AC-3439). Resulting values thus indicate the fraction of microbial cell abundance associated with each sample, relative to the sample with the highest cell count. This calculation did not distinguish between Archaea and Bacteria, and overall microbial abundance scaling factors (**Table 2**) were applied to both Domains' diversity charts (**Figures 2**, **3**).

PHYLOGENETIC ANALYSIS

To assess 16S rRNA gene diversity, the following workflow was performed for all 12 samples. DNA was extracted from ∼0.5 g of sediment or pulverized nodule/carbonate material using the UltraClean Soil DNA isolation kit (Mo Bio Laboratories, Carlsbad, CA). Bacterial and archaeal 16S rRNA genes were amplified in separate Polymerase Chain Reactions (PCR) with 27F (5′-AGAGTTTGATCCTGGCTCAG-3′)/1492R (5′-GGYTACCTTGTTACGACTT-3′) and Arc8F (5′-TCCGGTTG ATCCTGCC-3′)/Arc958R (5′-YCCGGCGTTGAMTCCAATT-3′) primers, respectively (all primer concentrations were 0.4 μM, primers from Integrated DNA Technologies, Inc., Coralville, IA), New England BioLab's *Taq* DNA Polymerase (NEB, Ipswich, MA), 0.4 μM dNTP solution mix (NEB), and 1× ThermoPol Reaction Buffer (NEB). PCR was performed on an Eppendorf Mastercycler Ep Gradient S thermocycler with a 2-min 95°C initialization, followed by 35 cycles of a 30 s 94°C denaturation, 60 s 54°C annealing, and 90 s 72°C elongation. A final 7-min 72°C elongation completed the procedure, at which point the block was cooled to 4°C until samples were retrieved (<15 h). 16S rRNA gene amplicons were cleaned by filtration through a Millipore MultiScreen Filter Plate (Millipore Corp., Billerica, MA) and cloned using the TOPO TA Cloning Kit following the manufacturer's instructions (Invitrogen, Carlsbad, CA). For bacterial analysis, 288 transformants (colonies) were picked for each sample, an average of 233 of which contained appropriately sized inserts. For archaeal clone libraries, 192 colonies were picked for each analysis, and an average of 168 of these colonies contained the correctly sized insert. A random subset of clones in each library (Table S1) were selected and sequenced by Laragen, Inc. (Culver City, CA). Archaeal amplicons were sequenced in one direction (∼900 bp), using the T3 primer (5′-ATTAACCCTCACTAAAGGGA-3′), while bacterial inserts were sequenced bi-directionally, using the T3 primer and the T7 primer (5′-TAATACGACTCACTATAGGG-3′). Vector sequence was removed and contigs (∼1500 bp) were constructed (90% minimum match, 10 base minimum overlap) using forward and reverse sequences from the same clone; when one direction of sequence passed quality control inspection but the other did not, the low quality sequence was not used. Chimeric sequences were identified with the Slayer, Uchime, and Bellerophon programs; non-chimeric sequences were manually aligned in ARB

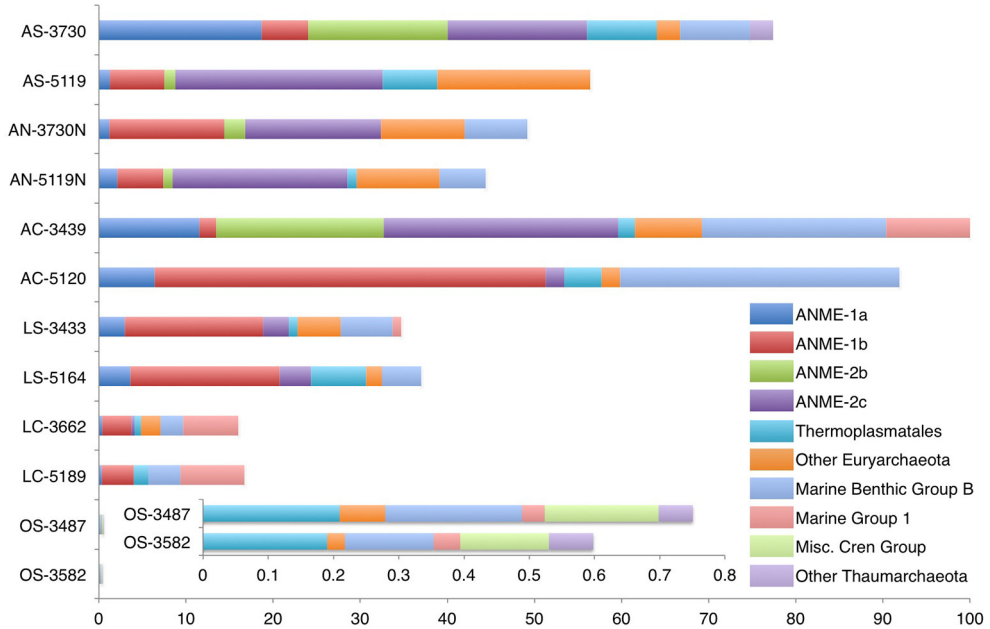

FIGURE 2 | Distribution of archaeal 16S rRNA gene sequences recovered from carbonate, nodule and sediment samples. Phylogenetic groups that account for at least 20% of overall abundance in one or more samples are shown. In all cases, bar lengths are scaled by the microbial abundance observed in each sample, with AC-3439, which has the highest microbial abundance, as the longest bar (see **Table 2**). Each bar segment length represents the microbial abundance-weighted proportion of that sample's clones falling within the phylogenetic group in question. Inset: Off-seep samples OS-3487 and OS-3582 have biomass values orders of magnitude lower than those of seep-associated samples.

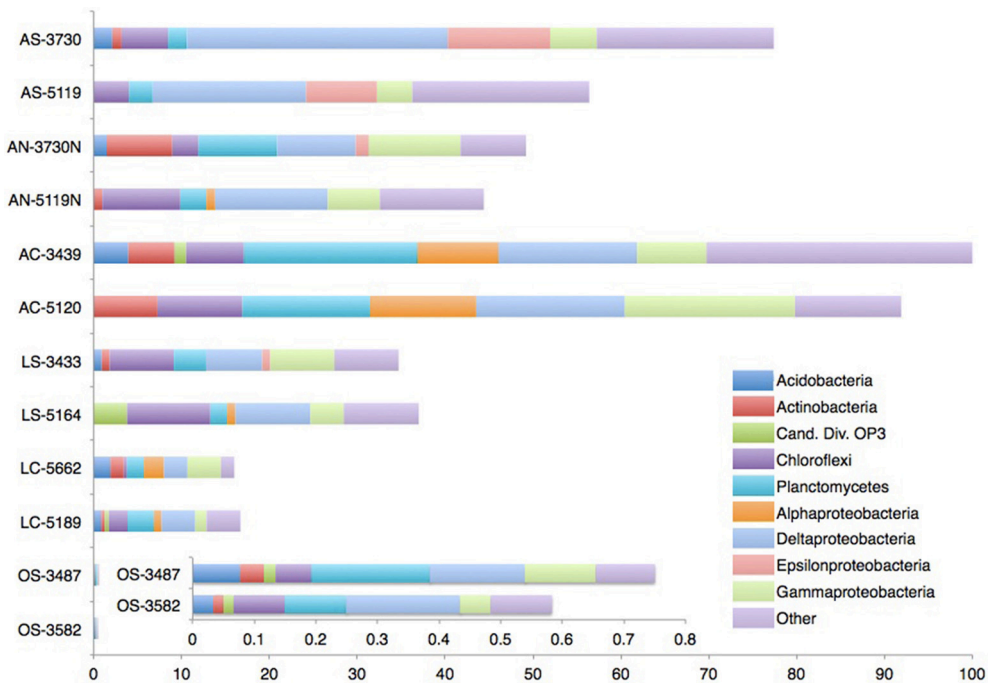

FIGURE 3 | Distribution of bacterial 16S rRNA gene sequences recovered from carbonate, nodule and sediment samples. Phylogenetic categories representing phyla (or class, in the case of *Proteobacteria*) that account for at least 10% of overall abundance in one or more samples are shown. Bar lengths are scaled as in **Figure 2**.

(Ludwig et al., 2004) in reference to the Silva 111 NR98040812 database and used for subsequent phylogenetic analysis. The sequences were submitted to Genbank with the following accession numbers: KF616551-KF616600; KF616676-KF616751; KM356307-KM357226. See Table S1 for the number of sequences involved at each stage of analysis.

Non-metric multidimensional scaling (MDS) treatments and analysis of similarity (ANOSIM) were performed on these sequences in Primer 6.1.13 (Clarke and Primer, 2006) using Bray-Curtis similarity matrices that had been square-root transformed to prevent artificial over-emphasis of abundant taxa on community structure (Legendre and Legendre, 1998). Chao, Inverse Simpson, Bray-Curtis, and Weighted Unifrac indices were calculated from 97% sequence similarity OTUs in reference to the Silva 104 NR99100211 database using the Mothur platform (Schloss et al., 2009).

RESULTS AND DISCUSSION

In this study, the microbial abundance and diversity of 12 samples representing six classes of methane seep habitats (**Table 1**) are assessed with the aim of establishing the influence of seepage activity and physical substrate type on the microbial community. Mineralogical examination, cell abundance calculations, and 16S rRNA gene archaeal and bacterial sequences, as well as statistical analyses of sequence diversity, reveal distinct patterns in, and raise intriguing questions about, the forcing of microbial community structure at methane seep-associated habitats.

MINERALOGY OF AUTHIGENIC CARBONATES IN THE SEEP ENVIRONMENT

XRD analysis of the 12 samples considered in this study supports four broad categories of mineralogical identification (**Figure S1**): sediments containing a dominant siliciclastic component identified as quartz (AS-3730, AS-5119, LS-3433, LS-5164, OS-3487, OS-3582); quartz, aragonite, and calcite mixtures (AN-3730N, AN-5119N, LC-5189); aragonitic carbonate rocks (AC-3439, LC-3662); and a dolomitic carbonate (AC-5120). Sediment with a low carbonate component was also reported by Orphan et al. (2004); the high proportion of quartz suggests a significant contribution from continental silicate weathering products, while other components including iron sulfide minerals are also likely present (Jørgensen et al., 2004; Van Dongen et al., 2007).

Changes in porewater chemistry with depth in the sediment column, particularly sulfate concentration, are hypothesized to influence mineralogy during precipitation (Burton, 1993; Savard et al., 1996; Naehr et al., 2007). Among carbonate precipitates, aragonite is the most thermodynamically favored pseudomorph in high-sulfate, high-alkalinity conditions above the SMTZ (Burton, 1993; Savard et al., 1996), and, in particular, at Hydrate Ridge seafloor environmental conditions (Greinert et al., 2001). Calcite is believed to form lower in the sediment column where sulfate is depleted (Naehr et al., 2007), and seep-associated dolomites have $\delta^{13}C$ and $\delta^{18}O$ values that have been interpreted as consistent with formation in deeper methanogenic sediment horizons (Naehr et al., 2007; Meister et al., 2011). Mineralogical differences may thereby record information about the depth and local porewater composition during precipitation.

RELATIVE MICROBIAL ABUNDANCE

Relative cell abundance calculations (**Table 2**) demonstrate that active carbonates, which contained more abundant and larger, but less densely packed cell aggregates, exhibited the highest cell counts of all sample types, with AC-3439 containing the highest cell abundance of the sample set. Active seep sediment samples contained 77% (AS-3730) and 56% (AS-5119) as many visible cells as the active carbonate AC-3439. Active carbonate nodule microbial abundance was roughly half that of active carbonates (49 and 44%, compared with 100 and 92% for active carbonate samples). Both nodule samples (AN-3730 and AN-5119) contained more (though less densely-packed) aggregates than the corresponding sediment horizons (AS-3730 and AS-5119) from which they were collected. Samples collected from areas of lower seepage activity had fewer microbial aggregates and larger numbers of single cells, resulting in relative cell abundance values of 35 and 37% for low-activity sediments (LS-3433 and LS-5164, respectively) and 16 and 17% for low-activity carbonates (LC-3662 and LC-5189, respectively). The microbial abundance of off-seep background sediments was approximately two orders of magnitude lower than active seep and low-activity samples and was comprised almost exclusively of single cells.

Archaeal and bacterial diversity in seafloor methane seep sediments, carbonate nodules, and carbonate slabs were characterized by 16S rRNA gene clone libraries. Supplementary Data files 1 and 2 provide the genus-level phylogenetic assignments of each sequence. Combining the relative abundance of 16S rRNA genes from archaeal and bacterial clone libraries with bulk microbial abundance data of unknown domain-level distribution (**Table 2**), abundance-scaled charts of phylogenetic distributions were generated (**Figures 2**, **3**).

ARCHAEAL COMMUNITY CHARACTERIZATION

Euryarchaeota belonging to diverse ANME groups dominated the archaeal 16S rRNA gene sequences recovered from active seep sediments (82.4% of all archaeal clones; percentages compiled from pooled sequences of a given sample type, see Supplementary Data file 1c). Similarly, ANME sequences comprised 84.3% of the total archaeal diversity from active nodules; this proportion was 59.6% for archaeal sequences recovered from active carbonates and 71.1% for archaeal sequences from low-activity sediments. Archaeal clone libraries constructed from low-activity carbonates showed a smaller proportion of ANME sequences, representing 24.7% of all archaeal sequences, while ANME sequences were not recovered in off-seep background sediment clone libraries, which instead contained abundant representatives of the uncultured Thaumarchaeotal lineage Marine Benthic Group B (MBGB) (Vetriani et al., 1999).

Among ANME representatives, ANME-1—predominantly the ANME-1b subgroup (Teske et al., 2002)—were more abundant in low-activity samples (83.1% of all ANME sequences from low-activity sediments and carbonates; Supplementary Data file 1e) than samples associated with actively venting seeps (34.2% of pooled ANME sequences from active sediments, nodules, and carbonates). ANME-2—mostly the ANME-2c subgroup (Orphan et al., 2001a)—exhibited the opposite pattern, accounting for 58.3% of ANME sequences recovered from active samples and

13% from low-activity samples. The exception to this trend is the phylogenetic distribution of sequences recovered from the active dolomitic sample AC-5120, whose archaeal clone library contained 48.8% ANME-1b and 2.3% ANME-2c representatives. Members of the ANME-3 group were observed in most active and low-activity seep sediment samples and carbonate nodules (6.8% of total archaeal diversity on average among these samples), but were not recovered from any of the seafloor exposed carbonate rock samples or off-seep sediments (Supplementary Data file 1).

Members of the ANME lineages are the dominant Archaea linked to sulfate-coupled methane oxidation at marine methane seeps (Knittel and Boetius, 2009), and their environmental abundances often correlate with methane flux in sulfate-perfused, anoxic sediment near the seabed. When compared with 16S rRNA gene sequences recovered from active seep sediments, our data demonstrate that the carbonate rock substrate variable accounted for an approximate 25% decrease in ANME sequence abundance relative to active sediments. [To make this calculation, active carbonate archaeal sequences were pooled ($n = 94$ sequences), relative abundance was determined, and this value was compared with the analogous value derived from combined active seep sediment samples ($n = 74$ sequences); see Supplementary Data file 1c]. Low seepage activity accounted for a 14% decrease (pooled low-activity sediment sequences compared with combined active seep sediment sequences). When low-activity carbonate samples' sequences were pooled, a 70% decrease in ANME relative abundance (compared with active sediment samples) was observed. This finding suggests that the combination of factors relating to methane seepage activity (low-activity) and physical substrate (carbonate) negatively impacts the relative ANME abundance more than the sum of each factor individually. For example, in low-activity carbonate habitats, anaerobic archaeal methanotrophs may become energy or carbon limited as a result of self-entombment (e.g., Luff et al., 2004). Additionally, unfavorable geochemical conditions associated with decreased methane flux and/or the intrusion of oxygenated seawater after exposure on the seafloor may limit the successful persistence of these obligate anaerobes. Other archaeal groups—most notably marine group 1 (MG 1) Thaumarchaeota—were more prevalent in low-activity carbonate communities, which may be attributable to their colonization of a habitat less suitable for anaerobic methanotrophs and/or a diminished ability of MG 1 to inhabit the reducing active seep settings.

ANME-1 are believed to be better adapted to lower sulfate and/or methane conditions than their ANME-2 counterparts based on observations of niche differentiation in Japan Sea sediments (Yanagawa et al., 2011), Black Sea mats (Blumenberg et al., 2004), diffusion driven continental margin sediments (Harrison et al., 2009), and other environmental comparisons (Nauhaus et al., 2005; Rossel et al., 2011). Our findings corroborate this trend: ANME-1 representatives constituted 25.5% of archaeal sequences from active seep sites and 37.9% of combined archaeal sequences recovered from low-activity sediment and carbonate samples (Supplementary Data file 1d). It remains unclear whether all members of the ANME-1 are methanotrophs physiologically adapted for low-methane conditions, or facultative methanogens (Reitner et al., 2005; House et al., 2009; Lloyd et al., 2011), a metabolic plasticity that would confer a competitive advantage in zones of limited methane. The relative abundance of ANME-1 sequences recovered from AC-5120 is markedly higher than that of other active-site samples, an observation that may suggest a contributing role of mineralogy in community structure (**Figure 2**, see discussion below). ANME-3 representatives were not recovered in our carbonate rock diversity surveys. Whether this is due to their relative low abundance in the Hydrate Ridge ecosystem overall (∼9% of archaeal sequences in active seep sediments) or if the apparent absence of ANME-3 in carbonates is indicative of habitat preference requires further investigation (Supplementary Data file 1). Members of the ANME-3 are typically reported as minor constituents from diverse seep sediment habitats and have only been reported as a dominant member from one site (Haakon Mosby mud volcano) to date (Lösekann et al., 2007).

Archaeal lineages not traditionally linked to methane oxidation also demonstrate activity-based trends. Euryarchaeotal Thermoplasmata were detected in 11 of the 12 samples, comprising a low percentage of the total archaeal sequences in active seep (5.2%) and low-activity samples (9.5%), and were observed at substantially higher proportions in off-seep background samples (31%; Supplementary Data file 1d). Sequences from the Halobacteria class, related to sequences from methane seep sediments (Harrison et al., 2009) or hydrothermal vents (Schauer et al., 2009), were recovered in low abundance (2.5% average of archaeal sequences, across all samples) from nearly all sample types with the exception of active carbonates.

The most prevalent thaumarchaeotal classes included MBGB and MG1. Sequences most closely related to the MBGB family, whose representatives are common in anoxic sediments (Vetriani et al., 1999), including those influenced by methane (Biddle et al., 2006), were abundant in clone libraries from all carbonates and low-activity and off-seep sediments (20.9% of pooled archaeal sequences recovered from these samples). The relative proportion of recovered MBGB sequences was lower in sediment and nodules from active seeps (8.9%). MG1 accounted for 39.5% (LC-3662) and 44% (LC-5189) of the total archaeal sequences of the two low-activity carbonate samples recovered from the seabed outside of active seepage areas; this proportion never exceeded 13.7% (AC-3439) in any of the other 10 samples.

The thaumarchaeotal class MG1 is pervasive in the deep-water column (Massana et al., 1997; Karner et al., 2001), and its high relative abundance in archaeal diversity surveys of the low-activity carbonates is likely reflective of seawater infiltration of these exposed carbonates at the seabed. Neither surface-exposed carbonates from active seep sites nor low-activity/off-seep sediments display the same MG1 abundance. This observation indicates that both low seepage activity (with low corresponding levels of methane and sulfide) and carbonate rock substrate appear to be necessary factors for MG1 prevalence, a finding that is consistent with MG1 acting as a passive colonizer of seawater-infused carbonates. In hydrothermal vent-associated basalt, MG1 representatives appear to be more abundant in weathered, off-vent samples (Lysnes et al., 2004) compared with initial communities in subseafloor hydrothermal environments (Huber et al., 2002). Channels of concentrated fluid flow developed by faulting and

exploited by upward advection of methane-rich fluids during periods of seep activity may serve as conduits for downward, tidally-enhanced fluid delivery (Tryon et al., 2002) during subsequent periods of quiescence. Convection (Aloisi et al., 2004) and hydrologic recharge mechanisms at mound bases (Paull et al., 1991; Teichert et al., 2005) may also remain active. These processes may have preferentially seeded carbonate rocks from low-activity settings, where upward advection is less prominent, with MG1 representatives from bottom water. Alternatively, the presence of MG1 organisms may represent a secondary colonization resulting from carbonate exposure to bottom water following exhumation. The low-activity and off-seep sediment samples encompassing the 0–6 cmbsf horizon (LS-3433 and OS-3487) displayed minimal MG1 representation, suggesting that they may be outcompeted in the sediment habitat. MG1 representatives have been implicated in ammonium oxidation (Konneke et al., 2005; Nicol and Schleper, 2006), but the metabolic proclivities of carbonate-associated MG1 is not currently known.

BACTERIAL COMMUNITY CHARACTERIZATION

Among bacterial sequences, Deltaproteobacteria was the most abundant class recovered from 8 of the 12 samples (AS-3730, AS-5119, AN-5119N, AC-3439, LS-5164, LC-5189, OS-3487, and OS-3582), and the second most abundant class detected in the remaining samples, with the exception of LS-3433 (Supplementary Data file 2c). Desulfobacteraceae and Desulfobulbaceae representatives were the most abundant deltaproteobacterial families recovered in active-seep samples (sediments, nodules, and carbonates), which likely reflects these taxa's role in AOM (e.g., Orphan et al., 2001a; Schreiber et al., 2010; Kleindienst et al., 2012; Green-Saxena et al., 2014). These families were abundant in bacterial diversity surveys from low-activity sediments as well (accounting for 75% of Deltaproteobacteria; Supplementary Data file 2d) but significantly less so in low-activity carbonates and off-seep sediments (15%), where members of the uncultured deltaproteobacterial groups SAR324 and SH765B-TzT-29 were more prevalent. Relatives from the SAR324 and SH765B-TzT-29 groups have been described from seafloor lavas (Santelli et al., 2008), South Atlantic Ocean sediment (Schauer et al., 2009), and river estuaries (Jiang et al., 2009). This geographic range suggests that these groups are widely distributed and have no particular dependence on methane geochemistry, though SAR324 methanotrophy has been proposed (Swan et al., 2011). Cultured representatives of these clades are lacking, but recent meta-omics approaches have begun to shed light on their physiological capabilities; members of the SAR324 clade associated with hydrothermal vent plumes, for example, have been implicated in several facultative metabolic modes, including sulfur and hydrocarbon oxidation (Sheik et al., 2014).

Epsilonproteobacteria most closely related to *Sulfurovum* sp. recovered from other methane seeps (Mills et al., 2005; Pernthaler et al., 2008; Beal et al., 2009) were prevalent in sediment samples from active seeps, but were detected at very low relative abundances in other active seep habitats including nodules and carbonate rocks. This observation potentially reflects a substrate-based control on diversity (Supplementary Data files 2b,c). Similar trends between seep sediments and their associated carbonate nodules were observed in an additional set of cores from Hydrate Ridge and Eel River Basin seeps (Mason and Orphan, personal observation). *Sulfurovum* from deep-sea hydrothermal vents are capable of multiple sulfur oxidation pathways (Yamamoto et al., 2010), and representatives of this genus have been described from methane seep sediments (Arakawa et al., 2006; Roalkvam et al., 2011) and methane-impacted terrestrial mud volcanoes (Green-Saxena et al., 2012). In this study, the near-exclusive presence of *Sulfurovum* in active sediments—even in horizons 6+ cm beneath the seafloor (AS-5119)—suggests that these environments contain dynamic sulfur cycles, with sulfide produced through sulfate-coupled AOM potentially being re-oxidized to sulfate by members of the Epsilonproteobacteria and Gammaproteobacteria.

Aerobic methanotrophic activity has been documented using radiotracer methods in sediments and carbonates from both actively seeping and low-activity locations at Hydrate Ridge (Marlow et al., 2014). Surprisingly, the majority of samples lacked 16S rRNA evidence of known aerobic methanotrophs with the exception of AC-5120, a dolomite sample collected from an active seep site, where sequences affiliated with gammaproteobacterial Methylococcales comprised 8% of recovered sequences (Supplementary Data file 2a). In contrast to the 16S rRNA findings, previous studies have reported the common occurrence of diverse particulate methane monooxygenase (*pmo*) genes related to gammaproteobacterial aerobic methanotrophs in surface sediments within seeps (Tavormina et al., 2008) as well as from the water column overlying seeps, at more than 50 times the abundance of sites over non-seep locations (Tavormina et al., 2010). Whether this general discrepancy between 16S rRNA and *pmo* findings is due to primer bias, low gammaproteobacterial methanotroph abundance, or the occurrence of as yet unidentified methane-oxidizing bacteria requires further investigation.

Verrucomicrobia—some of whose members have been implicated in aerobic methanotophic metabolism (Op den Camp et al., 2009)—were recovered only from active seep carbonates, comprising 7% of pooled active carbonate bacterial sequences (Supplementary Data file 2c). This sample-based specificity may suggest a dependence on methane or other geochemical components associated with active seeps. In addition, an indirect stimulation of heterotrophy (Freitas et al., 2012) associated with the high microbial abundances linked to active carbonates could sustain members of this phylum. The most closely related Verrucomicrobia sequences were reported from deep-sea sediment unaffiliated with methane seepage (Schauer et al., 2009), though some members of the phylum have been recovered from authigenic carbonate crusts linked to mud volcano AOM (Heijs et al., 2006).

DIVERSITY ANALYSIS: ENVIRONMENTAL CONTROLS ON COMMUNITY STRUCTURE

Alpha (within sample) and beta (between sample) diversity statistics demonstrate how communities are structured and how they relate to each other (**Table 3**). Examining how environmental variables such as seep activity and substrate type map onto these

Table 3 | Chao-1 and Inverse Simpson values for Archaeal and Bacterial clone libraries made from each of the 12 samples examined in this study.

Sample	Archaea				Bacteria			
	Chao-1	Chao-1 LCI, HCI	Inv simpson	Inv simpson LCI, HCI	Chao-1	Chao-1 LCI, HCI	Inv simpson	Inv simpson LCI, HCI
AS-3730	10	9.1, 19.7	7.3	5.2, 11.9	109	56.0, 279.4	14.5	10, 25.9
AS-5119	8.5	8, 16.3	4.4	3.1, 7.2	41.1	29.2, 80.5	16.6	9.5, 64.1
AN-3730N	8.5	8, 16.3	5.2	3.9, 7.7	28.3	19.7, 64.7	13.8	8.7, 33.1
AN-5119N	8.5	8, 16.3	4.1	2.9, 7.4	58	34.1, 138.4	15	9.2, 40.2
AC-3439	11	10.1, 20.7	6.2	4.9, 8.5	103.1	71.6, 178.4	49.1	30.9, 120.5
AC-5120	6.5	6, 14.3	2.8	2.2, 3.8	52.2	33.3, 114.5	28.3	17.4, 74.8
LS-3433	10	9.1, 19.7	4.5	3, 9	61.2	37.8, 135.1	41.1	24.7, 121.8
LS-5164	9	8.1, 21.9	4.1	2.8, 7.5	32.4	25.5, 58.9	29.3	19, 63.9
LC-3662	15	10.8, 42.1	4.6	3.3, 7.5	86.8	47.6, 208	41	24.1, 137.6
LC-5189	7	6.1, 19.7	3.5	2.8, 4.8	97	54.7, 218.5	78	41.2, 720.7
OS-3487	20.5	14.3, 55.5	7.9	5.5, 13.9	45.4	32.1, 88.3	32.8	19.6, 101.4
OS-3582	14.5	13.2, 25.5	8.9	6.4, 14.7	60.2	36.8, 134.1	32.2	18.4, 127.3

Larger values indicate higher alpha diversity. LCI and HCI indicate the 95% low-end and high-end confidence intervals, respectively.

relationships can help reveal factors that may play a role in determining microbial community structure. Such analysis may also help us understand the ecology of animal consumers, which exhibit trophic partitioning of microbial resources at Hydrate Ridge (Thurber et al., 2012; Levin et al., 2013).

Alpha diversity analyses, as computed by Chao-1 and Inverse Simpson values, provide comparative information capturing the two main components of community diversity: richness and evenness. Inverse Simpson values, which incorporate both parameters, reveal higher diversity in recovered bacterial sequences compared with archaeal sequences, a finding in agreement with Heijs et al.'s (2006) analysis of carbonate crust-associated microbial communities from Mediterranean mud volcanoes. A high degree of localized heterogeneity among Bacteria at the 97% sequence similarity OTU level was also observed, and archaeal diversity was substantially higher at off-seep locations compared with seep-associated sites, suggesting a larger range of niches available to Archaea in such environments (**Table 3**). There is no clear distinction in Chao-1 values between active and low-activity samples for archaeal and bacterial communities in sediment and carbonates, but bacterial communities in low-activity sediments and carbonates do exhibit higher Inverse Simpson values than their active-site counterparts. This finding suggests that bacterial communities in active seep habitats are dominated by lineages dependent upon seep-based physico-chemical conditions and/or groups associated with methanotrophic archaea. However, with longer residence time on the seafloor—during which alteration products or additional mineral phases can develop and the reducing, anoxic conditions related to active seep environments can dissipate—a broader range of methane-independent metabolic (or physical) niches may become available. A similar link between bacterial diversity and the degree of substrate alteration in weathered seafloor basalts was observed by Santelli et al. (2009). We observed no correspondence between sample-specific archaeal and bacterial alpha diversity metrics (linear best fit R^2 values were 2.8×10^{-5} and 0.029 for Chao-1 and Inverse Simpson inter-domain comparisons, respectively), suggesting that the two Domains respond differently to physico-chemical and ecological drivers of diversity (**Figure S2**).

Beta diversity analyses were used to characterize community differences among different habitat types. After sequences were combined by either activity level or substrate type, the dependence of community structure on these environmental variables was evaluated. Through our assessment of seep activity, we established a scale from most methane seep activity ("active") to least ("off-seep"), with "low-activity" occupying an intermediate position. If seep activity is an important control on diversity, active and low-activity communities would be more similar than active and off-seep communities as judged by beta diversity metrics. Similarly, off-seep and low-activity communities would be less divergent than off-seep and active communities. Equivalent expectations can be stated regarding substrate type, along the sliding scale of lithification, from least ("sediment") to most consolidated ("carbonate"), with "nodules" as the intermediate group.

Beta diversity statistics were used in order to evaluate not only significant differences between communities, but also the relative magnitude of such differences (**Figure 4**). Bray-Curtis analysis (Bray and Curtis, 1957) quantifies the similarity between samples based on the relative abundances of constituent OTUs, while weighted UniFrac (Lozupone et al., 2007) statistics incorporate phylogenetic distances between constituent 16S rRNA gene sequences; both approaches can be used as distance measures (Faith et al., 1987; Lozupone et al., 2011). Our results indicate that off-seep and low-activity archaeal and bacterial communities are more similar than off-seep and active communities. Similarly, active and low-activity archaeal and bacterial communities are more similar than active and off-seep communities (**Figures 4A,C**). The wide range in archaeal beta diversity comparison values, particularly noticeable in **Figure 4A**, suggests that archaeal communities are more strongly shaped by seepage, and that even low apparent methane flux moves the community away

Seep Activity

A

Bray-Curtis distance

	Active	Low-Activity	Off-Seep
Active		38.3	22.1
Low-Activity	44.7		36.3
Off-Seep	4.9	8.1	

C

Weighted Unifrac

	Active	Low-Activity	Off-Seep
Active		32	27
Low-Activity	64		30
Off-Seep	50	58	

Physical Substrate

B

	Sediment	Nodule	Carbonate
Sediment		38.9	20.1
Nodule	50.2		25.5
Carbonate	35.8	46.1	

D

	Sediment	Nodule	Carbonate
Sediment		33	24
Nodule	72		25
Carbonate	71	65	

FIGURE 4 | Results from beta diversity analyses of sequences binned by seep activity (A,C) or physical substrate (B,D). (A,B) provide Bray-Curtis similarities derived from comparison of proportional abundances of 97% sequence similarity OTUs. **(C,D)** Show weighted UniFrac-derived data for which all pairwise *P*-values are < 0.001. Green-shaded fields contain data from archaeal sequences; blue-shaded fields contain Bacteria-specific data. Weighted UniFrac values were subtracted from 1 and multiplied by 100 to provide a more intuitive statistic; in all cases, higher numbers indicate more similar communities.

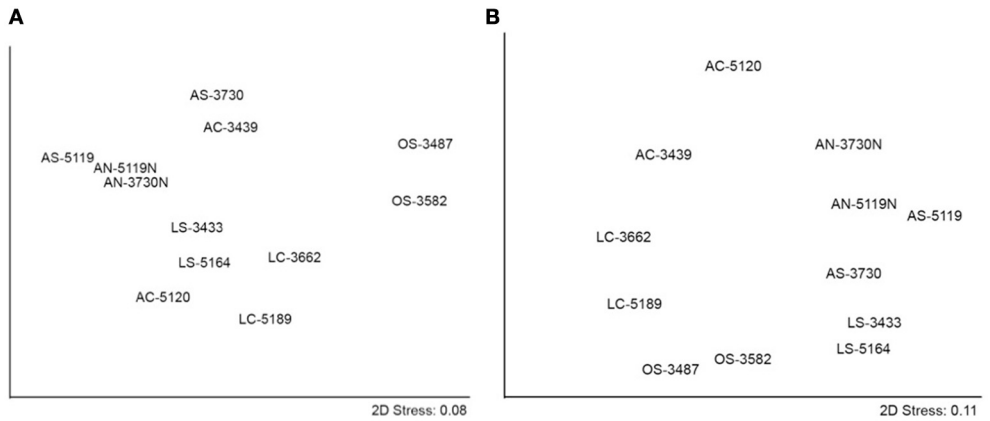

FIGURE 5 | Non-metric MDS showing (A) archaeal and (B) bacterial communities derived from genus-level relative abundances.

from background off-seep composition. High lateral heterogeneity in geochemistry, microbial assemblages, as well as in rates of sulfate reduction and methane oxidation, have been reported on sub-meter scales within and adjacent to seep-associated sulfide-oxidizing microbial mats and chemosynthetic invertebrate communities, illustrating the importance of seepage activity as a dominant control on the sediment-hosted microbial community (e.g., Barry et al., 1996; Lloyd et al., 2010). When substrate type is examined, both beta diversity measurements demonstrate that sediment and nodule communities are more similar than sediment and carbonate communities (**Figures 4B,D**). This finding may be partially attributable to spatial proximity, as the sediment-hosted nodules were recovered directly from the active seep sediment cores analyzed in this study. Weighted UniFrac analysis indicates that bacterial communities in carbonates and nodules are more similar than those in carbonates and sediment. However, the reverse was observed for archaeal communities, suggesting that bacterial diversity may be more dependent on substrate type than seepage level.

Non-metric MDS assessments (**Figure 5**) visualize Bray-Curtis community similarities between the 12 samples. In the two-dimensional plot of archaeal data, communities cluster primarily by seepage activity (**Figure 5A**). (The dolomitic sample AC-5120 is the single exception to this framework, which may be related to its unique mineralogy, discussed below.) This observation corroborates the Bray-Curtis and weighted UniFrac data that point to seepage activity as the primary determinant of archaeal community structure in and around methane seeps; similar qualitative observations have been reported at a number of seep habitats (e.g., Lloyd et al., 2010). ANOSIM supports the finding that seepage activity is a significant determinant of archaeal community structure (global $R = 0.65$, p-value $= 0.002$) rather than physical substrate (e.g., sediment, nodule, carbonate; $R = -0.04$, $p = 0.509$; see Table S2a for all pairwise values).

The bacterial non-metric MDS plot (**Figure 5B**) suggests a primary dependence on substrate type: sediments are distributed in the lower/lower right portion of the coordinate system, sediment-hosted nodules are positioned to the upper right, and

seafloor carbonates to the left. ANOSIM reveals that physical substrate is a significant driver of bacterial community structure (global $R = 0.41$, $p = 0.021$), while seep activity level is not (global $R = 0.215$, $p = 0.094$; Table S2b). The fact that substrate appears to discriminate among bacterial inhabitants is counter to an analogous study of seafloor basalts showing that the majority of clades are represented in both seafloor basalts and sediments (Mason et al., 2007). This discrepancy may be attributable to other environmental aspects distinctive of methane seep carbonates, such as fluid chemistry, mineralogy, predation pressure, permeability, or authigenic mineral formation (Heijs et al., 2006; Thurber et al., 2012). Indeed, activity appears to play a secondary role in separating bacterial communities, with active samples at the upper segment of the plot, off-seep samples to the bottom, and low-activity samples in between.

Mineralogy is another potential determinant of diversity. The geochemical association of sulfate-coupled AOM with carbonate minerals provides a direct link between microbial metabolism and authigenic mineral precipitation, a feedback that may, in turn, influence microbial community structure through physical constraints (Luff et al., 2004) and/or thermodynamic forcing (Knab et al., 2008). Specific links between diversity and carbonate mineralogy were difficult to discern with the relatively limited sample set included in this study. Aragonitic carbonates (AC-3439 and LC-3662) both contained abundant ANME sequences, an observation that is consistent with initial precipitation in zones of both high sulfate concentrations and high rates of AOM near the seabed (Burton, 1993; Savard et al., 1996; Greinert et al., 2001; Teichert et al., 2005). The lack of sulfate-reducing deltaproteobacteria in the calcitic LC-5189 is consistent with both a low-sulfate calcite formation environment (Naehr et al., 2007) as well as its current low methane seepage habitat, but it is difficult to parse the relative magnitudes of these influences. Sample AC-5120, a dolomite, may have formed in a deeper sediment horizon exhibiting low relative rates of AOM, as has been hypothesized on the basis of dolomite $\delta^{13}C$ and $\delta^{18}O$ isotopic signatures (Naehr et al., 2007; Meister et al., 2011). The divergence of this sample's archaeal community from those of other active site samples, characterized by the relative abundance of ANME-1 and lack of ANME-2 phylotypes, is consistent with formation in deeper sediment horizons (Knittel et al., 2005; Harrison et al., 2009), or may be uniquely influenced by the dolomitic mineralogy. In general, however, microbial community composition appears to be more dependent upon current environmental context rather than the original precipitation environment, as interpreted from mineralogical signatures. Indeed, when sample mineralogy is specifically plotted within the archaeal and bacterial MDS plots (**Figure S3**), the partitioning of communities is less clear than when only seepage activity or the degree of lithification (sediment, nodule, or carbonate, irrespective of mineralogy) is considered (**Figure 5**). The subsidiary importance of mineralogy in conveying microbial community relationships in our dataset suggests that this parameter is less significant than both methane seepage activity and lithification, which likely exert stronger influences over nutrient supply and metabolic intermediate exchange. The importance of mineralogy as a determinant of community composition has been documented at inactive hydrothermal vent deposits (Toner et al., 2012); with a more extensive dataset focused on mineralogy, it remains possible that this variable may help to explain additional microbial community differences unaccounted for by methane seepage activity or substrate type.

CONCLUSIONS

The analysis of mineralogy, microbial abundance, and archaeal and bacterial community structure across a range of habitats within and surrounding marine methane seeps reveals several key findings with implications for microbial ecology and seep development beyond what has been previously reported for marine sediment habitats.

Microbial community composition, as determined by 97% sequence similarity OTU-level 16S rRNA gene clone libraries, was remarkably similar among samples with similar seep activity levels and substrates—even if separated by several kilometers and acquired from different sediment depth horizons. This finding suggests that divergence owing to spatial heterogeneity, which has been reported in isotopic, geochemical, and community composition at the cm-scale in seep sediment (Orphan et al., 2004; House et al., 2009; Lloyd et al., 2010), is a less significant driver of bulk microbial diversity on its own than methane flux and/or substrate type.

The persistence of ANME Archaea and microbial aggregates typically associated with AOM in low-activity samples suggests that even at fluxes that do not support established sulfide-based chemosynthetic communities at the seabed (microbial mats or chemosynthetic clam beds), potential for anaerobic methanotrophy remains (Marlow et al., 2014). These findings imply that methanotrophic potential is pervasive on and below the seafloor across substrate types, and the degree to which ancient seep deposits preserve signals of microbial community succession is unknown. Studies of carbonate crusts from active mud volcanoes (Stadnitskaia et al., 2005) and of Black Sea AOM mats (Blumenberg et al., 2004) demonstrated an imperfect link between recovered lipids and 16S rRNA gene sequences, in which higher complexity lipid profiles suggested a more diverse microbial assemblage. In this context, lipid biomarkers, which are commonly used in geobiological studies to constrain communities or environmental conditions (e.g., Vestal and White, 1989; Turich and Freeman, 2011), may represent a time-integrated signal of microbial constituents and/or an accumulation of exogenous material rather than a faithful snapshot of a single community.

Statistical analyses of recovered 16S rRNA phylotypes reveal differences between sample types and point to distinct physicochemical determinants of microbial diversity. Archaeal communities, dominated by anaerobic methanotrophs, sort strongly by seep activity; whereas bacterial communities show a preferential association with physical substrate type. This discrepancy suggests that methane influx, while influencing the distribution of anaerobic archaeal methanotrophs, has less of an effect on bacterial diversity and serves as an overlaid imprint on, not a sole arbiter of, community structure. Rather, the physical nature of the habitat—a combination of factors likely including permeability, mineralogy, and hydrology—plays a more significant role in determining bacterial assemblages around methane seeps. Several

archaeal and bacterial lineages also appear to demonstrate specific activity-substrate pairing preferences, reflecting the interplay between seepage activity, environmental variation and succession, and microbial community structure. Our analysis exposes and begins to parse the intricate coupling of physical substrate and methane seepage as factors in environmental pressure and ecological determination; understanding the precise nature of these influences represents a fruitful area for continued research in microbial ecology.

AUTHOR CONTRIBUTIONS

Jeffrey J. Marlow, Victoria J. Orphan, Joshua A. Steele, and Lisa A. Levin designed the study; Jeffrey J. Marlow, David H. Case, and Joshua A. Steele performed the experiments and data analysis; Stephanie A. Connon processed much of the sequencing data; Jeffrey J. Marlow prepared the manuscript; all authors contributed to the editing of this work.

ACKNOWLEDGMENTS

We thank the Captains, Crew, *Alvin* group, *Jason* group, and Science party members from *RV Atlantis* legs AT-15-68, and AT-18-10. Patricia Tavormina and Alexis Pasulka provided useful suggestions on the manuscript. This study was funded by grants from the National Science Foundation (OCE-0825791 and OCE-0939559 to Victoria J. Orphan; OCE-0826254 and OCE-0939557 to Lisa A. Levin), the National Aeronautics and Space Administration (NASA) Astrobiology Institute under NASA-Ames Cooperative Agreement NNA04CC06A (to Victoria J. Orphan). Jeffrey J. Marlow was partially supported by a National Energy Technology Laboratory Methane Hydrate Research Fellowship funded by the National Research Council of the National Academies.

SUPPLEMENTARY MATERIAL

The Supplementary Material for this article can be found online at: http://www.frontiersin.org/journal/10.3389/fmars.2014.00044/abstract

Figure S1 | X-ray diffraction data from the 12 samples analyzed in this study. Each panel shows an experimental spectrum and peak placements of the top database matches. Qualitative mineralogical assignments based on relative peak heights are provided below the sample identifier.

Figure S2 | Bacterial Chao-1 (blue) and Inverse Simpson (red) values vs. archaeal Chao-1 and Inverse Simpson values. The wide scatter of both blue and red points suggests no significant correlation between domain-level diversity indices. R^2 of the linear best fit is 2.8×10^{-5} for Chao-1 and 0.029 for Inverse Simpson.

Figure S3 | Non-metric MDS results of (A) archaeal and (B) communities, where samples are labeled by mineralogical type.

REFERENCES

Aloisi, G., Bouloubassi, I., Heijs, S., Pancost, R., Pierre, C., Damste, J., et al. (2002). CH4-consuming microorganisms and the formation of carbonate crusts at cold seeps. *Earth Planet. Sci. Lett.* 203, 195–203. doi: 10.1016/S0012-821X(02)00878-6

Aloisi, G., Wallmann, K., Haese, R., and Saliege, J. (2004). Chemical, biological and hydrological controls on the 14C content of cold seep carbonate crusts: numerical modeling and implications for convection at cold seeps. *Chem. Geol.* 213, 359–383. doi: 10.1016/j.chemgeo.2004.07.008

Arakawa, S., Sato, T., Sato, R., Zhang, J., Gamo, T., Tsunogai, U., et al. (2006). Molecular phylogenetic and chemical analyses of the microbial mats in deep-sea cold seep sediments at the northeastern Japan Sea. *Extremophiles* 10, 311–319. doi: 10.1007/s00792-005-0501-0

Bahr, A., Pape, T., Bohrmann, G., Mazzini, A., Haeckel, M., Reitz, A., et al. (2009). Authigenic carbonate precipitates from the NE Black Sea: a mineralogical, geochemical, and lipid biomarker study. *Int. J. Earth Sci.* 98, 677–695. doi: 10.1007/s00531-007-0264-1

Barry, J., Greene, H., Orange, D., Baxter, C., Robison, B., Kochevar, R., et al. (1996). Biologic and geologic characteristics of cold seeps in Monterey Bay, California. *Deep Sea Res. Part I Oceanogr. Res. Pap.* 43, 1739–1762. doi: 10.1016/S0967-0637(96)00075-1

Beal, E. J., House, C. H., and Orphan, V. J. (2009). Manganese- and iron-dependent marine methane oxidation. *Science* 325, 184–187. doi: 10.1126/science.1169984

Bergmann, K. D. (2013). *Constraints on the Carbon Cycle and Climate During the Early Evolution of Animals*. Ph.D. dissertation, California Institute of Technology, Pasadena, CA.

Bian, Y., Feng, D., Roberts, H., and Chen, D. (2013). Tracing the evolution of seep fluids from authigenic carbonates: Green Canyon, northern Gulf of Mexico. *Mar. Petrol. Geol.* 44, 71–81. doi: 10.1016/j.marpetgeo.2013.03.010

Biddle, J. F., Lipp, J. S., Lever, M. A., Lloyd, K. G., Sorensen, K. B., Anderson, R., et al. (2006). Heterotrophic Archaea dominate sedimentary subsurface ecosystems off Peru. *Proc. Natl. Acad. Sci. U.S.A.* 103, 3846–3851. doi: 10.1073/pnas.0600035103

Blumenberg, M., Seifert, R., Reitner, J., Pape, T., and Michaelis, W. (2004). Membrane lipid patterns typify distinct anaerobic methanotrophic consortia. *Proc. Natl. Acad. Sci. U.S.A.* 101, 11111–11116. doi: 10.1073/pnas.0401188101

Boetius, A., Ravenschlag, K., Schubert, C., Rickert, D., Widdel, F., Gieseke, A., et al. (2000). A marine microbial consortium apparently mediating anaerobic oxidation of methane. *Nature* 407, 623–626. doi: 10.1038/35036572

Boetius, A., and Suess, E. (2004). Hydrate Ridge: a natural laboratory for the study of microbial life fueled by methane from near-surface gas hydrates. *Chem. Geol.* 205, 291–310. doi: 10.1016/j.chemgeo.2003.12.034

Bray, J. R., and Curtis, J. T. (1957). An ordination of the upland forest communities of southern Wisconsin. *Ecol. Monogr.* 27, 325–349. doi: 10.2307/1942268

Burton, E. A. (1993). Controls on marine carbonate cement mineralogy: review and reassessment. *Chem. Geol.* 105, 163–179. doi: 10.1016/0009-2541(93)90124-2

Clarke, K., and Primer, G. R. (2006). *V6: User Manual/Tutorial.* Plymouth: Primer-E Ltd. Plymouth–2006.

Claypool, G. E., and Kvenvolden, K. A. (1983). Methane and other hydrocarbon gases in marine sediment. *Annu. Rev. Earth Planet. Sci.* 11, 299. doi: 10.1146/annurev.ea.11.050183.001503

Daims, H., Lucker, S., and Wagner, M. (2006). Daime, a novel image analysis program for microbial ecology and biofilm research. *Environ. Microbiol.* 8, 200–213. doi: 10.1111/j.1462-2920.2005.00880.x

Faith, D., Minchin, P., and Belbin, L. (1987). Compositional dissimilarity as a robust measure of ecological distance. *Vegetatio* 69, 57–68. doi: 10.1007/BF00038687

Freitas, S., Hatosy, S., Fuhrman, J., Huse, S., Welch, D., Sogin, M., et al. (2012). Global distribution and diversity of marine Verrucomicrobia. *ISME J.* 6, 1499–1505. doi: 10.1038/ismej.2012.3

Gontharet, S., Stadnitskaia, A., Bouloubassi, I., Pierre, C., and Damste, J. (2009). Palaeo methane-seepage history traced by biomarker patterns in a carbonate crust, Nile deep-sea fan (Eastern Mediterranean Sea). *Mar. Geol.* 261, 105–113. doi: 10.1016/j.margeo.2008.11.006

Green-Saxena, A., Dekas, A. E., Dalleska, N. F., and Orphan, V. J. (2014). Nitrate-based niche differentiation by distinct sulfate-reducing bacteria involved in the anaerobic oxidation of methane. *ISME J.* 8, 150–163. doi: 10.1038/ismej.2013.147

Green-Saxena, A., Feyzullayev, A., Hubert, C., Kallmeyer, J., Krueger, M., Sauer, P., et al. (2012). Active sulfur cycling by diverse mesophilic and thermophilic microorganisms in terrestrial mud volcanoes of Azerbaijan. *Environ. Microbiol.* 14, 3271–3286. doi: 10.1111/1462-2920.12015

Greinert, J., Bohrmann, G., and Suess, E. (2001). "Gas hydrate-associated carbonates and methane-venting at Hydrate Ridge: classification, distribution, and origin of authigenic lithologies," in *Natural Gas Hydrates: Occurrence,*

Distribution, and Detection, Geophysical Monograph Series, eds C. K. Paull and W. P. Dillon (Washington, DC: AGU), 99–113.

Hallam, S., Putnam, N., Preston, C., Detter, J., Rokhsar, D., Richardson, P., et al. (2004). Reverse methanogenesis: testing the hypothesis with environmental genomics. *Science* 305, 1457–1462. doi: 10.1126/science.1100025

Harrison, B. K., Zhang, H., Berelson, W., and Orphan, V. J. (2009). Variations in archaeal and bacterial diversity associated with the sulfate-methane transition zone in continental margin sediments (Santa Barbara Basin, California). *Appl. Environ. Microbiol.* 75, 1487–1499. doi: 10.1128/AEM.01812-08

Heijs, S. K., Aloisi, G., Bouloubassi, I., Pancost, R., Pierre, C., Damste, J., et al. (2006). Microbial community structure in three deep-sea carbonate crusts. *Microb. Ecol.* 52, 451–462. doi: 10.1007/s00248-006-9099-8

Hinrichs, K., Hayes, J., Sylva, S., Brewer, P., and DeLong, E. (1999). Methane-consuming archaebacteria in marine sediments. *Nature* 398, 802–805. doi: 10.1038/19751

Hoehler, T., Alperin, M., Albert, D., and Martens, C. (1994). Field and laboratory studies of methane oxidation in an anoxic marine sediment: evidence for a methanogen-sulfate reducer consortium. *Global Biogeochem. Cycles* 8, 451–463. doi: 10.1029/94GB01800

Holler, T., Widdel, F., Knittel, K., Amann, R., Kellermann, M., Hinrichs, K., et al. (2011). Thermophilic anaerobic oxidation of methane by marine microbial consortia. *ISME J.* 5, 1946–1956. doi: 10.1038/ismej.2011.77

House, C. H., Orphan, V. J., Turk, K. A., Thomas, B., Pernthaler, A., Vrentas, J., et al. (2009). Extensive carbon isotopic heterogeneity among methane seep microbiota. *Environ. Microbiol.* 11, 2207–2215. doi: 10.1111/j.1462-2920.2009.01934.x

Huber, J. A., Butterfield, D. A., and Baross, J. A. (2002). Temporal Changes in archaeal diversity and chemistry in a mid-ocean ridge subseafloor habitat. *Appl. Environ. Microbiol.* 68, 1585–1594. doi: 10.1128/AEM.68.4.1585-1594.2002

Jiang, L., Zheng, Y., Peng, X., Zhou, H., Zhang, C., Xiao, Z., et al. (2009). Vertical distribution and diversity of sulfate−reducing prokaryotes in the Pearl River estuarine sediments, Southern China. *FEMS Microbiol. Ecol.* 70, 249–262. doi: 10.1111/j.1574-6941.2009.00758.x

Jørgensen, B. B., Bottcher, M., Luschen, H., Neretin, L., and Volkov, I. (2004). Anaerobic methane oxidation and a deep H2S sink generate isotopically heavy sulfides in Black Sea sediments. *Geochim. Cosmochim. Acta* 68, 2095–2118. doi: 10.1016/j.gca.2003.07.017

Karner, M. B., DeLong, E., and Karl, D. (2001). Archaeal dominance in the mesopelagic zone of the Pacific Ocean. *Nature* 409, 507–510. doi: 10.1038/35054051

Kleindienst, S., Ramette, A., Amann, R., and Knittel, K. (2012). Distribution and *in situ* abundance of sulfate-reducing bacteria in diverse marine hydrocarbon seep sediments. *Environ. Microbiol.* 14, 2689–2710. doi: 10.1111/j.1462-2920.2012.02832.x

Knab, N. J., Dale, A., Lettmann, K., Fossing, H., and Jorgensen, B. B. (2008). Thermodynamic and kinetic control on anaerobic oxidation of methane in marine sediments. *Geochim. Cosmochim. Acta* 72, 3746–3757. doi: 10.1016/j.gca.2008.05.039

Knittel, K., and Boetius, A. (2009). Anaerobic oxidation of methane: progress with an unknown process. *Annu. Rev. Microbiol.* 63, 311–334. doi: 10.1146/annurev.micro.61.080706.093130

Knittel, K., Losekann, T., Boetius, A., Kort, R., and Amann, R. (2005). Diversity and distribution of methanotrophic archaea at cold seeps. *Appl. Environ. Microbiol.* 71, 467–479. doi: 10.1128/AEM.71.1.467-479.2005

Konneke, M., Bernhard, A., de la Torre, J., Walker, C., Waterbury, J., and Stahl, D. (2005). Isolation of an autotrophic ammonia-oxidizing marine archaeon. *Nature* 437, 543–546. doi: 10.1038/nature03911

Kontoyannis, C. G., and Vagenas, N. V. (2000). Calcium carbonate phase analysis using XRD and FT-Raman spectroscopy. *Analyst* 125, 251–255. doi: 10.1039/a908609i

Legendre, P., and Legendre, L. (1998). "Numerical ecology: second English edition," in *Developments in Environmental Modelling* (New York, NY: Elsevier Science), 20.

Levin, L. A. (2005). Ecology of cold seep sediments: Interactions of fauna with flow, chemistry, and microbes. *Oceanogr. Mar. Biol.* 43, 1–46. doi: 10.1201/9781420037449.ch1

Levin, L. A., Ziebis, W., Mendoza, G. F., Bertics, V. J., Washington, T., Gonzalez, J., et al. (2013). Ecological release and niche partitioning under stress: lessons from dorvilleid polychaetes in sulfidic sediments at methane seeps. *Deep Sea Res. II* 92, 214–233. doi: 10.1016/j.dsr2.2013.02.006

Lloyd, K. G., Albert, D., Biddle, J., Chanton, J., Piarro, O., and Teske, A. (2010). Spatial structure and activity of sedimentary microbial communities underlying a Beggiatoa spp. mat in a Gulf of Mexico hydrocarbon seep. *PLoS ONE* 5:e8738. doi: 10.1371/journal.pone.0008738

Lloyd, K. G., Alperin, M., and Teske, A. (2011). Environmental evidence for net methane production and oxidation in putative ANaerobic MEthanotrophic (ANME) archaea. *Environ. Microbiol.* 13, 2548–2564. doi: 10.1111/j.1462-2920.2011.02526.x

Lösekann, T., Knittel, K., Nadalig, T., Fuchs, B., Niemann, H., Boetius, A., et al. (2007). Diversity and abundance of aerobic and anaerobic methane oxidizers at the Haakon Mosby Mud Volcano, Barents Sea. *Appl. Environ. Microbiol.* 73, 3348–3362. doi: 10.1128/AEM.00016-07

Lozupone, C., Hamady, M., Kelley, S., and Knight, R. (2007). Quantitative and qualitative β diversity measures lead to different insights into factors that structure microbial communities. *Appl. Environ. Microbiol.* 73, 1576–1585. doi: 10.1128/AEM.01996-06

Lozupone, C., Lladser, M., Knights, D., Stombaugh, J., and Knight, R. (2011). UniFrac: an effective distance metric for microbial community comparison. *ISME J.* 5, 169. doi: 10.1038/ismej.2010.133

Ludwig, W., Strunk, O., Westram, R., Richter, L., Meier, H., Buchner, A., et al. (2004). ARB: a software environment for sequence data. *Nucleic Acids Res.* 32, 1363–1371. doi: 10.1093/nar/gkh293

Luff, R., Wallmann, K., and Aloisi, G. (2004). Numerical modeling of carbonate crust formation at cold vent sites: significance for fluid and methane budgets and chemosynthetic biological communities. *Earth Planet. Sci. Lett.* 221, 337–353. doi: 10.1016/S0012-821X(04)00107-4

Lysnes, K., Thorseth, I., Steinsbu, B., Ovreas, L., Torsvik, T., and Pedersen, R. (2004). Microbial community diversity in seafloor basalt from the Arctic spreading ridges. *FEMS Microbiol. Ecol.* 50, 213–230. doi: 10.1016/j.femsec.2004.06.014

Marlow, J. J., Steele, J. A., Ziebis, W., Thurber, A. R., Levin, L. A., and Orphan, V. J. (2014). Carbonate-hosted methanotrophy represents an unrecognized methane sink in the deep sea. *Nat. Commun.* 5:5094. doi: 10.1038/ncomms6094

Mason, O. U., Stingl, U., Wilhelm, L., Moeseneder, M., Di Meo-Savoie, C., Fisk, M., et al. (2007). The phylogeny of endolithic microbes associated with marine basalts. *Environ. Microbiol.* 9, 2539–2550. doi: 10.1111/j.1462-2920.2007.01372.x

Massana, R., Murray, A., Preston, C., and DeLong, E. (1997). Vertical distribution and phylogenetic characterization of marine planktonic Archaea in the Santa Barbara Channel. *Appl. Environ. Microbiol.* 63, 50–56.

Meister, P., Gutjahr, M., Frank, M., Bernasconi, S., Vasconcelos, C., and McKenzie, J. (2011). Dolomite formation within the methanogenic zone induced by tectonically driven fluids in the Peru accretionary prism. *Geology* 39, 563–566. doi: 10.1130/G31810.1

Meyerdierks, A., Kube, M., Lombardot, T., Knittel, K., Bauer, M., Glockner, F., et al. (2005). Insights into the genomes of archaea mediating the anaerobic oxidation of methane. *Environ. Microbiol.* 7, 1937–1951. doi: 10.1111/j.1462-2920.2005.00844.x

Mills, H. J., Martinez, R. J., Story, S., and Sobecky, P. (2005). Characterization of microbial community structure in Gulf of Mexico gas hydrates: comparative analysis of DNA-and RNA-derived clone libraries. *Appl. Environ. Microbiol.* 71, 3235–3247. doi: 10.1128/AEM.71.6.3235-3247.2005

Milucka, J., Ferdelman, T., Polerecky, L., Franzke, D., Wegener, G., Schmid, M., et al. (2012). Zero-valent sulphur is a key intermediate in marine methane oxidation. *Nature* 491, 541–546. doi: 10.1038/nature11656

Naehr, T. H., Eichhubl, P., Orphan, V., Hovland, M., Paull, C., Ussler, W., et al. (2007). Authigenic carbonate formation at hydrocarbon seeps in continental margin sediments: a comparative study. *Deep Sea Res. Part II Top. Stud. Oceanogr.* 54, 1268–1291. doi: 10.1016/j.dsr2.2007.04.010

Nauhaus, K., Boetius, A., Kruger, M., and Widdel, F. (2002). *In vitro* demonstration of anaerobic oxidation of methane coupled to sulphate reduction in sediment from a marine gas hydrate area. *Environ. Microbiol.* 4, 296–305. doi: 10.1046/j.1462-2920.2002.00299.x

Nauhaus, K., Treude, T., Boetius, A., and Kruger, M. (2005). Environmental regulation of the anaerobic oxidation of methane: a comparison of ANME-I and ANME-II communities. *Environ. Microbiol.* 7, 98–106. doi: 10.1111/j.1462-2920.2004.00669.x

Nicol, G. W., and Schleper, C. (2006). Ammonia-oxidising Crenarchaeota: important players in the nitrogen cycle? *Trends Microbiol.* 14, 207–212. doi: 10.1016/j.tim.2006.03.004

Niemann, H., Linke, P., Knittel, K., MacPherson, E., Boetius, A., Bruckmann, W., et al. (2013). Methane-carbon flow into the benthic food web at cold seeps–a case study from the Costa Rica subduction zone. *PLoS ONE* 8:e74894. doi: 10.1371/journal.pone.0074894

Op den Camp, H. J. M., Islam, T., Stott, M., Harhangi, H., Hynes, A., Schouten, S., et al. (2009). Environmental, genomic and taxonomic perspectives on methanotrophic Verrucomicrobia. *Environ. Microbiol. Rep.* 1, 293–306. doi: 10.1111/j.1758-2229.2009.00022.x

Orcutt, B. N., Sylvan, J., Knab, N., and Edwards, K. (2011). Microbial Ecology of the Dark Ocean above, at, and below the Seafloor. *Microbiol. Mol. Biol. Rev.* 75, 361–422. doi: 10.1128/MMBR.00039-10

Orphan, V. J., Hinrichs, K., Ussler, W., Paull, C., Taylor, L., Sylva, S., et al. (2001a). Comparative analysis of methane-oxidizing archaea and sulfate-reducing bacteria in anoxic marine sediments. *Appl. Environ. Microbiol.* 67, 1922–1934. doi: 10.1128/AEM.67.4.1922-1934.2001

Orphan, V. J., House, C. H., Hinrichs, K. U., McKeegan, K. D., and DeLong, E. F. (2001b). Methane-consuming archaea revealed by directly coupled isotopic and phylogenetic analysis. *Science* 293, 484–487. doi: 10.1126/science.1061338

Orphan, V. J., House, C. H., Hinrichs, K. U., McKeegan, K. D., and DeLong, E. F. (2002). Multiple archaeal groups mediate methane oxidation in anoxic cold seep sediments. *Proc. Natl. Acad. Sci. U.S.A.* 99, 7663–7668. doi: 10.1073/pnas.072210299

Orphan, V. J., Ussler, W., Naehr, T. H., House, C. H., Hinrichs, K. U., and Paull, C. K. (2004). Geological, geochemical, and microbiological heterogeneity of the seafloor around methane vents in the Eel River Basin, offshore California. *Chem. Geol.* 205, 265–289. doi: 10.1016/j.chemgeo.2003.12.035

Paull, C., Chanton, J., Martens, C., Fullagar, P., Neumann, A., and Coston, J. (1991). Seawater circulation through the flank of the Florida Platform: evidence and implications. *Mar. Geol.* 102, 265–279. doi: 10.1016/0025-3227(91)90011-R

Pernthaler, A., Dekas, A., Brown, T., Goffredi, S., Embaye, T., and Orphan, V. (2008). Diverse syntrophic partnerships from deep-sea methane vents revealed by direct cell capture and metagenomics. *Proc. Natl. Acad. Sci. U.S.A.* 105, 7052–7057. doi: 10.1073/pnas.0711303105

Reeburgh, W. S. (1983). Rates of biogeochemical processes in anoxic sediments. *Annu. Rev. Earth Planet. Sci.* 11, 269–298. doi: 10.1146/annurev.ea.11.050183.001413

Reeburgh, W. S. (2007). Oceanic methane biogeochemistry. *Chem. Rev.* 107, 486–513. doi: 10.1021/cr050362v

Reitner, J., Peckmann, J., Blumenberg, M., Michaelis, W., Reimer, A., and Thiel, V. (2005). Concretionary methane-seep carbonates and associated microbial communities in Black Sea sediments. *Palaeogeogr. Palaeoclimatol. Palaeoecol.* 227, 18–30. doi: 10.1016/j.palaeo.2005.04.033

Roalkvam, I., Jorgensen, S., Chen, Y., Stokke, R., Dahle, H., Hocking, W., et al. (2011). New insight into stratification of anaerobic methanotrophs in cold seep sediments. *FEMS Microbiol. Ecol.* 78, 233–243. doi: 10.1111/j.1574-6941.2011.01153.x

Rossel, P. E., Elvert, M., Ramette, A., Boetius, A., and Hinrichs, K. U. (2011). Factors controlling the distribution of anaerobic methanotrophic communities in marine environments: evidence from intact polar membrane lipids. *Geochim. Cosmochim. Acta* 75, 164–184. doi: 10.1016/j.gca.2010.09.031

Ryan, W. B., Carbotte, S. M., Coplan, J. O., O'Hara, S., Melkonian, A., Arko, R., et al. (2009). Global multi-resolution topography synthesis. *Geochem. Geophys. Geosyst.* 10:Q03014. doi: 10.1029/2008GC002332

Santelli, C., Edgcomb, V., Bach, W., and Edwards, K. (2009). The diversity and abundance of bacteria inhabiting seafloor lavas positively correlate with rock alteration. *Environ. Microbiol.* 11, 86–98. doi: 10.1111/j.1462-2920.2008.01743.x

Santelli, C., Orcutt, B., Banning, E., Bach, W., Moyer, C., Sogin, M., et al. (2008). Abundance and diversity of microbial life in ocean crust. *Nature* 453, 653–656. doi: 10.1038/nature06899

Savard, M., Beauchamp, B., and Veizer, J. (1996). Significance of aragonite cements around Cretaceous marine methane seeps. *J. Sediment. Res.* 66, 430–438.

Schauer, R., Bienhold, C., Ramette, A., and Harder, J. (2009). Bacterial diversity and biogeography in deep-sea surface sediments of the South Atlantic Ocean. *ISME J.* 4, 159–170. doi: 10.1038/ismej.2009.106

Schloss, P., Westcott, S., Ryabin, T., Hall, J., Hartmann, M., Hollister, E., et al. (2009). Introducing mothur: open-source, platform-independent, community-supported software for describing and comparing microbial communities. *Appl. Environ. Microbiol.* 75, 7537–7541. doi: 10.1128/AEM.01541-09

Schreiber, L., Holler, T., Knittel, K., Meyerdierks, A., and Amann, R. (2010). Identification of the dominant sulfate−reducing bacterial partner of anaerobic methanotrophs of the ANME−2 clade. *Environ. Microbiol.* 12, 2327–2340. doi: 10.1111/j.1462-2920.2010.02275.x

Sheik, C., Jain, S., and Dick, G. (2014). Metabolic flexibility of enigmatic SAR324 revealed through metagenomics and metatranscriptomics. *Environ. Microbiol.* 16, 304–317. doi: 10.1111/1462-2920.12165

Stadnitskaia, A., Bouloubassi, I., Elvert, M., Hinrichs, K., and Damste, J. (2008). Extended hydroxyarchaeol, a novel lipid biomarker for anaerobic methanotrophy in cold seepage habitats. *Org. Geochem.* 39, 1007–1014. doi: 10.1016/j.orggeochem.2008.04.019

Stadnitskaia, A., Muyzer, G., Abbas, B., Coolen, M., Hopmans, E., Baas, M., et al. (2005). Biomarker and 16S rDNA evidence for anaerobic oxidation of methane and related carbonate precipitation in deep-sea mud volcanoes of the Sorokin Trough, Black Sea. *Mar. Geol.* 217, 67–96. doi: 10.1016/j.margeo.2005.02.023

Steinhaus, H. (1999). *Mathematical Snapshots*. Mineola, NY: Courier Dover Publications.

Suess, E., Torres, M., Bohrmann, G., Collier, R., Greinert, J., Linke, P., et al. (1999). Gas hydrate destabilization: enhanced dewatering, benthic material turnover and large methane plumes at the Cascadia convergent margin. *Earth Planet. Sci. Lett.* 170, 1–15. doi: 10.1016/S0012-821X(99)00092-8

Swan, B. K., Martinez-Garcia, M., Preston, C. M., Sczyrba, A., Woyke, T., Lamy, D., et al. (2011). Potential for chemolithoautotrophy among ubiquitous bacteria lineages in the Dark Ocean. *Science* 333, 1296–1300. doi: 10.1126/science.1203690

Tavormina, P., Ussler, W., Joye, S., Harrison, B., and Orphan, V. (2010). Distributions of putative aerobic methanotrophs in diverse pelagic marine environments. *ISME J.* 4, 700–710. doi: 10.1038/ismej.2009.155

Tavormina, P., Ussler, W., and Orphan, V. (2008). Planktonic and sediment-associated aerobic methanotrophs in two seep systems along the North American margin. *Appl. Environ. Microbiol.* 74, 3985–3995. doi: 10.1128/AEM.00069-08

Teichert, B., Bohrmann, G., and Suess, E. (2005). Chemoherms on Hydrate Ridge—Unique microbially-mediated carbonate build-ups growing into the water column. *Palaeogeogr. Palaeoclimatol. Palaeoecol.* 227, 67–85. doi: 10.1016/j.palaeo.2005.04.029

Tennant, C., and Berger, R. (1957). X-ray determination of dolomite-calcite ratio of a carbonate rock. *Am. Mineral.* 42, 23–29.

Teske, A., Hinrichs, K., Edgcomb, V., de Vera Gomez, A., Kysela, D., Sylva, S., et al. (2002). Microbial diversity of hydrothermal sediments in the guaymas basin: evidence for anaerobic methanotrophic communities. *Appl. Environ. Microbiol.* 68, 1994–2007. doi: 10.1128/AEM.68.4.1994-2007.2002

Thamdrup, B., and Dalsgaard, T. (2002). Production of N2 through anaerobic ammonium oxidation coupled to nitrate reduction in marine sediments. *Appl. Environ. Microbiol.* 68, 1312–1318. doi: 10.1128/AEM.68.3.1312-1318.2002

Thurber, A. R., Levin, L. A., Orphan, V. J., and Marlow, J. J. (2012). Archaea in metazoan diets: implications for food webs and biogeochemical cycling. *ISME J.* 6, 1602–1612. doi: 10.1038/ismej.2012.16

Toner, B., Lesniewski, R., Marlow, J., Briscoe, L., Santelli, C., Bach, W., et al. (2012). Mineralogy drives bacterial biogeography of hydrothermally inactive seafloor sulfide deposits. *Geomicrobiol. J.* 30, 313–326. doi: 10.1080/01490451.2012.688925

Treude, T., Boetius, A., Knittel, K., Wallmann, K., and Jorgensen, B. (2003). Anaerobic oxidation of methane above gas hydrates at Hydrate Ridge, NE Pacific Ocean. *Mar. Ecol. Prog. Ser.* 264, 1–14. doi: 10.3354/meps264001

Treude, T., Orphan, V., Knittel, K., Gieseke, A., House, C., and Boetius, A. (2007). Consumption of methane and CO2 by methanotrophic microbial mats from gas seeps of the Anoxic Black Sea. *Appl. Environ. Microbiol.* 73, 2271–2283. doi: 10.1128/AEM.02685-06

Tryon, M., Brown, K., and Torres, M. (2002). Fluid and chemical flux in and out of sediments hosting methane hydrate deposits on Hydrate Ridge, OR, II: hydrological processes. *Earth Planet. Sci. Lett.* 201, 541–557. doi: 10.1016/S0012-821X(02)00732-X

Turich, C., and Freeman, K. H. (2011). Archaeal lipids record paleosalinity in hypersaline systems. *Org. Geochem.* 42, 1147–1157. doi: 10.1016/j.orggeochem.2011.06.002

Ussler, W., and Paull, C. K. (2008). Rates of anaerobic oxidation of methane and authigenic carbonate mineralization in methane-rich deep-sea sediments inferred from models and geochemical profiles. *Earth Planet. Sci. Lett.* 266, 271–287. doi: 10.1016/j.epsl.2007.10.056

Van Dongen, B. E., Roberts, A., Schouten, S., Jiang, W., Florindo, F., and Pancost, R. (2007). Formation of iron sulfide nodules during anaerobic oxidation of methane. *Geochim. Cosmochim. Acta* 71, 5155–5167. doi: 10.1016/j.gca.2007.08.019

Van Dover, C. L., Aharon, P., Bernhard, J., Caylor, E., Doerries, M., Flickinger, W., et al. (2003). Blake Ridge methane seeps: characterization of a soft-sediment, chemosynthetically based ecosystem. *Deep Sea Res. Part I Oceanogr. Res. Pap.* 50, 281–300. doi: 10.1016/S0967-0637(02)00162-0

Vestal, J. R., and White, D. C. (1989). Lipid analysis in microbial ecology. *Bioscience* 39, 535–541. doi: 10.2307/1310976

Vetriani, C., Jannasch, H., MacGregor, B., Stahl, D., and Reysenbach, A. (1999). Population structure and phylogenetic characterization of marine benthic archaea in deep-sea sediments. *Appl. Environ. Microbiol.* 65, 4375–4384.

Watanabe, Y., Nakai, S., Hiruta, A., Matsumoto, R., and Yoshido, K. (2008). U–Th dating of carbonate nodules from methane seeps off Joetsu, Eastern Margin of Japan Sea. *Earth Planet. Sci. Lett.* 272, 89–96. doi: 10.1016/j.epsl.2008.04.012

Yamamoto, M., Nakagawa, S., Shimamura, S., Takai, K., and Horikoshi, K. (2010). Molecular characterization of inorganic sulfur-compound metabolism in the deep-sea epsilonproteobacterium Sulfurovum sp. NBC37-1. *Environ. Microbiol.* 12, 1144–1153. doi: 10.1111/j.1462-2920.2010.02155.x

Yanagawa, K., Sunamura, M., Lever, M., Morono, Y., Hiruta, A., Ishizaki, O., et al. (2011). Niche separation of methanotrophic archaea (ANME-1 and -2) in methane-seep sediments of the Eastern Japan Sea Offshore Joetsu. *Geomicrobiol. J.* 28, 118–129. doi: 10.1080/01490451003709334

Zhang, F., Xu, H., Konishi, H., and Roden, E. (2010). A relationship between d104 value and composition in the calcite-disordered dolomite solid-solution series. *Am. Mineral.* 95, 1650–1656. doi: 10.2138/am.2010.3414

Conflict of Interest Statement: The authors declare that the research was conducted in the absence of any commercial or financial relationships that could be construed as a potential conflict of interest.

Received: 04 July 2014; accepted: 08 September 2014; published online: 28 October 2014.

*Citation: Marlow JJ, Steele JA, Case DH, Connon SA, Levin LA and Orphan VJ (2014) Microbial abundance and diversity patterns associated with sediments and carbonates from the methane seep environments of Hydrate Ridge, OR. Front. Mar. Sci. **1**:44. doi: 10.3389/fmars.2014.00044*

This article was submitted to Aquatic Microbiology, a section of the journal Frontiers in Marine Science.

frontiers in MICROBIOLOGY

ORIGINAL RESEARCH ARTICLE
published: 08 January 2015
doi: 10.3389/fmicb.2014.00743

Benthic ammonia oxidizers differ in community structure and biogeochemical potential across a riverine delta

Julian Damashek, Jason M. Smith†, Annika C. Mosier† and Christopher A. Francis*

Department of Environmental Earth System Science, Stanford University, Stanford, CA, USA

Edited by:
Anne Bernhard, Connecticut College, USA

Reviewed by:
Annette Bollmann, Miami University, USA
Xiang Xiao, Shanghai JiaoTong University, China

****Correspondence:***
Christopher A. Francis, Department of Environmental Earth System Science, Stanford University, 473 Via Ortega, Room 140, Stanford, CA 94305-4216, USA
e-mail: caf@stanford.edu

†Present address:
Jason M. Smith, Monterey Bay Aquarium Research Institute, Moss Landing, CA, USA;
Annika C. Mosier, Department of Integrative Biology, University of Colorado Denver, Denver, CO, USA

Nitrogen pollution in coastal zones is a widespread issue, particularly in ecosystems with urban or agricultural watersheds. California's Sacramento-San Joaquin Delta, at the landward reaches of San Francisco Bay, is highly impacted by both agricultural runoff and sewage effluent, leading to chronically high nutrient loadings. In particular, the extensive discharge of ammonium into the Sacramento River has altered this ecosystem by vastly increasing ammonium concentrations and thus changing the stoichiometry of inorganic nitrogen stocks, with potential effects throughout the food web. This debate surrounding ammonium inputs highlights the importance of understanding the rates of, and controls on, nitrogen (N) cycling processes across the delta. To date, however, there has been little research examining N biogeochemistry or N-cycling microbial communities in this system. We report the first data on benthic ammonia-oxidizing microbial communities and potential nitrification rates for the Sacramento-San Joaquin Delta, focusing on the functional gene *amoA* (which codes for the α-subunit of ammonia monooxygenase). There were stark regional differences in ammonia-oxidizing communities, with ammonia-oxidizing bacteria (AOB) outnumbering ammonia-oxidizing archaea (AOA) only in the ammonium-rich Sacramento River. High potential nitrification rates in the Sacramento River suggested these communities may be capable of oxidizing significant amounts of ammonium, compared to the San Joaquin River and the upper reaches of San Francisco Bay. Gene diversity also showed regional patterns, as well as phylogenetically unique ammonia oxidizers in the Sacramento River. The benthic ammonia oxidizers in this nutrient-rich aquatic ecosystem may be important players in its overall nutrient cycling, and their community structure and biogeochemical function appear related to nutrient loadings. Unraveling the microbial ecology and biogeochemistry of N cycling pathways, including benthic nitrification, is a critical step toward understanding how such ecosystems respond to the changing environmental conditions wrought by human development and climate change.

Keywords: nitrification, archaea, bacteria, amoA, estuary, river, salinity, ammonium

INTRODUCTION

In the past century, widespread synthetic ammonia production has profoundly perturbed the global nitrogen (N) cycle (Erisman et al., 2008). Industrial N fixation rates are now comparable to or even greater than natural sources, leading to a doubling of the planet's fixed N inventory (Galloway et al., 2004; Billen et al., 2013; Erisman et al., 2013). Local ecological effects of this global phenomenon have been drastic. In particular, agricultural runoff and sewage treatment effluent can greatly enrich aquatic habitats with respect to N, often stimulating primary production and leading to eutrophication (Erisman et al., 2013), the consequences of which can include hypoxia (Rabalais et al., 2010) and harmful algal blooms (Anderson et al., 2002), among others. However, a substantial fraction of fixed N inputs to rivers and estuaries is removed *in situ* by two microbial pathways: denitrification and the anaerobic oxidation of ammonia (anammox; Boynton and Kemp, 2008; Ward, 2013). In well-mixed rivers and estuaries, these N loss pathways are typically active only within anoxic sediments, and ultimately provide an ecological N sink by converting fixed N to nitrogen gas (N_2). In this way, microbes provide a tremendous "ecosystem service" by shuttling N out of aquatic ecosystems and back to the atmosphere.

The N cycle is a set of coupled reactions that transform N from one compound into another (Ward, 2012). One particularly important component is nitrification, the microbially-catalyzed conversion of ammonia (NH_3) to nitrate (NO_3^-). This process occurs in two steps: (1) ammonia oxidation, typically the rate-limiting step, converts NH_3 to nitrite (NO_2^-); and (2) nitrite oxidation further converts NO_2^- to NO_3^-. Importantly, NO_3^- and NO_2^- are substrates for denitrification and anammox. Since nitrification is the only process that transforms remineralized ammonium (NH_4^+) into the inorganic forms that feed N loss, it is the crucial link between fixed N inputs and outputs in an ecosystem. Therefore, understanding environmental controls on

the microbial ecology and biogeochemistry of ammonia oxidation is critical for understanding how N is cycled through, and ultimately lost from, any aquatic ecosystem.

For over a century, it was believed the capacity for ammonia oxidation was confined to the phylum *Proteobacteria* (Kowalchuk and Stephen, 2001). Recently, the discovery of ammonia-oxidizing archaea (AOA; Könneke et al., 2005), now known as "Thaumarchaeota" (Brochier-Armanet et al., 2008), made this story more complex. AOA are present in many environments (Francis et al., 2005; Treusch et al., 2005; Beman et al., 2007; Spear et al., 2007; De Corte et al., 2008; Biller et al., 2012), frequently outnumber AOB in marine and terrestrial systems (Leininger et al., 2006; Wuchter et al., 2006; Beman et al., 2008; Weidler et al., 2008; Santoro et al., 2010; Nicol et al., 2011), and appear to drive nitrification rates throughout the marine water column (Wuchter et al., 2006; Beman et al., 2012; Newell et al., 2013; Smith et al., 2014a). However, the complexity of ammonia-oxidizing communities in estuaries has precluded efforts to uncover broad estuarine trends. Some estuaries are dominated by AOA (Beman and Francis, 2006; Caffrey et al., 2007; Moin et al., 2009), others by AOB (Abell et al., 2010; Bernhard et al., 2010), and some have alternating zones of AOA and AOB dominance (Mosier and Francis, 2008; Santoro et al., 2008; Bouskill et al., 2012a; Zheng et al., 2014). Additionally, studies of ammonia oxidizers in freshwater ecosystems are relatively rare, and rivers are particularly understudied (Biller et al., 2012), though the handful of studies published to date have indicated the ammonia-oxidizing communities in river sediments are often quite complex (Liu et al., 2013; Sonthiphand et al., 2013; Wang et al., 2014).

The Sacramento-San Joaquin River Delta ("the Delta") is a network of tidally influenced freshwater marshes, rivers, and islands where the Sacramento and San Joaquin rivers meet San Francisco Bay (**Figure 1**). The Delta drains a 153,000 km^2 watershed encompassing 40% of the area of California, including the entire Central Valley (Conomos et al., 1985), and receives high nutrient loads from agricultural runoff and wastewater effluent (Cloern and Jassby, 2012). In the past two centuries, anthropogenic development throughout California has led to massive alterations within the Delta: huge swaths of wetlands have been diked and drained to create arable farmland, massive volumes of water are pumped south for agricultural and urban use, and increased wastewater discharge has elevated nutrient concentrations (Lund et al., 2010). The recent collapse of numerous fish populations, termed the "pelagic organism decline" (Sommer et al., 2007), has focused considerable scientific and political attention on water quality issues in the Delta. While the piscine population crashes appear to be caused by a complex array of environmental forces (MacNally et al., 2010; Thomson et al., 2010), two potential stressors have come under particular scrutiny, due to their implications for management: freshwater exports from the Delta (Kimmerer, 2008), and the massive discharge of NH_4^+ into the Sacramento River by the Sacramento

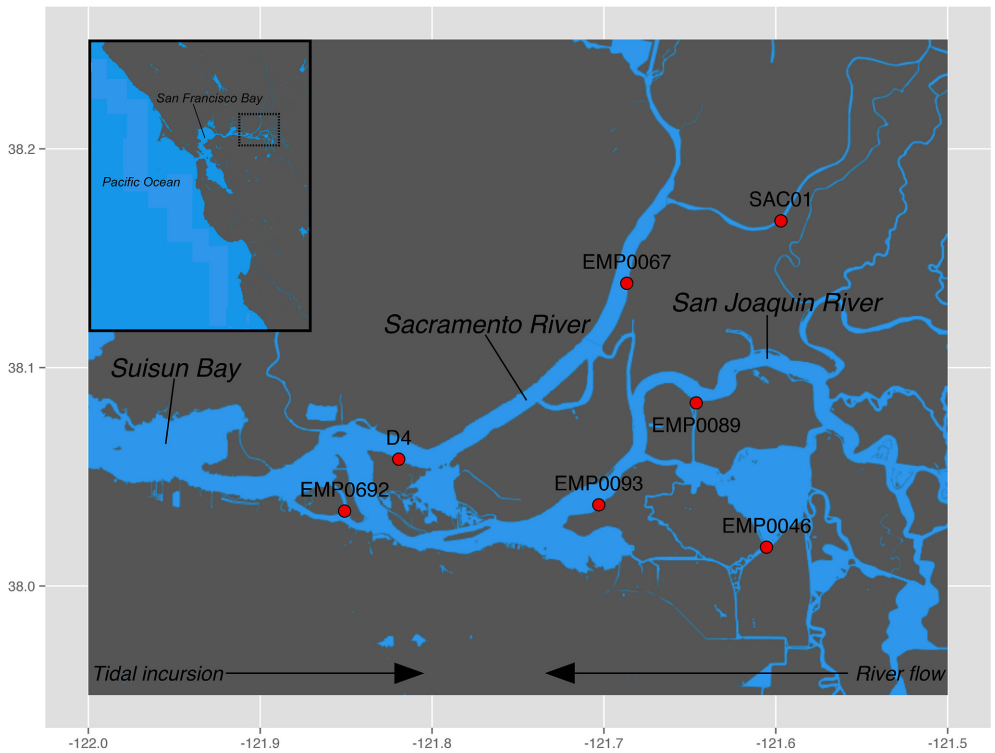

FIGURE 1 | Sampling locations in the Sacramento-San Joaquin Delta. Regions sampled were the Sacramento River (stations SAC01 and EMP0067), the San Joaquin River (stations EMP0089 and EMP0093), Franks Tract (station EMP0046), and the upper oligohaline region of the estuary (San Francisco Bay) at the confluence of the two rivers (stations D4 and EMP0692). Generally, river flow moves westward while tides propagate eastward. Inset shows the greater region of San Francisco Bay, with the dotted black box denoting the Delta.

Regional Wastewater Treatment Plant (Glibert, 2010; Glibert et al., 2011). While this debate highlights the importance of understanding the sources, sinks, and transformation rates of NH_4^+ in the Delta, little is known about a key aspect of the N cycle in this system: benthic nitrification and the associated ammonia-oxidizing microbial assemblages. A recent study measuring rates of benthic N_2, NH_4^+, and NO_3^- fluxes across northern San Francisco Bay and the Delta showed high but seasonally-variable rates of coupled nitrification-denitrification, with high rates reported from Delta sediments, compared to the brackish sediments further downstream (Cornwell et al., 2014). Therefore, benthic nitrification may be an important driver of N loss in the Delta. Here, we assess the diversity, abundance, and biogeochemical potential of benthic ammonia-oxidizing communities throughout the Delta. This work is the first analysis of ammonia-oxidizing communities and benthic potential nitrification rates in this ecosystem.

MATERIALS AND METHODS

SEDIMENT AND BOTTOM WATER DATA COLLECTION

Sampling stations were selected to encompass both riverine systems (Sacramento, San Joaquin) as well as the confluence of the rivers in the "upper estuary" oligohaline region of San Francisco Bay. Additionally, one station was located in Franks Tract, a slowly flushed tidal lake adjacent to the San Joaquin river (**Figure 1**). Samples were collected in September and October 2007 onboard the R/V *Endeavor*. Surface sediment was retrieved using a modified Van Veen grab. Duplicate cores were taken from each grab sample using sterile, cut-off 5 mL syringes and immediately placed on dry ice prior to storage at −80°C. Bottom water nutrient samples were collected it duplicate using a hand-held Niskin bottle, immediately filtered (0.2 μm pore size), and frozen on dry ice prior to storage at −20°C. Nutrient (NH_4^+, NO_2^-, and NO_3^-) concentrations were measured using a QuikChem 8000 Flow Injection Analyzer (Lachat Instruments). Bottom water alkalinity, conductivity, dissolved oxygen, pH, and temperature data were collected by the California Water Resources Control Board's sediment quality objectives program, in collaboration with the Department of Water Resources, and were provided by the Southern California Coastal Water Research Project (Steve Bay, personal communication). Dayflow data were downloaded from the California Department of Water Resources database (http://www.water.ca.gov/dayflow/).

POTENTIAL NITRIFICATION RATES

Sediment samples for potential nitrification rate measurements were collected in triplicate into the barrels of cut-off 60 mL syringes, which were sealed with parafilm and transported to the laboratory on ice. Potential rates were measured using amended sediment slurries (Hansen et al., 1981; Henriksen et al., 1981). Slurries included 5 g of sediment (top 2 cm) homogenized in 50 mL artificial seawater (adjusted to site-specific salinities) augmented with a final concentration of 500 μM ammonium sulfate. Amended slurries were shaken (200 rpm) in the dark for 24 h at room temperature (∼22°C). Aliquots for the determination of NO_3^- plus NO_2^- (NO_X) were collected at evenly spaced intervals through the incubation period and stored at −20°C. Prior to analysis, aliquots were thawed and passed through Whatman No. 42 filter paper, and the filtrate was analyzed for the accumulation of NO_X over time, using a SmartChem 200 Discrete Analyzer (Unity Scientific). Rates were determined by linear regression of NO_X concentrations over time.

DNA EXTRACTION AND FUNCTIONAL GENE ANALYSES

DNA was extracted from approximately 0.5 g of surface sediments by extruding and cutting the top 0.5 cm from frozen cores with a sterile scalpel and immediately proceeding with the FastDNA SPIN Kit for Soil (MP Biomedicals), including a bead beating step of 30 s at speed 5.5. All DNA extracts were visually checked by gel electrophoresis and quantified using the Qubit dsDNA BR assay (Life Technologies).

AOA and AOB *amoA* genes were quantified using gene-specific SYBR qPCR assays on a StepOnePlus Real-Time PCR System (Life Technologies). AOA *amoA* reactions contained iTaq SYBR Green Supermix with ROX (Bio-Rad Laboratories), 0.4 μM primers Arch-amoAF/Arch-amoAR (Francis et al., 2005) and 1 μL template DNA. AOA qPCR program details were identical to previously published protocols (Mosier and Francis, 2008) but with a 10 s detection step at 78.5°C. AOB *amoA* qPCR reactions used primers amoA1F/amoA2R (Rotthauwe et al., 1997), and were set up following Mosier and Francis (2008) but with a 10 s detection step at 83°C. Each plate included a standard curve (5–10^6 copies/reaction) made by serial dilution of linearized plasmids extracted from previously sequenced clones, and negative controls that substituted sterile water for DNA. All standard curves had $R^2 \geq 0.99$, and reaction efficiency ranged from 90.9 to 94.3% (AOA) and 86.0 to 88.3% (AOB). Specificity was determined using melt curves. Data were discarded if the standard deviation between triplicate reactions was >15%; occasionally, obvious outliers were excluded and the midpoint of duplicate values was used.

The diversity of ammonia oxidizing communities was determined by cloning and sequencing of PCR-amplified *amoA* genes using primers Arch-amoAF/Arch-amoAR (Francis et al., 2005) and amoA1F∗/amoA2R (Rotthauwe et al., 1997; Stephen et al., 1999) for AOA and AOB, respectively. Reaction conditions and PCR programs followed previously published protocols (Mosier and Francis, 2008). Triplicate reactions were qualitatively checked by gel electrophoresis, pooled, and purified using the MinElute PCR Purification Kit or MinElute Gel Extraction Kit (Qiagen), following the manufacturer's instructions. Purified products were cloned using the pGEM-T Vector System II (Promega), and sequenced by Elim Biopharmaceuticals on a 3730xl capillary sequencer (Life Technologies), using the M13R primer. Sequences were imported into Geneious (version 6.1.6 created by Biomatters, available from http://www.geneious.com) and manually cleaned prior to operational taxonomic unit (OTU) grouping (≥95% sequence similarity) using mothur (Schloss et al., 2009). Rarefaction curves and diversity/richness estimators (Chao1 and Shannon indices) were calculated using mothur. OTUs were aligned with reference sequences using the MUSCLE alignment package within Geneious, using a gap open score of −750. Alignments were manually checked and used to build neighbor-joining bootstrap trees (Jukes-Cantor distance model,

1000 neighbor joining bootstrap replicates) within Geneious. The *amoA* sequences generated in this study have been deposited into GenBank with accession numbers KM000240–KM000508 (AOB) and KM000509–KM000784 (AOA).

STATISTICAL ANALYSES

Due to the low number of samples ($n = 7$), standard statistical analyses such as *t*-tests and ANOVAs could not be used to compare environmental data between stations or regions, due to a lack of statistical power. Two-tailed Spearman rank correlation coefficients (ρ) were calculated using R (R Core Team, 2014) to determine correlations between variables, using the suggested critical value of $\rho \geq 0.786$ for 5% significance with a sample size of 7 (Zar, 1972).

Principal component and non-metric multidimensional scaling analyses were performed using the vegan package in R (Borcard et al., 2011; Oksanen, 2013). Environmental variables were z-transformed to standardize across different scales and units by subtracting the population mean from each measurement and dividing by the standard deviation. OTU count data were Hellinger-transformed to standardize to relative abundances (Legendre and Legendre, 2012). Other than unweighted UniFrac distances, which were calculated using the online UniFrac portal (Lozupone et al., 2006), distance/dissimilarity indices were calculated using the vegan package in R. All principle component analyses are presented using scaling 1; therefore, the distance between sites on the biplot represents their Euclidean distance, and the right-angle projection of a site onto a descriptor vector shows the approximate position of that site on the vector (Legendre and Legendre, 2012).

RESULTS AND DISCUSSION

BOTTOM WATER CHEMISTRY

Conductivity generally increased downriver, with upper estuary stations EMP0692 and D4 approximately 100 μS cm^{-1} greater than stations further up either river (**Table 1**). This change in conductivity was reflected in a marginal correlation with station longitude ($\rho = -0.71$, $p = 0.088$), as both rivers generally flow westward. Freshwater flows in the Delta are typically high in late winter and spring, followed by a prolonged dry season, during which brackish water from San Francisco Bay gradually moves upriver (eastward; Kimmerer, 2004). During and after periods of high freshwater flow, the conductivity gradient between the rivers to the upper estuary would likely be more pronounced. In contrast, since our samples were collected after months of low precipitation and therefore low Delta outflow (Supplementary Figure A1), it is not surprising that conductivity is only marginally higher in the oligohaline upper estuary than in the rivers.

Bottom water nutrient concentrations were generally in the range of values previously reported from northern San Francisco Bay and the Delta (Wankel et al., 2006; Mosier and Francis, 2008; Parker et al., 2012), though with substantial geographical variation (**Table 1**). NH_4^+ was higher in the Sacramento River (stations EMP0067 and SAC01; 15.43 and 27.12 μM, respectively) than in other regions, where NH_4^+ ranged from 1.08 to 7.34 μM. NO_3^- was slightly higher in the upper estuary and San Joaquin River stations (14.16–22.57 μM) compared to the rest of the Delta (1.79–10.76 μM). All nutrients were lowest at station EMP0046, located at the southern tip of Franks Tract, a shallow tidal lake connected to the San Joaquin River (Lucas et al., 2002). Compared to the surrounding channels, Franks Tract generally has low turbidity and high productivity (Jassby and Cloern, 2000), which was supported by the relatively high pH (8.0) and low macronutrient concentrations, compared to other sites (**Table 1**).

NITRIFICATION

Potential nitrification rates were quantified by measuring the change in NO_X concentrations in amended sediment slurries over time. In contrast to measuring rates that more closely approximate *in situ* conditions (i.e., intact core incubations), potential rates estimate the maximal capability of the viable ammonia-oxidizing populations in the slurry, by alleviating any NH_4^+ or oxygen limitation. While potential rate measurements are not a perfect proxy for *in situ* processes, rates determined under "optimal" conditions yield insightful information about differences in the maximum sustainable nitrification rate between sites. NO_X

Table 1 | Bottom water chemistry and benthic potential nitrification rates.

Station	Region	Lat.	Lon.	Conductivity	Dissolved oxygen	pH	Temp.	Alkalinity	NH_4^+	NO_3^-	NO_2^-	Potential nitrification
		°N	°W	μS cm^{-1}	mg L^{-1}		°C	mg L^{-1} $CaCO_3$	μM	μM	μM	nmol NO_X g^{-1} h^{-1}
EMP0093	SJ	38.037	121.703	686	6.31	7.7	22.1	119	2.69	14.16	0.43	55.41 (± 2.49)
EMP0089	SJ	38.084	121.646	665	5.83	7.6	22.1	110	4.48	16.00	0.72	8.29 (± 1.01)
EMP0046	FT	38.018	121.605	704	5.62	8.0	23.1	129	1.08	1.79	0.14	11.38 (± 0.66)
EMP0067	Sac	38.139	121.687	675	5.61	7.8	22.1	119	15.43	10.76	0.58	118.74 (± 24.86)
SAC01	Sac	38.167	121.597	674	5.62	7.8	22.1	131	27.12	9.71	0.50	146.00 (± 70.97)
EMP0692	Est	38.034	121.851	783	7.21	7.6	22.5	120	7.34	22.57	0.62	47.97 (± 2.6)
D4	Est	38.058	121.819	775	6.38	7.2	22.4	115	6.55	16.50	0.64	20.33 (± 2.2)

SJ, San Joaquin River; FT, Franks Tract; Sac, Sacramento River; Est, Upper Estuary. Potential nitrification rates were normalized to sediment wet weight; values in parentheses show the standard deviation of triplicate measurements. All data other than nutrient concentrations and potential nitrification rates were provided courtesy of the Southern California Coastal Water Research Project.

increased linearly over the incubation period in all Delta samples ($R^2 = 0.92$–0.99, mean ± SD = 0.98 ± 0.02, $n = 21$). Potential nitrification ranged from 8.3 to 146.0 nmol NO_X g^{-1} h^{-1} (58.3 ± 54.2, rates normalized to wet sediment weight; **Table 1**). Though quite wide, this range was similar to those reported by previous studies using similar methods (Kemp et al., 1990; Joye and Hollibaugh, 1995; Dollhopf et al., 2005; Smith et al., 2014b).

Potential rates at the two Sacramento River stations were an order of magnitude higher than rates from the other study sites (**Table 1**). This was particularly interesting because of the high concentrations of NH_4^+ in the Sacramento River: the correlation between potential nitrification and NH_4^+ was positive and at the margins of significance ($\rho = 0.71$, $p = 0.088$). Due to the recent controversy over the ecological impacts of elevated NH_4^+ concentrations in the Sacramento River (Glibert, 2010; Brooks et al., 2012; Cloern et al., 2012; Lancelot et al., 2012), there is substantial interest in quantifying the rates of NH_4^+ transformations throughout the Delta. While previous work has inferred high nitrification rates in the Sacramento River due to longitudinal decreases in NH_4^+ and increases in NO_3^- concentrations (Parker et al., 2012), no measurements of nitrification rates in the Delta exist to date. Although the potential nitrification rates reported here do not yet allow for an estimate of the *in situ* benthic nitrification rates, they nevertheless suggest that such rates may be higher in the Sacramento River than in the rest of the Delta. Throughout the Delta, there is a clear need to accurately quantify the contribution of nitrification (both benthic and pelagic) to NH_4^+ depletion, under conditions that more closely approximate those observed *in situ*. Such an effort would confirm whether the sediments of the Sacramento River are a significant sink for the NH_4^+ present in its waters, as our data suggest.

We used principal component analysis (PCA) to cluster stations according to a combination of environmental variables and nitrification potentials. Combined, the first two eigenvectors explained 78.8% of the variance in bottom water physicochemical parameters, and suggested strong geographical clustering of stations (**Figure 2**). The upper estuary stations D4 and EMP0692 clustered together, due to higher conductivity, dissolved oxygen, and NO_3^-. High NH_4^+ and potential nitrification rates separated SAC01 and EMP0067, the two Sacramento River stations, from the rest of the study sites. EMP0046 appeared distinct from all other sites, while EMP0093 and EMP0089 from the San Joaquin River also clustered with one another. Overall, the PCA suggested the four sampled geographical regions of the Delta

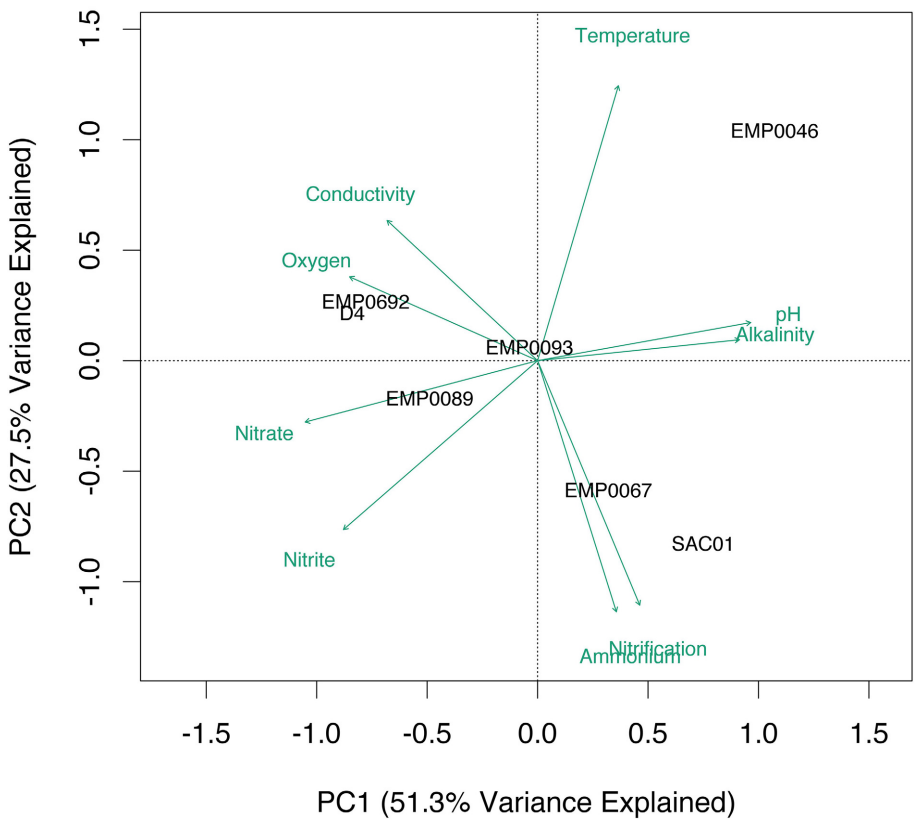

FIGURE 2 | PCA biplot (scaling 1) of environmental data at the sampled Delta stations. Data were z-transformed prior to the analysis to standardize across varying units and scales. Distance between stations on the biplot represents Euclidean distance in multidimensional space. Projections of a station onto a green environmental vector indicate its position along that vector.

may be considered distinct physicochemical and biogeochemical regimes.

AMMONIA OXIDIZER ABUNDANCES

Abundance of AOA and AOB in surface sediments was determined by domain-specific *amoA* qPCR assays. Genes associated with both groups were detectable at all sites, but their abundances varied substantially: AOA *amoA* was present at 7.28×10^4 to 6.42×10^5 copies g^{-1}, while AOB *amoA* ranged between 1.09×10^4 and 1.03×10^6 copies g^{-1} (**Figure 3**; gene copies are normalized to wet sediment weight). As with potential nitrification rates, ammonia oxidizer abundances showed regional patterns: the average log ratio of AOA:AOB *amoA* in the Sacramento River was -0.76, compared to 1.11 in the San Joaquin River and 0.16 in the upper estuary. In other words, AOA outnumbered AOB in the San Joaquin River by 2- to 18-fold, AOB outnumbered AOA in the Sacramento River by 3- to 14-fold, and their abundances were practically equal in the upper reaches of San Francisco Bay. Prior work in the upper estuary also found AOA present at an equal or greater abundance than AOB over multiple summers, though with some site-specific differences in overall abundance values (Mosier and Francis, 2008).

The correlation between AOA abundances and potential nitrification rates was negative but statistically insignificant ($\rho = -0.64$, $p = 0.139$), while AOB abundances and potential rates were positively correlated at the margins of significance ($\rho = 0.71$, $p = 0.088$). Although the *in situ* biogeochemical rates and the levels of ammonia oxidizer gene expression are still unknown, these correlations suggest that AOB may have been driving nitrification at those sites in the Delta where benthic nitrification rates were highest. Such a relationship between AOB gene abundance and potential nitrification rates agrees with observations from intertidal sediments in polyhaline Elkhorn Slough, where AOB abundances also strongly correlated with potential rates, while the relationship between AOA abundances and potential rates was much weaker (Smith et al., 2014b). Therefore, AOB appear to be

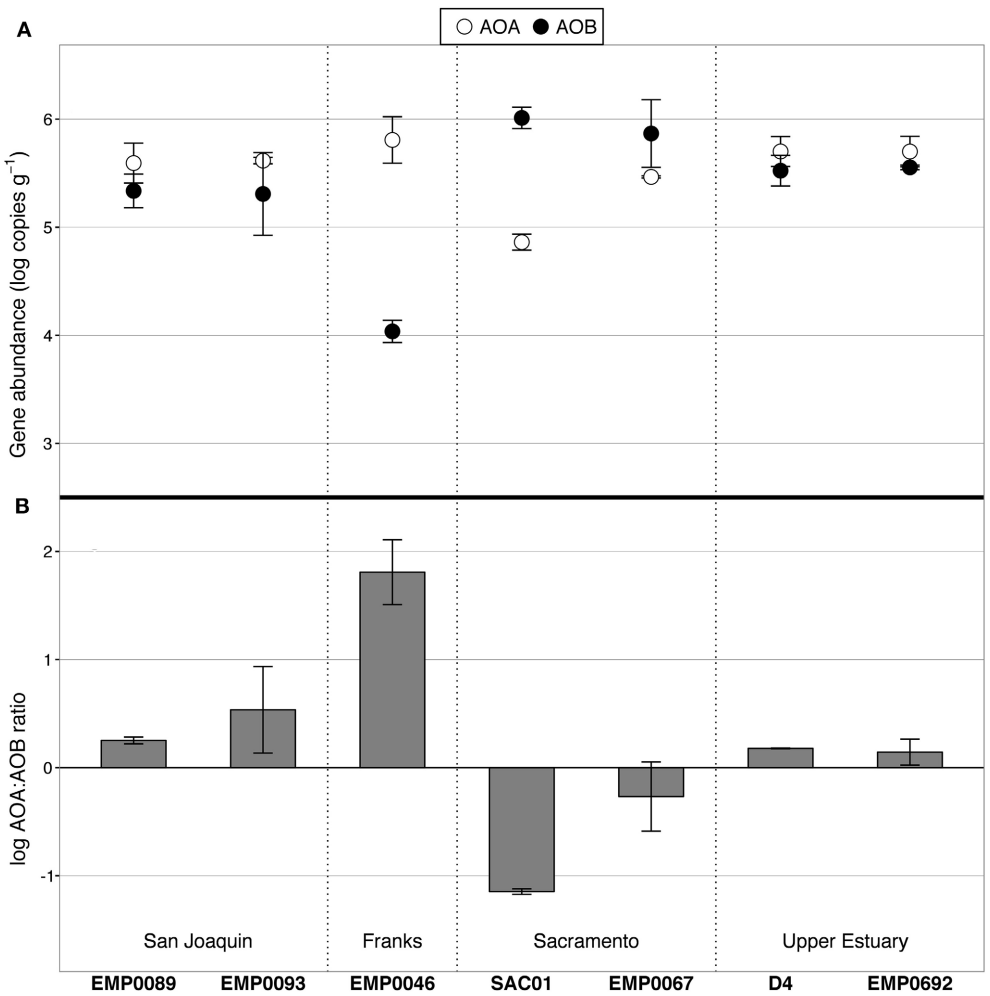

FIGURE 3 | AOA and AOB *amoA* abundance, as determined by qPCR. (A) Average values of duplicate samples per site. Abundance data are normalized by wet weight of sediment. Error bars show the range of duplicate samples. AOA are shown in white, AOB in black. **(B)** Log-transformed ratio of AOA:AOB *amoA*. Values above zero indicate AOA abundance greater than AOB, and visa versa. Error bars show the range of values from duplicate extractions per station.

potentially important players in the N cycles of both polyhaline and oligohaline/freshwater estuarine sediments.

Interestingly, the site with the highest bottom water NH_4^+ concentration (27.1 μM; station SAC01 in the Sacramento River) also had the highest AOB abundance (1.03×10^6 copies g^{-1}). Across all sites, the rank correlation between AOB abundance and bottom water NH_4^+ concentration was perfectly positive ($\rho = 1$, $p < 0.001$). AOB have previously been found to outnumber AOA in the sediments of other eutrophic systems, including Elkhorn Slough (Wankel et al., 2011; Smith et al., 2014b), the organic-rich regions of Lake Taihu (Wu et al., 2010), Fuyang River surface sediments (Wang et al., 2014), and freshwater flow channels fertilized with high doses of NH_4^+ (Herrmann et al., 2011). AOB also vastly outnumbered AOA in the extremely NH_4^+-rich activated sludge of the Palo Alto wastewater treatment plant (Wells et al., 2009). The numerical dominance of AOB over AOA in NH_4^+-rich ecosystems may not be a universal trend, as numerous studies have reported AOA outnumbering AOB in sediments under diverse nutrient regimes (Caffrey et al., 2007; Moin et al., 2009; Abell et al., 2010; Liu et al., 2013); however, the occurrence of such a relationship in numerous ecosystems suggests there is a relationship between benthic AOB abundance and NH_4^+ loadings in at least some freshwater and estuarine ecosystems.

Table 2 | Diversity (Chao1 index) and richness (Shannon index) data for Delta *amoA* OTU data.

	No. Clones	No. OTUs	Unique OTUs	Chao1	Shannon
AOA					
All Sites	276	52		76 (69.7%)	3.1
EMP0093	41	15	6	16 (93.8%)	2.4
EMP0089	24	1	0	1 (100%)	0
EMP0046	45	12	9	15 (80.0%)	2.1
EMP0067	44	10	2	12 (83.3%)	1.9
SAC01	39	15	10	24 (62.5%)	2.3
EMP0692	41	10	4	12 (83.3%)	1.9
D4	43	9	3	12 (75.0%)	1.6
AOB					
All Sites	269	39		52 (75.0%)	2.9
EMP0093	35	8	0	9 (88.9%)	1.6
EMP0089	24	9	3	12 (75.0%)	1.7
EMP0046	19	3	1	3 (100%)	0.8
EMP0067	41	19	8	22 (86.4%)	2.8
SAC01	40	8	0	11 (72.7%)	1.8
EMP0692	80	16	7	34 (47.1%)	1.8
D4	30	13	2	27 (48.1%)	2.3

Parenthetical numbers next to the Chao1 indices show the percent of estimated (Chao1) diversity actually recovered (number of OTUs). "Unique" OTUs for each station show the number of OTUs exclusively containing sequences from that station. OTUs were defined as ≥95% sequence similarity.

AOA AND AOB COMMUNITY DIVERSITY

The *amoA* clone libraries in this study are the first exploration of the ammonia-oxidizing communities in the Sacramento-San Joaquin Delta, expanding the database of *amoA* sequences from the San Francisco Bay estuary system (Francis et al., 2005; Mosier and Francis, 2008; Lund et al., 2012) upstream into the Sacramento and San Joaquin rivers. Furthermore, ammonia-oxidizing communities in rivers are undersampled compared to coastal sediments, soils, and marine waters (Biller et al., 2012; Cao et al., 2013), and the data in this study help to expand our understanding of the diversity of *amoA* and ammonia-oxidizing microorganisms in riverine sediments.

Both archaeal and bacterial *amoA* sequences were obtained from all 7 Delta sites. The richness of AOA *amoA* was greater than for AOB: when analyzed using a 95% sequence similarity cutoff, the 276 total AOA *amoA* sequences formed 52 OTUs, while the 269 AOB *amoA* sequences formed 39 OTUs (**Table 2**). Rarefaction analysis of AOA OTUs suggested the highest richness at stations SAC01 in the upper Sacramento River and EMP0093 in the lower San Joaquin (**Figure 4A**), while richness was remarkably low at EMP0089, further up the San Joaquin River. It is unclear why this station showed such a marked lack of AOA diversity, especially since AOB *amoA* sequences obtained here were far more diverse (see below). Rarefaction curves of AOB OTUs differed from those of AOA: stations EMP0067 and D4 had the highest richness, while EMP0046 had the lowest (**Figure 4B**). Curves generated with all combined sequences appeared to be leveling off but not yet at a plateau, indicating that we characterized the majority, but not the fullest extent, of the total ammonia oxidizer diversity in the Delta (**Figure 4C**), and that many OTUs present were shared between sites.

To further assess the richness and diversity of the Delta sediments, Chao1 and Shannon indices were calculated for individual sites (**Table 2**). The Chao1 richness index, which estimates the total theoretical number of OTUs in a sample (Chao, 1984), ranged from 1 to 24 for AOA (mean ± SD = 13 ± 7 OTUs), and indicated that Sacramento River station SAC01 harbored the highest AOA richness. Station SAC01 also had the highest number (10) of unique AOA OTUs. Chao1 suggested 3 to 34 AOB OTUs should be present at Delta sites (17 ± 11 OTUs), with the two upper estuary stations having the greatest estimated richness. The fraction of estimated OTUs observed in the combined data sets was 69.7% for AOB and 75% for AOA, supporting the conclusion that a substantial number of OTUs from the Delta may yet be unrecovered (**Figure 4C**). The percentage of richness recovered at each individual station ranged from 62.5 to 100% (83.0 ± 13.3%) for AOA and 47.1–100% (74.2 ± 18.7%) for AOB.

The Shannon diversity index estimates the "entropy" associated with OTU composition in a data set, or the uncertainty of predicting the identity of a randomly selected OTU (Legendre and Legendre, 2012). While richness indices estimate the total number of OTUs in a sample, diversity indices also account for the relative abundance ("evenness") of OTUs within sites. Shannon analysis generally supported the conclusions of the Chao1 index, though with a few interesting differences. While the Sacramento River station SAC01 had the highest AOA richness as estimated by the Chao1 index, the Shannon index matched the AOA rarefaction analyses in suggesting that the San Joaquin River station EMP0093 (Shannon = 2.4), as well as SAC01 (Shannon = 2.3), had relatively high diversity (**Table 2**; **Figure 4A**). For AOB data, Shannon indices indicated *amoA* diversity at Sacramento

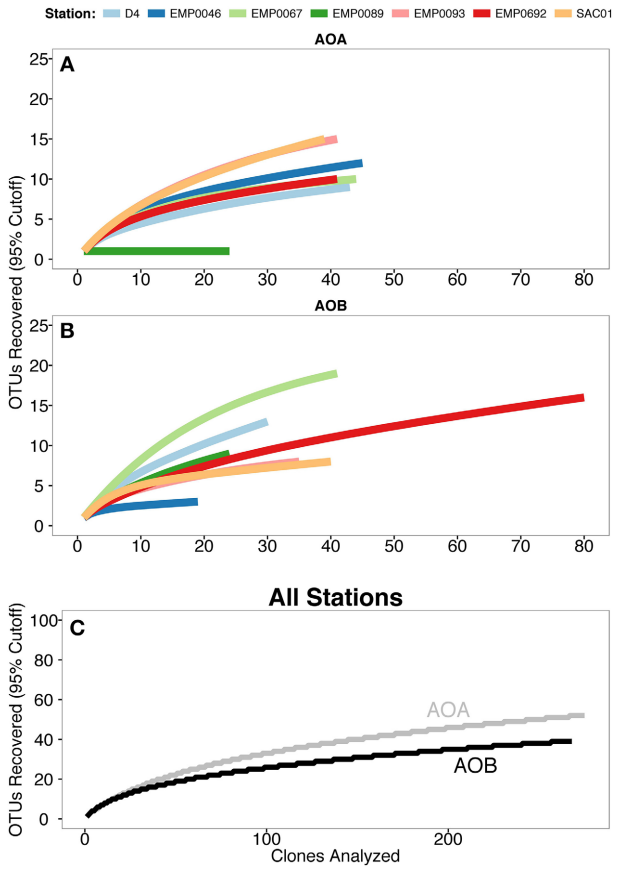

FIGURE 4 | Rarefaction curves of *amoA* OTU (≥95% similarity) data. **(A)** AOA and **(B)** AOB, with color denoting sampling site. **(C)** Combined OTU data from all stations, with AOA *amoA* data in gray and AOB *amoA* in black.

River station EMP0067 and upper estuary station D4 was high (Shannon = 2.8 and 2.3, respectively; **Table 2**), matching the AOB rarefaction curve (**Figure 4B**). Both Chao1 and Shannon indices were in the general range of other estuarine and riverine sediments, though on the higher side (e.g., Mosier and Francis, 2008; Liu et al., 2013; Zheng et al., 2014). Neither Shannon nor Chao1 indices were significantly correlated with potential nitrification rates.

AOA *amoA* COMPOSITION

Years after the discovery of "Marine Group I" Crenarchaeota in the ocean (DeLong, 1992; Fuhrman et al., 1992), these archaea have been broadly (though not exclusively) split into "group I.1a" (marine water and sediment) and "group I.1b" (soil) clades, and appear to be abundant members of the microbial communities in soils, sediments, freshwaters, and marine waters. Numerous cultures and enrichments have documented their ability to sustain autotrophic growth by oxidizing ammonia (Könneke et al., 2005; Santoro and Casciotti, 2011; Tourna et al., 2011; French et al., 2012; Mosier et al., 2012b). In initial studies of AOA *amoA* in San Francisco Bay, many sequences from freshwater and oligohaline sediments grouped together in a distinct and presumably "low-salinity" I.1a clade (Francis et al., 2005; Mosier and Francis, 2008); sequences in this clade are commonly found in diverse freshwater and oligohaline estuarine environments (Mosier and Francis, 2008; Hu et al., 2010; Wu et al., 2010; Wankel et al., 2011; Liu et al., 2013; Sonthiphand et al., 2013). A number of putative low-salinity AOA have been enriched from environmental samples, including *Nitrosoarchaeum limnia* strain SFB1 (Blainey et al., 2011; Mosier et al., 2012b), *N. limnia* strain BG20 (Mosier et al., 2012a), *N. koreensis* (Jung et al., 2011), and freshwater enrichment AC2 (French et al., 2012).

In our clone libraries, 25% (13/52) of AOA OTUs fell within the "low-salinity" clade (**Figure 5**). The only AOA OTU that contained sequences from all 7 Delta sites ("A1") clustered within this clade, near another OTU ("A5") containing sequences from all 5 riverine stations. Both of these ubiquitous OTUs were similar to *N. limnia* (94.9–95.3% nucleotide similarity to the *N. limnia* reference *amoA* sequence). OTU "A1" was the most populous Delta OTU, containing 86/276 (31%) of Delta AOA sequences, and the combined OTUs within the "low-salinity" clade included 152/276 (55%) of the Delta AOA sequences. Numerous OTUs (8/52; 15.4%), all of which contained sequences from the upper estuary stations, grouped near *N. koreensis* and freshwater enrichment AC2, suggesting this clade may be well suited to live in oligohaline sediments.

Nearly half the AOA OTUs obtained from the Delta (25/52; 48%) grouped with I.1a AOA sequences from marine, estuarine, and freshwater sediments (related to *Nitrosopumilus maritimus*) to form three major "sediment" clades (**Figure 5**). No Delta OTUs clustered closely with *N. maritimus*, despite previous detection of *N. maritimus*-like sequences in San Francisco Bay sediments (Mosier and Francis, 2008) and other estuaries (Cao et al., 2013), which suggests this clade of AOA does not penetrate inland to the rivers upstream of San Francisco Bay. Within the sediment clades, 11 OTUs (21% total) clustered in a clade (90% bootstrap support) containing freshwater enrichments "AC5" and "DW" (both isolated from lakes in Ohio, USA). Physiological experiments showed these strains grow well at relatively low NH_4^+ concentrations and are not impaired by low or fluctuating oxygen concentrations, perhaps as a specialization for living at the sedimentary oxic/anoxic interface (French et al., 2012). These organisms appeared to be consistent members of the benthic AOA communities throughout all stations in the Delta. Notably, OTU "A4," containing sequences from both rivers and the upper estuary, clustered tightly with enrichment "DW" (100% bootstrap support and 98.4% nucleotide similarity). This AOA strain therefore appears to be common in the Delta, and may be a generally important player in N cycling in freshwater and oligohaline sediments.

AOA group I.1b, typically recovered from soils (Gubry-Rangin et al., 2011; Pester et al., 2012), was also well represented in our libraries. In total, 27% (14/52) of OTUs from the Delta were related to two distinct I.1b clades: one contained *Nitrososphaera* spp. (Hatzenpichler et al., 2008; Tourna et al., 2011), while the other included soil fosmid 54d9, the first metagenomic linkage between an archaeal *amoA* gene and a 16S rRNA gene (**Figure 5**; Treusch et al., 2005). A small number of OTUs (8%, 4/52), comprising only sequences obtained from Sacramento

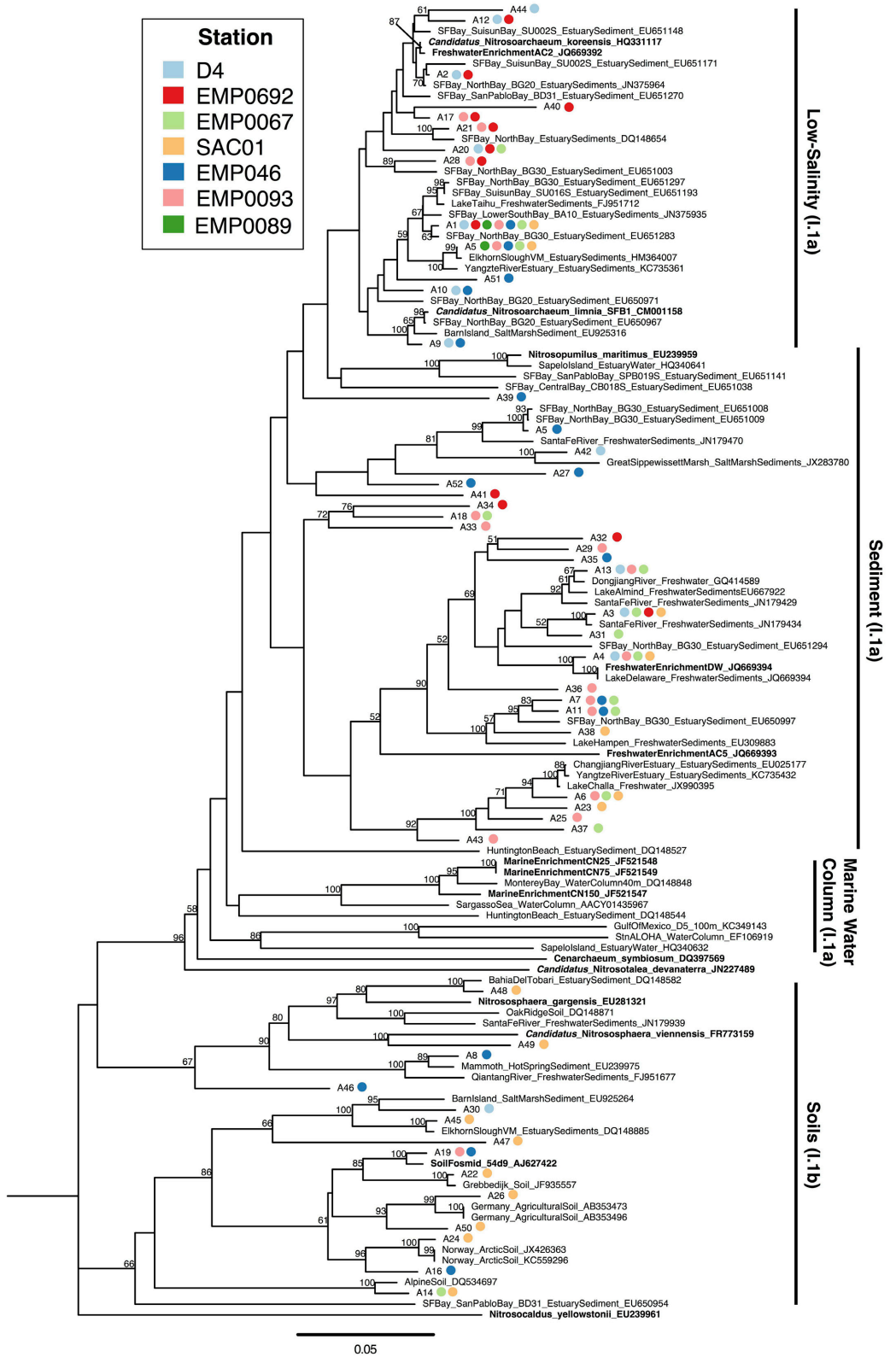

FIGURE 5 | Neighbor joining tree of AOA *amoA* OTUs (≥95% similarity) from the Delta. Colored points next to each OTU indicate the composition of the OTU by station. Values at nodes indicate bootstrap support ≥50% (1000 neighbor-joining bootstrap replicates). Reference sequences from named organisms are indicated in bold. Clades referred to in the text are marked to the right of the tree.

River station SAC01 or Franks Tract station EMP0046, grouped with the *Nitrososphaera* sequences. Interestingly, these stations appear to harbor common AOA lineages despite the markedly different physicochemical conditions between them (**Table 1**). On the other hand, the clade containing fosmid 54d9 contained 10/52 Delta OTUs (19%), and was geographically widespread, including sequences from all regions in the Delta. It is possible some uncultured group I.1b AOA have simply been transported into the Delta from soils in its agricultural watershed, as much of the Delta itself is active farmland (Lund et al., 2010) and group I.1b AOA are commonly found in agricultural soils (Nicol et al., 2008; Pratscher et al., 2011); however, without sequencing *amoA* mRNA transcripts, we could not determine whether their presence within clone libraries was not due to inactive passage through the Delta. Nevertheless, the presence of I.1b AOA in many other estuarine and riverine sediments (Mosier and Francis, 2008; Moin et al., 2009; Abell et al., 2010; Wankel et al., 2011; Liu et al., 2013) implies that they are at least a common member of ammonia-oxidizing communities in these systems.

Sequences clustering with *Nitrosotalea devanaterra* have been found in numerous freshwater environments, including lakes and rivers, and are occasionally found in estuary sediments (Cao et al., 2013). The lack of this clade in our AOA *amoA* clone libraries is curious. As *N. devanaterra* was originally isolated from, and commonly found in, acidic soils (Gubry-Rangin et al., 2011; Lehtovirta-Morley et al., 2011), these AOA may be poorly adapted to the pH-neutral regions of the Delta (**Table 1**). However, while a negative correlation between *Nitrosotalea* relative abundance and pH was documented from lakes in the Pyrenees (Auguet and Casamayor, 2013), *Nitrosotalea* sequences have also been reported from numerous non-acidic freshwater ecosystems (Auguet et al., 2012; Liu et al., 2013; Bollmann et al., 2014). It is unclear what factors other than pH may regulate the abundance or activity of *Nitrosotalea* AOA in freshwater ecosystems. If the lack of this clade in the Delta is not merely an artifact of our limited number of sequenced clones, comparing the environmental conditions of the Delta with sediments with abundant *Nitrosotalea* may be useful for identifying factors that potentially affect its distribution.

Overall, our data showed a diverse AOA community in the Delta, including many of the clades commonly found in estuary and freshwater sediments. Unlike other ecosystems where AOA *amoA* is restricted to a small number of clades (e.g., the marine water column and terrestrial soils), AOA diversity in estuary sediments is often quite complex, typically including sequences from marine, low-salinity, and soil clades (Biller et al., 2012; Cao et al., 2013). Previous work from a range of sites in San Francisco Bay found the majority of AOA sequences clustering in either the "low-salinity" clade (now including *Nitrosoarchaeum* spp.), one of the major soil clades, and a diverse sediment clade including *Nitrosopumilus maritimus*, though numerous additional sequences fell in other less populous clades (Francis et al., 2005; Mosier and Francis, 2008). Similarly diverse benthic archaeal communities have been reported from other estuaries, including Plum Island Sound (Bernhard et al., 2010), the Westerschelde estuary (Sahan and Muyzer, 2008), Elkhorn Slough (Francis et al., 2005; Wankel et al., 2011; Smith et al., 2014b), and the Changjiang Estuary (Dang et al., 2008), among others. However, the geographic positioning of the Delta at the upstream reaches of San Francisco Bay was reflected in AOA communities largely dominated by OTUs grouping in the soil and freshwater clades, with fewer OTUs grouping in typical marine clades. For example, the preponderance of Delta sequences related to *Nitrosoarchaeum* spp., as well as sequences grouping with freshwater enrichments "DW" and "AC5," indicated the widespread presence of these strains in this upper estuary and riverine ecosystem, while the absence of OTUs closely related to *Nitrosopumilus maritimus* suggested this organism is less common in freshwater sediments than in estuarine or marine sediments. Compared to estuary and marine sediments, AOA community composition in freshwater (and especially river) sediments is relatively understudied (Cao et al., 2013). It is therefore difficult to assess the "typical" diversity of freshwater sediments. However, a handful of studies have documented diverse benthic freshwater AOA communities, commonly including the soil, "low-salinity," and some marine/estuary sediment clades (Herrmann et al., 2009; Wu et al., 2010; Liu et al., 2013; Bollmann et al., 2014), suggesting the clades of AOA recovered from the riverine Delta stations may include common members of benthic freshwater AOA communities. Compared to marine waters and sediments, the presence of group I.1b *amoA* OTUs in the Delta may reflect the proximity of this river-dominated system to terrestrial influences.

AOB *amoA* COMPOSITION

In estuary sediments, AOB often show distinct phylogenetic partitioning along salinity gradients (e.g., Francis et al., 2003; Bernhard et al., 2005), with communities in marine-influenced regions generally dominated by *Nitrosospira*-like *amoA* sequences and those in oligohaline/freshwater regions by a mix of *Nitrosospira*-like and *Nitrosomonas*-like sequences (Bernhard and Bollmann, 2010). These two major AOB clades appear physiologically distinct. For example, both lab and field experiments have suggested *Nitrosospira*-like AOB can be more active or abundant in low NH_4^+ environments, whereas *Nitrosomonas*-like AOB may be adapted to grow in high NH_4^+ environments (Taylor and Bottomley, 2006; Peng et al., 2013), although modeling experiments have suggested cultured *Nitrosospira* may grow rapidly in response to large NH_4^+ pulses (Bouskill et al., 2012b). *Nitrosospira*-like AOB are common in marine and soil ecosystems (Stephen et al., 1996; Rotthauwe et al., 1997; Freitag and Prosser, 2003; O'Mullan and Ward, 2005), and often found in estuaries, as well (Francis et al., 2003; Bernhard et al., 2005; Freitag et al., 2006; Mosier and Francis, 2008; Smith et al., 2014b). However, only 7/39 (17.9%) Delta OTUs grouped with *Nitrosospira* or *Nitrosospira*-like sequences. Along with sequences previously recovered from soils and estuary sediments, 3/39 OTUs (7.7%) clustered near cultured *Nitrosospira* sequences, including *N. multiformis* and *N. briensis*. OTU "B34" was very closely related to *Nitrosospira.* sp. 40K1 (96.9% nucleotide identity), originally isolated from loam soil (Jiang and Bakken, 1999). Only one OTU ("B33") was within the mesohaline *Nitrosospira*-like clade ("B") common in estuaries, while 3/39 OTUs (7.7%) grouped in the low-salinity *Nitrosospira*-like clade ("A") (**Figure 6**). Overall, *Nitrosospira*-like OTUs contained sequences from 5 of 7 sites,

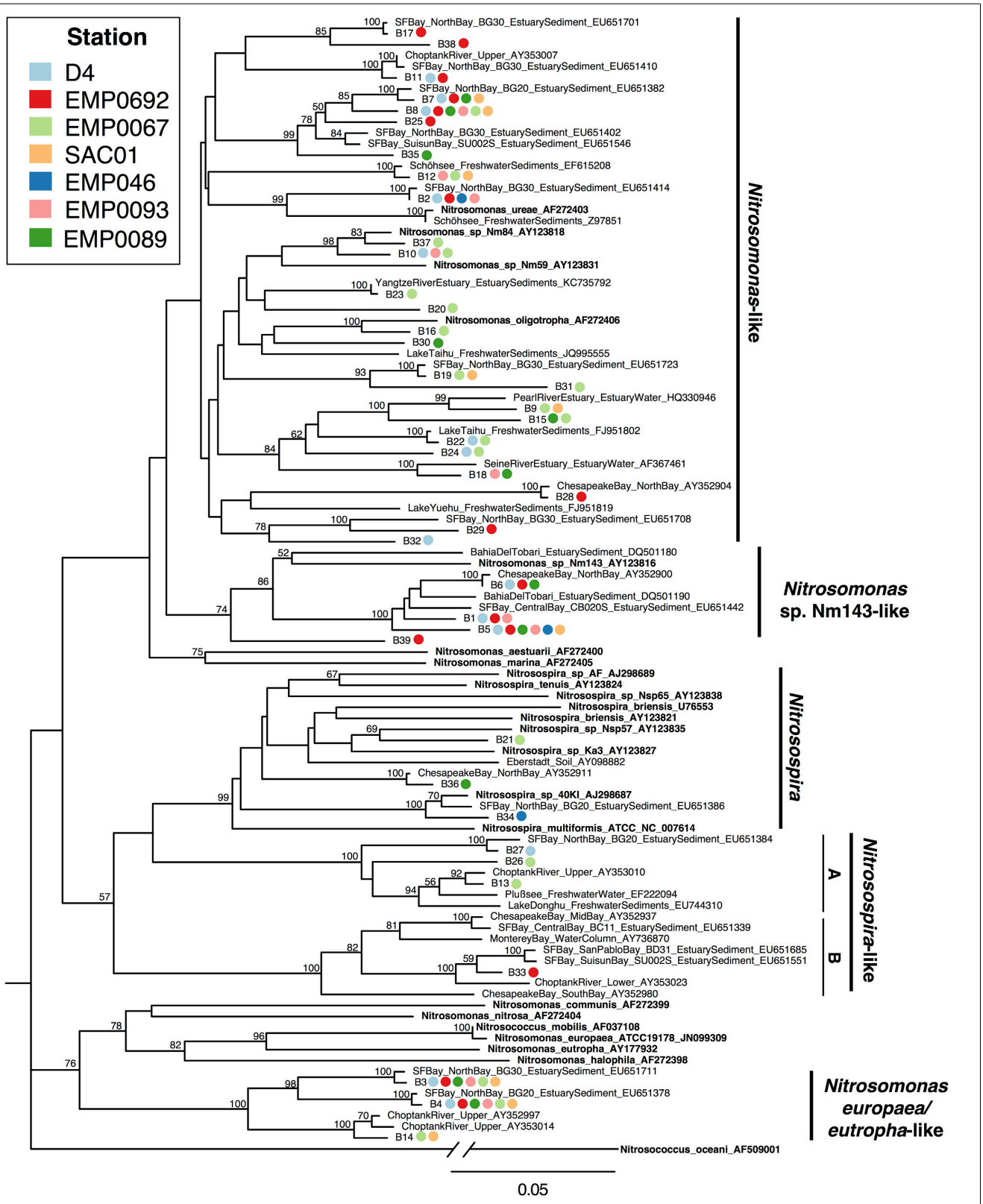

FIGURE 6 | Neighbor joining tree of AOB *amoA* OTUs (≥95% similarity) from the Delta. Colored points next to each OTU indicate the composition of the OTU by station. Values at nodes indicate bootstrap support ≥50% (1000 neighbor-joining bootstrap replicates). Reference sequences from named organisms are indicated in bold. Clades referred to in the text are marked to the right of the tree.

and were therefore relatively widespread throughout the Delta. However, no OTUs in this clade contained sequences from more than one station, suggesting the *Nitrosospira*-like AOB in the Delta may be sensitive to site-specific environmental conditions.

Three AOB OTUs fell in a well-supported clade that grouped, with moderate support, next to a cluster of *Nitrosomonas* species (*Nitrosomonas europaea*, *N. eutropha*, *N. communis, N. nitrosa, N. halophila*, etc.) generally adapted to high-N environments (Koops et al., 1991; Stehr et al., 1995; Mortimer et al., 2004; Stein et al., 2007; Dang et al., 2010). This as yet-uncultivated clade, referred to here as "*Nitrosomonas europaea/eutropha*-like," has been found in a range of nutrient-rich ecosystems (Sahan and Muyzer, 2008; Wankel et al., 2011; Zheng et al., 2014). OTUs "B3" and "B4" contained sequences from all Delta sites other than Franks Tract, and were nearly identical (>99% nucleotide identity) to sequences within this clade previously obtained from northern San Francisco Bay (Mosier and Francis, 2008). Notably, all three *Nitrosomonas europaea/eutropha*-like OTUs included sequences from both NH_4^+-rich Sacramento River stations (**Figure 6**). Closely related sequences have also been obtained from low-salinity, high-nutrient sediments in the upper Choptank River, Maryland, though NH_4^+ in the Choptank was lower than the Sacramento River (Francis et al., 2003). These OTUs appear to represent organisms broadly adapted to oligohaline and relatively N-rich environments, and the absence of sequences from Franks Tract suggests its relatively oligotrophic (see **Table 1**, **Figure 2**) conditions may not be hospitable to *N. europaea/eutropha*-like AOB.

The majority of AOB OTUs from the Delta (29/39; 74%) were in a broad group referred to here as "*Nitrosomonas*-like" (**Figure 6**), closely related to cultivated strains including *N. oligotropha* and *N. ureae*. Nucleotide identity between Delta OTUs and sequences from *Nitrosomonas* spp. was 81.3 to 98.0%. *Nitrosomonas ureae* and *N. oligotropha* have relatively high affinity for NH_4^+ (Koops and Pommerening-Röser, 2001; Bollmann et al., 2002); thus, these bacteria may be able to thrive in low-NH_4^+ environments. Related sequences are commonly found in freshwater and estuarine sediments (Speksnijder et al., 1998; de Bie et al., 2001; Cébron et al., 2003; Bernhard et al., 2005; Peng et al., 2013), including the northern reaches of San Francisco Bay (Mosier and Francis, 2008), and have also been recovered from marine environments (Ward et al., 2007). Some *Nitrosomonas*-like OTUs, such as OTU "B8," appeared widely distributed across the Delta. However, others were region-specific: OTUs "B11," "B17," and "B38" exclusively contained sequences from the upper estuary, and OTU "B2" contained sequences from all regions other than the Sacramento River (**Figure 6**). *Nitrosomonas*-like OTUs therefore appeared to be common in Delta sediments, but with geographical distributions differing between OTUs.

Multiple AOB OTUs grouped in a clade (86% bootstrap support) containing *Nitrosomonas* sp. Nm143, a strongly-supported, novel AOB lineage (Purkhold et al., 2003) commonly found in marine and estuarine sediments (e.g., Bernhard et al., 2005; Mosier and Francis, 2008). Nucleotide identity between these OTUs and *Nitrosomonas* sp. Nm143 was 86.4–88.0%. All OTUs in this group contained sequences from one or both upper estuary stations, and two contained sequences from both estuarine stations and a San Joaquin River station (**Figure 6**). OTU "B5" was widely distributed throughout the Delta, containing sequences from all Delta sites other than station EMP0067 (although sequences from SAC01, further up the Sacramento River, were present). These data suggested *Nitrosomonas* sp. Nm143-like AOB were common members of microbial communities of the Delta.

Similar to AOA diversity in the Delta, its diverse AOB communities included many common estuary and freshwater clades, but were distinct from typical benthic meso/polyhaline estuary communities. In estuaries, common AOB clades include those related to *Nitrosomonas ureae/oligotropha/aestuarii*, as well as yet-uncultivated clades close to *Nitrosomonas* sp. Nm143 and *Nitrosospira* (Francis et al., 2003; Bernhard et al., 2005; Mosier and Francis, 2008; Bernhard and Bollmann, 2010; Peng et al., 2013). In freshwater sediments, trophic status and nutrient loading are frequently thought to affect AOB diversity, with *Nitrosomonas europaea/eutropha*-like AOB typically found in eutrophic sediments, *Nitrosospira*-like AOB in lower nutrient sediments, and *Nitrosomonas oligotropha/ureae* generally widespread (Zhang et al., 2007; Chen et al., 2009; Herrmann et al., 2009; Wu et al., 2010; Bollmann et al., 2014). While some common estuary AOB sequences were found in the Delta, few Delta sequences grouped in the *Nitrosospira*-like clade. A number of OTUs, however, grouped with *Nitrosomonas* sp. Nm143-like AOB. All three OTUs in this clade included sequences from both upper estuary stations, as well as at least one river, suggesting the AOB represented by these OTUs are widespread in the upper estuary but also sometimes present in the fresher regions of the Delta, as well. Interestingly, sequences from all regions of the Delta fell in the *Nitrosomonas europaea/eutropha*-like clade, despite the clear physicochemical and trophic differences between the two rivers (**Table 1**; **Figure 2**), and a number of Delta OTUs similar to *N. oligotropha/ureae* (though not all) were also widely distributed throughout the Delta. These ubiquitous OTUs, typical of either eutrophic or oligotrophic freshwater sediments, suggest AOB communities in the Delta may be structured by more than just trophic status.

GEOGRAPHICAL CLUSTERING OF AMMONIA-OXIDIZING POPULATIONS

To assess whether ammonia oxidizer diversity in the Delta differed by region, we performed PCA on Hellinger-transformed OTU counts of combined AOA and AOB data from each site (analyses of each separate gene showed similar results; Supplementary Figure A2). The Hellinger transformation maintains information on relative abundance between sites, while removing potential effects of differences in total abundance (Legendre and Gallagher, 2001; Legendre and Legendre, 2012). Since clone library data is considered semi-quantitative at best (PCR and cloning biases may cause some clades to be over-represented), we believed transformed OTU counts were a reasonable, if imperfect, representation of relative abundance (a PCA using OTU presence/absence produced similar results; Supplementary Figure A3). The first two principal component axes of the PCA explained 54.8% of the variance in *amoA* diversity between stations. Station EMP0046 grouped alone, due to the effects of numerous archaeal and bacterial OTUs (**Figure 7**). The distinct ammonia-oxidizing

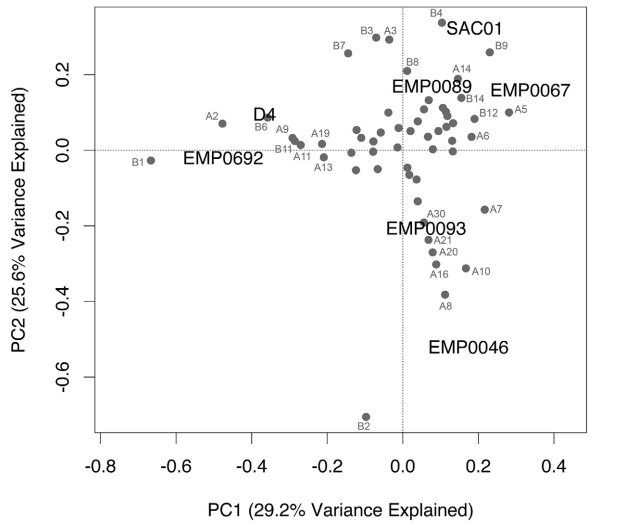

FIGURE 7 | PCA biplot (scaling 1) of combined, Hellinger-transformed AOA and AOB *amoA* OTU counts. Distance between stations on the biplot represents Euclidean distance in multidimensional space. Projections of a station onto an OTU vector indicate its position along that vector. Identity of OTUs is indicated, using the same names as **Figures 5**, **6** (AOA *amoA* OTUs are labeled "A" and AOB *amoA* OTUs are labeled "B"). OTUs clustered near the center are unnamed, for legibility.

community here may reflect the environmental uniqueness (i.e., low nutrient concentrations and elevated pH) of Franks Tract compared to the other sampled regions (**Table 1**; **Figure 2**). The upper estuary stations EMP0692 and D4 clustered together, driven by the presence of multiple OTUs, most notably "B1" and "A2." Therefore, ammonia oxidizer community composition shifted between the rivers and the upper reaches of San Francisco Bay: even though stations D4 and EMP0692 were only in the low-salinity estuary regime, there is a clear difference between these sites and those in the fresher regions of the Delta. Previous research showed stark differences between ammonia-oxidizing communities along the entire salinity gradient of San Francisco Bay (Mosier and Francis, 2008), and our data suggest that communities in the oligohaline upper estuary were also distinct from those in river sediments. Such partitioning fits the general pattern of distinct ammonia-oxidizing communities along salt gradients (Bernhard and Bollmann, 2010). Additionally, this finding is important in light of recent research suggesting a landward increase in salinity throughout San Francisco Bay and the Delta, due to expected sea level rise and altered precipitation/snowmelt brought on by climate change (Cloern et al., 2011). Understanding the distribution of biogeochemically-relevant microbes throughout this system, and ultimately the controls on their distribution and activity, are crucial aspects of understanding how the ecosystem will respond to environmental changes.

Because the Sacramento River sites had high NH_4^+ concentrations and high potential nitrification rates (**Table 1**), we were particularly interested in whether the ammonia-oxidizing communities in these sediments were distinct from other regions. However, this was not entirely the case: the San Joaquin station EMP0089 grouped near both Sacramento stations (**Figure 7**), though the Sacramento River stations were more strongly separated when OTU presence/absence data were used (Supplementary Figure A3). Therefore, ammonia oxidizer community composition may not be a strong indicator of biogeochemical potential in sediments in the Delta. However, given the high AOB abundance in the Sacramento River (**Figure 3**), it is likely that OTUs "B4" and "B9" are particularly important ammonia oxidizers here, as these two bacterial OTUs contributed to the clustering of these three stations in the combined PCA. These OTUs are quite phylogenetically distinct (only 74.7% nucleotide identity): one grouped in the "*Nitrosomonas europaea/eutropha*-like" clade, and the other in an unresolved but distinct "*Nitrosomonas*-like" clade (**Figure 6**).

In addition to the PCA using OTU count data, we analyzed the phylogenetic uniqueness of the Delta stations using non-metric multidimensional scaling (NMDS) of unweighted UniFrac distances (Lozupone and Knight, 2005). While analyses of OTU counts separate sites due to the presence and/or relative abundance of OTUs, UniFrac estimates the fraction of tree branch lengths unique to each site. NMDS compares calculated pairwise distances between sites (in this case, UniFrac distances) to distances between points in ordination space, rearranging the points to maximize the correlation between these two distances and thus minimize a "stress" statistic. Therefore, clustering of sites indicates similarity, but ordination distances do not necessarily reflect the original pairwise distances (Ramette, 2007; Legendre and Legendre, 2012). In contrast to the OTU-count PCA, both AOA and AOB UniFrac NMDS analyses grouped the Sacramento River stations SAC01 and EMP067 separately from the other stations (**Figure 8**). Thus, even if relative OTU abundance did not clearly separate these stations from other regions, it appears the Sacramento River sediments harbored phylogenetically distinct ammonia-oxidizing populations. In light of their high NH_4^+ exposure and potential nitrification rates, the separation of the Sacramento River stations in UniFrac analyses for both genes, combined with the distinct prevalence of large AOB populations, suggested the unique diversity of ammonia oxidizers here may be responsible for the enhanced potential biogeochemical functioning in this river. The upper estuary stations, however, did not group as distinctly in NMDS analyses as in the OTU-count PCA: while the AOA NMDS grouped D4 and EMP0692 somewhat close together, the AOB NMDS did not, grouping them instead with the San Joaquin River stations (**Figure 8**). While the relative abundances of ammonia-oxidizing OTUs in the upper estuary separated upper estuary stations from the other regions of the Delta (**Figure 7**), the OTUs driving this separation may not have been phylogenetically unique to this region.

CONCLUSIONS

This study of the Sacramento/San Joaquin Delta indicated benthic ammonia oxidizers are likely important players in the N cycle within this ecosystem, particularly in the NH_4^+-replete Sacramento River. The high abundance of AOB in this river (outnumbering AOA), combined with elevated potential nitrification

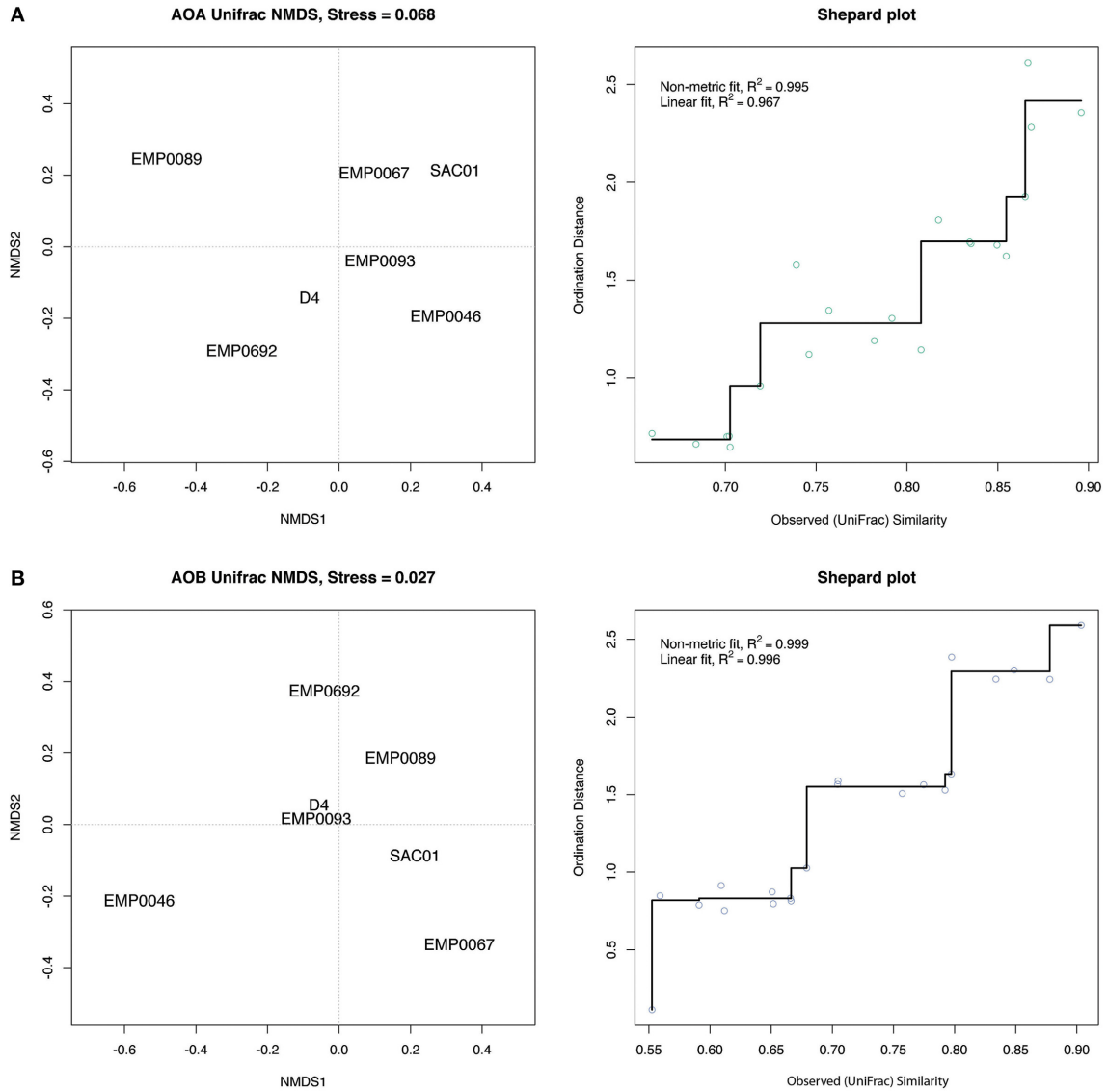

FIGURE 8 | Unweighted UniFrac distance-based NMDS plots. (A) AOA and **(B)** AOB *amoA*. Proximity between stations represents similarity but is not necessarily equal to original distances. For each gene, the NMDS plot is shown on the left, and a Shepard plot, showing the correlation between observed similarity (i.e., UniFrac distance) and ordination distance, is shown on the right. Each point corresponds to pairwise distances between two sites, and the fit between the UniFrac distances and ordination distances is drawn as a line. Values of R^2 are shown for a linear correlation and a non-metric fit based on the stress statistic (see Oksanen, 2013).

rates, suggested AOB may be driving nitrification in the benthic regions of the Delta most directly affected by anthropogenic NH_4^+ pollution. Our clone libraries vastly expanded the database of *amoA* sequences from the San Francisco Bay ecosystem, as well as from freshwater and riverine sediments in general. Across the regions of the Delta, relative abundance of ammonia oxidizer OTUs showed a distinction between the oligohaline estuary and the riverine regions, without clear partitioning of the two rivers. However, there was a marked difference in phylogenetic uniqueness for both AOA and AOB between the Sacramento River and the other regions. Benthic nitrification is likely a key link in the N cycle of estuarine and riverine ecosystems that are strongly affected by anthropogenic nutrient inputs, including the Delta. Understanding the controls on biogeochemical cycles and the associated microbial communities, as well as the relationships between the two, is vital for understanding how aquatic ecosystems will be affected by the climatic changes and increased human development associated with the twenty-first century.

ACKNOWLEDGMENTS

We thank Paul Salop, Sarah Lowe, Applied Marine Sciences, the San Francisco Estuary Institute, and the crew of the R/V *Endeavor* for allowing us to participate in the sediment cruises and assisting in sample collection. We are grateful to Steve Bay for providing

water quality data. Marie Lund provided valuable assistance and advice in the lab. This work was funded by NSF Biological Oceanography grant OCE-0847266 to Christopher A. Francis. Salary support came from a Stanford University DARE Doctoral Fellowship and EPA STAR Graduate fellowship for Annika C. Mosier, and from the Northern California chapter of the ARCS Foundation for Jason M. Smith.

SUPPLEMENTARY MATERIAL

The Supplementary Material for this article can be found online at: http://www.frontiersin.org/journal/10.3389/fmicb.2014.00743/abstract

REFERENCES

Abell, G. C. J., Revill, A. T., Smith, C., Bissett, A. P., Volkman, J. K., and Robert, S. S. (2010). Archaeal ammonia oxidizers and *nirS*-type denitrifiers dominate sediment nitrifying and denitrifying populations in a subtropical macrotidal estuary. *ISME J.* 4, 286–300. doi: 10.1038/ismej.2009.105

Anderson, D. M., Glibert, P. M., and Burkholder, J. M. (2002). Harmful algal blooms and eutrophication: nutrient sources, composition, and consequences. *Estuar. Coasts* 25, 704–726. doi: 10.1007/BF02804901

Auguet, J. C., and Casamayor, E. O. (2013). Partitioning of *Thaumarchaeota* populations along environmental gradients in high mountain lakes. *FEMS Microbiol. Ecol.* 84, 154–164. doi: 10.1111/1574-6941.12047

Auguet, J. C., Triadó-Margarit, X., Nomokonova, N., Camarero, L., and Casamayor, E. O. (2012). Vertical segregation and phylogenetic characterization of ammonia-oxidizing Archaea in a deep oligotrophic lake. *ISME J.* 6, 1786–1797. doi: 10.1038/ismej.2012.33

Beman, J. M., and Francis, C. A. (2006). Diversity of ammonia-oxidizing archaea and bacteria in the sediments of a hypernutrified subtropical estuary: Bahía del Tobarí, Mexico. *Appl. Environ. Microbiol.* 72, 7767–7777. doi: 10.1128/AEM.00946-06

Beman, J. M., Popp, B. N., and Alford, S. E. (2012). Quantification of ammonia oxidation rates and ammonia-oxidizing archaea and bacteria at high resolution in the Gulf of California and eastern tropical North Pacific Ocean. *Limnol. Oceanogr.* 57, 711–726. doi: 10.4319/lo.2012.57.3.0711

Beman, J. M., Popp, B. N., and Francis, C. A. (2008). Molecular and biogeochemical evidence for ammonia oxidation by marine Crenarchaeota in the Gulf of California. *ISME J.* 2, 429–441. doi: 10.1038/ismej.2007.118

Beman, J. M., Roberts, K. J., Wegley, L., Rohwer, F., and Francis, C. A. (2007). Distribution and diversity of archaeal ammonia monooxygenase genes associated with corals. *Appl. Environ. Microbiol.* 73, 5642–5647. doi: 10.1128/AEM.00461-07

Bernhard, A. E., and Bollmann, A. (2010). Estuarine nitrifiers: new players, patterns and processes. *Estuar. Coast. Shelf Sci.* 88, 1–11. doi: 10.1016/j.ecss.2010.01.023

Bernhard, A. E., Donn, T., Giblin, A. E., and Stahl, D. A. (2005). Loss of diversity of ammonia-oxidizing bacteria correlates with increasing salinity in an estuary system. *Environ. Microbiol.* 7, 1289–1297. doi: 10.1111/j.1462-2920.2005.00808.x

Bernhard, A. E., Landry, Z. C., Blevins, A., de la Torre, J. R., Giblin, A. E., and Stahl, D. A. (2010). Abundance of ammonia-oxidizing *Archaea* and *Bacteria* along an estuarine salinity gradient in relation to potential nitrification rates. *Appl. Environ. Microbiol.* 76, 1285–1289. doi: 10.1128/AEM.02018-09

Billen, G., Garnier, J., and Lassaletta, L. (2013). The nitrogen cascade from agricultural soils to the sea: modelling nitrogen transfers at regional watershed and global scales. *Philos. Trans. R. Soc. B Biol. Sci.* 368, 20130123. doi: 10.1038/nature11069

Biller, S. J., Mosier, A. C., Wells, G. F., and Francis, C. A. (2012). Global biodiversity of aquatic ammonia-oxidizing archaea is partitioned by habitat. *Front. Microbiol.* 3:252. doi: 10.3389/fmicb.2012.00252

Blainey, P. C., Mosier, A. C., Potanina, A., Francis, C. A., and Quake, S. R. (2011). Genome of a low-salinity ammonia-oxidizing archaeon determined by single-cell and metagenomic analysis. *PLoS ONE* 6:e16626. doi: 10.1371/journal.pone.0016626

Bollmann, A., Bar-Gilissen, M. J., and Laanbroek, H. J. (2002). Growth at low ammonium concentrations and starvation response as potential factors involved in niche differentiation among ammonia-oxidizing bacteria. *Appl. Environ. Microbiol.* 68, 4751–4757. doi: 10.1128/AEM.68.10.4751-4757.2002

Bollmann, A., Bullerjahn, G. S., and McKay, R. M. (2014). Abundance and diversity of ammonia-oxidizing archaea and bacteria in sediments of trophic end members of the Laurentian Great Lakes, Erie and Superior. *PLoS ONE* 9:e97068. doi: 10.1371/journal.pone.0097068

Borcard, D., Gillet, F., and Legendre, P. (2011). *Numerical Ecology with R*. New York, NY: Springer.

Bouskill, N. J., Eveillard, D., Chien, D., Jayakumar, A., and Ward, B. B. (2012a). Environmental factors determining ammonia-oxidizing organism distribution and diversity in marine environments. *Environ. Microbiol.* 14, 714–729. doi: 10.1111/j.1462-2920.2011.02623.x

Bouskill, N. J., Tang, J., Riley, W. J., and Brodie, E. L. (2012b). Trait-based representation of biological nitrification: model development, testing, and predicted community composition. *Front. Microbiol.* 3:364. doi: 10.3389/fmicb.2012.00364

Boynton, W. R., and Kemp, W. M. (2008). "Estuaries," in *Nitrogen in the Marine Environment*, eds D. G. Capone, D. A. Bronk, M. R. Mulholland, and E. J. Carpenter (Oxford, UK: Elsevier), 809–866.

Brochier-Armanet, C., Boussau, B., Gribaldo, S., and Forterre, P. (2008). Mesophilic crenarchaeota: proposal for a third archaeal phylum, the Thaumarchaeota. *Nat. Rev. Microbiol.* 6, 245–252. doi: 10.1038/nrmicro1852

Brooks, M. L., Fleishman, E., Brown, L. R., Lehman, P. W., Werner, I., Scholz, N., et al. (2012). Life histories, salinity zones, and sublethal contributions of contaminants to pelagic fish declines illustrated with a case study of San Francisco Estuary, California, USA. *Estuar. Coasts* 35, 603–621. doi: 10.1007/s12237-011-9459-6

Caffrey, J. M., Bano, N., Kalanetra, K., and Hollibaugh, J. T. (2007). Ammonia oxidation and ammonia-oxidizing bacteria and archaea from estuaries with differing histories of hypoxia. *ISME J.* 1, 660–662. doi: 10.1038/ismej.2007.79

Cao, H., Auguet, J. C., and Gu, J. D. (2013). Global ecological pattern of ammonia-oxidizing archaea. *PLoS ONE* 8:e52853. doi: 10.1371/journal.pone.0052853

Cébron, A., Berthe, T., and Garnier, J. (2003). Nitrification and nitrifying bacteria in the lower Seine River and estuary (France). *Appl. Environ. Microbiol.* 69, 7091–7100. doi: 10.1128/AEM.69.12.7091-7100.2003

Chao, A. (1984). Nonparametric estimation of the number of classes in a population. *Scand. J. Stat.* 11, 265–270.

Chen, G. Y., Qiu, S. L., and Zhou, Y. Y. (2009). Diversity and abundance of ammonia-oxidizing bacteria in eutrophic and oligotrophic basins of a shallow Chinese lake (Lake Donghu). *Res. Microbiol.* 160, 173–178. doi: 10.1016/j.resmic.2009.01.003

Cloern, J. E., and Jassby, A. D. (2012). Drivers of change in estuarine-coastal ecosystems: Discoveries from four decades of study in San Francisco Bay. *Rev. Geophys.* 50, RG4001. doi: 10.1029/2012RG000397

Cloern, J. E., Jassby, A. D., Carstensen, J., Bennett, W. A., Kimmerer, W., MacNally, R., et al. (2012). Perils of correlating CUSUM-transformed variables to infer ecological relationships (Breton et al. 2006, Glibert 2010). *Limnol. Oceanogr.* 57, 665–668. doi: 10.4319/lo.2012.57.2.0665

Cloern, J. E., Knowles, N., Brown, L. R., Cayan, D., Dettinger, M. D., Morgan, T. L., et al. (2011). Projected evolution of California's San Francisco bay-delta-river system in a century of climate change. *PLoS ONE* 6:e24465. doi: 10.1371/journal.pone.0024465

Conomos, T. J., Smith, R. E., and Gartner, J. W. (1985). Environmental setting of San Francisco Bay. *Hydrobiologia* 129, 1–12. doi: 10.1007/BF00048684

Cornwell, J. C., Glibert, P. M., and Owens, M. S. (2014). Nutrient fluxes from sediments in the San Francisco Bay Delta. *Estuar. Coasts* 37, 1120–1133. doi: 10.1007/s12237-013-9755-4

Dang, H., Li, J., Chen, R., Wang, L., Guo, L., Zhang, Z., et al. (2010). Diversity, abundance, and spatial distribution of sediment ammonia-oxidizing betaproteobacteria in response to environmental gradients and coastal eutrophication in Jiaozhou Bay, China. *Appl. Environ. Microbiol.* 76, 4691–4702. doi: 10.1128/AEM.02563-09

Dang, H., Zhang, X., Sun, J., Li, T., Zhang, Z., and Yang, G. (2008). Diversity and spatial distribution of sediment ammonia-oxidizing crenarchaeota in response to estuarine and environmental gradients in the Changjiang Estuary and East China Sea. *Microbiology* 154, 2084–2095. doi: 10.1099/mic.0.2007/013581-0

de Bie, M. J. M., Speksnijder, A. G. C. L., Kowalchuk, G. A., Schuurman, T., Zwart, G., Stephen, J. R., et al. (2001). Shifts in the dominant populations

of ammonia-oxidizing ß-subclass Proteobacteria along the eutrophic Schelde estuary. *Aquat. Microb. Ecol.* 23, 225–236. doi: 10.3354/ame023225

De Corte, D., Yokokawa, T., Varela, M. M., Agogué, H., and Herndl, G. J. (2008). Spatial distribution of *Bacteria* and *Archaea* and *amoA* gene copy numbers throughout the water column of the Eastern Mediterranean Sea. *ISME J.* 3, 147–158. doi: 10.1038/ismej.2008.94

DeLong, E. F. (1992). Archaea in coastal marine environments. *Proc. Natl. Acad. Sci. U.S.A.* 89, 5685–5689.

Dollhopf, S. L., Hyun, J. H., Smith, A. C., Adams, H. J., O'Brien, S., and Kostka, J. E. (2005). Quantification of ammonia-oxidizing bacteria and factors controlling nitrification in salt marsh sediments. *Appl. Environ. Microbiol.* 71, 240–246. doi: 10.1128/AEM.71.1.240-246.2005

Erisman, J. W., Galloway, J. N., Seitzinger, S., Bleeker, A., Dise, N. B., Petrescu, A. M. R., et al. (2013). Consequences of human modification of the global nitrogen cycle. *Philos. Trans. R. Soc. B Biol. Sci.* 368, 20130116. doi: 10.1126/science.1176985

Erisman, J. W., Sutton, M. A., Galloway, J., Klimont, Z., and Winiwarter, W. (2008). How a century of ammonia synthesis changed the world. *Nat. Geosci.* 1, 636–639. doi: 10.1038/ngeo325

Francis, C. A., O'Mullan, G. D., and Ward, B. B. (2003). Diversity of ammonia monooxygenase (*amoA*) genes across environmental gradients in Chesapeake Bay sediments. *Geobiology* 1, 129–140. doi: 10.1046/j.1472-4669.2003.00010.x

Francis, C. A., Roberts, K. J., Beman, J. M., Santoro, A. E., and Oakley, B. B. (2005). Ubiquity and diversity of ammonia-oxidizing archaea in water columns and sediments of the ocean. *Proc. Natl. Acad. Sci. U.S.A.* 102, 14683–14688. doi: 10.1073/pnas.0506625102

Freitag, T. E., and Prosser, J. I. (2003). Community structure of ammonia-oxidizing bacteria within anoxic marine sediments. *Appl. Environ. Microbiol.* 69, 1359–1371. doi: 10.1128/AEM.69.3.1359-1371.2003

Freitag, T. E., Chang, L., and Prosser, J. I. (2006). Changes in the community structure and activity of betaproteobacterial ammonia-oxidizing sediment bacteria along a freshwater-marine gradient. *Environ. Microbiol.* 8, 684–696. doi: 10.1111/j.1462-2920.2005.00947.x

French, E., Kozlowski, J. A., Mukherjee, M., Bullerjahn, G., and Bollmann, A. (2012). Ecophysiological characterization of ammonia-oxidizing archaea and bacteria from freshwater. *Appl. Environ. Microbiol.* 78, 5773–5780. doi: 10.1128/AEM.00432-12

Fuhrman, J. A., McCallum, K., and Davis, A. A. (1992). Novel major archaebacterial group from marine plankton. *Nature* 356, 148–149. doi: 10.1038/356148a0

Galloway, J. N., Dentener, F. J., Capone, D. G., Boyer, E. W., Howarth, R. W., Seitzinger, S. P., et al. (2004). Nitrogen cycles: past, present, and future. *Biogeochemistry* 70, 153–226. doi: 10.1007/s10533-004-0370-0

Glibert, P. M. (2010). Long-term changes in nutrient loading and stoichiometry and their relationships with changes in the food web and dominant pelagic fish species in the San Francisco Estuary, California. *Rev. Fisher. Sci.* 18, 211–232. doi: 10.1080/10641262.2010.492059

Glibert, P. M., Fullerton, D., Burkholder, J. M., Cornwell, J. C., and Kana, T. M. (2011). Ecological stoichiometry, biogeochemical cycling, invasive species, and aquatic food webs: San Francisco estuary and comparative systems. *Rev. Fisher. Sci.* 19, 358–417. doi: 10.1080/10641262.2011.611916

Gubry-Rangin, C., Hai, B., Quince, C., Engel, M., Thomson, B. C., James, P., et al. (2011). Niche specialization of terrestrial archaeal ammonia oxidizers. *Proc. Natl. Acad. Sci. U.S.A.* 108, 21206–21211. doi: 10.1073/pnas.1109000108

Hansen, J. I., Henriksen, K., and Blackburn, T. H. (1981). Seasonal distribution of nitrifying bacteria and rates of nitrification in coastal marine sediments. *Microb. Ecol.* 7, 297–304. doi: 10.1007/BF02341424

Hatzenpichler, R., Lebedeva, E. V., Spieck, E., Stoecker, K., Richter, A., Daims, H., et al. (2008). A moderately thermophilic ammonia-oxidizing crenarchaeote from a hot spring. *Proc. Natl. Acad. Sci. U.S.A.* 105, 2134–2139. doi: 10.1073/pnas.0708857105

Henriksen, K., Hansen, J. I., and Blackburn, T. H. (1981). Rates of nitrification, distribution of nitrifying bacteria, and nitrate fluxes in different types of sediment from Danish waters. *Mar. Biol.* 61, 299–304. doi: 10.1007/BF00401569

Herrmann, M., Saunders, A. M., and Schramm, A. (2009). Effect of lake trophic status and rooted macrophytes on community composition and abundance of ammonia-oxidizing prokaryotes in freshwater sediments. *Appl. Environ. Microbiol.* 75, 3127–3136. doi: 10.1128/AEM.02806-08

Herrmann, M., Scheibe, A., Avrahami, S., and Kusel, K. (2011). Ammonium availability affects the ratio of ammonia-oxidizing bacteria to ammonia-oxidizing archaea in simulated creek ecosystems. *Appl. Environ. Microbiol.* 77, 1896–1899. doi: 10.1128/AEM.02879-10

Hu, A., Yao, T., Jiao, N., Liu, Y., Yang, Z., and Liu, X. (2010). Community structures of ammonia-oxidising archaea and bacteria in high-altitude lakes on the Tibetan Plateau. *Freshwater Biol.* 55, 2375–2390. doi: 10.1111/j.1365-2427.2010.02454.x

Jassby, A. D., and Cloern, J. E. (2000). Organic matter sources and rehabilitation of the Sacramento-San Joaquin Delta (California, USA). *Aquat. Conserv. Mar. Freshwater Ecosyst.* 10, 323–352. doi: 10.1002/1099-0755(200009/10)10:5<323::AID-AQC417>3.0.CO;2-J

Jiang, Q. Q., and Bakken, L. R. (1999). Comparison of *Nitrosospira* strains isolated from terrestrial environments. *FEMS Microbiol. Ecol.* 30, 171–186. doi: 10.1111/j.1574-6941.1999.tb00646.x

Joye, S. B., and Hollibaugh, J. T. (1995). Influence of sulfide inhibition of nitrification on nitrogen regeneration in sediments. *Science* 270, 623–625. doi: 10.1126/science.270.5236.623

Jung, M. Y., Park, S. J., Min, D., Kim, J. S., Rijpstra, W. I. C., Sinninghe Damsté, J. S., et al. (2011). Enrichment and characterization of an autotrophic ammonia-oxidizing archaeon of mesophilic crenarchaeal group I.1a from an agricultural soil. *Appl. Environ. Microbiol.* 77, 8635–8647. doi: 10.1128/AEM.05787-11

Kemp, W. M., Sampou, P., Caffrey, J., Mayer, M., Henriksen, K., and Boynton, W. R. (1990). Ammonium recycling versus denitrification in Chesapeake Bay sediments. *Limnol. Oceanogr.* 35, 1545–1563.

Kimmerer, W. (2004). Open water processes of the San Francisco Estuary: from physical forcing to biological responses. *San Francisco Estuary Watershed Sci.* 2:1.

Kimmerer, W. J. (2008). Losses of Sacramento River Chinook salmon and delta smelt to entrainment in water diversions in the Sacramento-San Joaquin Delta. *San Francisco Estuary Watershed Sci.* 6:2.

Koops, H. P., and Pommerening-Röser, A. (2001). Distribution and ecophysiology of the nitrifying bacteria emphasizing cultured species. *FEMS Microbiol. Ecol.* 37, 1–9. doi: 10.1111/j.1574-6941.2001.tb00847.x

Koops, H. P., Böttcher, B., Möller, U. C., Pommerening-Röser, A., and Stehr, G. (1991). Classification of eight new species of ammonia-oxidizing bacteria: *Nitrosomonas communis* sp. nov., *Nitrosomonas ureae* sp. nov., *Nitrosomonas aestuarii* sp. nov., *Nitrosomonas marina* sp. nov., *Nitrosomonas nitrosa* sp. nov., *Nitrosomonas eutropha* sp. nov., *Nitrosomonas oligotropha* sp. nov. and *Nitrosomonas halophila* sp. nov. *J. Gen. Microbiol.* 137, 1689–1699. doi: 10.1099/00221287-137-7-1689

Kowalchuk, G. A., and Stephen, J. R. (2001). Ammonia-oxidizing bacteria: a model for molecular microbial ecology. *Annu. Rev. Microbiol.* 55, 485–529. doi: 10.1146/annurev.micro.55.1.485

Könneke, M., Bernhard, A. E., de la Torre, J. R., Walker, C. B., Waterbury, J. B., and Stahl, D. A. (2005). Isolation of an autotrophic ammonia-oxidizing marine archaeon. *Nature* 437, 543–546. doi: 10.1038/nature03911

Lancelot, C., Grosjean, P., Rousseau, V., Breton, E., and Glibert, P. M. (2012). Rejoinder to "Perils of correlating CUSUM-transformed variables to infer ecological relationships (Breton et al., 2006; Glibert 2010)." *Limnol. Oceanogr.* 57, 669–670. doi: 10.4319/lo.2012.57.2.0669

Legendre, P., and Gallagher, E. (2001). Ecologically meaningful transformations for ordination of species data. *Oecologia* 129, 271–280. doi: 10.1007/s004420100716

Legendre, P., and Legendre, L. (2012). *Numerical Ecology*, *3rd Edn.* San Francisco, CA: Elsevier.

Lehtovirta-Morley, L. E., Stoecker, K., Vilcinskas, A., Prosser, J. I., and Nicol, G. W. (2011). Cultivation of an obligate acidophilic ammonia oxidizer from a nitrifying acid soil. *Proc. Natl. Acad. Sci. U.S.A.* 108, 15892–15897. doi: 10.1073/pnas.1107196108

Leininger, S., Urich, T., Schloter, M., Schwark, L., Qi, J., Nicol, G. W., et al. (2006). Archaea predominate among ammonia-oxidizing prokaryotes in soils. *Nature* 442, 806–809. doi: 10.1038/nature04983

Liu, S., Shen, L., Lou, L., Tian, G., Zheng, P., and Hu, B. (2013). Spatial distribution and factors shaping the niche segregation of ammonia-oxidizing microorganisms in the Qiantang River, China. *Appl. Environ. Microbiol.* 79, 4065–4071. doi: 10.1128/AEM.00543-13

Lozupone, C., and Knight, R. (2005). UniFrac: a new phylogenetic method for comparing microbial communities. *Appl. Environ. Microbiol.* 71, 8228–8235. doi: 10.1128/AEM.71.12.8228-8235.2005

Lozupone, C., Hamady, M., and Knight, R. (2006). UniFrac - An online tool for comparing microbial community diversity in a phylogenetic context. *BMC Bioinformatics* 7:371. doi: 10.1186/1471-2105-7-371

Lucas, L. V., Cloern, J. E., Thompson, J. K., and Monsen, N. E. (2002). Functional variability of habitats within the Sacramento-San Joaquin delta: restoration implications. *Ecol. Appl.* 12, 1528–1547. doi: 10.1890/1051-0761(2002)012[1528:FVOHWT]2.0.CO;2

Lund, J. R., Hanak, E., Fleenor, W. E., Bennett, W. A., Howitt, R. E., Mount, J. F., et al. (2010). *Comparing Futures for the Sacramento-San Joaquin Delta*. Berkeley, CA: University of California Press.

Lund, M. B., Smith, J. M., and Francis, C. A. (2012). Diversity, abundance and expression of nitrite reductase (*nirK*)-like genes in marine thaumarchaea. *ISME J.* 6, 1966–1977. doi: 10.1038/ismej.2012.40

MacNally, R., Thomson, J. R., Kimmerer, W. J., Feyrer, F., Newman, K. B., Sih, A., et al. (2010). Analysis of pelagic species decline in the upper San Francisco Estuary using multivariate autoregressive modeling (MAR). *Ecol. Appl.* 20, 1417–1430. doi: 10.1890/09-1724.1

Moin, N. S., Nelson, K. A., Bush, A., and Bernhard, A. E. (2009). Distribution and diversity of archaeal and bacterial ammonia oxidizers in salt marsh sediments. *Appl. Environ. Microbiol.* 75, 7461–7468. doi: 10.1128/AEM.01001-09

Mortimer, R. J. G., Harris, S. J., Krom, M. D., Freitag, T. E., Prosser, J. I., Barnes, J., et al. (2004). Anoxic nitrification in marine sediments. *Mar. Ecol. Prog. Ser.* 276, 37–51. doi: 10.3354/meps276037

Mosier, A. C., Allen, E. E., Kim, M., Ferriera, S., and Francis, C. A. (2012a). Genome sequence of "*Candidatus* Nitrosoarchaeum limnia" BG20, a low-salinity ammonia-oxidizing archaeon from the San Francisco Bay estuary. *J. Bacteriol.* 194, 2119–2120. doi: 10.1128/JB.00007-12

Mosier, A. C., and Francis, C. A. (2008). Relative abundance and diversity of ammonia-oxidizing archaea and bacteria in the San Francisco Bay estuary. *Environ. Microbiol.* 10, 3002–3016. doi: 10.1111/j.1462-2920.2008.01764.x

Mosier, A. C., Lund, M. B., and Francis, C. A. (2012b). Ecophysiology of an ammonia-oxidizing archaeon adapted to low-salinity habitats. *Microb. Ecol.* 64, 955–963. doi: 10.1007/s00248-012-0075-1

Newell, S. E., Fawcett, S. E., and Ward, B. B. (2013). Depth distribution of ammonia oxidation rates and ammonia-oxidizer community composition in the Sargasso Sea. *Limnol. Oceanogr.* 58, 1491–1500. doi: 10.4319/lo.2013.58.4.1491

Nicol, G. W., Leininger, S., and Schleper, C. (2011). "Distribution and activity of ammonia-oxidizing archaea in natural environments," in *Nitrification*, eds B. B. Ward, D. J. Arp, and M. G. Klotz (Washington, DC: ASM Press), 157–178.

Nicol, G. W., Leininger, S., Schleper, C., and Prosser, J. I. (2008). The influence of soil pH on the diversity, abundance and transcriptional activity of ammonia oxidizing archaea and bacteria. *Environ. Microbiol.* 10, 2966–2978. doi: 10.1111/j.1462-2920.2008.01701.x

O'Mullan, G. D., and Ward, B. B. (2005). Relationship of temporal and spatial variabilities of ammonia-oxidizing bacteria to nitrification rates in Monterey Bay, California. *Appl. Environ. Microbiol.* 71, 697–705. doi: 10.1128/AEM.71.2.697-705.2005

Oksanen, J. (2013). *Multivariate Analysis of Ecological Communities in R: Vegan Tutorial*. Available online at: http://cc.oulu.fi/~jarioksa/opetus/metodi/vegantutor.pdf

Parker, A. E., Dugdale, R. C., and Wilkerson, F. P. (2012). Elevated ammonium concentrations from wastewater discharge depress primary productivity in the Sacramento River and the Northern San Francisco estuary. *Mar. Pollut. Bull.* 64, 574–586. doi: 10.1016/j.marpolbul.2011.12.016

Peng, X., Yando, E., Hildebrand, E., Dwyer, C., Kearney, A., Waciega, A., et al. (2013). Differential responses of ammonia-oxidizing archaea and bacteria to long-term fertilization in a New England salt marsh. *Front. Microbiol.* 3:445. doi: 10.3389/fmicb.2012.00445

Pester, M., Rattei, T., Flechl, S., Gröngröft, A., Richter, A., Overmann, J., et al. (2012). *amoA*-based consensus phylogeny of ammonia-oxidizing archaea and deep sequencing of *amoA* genes from soils of four different geographic regions. *Environ. Microbiol.* 14, 525–539. doi: 10.1111/j.1462-2920.2011.02666.x

Pratscher, J., Dumont, M. G., and Conrad, R. (2011). Ammonia oxidation coupled to CO_2 fixation by archaea and bacteria in an agricultural soil. *Proc. Natl. Acad. Sci. U.S.A.* 108, 4170–4175. doi: 10.1073/pnas.1010981108

Purkhold, U., Wagner, M., Timmermann, G., Pommerening-Röser, A., and Koops, H. P. (2003). 16S rRNA and *amoA*-based phylogeny of 12 novel betaproteobacterial ammonia-oxidizing isolates: extension of the dataset and proposal of a new lineage within the nitrosomonads. *Int. J. Syst. Evolut. Microbiol.* 53, 1485–1494. doi: 10.1099/ijs.0.02638-0

Rabalais, N. N., Díaz, R. J., Levin, L. A., Turner, R. E., Gilbert, D., and Zhang, J. (2010). Dynamics and distribution of natural and human-caused hypoxia. *Biogeosciences* 7, 585–619. doi: 10.5194/bg-7-585-2010

Ramette, A. (2007). Multivariate analyses in microbial ecology. *FEMS Microbiol. Ecol.* 62, 142–160. doi: 10.1111/j.1574-6941.2007.00375.x,

R Core Team. (2014). *R: A Language and Environment for Statistical Computing*. Vienna: R Foundation for Statistical Computing. Available online at: http://www.R-project.org/

Rotthauwe, J. H., Witzel, K. P., and Liesack, W. (1997). The ammonia monooxygenase structural gene *amoA* as a functional marker: molecular fine-scale analysis of natural ammonia-oxidizing populations. *Appl. Environ. Microbiol.* 63, 4704–4712.

Sahan, E., and Muyzer, G. (2008). Diversity and spatio-temporal distribution of ammonia-oxidizing *Archaea* and *Bacteria* in sediments of the Westerschelde estuary. *FEMS Microbiol. Ecol.* 64, 175–186. doi: 10.1111/j.1574-6941.2008.00462.x

Santoro, A. E., and Casciotti, K. L. (2011). Enrichment and characterization of ammonia-oxidizing archaea from the open ocean: phylogeny, physiology and stable isotope fractionation. *ISME J.* 5, 1796–1808. doi: 10.1038/ismej.2011.58

Santoro, A. E., Casciotti, K. L., and Francis, C. A. (2010). Activity, abundance and diversity of nitrifying archaea and bacteria in the central California Current. *Environ. Microbiol.* 12, 1989–2006. doi: 10.1111/j.1462-2920.2010.02205.x

Santoro, A. E., Francis, C. A., de Sieyes, N. R., and Boehm, A. B. (2008). Shifts in the relative abundance of ammonia-oxidizing bacteria and archaea across physicochemical gradients in a subterranean estuary. *Environ. Microbiol.* 10, 1068–1079. doi: 10.1111/j.1462-2920.2007.01547.x

Schloss, P. D., Westcott, S. L., Ryabin, T., Hall, J. R., Hartmann, M., Hollister, E. B., et al. (2009). Introducing mothur: open-source, platform-independent, community-supported software for describing and comparing microbial communities. *Appl. Environ. Microbiol.* 75, 7537–7541. doi: 10.1128/AEM.01541-09

Smith, J. M., Casciotti, K. L., Chavez, F. P., and Francis, C. A. (2014a). Differential contributions of archaeal ammonia oxidizer ecotypes to nitrification in coastal surface waters. *ISME J.* 8, 1704–1714. doi: 10.1038/ismej.2014.11

Smith, J. M., Mosier, A. C., and Francis, C. A. (2014b). Spatiotemporal relationships between the abundance, distribution, and potential activities of ammonia-oxidizing and denitrifying microorganisms in intertidal sediments. *Microb. Ecol.* doi: 10.1007/s00248-014-0450-1. [Epub ahead of print].

Sommer, T., Armor, C., Baxter, R., Breuer, R., Brown, L., Chotkowski, M., et al. (2007). The collapse of pelagic fishes in the upper San Francisco estuary. *Fisheries* 32, 270–277. doi: 10.1577/1548-8446(2007)32[270:TCOPFI]2.0.CO;2

Sonthiphand, P., Cejudo, E., Schiff, S. L., and Neufeld, J. D. (2013). Wastewater effluent impacts ammonia-oxidizing prokaryotes of the Grand River, Canada. *Appl. Environ. Microbiol.* 79, 7454–7465. doi: 10.1128/AEM.02202-13

Spear, J. R., Barton, H. A., Robertson, C. E., Francis, C. A., and Pace, N. R. (2007). Microbial community biofabrics in a geothermal mine adit. *Appl. Environ. Microbiol.* 73, 6172–6180. doi: 10.1128/AEM.00393-07

Speksnijder, A. G. C. L., Kowalchuk, G. A., Roest, K., and Laanbroek, H. J. (1998). Recovery of a *Nitrosomonas*-like 16S rDNA sequence group from freshwater habitats. *Syst. Appl. Microbiol.* 21, 321–330. doi: 10.1016/S0723-2020(98)80040-4

Stehr, G., Böttcher, B., Dittberner, P., Rath, G., and Koops, H. P. (1995). The ammonia−oxidizing nitrifying population of the River Elbe estuary. *FEMS Microbiol. Ecol.* 17, 177–186. doi: 10.1111/j.1574-6941.1995.tb00141.x

Stein, L. Y., Arp, D. J., Berube, P. M., Chain, P. S. G., Hauser, L., Jetten, M. S. M., et al. (2007). Whole-genome analysis of the ammonia-oxidizing bacterium, *Nitrosomonas eutropha* C91: implications for niche adaptation. *Environ. Microbiol.* 9, 2993–3007. doi: 10.1111/j.1462-2920.2007.01409.x

Stephen, J. R., Chang, Y. J., Macnaughton, S. J., Kowalchuk, G. A., Leung, K. T., Flemming, C. A., et al. (1999). Effect of toxic metals on indigenous soil ß-subgroup proteobacterium ammonia oxidizer community structure and protection against toxicity by inoculated metal-resistant bacteria. *Appl. Environ. Microbiol.* 65, 95–101.

Stephen, J. R., McCaig, A. E., Smith, Z., Prosser, J. I., and Embley, T. M. (1996). Molecular diversity of soil and marine 16S rRNA gene sequences to ß-subgroup ammonia-oxidizing bacteria. *Appl. Environ. Microbiol.* 62, 4147–4154.

Taylor, A. E., and Bottomley, P. J. (2006). Nitrite production by *Nitrosomonas europaea* and *Nitrosospira* sp. AV in soils at different solution concentrations of ammonium. *Soil Biol. Biochem.* 38, 828–836. doi: 10.1016/j.soilbio.2005.08.001

Thomson, J. R., Kimmerer, W. J., Brown, L. R., Newman, K. B., MacNally, R., Bennett, W. A., et al. (2010). Bayesian change point analysis of abundance trends for pelagic fishes in the upper San Francisco estuary. *Ecol. Appl.* 20, 1431–1448. doi: 10.1890/09-0998.1

Tourna, M., Stieglmeier, M., Spang, A., Könneke, M., Schintlmeister, A., Urich, T., et al. (2011). *Nitrososphaera viennensis*, an ammonia oxidizing archaeon from soil. *Proc. Natl. Acad. Sci. U.S.A.* 108, 8420–8425. doi: 10.1073/pnas.1013488108

Treusch, A. H., Leininger, S., Kletzin, A., Schuster, S. C., Klenk, H. P., and Schleper, C. (2005). Novel genes for nitrite reductase and Amo-related proteins indicate a role of uncultivated mesophilic crenarchaeota in nitrogen cycling. *Environ. Microbiol.* 7, 1985–1995. doi: 10.1111/j.1462-2920.2005.00906.x

Wang, Z., Wang, Z., Huang, C., and Pei, Y. (2014). Vertical distribution of ammonia-oxidizing archaea (AOA) in the hyporheic zone of a eutrophic river in North China. *World J. Microbiol. Biotechnol.* 30, 1335–1346. doi: 10.1007/s11274-013-1559-y

Wankel, S. D., Kendall, C., Francis, C. A., and Paytan, A. (2006). Nitrogen sources and cycling in the San Francisco Bay estuary: a nitrate dual isotopic composition approach. *Limnol. Oceanogr.* 51, 1654–1664. doi: 10.4319/lo.2006.51.4.1654

Wankel, S. D., Mosier, A. C., Hansel, C. M., Paytan, A., and Francis, C. A. (2011). Spatial variability in nitrification rates and ammonia-oxidizing microbial communities in the agriculturally impacted Elkhorn Slough Estuary, California. *Appl. Environ. Microbiol.* 77, 269–280. doi: 10.1128/AEM.01318-10

Ward, B. B. (2013). How nitrogen is lost. *Science* 341, 352–353. doi: 10.1126/science.1240314

Ward, B. B. (2012). "The global nitrogen cycle," in *Fundamentals of Geobiology*, eds A. H. Knoll, D. E. Canfield, and K. O. Konhauser (West Sussex, UK: Blackwell Publishing Ltd), 36–48.

Ward, B. B., Eveillard, D., Kirshtein, J. D., Nelson, J. D., Voytek, M. A., and Jackson, G. A. (2007). Ammonia-oxidizing bacterial community composition in estuarine and oceanic environments assessed using a functional gene microarray. *Environ. Microbiol.* 9, 2522–2538. doi: 10.1111/j.1462-2920.2007.01371.x

Weidler, G. W., Gerbl, F. W., and Stan-Lotter, H. (2008). *Crenarchaeota* and their role in the nitrogen cycle in a subsurface radioactive thermal spring in the Austrian Central Alps. *Appl. Environ. Microbiol.* 74, 5934–5942. doi: 10.1128/AEM.02602-07

Wells, G. F., Park, H. D., Yeung, C. H., Eggleston, B., Francis, C. A., and Criddle, C. S. (2009). Ammonia-oxidizing communities in a highly aerated full-scale activated sludge bioreactor: betaproteobacterial dynamics and low relative abundance of Crenarchaea. *Environ. Microbiol.* 11, 2310–2328. doi: 10.1111/j.1462-2920.2009.01958.x

Wu, Y., Xiang, Y., Wang, J., Zhong, J., He, J., and Wu, Q. L. (2010). Heterogeneity of archaeal and bacterial ammonia-oxidizing communities in Lake Taihu, China. *Environ. Microbiol. Rep.* 2, 569–576. doi: 10.1111/j.1758-2229.2010.00146.x

Wuchter, C., Abbas, B., Coolen, M. J. L., Herfort, L., van Bleijswijk, J., Timmers, P., et al. (2006). Archaeal nitrification in the ocean. *Proc. Natl. Acad. Sci. U.S.A.* 103, 12317–12322. doi: 10.1073/pnas.0600756103

Zar, J. H. (1972). Significance testing of the Spearman rank correlation coefficient. *J. Am. Stat. Assoc.* 67, 578–580. doi: 10.2307/2284441

Zhang, Y., Ruan, X. H., Op den Camp, H. J. M., Smits, T. J. M., Jetten, M. S. M., and Schmid, M. C. (2007). Diversity and abundance of aerobic and anaerobic ammonium-oxidizing bacteria in freshwater sediments of the Xinyi River (China). *Environ. Microbiol.* 9, 2375–2382. doi: 10.1111/j.1462-2920.2007.01357.x

Zheng, Y., Hou, L., Newell, S., Liu, M., Zhou, J., Zhao, H., et al. (2014). Community dynamics and activity of ammonia-oxidizing prokaryotes in intertidal sediments of the yangtze estuary. *Appl. Environ. Microbiol.* 80, 408–419. doi: 10.1128/AEM.03035-13

Conflict of Interest Statement: The authors declare that the research was conducted in the absence of any commercial or financial relationships that could be construed as a potential conflict of interest.

Received: 10 July 2014; accepted: 08 December 2014; published online: 08 January 2015.

Citation: Damashek J, Smith JM, Mosier AC and Francis CA (2015) Benthic ammonia oxidizers differ in community structure and biogeochemical potential across a riverine delta. Front. Microbiol. ***5****:743. doi: 10.3389/fmicb.2014.00743*

This article was submitted to Aquatic Microbiology, a section of the journal Frontiers in Microbiology.

frontiers in MICROBIOLOGY

ORIGINAL RESEARCH ARTICLE
published: 20 May 2014
doi: 10.3389/fmicb.2014.00230

Loss of diversity in wood-inhabiting fungal communities affects decomposition activity in Norway spruce wood

Lara Valentín[1,2], Tiina Rajala[1], Mikko Peltoniemi[1], Jussi Heinonsalo[3], Taina Pennanen[1] and Raisa Mäkipää[1]*

[1] *Vantaa Research Unit, Finnish Forest Research Institute, Vantaa, Finland*
[2] *Department of Chemical Engineering, Technical School of Engineering, Universitat Autònoma de Barcelona, Barcelona, Spain*
[3] *Department of Food and Environmental Sciences, University of Helsinki, Helsinki, Finland*

Edited by:
John J. Kelly, Loyola University Chicago, USA

Reviewed by:
Stefan Bertilsson, Uppsala University, Sweden
Petra Fransson, Swedish University of Agricultral Sciences, Sweden

***Correspondence:**
Raisa Mäkipää, Vantaa Research Unit, Finnish Forest Research Institute, PO Box 18, Jokiniemenkuja 1, FI-01301 Vantaa, Finland
e-mail: raisa.makipaa@metla.fi

Hundreds of wood-inhabiting fungal species are now threatened, principally due to a lack of dead wood in intensively managed forests, but the consequences of reduced fungal diversity on ecosystem functioning are not known. Several experiments have shown that primary productivity is negatively affected by a loss of species, but the effects of microbial diversity on decomposition are less studied. We studied the relationship between fungal diversity and the *in vitro* decomposition rate of slightly, moderately and heavily decayed *Picea abies* wood with indigenous fungal communities that were diluted to examine the influence of diversity. Respiration rate, wood-degrading hydrolytic enzymes and fungal community structure were assessed during a 16-week incubation. The number of observed OTUs in DGGE was used as a measure of fungal diversity. Respiration rate increased between early- and late-decay stages. Reduced fungal diversity was associated with lower respiration rates during intermediate stages of decay, but no effects were detected at later stages. The activity of hydrolytic enzymes varied among decay stages and fungal dilutions. Our results suggest that functioning of highly diverse communities of the late-decay stage were more resistant to the loss of diversity than less diverse communities of early decomposers. This indicates the accumulation of functional redundancy during the succession of the fungal community in decomposing substrates.

Keywords: biodiversity, woody debris, respiration activity, functional redundancy, enzymes

INTRODUCTION

The loss of species diversity alters ecosystem function, stability and the ability to provide goods and services to society (Loreau et al., 2001; Hooper et al., 2005; Wertz et al., 2006; Cardinale et al., 2012). Several experiments have shown that primary productivity is negatively affected by a loss of plant species (Loreau et al., 2001; Hooper et al., 2012) and ecosystem stability is reduced by decreasing functional diversity (Hooper et al., 2005). Biodiversity affects the rate of key ecosystem processes such as decomposition and nutrient cycling (Loreau et al., 2001; Hättenschwiler et al., 2005; Gessner et al., 2010). In boreal forests, where fungal communities are major decomposers (Rayner and Boddy, 1988; Lindahl and Boberg, 2008; Stenlid et al., 2008), a high diversity of soil fungi can enhance the decomposition rate (Tiunov and Scheu, 2005), especially under environmental fluctuations such as variations in temperature regimes (Toljander et al., 2011). Hundreds of fungal species in Fennoscandian forests are now threatened, principally due to a lack of dead wood in a forest landscape that is intensively managed (Siitonen, 2001). The consequences of reduced fungal diversity on decomposition are unknown. Furthermore, the stability and function of forest ecosystems might be dramatically affected if the fungal capacity to resist habitat perturbation is continuously exceeded, as is the case for many species in managed forests (Stenlid et al., 2008).

Since fungal species produce complementary enzymes, the presence of many species can improve the communities' efficiency to degrade a wide range of litter constituents and thus enhance decomposition rate (Gessner et al., 2010). Experiments with selected fungal species and their combinations revealed a strong positive relationship between fungal diversity and decomposition rate, which became asymptotic at a relatively low level of diversity (Setälä and McLean, 2004; Tiunov and Scheu, 2005). In experiments involving a few species, facilitation and resource partitioning have been observed (Tiunov and Scheu, 2005). In more diverse terrestrial fungal communities, antagonistic mechanisms might prevail (Boddy, 2000; Gessner et al., 2010) and the colonization sequence of wood-degrading fungi can further affect decomposition (Fukami et al., 2010). Studies of the decomposition rate in manipulated fungal communities are mostly performed with a few cultured species, and the results might be a poor reflection of natural communities, especially if certain community members have a greater proportional influence on the decomposition rate than the totality of the fungal community (Robinson et al., 2005).

Decaying Norway spruce logs harbor diverse fungal communities (Ovaskainen et al., 2010; Rajala et al., 2011; Kubartová et al., 2012), where the number of active species is far higher than that considered in experimental studies. Species number

tends to increase with mass loss (and related changes in the substrate quality) and peaks in the most decayed logs (Rajala et al., 2012). Decomposition of cell wall polymers in wood is a complex process that is driven by a succession of species with different litter-degrading enzymes (Baldrian, 2008; Stenlid et al., 2008). During the decay process of dead wood over several decades, the fungal decomposer community changes from one dominated by ascomycetes to one of white- and brown-rot basidiomycetes, before slowly becoming one composed mainly by the mycorrhizal species found in the underlying soil (Rajala et al., 2010, 2012). Wood-degrading fungi (white-rot and brown-rot fungi) decompose polysaccharides by producing hydrolases, but only white-rot fungi efficiently degrade lignin via oxidative metalloenzymes (e.g., laccase and manganese peroxidase) (Lundell et al., 2010). Experiments with decomposing leaves and needles have linked enzyme activities (EA) with fungal communities (Šnajdr et al., 2011; Žifčáková et al., 2011), but to our knowledge, no study has yet analyzed such a relationship with the fungal community in decomposing wood. Therefore, we studied wood substrates in different stages of decay to examine the effects of manipulated fungal diversity on enzyme production and decomposition rate during the entire process.

The overall objective of this study was to examine the relationship between fungal diversity and decomposition rate by manipulating fungal communities obtained from decaying Norway spruce wood. We designed a microcosm experiment to investigate: (1) whether a reduced diversity of wood-inhabiting fungi affects the decomposition of Norway spruce wood and, if so, (2) whether functional redundancy and stability of the decomposition process varies among decay stages, and (3) whether changes in fungal diversity and rate of decomposition are related to changes in hydrolytic enzyme production. We tested the hypothesis that CO_2 production and enzyme activity in the dead wood are affected by the decay stage of the substrate and diversity of the decomposing species. Furthermore, we hypothetisized that the decomposition activity (measured as CO_2 production) is correlated to overall variation of the fungal community and the decomposition increases to direction that is parallel to increasing species diversity (measured as number of detected OTUs).

MATERIALS AND METHODS

WOOD SAMPLES

The study material was collected from an unmanaged forest in Lapinjärvi (Southern Finland, 60°39.413′N, 26°7.352′E, altitude 50 m, temperature sum 1300°C d; further details are provided in Rajala et al., 2012). Wood samples were obtained from stem discs sawn on site from 46 fallen Norway spruce (*Picea abies*) logs (diameter >5 cm at breast height). Logs were classified as early, intermediate or late stages of decay (I, III, and V according to Mäkinen et al., 2006). Sample discs were sawn in May 2011 and stored in plastic bags at −18°C until processing in the laboratory. The properties of the wood (C/N ratio, lignin content and density) for individual discs were analyzed as described in Rajala et al. (2010) and the mean values of 14 discs from early-decay stages, 12 discs from intermediate-decay stages and 16 discs from late-decay stages were calculated (**Table 1**).

Bark from the outermost layer of each frozen sample disc was removed with a flame-sterilized knife. Frozen discs were then drilled with a flame-sterilized and cooled bit (Ø = 10 mm) from the surface through the sapwood and heartwood. Shavings and sawdust of each decay stage were pooled into a single sample and stored in a plastic bag at −18°C prior to use as a fungal inoculum. A few active fungi might be suppressed during the processing of the samples, but species inhabiting dead wood in boreal forests are acclimated to varying temperatures and the fungal community obtained from the inocula was considered to reflect species composition in each decay phase.

The experimental growth medium (i.e., sawdust) was prepared by milling five discs from each decay stage that had been debarked and dried at 105°C for 48 h. Dry sawdust from each stage was pooled into a single sample and sterilized twice by autoclaving (121°C for 20 min) with a 3-day interval.

EXPERIMENTAL SET-UP

The incubation took place in sterile 100-mL glass flasks containing different amounts of inoculum and autoclaved substrate (**Table 2**). Sterile distilled water was added to each flask to remoisten the culture to a dry matter content similar to that at sampling, i.e., 77% for early, 59% for intermediate and 21% for late decay stages (**Tables 1**, **2**). Flasks were then sealed with rubber septa and a one-way stopcock was connected to a 50 mm needle. The stopcock system was designed to ventilate air and prevent anoxic conditions in the microcosm. The stopcock was opened only when the ventilation was performed after measurement of CO_2 (see below). The air in the flasks was ventilated by connecting the capstock to a diaphragm vacuum pump (type N 022 AN.18, KNF Neuberger GmbH, Germany) for 2 min 30 s. The capstock was then closed and reopened to flush the flasks for 5 min with moist air previously channeled through an autoclaved vent filter (0.2 μm, Millipore, USA). The evacuation-flushing system prevented oxygen depletion and drought in the microcosms.

PREPARATION OF MICROCOSMS AND EXPERIMENTAL DESIGN OF DECOMPOSITION STUDY (EXPERIMENT 1)

The effect of fungal diversity on respiration activity was assessed in microcosms by exposing the inoculum to a dilution procedure (Wertz et al., 2007). We tested four levels of fungal diversity (i.e., dilutions) on triplicate substrates of three different qualities (i.e., decay stages). Experimental conditions in microcosms were as follows: (1) undiluted (UD) inoculum prepared with non-sterile sawdust; (2) a dilution of approximately 1 g inoculum (dry matter, dm) per 10 g of substrate (dm) was prepared by first mixing non-sterile sawdust with sterile distilled water to create slurries with dry matter of 27% (i.e., early), 14% (i.e., intermediate), or 3% (i.e., late), then adding aliquots of 540 mg dm (early), 400 mg dm (intermediate), and 150 mg dm (late) to the corresponding dry substrate to yield a final inoculum dilution of 10^{-1} (**Table 2**); (3) a dilution of approximately 1 g inoculum (dm) per 100 g of substrate (dm) was prepared similarly, but slurry dry matter was 0.8% (early), 0.5% (intermediate) or 0.3% (late), and aliquots of 15 mg (dm) of each slurry were added to the corresponding dry substrate (**Table 2**); (4) autoclaved sawdust was used as a control

Table 1 | Properties of Norway spruce (*Picea abies*) wood of different decay stages (early, intermediate and late) and the number of pooled discs used to prepare the inoculum (non-sterile sawdust) or the autoclaved sawdust for the microcosms.

Wood decay stage	C/N	Lignin (%)	Density kg/dm	[a]Dry matter (%)	[b]Water content (%)	No of pooled discs	
						inoculum	Substrate
Early	352 ± 41	32 ± 5	0.42 ± 0.02	77 ± 0	30 ± 1	14	5
Intermediate	328 ± 63	37 ± 10	0.28 ± 0.01	59 ± 1	71 ± 3	12	5
Late	136 ± 42	51 ± 19	0.15 ± 0.02	21 ± 1	376 ± 16	16	5

The C/N ratio, lignin, diameter, and density (determined as described in Rajala et al., 2010) are the mean values (±SD) of 14 discs from early-decay stages, 12 discs from intermediate-decay stages and 16 discs from late-decay stages. Dry matter and water content were determined by drying fresh sawdust at 105° C for 24 h.

*[a] Dry matter (%) was calculated as: weight of dry sawdust (g)/weight of wet sawdust (g) * 100.*

*[b] Water content (%) was calculated as: [weight of wet sawdust (g)—weight of dry sawdust (g)]/weight of dry sawdust (g) * 100.*

Table 2 | Amount of inoculum (non-sterile sawdust) or autoclaved sawdust in dry form added to 100-mL glass flasks to assess the effect of fungal diversity on the decomposition activities of Norway spruce sawdust in early, intermediate and late stages of decay.

Dilutions of the inoculum	[a]Inoculum (non-sterile sawdust)		Autoclaved sawdust		Added water	Total initial dry weight of the incubated sample	Initial dry matter content
	Decay stage	Amount (g, dm)	Decay stage	Amount (g, dm)	(ml)	(g, dm)	(%)
Undiluted	Early	5.0	–	–	0	5.9	79
	Intermediate	3.8	–	–	0	3.8	59
	Late	1.4	–	–	0	1.4	21
Dilution 10^{-1}	Early	0.54	Early	4.7	5.0	5.24	73
	Intermediate	0.4	Intermediate	3.5	3.0	3.9	52
	Late	0.15	Late	1.3	1.6	1.45	24
Dilution 10^{-2}	Early	0.013	Early	4.7	5.0	4.71	66
	Intermediate	0.015	Intermediate	3.5	3.0	3.52	45
	Late	0.015	Late	1.3	1.6	1.32	23
Control (Ctrl)	–	–	Early	5.2	1.9	5.2	65
	–	–	Intermediate	3.8	3.5	3.8	46
	–	–	Late	1.5	5.7	1.5	21

The same amounts were used in a parallel experiment for the assessment of wood-degrading enzymes.

*[a] Dry matter (dm) content of inoculum that was added as wet sawdust (water content according to field conditions, reported in **Table 1**).*

(Ctrl). The initial fungal diversity of the microcosms was tested with the DGGE (Rajala et al., 2010 and description below) and the number of observed OTUs was used as a measure of fungal diversity. The test showed that the dilution procedure reduced the number of observed fungal OTU in the inocula (**Figure 1**). All treatments were performed in triplicate, yielding a total of 36 flasks (four levels of fungal diversity * three decay stages * three replicates = 36 flasks). Sealed flasks were incubated at 21°C in total darkness for 16 weeks. The cumulative CO_2 was measured periodically (see below) and the airspace of the incubation flasks was ventilated immediately after CO_2 measurement.

At the end of the incubation, the substrate from each replicate was pooled into a single sample and stored at –18°C prior to the extraction of total DNA.

MEASUREMENT OF CO_2, EVACUATION AND CALCULATION OF CARBON LOSS

An air sample (100 μL) was collected from the sealed flask with a Hamilton Microfilter™ glass syringe, previously wiped with 95% ethanol, and injected manually into a gas chromatograph (Hewlett-Packard 6890, Finland) to analyse CO_2 (assuming that most of the produced CO_2 was transferred to the gas phase). The chromatograph was equipped with a capillary column (Agilent 19095P-MS6 HP-PLOT MoleSieve 5 Å, length 30 m and diameter 530 μm) and a temperature conductor detector at 250°C for detecting CO_2. Helium was used as carrier gas at a split ratio of 10:1 and flow rate of 7.9 mL min^{-1}. Injector and oven temperatures were 120 and 40°C, respectively.

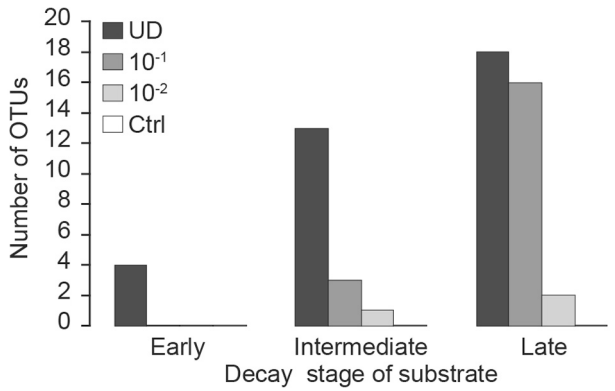

FIGURE 1 | Number of ITS1F-GC/ITS2 fungal DNA-derived DGGE bands (Operational Taxonomic Units; OTUs) in Norway spruce pooled substrate samples at the beginning of incubation under a range of inoculum dilutions (UD, undiluted fungal inoculum; dilution 10^{-1} g inoculum/g substrate (dm); dilution 10^{-2} g inoculum/g substrate (dm); Ctrl, autoclaved sawdust) for early, intermediate and late stages of decay.

The CO_2 level was measured weekly at the beginning of the incubation and every 2 weeks after week five. Estimated carbon loss (*C loss*, %) from microcosms was calculated using cumulative CO_2 at the end of the incubation following equations (1) and (2):

$$\text{C loss}(\%) = \text{cumulative } CO_2\ (\text{g})/\text{Max } CO_2\ (\text{g}) * 100 \quad (1)$$

$$\text{Max } CO_2\ (\text{g}) = \text{mass sawdust (g)} * \text{C (\%)}/100 * M_{CO_2} (\text{g mol}^{-1})/M_C\ (\text{g mol}^{-1}) \quad (2)$$

where *Max* CO_2 is the maximum production of CO_2 from each microcosm, *mass sawdus*t is the amount of sawdust in the flask (in dm), *C* is total carbon content in the sawdust, and M_{CO2} and M_C are the molecular masses of CO_2 (44 g mol^{-1}) and carbon (12 g mol^{-1}), respectively.

PREPARATION OF MICROCOSMS AND EXPERIMENTAL DESIGN OF THE HYDROLYTIC ENZYME STUDY (EXPERIMENT 2)

The activity of several wood-degrading hydrolytic enzymes was measured from flasks incubated in parallel with the microcosms in Experiment 1. The experimental design was similar to that in Experiment 1 (i.e., four levels of fungal diversity * three decay stages * three replicates = 36 flasks). In this study, each flask was opened under sterile conditions after weeks 4, 6, 9, 11, 13, and 16 to collect about 1 g (wet weight, ww) of the substrate. Half of the sample was subjected immediately to enzyme activity assays and the other half was stored at −18°C prior to DNA extraction (samples from weeks 9 and 13).

EXTRACTION OF ENZYMES AND ACTIVITY ASSAYS

Four glycoside hydrolases [β-glucuronidase (EC 3.2.1.31), β-xylosidase (EC 3.2.1.37), β-glucosidase (EC 3.2.1.21), and cellobiohydrolase (EC 3.2.1.37)] were recovered from the substrate samples following a recently described enzyme extraction method with slight modifications (Heinonsalo et al., 2012). The method is based on the recovery of extracellular enzymes by centrifuging a small amount of substrate (∼155 mg, ww) placed into a centrifuge tube filter (0.45 μm pore size; 500 μL working volume; Costar® Spin-X® CLS8162; Corning Inc., NY, USA). The centrifugation speed was 15,700 *g* for 30 min. To obtain enough enzyme solution to run the assays, three sub-samples were prepared from each flask. The day before extraction, 200 μL sterile distilled water was added to each substrate sub-sample. After centrifugation, approximately 250 μL enzyme solution was recovered, pooled with that from the other three sub-samples, adjusted to a total volume of 2 mL with water and used directly for the activity assays. Once all the tubes were centrifuged, the inner filter tube was placed in an oven at 70°C for 48 h to measure substrate dry matter.

Hydrolytic enzymes were measured by a fluorimetric assay (Pritsch et al., 2004, 2011) and modified according to the requirements of this study. Three solutions were prepared: (1) incubation buffer (pH 4.5) containing 7.2 mM maleic acid, 7.3 mM citric acid, 10 mM boric acid, 10 mM Tris (2-amino-2(hydroxymethyl)-1,3-propanediol), and 48.8 mM sodium hydroxide; (2) different fluorogenic substrate solutions based on 4-methylumbelliferone (MU) for the detection of each glycosidic enzyme were prepared from 5 mM stock solutions in 2-methoxyethanol. The concentration of each fluorogenic substrate in the working solution was 1500 μM of MU-β-D-glucuronide (for detection of β-glucuronidase), 1500 μM of MU-β-D-xyloside (for detection of β-xylosidase), 1500 μM of MU-β-D-glucoside (for detection of β-glucosidase), and 1200 μM of MU-β-D-cellobioside (for detection of cellobiohydrolase); (3) the stop solution was 1 M Tris at pH 10-11 to enhance the fluorescence response. Triplicate assays were performed in black flat-bottom 96-well microplates, with each well-containing a reaction mixture of 50 μL enzyme solution, 50 μL incubation buffer and 50 μL of the respective fluorogenic substrate solution. Plates were incubated at 20°C on a microplate shaker for 30 min, except for β-glucosidase where 15 min was used. At the end of incubation, 150 μlL stop solution was added to all wells and the fluorescence response was measured with a Wallac 1430 Victor^3 (PerkinElmer, Inc., USA) multilabel plate reader at an excitation wavelength of 364 nm and emission wavelength of 450 nm. Calibration wells were prepared by adding 100 μL stop solution, 100 μL incubation buffer and 50 μL stock solution mixed with water to give final MU concentrations of 0, 0.4, 0.8, 1.2, 1.6, and 2 μM.

Enzyme activities (EA) were expressed as picokatals per gram of substrate (in dm). A picokatal is one picomol of reacted fluorogenic substrate per second. *EA* were calculated using the equation (3). Total hydrolytic activity was estimated by summing that of the four measured enzymes.

$$\text{EA (pkat g}^{-1}) = (\text{sample} - \text{negative control})/(a^*t)^*V_a/V_s^*1/m_s \quad (3)$$

where *sample* is the fluorescence response (counts) of the enzyme solution and *negative control* is the response without enzyme (fluorogenic substrate without sample), *a* is the slope of the regression line of the calibration curve (counts/pmol), *t* is the incubation time (sec), V_a is the adjusted volume of the three sub-samples (2000 μL), V_s is the volume of the enzyme solution in the

well (50 μL), and m_s is the sum of the extracted substrate mass of the three sub-samples (g, dm).

MOLECULAR ANALYSIS OF THE FUNGAL COMMUNITY

Total DNA was extracted from substrates (100–150 mg, ww) at the beginning, after weeks 9 and 13 (only from the microcosms subjected to enzyme analyses) and at the end of incubation (week 16) using the NucleoSpin® 96 Soil Kit (Macherey-Nagel, Germany). Extracted total DNA was amplified using polymerase chain reaction (PCR) with the GC-clamped internal transcribed spacer 1 (ITS1F) primer (Gardes and Bruns, 1993) and the ITS2 primer pair (White et al., 1990) typical of fungal ribosomal DNA. PCR was performed in a 50 μL reaction containing 25 μL MyTaq™ HS Red Mix (which included reaction buffer, dNTP, DNA Polymerase and loading dye; Bioline, Germany), 1 μL each 25 μM primer, 2.5 μL template and 20.5 μL sterile distilled water. The thermal profile for the PCR was: 1 min at 95°C for initial denaturation, 34 cycles of denaturation for 15 s at 95°C, annealing for 15 s at 58°C and extension for 10 s at 72°C, and a final extension of 72°C for 10 s. Equal concentrations of PCR products were resolved by denaturing gradient gel electrophoresis (DGGE) as described in Rajala et al. (2010). Briefly, the denaturing gradient in an acrylamide gel was 18–58% and running conditions were 75 V at 60°C for 16 h. Gels were stained with SYBR® Gold (Molecular Probes, Eugene, Oregon) and visualized with blue light on a SafeImager™ transilluminator (Invitrogen, Carlsbad, California). The DGGE gels were analyzed using GelCompar II software (Applied Maths BVBA, Belgium). The bands at the same position in the DGGE gel were considered the same operational taxonomic unit (OTU). Thus, this step generated a presence–absence matrix of fungal taxa (OTUs) in each microcosm and we used the number of the detected OTUs as a measure of fungal diversity in this experiment.

STATISTICAL ANALYSIS

We analyzed the effects of inoculum dilution (undiluted, 10^{-1} and 10^{-2}) and decay stage on CO_2 production and enzymes activities measured from samples during the incubation period using the methods of longitudinal data analysis (Diggle et al., 2002). We also performed some additional analyses of cumulative CO_2 production during the entire incubation period and on EA at the end of the experiment (week 16) using ANOVA, where longitudinal data analysis was not needed. In addition, we tested correlation between the number of observed OTUs and the cumulative CO_2 production at the end of the experiment.

In the longitudinal analyses of consecutive weekly CO_2 production and log-transformed total hydrolytic EA of the samples, we used a mixed model where replicates (r) represented random effects [$\sim N(0, \sigma_r^2)$]. The fixed part of the model consisted of the decay stage and dilution factors, and their interaction, i.e., the effects we were interested in. Serial correlation of repeated measurements in the time series of replicates was treated with a continuous autoregressive covariance structure AR(1).

Residuals of the fitted models were inspected visually for normality and homoscedasticity. In all cases, we found that the residuals of the CO_2 fit were normally distributed by fitted values, and the distributions were also normal and fairly similar by explanatory variables. Random effects were distributed approximately normally as well. To fulfil these requirements for the total hydrolytic EA, we converted them to a log-scale.

Strong interactions in the fixed part of the model can make it difficult to interpret the model. Therefore, if we found significant interactions between the fixed effects, we simplified the model by either regrouping the dilution and decay stage to a single factor, or by fitting the model for dilution factor by the decay-stage factor, or the other way around.

We also investigated the trends of log-transformed total hydrolytic enzyme activity, and the ratio of hydrolytic activity to CO_2 production during the incubation period. In these cases, we added a slope parameter for incubation week to the fixed part of the model. The trends for these variables were tested for each decay stage separately, so that we allowed the trend to vary by dilution. For the ratio of hydrolytic activity and CO_2 production, the results are presented for the early decay stage by dilution.

Longitudinal analyses were implemented using the lme function of the nlme library of R, using the maximum likelihood method. Parameter significance was estimated by the lme-function.

When a time-series approach was not needed, we used a type II ANOVA with interaction between the decay stage. These analyses were conducted using the ANOVA function in the car-library (Fox and Weisberg, 2011) of R (R Development Core Team, 2011). The same principles of examining the residuals and splitting the model into parts if interactions were present, were applied as with the longitudinal approach. Pairwise comparisons were made with the Tukey Honestly Significant Difference (HSD) test.

Fungal community composition (i.e., the presence/absence of OTUs) was visualized by non-metric multidimensional scaling (NMDS) using metaMDS of the vegan library (Oksanen et al., 2008). We generated a dissimilarity matrix (n_{sample}*n_{sample}) of Bray-Curtis coefficients and used NMDS to create a graph where the distances between points (representing samples) corresponded as closely as possible to the original dissimilarity matrix. Arrows that indicate the direction of maximum correlation of cumulative CO_2 and OTU number with the ordinated samples were superimposed onto the ordination graph. The significance of these correlations was assessed with a permutation test implemented in the envfit function of vegan library (Oksanen et al., 2008). The NMDS was performed separately for each incubation time. The analyses made for week 0 and 16 corresponded to the experiment where flasks were closed during incubation (Experiment 1), whereas those made for week 9 and 13 corresponded to the microcosms in which flasks were opened to collect samples (Experiment 2).

RESULTS

EFFECTS OF SUBSTRATE AND REDUCED DIVERSITY ON DECOMPOSITION

The wood decay stage was an important factor to explain CO_2 production during the experiment (**Figure 2**, Supplementary Material). When we analyzed the consecutive CO_2 observations and their association with the decay stage with longitudinal analysis, we found that late- and intermediate-decay substrates were associated with significantly higher CO_2 production rates than early-decay substrates ($t = 8.0$, $df = 17$, $p \leq 0.001$, and $t = 5.7$,

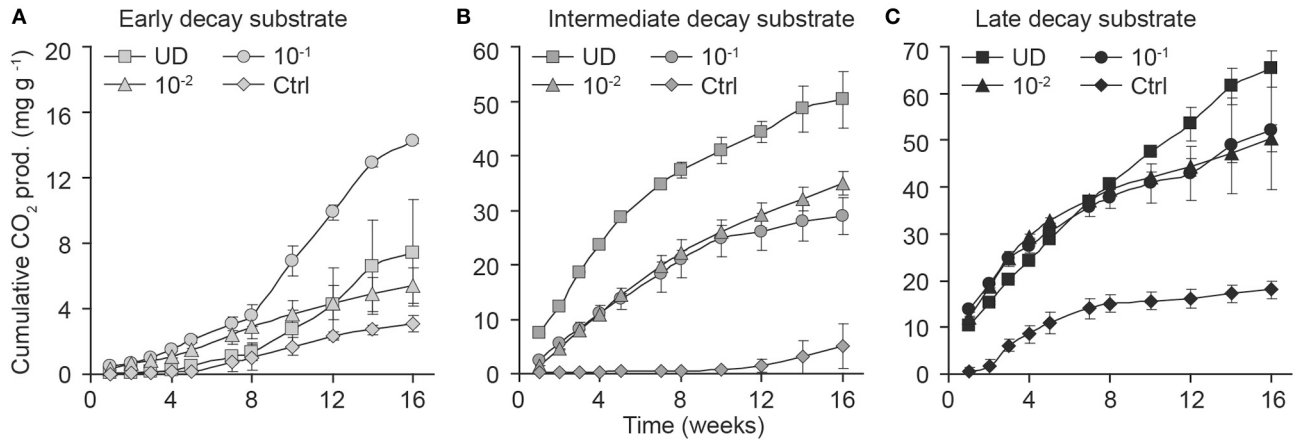

FIGURE 2 | Effect of dilution on the production of CO_2 (cumulative mg of CO_2 per g of substrate; in dm) within early- (A), intermediate- (B), and late- (C) decay stages. Dilution of fungal diversity is shown by symbols as undiluted fungal inoculum (squares), dilution 10^{-1} g inoculum/g substrate (circles), dilution 10^{-2} g inoculum/g substrate (triangles), and controls (diamonds). Error bars indicate the *SD* of the mean for observations and were calculated for each decay stage and dilution separately.

$df = 17, p < 0.001$, respectively). This effect was present when we analyzed each inoculum separately ($p < 0.02$ for decay-stage differences within inocula), although the 10^{-1} inoculum responded significantly differently from other inocula in the full model with interactions.

When we analyzed the effect of inoculum (which had different number of fungal OTUs) according to decay stage with longitudinal analysis, we found that the weekly CO_2 production of diluted 10^{-1} g and 10^{-2} g inocula differed from that of undiluted inoculum in intermediate-decay substrates ($t = -5.5$, $p = 0.002$ and $t = -3.9$, $p = 0.008$, respectively). The ANOVA of cumulative CO_2 at week 16 supported these findings. When fungal diversity (OTU) was added to the previous model, it was also significant ($F = 4.4$, $df = 1$, $p = 0.05$). After 16 weeks, the cumulative production of CO_2 from undiluted inoculum in late-decay substrates reached 65 mg CO_2 g^{-1} substrate (dm), corresponding to a C loss of 3.1%, whereas C loss from undiluted intermediate- and early-decay substrates were 2.6 and 0.2%, respectively (**Figures 2C**, **3**). At the end of the experiment, the cumulative CO_2 production was correlated with the observed number of OTUs ($r = 0.83$, $p < 0.001$).

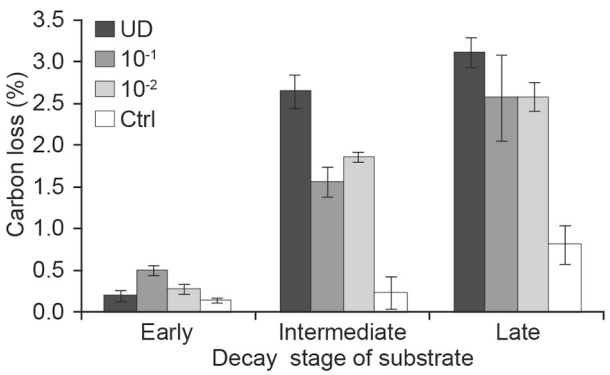

FIGURE 3 | Cumulative carbon loss (means of three replicates) during the incubation of early, intermediate and late stages of decay and receiving various dilutions of fungal inoculum [UD, undiluted; dilution 10^{-1} g inoculum/g substrate (dm); dilution 10^{-2} g inoculum/g substrate (dm); Ctrl, autoclaved sawdust].

EFFECTS OF SUBSTRATE AND REDUCED DIVERSITY ON ENZYME ACTIVITY

Differences in total hydrolytic EA depended on the substrate, therefore, we performed the analyses by substrate and by dilution (**Figure 4**).

When we analyzed the consecutive total hydrolytic activity of replicates with longitudinal analysis, we found that it was higher in preparations containing the 10^{-2} dilution than in the undiluted inoculum in early- ($t = 3.6$, $df = 5$, $p = 0.02$) and late-decay substrates ($t = 6.0$, $df = 6$, $p = 0.001$). Moreover, the hydrolytic activities were also significantly different between early decayed and other substrates in undiluted inocula (both $t > 4.0$, $df = 6$, $p < 0.005$) and in the 10^{-1} dilution (both $t > 3.2$, $df = 5$, $p < 0.03$).

When we analyzed the total hydrolytic enzyme activity measurements at the end of the experiment with ANOVA, we also found that the activities depended on the dilution-substrate combination (interaction $F = 10.2$, $df = 6$, $p < 0.001$). We then grouped the inoculum and substrate into a compounded factor, performed an ANOVA and conducted a pair-wise comparison of factors, which showed that the mean hydrolytic activity of the most diluted (10^{-2}) inoculum of the late-decayed substrate was greater than that in any of the other inoculum decay-stage combinations ($p < 0.0001$ for all pairs).

Furthermore, the number of fungal OTUs appeared to influence the enzyme activity at the end of the experiment ($F = 14.2$, $df = 1$, $p = 0.09$).

In all dilutions of the intermediate-decay inoculum, a negative trend in total hydrolytic activity was recorded toward the end of the incubation (**Figure 4B**). According to the longitudinal

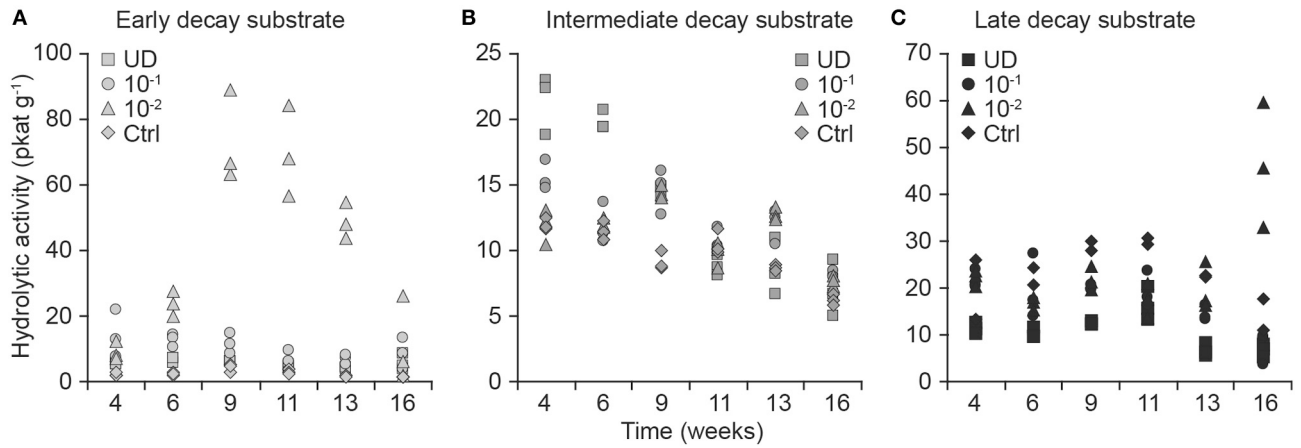

FIGURE 4 | Effect of fungal community dilution on total hydrolytic activity (pkat/g of substrate; in dm) as the sum of 1,4-β-glucuronidase, 1,4-β-xylosidase, cellobiohydrolase, and 1,4-β-glucosidase from early-decayed (A), intermediate-decayed (B), and late-decayed substrate (C). The dilution of fungal diversity is shown by symbols as undiluted fungal inoculum (squares), dilution 10^{-1} g inoculum/g substrate (circles), dilution 10^{-2} g inoculum/g substrate (triangles), and controls (diamonds).

analysis, the higher intercept and stronger negative trend of hydrolytic activity in undiluted inoculum than in either of the diluted inocula (the model intercept differences in comparison to the undiluted inoculum both had $t < -3.0$, $df = 6$, $p < 0.02$ and for the trend coefficient, they had $t > 3.4$, $df = 42$, $p < 0.001$, respectively) were coincident with the measured respiration rates that started at the highest values ($t < -3.9$, $df = 6$, $p < 0.01$) and then decreased the quickest ($t > 2.3$, $df = 42$, $p < 0.02$) in the undiluted inoculum in comparison with other dilutions in the intermediate-decay substrate (**Figures 2B**, **4B**).

The ratio of hydrolytic activity to respiration (Hydrolytic activity/CO_2) clearly decreased toward the end of the incubation in the early decay substrate that received undiluted ($t = -3, 4$, $df = 13$, $p = 0.005$), as well as diluted inocula (10^{-1} dilution: $t = -2.9$, $df = 9$, $p < 0.02$) (**Figure 5**). The same phenomenon did not occur in more decayed substrates (data not shown).

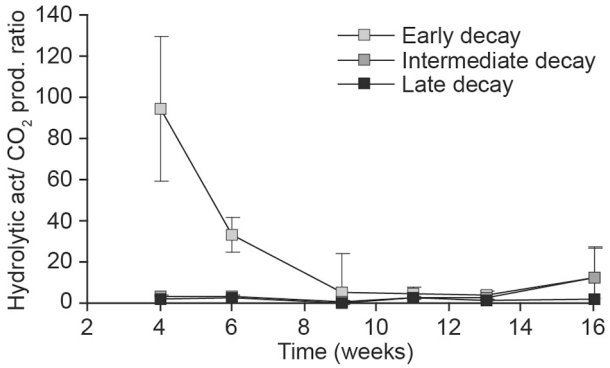

FIGURE 5 | Relationship of carbohydrate degradation (pkat/g) and weekly CO_2 production (mg/g substrate, dm) in the treatments receiving undiluted fungal inoculum of early- (light gray), intermediate- (dark gray), and late- (black) decay substrate during the 16-week incubation.

FUNGAL COMMUNITY STRUCTURE AND RESPIRATION ACTIVITY IN DIFFERENT DECAY STAGES

Fungal communities of different decay stages differed at the start of the experiment (**Figure 6A**) and community structures changed during the incubation period (**Figure 6**). In conjunction with observed differences between undiluted and diluted fungal communities in the intermediate decay substrate (**Figure 6B**), we measured higher respiration activity in the microcosm prepared with the undiluted inoculum, especially during the first 6 weeks (**Figure 2B**). In the early decay substrate, the slightly diluted (10^{-1}) fungal community, which had the highest respiration rate (**Figure 2A**), appeared to deviate from all other communities after 13 weeks of incubation (**Figure 6C**).

At the end of the experiment, cumulative CO_2 ($r = 0.91$, $p < 0.001$) and the number of OTUs ($r = 0.87$, $p < 0.001$) increased in the communities composed of intermediate- and late-decay stage species, as shown by the linear fit superimposed on the NMDS graph (**Figure 6D**).

DISCUSSION

EFFECTS OF FUNGAL DIVERSITY ON WOOD DECOMPOSITION

The main findings of the experiment confirmed our hypothesis that fungal diversity affects decomposition rate and that resistance of the decomposition process to the loss of diversity depends on the decomposition stage of woody substrates. We used inocula that originated from actively decaying wood, where the number of OTUs is higher than in previous experiments using selected species from pure cultures (Setälä and McLean, 2004; Tiunov and Scheu, 2005). These studies with communities created by combining cultured fungal species have shown how the decomposition rate becomes asymptotic with relatively few decomposer species, and our results on late-decay communities with initially high number of fungal OTUs support this finding. However, we observed that the functioning of the decomposers of the intermediate-decay stage, where the initial number of OTUs was

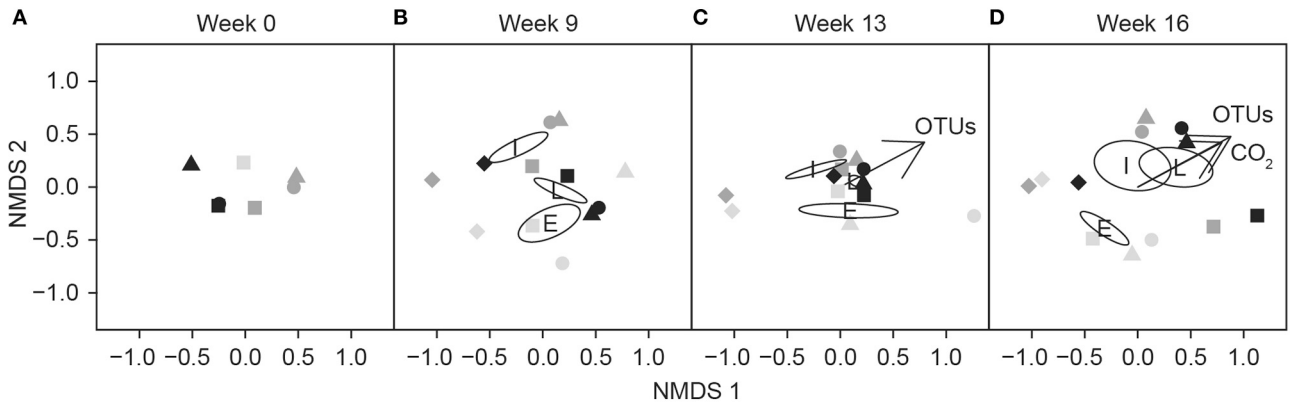

FIGURE 6 | Non-metric multidimensional scaling (NMDS) ordination showing the separation of fungal communities at the beginning (A), after 9 weeks (B), 13 weeks (C), and 16 weeks (D) in the different dilutions or controls (autoclaved sawdust) according to the decay stage of substrate. Symbols represent the dilution of the fungal community: undiluted (squares), dilution 10^{-1} g inoculum/g substrate (circles), dilution 10^{-2} g inoculum/g substrate (triangles) and controls (diamonds). The intensity of the symbol indicates the decay stage. Vectors indicate the direction of maximum correlation of CO_2 production and number of OTUs with ordinated samples ($p < 0.01$). Ellipses indicate the mean location of each decay stage: E, early; I, intermediate; and L, late.

lower than in the late-decay wood, was less resistant to the loss of diversity. In the intermediate-decay stage, decomposition activity was highest in non-diluted communities and the experimental dilution of the fungal community was associated with a lower respiration rate.

This study showed that CO_2 production, as an indicator of decomposition, increased in relation to the decay stage of Norway spruce wood and peaked during the late-decay stage, where fungal diversity (measured as the number of observed OTUs) was also maximal. The observed increase in decomposition activity with increasing OTU diversity is in agreement with our hypothesis. Earlier studies, where decay models were fitted to empirical field data, predicted that the rate of decay is highest during intermediate phases of decomposition (Harmon et al., 2000; Mäkinen et al., 2006; Tuomi et al., 2011), which coincides with the period when white- and brown-rot fungi are at their peak prevalence (Rajala et al., 2011, 2012). However, we suggest that decomposition activity is also maintained in the late-decay stage wood that might be under-represented in previous studies (i.e., they used a relatively small number of late-decay samples, which are difficult to date). In addition, our results indicate that lowering fungal diversity, especially in the intermediate-decay stage, has a direct impact on fungal community function, and thereby on the decomposition of woody litter.

We showed that in the most diverse fungal community inhabiting the late-decay substrate, lowering the diversity with dilution of the inocula had only a slight impact on decomposition rate. This suggests that the community that remained after dilution was sufficiently diverse to provide the same ecological function as that of the undiluted system, which agrees well with earlier studies of the diversity-function relationship in soil microbes (Wertz et al., 2006), whereas the less diverse communities were more affected by random selection. Consequently, we predict a stronger resilience of the diverse fungal community found in advanced stages of wood decay.

In the less diverse community inhabiting the early decay substrate, a 10^{-1} dilution caused an unexpected result in that CO_2 production increased. It appears that loss of diversity in a low-density community affects competitive interactions and decomposition in unpredictable ways. The response is highly sensitive to the activity of the remaining species and the functional redundancy in the fungal community of early-stage decomposers is lower than that found in later stages.

The use of indigenous fungal communities as inocula to study the relationship between diversity and function of terrestrial fungal communities is novel and was applied for the first time to wood-inhabiting fungi in this study. Previous laboratory studies have assessed the ability of cultured fungi to degrade woody substrates (Boddy et al., 1989; Tiunov and Scheu, 2005; Toljander et al., 2011) and compete with natural wood-inhabiting fungi (Holmer and Stenlid, 1997; Holmer et al., 1997). According to the method proposed by Wertz et al. (2006), the dilution procedure reduced the number of fungal taxa detected in the inoculum. Prior to our experiment, we tested different ratios of dilutions and found that a relatively high (1/100) dilution is needed for a remarkable reduction of OTUs in highly diverse inocula. However, for a moderate reduction in the OTU diversity, we chose to apply a dilution ratio (1/10) that was optimal for the intermediate decay stage, but compromised late decay, where the resulting reduction in OTU diversity was only slight.

As expected, the number of detected fungal species increased in all treatments with the progression of the incubation, since the applied PCR-DGGE method cannot identify infrequent fungi and only after replication of DNA during the incubation they became visible. Our sterilization procedure of the control substrate was apparently sufficient to destroy most of the fungal DNA, as OTUs were not detectable via DGGE at the start of the experiment (**Figure 1**). However, slight CO_2 production during the incubation indicated that some microbes survived autoclaving (**Figure 2**), as it is known that some spores might be resistant

to this form of sterilization (Cheng et al., 2008). This was the reason to detect a few fungal OTUs in the controls after 9 weeks (data not shown). However, NMDS showed the community structure in controls to be distinct from that of other microcosms. This suggests that the key species involved in decomposition did not survive autoclaving, although we cannot totally deny that some species originated from autoclaved sawdust. However, CO_2 production in controls was far lower than in any of the treatments and therefore we believe that effect of contaminant species in dilution treatments is minor. The fact that sterilization of wood, soil or other substrate by autoclaving is practically impossible should still be considered in this kind of dilution procedures.

ENZYME ACTIVITY DURING WOOD DECOMPOSITION IN RESPONSE TO FUNGAL DIVERSITY

Contrary to our hypothesis, the most diluted (10^{-2}) inoculum was associated with a higher activity of hydrolytic enzymes than treatments of the same substrate receiving inoculum with a higher fungal richness (**Figure 4**). This might be explained by less competition in the diluted communities involving species specializing in the production of carbohydrate-degrading enzymes (e.g., brown- and soft-rot fungi). We also found that the ratio of hydrolytic activity and production of CO_2 per week in early-decay substrates was initially high and gradually decreased. The negative slope of the relationship between hydrolytic activity and weekly CO_2 production suggests that fungal taxa that are active during the early phases of decomposition must produce hydrolytic enzymes to release the wide variety of carbohydrates that are metabolized in later stages.

The enzyme recovery method, based on a filter centrifugation approach, has been validated in agar media supplemented with different organic products (Heinonsalo et al., 2012), but has never been applied to a more complex substrate such as one composed of decomposing spruce wood. A standard and universal protocol for extracting and measuring enzymes from environmental samples does not exist (Baldrian, 2009). Common practice is to soak the samples in buffer (e.g., acetate or sulfate buffers) and extract the enzymes by agitating the slurry, but such treatment might negatively affect EA (Vepsäläinen, 2001). In our study, the level of enzyme activity was in the range 10–100 pkat g^{-1} dry substrate. Previous studies that reported activities as high as 1000 pkat g^{-1} (dm) in Norway spruce needles used pure fungal inoculum from a cultured isolate (Žifčáková et al., 2011). Our results indicate that extracellular EA in spruce wood that has not received a pure and concentrated inoculum are much lower. It is known that spruce wood is a complex substrate for the recovery of wood-degrading enzymes, since water-soluble constituents such as phenols, sugars, organic acids, xylo-oligosaccharides and proteins all act as inhibitors of hydrolytic enzymes (e.g., Lagaert et al., 2009; Kim et al., 2011). Nevertheless, the effect of wood extracts on enzyme recovery in this study was expected to be minimal as was previously reported by Valentín et al. (2010).

CONCLUSIONS

Dilution of fungal inocula recovered from *Picea abies* logs in three different decay stages revealed a stage-dependent response in decomposition rate. Reduced fungal diversity was associated with lower respiration rates during the intermediate stages of decay, but no diversity effects were detected in later stages, where initial number of detected species was high. This suggested that the highly diverse community of the late-decay stage was more resistant to the loss of diversity than less diverse communities of early decomposers. In early-decay communities, dilution caused unexpected changes to the decomposition process, probably due to the strong stochastic effect of dilution on less diverse communities. The results of this study also showed that the decomposition rate and the fungal diversity increased as decay advanced. We suggest that fungal activity and the functional redundancy of the fungal community in decaying wood increase during the fungal succession from intermediate- to late-decay stages.

ACKNOWLEDGMENTS

We are grateful to the forest and laboratory personnel of the Finnish Forest Research Institute for their assistance in field work and the preparation of samples for chemical, enzymatic and molecular analyses. The study was funded by the Academy of Finland (project numbers 121630 and 257701).

SUPPLEMENTARY MATERIAL

The Supplementary Material for this article can be found online at: http://www.frontiersin.org/journal/10.3389/fmicb.2014.00230/abstract

REFERENCES

Baldrian, P. (2008). "Enzymes of saprotrophic basidiomycetes," in *Ecology of Saprotrophic Basidiomycetes*, eds L. Boddy, J. C. Frankland, and P. van West (London: Academic Press), 19–41.

Baldrian, P. (2009). Microbial enzyme-catalyzed processes in soils and their analysis. *Plant Soil Environ.* 55, 370–378. Available online at: http://www.agriculturejournals.cz/web/pse.htm?volume=55&firstPage=370&type=publishedArticle

Boddy, L. (2000). Interspecific combative interactions between wood-decaying basidiomycetes. *FEMS Microbiol. Ecol.* 31, 185–194. doi: 10.1111/j.1574-6941.2000.tb00683.x

Boddy, L., Owens, E., and Chapela, I. (1989). Small scale variation in decay rate witin logs one year after felling: effect of fungal community structure and moisture content. *FEMS Microbiol. Lett.* 62, 173–184. doi: 10.1111/j.1574-6968.1989.tb03691.x

Cardinale, B. J., Duffy, J. E., Gonzalez, A., Hooper, D. U., Perrings, C., Venail, P., et al. (2012). Biodiversity loss and its impact on humanity. *Nature* 486, 59–67. doi: 10.1038/nature11148

Cheng, J. Y. W., Lau, A. P. S., and Fang, M. (2008). Assessment of the atmospheric fungal prevalence through field ergosterol measurement I - Determination of the specific ergosterol content in common ambient fungal spores and yeast cells. *Atmos. Environ.* 42, 5526–5533. doi: 10.1016/j.atmosenv.2008.03.021

Diggle, P. J., Heagerty, P., Liang, K. Y., and Zeger, S. L. (2002). *Analysis of Longitudinal Data, 2nd Edn.* Oxford: Oxford University Press.

Fox, J., and Weisberg, S. (2011). *An R Companion to Applied Regression, 2nd Edn.* Sage Publications. Available online at: http://socserv.socsci.mcmaster.ca/jfox/Books/Companion/ (Accessed December 19, 2013).

Fukami, T., Dickie, I. A., Paula Wilkie, J., Paulus, B. C., Park, D., et al. (2010). Assembly history dictates ecosystem functioning: evidence from wood decomposer communities. *Ecol. Lett.* 13, 675–684. doi: 10.1111/j.1461-0248.2010.01465.x

Gardes, M., and Bruns, T. D. (1993). ITS primers with enhanced specificity for basidiomycetes - application to the identification of mycorrhizae and rusts. *Mol. Ecol.* 2, 113–118. doi: 10.1111/j.1365-294X.1993.tb00005.x

Gessner, M. O., Swan, C. M., Dang, C. K., McKie, B. G., Bardgett, R. D., Wall, D. H., et al. (2010). Diversity meets decomposition. *Trends Ecol. Evol.* 25, 372–380. doi: 10.1016/j.tree.2010.01.010

Harmon, M., Krankina, O., and J, S. (2000). Decomposition vectors: a new approach to estimating woody detritus decomposition dynamics. *Can. J. For. Res.* 30, 76–84. doi: 10.1139/cjfr-30-1-76

Hättenschwiler, S., Tiunov, A. V., and Scheu, S. (2005). Biodiversity and litter decomposition in terrestrial ecosystems. *Annu. Rev. Ecol. Evol. Syst.* 36, 191–218. doi: 10.1146/annurev.ecolsys.36.112904.151932

Heinonsalo, J., Kabiersch, G., Niemi, R. M., Simpanen, S., Ilvesniemi, H., Hofrichter, M., et al. (2012). Filter centrifugation as a sampling method for miniaturization of extracellular fungal enzyme activity measurements in solid media. *Fungal Ecol.* 5, 261–269. doi: 10.1016/j.funeco.2011.07.008

Holmer, L., Renvall, P., and Stenlid, J. (1997). Selective replacement between species of wood-rotting basidiomycetes, a laboratory study. *Mycol. Res.* 101, 714–720. doi: 10.1017/S0953756296003243

Holmer, L., and Stenlid, J. (1997). Competitive hierarchies of wood decomposing basidiomycetes in artificial systems based on variable inoculum sizes. *Oikos* 79, 77–84. doi: 10.2307/3546092

Hooper, D., Chapin, F. III., Ewel, J., Hector, A., Inchausti, P., Lavorel, S., et al. (2005). Effects of biodiversity on ecosystem functioning a consensus of current knowledge. *Ecol. Monogr.* 75, 3–35. doi: 10.1890/04-0922

Hooper, D. U., Adair, E. C., Cardinale, B. J., Byrnes, J. E. K., Hungate, B. A., Matulich, K. L., et al. (2012). A global synthesis reveals biodiversity loss as a major driver of ecosystem change. *Nature* 486, 105–108. doi: 10.1038/nature11118

Kim, Y., Ximenes, E., Mosier, N. S., and Ladisch, M. R. (2011). Soluble inhibitors/deactivators of cellulase enzymes from lignocellulosic biomass. *Enzyme Microb. Technol.* 48, 408–415. doi: 10.1016/j.enzmictec.2011.01.007

Kubartová, A., Ottosson, E., Dahlberg, A., and Stenlid, J. (2012). Patterns of fungal communities among and within decaying logs revealed by 454 sequencing. *Mol. Ecol.* 21, 4514–4532. doi: 10.1111/j.1365-294X.2012.05723.x

Lagaert, S., Beliën, T., and Volckaert, G. (2009). Plant cell walls: protecting the barrier from degradation by microbial enzymes. *Semin. Cell Dev. Biol.* 20, 1064–1073. doi: 10.1016/j.semcdb.2009.05.008

Lindahl, B., and Boberg, J. (2008). "Distribution and function of litter basidiomycetes in coniferous forests," in *Ecology of Saprotrophic Basidiomycetes*, eds L. Boddy, J. C. Frankland, and P. van West (London: Academic Press), 183–196.

Loreau, M., Naeem, S., Inchausti, P., Bengtsson, J., Grime, J. P., Hector, A., et al. (2001). Biodiversity and ecosystem functioning: current knowledge and future challenges. *Science* 294, 804–808. doi: 10.1126/science.1064088

Lundell, T. K., Mäkelä, M. R., and Hildén, K. (2010). Lignin-modifying enzymes in filamentous basidiomycetes - ecological, functional and phylogenetic review. *J. Basic Microbiol.* 50, 5–20. doi: 10.1002/jobm.200900338

Mäkinen, H., Hynynen, J., Siitonen, J., and Sievänen, R. (2006). Predicting the decomposition of Scots pine, Norway spruce, and birch stems in Finland. *Ecol. Appl.* 16, 1865–1879. doi: 10.1890/1051-0761(2006)016[1865:PTDOSP]2.0.CO;2

Oksanen, J., Kindt, R., Legendre, P., Simpson, G., Sólymos, P., Stevens, M. H., et al. (2008). *Vegan: Community ecology package - R package version 1.15-2.* Available online at: http://cran.r-project.org (Accessed December 19, 2013).

Ovaskainen, O., Nokso-Koivisto, J., Hottola, J., Rajala, T., Pennanen, T., Ali-Kovero, H., et al. (2010). Identifying wood-inhabiting fungi with 454 sequencing – what is the probability that BLAST gives the correct species? *Fungal Ecol.* 3, 274–283. doi: 10.1016/j.funeco.2010.01.001

Pritsch, K., Courty, P. E., Churin, J.-L., Cloutier-Hurteau, B., Ali, M. A., Damon, C., et al. (2011). Optimized assay and storage conditions for enzyme activity profiling of ectomycorrhizae. *Mycorrhiza* 21, 589–600. doi: 10.1007/s00572-011-0364-4

Pritsch, K., Raidl, S., Marksteiner, E., Blaschke, H., Agerer, R., Schloter, M., et al. (2004). A rapid and highly sensitive method for measuring enzyme activities in single mycorrhizal tips using 4-methylumbelliferone-labelled fluorogenic substrates in a microplate system. *J. Microbiol. Methods* 58, 233–241. doi: 10.1016/j.mimet.2004.04.001

R Development Core Team. (2011). *R: A Language and Environment for Statistical Computing. R Foundation for Statistical Computing.* Available online at: http://www.r-project.org (Accessed December 19, 2013).

Rajala, T., Peltoniemi, M., Hantula, J., Mäkipää, R., and Pennanen, T. (2011). RNA reveals a succession of active fungi during the decay of Norway spruce logs. *Fungal Ecol.* 4, 437–448. doi: 10.1016/j.funeco.2011.05.005

Rajala, T., Peltoniemi, M., Pennanen, T., and Mäkipää, R. (2010). Relationship between wood-inhabiting fungi determined by molecular analysis (denaturing gradient gel electrophoresis) and quality of decaying logs. *Can. J. For. Res.* 40, 2384–2397. doi: 10.1139/X10-176

Rajala, T., Peltoniemi, M., Pennanen, T., and Mäkipää, R. (2012). Fungal community dynamics in relation to substrate quality of decaying Norway spruce (*Picea abies* [L.] Karst.) logs in boreal forests. *FEMS Microbiol. Ecol.* 81, 494–505. doi: 10.1111/j.1574-6941.2012.01376.x

Rayner, A. D. M., and Boddy, L. (1988). *Fungal Decomposition of Wood. Its Biology and Ecology.* Chichester: John Wiley & Sons Ltd.

Robinson, C. H., Miller, E. J. P., and Deacon, L. J. (2005). "Biodiversity of saprotrophic fungi in relation to their function: Do fungi obey the rules?," in *Biological Diversity and Function in Soils*, eds R. Bardgett, M. Usher, and D. Hopkins (Cambridge: Cambridge University Press), 189–215. doi: 10.1017/CBO9780511541926

Setälä, H., and McLean, M. A. (2004). Decomposition rate of organic substrates in relation to the species diversity of soil saprophytic fungi. *Oecologia* 139, 98–107. doi: 10.1007/s00442-003-1478-y

Siitonen, J. (2001). Forest management, coarse woody debris and saproxylic organisms: Fennoscandian boreal forests as an example. *Ecol. Bull.* 49, 11–41.

Šnajdr, J., Cajthaml, T., Valášková, V., Merhautová, V., Petránková, M., Spetz, P., et al. (2011). Transformation of *Quercus petraea* litter: successive changes in litter chemistry are reflected in differential enzyme activity and changes in the microbial community composition. *FEMS Microbiol. Ecol.* 75, 291–303. doi: 10.1111/j.1574-6941.2010.00999.x

Stenlid, J., Penttilä, R., and Dahlberg, A. (2008). "Wood-decay basidiomycetes in boreal forests: Distribution and community development," in *Ecology of Saprotrophic Basidiomycetes,* eds L. Boddy, J. C. Frankland, and P. van West (London: Academic Press), 239–262.

Tiunov, A. V., and Scheu, S. (2005). Facilitative interactions rather than resource partitioning drive diversity-functioning relationships in laboratory fungal communities. *Ecol. Lett.* 8, 618–625. doi: 10.1111/j.1461-0248.2005.00757.x

Toljander, Y. K., Lindahl, B. J. D., Holmer, L., and Högberg, N. O. S. (2011). Environmental fluctuations facilitate species co-existence and increase decomposition. *Oecologia* 148, 625–631. doi: 10.1007/s00442-006-0406-3

Tuomi, M., Laiho, R., Repo, A., and Liski, J. (2011). Wood decomposition model for boreal forests. *Ecol. Model.* 222, 709–718. doi: 10.1016/j.ecolmodel.2010.10.025

Valentín, L., Kluczek-Turpeinen, B., Willför, S., Hemming, J., Hatakka, A., Steffen, K., et al. (2010). Scots pine (*Pinus sylvestris*) bark composition and degradation by fungi: potential substrate for bioremediation. *Bioresour. Technol.* 101, 2203–2209. doi: 10.1016/j.biortech.2009.11.052

Vepsäläinen, M. (2001). Poor enzyme recovery by extraction from soils. *Soil Biol. Biochem.* 33, 1131–1135. doi: 10.1016/S0038-0717(00)00240-6

Wertz, S., Degrange, V., Prosser, J. I., Poly, F., Commeaux, C., Freitag, T., et al. (2006). Maintenance of soil functioning following erosion of microbial diversity. *Environ. Microbiol.* 8, 2162–2169. doi: 10.1111/j.1462-2920.2006.01098.x

Wertz, S., Degrange, V., Prosser, J. I., Poly, F., Commeaux, C., Guillaumaud, N., et al. (2007). Decline of soil microbial diversity does not influence the resistance and resilience of key soil microbial functional groups following a model disturbance. *Environ. Microbiol.* 9, 2211–2219. doi: 10.1111/j.1462-2920.2007.01335.x

White, T. J., Bruns, S., Lee, S., and Taylor, J. (1990). "Amplification and direct sequencing of fungal ribosomal RNA genes for phylogenetics," in *PCR Protocols: A Guide to Methods and Applications*, eds M. A. Innis, D. H. Gelfand, J. J. Sninsky, and T. J. White (San Diego, CA: Academic Press), 315–322.

Žifčáková, L., Dobiášová, P., Koláøová, Z., Koukol, O., and Baldrian, P. (2011). Enzyme activities of fungi associated with *Picea abies* needles. *Fungal Ecol.* 4, 427–436. doi: 10.1016/j.funeco.2011.04.002

Conflict of Interest Statement: The authors declare that the research was conducted in the absence of any commercial or financial relationships that could be construed as a potential conflict of interest.

Received: 24 January 2014; accepted: 29 April 2014; published online: 20 May 2014.
*Citation: Valentín L, Rajala T, Peltoniemi M, Heinonsalo J, Pennanen T and Mäkipää R (2014) Loss of diversity in wood-inhabiting fungal communities affects decomposition activity in Norway spruce wood. Front. Microbiol. **5**:230. doi: 10.3389/fmicb.2014.00230*
This article was submitted to Terrestrial Microbiology, a section of the journal Frontiers in Microbiology.

frontiers in
MICROBIOLOGY

ORIGINAL RESEARCH ARTICLE
published: 02 June 2014
doi: 10.3389/fmicb.2014.00263

Lignocellulose-responsive bacteria in a southern California salt marsh identified by stable isotope probing

Lindsay E. Darjany, Christine R. Whitcraft and Jesse G. Dillon*

Department of Biological Sciences, California State University, Long Beach, CA, USA

Edited by:
Anne Bernhard, Connecticut College, USA

Reviewed by:
Vanessa Karel Michelou, University of Hawaii, USA
Vinicius Fortes Farjalla, Universidade Federal do Rio de Janeiro, Brazil

***Correspondence:**
Jesse G. Dillon, Department of Biological Sciences, California State University, 1250 Bellflower Boulevard, Long Beach, CA 90840, USA
e-mail: jesse.dillon@csulb.edu

Carbon cycling by microbes has been recognized as the main mechanism of organic matter decomposition and export in coastal wetlands, yet very little is known about the functional diversity of specific groups of decomposers (e.g., bacteria) in salt marsh benthic trophic structure. Indeed, salt marsh sediment bacteria remain largely in a black box in terms of their diversity and functional roles within salt marsh benthic food web pathways. We used DNA stable isotope probing (SIP) utilizing ^{13}C-labeled lignocellulose as a proxy to evaluate the fate of macrophyte-derived carbon in benthic salt marsh bacterial communities. Overall, 146 bacterial species were detected using SIP, of which only 12 lineages were shared between enriched and non-enriched communities. Abundant groups from the ^{13}C-labeled community included *Desulfosarcina*, *Spirochaeta*, and *Kangiella*. This study is the first to use heavy-labeled lignocellulose to identify bacteria responsible for macrophyte carbon utilization in salt marsh sediments and will allow future studies to target specific lineages to elucidate their role in salt marsh carbon cycling and ultimately aid our understanding of the potential of salt marshes to store carbon.

Keywords: salt marsh, bacteria, lignocellulose, stable isotope probing (SIP), food web, macrophytes, sediments

INTRODUCTION

Coastal wetlands provide a variety of key ecosystem functions that include food web support, nutrient cycling, sediment stabilization, and long-term carbon sequestration (Minello et al., 2003; Mitsch and Gosselink, 2007). Many of these functions are tied to macrophyte abundance, microbial decomposition rates and the accumulation of biomass or soil organic matter (Newell, 1993; Megonigal et al., 2004). Carbon cycling by microbial communities has been recognized as the main mechanism of organic matter decomposition in coastal wetland systems in the United States (Benner et al., 1986; Paerl and Pinckney, 1996; Wagner et al., 2008), although most of these studies have been performed on the East Coast (Kowalchuk et al., 2002; Blum et al., 2004; Aneja et al., 2006). A number of East Coast U.S.A. studies have identified sulfate-reducing bacteria as key anaerobic degraders in salt marshes (Howarth and Teal, 1979; Hines et al., 1989; Rooney-Varga et al., 1998), although the diverse functional roles of salt marsh bacteria remain poorly characterized. In addition, West Coast marshes are typically smaller and drier with reduced precipitation and less freshwater input than their East Coast counterparts, suggesting that ecological and biogeochemical functional diversity may differ. It has recently been hypothesized that these factors lead to differences in decomposition rates and long-term carbon storage in southern California coastal marshes (Keller et al., 2012). An understanding of key microbial participants in carbon cycling will improve our overall understanding of ecosystem functioning in southern California coastal salt marshes.

While aboveground and belowground plant material and root exudates are all known to be important carbon sources in salt marsh systems (e.g., Hodson et al., 1984; Hemminga et al., 1988), our study focuses on the role of lignocellulose as a major component of aboveground litter and as an important substrate for microbial degradation in the marsh ecosystem. Earlier studies have found a close coupling between macrophyte productivity and microbial processes in salt marsh ecosystems (Howarth, 1993; Boschker et al., 1999). Specifically, East Coast studies revealed that lignocellulose-rich *Spartina* spp. contribute the bulk of dissolved organic carbon (DOC) in the most productive marshes (Gallagher et al., 1976; Moran and Hodson, 1990) and that bacteria are the primary degraders of decaying *Spartina* (Benner et al., 1986). As macrophyte carbon (plant lignocellulose) is broken down into cellulose and other simpler carbon compounds, this leads to a succession of food source availability (Peterson et al., 1985; Choi et al., 2001), which in turn can lead to changing communities of bacteria and fungi that preferentially consume the more labile components of dissolved organic matter (Coffin et al., 1990; Blum et al., 2004). This study focuses on the influence of macrophyte carbon on near surface sediment bacterial communities (Buchan et al., 2003), because of their known ability to degrade complex carbon-rich litter in salt marsh systems (Lydell et al., 2004; Romani et al., 2006; Das et al., 2007).

In general, little is known about salt marsh plant-microbe interactions in southern California where *Spartina foliosa* (cordgrass) and *Sarcocornia pacifica* (pickleweed) are key components of marsh foodwebs (Kwak and Zedler, 1997). Characterizing the role of specific microbial groups in the salt marsh benthic food web is difficult despite the recognition that their connection with organic matter cycling is integral to trophic structuring (Neutel et al., 2002, 2007). DNA stable isotope probing (SIP) overcomes some of the challenges inherent in using traditional culturing and environmental molecular methods to study microbes in the

environment by directly linking substrate utilization to microbial identity (Radajewski et al., 2000; Buckley et al., 2007). The SIP method follows heavy-labeled carbon isotopes into the nucleic acids of microbes, providing an unambiguous identification of microbial consumers of plant carbon (Prosser et al., 2006). SIP has been used to identify bacteria actively degrading cellulose in habitats such as agricultural soils, prescribed-burned forest soils and cellulose-responsive bacteria and fungi in pine forest grasslands (Haichar et al., 2007; Bastias et al., 2009; Eichorst and Kuske, 2012). In this study, our objective was to use DNA SIP with ^{13}C-labeled lignocellulose to identify salt marsh sediment bacteria capable of incorporating macrophyte carbon. Specifically, we performed stable isotope incubations with salt marsh sediments followed by 16S rRNA gene amplification, T-RFLP and gene sequencing to identify and compare lignocellulose-responsive and non-responsive bacterial communities.

MATERIALS AND METHODS

SITE DESCRIPTION

Salt marsh sediment cores were collected from a 1 m^2 quadrat placed on sediments around the base of live *Spartina foliosa* plants in the Talbert salt marsh in Huntington Beach, California (33°38′ 0.52″ N, 117°57′ 70.3″ W). Samples were taken in the low *Spartina* marsh zone that possessed ∼80% *Spartina foliosa* cover with the remaining area covered in microalgae. Using the hydrometer method (Bouyoucos, 1962) and loss on ignition to determine grain size and organic matter content, the sediment in the sampled area was found to be 60% mud and 30% sand with 30% organic matter. Redox potential was measured to be 30 mV at 1 cm depth with a millivolt meter (Mettler-Toledo, Columbus, OH, USA). Salinity was measured to be 48 ppt with a portable refractometer (VWR, West Chester, PA, USA), and atmospheric humidity in the plot area at the base of *Spartina* plants was 71%, measured with a humidity reader (Fisher Scientific, Waltham, MA, USA). Sediment pH was found to be 7.2 using a pH meter (Mettler-Toledo).

CORE SAMPLE PROCESSING

Triplicate sediment cores (2 cm diameter × 1 cm deep) were collected for SIP from within the quadrat using a sterile syringe with the tip cut off and returned to California State University, Long Beach where they were equilibrated at room temperature for 10 h. In the laboratory, 5 g (wet weight) of each core was placed in 20 ml sterile scintillation vials and homogenized with 2.5 ml of sterile 0.2 μm filtered seawater. The resulting slurries were labeled with 5 mg of ^{13}C lignocellulose (Isolife, Netherlands; Benner et al., 1984; Hodson et al., 1984; Wilson, 1985). Samples were incubated at 21°C in the dark for 30 days and then frozen at −20°C to stop the experiment. A 30 day incubation was used to ensure label was incorporated based on previous findings of lignocellulose degradation rates (Benner et al., 1984). A 4 mg sediment subsample from each scintillation vial microcosm was sent to the University of California, Davis Stable Isotope Facility and analyzed for ^{13}C on a PDZ Europa ANCA-GSL elemental analyzer followed by a PDZ Europa 20–20 isotope ratio mass spectrometer (Sercon Ltd., Cheshire, UK). These measurements are accurate to 0.2% for ^{13}C[1].

[1]http://stableisotopefacility.ucdavis.edu/

NUCLEIC ACID EXTRACTION AND PCR AMPLIFICATION

Four 0.5 g subsamples from each ^{13}C lignocellulose microcosm were used for DNA extractions using a FastDNA Spin Kit for soil (MPBIO, Solon, OH, USA) following manufacturer's instructions and then pooled to yield ∼5 μg of DNA per microcosm sample. DNA from each of the triplicate microcosms was processed immediately for SIP following the protocol of Neufeld et al. (2007). Briefly, DNA was mixed with a CsCl solution (initial density of 1.725 g ml^{-1}). Samples were loaded into 5.1 ml centrifuge tubes (Beckman Coulter, Brea, CA, USA) and enriched DNA was separated from non-enriched by ultracentrifugation (Vti 65.2 rotor, Avanti J-E centrifuge, Beckman Coulter, Indianapolis, IN, USA) for 40 h at ∼177,000 *g* at 20°C with no braking. A syringe pump (Braintree Scientific, Braintree, MA, USA) was calibrated and used to dispense 12 × 425 μl fractions, which were collected from the bottom of the pierced centrifuge tube, with heavy, enriched fractions coming off first and light, non-enriched fractions coming off last. The density of each fraction was calculated by weighing fractions of known volume on an analytical balance (Denver Instrument, Bohemia, NY, USA). Gradient formation was confirmed for the fractions and varied from 1.80 to 1.68 g ml^{-1} for replicate three, for example. DNA was precipitated via centrifugation after overnight addition of molecular grade glycogen (Thermo Fisher Scientific, Waltham, MA, USA) and polyethylene glycol (Sigma–Aldrich, Miamisburg, OH, USA) and the resulting pellet was washed with 70% ethanol. DNA was resuspended in 50 μl TE (10 mM Tris–HCl and 1 mM EDTA) buffer and run on a 1% agarose gel to confirm recovery of DNA from each fraction. Bacterial 16S rRNA genes were amplified from enriched and non-enriched fractions in 20 μl reaction volumes using GM3 and GM4 primers (Muyzer et al., 1995) as previously described (Dillon et al., 2009a). Briefly, 1 mM $MgCl_2$, 10 pmol of each primer (Operon, Huntsville, AL, USA), 50 nmol of each dNTP (Promega, Madison, WI, USA), 1× PCR buffer and 1.5 units of GoTaq DNA Polymerase (Promega), 4 μl of 0.4% (w/v) Bovine Serum Albumin and 50–100 ng of extracted nucleic acids. Reaction conditions were as follows: 5 min initial denaturation at 94°C, followed by 30 cycles of denaturation (94°C for 30 s), annealing (53°C for 30 s) and elongation (72°C for 90 s), and a final extension (72°C for 10 min) carried out in an Eppendorf Mastercycler (Brinkmann Instruments, Westbury, NY, USA).

T-RFLP ANALYSIS

Terminal restriction fragment polymorphism (T-RFLP; Liu et al., 1997) was used to screen SIP fractions for community differences. Briefly, bacterial amplicons from a 30-cycle PCR as described above were amplified for another 5–10 cycles using a WellRed fluorescently labeled GM3 forward primer (Beckman Coulter; Dillon et al., 2009b; Harrison and Orphan, 2012). 100 ng of resulting amplicons were digested with Hae III restriction endonuclease (Promega, Madison, WI, USA) in 20 μl reactions at 37°C for 4 h following manufacturer's instructions. Terminal restriction fragments (T-RFs) from each SIP fraction of the triplicate microcosms were determined via capillary gel electrophoresis using a CEQ800 sequence analyzer (Beckman Coulter, Fullerton, CA, USA) with a two-base pair bin size used to group peaks above a

1% peak-area threshold. Visual inspections of T-RFLP traces from enriched and non-enriched fractions (see below) from the triplicate microcosms revealed similar peak patterns (data not shown), so the fractions from a single replicate microcosm (number 3) were chosen for further analyses. T-RFLP data were analyzed using PRIMER v6.2 (Primer-E Ltd., Plymouth, UK) by cluster analyses and a multidimensional scaling (MDS) plot based on presence/absence of peaks to elucidate differences in community composition among fractions. Permutational multivariate analyses of variance (perMANOVA) based on presence or absence of peaks using Bray–Curtis dissimilarity of relative peak area percentages were performed on enriched and non-enriched community data using fractions 5–8 (representative of enriched) and 9–12 (representative of non-enriched).

CLONING, SEQUENCING, AND DIVERSITY

Positive PCR amplicons were pooled for representative enriched (fractions 07 and 08) and non-enriched SIP fractions (fractions 11 and 12) identified by T-RFLP and cloned using pcr4-TOPO vector and TOP10 competent cells (Invitrogen, Carlsbad, CA, USA) following manufacturer's instructions. Each clone was screened via PCR for successful insertion of amplicons using M13 vector primers. Plasmids were extracted using a miniprep extraction kit (Epoch Life Sciences, Sugar Land, TX, USA) following the manufacturer's instructions then sequenced using M13 forward and reverse vector primers by the University of Washington High-Throughput Genomics Unit (Seattle, WA, USA). Vector sequence was trimmed using 4Peaks software[2] and forward and reverse contigs were merged using Seqman software program (DNASTAR, Madison, WI, USA). Chimeric sequences were identified using Mallard v.1.0 (Ashelford et al., 2006) and removed. The remaining 214 sequences were aligned using the online SINA aligner (v1.2.9; Pruesse et al., 2012) and manually refined in ARB (v5.2; Ludwig et al., 2004) with nearest neighbors from the SILVA reference database 102. Sequences were deposited in Genbank with accession numbers KF41379-KF41593.

Diversity analyses were performed on the clone library sequence data. Specifically, a pair-wise sequence distance matrix was exported and analyzed using the average neighbor method in MOTHUR (Schloss et al., 2009) for operational taxonomic units (OTUs) assigned based on an evolutionary distance of 3 and 7%, corresponding to 97 and 93% similarity cutoffs commonly used to define species and genus level diversification, respectively (Stackebrandt and Goebel, 1994). Rarefaction curves were generated, and alpha diversity indices (Chao, ACE, Shannon-Wiener, Simpson's D) and evenness were calculated. Percent coverage of the libraries was calculated as in (Good, 1953). The beta diversity tests $\int$-Libshuff and AMOVA were used to test for community differences between the enriched and non-enriched fractions. AMOVA tests whether the genetic diversity within communities is significantly different from their pooled genetic diversity (Schloss, 2008) while $\int$-Libshuff is a Cramér-von Mises-type statistic and a Monte Carlo procedure to determine if two libraries are significantly different (Singleton et al., 2001). A Bonferroni correction to account for reciprocal pair-wise comparisons of two groups was applied for the $\int$-Libshuff statistic, which was deemed to be significant at the $p = 0.025$ level.

RESULTS

Elemental analysis confirmed successful labeling of the enriched sediment ($\delta^{13}C = 579.0\%$) to ~5 times the non-enriched sediments. An MDS plot using dissimilarity based on the presence or absence of peak composition from T-RFLP data for each fraction showed clustering of heavy (enriched) and light (non-enriched) communities (PerMANOVA Pseudo-$F = 2.548$, $p(MC) = 0.0859$, unique permutations = 35; **Figure 1**) and allowed us to identify samples for downstream molecular sequencing. Among 16S rRNA sequences analyzed at the species level (3% distance), 146

[2]http://nucleobytes.com/index.php/4peaks

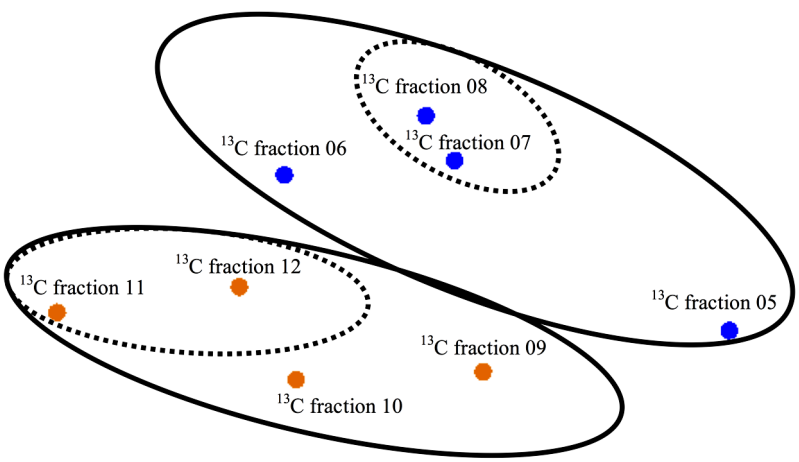

FIGURE 1 | Multidimensional scaling (MDS) plot of T-RFLP data based on presence or absence of TRFs. Orange symbols show light, non-enriched fractions and blue symbols show heavy, enriched fractions. Solid ellipses drawn on graph illustrate different groups at the $p = 0.086$ level (perMANOVA). Traditionally, enriched DNA is found in fractions 5–8 and light fractions found in 9–12 (Neufeld et al., 2007). Fractions 7/8 and 11/12 (dashed ellipses) were pooled as representatives of enriched and non-enriched DNA, respectively, to use for molecular sequencing.

total OTUs were detected (**Table 1**) of which only 12 were shared between the lignocellulose-responsive and non-responsive communities (**Figure 2D**). At the genus level (7% distance), 101 OTUs were detected of which 19 were found in both clone libraries (**Figure 2C**), further illustrating the differences even at higher taxonomic levels.

Rarefaction curves for non-responsive and lignocellulose-responsive bacterial communities were similar at both the genus and species level cutoffs (**Figures 2A,B**). Percent coverage values were also similar (**Table 1**). Comparable bacterial richness was observed between responsive and non-responsive bacterial communities; for example 82 and 76 OTUs were observed at the 3% distance level for the non-enriched and enriched bacterial communities, respectively (**Table 1**). Indeed, the richness and diversity estimators Chao, ACE, Shannon and Simpson's (Chao, 1984; Chao et al., 1992) were not statistically different between the two communities as indicated by the overlapping confidence intervals at both cutoffs. High evenness was observed as well (above 0.9 for both cutoffs), indicating no taxon was too rare or too common in either community (**Table 1**).

Despite the similarities in alpha diversity metrics, beta diversity comparisons revealed differences in community diversity between the lignocellulose-responsive and non-responsive bacterial communities. Significant statistical differences were observed only in one direction for the $\int$-Libshuff pair-wise comparisons at both the 3% (XY $p = 0.0003$, YX $p = 0.1007$) and 7% cutoffs (Libshuff, XY $p = 0.0002$, YX $p = 0.110$), which using the strict definition for this method does not provide evidence of significant differences between the two communities (Schloss, 2008). However, AMOVA ($p = 0.029$; Excoffier et al., 1992) results were significant indicating

Table 1 | Calculated alpha diversity indices for lignocellulose-responsive and non-responsive bacterial communities at the 3 and 7% evolutionary distance level.

Level	Group	*N*	OTUs [% Coverage]	Chao	ACE	Shannon-Wiener	Evenness	Simpson's D
Species (0.03)	Non-enriched	111	82 [26][1]	316.6 (257)[2]	322.56 (255.4)	4.2 (0.2)	0.95	0.01 (0.01)
	Enriched	108	76 [30]	175.0 (105.3)	193 (120.5)	4.2 (0.2)	0.97	0.01 (0.00)
Genus (0.07)	Non-enriched	111	63 [43]	149.3 (104)	305 (151.8)	3.7 (0.2)	0.90	0.04 (0.02)
	Enriched	108	57 [47]	120.9 (85.5)	247.4 (95.6)	3.7 (0.2)	0.92	0.03 (0.01)

[1] *Numbers in brackets denote percent coverage.*
[2] *Numbers in parentheses show 95% confidence intervals.*

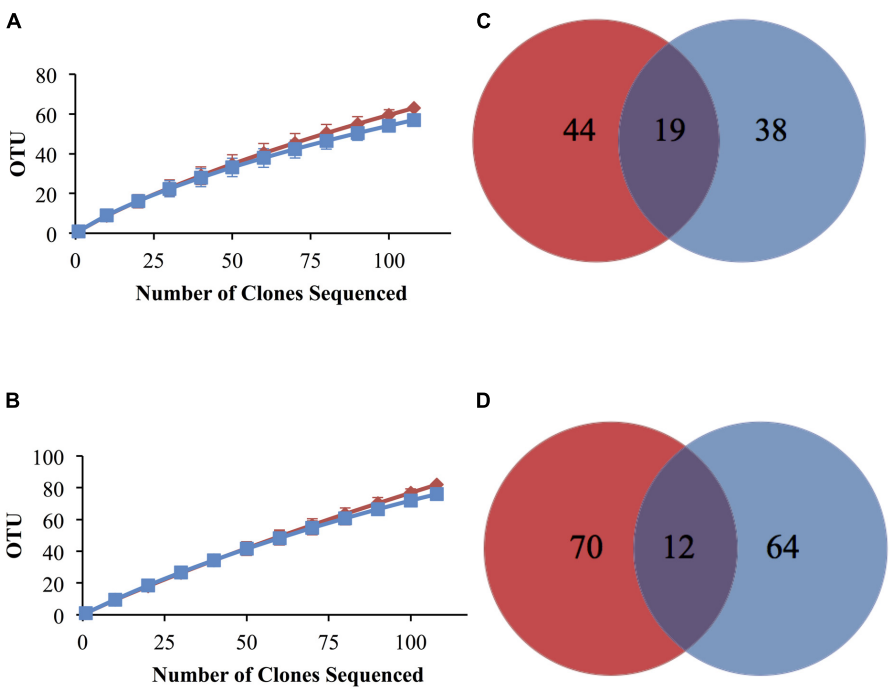

FIGURE 2 | Rarefaction analysis of bacterial 16S rRNA gene clone sequence data and Venn diagrams showing distribution of total and shared OTUs at 7% (A,C) and 3% (B,D) distance cutoff in lignocellulose-responsive (blue) and non-responsive (red) bacterial communities. Error bars are 95% confidence intervals.

that the genetic diversity within the individual communities was significantly different from their pooled genetic diversity.

Overall, 43% of bacterial species-level OTUs were unique to the enriched fraction, indicating a large portion of the total sediment community is lignocellulose-responsive. When we examined the specific bacterial taxa identified, we found a diverse bacterial community in both the lignocellulose-responsive and non-responsive communities, which both included diverse members of the Alpha-, Delta-, and Gamma-proteobacteria and Bacteroidetes. Among genera representing 4% of the community or greater that were only found in the ^{13}C-lignocellulose-responsive community, we identified members of the *Desulfosarcina*, *Kangiella*, *Spirochaeta*, and an uncultured group NKB5 (**Figure 3A**). Lineages that represented 4% or more and were only found in the non-responsive community were JTB148 (an unclassified member of Chromatiaceae), JG37-AG-15 (unclassified Myxococcales), *Haliea* and *Desulfobulbus* (**Figure 3B**). Notably, sequences assigned to the Flavobacterial genus *Sediminibacter* were abundant in both the

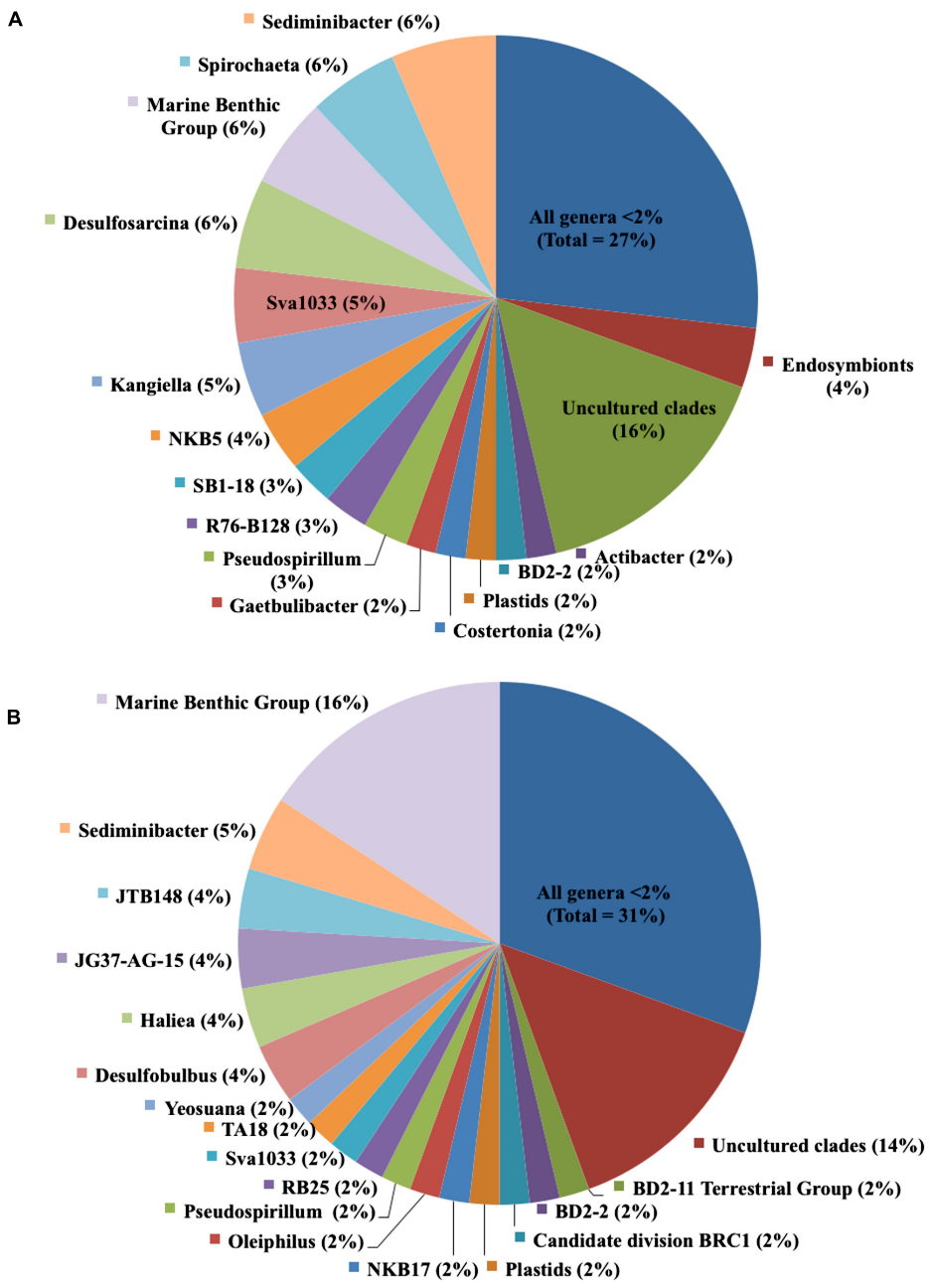

FIGURE 3 | Relative contributions of genera in (A) lignocellulose-responsive bacterial community and (B) non-responsive bacterial community. Cultured genera and uncultured lineages that comprised less than 2% of clones, respectively, were separately grouped.

responsive and non-responsive communities (6 vs. 5%, respectively; **Figure 3**). However, when viewed more generally at the Class level, there was roughly twice the percentage of Flavobacteria (19%) clones in the enriched community as in the non-enriched community (10%; data not shown).

DISCUSSION

Lignocellulose-degrading and utilizing bacteria are ecologically important in any plant-dominated ecosystem (McCarthy, 1987; Romani et al., 2006), and in salt marshes bacterial communities are thought to be largely supported by *Spartina*-derived carbon (Bushaw-Newton et al., 2008). Recent SIP studies utilizing ^{13}C-labeled substrates have uncovered active microbial cellulose degraders or carbon utilizers in environmental samples (Haichar et al., 2007; Bastias et al., 2009; Eichorst and Kuske, 2012). However, this is the first study to report the successful use of SIP with lignocellulose, a more realistic proxy for plant carbon than cellulose alone, to identify microbes responsive to macrophyte-derived carbon.

Sediment bacterial diversity has often been measured as an indicator of general ecosystem community response, since changes in the metabolic activity of microbes have the potential to impact system stability (Hunter-Cevera, 1998). The main goal of this study was to identify the specific microbial communities capable of contributing to carbon cycling by degrading lignocellulose or incorporating its breakdown products. Members of the deltaproteobacterial genus *Desulfosarcina* made up 6% of the enriched community. This group of sulfate-reducing bacteria (SRB) is commonly found in salt marshes, mud flats, hypersaline mats, and marine microbial biofilms (So and Young, 1999; Bahr et al., 2005; Mussmann et al., 2005; Buhring et al., 2009). Diverse SRB communities have been identified as key remineralizers in salt marsh sediments (Klepac-Ceraj et al., 2004; Bahr et al., 2005), and rates of sulfate reduction have been indirectly linked with seasonal changes in *Spartina* primary production (Howarth and Teal, 1979). However, SRB typically respire simpler carbon substrates such as fatty acids that have been produced by fermenters, suggesting that these may be end users of the decomposing macrophyte carbon. Nevertheless, our findings provide a direct link between plant-derived carbon and these SRB in salt marsh sediments. In addition, the prevalence of members of the SRB lineage *Desulfobulbus* in the non-responsive fraction indicates that not all SRB lineages were end users of plant carbon in this study.

In the responsive fraction, 5% of the bacterial sequences were most closely related to *Kangiella*, a genus of non-motile, gram-negative Gammaproteobacteria (Yoon et al., 2004; Han et al., 2009) found in marine sediments (Romanenko et al., 2010). Cultured members of this group have not previously been shown to degrade complex carbon (Yoon et al., 2004; Jean et al., 2012) suggesting possible new roles for *Kangiella* either directly using lignocellulose or indirectly using lignocellulose-derived degradation by-products in the HBW marsh. Alternatively, we cannot rule out the possibility that during the 30-day incubation period, cross feeding among bacterial groups occurred in this microcosm, which could also result in labeling of unexpected lineages such as *Kangiella*. Nevertheless, these findings indicate that unexpected sediment groups benefit at least indirectly from plant carbon.

Six percent of the enriched fraction sequences were identified as Spirochetes, which were not found in the non-enriched bacterial community. Free-living anaerobic spirochetes are common in marine sediments and microbial mats including those found in salt marshes (Teal et al., 1996; Margulis et al., 2010) and have been found to respond chemotactically to cellobiose in lab cultures (Breznak and Warnecke, 2008). They have also been shown to exist as symbionts in the guts of insects (Droge et al., 2008; Berlanga et al., 2010), likely aiding in the breakdown of lignocellulose components. While we have not specifically identified gut contents of invertebrates in this study, it is possible that some of the bacteria in the HBW marsh are associated with larval insects that commonly inhabit salt marsh sediments.

In the non-responsive community, unclassified members of Chromatiaceae and Myxococcales were abundant. These two groups would not be predicted to be lignocellulose utilizers as purple sulfur photoautotrophs fix their own carbon and Myxococcales typically prey upon other bacteria. At this point it is unknown if they are unable to incorporate plant-derived carbon or perhaps they were outcompeted for lignocellulose-derived substrates in our study.

Members of the Flavobacterial genus *Sediminibacter* were commonly recovered from both responsive and non-responsive fractions. This is a poorly characterized genus named for a single species of gram-negative chemoheterotrophic bacteria isolated from marine sediments in Japan (Khan et al., 2007). However, not all members of the Flavobacteria were abundant in both fractions. Overall, there was roughly twice the percentage of Flavobacteria in the lignocellulose-responsive community compared to the non-enriched community. Flavobacteria have been found to be associated with decaying *Spartina* blades in southeastern U.S. coastal salt marshes (Buchan et al., 2003), potentially because of their ability to degrade complex carbon-rich litter in salt marshes (Lydell et al., 2004; Das et al., 2007). Flavobacteria have also been identified as cellulose-responsive via SIP in cellulose-amended pine forest soils (Eichorst and Kuske, 2012) and as members of a lignocellulytic consortium in biofuel experiments (DeAngelis et al., 2010). Our study in salt marsh sediments corroborates these findings by directly linking lignocellulose-derived carbon to some members of the Flavobacteria.

These findings have identified key lignocellulose-responsive groups in the Huntington Beach Wetland. However, this should not be considered an exhaustive study as we have not fully analyzed (i.e., sequenced) replicate samples, and the clone libraries we obtained did not fully capture the diversity of lignocellulose-responsive bacteria as seen in our rarefaction analyses, which indicated that a higher sampling effort is needed to fully uncover the diversity of these samples. High levels of species richness and diversity are common for sediment microbial communities (Hughes et al., 2001; Hughes and Hellmann, 2005). However, the fact that significantly different communities were observed between the labeled and non-labeled fractions indicates that even these relatively small libraries were sufficient to identify community differences and redundancy of species-level OTUs up to 6% was seen in these libraries. Future studies combining SIP with next generation sequencing approaches will more thoroughly sample the biodiversity of carbon utilizers in salt marsh sediments.

CONCLUSION

Despite the importance of understanding food web structure and carbon storage potential in the environment, the role of microbes, especially diverse bacteria, within ecosystems like this can be difficult to detect and quantify (Neutel et al., 2002, 2007). Indeed little is known about the linkage between plants and microorganisms in highly productive ecosystems such as salt marshes (Koretsky et al., 2005). Our application of DNA SIP to identify lignocellulose-responsive bacteria has provided a direct link between the source and fate of macrophyte carbon in salt marshes for the first time, a key step in understanding the full spectrum of carbon cycling in these important ecosystems. In addition, regional variability has been observed in carbon storage potential among marshes (Chmura et al., 2003). Studies such as ours, which identify potential bacterial decomposer communities in southern California salt marshes, advance our understanding of the value of marshes in this region for long-term carbon sequestration. This study represents a first step in identifying lignocellulose-responsive bacterial communities, demonstrating the efficacy of the SIP approach with lignocellulose and in salt marshes. Future studies in this and other California coastal salt marshes should specifically target these identified lignocellulose-responsive bacterial groups to further elucidate their role in salt marsh carbon degradation and utilization.

ACKNOWLEDGMENTS

Funding for this project was provided by California Seagrant #R/ENV-215EPD to Jesse G. Dillon and Christine R. Whitcraft, CSU-COAST Summer Research Grant and Reish Research Grant to Lindsay E. Darjany. Lindsay E. Darjany would also like to acknowledge the CSULB Handloser tuition remission award, which provided support. The authors would like to thank the Huntington Beach Wetland Conservancy for allowing us to access the field site and for facilitating our research and Jazmyne Gill for assistance with this research and the NIH Minority Bridges Summer Program grant (5R25GM50089-12) for supporting her.

REFERENCES

Aneja, M. K., Sharma, S., Fleischmann, F., Stich, S., Heller, W., Bahnweg, G., et al. (2006). Microbial colonization of beech and spruce litter – Influence of decomposition site and plant litter species on the diversity of microbial community. *Microb. Ecol.* 52, 127–135. doi: 10.1007/s00248-006-9006-3

Ashelford, K. E., Chuzhanova, N. A., Fry, J. C., Jones, A. J., and Weightman, A. J. (2006). New screening software shows that most recent large 16S rRNA gene clone libraries contain chimeras. *Appl. Environ. Microbiol.* 72, 5734–5741. doi: 10.1128/AEM.00556-06

Bahr, M., Crump, B. C., Klepac-Ceraj, V., Teske, A., Sogin, M. L., and Hobbie, J. E. (2005). Molecular characterization of sulfate-reducing bacteria in a New England salt marsh. *Environ. Microbiol.* 7, 1175–1185. doi: 10.1111/j.1462-2920.2005.00796.x

Bastias, B. A., Anderson, I. C., Rangel-Castro, J. I., Parkin, P. I., Prosser, J. I., and Cairney, J. W. G. (2009). Influence of repeated prescribed burning on incorporation of 13C from cellulose by forest soil fungi as determined by RNA stable isotope probing. *Soil Biol. Biochem.* 41, 467–472. doi: 10.1016/j.soilbio.2008.11.018

Benner, R., Moran, M. A., and Hodson, R. E. (1986). Biogeochemical cycling of lignocellulosic carbon in marine and freshwater ecosystems relative contributions of prokaryotes and eukaryotes. *Limnol. Oceanogr.* 31, 89–100. doi: 10.4319/lo.1986.31.1.0089

Benner, R., Newell, S. Y., Maccubbin, A. E., and Hodson, R. E. (1984). Relative contributions of bacteria and fungi to rates of degradation of lignocellulosic detritus in salt-marsh sediments. *Appl. Environ. Microbiol.* 48, 36–40.

Berlanga, M., Paster, B. J., and Guerrero, R. (2010). Coevolution of symbiotic spirochete diversity in lower termites. *Int. Microbiol.* 10, 133–139.

Blum, L. K., Roberts, M. S., Garland, J. L., and Mills, A. L. (2004). Distribution of microbial communities associated with the dominant high marsh plants and sediments of the United States east coast. *Microb. Ecol.* 48, 375–388. doi: 10.1007/s00248-003-1051-6

Boschker, H. T. S., De Brouwer, J. F. C., and Cappenberg, T. E. (1999). The contribution of macrophyte-derived organic matter to microbial biomass in salt-marsh sediments: stable carbon isotope analysis of microbial biomarkers. *Limnol. Oceanogr.* 44, 309–319. doi: 10.4319/lo.1999.44.2.0309

Bouyoucos, G. J. (1962). Hydrometer method improved for making particle size analyses of soil. *Agron. J.* 54, 464–465. doi: 10.2134/agronj1962.00021962005400050028x

Breznak, J. A., and Warnecke, F. (2008). *Spirochaeta cellobiosiphila* sp. nov., a facultatively anaerobic, marine spirochaete. *Int. J. Syst. Evol. Microbiol.* 58, 2762–2768. doi: 10.1099/ijs.0.2008/001263-0

Buchan, A., Newell, S. Y., Butler, M., Biers, E. J., Hollibaugh, J. T., and Moran, M. A. (2003). Dynamics of bacterial and fungal communities on decaying salt marsh grass. *Appl. Environ. Microbiol.* 69, 6676–6687. doi: 10.1128/AEM.69.11.6676-6687.2003

Buckley, D. H., Huangyutitham, V., Hsu, S.-F., and Nelson, T. A. (2007). Stable isotope probing with 15N2 reveals novel noncultivated diazotrophs in soil. *Appl. Environ. Microbiol.* 73, 3196–3204. doi: 10.1128/AEM.02610-06

Buhring, S., Smittenberg, R., Sachse, D., Lipp, J., Golubic, S., Sachs, J., et al. (2009). A hypersaline microbial mat from the Pacific Atoll Kiritimati: insights into composition and carbon fixation using biomarker analyses and a 13C-labeling approach. *Geobiology* 7, 308–323. doi: 10.1111/j.1472-4669.2009.00198.x

Bushaw-Newton, K. L., Kreeger, D. A., Doaty, S., and Velinsky, D. J. (2008). Utilization of Spartina-and Phragmites-derived dissolved organic matter by bacteria and ribbed mussels (Geukensia demissa) from Delaware Bay salt marshes. *Estuar. Coasts* 31, 694–703. doi: 10.1007/s12237-008-9061-8

Chao, A. (1984). Nonparametric estimation of the number of classes in a population. *Scand. J. Stat.* 265–270.

Chao, A., Lee, S. M., and Jeng, S. L. (1992). Estimating population size for capture-recapture data when capture probabilities vary by time and individual animal. *Biometrics* 201–216. doi: 10.2307/2532750

Chmura, G. L., Anisfeld, S. C., Cahoon, D. R., and Lynch, J. C. (2003). Global carbon sequestration in tidal, saline wetland soils. *Global Biogeochem. Cycles* 17. doi: 10.1029/2002GB001917

Choi, Y., Wang, Y., Hsieh, Y. Ä., and Robinson, L. (2001). Vegetation succession and carbon sequestration in a coastal wetland in northwest Florida: evidence from carbon isotopes. *Global Biogeochem. Cycles* 15, 311–319. doi: 10.1029/2000GB001308

Coffin, R. B., Velinsky, D. J., Devereux, R., Price, W. A., and Cifuentes, L. A. (1990). Stable carbon isotope analysis of nucleic acids to trace sources of dissolved substrates used by estuarine bacteria. *Appl. Environ. Microbiol.* 56, 2012–2020.

Das, M., Royer, T. V., and Leff, L. G. (2007). Diversity of fungi, bacteria, and actinomycetes on leaves decomposing in a stream. *Appl. Environ. Microbiol.* 73, 756–767. doi: 10.1128/AEM.01170-06

DeAngelis, K. M., Gladden, J. M., Allgaier, M., D'Haeseleer, P., Fortney, J. L., Reddy, A., et al. (2010). Strategies for enhancing the effectiveness of metagenomic-based enzyme discovery in lignocellulolytic microbial communities. *Bioenerg. Res.* 3, 146–158. doi: 10.1007/s12155-010-9089-z

Dillon, J. G., Mcmath, L. M., and Trout, A. L. (2009a). Seasonal changes in bacterial diversity in the Salton Sea. *Hydrobiologia* 632, 49–64. doi: 10.1007/s10750-009-9827-4

Dillon, J. G., Miller, S., Bebout, B., Hullar, M., Pinel, N., and Stahl, D. A. (2009b). Spatial and temporal variability in a stratified hypersaline microbial mat community. *FEMS Microbiol. Ecol.* 68, 46–58. doi: 10.1111/j.1574-6941.2009.00647.x

Droge, S., Rachel, R., Radek, R., and Konig, H. (2008). *Treponema isoptericolens* sp. nov., a novel spirochaete from the hindgut of the termite Incisitermes tabogae. *Int. J. Syst. Evol. Microbiol.* 58, 1079–1083. doi: 10.1099/ijs.0.64699-0

Eichorst, S. A., and Kuske, C. R. (2012). Identification of cellulose-responsive bacterial and fungal communities in geographically and edaphically different soils by using stable isotope probing. *Appl. Environ. Microbiol.* 78, 2316–2327. doi: 10.1128/AEM.07313-11

Excoffier, L., Smouse, P. E., and Quattro, J. M. (1992). Analysis of molecular variance inferred from metric distances among DNA haplotypes: application to human mitochondrial DNA restriction data. *Genetics* 131, 479–491.

Gallagher, J. L., Pfeiffer, W. J., and Pomeroy, L. R. (1976). Leaching and microbial utilization of dissolved organic carbon from leaves of Spartina alterniflora. *Estuar. Coast. Mar. Sci.* 4, 467–471. doi: 10.1016/0302-3524(76)90021-9

Good, I. J. (1953). The population frequencies of species and the estimation of population parameters. *Biometrika* 40, 237–264. doi: 10.1093/biomet/40.3-4.237

Haichar, F. E. Z., Achouak, W., Christen, R., Heulin, T., Marol, C., Marais, M.-F., et al. (2007). Identification of cellulolytic bacteria in soil by stable isotope probing. *Environ. Microbiol.* 9, 625–634. doi: 10.1111/j.1462-2920.2006.01182.x

Han, C., Sikorski, J., Lapidus, A., Nolan, M., Del Rio, T. G., Tice, H., et al. (2009). Complete genome sequence of *Kangiella koreensis* type strain (SW-125T). *Stand. Genomic Sci.* 1, 226. doi: 10.4056/sigs.36635

Harrison, B. K., and Orphan, V. J. (2012). Method for assessing mineral composition-dependent patterns in microbial diversity using magnetic and density separation. *Geomicrobiol. J.* 29, 435–449. doi: 10.1080/01490451.2011.581327

Hemminga, M., Kok, C., and De Munck, W. (1988). Decomposition of Spartina anglica roots and rhizomes in a salt marsh of the Westerschelde estuary. *Mar. Ecol. Prog. Ser.* 48.

Hines, M. E., Knollmeyer, S. L., and Tugel, J. B. (1989). Sulfate Reduction and Other Sedimentary Biogeochemistry in a Northern New England Salt Marsh. *Limnol. Oceanogr.* 34, 578–590. doi: 10.4319/lo.1989.34.3.0578

Hodson, R. E., Christian, R. R., and Maccubbin, A. E. (1984). Lignocellulose and lignin in the salt marsh grass Spartina alterniflora: initial concentrations and short-term, post-depositional changes in detrital matter. *Mar. Biol.* 81, 1–7. doi: 10.1007/BF00397619

Howarth, R. (1993). "Microbial processes in salt-marsh sediments," in *Aquatic Microbiology,* ed. T. E. Ford (Boston: Blackwell Scientific), 239–259.

Howarth, R. W., and Teal, J. M. (1979). Sulfate reduction in a New England USA salt marsh. *Limnol. Oceanogr.* 24, 999–1013. doi: 10.4319/lo.1979.24.6.0999

Hughes, J. B., and Hellmann, J. J. (2005). The application of rarefaction techniques to molecular inventories of microbial diversity. *Methods Enzymol.* 397, 292–308. doi: 10.1016/S0076-6879(05)97017-1

Hughes, J. B., Hellmann, J. J., Ricketts, T. H., and Bohannan, B. J. M. (2001). Counting the uncountable: statistical approaches to estimating microbial diversity. *Appl. Environ. Microbiol.* 67, 4399–4406. doi: 10.1128/AEM.67.10.4399-4406.2001

Hunter-Cevera, J. C. (1998). The value of microbial diversity. *Curr. Opin. Microbiol.* 1, 278–285. doi: 10.1016/S1369-5274(98)80030-1

Jean, W. D., Huang, S.-P., Chen, J.-S., and Shieh, W. Y. (2012). *Kangiella taiwanensis* sp. nov. and *Kangiella marina* sp. nov., marine bacteria isolated from shallow coastal water. *Int. J. Syst. Evol. Microbiol.* 62, 2229–2234. doi: 10.1099/ijs.0.037010-0

Keller, J. K., Takagi, K. K., Brown, M. E., Stump, K. N., Takahashi, C. G., Joo, W., et al. (2012). Soil organic carbon storage in restored salt marshes in Huntington Beach, California. *Bull. South. Calif. Acad. Sci.* 111, 153–161. doi: 10.3160/0038-3872-111.2.153

Khan, S. T., Nakagawa, Y., and Harayama, S. (2007). *Sediminibacter furfurosus* gen. nov., sp. nov. and *Gilvibacter sediminis* gen. nov., sp. nov., novel members of the family Flavobacteriaceae. *Int. J. Syst. Evol. Microbiol.* 57, 265–269. doi: 10.1099/ijs.0.64628-0

Klepac-Ceraj, V., Bahr, M., Crump, B. C., Teske, A. P., Hobbie, J. E., and Polz, M. F. (2004). High overall diversity and dominance of microdiverse relationships in salt marsh sulphate-reducing bacteria. *Environ. Microbiol.* 6, 686–698. doi: 10.1111/j.1462-2920.2004.00600.x

Koretsky, C. M., Van Cappellen, P., Dichristina, T. J., Kostka, J. E., Lowe, K. L., Moore, C. M., et al. (2005). Salt marsh pore water geochemistry does not correlate with microbial community structure. *Estuar. Coast. Shelf Sci.* 62, 233–251. doi: 10.1016/j.ecss.2004.09.001

Kowalchuk, G., Buma, D., De Boer, W., Klinkhamer, P., and Van Veen, J. (2002). Effects of above-ground plant species composition and diversity on the diversity of soil-borne microorganisms. *Anton. Leeuw.* 81, 509–520. doi: 10.1023/A:1020565523615

Kwak, T. J., and Zedler, J. B. (1997). Food web analysis of southern California coastal wetlands using multiple stable isotopes. *Oecologia (Berlin)* 110, 262–277. doi: 10.1007/s004420050159

Liu, W., Marsh, T., Cheng, H., and Forney, L. (1997). Characterization of microbial diversity by determining terminal restriction fragment length polymorphisms of genes encoding 16S rRNA. *Appl. Environ. Microbiol.* 63, 4516–4522.

Ludwig, W., Strunk, O., Westram, R., Richter, L., Meier, H., Kumar, Y., et al. (2004). ARB: a software environment for sequence data. *Nucleic Acids Res.* 32, 1363–1371. doi: 10.1093/nar/gkh293

Lydell, C., Dowell, L., Sikaroodi, M., Gillevet, P., and Emerson, D. (2004). A population survey of members of the phylum Bacteroidetes isolated from salt marsh sediments along the East Coast of the United States. *Microb. Ecol.* 48, 263–273. doi: 10.1007/s00248-003-1068-x

Margulis, L., Navarrete, A., and Sole, M. (2010). Cosmopolitan distribution of the large composite microbial mat spirochete, *Spirosymplokos deltaeiberi*. *Int. Microbiol.* 1, 27–34.

McCarthy, A. J. (1987). Lignocellulose-degrading actinomycetes. *FEMS Microbiol. Lett.* 46, 145–163. doi: 10.1111/j.1574-6968.1987.tb02456.x

Megonigal, J. P., Hines, M. E., and Visscher, P. T. (2004). "Anaerobic metabolism: linkages to trace gases and aerobic processes," in *Biogeochemistry*, ed. W. H. Schlesinger (Oxford: Elsevier-Pergamon), 317–434.

Minello, T. J., Able, K. W., Weinstein, M. P., and Hays, C. G. (2003). Salt marshes as nurseries for nekton: testing hypotheses on density, growth and survival through meta-analysis. *Mar. Ecol. Prog. Ser.* 246, 39–59. doi: 10.3354/meps246039

Mitsch, W. J., and Gosselink, J. G. (2007). *Wetlands. Hoboken.* New Jersey: Wiley.

Moran, M. A., and Hodson, R. E. (1990). Contributions of degrading Spartina alterniflora lignocellulose to the dissolved organic carbon pool of a salt marsh. *Mar. Ecol. Prog. Ser.* 62, 161–168. doi: 10.3354/meps062161

Mussmann, M., Ishii, K., Rabus, R., and Amann, R. (2005). Diversity and vertical distribution of cultured and uncultured Deltaproteobacteria in an intertidal mud flat of the Wadden Sea. *Environ. Microbiol.* 7, 405–418. doi: 10.1111/j.1462-2920.2005.00708.x

Muyzer, G., Teske, A., Wirsen, C. O., and Jannasch, H. W. (1995). Phylogenetic-relationships of Thiomicrospira species and their identification in deep-sea hydrothermal vent samples by denaturing gradient gel-electrophoresis of 16S rDNA fragments. *Arch. Microbiol.* 164, 165–172. doi: 10.1007/BF02529967

Neufeld, J. D., Vohra, J., Dumont, M. G., Lueders, T., Manefield, M., Friedrich, M. W., et al. (2007). DNA stable-isotope probing. *Nat. Protoc.* 2, 860–866. doi: 10.1038/nprot.2007.109

Neutel, A. M., Heesterbeek, J. A. P., and De Ruiter, P. C. (2002). Stability in real food webs: weak links in long loops. *Science* 296, 1120–1123. doi: 10.1126/science.1068326

Neutel, A. M., Heesterbeek, J. A. P., Van De Koppel, J., Hoenderboom, G., Vos, A., Kaldeway, C., et al. (2007). Reconciling complexity with stability in naturally assembling food webs. *Nature* 449, 599–602. doi: 10.1038/nature06154

Newell, S. Y. (1993). Decomposition of shoots of a salt-marsh grass: methodology and dynamics of microbial assemblages. *Adv. Microb. Ecol.* 13, 301–326. doi: 10.1007/978-1-4615-2858-6_7

Paerl, H. W., and Pinckney, J. L. (1996). A mini-review of microbial consortia: their roles in aquatic production and biogeochemical cycling. *Microb. Ecol.* 31, 225–247. doi: 10.1007/BF00171569

Peterson, B. J., Howarth, R. W., and Garritt, R. H. (1985). Multiple stable isotopes used to trace the flow of organic matter in estuarine food webs. *Science* 227, 1361–1363. doi: 10.1126/science.227.4692.1361

Prosser, J., Rangelcastro, J., and Killham, K. (2006). Studying plant–microbe interactions using stable isotope technologies. *Curr. Opin. Biotechnol.* 17, 98–102. doi: 10.1016/j.copbio.2006.01.001

Pruesse, E., Peplies, J., and Gloeckner, F. O. (2012). SINA: accurate high-throughput multiple sequence alignment of ribosomal RNA genes. *Bioinformatics* 28, 1823–1829. doi: 10.1093/bioinformatics/bts252

Radajewski, S., Ineson, P., Parekh, N. R., and Murrell, J. C. (2000). Stable-isotope probing as a tool in microbial ecology. *Nature* 403, 646–649. doi: 10.1038/35001054

Romanenko, L. A., Tanaka, N., Frolova, G. M., and Mikhailov, V. V. (2010). *Arenicella xantha* gen. nov., sp. nov., a Gammaproteobacterium isolated from

a marine sandy sediment. *Int. J. Syst. Evol. Microbiol.* 60, 1832–1836. doi: 10.1099/ijs.0.017194-0

Romani, A. M., Fischer, H., Mille-Lindblom, C., and Tranvik, L. J. (2006). Interactions of bacteria and fungi on decomposing litter: differential extracellular enzyme activities. *Ecology* 87, 2559–2569. doi: 10.1890/0012-9658(2006)87[2559:IOBAFO]2.0.CO;2

Rooney-Varga, J. N., Genthner, B. R. S., Devereux, R., Willis, S. G., Friedman, S. D., and Hines, M. E. (1998). Phylogenetic and physiological diversity of sulphate-reducing bacteria isolated from a salt marsh sediment. *Syst. Appl. Microbiol.* 21, 557–568. doi: 10.1016/S0723-2020(98)80068-4

Schloss, P. D. (2008). Evaluating different approaches that test whether microbial communities have the same structure. *ISME J.* 2, 265–275. doi: 10.1038/ismej.2008.5

Schloss, P. D., Westcott, S. L., Ryabin, T., Hall, J. R., Hartmann, M., Hollister, E. B., et al. (2009). Introducing mothur: open-source, platform-independent, community-supported software for describing and comparing microbial communities. *Appl. Environ. Microbiol.* 75, 7537–7541. doi: 10.1128/AEM.01541-09

Singleton, D. R., Furlong, M. A., Rathbun, S. L., and Whitman, W. B. (2001). Quantitative comparisons of 16S rRNA gene sequence libraries from environmental samples. *Appl. Environ. Microbiol.* 67, 4374–4376. doi: 10.1128/AEM.67.9.4374-4376.2001

So, C. M., and Young, L. Y. (1999). Isolation and characterization of a sulfate-reducing bacterium that anaerobically degrades alkanes. *Appl. Environ. Microbiol.* 65, 2969–2976.

Stackebrandt, E., and Goebel, B. M. (1994). Taxonomic note: a place for DNA-DNA reassociation and 16S rRNA sequence analysis in the present species definition in bacteriology. *Int. J. Syst. Bacteriol.* 44, 846–849. doi: 10.1099/00207713-44-4-846

Teal, T. H., Chapman, M., Guillemette, T., and Margulis, L. (1996). Free-living spirochetes from Cape Cod microbial mats detected by electron microscopy. *Microbiologia* 12, 571–584.

Wagner, K. I., Gallagher, S. K., Hayes, M., Lawrence, B. A., and Zedler, J. B. (2008). Wetland restoration in the new millennium: do research efforts match opportunities? *Restor. Ecol.* 16, 367–372. doi: 10.1111/j.1526-100X.2008.00433.x

Wilson, J. O. (1985). Decomposition of [14C] lignocelluloses of Spartina alterniflora and a comparison with field experiments. *Appl. Environ. Microbiol.* 49, 478–484.

Yoon, J. H., Oh, T. K., and Park, Y. H. (2004). *Kangiella koreensis* gen. nov., sp. nov. and *Kangiella aquimarina* sp. nov., isolated from a tidal flat of the Yellow Sea in Korea. *Int. J. Syst. Evol. Microbiol.* 54, 1829–1835. doi: 10.1099/ijs.0.63156-0

Conflict of Interest Statement: The authors declare that the research was conducted in the absence of any commercial or financial relationships that could be construed as a potential conflict of interest.

Received: 31 January 2014; accepted: 13 May 2014; published online: 02 June 2014.
*Citation: Darjany LE, Whitcraft CR and Dillon JG (2014) Lignocellulose-responsive bacteria in a southern California salt marsh identified by stable isotope probing. Front. Microbiol. **5**:263. doi: 10.3389/fmicb.2014.00263*
This article was submitted to Aquatic Microbiology, a section of the journal Frontiers in Microbiology.

frontiers in Microbiology

ORIGINAL RESEARCH
published: 16 March 2015
doi: 10.3389/fmicb.2015.00197

The transcriptional response of microbial communities in thawing Alaskan permafrost soils

Marco J. L. Coolen[1,2*†] *and William D. Orsi*[1†]

[1] *Marine Chemistry and Geochemistry Department, Woods Hole Oceanographic Institution, Woods Hole, MA, USA,* [2] *Western Australia Organic and Isotope Geochemistry Centre, Department of Chemistry, Curtin University, Perth, WA, Australia*

Thawing of permafrost soils is expected to stimulate microbial decomposition and respiration of sequestered carbon. This could, in turn, increase atmospheric concentrations of greenhouse gasses, such as carbon dioxide and methane, and create a positive feedback to climate warming. Recent metagenomic studies suggest that permafrost has a large metabolic potential for carbon processing, including pathways for fermentation and methanogenesis. Here, we performed a pilot study using ultrahigh throughput Illumina HiSeq sequencing of reverse transcribed messenger RNA to obtain a detailed overview of active metabolic pathways and responsible organisms in up to 70 cm deep permafrost soils at a moist acidic tundra location in Arctic Alaska. The transcriptional response of the permafrost microbial community was compared before and after 11 days of thaw. In general, the transcriptional profile under frozen conditions suggests a dominance of stress responses, survival strategies, and maintenance processes, whereas upon thaw a rapid enzymatic response to decomposing soil organic matter (SOM) was observed. Bacteroidetes, Firmicutes, ascomycete fungi, and methanogens were responsible for largest transcriptional response upon thaw. Transcripts indicative of heterotrophic methanogenic pathways utilizing acetate, methanol, and methylamine were found predominantly in the permafrost table after thaw. Furthermore, transcripts involved in acetogenesis were expressed exclusively after thaw suggesting that acetogenic bacteria are a potential source of acetate for acetoclastic methanogenesis in freshly thawed permafrost. Metatranscriptomics is shown here to be a useful approach for inferring the activity of permafrost microbes that has potential to improve our understanding of permafrost SOM bioavailability and biogeochemical mechanisms contributing to greenhouse gas emissions as a result of permafrost thaw.

Keywords: permafrost, metatranscriptomics, hydrolysis of biopolymers, acetoclastic methanogenesis, biofilm formation, DNA repair, cellular defense mechanisms

OPEN ACCESS

Edited by:
Anne Bernhard, Connecticut College, USA

Reviewed by:
Matthew Wallenstein, Colorado State University, USA
Nathan Basiliko, Laurentian University, Canada

***Correspondence:**
Marco J. L. Coolen, Western Australia Organic and Isotope Geochemistry Centre, Department of Chemistry, Curtin University, GPO Box U1987, Perth, WA 6845, Australia
marco.coolen@curtin.edu.au

† *These authors have contributed equally to this work.*

Specialty section:
This article was submitted to Terrestrial Microbiology, a section of the journal Frontiers in Microbiology

Received: *06 January 2015*
Accepted: *24 February 2015*
Published: *16 March 2015*

Citation:
Coolen MJL and Orsi WD (2015) The transcriptional response of microbial communities in thawing Alaskan permafrost soils. Front. Microbiol. 6:197. doi: 10.3389/fmicb.2015.00197

Introduction

The northern permafrost region contains ~1672 gigatonnes (Gt) of organic carbon, nearly twice the amount of atmospheric carbon. Roughly 1470 Gt or 88% of this carbon occurs in perennially frozen soils and deposits (Tarnocai et al., 2009). The majority of permafrost organic matter is derived from (partially decomposed) plant material and was buried by dust deposition, sedimentation in flood plains and peat development on time scales of decades to millennia

(Zimov et al., 2006; Schuur et al., 2008). Permafrost is overlain by a soil horizon that varies in thickness from a few centimeters to several meters, which experiences seasonal freeze–thaw cycles (i.e., the active layer). Owing to atmospheric warming, the depth of the active layer has been increasing in many locations over the past few decades, resulting in a subsequent decline in the underlying permafrost (Kane et al., 1991; Anisimov et al., 1999; Jorgenson et al., 2001; Zhang et al., 2005; Pautler et al., 2010). This warming-induced thickening of the active layer is expected to enhance microbially mediated soil organic matter (SOM) decomposition, and release of carbon from the upper permafrost to the atmosphere (Dutta et al., 2006; Uhlirova et al., 2007; Schuur et al., 2008; Pautler et al., 2010).

Despite subfreezing temperatures and low water availability, permafrost soils up to 3 million years in age harbor a large diversity of bacteria, archaea, and fungi as revealed by sequencing of environmental ribosomal RNA (rRNA) genes (Vishnivetskaya et al., 2006; Liebner et al., 2008; Waldrop et al., 2010; Coolen et al., 2011; Penton et al., 2013; Bakermans et al., 2014; Frank-Fahle et al., 2014; Ganzert et al., 2014). A variety of microbes have retained viability in frozen permafrost over geological time periods and, upon thawing, could renew or accelerate their physiological activity. Many permafrost bacterial isolates are cold-adapted heterotrophs belonging to the phyla Firmicutes, Actinobacteria, Proteobacteria, and Bacteroidetes, while many of the archaeal isolates are methane (CH_4)-producers (methanogens) growing on hydrogen (H_2) and carbon dioxide (CO_2) with some species also growing on formate, methanol, or methylamine (Jansson and Tas, 2014 and references therein).

Genomes of bacterial isolates have also revealed insights into strategies for survival in subzero conditions. For example, the genome of the Siberian permafrost isolate *Psychrobacter arcticus* 273-4 revealed three cold shock proteins, which operate as RNA chaperones that enhance translation processes by eliminating the formation of secondary structures in the messenger RNA (mRNA) (Ayala-Del-Rio et al., 2010). This adaptation is important for *P. arcticus*, and possibly other permafrost bacteria, because subzero temperatures make mRNA more stable and less efficient for translation. Furthermore, *P. arcticus* uses acetate, which can diffuse into the cell without an energetically costly transport system, as the basis for its biosynthesis and energy metabolism (Ayala-Del-Rio et al., 2010). However, cultured species isolated from permafrost are not necessarily representative of active microbial community *in situ*, and the ability of some members to form spores (e.g., Firmicutes) may bias phylogenetic representation in culture (Steven et al., 2008; Niederberger et al., 2009).

Recent pioneering metagenomic studies have helped to circumvent some cultivation-biased interpretations of *in situ* activity, and revealed cultivation-independent insights into which biochemical pathways are present and potentially expressed by permafrost microbiota. Overall, these studies suggest that permafrost microbial communities have a large metabolic potential for carbon processing, including pathways for fermentation, methanogenesis, and nitrogen cycling (Yergeau et al., 2010; Mackelprang et al., 2011; Lipson et al., 2013). However, metagenomic surveys do not provide information on the relative importance and the exact timing of biochemical processes, as cells need to replicate their genomes first to monitor an increase in metabolic potential. In addition, in pristine frozen soil samples it is difficult to distinguish between genes involved in ongoing vs. past microbial processes using DNA-based metagenomic datasets because bacterial, fungal, and plant DNA can be preserved for thousands of years in permafrost soils (Willerslev et al., 2003, 2004; Bellemain et al., 2013). However, metatransciptomic analysis of extremely short-lived mRNA would provide information on microbial activities that occurred in the permafrost soils at the time of sampling.

Here, we performed a pilot study using ultrahigh throughput Illumina HiSeq sequencing of reverse transcribed mRNA (e.g., Orsi et al., 2013; Huang et al., 2014) to obtain a detailed overview of active metabolic pathways and responsible organisms in permafrost soils under pristine frozen conditions and transcriptional responses after 11 days of thaw. The permafrost soil horizons analyzed (up to 70-cm-deep) are expected to thaw in the Alaskan Arctic within decades as a result of continuing Arctic warming (Osterkamp, 2007). For our analysis, we were particularly interested in the expression of biochemical pathways that are hypothesized to play an important role in mediating the release of greenhouse gasses from thawing permafrost (e.g., CO_2 and CH_4). We sought to provide the first transcriptional data supporting the hypothesis that microbial degradation of SOM biopolymers leads to increased CO_2 production and methanogenesis, and to elucidate the biochemical mechanisms underlying these processes. Parallel geochemical analysis of soil age, carbon and nitrogen content, and lipid biomarkers provided additional information on the sources and composition of permafrost SOM.

Methods

Site Description and Sample Collection

Using a SIPRE style auger system (Jon's Machine Shop, Fairbanks, AK), a 130-cm-long (8 cm diameter) core was recovered on July 27, 2008 from moist acidic tundra (MAT) near the Kuparuk River at the Toolik Long Term Ecological Research (LTER) Field Station, Alaska (68°38′41.455″N:149°24′09.682″W) (Coolen et al., 2011). The pH of the soils was not determined, but a pH of 3–4 has been reported from comparable North Alaskan MAT soils (Hobbie and Gough, 2004). According to the Alaska Tundra Vegetation Map (Walker and Maier, 2008), the coring location was located in bioclimate subzone E where mean July temperatures are between 9 and 12°C and the tundra vegetation covering the coring site is defined as Class 4.1 Tussock-sedge, dwarf shrub, moss communities on mesic, acidic loess. This is the most common type of vegetation, covering 100,000 km^2 or 25% of the land surface in Arctic Alaska. The thickness of the active layer was 26 cm at the time of coring. Core sections were described in the field and immediately wrapped in sterile, baked (500°C, 8 h) aluminum foil and kept frozen inside coolers with deeply frozen blue ice packs. At the Toolik Field Station, the melted active layer was kept inside the cooler and the frozen core sections were kept in a freezer at −5°C for up to 2 h until subsampling was completed: within 2 h after coring an uncontaminated subsampling surface area was created by removing the outer 1 cm of frozen

soil with a sterile knife. Cores were split laterally at the desired depths using a sterilized hammer and a chisel, and subsamples were obtained only from the central part of each interval with sterilized scalpel and tweezers. Thus, the distance between the core liner and subsampled sediment was at least 2 cm to avoid cross contamination.

Soil samples were collected immediately after coring on July 27, 2008 from two active layer horizons (12 ± 2 and 24 ± 2 cm), and five depth intervals from the underlying permafrost (33.5 ± 2, 49 ± 2, 68 ± 2, 109 ± 2, and 126 ± 2 cm). For lipid analysis, subsamples (~2 g) were stored frozen at −20°C at the Woods Hole Oceanographic Institution (WHOI) until subsequent lipid extraction. For the subsequent extraction of RNA, ~2 g aliquots of pristine soils were transferred to 5 ml cryovials and immediately flash frozen in liquid nitrogen. In addition, 20 ml sterile serum flasks were completely filled with soil leaving no headspace, capped airtight, and incubated in the dark at 4°C. As samples were capped airtight with no headspace, they remained anoxic for the duration of the incubation. Subsamples for RNA extraction were also obtained on the last day of fieldwork (i.e., after 11 days of thaw/incubation). All samples for RNA work were stored in liquid nitrogen during airfreight transport to WHOI and RNA was extracted immediately upon arrival as detailed below.

Radiocarbon dates and bulk geochemical analysis (%TOC, %TN, $\delta^{13}C$, $\delta^{15}N$) from the exact same intervals were provided previously (Coolen et al., 2011), and compared with the lipid biomarker results from the present study (**Figure 1**).

Soil Organic Matter Composition

Lipid biomarker compounds were extracted from soils collected from the 7 depth horizons with a methylene chloride:methanol mixture (9:1, v:v) using a microwave-accelerated reaction system (MARS6) (CEM, Matthews, NC) in which samples were heated at 100°C for 15 min with continuous stirring (Osburn et al., 2011). Following extraction, samples were filtered, dried under N_2 gas, and saponified with aqueous 0.5 M sodium hydroxide at 70°C for 4 h. Cooled samples were acidified with 3N hydrochloric acid (pH < 3) before being extracted 3 times with methyl tert-butyl ether. Subsequently, elemental sulfur was removed by filtering extracts through acid-washed copper. Samples were resuspended in hexane prior to separation of compound classes by solid phase extraction. Discovery DSC-NH2 stationary phase (Sigma-Aldrich, St. Louis, MO) (1 g) was packed into glass columns and samples were separated into five fractions: F1 5 ml hexane; F2 8 ml of 4:1 hexane/methylene chloride; F3 10 ml of 9:1 methylene chloride/acetone; F4 15 ml of 2% formic acid in methylene chloride (Sessions, 2006). Fatty acids (F4) were methylated with acidic methanol (95:5 methanol/HCl) and heated overnight at 70°C to form fatty acids methyl esters. Fractions containing hydrocarbons (F1) and fatty acids (F4) were concentrated and an internal standard was added prior to analysis by gas chromatography—mass spectrometry (GC-MS). One microliter of sample was injected into an Agilent 7890 GC (Agilent Technologies, Santa Clara, CA) with an effluent split ~70:30 between a 5975C mass spectrometer and a flame ionizing detector. Peaks were separated on a DB-5 ms column (60 m long, 0.25 mm ID, 0.25 μm film thickness). Data from hydrocarbon (F1) and fatty acid (F4) fractions are presented here for all samples except the 68 cm horizon, due to sample loss. From *n*-alkane concentrations (hydrocarbon fraction) we calculated the carbon preference index (CPI), P_{aq} index, and P_{wax} index. CPI_{alkane} reflects relative inputs of higher plants vs. algae and bacteria since the former have a strong odd/even predominance. Consequently, high CPI_{alkane} values (>5) reflect mainly contributions from higher plants (Cranwell et al., 1987).

$$CPI_{alkane} = \left(\Sigma(C_{21}-C_{29})_{odd}+\Sigma(C_{23}-C_{31})_{odd}\right)/\left(2*\Sigma(C_{22}-C_{30})_{even}\right).$$

The P_{aq} index reflects relative contributions of alkanes from aquatic macrophytes vs. higher plants (Ficken et al., 2000). High P_{aq} values (>0.5) indicate inputs from submerged or floating macrophytes and may reflect wet conditions.

$$P_{aq} = (C_{23}+C_{25}) / (C_{23}+C_{25}+C_{29}+C_{31}).$$

A high P_{wax} index value (>0.7) reflects waxy inputs from higher plants and may indicate drier conditions (Zheng et al., 2007):

$$P_{wax} = (C_{27}+C_{29}+C_{31}) / (C_{23}+C_{25}+C_{27}+C_{29}+C_{31}).$$

RNA Extraction and Purification

Immediately after arrival of the flash frozen soil samples at WHOI, RNA was extracted in triplicate from ~2 g of soil using the Power Soil™ Total RNA Isolation kit (MoBio Laboratories, Inc., Carlsbad, CA) following the instructions of the manufacturer. The homogenization step started while the soil was still frozen to minimize degradation of RNA during thawing of the flash frozen soil samples. Standard procedures to further minimize degradation of RNA during the extraction process involved the use of filter tips and certified RNAse free disposables and reagents. Surfaces were cleaned with RNase AWAY™ (Life Technologies, Grand Island, NY), and all extraction procedures were performed in a HEPA-filtered horizontal laminar flow hood (Labconco, Kansas City, MO) inside a HEPA-filtered and positive-pressured ancient DNA dedicated lab at WHOI to eliminate aerosol contamination by bacterial and fungal cells/spores. DNA was removed using the Turbo DNA-free® kit (Life Technologies), increasing the incubation time to 1 h to ensure rigorous DNA removal. Extraction blanks were performed (adding sterile water instead of sample) to ensure that aerosolized contaminants did not enter sample and reagent tubes during the extraction process. Short RNA fragments (mostly produced during the extraction protocol) and residual inhibitors (i.e., humics) were removed from the extracted RNA using the MEGA-Clear® RNA Purification Kit (Life Technologies). We followed the protocol all the way through the optional precipitation/concentration step, resuspending the RNA pellet in 10 μl of certified RNAse free sterile water (Life Technologies). Prior to cDNA amplification, the removal of contaminating DNA in RNA extracts was confirmed by the absence of visible amplification of SSU rRNA genes after 35 cycles of PCR using the RNA extracts as template, and the quality of the RNA was

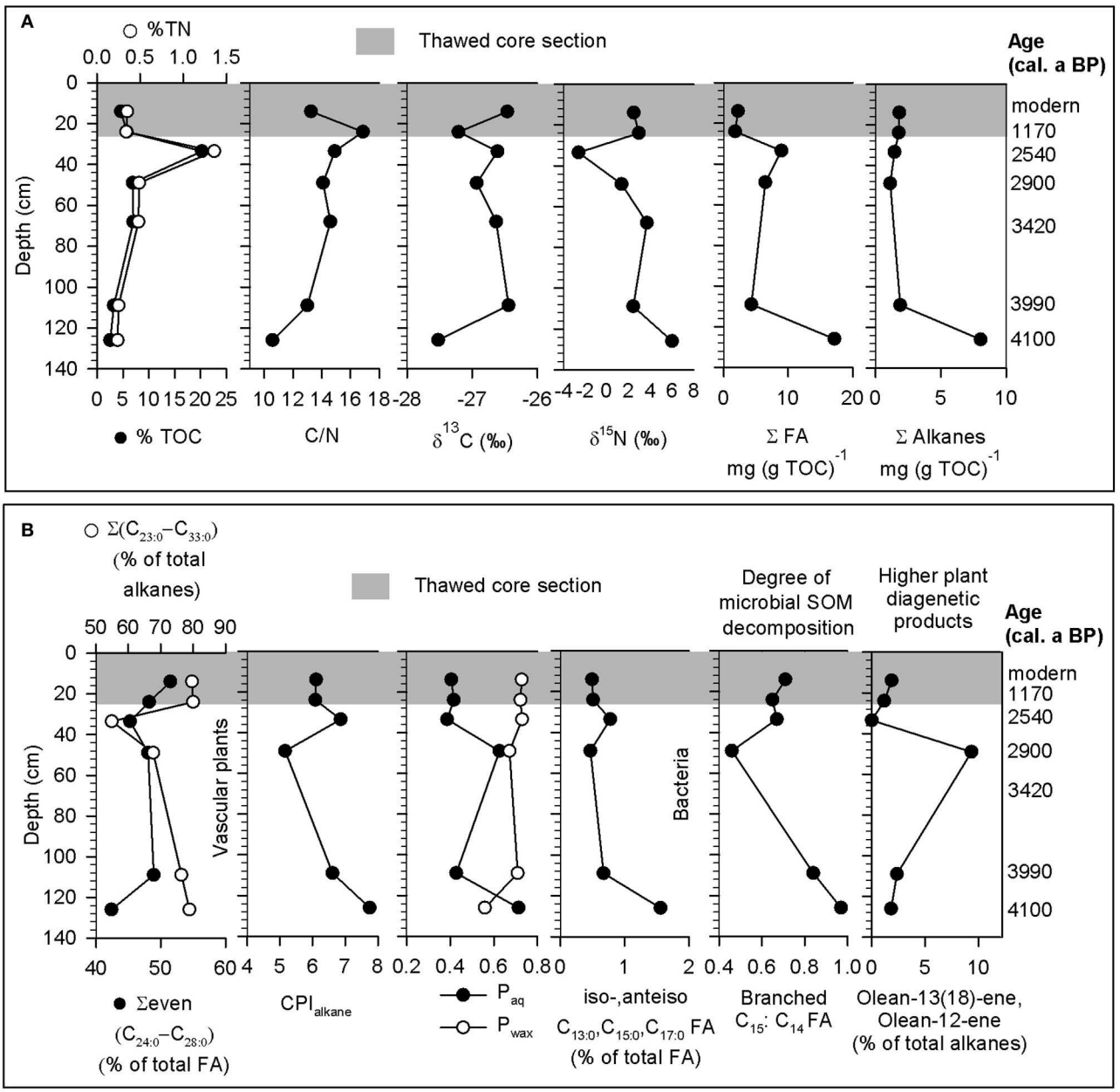

FIGURE 1 | Geochemistry of SOM in the 2 active layer (14 ± 2 and 24 ± 2 cm) and 5 permafrost soil horizons (33.5 ± 2 to 126 ± 2 cm) of core TL08S1C3. (A) Bulk geochemical and stable isotope data and total concentrations of FAs and alkanes. **(B)** Percent contributions and ratios from lipid sub-classes representing different biological sources.

verified by agarose gel electrophoresis. All downstream analyses (cDNA amplification, sequencing, and bioinformatic analyses) described briefly in the following sections followed the protocols developed and reported recently (Orsi et al., 2013, 2015).

Choice of Samples for Subsequent Metatranscriptomic Analysis

The permafrost soil horizons that were selected for cDNA amplification and Illumina sequencing (up to 70-cm-deep) are expected to thaw in the Alaskan Arctic as a result of continuing Arctic warming (Osterkamp, 2007). High quality RNA was extracted from the permafrost table (33.5 ± 2 cm) and from the horizon at 49 ± 2 cm before and after thaw. However, only after thaw the soil interval of 68 ± 2 cm yielded visible amounts of RNA on gel and subsequent cDNA amplification and Illumina sequencing was therefore not performed on the pristine frozen sample at this depth. The selected permafrost table was thought to contain relatively labile OM (Coolen et al., 2011) whereas the two deeper late-Holocene permafrost intervals (at 49 and 68 cm depth) potentially contained more recalcitrant SOM. Unfortunately, for budgetary reasons we were not able to sequence the metranscriptomes from the overlying active

layers. However, parallel analysis of the microbial community composition (ribosomal RNA genes and transcripts) and microbial ectoenzyme activities involved in the hydrolysis of complex soil biopolymers, previously revealed that the most dramatic response in microbial activities and communities occurred in the permafrost intervals after 11 days of thaw while activities and microbial communities underwent little variation in the active layers over the course of incubation (Coolen et al., 2011). For the above reasons, subsequent Illumina sequencing of the reverse transcribed mRNA (this study) was only performed from depth horizons 33.5 ± 2 and 49 ± 2 cm (before and after 11 days of thaw) and 68 ± 2 cm (after 11 days of thaw).

cDNA Amplification and Illumina Sequencing

Since Illumina HiSeq sequencing was not yet available in 2008, the following steps were performed 5 years after frozen storage (−80°) of the purified RNA: Five nanograms of purified high quality RNA as determined fluorometrically with Quant-iT™ RiboGreen® RNA reagent (Life Technologies) was used as template for selective mRNA amplification using the Ovation RNA-Seq v2 System® (NuGEN technologies, San Carlos, CA). We followed the manufacturers instructions for cDNA amplification, and the resulting quantity of cDNA was checked fluorometrically using the Quant-iT™ PicoGreen® dsDNA Assay Kit (Life Technologies). Quality of the amplified cDNA was checked on a Bioanalyzer (Agilent Technologies, Santa Clara, CA) prior to Illumina® sequencing. cDNA of the triplicate extracts were pooled and Illumina® library preparation and paired-end sequencing was performed at the University of Delaware Sequencing and Genotyping Center (Delaware Biotechnology Institute, Newark DE). We acknowledge that because the original RNA extracts were stored ∼5 years at −80°C prior to metatranscriptome construction, it is possible that some RNA could have been lost or partially degraded.

Quality Control and Assembly

Quality control of the dataset was performed using FastQC (http://www.bioinformatics.babraham.ac.uk/projects/fastqc/), with a quality score cutoff of 28. Approximately 375 million paired-end reads that passed quality control were imported into CLC Genomics Workbench 6.0® (CLC Bio Inc., Cambridge, MA) and assembled using the paired-end Illumina assembler. Contigs were assembled over a range of kmer sizes (20, 50, 60, 64) with a minimum contig size cutoff of 300 nucleotides. The kmer size of 50 resulted in the highest number of contigs and thus these contigs were chosen for use in downstream bioinformatics analyses. To reduce the formation of chimeric assemblies, we used a 2 × 105 paired-end sequencing approach on the Illumina HiSeq platform and performed assemblies without scaffolding. Reads were mapped onto the contigs using the read mapping option in CLC Genomics Workbench to retain information on relative abundance of contigs.

Functional Annotation of Contigs

Contigs were submitted to CAMERA (Community Cyber infrastructure for Advanced Microbial Ecology Research and Analysis, http://camera.calit2.net/) and assigned to clusters of orthologous gene (COG) families using the Rapid Analysis of Multiple Metagenomes with a Clustering and Annotation Pipeline (RAMMCAP) (Li, 2009) using the 6 reading frame translation option for open reading frame (ORF) prediction and BLASTn for rRNA identifications. The cutoff criterion *E*-value of 10^{-5} was used for RPS BLAST searches the COG database. For identification of bacterial and archaeal ORFs, the RAMMCAP analyses were performed using the bacterial and archaeal genetic code (-t 11 in advanced options). For identification of fungal ORFs, additional RAMMCAP analyses were performed using the standard genetic code for eukaryotes and the alternative yeast genetic code (−t 1 and −t 12 in advanced options). cDNA contigs were also submitted to MG-RAST (Meyer et al., 2008), and ORFs were detected and annotated according to their standard bioinformatics pipeline. Data have been deposited in in MG-RAST under accession numbers 4517418.3, 4517417.3, 4517416.3, 4517415.3, 4517414.3.

Taxonomic Annotation of Contigs

Contigs were assigned to high-level taxonomic groups (Class level and above) using a Naïve Baysien Classifier (NBC) that compares against a database containing all DNA sequences in NCBI that classified as either Bacteria, Archaea, Fungi, or viral (Rosen and Essinger, 2010). This approach was chosen because NBC has been found to outperform most other composition, similarity, and phylogeny based metagenomic classifiers in terms of sensitivity and precision (Bazinet and Cummings, 2012). Custom perl scripts were used to merge NBC taxonomic identifications of contigs, with COG and Pfam annotations from RPS-BLAST searches together with average coverage (read mapping) from assemblies.

Mapping of Metatranscriptomic Data to *M. barkeri* Methanogenesis Pathways

The bioinformatics pipeline for metatranscriptomic genome recruitment followed that described recently (Orsi et al., 2015). In brief, contigs from frozen and thawed metatranscriptomes were searched for homology in the genome of *M. barkeri* via BLASTx (e^{-5}, >60 amino acid identity) searches using the translated amino acid sequences of *M. barkeri* genes as a reference. Expressed genes with homology *M. barkeri* proteins were subjected to metabolic pathway mapping in KEGG (http://www.genome.jp/kegg/pathway.html). Expressed genes with homology to the *M. barkeri* genome involved in methanogenesis pathways were visualized using Adobe Illustrator (Adobe Systems Inc., San Jose, CA).

Analysis of Gene Overexpression in Frozen vs. Thawed Soil Samples

Analyses of gene overexpression in frozen vs. thawed samples was performed using the R statistical package (http://www.r-project.org/), with the MG-RAST matR library (metagenomics.anl.gov). To maintain abundance information, assembled contig sequences from each sample were uploaded to MG RAST with the read mapping abundance added to the fasta headers as specified on the MG RAST website. Differences in

overexpression between frozen and thawed permafrost samples were determined by a One-Way ANOVA test with a *P*-value cutoff of 0.025. The relatively low number of rRNA reads that were present in the dataset despite the selective amplification of mRNA using the Ovation RNA-Seq v2 System® were removed prior to comparison. Data were normalized in MG RAST with a log-based transformation [$Y_{s,i} = \log_2 (X_{s,i} + 1)$], where $X_{s,i}$ represents an abundance measure (*i*) in sample (*s*). Log transformed counts from each sample were then standardized (data centering) according to the equation [$Z_{s,i} = (Y_{s,i} - Y_s)/\sigma_s$)], where $Z_{s,i}$ is the standardized abundance of an individual measure $Y_{s,i}$ (log transformed from previous equation). From each log transformed measure of (*i*) in sample (*s*), the mean of all transformed values (Y_s) is subtracted and the difference is divided by the standard deviation (σ_s) of all log-transformed values for the given sample. After log transformation and standardization, the values for the functional categories within each sample were scaled from 0 (minimum value of all samples) to 1 (maximum value of all samples), which is a uniform scaling that does not affect the relative differences of values within or between samples. The top 100 processes which differed most substantially in the level of gene expression between frozen and thawed samples and which passed the One-Way ANOVA test were used as input for heatmap presentation, hypothetical proteins and proteins of unknown function were removed from the list of top 100 processes after creating the heatmap.

Results and Discussion

Composition of Permafrost SOM

SOM composition, as indicated by bulk metrics (TOC, TN, $\delta^{13}C$, $\delta^{15}N$) and lipid biomarkers (fatty acids [FAs] and alkanes), reflected mainly higher plant sources (**Figure 1**). %TOC and %TN were fairly constant throughout the soil core, with maximum values at 33.5 cm depth (**Figure 1A**). Elevated %TOC at 33.5 cm suggests that this horizon represents the permafrost table, assuming that cryoturbation under the tussock tundra and dwarf shrub vegetation has caused frost-churning of organic matter into the underlying mineral soil horizons, which then concentrated in the upper permafrost (Ping et al., 1997). Bulk soil $\delta^{13}C$ signatures ranged from −26 to −27‰, reflecting inputs from C_3 plants (**Figure 1A**). Soil $\delta^{15}N$ was most enriched in the deepest horizon (**Figure 1A**), which could be indicative of several processes including preferential mineralization and plant uptake of isotopically light nitrogen compounds, microbial production of ^{15}N enriched compounds during decomposition, and contributions from mycorrhizal fungi (Hogberg, 1997; Hobbie and Hobbie, 2008). The permafrost table was most depleted in $\delta^{15}N$, suggesting a lower degree of decomposition of plant organic matter than in the deeper soil horizons (Andersson et al., 2012). Concentrations of total alkanes and FAs were generally highest in the deepest soil horizon and lower at shallower depths. Long chain FAs [even Σ ($C_{24:0}$-$C_{28:0}$)] (Killops and Killops, 2005) and alkanes [Σ ($C_{22:0}$-$C_{33:0}$)] (Yunker et al., 1995) characteristic of vascular plants were important constituents of the total FA and alkane pools, accounting for 42–51 and 56–82%, respectively (**Figure 1B**). The CPI_{alkane} was >5, ranging from 5.17 at 49 cm to 7.75 at 126 cm, indicating that inputs from higher plants were important. The P_{wax} and P_{aq} indices suggested that contributions from higher plants were high while inputs from aquatic macrophytes were low at all depths except for 49 and 126 cm. In combination, the FAs and n-alkanes suggested that higher plants were the main source of SOM and likely deposited under drier conditions. However, aquatic macrophytes and mosses may have been important sources of SOM 2900 and 4100 calendar years before the present (cal. a BP) (**Figure 1B**) and conditions may have been wetter during those periods.

Lipid biomarkers reflecting bacterial inputs and processes indicated microbial decomposition occurred throughout the core. Contributions from bacterial FAs [iso-, anteiso- odd Σ ($C_{13:0}$-$C_{17:0}$)] (Meyers, 2003) were similar across depth horizons but were greatest at 126 cm (**Figure 1B**). Microbial decomposition of SOM occurred in all of the soil horizons, as indicated by the presence of Olean-13(18)-ene and Olean-12-ene, which are diagenetic products of higher plants (Yunker et al., 1995), and the ratio of branched C_{15}:C_{14} FAs (Lu and Meyers, 2009) (**Figure 1B**). Since iso- and anteiso-C_{15} compounds are produced by bacteria from straight chain C_{14} precursors, an increase in the ratio of branched C_{15}: straight chain C_{14} compounds may reflect organic matter decomposition (Lu and Meyers, 2009). Thus, SOM decomposition may be most extensive in the deepest soil horizon where branched C_{15}:C_{14}, contributions from bacterial FAs, and concentrations of total FAs and alkanes were the highest.

Overall, these results indicate that SOM was largely derived from vascular plants and microbial decomposition occurred throughout the soil column. Microbial breakdown of SOM may have occurred during deposition or after the soils were frozen, but we cannot distinguish between these possibilities based on the lipid biomarker results.

Overview of the Metatranscriptomic Datasets

An average of 29,022 contigs (SD = 8951) with an average length of 616 (*SD* = 52) were assembled *de-novo* from each Illumina-sequenced metatranscriptome, with 87% (*SD* = 3%) of original reads mapping to contigs per sample (Supplementary Table S1). Open reading frames (ORFs) on contigs were assigned to COG (Cluster of Orthologous Genes) functional classes and high-level taxonomic groups (Class level and above). Transcribed ORFs with homology to proteins representing 22 out of the 25 defined Clusters of Orthologous Genes (Tatusov et al., 1997) were detected in metatranscriptomes from both frozen and thawed permafrost. Similar to a previous study utilizing the same cDNA amplification and sequence classification procedures (Orsi et al., 2013), the majority of reads could be annotated (86 ± 6%) in each sample, with the majority (79 ± 7%) of annotated reads coding for proteins and a minimal representation (7 ± 2%) of ribosomal RNA reads (Supplementary Table S1).

Overexpressed Genes under Frozen Conditions

Amino acid transport and metabolism, energy production, and DNA repair, replication and recombination were amongst the

most relatively abundant COG categories expressed in the frozen permafrost (**Figure 2A**). The expression of genes corresponding to most major COG families in frozen permafrost suggests the *in situ* activity of microbes, even at subfreezing temperatures. The variability in relative abundances of COGs was markedly less in metatranscriptomes from frozen samples, compared to the metatranscriptomes from thawed permafrost (**Figure 2A**) Phylogenetic binning indicates that Proteobacteria (γ, β, α, and δ), Firmicutes, Acidobacteria, and Actinobacteria, as well as Euryarchaeota and ascomycetous Fungi were the most transcriptionally active microbial groups under frozen conditions in the permafrost table (**Figure 2B**). These taxa are frequently reported from Arctic soils (Jansson and Tas, 2014 and references therein).

Several transcripts encoding proteins involved in biofilm formation, virulence, and horizontal gene transfer had relatively higher expression levels under frozen conditions (**Figure 3**). Notably, expression of genes coding for pilus assembly proteins (COGs 2064, 1706, 4964, 3166) may indicate biofilm formation, which is a common feature among bacteria living under stressful conditions and causes a close interaction between cells that can promote virulence, bacterial signaling, and/or horizontal gene transfer (Varga et al., 2008). Biofilm formation in the frozen soils may be related to the small area available for growth in the permafrost microhabitat where the current consensus is that microbes inhabit very thin liquid brine veins surrounding frozen soil particles (Gilichinsky et al., 2003, 2005; Shcherbakova et al., 2005; Onstott et al., 2009; Pecheritsyna et al., 2012). Active defense against viral infection is indicated by the activity of a Type II restriction-modification system (i.e., site-specific DNA methylase COG0338; **Figure 3**), which can protect bacteria and archaea against invading foreign DNA (Pingoud et al., 2005). However, virulence-associated genes were also overexpressed in thawed soils, suggesting active viral defenses during both frozen and thawed conditions. Enzymes involved in DNA repair were also overexpressed in frozen soils (**Figure 3**). Uracil-DNA glycolases are involved in base excision repair, a process that removes damaged bases that could otherwise lead to mutations (Kim and Wilson, 2012). Recently, an ionization radiation (IR) experiment with a frozen culture of *Psychrobacter arcticus* suggested that, in the presence of long-term natural background IR, permafrost bacteria can repair double stranded DNA breaks in the absence of net growth (Dieser et al., 2013). Our results support this observation, and suggest that *in situ*, uracil-DNA glycolases play an important role in DNA repair incurred from long-term exposure to natural background IR sources in the permafrost environment. Compared to thawed soils, a gene sequence encoding a *Rec*A-mediated autopeptidase was relatively more abundant in the permafrost sequence datasets further suggesting that bacterial "Save Our Ship" (SOS)-response occurs in the frozen soils (**Figure 3**). SOS-response is a global response to DNA damage in which the cell cycle is arrested and DNA repair is induced (Michel, 2005). Such DNA repair and stress response mechanisms likely allow microbes to survive over geological timescales in permafrost until favorable conditions for growth are experienced, such as thawed conditions resulting from increasing atmospheric temperatures.

Overall Transcriptional Activity Stimulated Under Thawed Conditions

Compared to the frozen samples, all three thawed permafrost intervals exhibit relatively increased representation of transcripts involved in translation, ribosomal structure, and biogenesis, indicating a general increase in microbial activity and growth (**Figure 2A**). In thawed samples from the permafrost table, metatranscriptomes had an increased proportion of transcripts involved in coenzyme transport and metabolism compared to metatranscriptomes from frozen permafrost table samples (**Figure 2A**). The majority of transcripts falling into this functional category in permafrost table metatranscriptomes were assigned to Euryarchaeota (**Figure 2B**).

Overall, there was increased representation of Firmicutes, Bacteroidetes, Euryarchaeota, and ascomycetous Fungi in metatranscriptomes from thawed samples relative to Proteobacteria, Acidobacteria, and Actinobacteria (**Figure 2B**). The thawed permafrost table at 33.5 cm showed the largest relative increase in fungal-derived transcripts, compared to the frozen sample from this horizon. The thawed horizon at 49 cm, revealed the largest relative increase in transcripts assigned to Firmicutes compared to frozen permafrost at this depth, and a similar proportion of transcripts were assigned Firmicutes in thawed samples from 68 cm (**Figure 2B**). This may be due to the germination of spores in permafrost soils after thawed conditions (Steven et al., 2008; Niederberger et al., 2009). Transcripts assigned to Chloroflexi and Crenarchaeota involved in translation, ribosomal structure and biogenesis at 49 cm increased in relative abundance in metatranscriptomes from thawed samples (**Figure 2B**). Similar proportions of transcripts were assigned to Chloroflexi and Crenarchaeota in metatranscriptomes from thawed permafrost at 68 cm. Transcriptional activity of these phyla mainly increased in the deeper thawed soils, suggesting that they may be specialized in the initial decomposition of more complex, ancient SOM.

Relative to the frozen samples, thawed metatranscriptomes exhibit an upregulation of genes coding for enzymes involved in extracellular protein degradation (notably Aminopeptidase C) (**Figure 3**). This suggests microbial utilization of labile proteins as a source of N and C during thawed conditions. Thawed metatranscriptomes also had a relative increase in transcripts encoding proteins involved in uptake, transport, and degradation of carbohydrates (e.g., ABC type sugar transporter, a predicted sugar isomerase, 6-phosphogluconate dehydrogenase, fructose 1,7 biphosphatase, and a pyruvate formate lyase-activating enzyme) (**Figure 3**). Upon thawed conditions, some of the microbial metabolism appears to be anaerobic, as evidenced by the relative increased expression of the pyruvate-formate lyase-activating enzyme (**Figure 3**), which catalyzes the anaerobic conversion of pyruvate and coenzyme A into acetyl CoA and formate (Jiang et al., 2001).

Transcriptional Evidence for Enzymatic Decomposition of Complex Soil Biopolymers under Thawed Conditions

Genes encoding for all major classes of hydrolases involved in the cleavage of complex biopolymers into C1 and C2 substrates

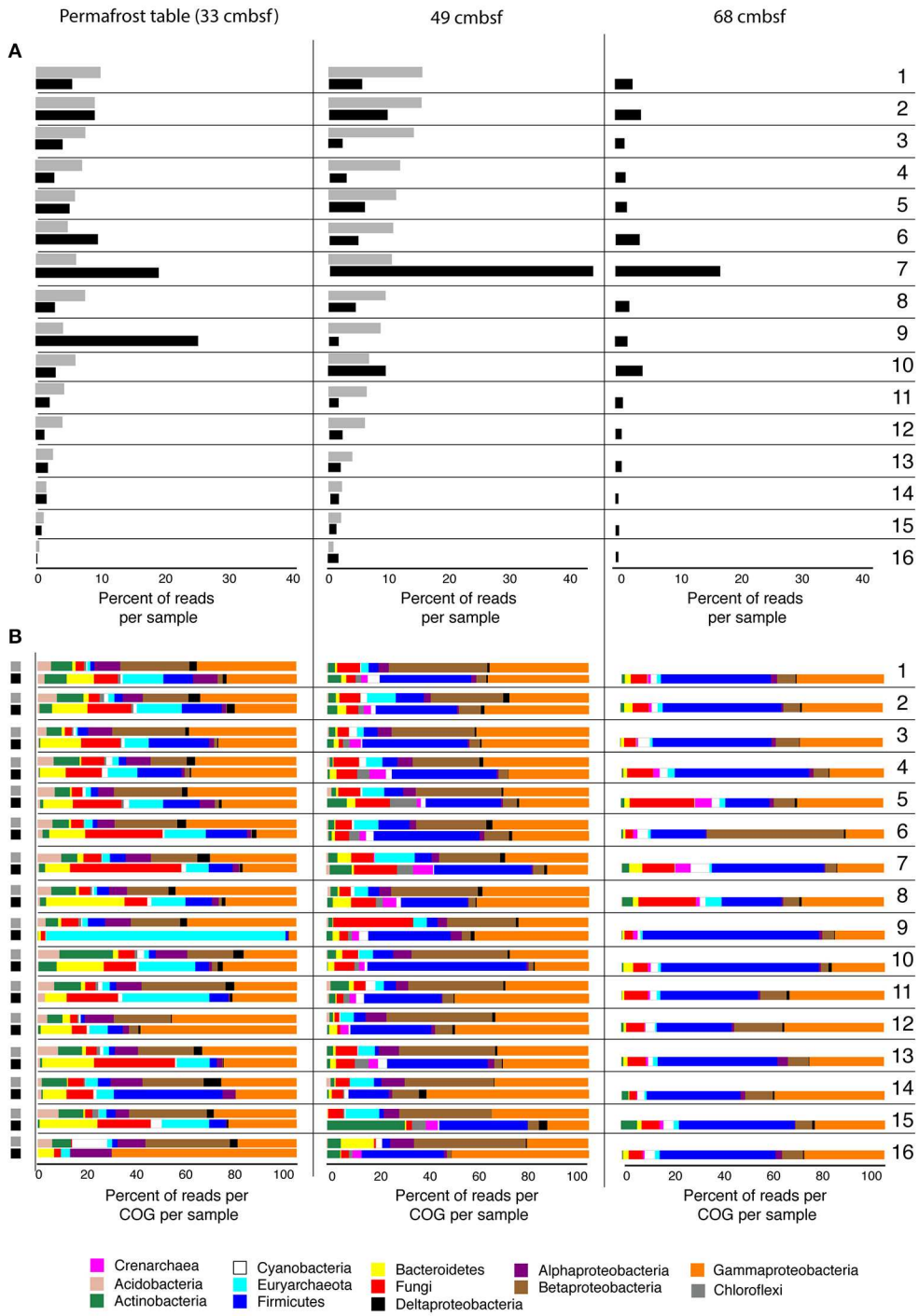

FIGURE 2 | (A) Relative abundance of reads assigned to COGs in metatranscriptomes from frozen (gray bars) permafrost soils of core TL08S1C3 at 33.5 ± 2 cm (permafrost table) and 49 ± 2 cm depth and at 33.5 ± 2, 49 ± 2, and 68 ± 2 cm after 11 days of incubation at 4°C (black bars). Only the 16 most (relative) abundant COGs are shown (excluding [R] General function prediction and [S] Function unknown). COGs detected in low abundance, but not shown, are [A] RNA processing and modification; [V] Defense mechanisms; [Z] Cytoskeleton. **(B)** The prokaryotic and fungal ORFs as percent of reads per COG per sample with homology to the following COG families: **1,** Amino acid transport and metabolism; **2,** Energy production and conversion; **3,** Inorganic ion transport and metabolism; **4,** Replication, recombination and repair; **5,** Transcription; **6,** Posttranslational modification, protein turnover, chaperones; **7,** Translation, ribosomal structure and biogenesis; **8,** Cell wall/membrane/envelope biogenesis; **9,** Coenzyme transport and metabolism; **10,** Carbohydrate transport and metabolism; **11,** Signal transduction mechanisms; **12,** Lipid transport and metabolism; **13,** Nucleotide transport and metabolism; **14,** Intracellular trafficking, secretion, and vesicular transport; **15,** Cell cycle control, cell division, chromosome partitioning; **16,** Cell motility.

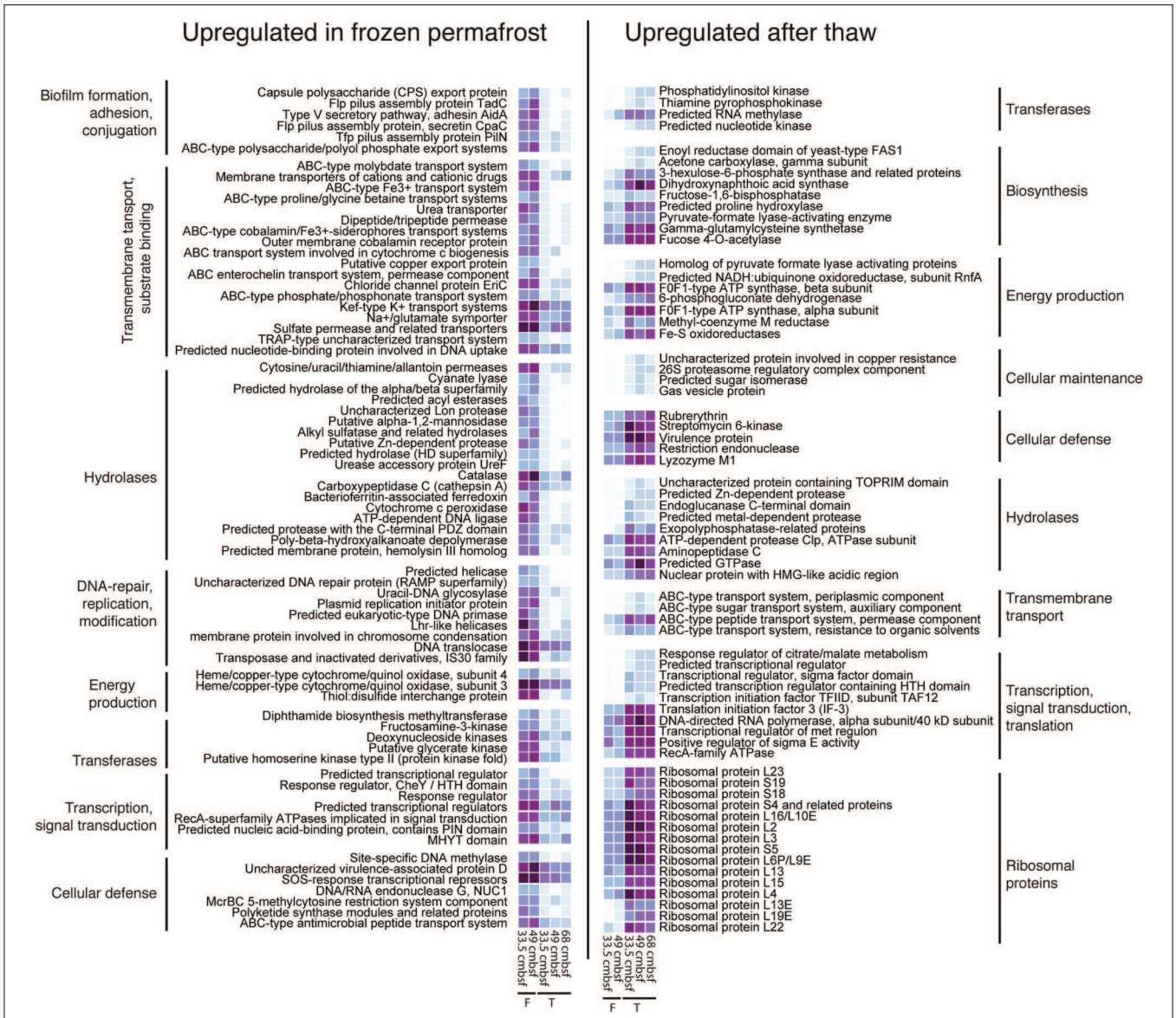

FIGURE 3 | Heatmap showing the most abundant overexpressed genes in frozen and thawed permafrost soils. Shown is the distribution of normalized reads mapping to contigs with homologous ORFs (>60% amino acid identity) to proteins in the COG database. The distribution of functional categories and the colors correspond to log transformed read abundance (dark purple is more, light blue is less).

were expressed in both frozen and thawed soils (**Figure 4A**). The relative distribution of hydrolase-encoding transcripts at the shallowest interval (permafrost table), revealed a relative increase in peptidase encoding transcripts in thawed samples (**Figure 4A**). This difference was not observed for the deeper permafrost sample (49 cm), and may indicate increased bioavailability of peptides at 33.5 cm after thaw. Most of this relative increase in peptidase encoding transcripts at 33.5 cm could be attributed to the activity of euryarchaea and bacteroidetes (**Figure 4A**). This confirms our earlier findings based on detectable activities of leucine aminopeptidase at this depth interval, indicating that the permafrost table contains relatively labile polypeptides or proteins as source of C and N (Coolen et al., 2011).

The diversity of taxa expressing hydrolase encoding transcripts in the deeper permafrost decreased markedly relative to 33.5 cm, with Firmicutes-derived hydrolase encoding transcripts increasing in relative representation after thaw (**Figure 4A**). A similar response was observed for crenarchaeal transcripts encoding glycosylases and peptidases, which were only observed in the two deepest thawed permafrost intervals (**Figure 4A**). Despite the overall increase in activity of Chloroflexi in the thawed soil interval at 49 cm (**Figure 2B**), transcripts homologous to Chloroflexi–derived hydrolases acting on complex soil biopolymers were not observed early after thaw (**Figure 4A**). Their role in the cycling of organic matter in permafrost soils requires further investigation.

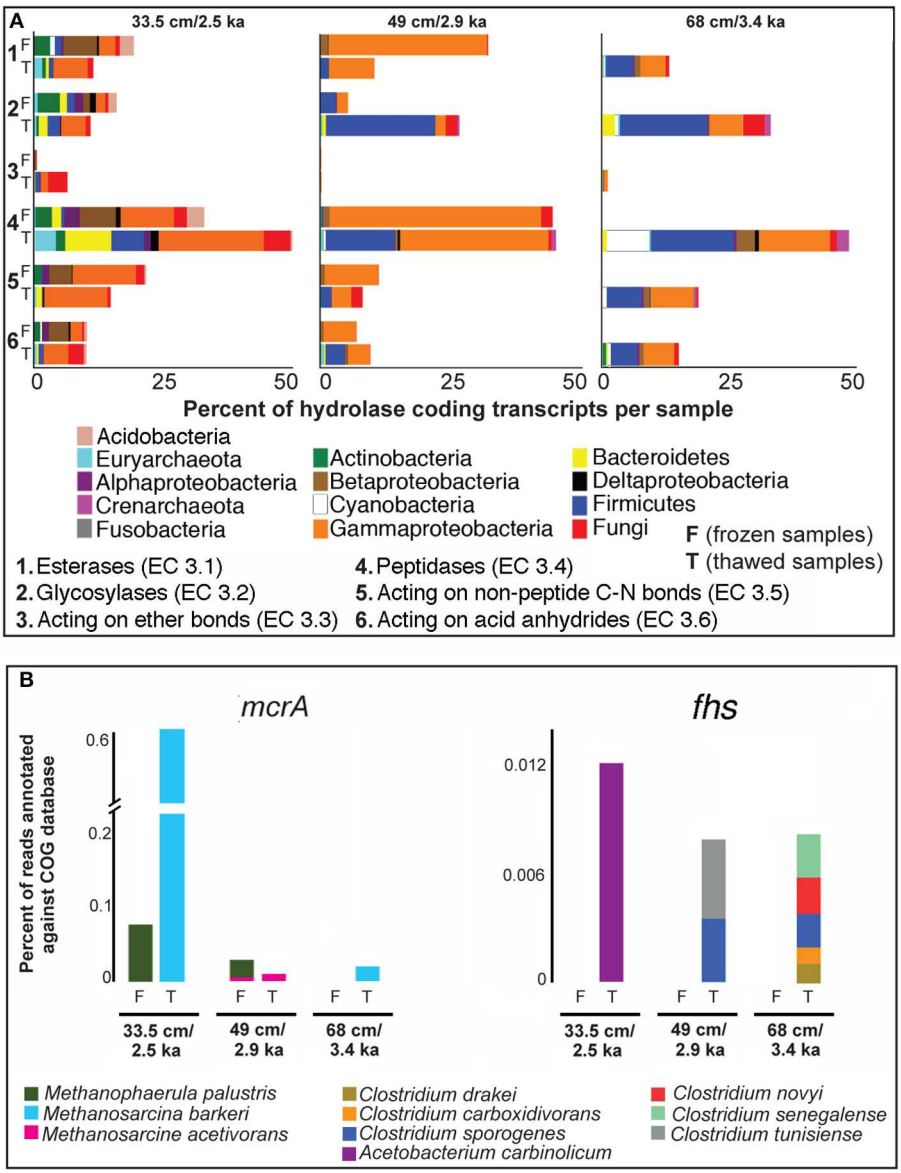

FIGURE 4 | Expressed homologs, (relative abundance) encoding (A) hydrolases potentially involved in the initial breakdown of of complex permafrost soil biopolymers, and (B) formyltetrahydrofolate synthetase (*fhs*) and methyl-coenzyme reductase A (*mcrA*) before and after 11 days of thaw. Note the predominance of concomitant *mcr*A (methanogenesis) and *fhs* (acetogenesis) expression in thawed samples relative to frozen samples.

Upon thawed conditions in the permafrost table, relative expression of fungal, γ-Proteobacterial, and Firmicutes genes encoding hydrolases acting on recalcitrant ether bonds increased (**Figure 4A**). Ether bonds occur in the tetraether membranes of yet unidentified soil bacteria (i.e., branched Glycerol Dialkyls Glycerol Tetraethers [branched GDGTs]), commonly found in peat soils (Weijers et al., 2007), as well as in isoprenoid GDGTs of (methanogenic) archaea (Schouten et al., 2000). The increased transcription of genes encoding hydrolases acting on ether bonds in the permafrost table upon thaw suggests that some permafrost microbiota at 33.5 cm decompose dead bacterial and/or archaeal biomass. Collectively these data suggest that thawed conditions stimulate growth and turnover of archaeal and bacterial biomass in soil permafrost.

Relative expression of genes with homology to cyanobacterial peptidases and hydrolases acting on non-peptide C-N bonds and anhydrides was highest in the deepest analyzed thawed permafrost interval (**Figure 4A**). The activity in permafrost soils in the absence of light seems counter-intuitive. However, oligopeptides and or amino acids may serve as nitrogen sources for cyanobacteria in permafrost soils, as they have been reported to assimilate organic compounds for biosynthesis during the dark

phase of their life cycle (Vernotte et al., 1992). Lay et al. (2013) reported the presence of cyanobacterial genes involved in the reduction of nitrate to ammonia in high-Arctic saline subzero spring sediments, and they suggested that this strategy might be advantageous for maintaining activity during the long-term darkness of the Arctic winter. Our results suggest that cyanobacteria may be dormant in the deeper permafrost soils for substantial periods of time and can regain activity under dark conditions within days after thaw.

Active Metabolic Pathways for Methanogenesis and Acetogenesis Stimulated under Thawed Conditions

Metatranscriptomes from thawed permafrost exhibited a marked relative increase in transcripts involved in coenzyme transport and metabolism (**Figure 2A**). In the permafrost table, metatranscriptomes in this category were mainly assigned to Euryarchaeota (**Figure 2B**). The most predominant transcript in this category was methyl coenzyme M reductase subunit A (*mcr*A), which catalyzes the last step in methanogenesis and is present in all methanogens (Ferry, 1999). More specifically, the *mcr*A transcripts in the thawed permafrost table were assigned to the versatile methanogen *Methanosarcina barkeri,* capable of using a variety of C_1 and C_2 compounds including acetate (Weimer and Zeikus, 1979; Jetten et al., 1992). The identification of *M. barkeri* as the main producer of *mcr*A transcripts is plausible since acetate concentrations in permafrost samples can be 50 times higher (Strauss et al., 2012) than the minimum acetate requirement (~200 μM) of *Methanosarcina* spp. (Jetten et al., 1992). Expression of methano phenazine-reducing hydrogenase (*mph*), which is indicative of heterotrophic methanogenic metabolism, was also detected after thaw, suggesting C1 and C2 substrates as sources of biogenic methane. Further metabolic mapping of expressed genes to the *M. barkeri* genome indicated an increase in active biochemical pathways utilizing acetate, trimethylamine, and methanol as methanogenic substrates (**Figure 5**). Expression of genes coding for formylmethanofuran-tetrahydromethanopterin N-formyltransferase (*ftr*) (a protein necessary completing the pathway from methanogenesis from CO_2), was not detected, suggesting a predominance of heterotrophic methanogenesis after thaw. A marked increase in acetoclastic methanogensis was recently also reported from thawed permafrost soils in northern Sweden (McCalley et al., 2014). In addition, recent biogeochemical examination of peat and dissolved organic matter (DOM) at northern Sweden permafrost sites that had been exposed to thaw for up to 40 years revealed a shift in CH_4 production pathway from CO_2-reduction to acetate cleavage, which was associated with (i) increased humification rates, (ii) DOM shifted

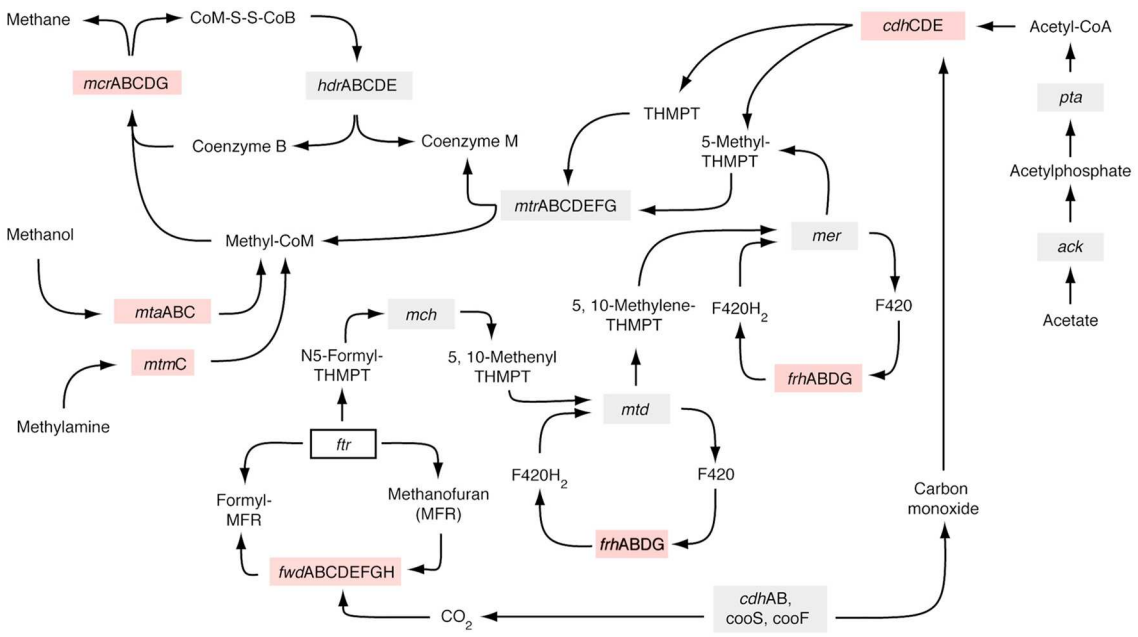

FIGURE 5 | Metabolic pathways actively expressed by the methanogen *Methanosarcina barkeri* in metatranscriptomes from frozen and thawed permafrost samples. The *M. barkeri* genome was chosen as a reference because it was found to be the dominant methanogen expressing *mcr*A after thaw (**Figure 4B**). Red boxes represent expressed genes that were only detected after thaw, gray boxes represent genes expressed before and after thaw, and clear boxes are genes that were not detected under any conditions. **CoM-S-S-CoB**, Coenzyme M 7-mercaptoheptanoylthreonine-phosphate heterodisulfide; **THMPT**, Tetrahydromethanopterin; **hcr**, Heterodisulfide reductase subunit A; **mcr**, Methyl-coenzyme reductase; **mtr**, Tetrahydromethanopterin S-methyltransferase; **CoM,** Coenzyme M; **mtm**, Monomethylamine corrinoid protein; **mta** Methanol-specific corrinoid protein; **cdh**; Acetyl-CoA decarbonylase/synthase complex; **frh**, Coenzyme F420 hydrogenase; **mer**, 5,10-methylenetetrahydromethanopterin reductase; **mch**, Methenyltetrahydromethanopterin cyclohydrolase; **mtd**, Methylenetetrahydromethanopterin dehydrogenase; **fwd**, Formylmethanofuran dehydrogenase; **pta**, Phosphate acetyltransferase; **ack**, Acetate kinase; **cooS/F**, Carbon monoxide dehydrogenase.

toward lower molecular weight compounds with lower aromaticity, (iii) lower organic oxygen content, and (iv) more abundant microbially produced compounds (Hodgkins et al., 2014).

In all thawed permafrost samples, an increase in *mcr*A expression was accompanied by an increase in expression of formyltetrahydrofolate synthetase (*fhs*) genes (not detected in frozen permafrost), which can serve as a proxy for acetogenesis (Lever, 2013) (**Figure 4B**). Transcripts encoding *fhs* in the upper permafrost were assigned predominantly to *Acetobacterium carbinolicum*, whereas various *Clostridium* species are likely involved in acetate production in deeper permafrost (**Figure 4B**). The genetic expression of the acetate-utilizing methanogenesis pathway (**Figure 5**) after thaw suggests that some of this acetate is then utilized as a substrate by methanogens, predominantly *M. barkeri* (**Figure 4B**). Acetogenic fermentation, which is also likely under anaerobic conditions in thawed permafrost, could be another source of acetate for acetoclastic methanogens. Bacterial genes encoding the two enzymes diagnostic for fermentative conversion of acetyl-CoA to acetate (acetate kinase, EC:2.7.2.1 and phosphotransacetylase EC:2.3.1.8) were not detected in thawed permafrost, suggesting that pyruvate fermentation to acetate may not be a dominant source of acetate, relative to homoacetogenesis. However, to substantiate the claim of homoacetogenesis dominating over fermentation as a source of acetate in thawing permafrost soils, it is necessary to perform radiotracer incubations or to analyze the stable isotopic composition of acetate in these soils (Rivkina et al., 2000; Bakermans and Skidmore, 2011).

Concluding Remarks

Our pilot study shows that the analysis of metatranscriptomes is a sensitive approach capable of identifying a wide spectrum of important metabolic processes in frozen and thawed permafrost. In general, the transcriptional profile under frozen conditions suggests a dominance of stress responses, survival strategies, and maintenance processes whereas upon thaw a rapid enzymatic response to decomposing SOM was observed. Furthermore, our analysis indicates that acetoclastic methanogenesis may be a dominant form of methanogenesis in thawing permafrost soils fueled, in part, by acetate production from acetogenic bacteria. Due to large heterogeneity in permafrost SOM and microbial composition, future metatranscriptome studies should be performed from a wider variety of permafrost soil types and locations, and in comparison with the active layer. Future studies comparing metatranscriptomes from thawing permafrost should also contain biological replicates to provide robust statistical power for hypothesis testing. Furthermore, paired geochemical analysis of isotopically labeled substrates and metabolites during thaw incubation experiments as well as the analysis of the stable isotopic composition and concentration of dissolved methane should be performed to validate mRNA-based inferences of metabolic pathways. Measurements of soil pH would further be useful to contextualize microbial responses to permafrost thaw at the transcriptional level. Metatranscriptomics is shown here to be a useful approach for inferring the activity of permafrost microbes, that has potential to improve our understanding of permafrost SOM bioavailability and biogeochemical mechanisms contributing to greenhouse gas emissions as a result of warming induced permafrost thaw.

Acknowledgments

We thank Dr. Amanda Spivak (WHOI) for the analysis of the permafrost organic matter composition and the interpretation of the lipid data as well as Dr. Cornelia Wuchter (WHOI) for helpful general discussions. This work was fostered by grants from WHOI's Arctic Research Initiative to MJLC and AS, as well as a Center for Dark Energy Biosphere Investigations (CDEBI) grant OCE-0939564 to WDO. This is C-DEBI Contribution 258.

Supplementary Material

The Supplementary Material for this article can be found online at: http://www.frontiersin.org/journal/10.3389/fmicb.2015.00197/abstract

References

Andersson, R. A., Meyers, P., Hornibrook, E., Kuhry, P., and Morth, C. M. (2012). Elemental and isotopic carbon and nitrogen records of organic matter accumulation in a Holocene permafrost peat sequence in the East European Russian Arctic. *J. Q. Sci.* 27, 545–552. doi: 10.1002/jqs.2541

Anisimov, O. A., Nelson, F. E., and Pavlov, A. V. (1999). Predicitive scenarios of permafrost development under conditions of global change in the XXI century. *Earth Cryol.* 3, 15–25.

Ayala-Del-Rio, H. L., Chain, P. S., Grzymski, J. J., Ponder, M. A., Ivanova, N., Bergholz, P. W., et al. (2010). The genome sequence of *Psychrobacter arcticus* 273-4, a psychroactive Siberian permafrost bacterium, reveals mechanisms for adaptation to low-temperature growth. *Appl. Environ. Microbiol.* 76, 2304–2312. doi: 10.1128/AEM.02101-09

Bakermans, C., and Skidmore, M. L. (2011). Microbial Metabolism in Ice and Brine at −5°C. *Environ. Microbiol.* 13, 2269–2278. doi: 10.1111/j.1462-2920.2011.02485.x

Bakermans, C., Skidmore, M. L., Douglas, S., and McKay, C. P. (2014). Molecular characterization of bacteria from permafrost of the Taylor Valley, Antarctica. *Fems Microbiol. Ecol.* 89, 331–346. doi: 10.1111/1574-6941.12310

Bazinet, A. L., and Cummings, M. P. (2012). A comparative evaluation of sequence classification programs. *BMC Bioinformatics* 13:92. doi: 10.1186/1471-2105-13-92

Bellemain, E., Davey, M. L., Kauserud, H., Epp, L. S., Boessenkool, S., Coissac, E., et al. (2013). Fungal palaeodiversity revealed using high-throughput metabarcoding of ancient DNA from arctic permafrost. *Environ. Microbiol.* 15, 1176–1189. doi: 10.1111/1462-2920.12020

Coolen, M. J. L., Van De Giessen, J., Zhu, E. Y., and Wuchter, C. (2011). Bioavailability of soil organic matter and microbial community dynamics upon permafrost thaw. *Environ. Microbiol.* 13, 2299–2314. doi: 10.1111/j.1462-2920.2011.02489.x

Cranwell, P. A., Eglinton, G., and Robinson, N. (1987). Lipids of aquatic organisms as potential contributors to lacustrine sediments.2. *Organ. Geochem.* 11, 513–527. doi: 10.1016/0146-6380(87)90007-6

Dieser, M., Battista, J. R., and Christner, B. C. (2013). DNA double-strand break repair at −15°C. *Appl. Environ. Microbiol.* 79, 7662–7668. doi: 10.1128/AEM.02845-13

Dutta, K., Schuur, E. A. G., Neff, J. C., and Zimov, S. A. (2006). Potential carbon release from permafrost soils of Northeastern Siberia. *Glob. Change Biol.* 12, 2336–2351. doi: 10.1111/j.1365-2486.2006.01259.x

Ferry, J. G. (1999). Enzymology of one-carbon metabolism in methanogenic pathways. *Fems Microbiol. Rev.* 23, 13–38. doi: 10.1111/j.1574-6976.1999.tb00390.x

Ficken, K. J., Li, B., Swain, D. L., and Eglinton, G. (2000). An n-alkane proxy for the sedimentary input of submerged/floating freshwater aquatic macrophytes. *Organ. Geochem.* 31, 745–749. doi: 10.1016/S0146-6380(00)00081-4

Frank-Fahle, B. A., Yergeau, E., Greer, C. W., Lantuit, H., and Wagner, D. (2014). Microbial functional potential and community composition in permafrost-affected soils of the NW canadian arctic. *PLoS ONE* 9:e84761. doi: 10.1371/journal.pone.0084761

Ganzert, L., Bajerski, F., and Wagner, D. (2014). Bacterial community composition and diversity of five different permafrost-affected soils of Northeast Greenland. *Fems Microbiol. Ecol.* 89, 426–441. doi: 10.1111/1574-6941.12352

Gilichinsky, D., Rivkina, E., Bakermans, C., Shcherbakova, V., Petrovskaya, L., Ozerskaya, S., et al. (2005). Biodiversity of cryopegs in permafrost. *FEMS Microbiol. Ecol.* 53, 117–128. doi: 10.1016/j.femsec.2005.02.003

Gilichinsky, D., Rivkina, E., Shcherbakova, V., Laurinavichuis, K., and Tiedje, J. (2003). Supercooled water brines within permafrost - An unknown ecological niche for microorganisms: a model for astrobiology. *Astrobiology* 3, 331–341. doi: 10.1089/153110703769016424

Hobbie, E. A., and Hobbie, J. E. (2008). Natural abundance of (15)N in nitrogen-limited forests and tundra can estimate nitrogen cycling through mycorrhizal fungi: a review. *Ecosystems* 11, 815–830. doi: 10.1007/s10021-008-9159-7

Hobbie, S. E., and Gough, L. (2004). Litter decomposition in moist acidic and non-acidic tundra with different glacial histories. *Oecologia* 140, 113–124. doi: 10.1007/s00442-004-1556-9

Hodgkins, S. B., Tfaily, M. M., McCalley, C. K., Logan, T. A., Crill, P. M., Saleska, S. R., et al. (2014). Changes in peat chemistry associated with permafrost thaw increase greenhouse gas production. *Proc. Natl. Acad. Sci. U.S.A.* 111, 5819–5824. doi: 10.1073/pnas.1314641111

Hogberg, P. (1997). Tansley review No 95. 15N natural abundance in soil-plant systems. *New Phytol.* 137, 179–203. doi: 10.1046/j.1469-8137.1997.00808.x

Huang, Q. Y., Briggs, B. R., Dong, H. L., Jiang, H. C., Wu, G., Edwardson, C., et al. (2014). Taxonomic and functional diversity provides insight into microbial pathways and stress responses in the saline Qinghai Lake, China. *PLoS ONE* 9:e116444. doi: 10.1371/journal.pone.0111681

Jansson, J. K., and Tas, N. (2014). The microbial ecology of permafrost. *Nat. Rev. Microbiol.* 12, 414–425. doi: 10.1038/nrmicro3262

Jetten, M. S. M., Stams, A. J. M., and Zehnder, A. J. B. (1992). Methanogenesis from acetate - a comparison of the acetate metabolism in *Methanothrix soehngenii* and *Methanosarcina* spp. *Fems Microbiol. Lett.* 88, 181–197. doi: 10.1111/j.1574-6968.1992.tb04987.x

Jiang, G. R. J., Nikolova, S., and Clark, D. P. (2001). Regulation of the ldhA gene, encoding the fermentative lactate dehydrogenase of *Escherichia coli*. *Microbiology* 147, 2437–2446.

Jorgenson, M. T., Racine, C. H., Walters, J. C., and Osterkamp, T. E. (2001). Permafrost degradation and ecological changes associated with a warming climate in central Alaska. *Clim. Change* 48, 551–579. doi: 10.1023/A:1005667424292

Kane, D. L., Hinzman, L. D., and Zarling, J. P. (1991). Thermal response of the active layer to climatic warming in a permafrost environment. *Cold Reg. Sci. Technol.* 19, 111–122. doi: 10.1016/0165-232X(91)90002-X

Killops, S., and Killops, V. (2005). *Introduction to Organic Geochemistry*. Oxford, UK: Blackwell Publishing Ltd.

Kim, Y. J., and Wilson, D. M. III. (2012). Overview of base excision repair biochemistry. *Curr. Mol. Pharmacol.* 5, 3–13. doi: 10.2174/1874467211205010003

Lay, C. Y., Mykytczuk, N. C. S., Yergeau, E., Lamarche-Gagnon, G., Greer, C. W., and Whyte, L. G. (2013). Defining the functional potential and active community members of a sediment microbial community in a high-Arctic hypersaline subzero spring. *Appl. Environ. Microbiol.* 79, 3637–3648. doi: 10.1128/AEM.00153-13

Lever, M. A. (2013). Functional gene surveys from ocean drilling expeditions – a review and perspective. *FEMS Microbiol. Ecol.* 84, 1–23. doi: 10.1111/1574-6941.12051

Li, W. Z. (2009). Analysis and comparison of very large metagenomes with fast clustering and functional annotation. *BMC Bioinformatics* 10:359. doi: 10.1186/1471-2105-10-359

Liebner, S., Harder, J., and Wagner, D. (2008). Bacterial diversity and community structure in polygonal tundra soils from Samoylov Island, Lena Delta, Siberia. *Int. Microbiol.* 11, 195–202. doi: 10.2436/20.1501.01.60

Lipson, D. A., Haggerty, J. M., Srinivas, A., Raab, T. K., Sathe, S., and Dinsdale, E. A. (2013). Metagenomic insights into anaerobic metabolism along an Arctic peat soil profile. *PLoS ONE* 8:e64659. doi: 10.1371/journal.pone.0064659

Lu, Y. H., and Meyers, P. A. (2009). Sediment lipid biomarkers as recorders of the contamination and cultural eutrophication of Lake Erie, 1909-2003. *Organ. Geochem.* 40, 912–921. doi: 10.1016/j.orggeochem.2009.04.012

Mackelprang, R., Waldrop, M. P., Deangelis, K. M., David, M. M., Chavarria, K. L., Blazewicz, S. J., et al. (2011). Metagenomic analysis of a permafrost microbial community reveals a rapid response to thaw. *Nature* 480, 368–U120. doi: 10.1038/nature10576

McCalley, C. K., Woodcroft, B. J., Hodgkins, S. B., Wehr, R. A., Kim, E.-H., Mondav, R., et al. (2014). Methane dynamics regulated by microbial community response to permafrost thaw. *Nature* 514, 478–481. doi: 10.1038/nature13798

Meyer, F., Paarmann, D., D'souza, M., Olson, R., Glass, E. M., Kubal, M., et al. (2008). The metagenomics RAST server - a public resource for the automatic phylogenetic and functional analysis of metagenomes. *BMC Bioinformatics* 9:386. doi: 10.1186/1471-2105-9-386

Meyers, P. A. (2003). Applications of organic geochemistry to paleolimnological reconstructions: a summary of examples from the Laurentian Great Lakes. *Organ. Geochem.* 34, 261–289. doi: 10.1016/S0146-6380(02)00168-7

Michel, B. (2005). After 30 years of study, the bacterial SOS response still surprises us. *PLoS Biol.* 3, 1174–1176. doi: 10.1371/journal.pbio.0030255

Niederberger, T. D., Steven, B., Charvet, S., Barbier, B., and Whyte, L. G. (2009). *Virgibacillus arcticus* sp nov., a moderately halophilic, endospore-forming bacterium from permafrost in the Canadian high Arctic. *Int. J. Syst. Evol. Microbiol.* 59, 2219–2225. doi: 10.1099/ijs.0.002931-0

Onstott, T. C., McGown, D. J., Bakermans, C., Ruskeeniemi, T., Ahonen, L., Telling, J., et al. (2009). Microbial communities in subpermafrost saline fracture water at the Lupin Au Mine, Nunavut, Canada. *Microb. Ecol.* 58, 786–807. doi: 10.1007/s00248-009-9553-5

Orsi, W. D., Edgcomb, V. P., Christman, G. D., and Biddle, J. F. (2013). Gene expression in the deep biosphere. *Nature* 499, 205–208. doi: 10.1038/nature12230

Orsi, W. D., Smith, J. M., Wilcox, H. M., Swalwell, J. E., Carini, P., Worden, A. Z., et al. (2015). Ecophysiology of uncultivated marine euryarchaea is linked to particulate organic matter. *ISME J.* 1–17. doi: 10.1038/ismej.2014.260

Osburn, M. R., Sessions, A. L., Pepe-Ranney, C., and Spear, J. R. (2011). Hydrogen-isotopic variability in fatty acids from Yellowstone National Park hot spring microbial communities. *Geochim. Cosmochim. Acta* 75, 4830–4845. doi: 10.1016/j.gca.2011.05.038

Osterkamp, T. E. (2007). Characteristics of the recent warming of permafrost in Alaska. *J. Geophys. Res. Earth Surf.* 112:F02S02. doi: 10.1029/2006JF000578

Pautler, B. G., Simpson, A. J., McNally, D. J., Lamoureux, S. F., and Simpson, M. J. (2010). Arctic permafrost active layer detachments stimulate microbialactivity and degradation of soil organic matter. *Environ. Sci. Technol.* 44, 4076–4082. doi: 10.1021/es903685j

Pecheritsyna, S. A., Rivkina, E. M., Akimov, V. N., and Shcherbakova, V. A. (2012). *Desulfovibrio arcticus* sp nov., a psychrotolerant sulfate-reducing bacterium from a cryopeg. *Int. J. Syst. Evol. Microbiol.* 62, 33–37. doi: 10.1099/ijs.0.021451-0

Penton, C. R., St Louis, D., Cole, J. R., Luo, Y., Wu, L., Schuur, E., et al. (2013). Fungal diversity in Permafrost and Tallgrass Prairie soils under experimental warming conditions. *Appl. Environ. Microbiol.* 79, 7063–7072. doi: 10.1128/AEM.01702-13

Ping, C. L., Michaelson, G. J., and Kimble, J. M. (1997). Carbon storage along a latitudinal transect in Alaska. *Nutr. Cycl. Agroecosys.* 49, 235–242. doi: 10.1023/A:1009731808445

Pingoud, A., Fuxreiter, M., Pingoud, V., and Wende, W. (2005). Type II restriction endonucleases: structure and mechanism. *Cell. Mol. Life Sci.* 62, 685–707. doi: 10.1007/s00018-004-4513-1

Rivkina, E. M., Friedmann, E. I., McKay, C. P., and Gilichinsky, D. A. (2000). Metabolic activity of permafrost bacteria below the freezing point. *Appl. Environ. Microbiol.* 66, 3230–3233. doi: 10.1128/AEM.66.8.3230-3233.2000

Rosen, G. L., and Essinger, S. D. (2010). Comparison of statistical methods to classify environmental genomic fragments. *IEEE Trans. Nanobiosci.* 9, 310–316. doi: 10.1109/TNB.2010.2081375

Schouten, S., Hopmans, E. C., Pancost, R. D., and Sinninghe Damsté, J. S. (2000). Widespread occurrence of structurally diverse tetraether membrane lipids: evidence for the ubiquitous presence of low-temperature relatives of hyperthermophiles. *Proc. Natl. Acad. Sci. U.S.A.* 97, 14421–14426. doi: 10.1073/pnas.97.26.14421

Schuur, E. A.G., Bockheim, J., Canadell, J. G., Euskirchen, E., Field, C. B., Zimov, S. A. et al. (2008). Vulnerability of permafrost carbon to climate change: implications for the global carbon cycle. *Bioscience* 58, 701–714. doi: 10.1641/B580807

Sessions, A. L. (2006). Seasonal changes in D/H fractionation accompanying lipid biosynthesis in *Spartina alternflora*. *Geochim. Cosmochim. Acta* 70, 2153–2162. doi: 10.1016/j.gca.2006.02.003

Shcherbakova, V. A., Chuvilskaya, N. A., Rivkina, E. M., Pecheritsyna, S. A., Laurinavichius, K. S., Suzina, N. E., et al. (2005). Novel psychrophilic anaerobic spore-forming bacterium from the overcooled water brine in permafrost: description *Clostridium algoriphilum* sp nov. *Extremophiles* 9, 239–246. doi: 10.1007/s00792-005-0438-3

Steven, B., Pollard, W. H., Greer, C. W., and Whyte, L. G. (2008). Microbial diversity and activity through a permafrost/ground ice core profile from the Canadian high Arctic. *Environ. Microbiol.* 10, 3388–3403. doi: 10.1111/j.1462-2920.2008.01746.x

Strauss, J., Schirrmeister, L., Wetterich, S., and, Mangelsdorf, K. (2012). "Old organic matter in Siberian permafrost deposits and its degradation features," in *Tenth International Conference on Permafrost-Resources and Risks of Permafrost Areas in a Changing World* (Salekhard).

Tarnocai, C., Canadell, J. G., Schuur, E. A. G., Kuhry, P., Mazhitova, G., and Zimov, S. (2009). Soil organic carbon pools in the northern circumpolar permafrost region. *Glob. Biogeochem. Cycles* 23, GB2023. doi: 10.1029/2008GB003327

Tatusov, R. L., Koonin, E. V., and Lipman, D. J. (1997). A genomic perspective on protein families. *Science* 278, 631–637. doi: 10.1126/science.278.5338.631

Uhlirova, E., Santruckova, H., and Davidov, S. P. (2007). Quality and potential biodegradability of soil organic matter preserved in permafrost of Siberian tussock tundra. *Soil Biol. Biochem.* 39, 1978–1989. doi: 10.1016/j.soilbio.2007.02.018

Varga, J. J., Therit, B., and Melville, S. B. (2008). Type IV pili and the CcpA protein are needed for maximal biofilm formation by the Gram-Positive anaerobic pathogen *Clostridium perfringens*. *Infect. Immun.* 76, 4944–4951. doi: 10.1128/IAI.00692-08

Vernotte, C., Picaud, M., Kirilovsky, D., Olive, J., Ajlani, G., and Astier, C. (1992). Changes in the photosynthetic apparatus in the cyanobacterium *Synechocystis* Sp Pcc-6714 following light-to-dark and dark-to-light transitions. *Photosyn. Res.* 32, 45–57. doi: 10.1007/BF00028797

Vishnivetskaya, T. A., Petrova, M. A., Urbance, J., Ponder, M., Moyer, C. L., Gilichinsky, D. A., et al. (2006). Bacterial community in ancient Siberian permafrost as characterized by culture and culture-independent methods. *Astrobiology* 6, 400–414. doi: 10.1089/ast.2006.6.400

Waldrop, M. P., Wickland, K. P., White, R., Berhe, A. A., Harden, J. W., and Romanovsky, V. E. (2010). Molecular investigations into a globally important carbon pool: permafrost-protected carbon in Alaskan soils. *Glob. Change Biol.* 16, 2543–2554. doi: 10.1111/j.1365-2486.2009.02141.x

Walker, D. A., and Maier, H. A. (2008). *Vegetation in the Vicinity of the Toolik Field Station, Alaska, No.28*. Fairbanks: Institute of Arctic Biology.

Weijers, J. W. H., Schouten, S., Van Den Donker, J. C., Hopmans, E. C., and Sinninghe Damsté, J. S. (2007). Environmental controls on bacterial tetraether membrane lipid distribution in soils. *Geochim. Cosmochim. Acta* 71, 703–713. doi: 10.1016/j.gca.2006.10.003

Weimer, P. J., and Zeikus, J. G. (1979). Acetate assimilation pathway of *Methanosarcina barkeri*. *J. Bacteriol.* 137, 332–339.

Willerslev, E., Hansen, A. J., Binladen, J., Brand, T. B., Gilbert, M. T. P., Shapiro, B., et al. (2003). Diverse plant and animal genetic records from Holocene and Pleistocene sediments. *Science* 300, 791–795. doi: 10.1126/science.1084114

Willerslev, E., Hansen, A. J., Ronn, R., Brand, T. B., Barnes, I., Wiuf, C., et al. (2004). Long-term persistence of bacterial DNA. *Curr. Biol.* 14, R9–R10. doi: 10.1016/j.cub.2003.12.012

Yergeau, E., Hogues, H., Whyte, L. G., and Greer, C. W. (2010). The functional potential of high Arctic permafrost revealed by metagenomic sequencing, qPCR and microarray analyses. *ISME J.* 4, 1206–1214. doi: 10.1038/ismej.2010.41

Yunker, M. B., Macdonald, R. W., Veltkamp, D. J., and Cretney, W. J. (1995). Terrestrial and marine biomarkers in a seasonally ice-covered arctic estuary - integration of multivariate and biomarker approaches. *Mar. Chem.* 49, 1–50. doi: 10.1016/0304-4203(94)00057-K

Zhang, T. J., Frauenfeld, O. W., Serreze, M. C., Etringer, A., Oelke, C., McCreight, J., et al. (2005). Spatial and temporal variability in active layer thickness over the Russian Arctic drainage basin. *J. Geophys. Res. Atmos.* 110:D16101. doi: 10.1029/2004JD005642

Zheng, Y., Zhou, W., Meyers, P. A., and Xie, S. (2007). Lipid biomarkers in the Zoigê-Hongyuan peat deposit: indicators of Holocene climate changes in West China. *Org. Geochem.* 38, 1927–1940. doi: 10.1016/j.orggeochem.2007.06.012

Zimov, S. A., Davydov, S. P., Zimova, G. M., Davydova, A. I., Schuur, E. A. G., Chapin, F. S. et al. (2006). Permafrost carbon: stock and decomposability of a globally significant carbon pool. *Geophys. Res. Lett.* 33, L20502. doi: 10.1029/2006GL027484

Conflict of Interest Statement: The authors declare that the research was conducted in the absence of any commercial or financial relationships that could be construed as a potential conflict of interest.

frontiers in Microbiology

ORIGINAL RESEARCH
published: 23 September 2015
doi: 10.3389/fmicb.2015.00966

Metagenomic analysis reveals that modern microbialites and polar microbial mats have similar taxonomic and functional potential

Richard Allen White III[1†], *Ian M. Power*[2], *Gregory M. Dipple*[2], *Gordon Southam*[3] and *Curtis A. Suttle*[1, 2, 4, 5*]

[1] Department of Microbiology and Immunology, University of British Columbia, Vancouver, BC, Canada, [2] Department of Earth, Ocean and Atmospheric Sciences, University of British Columbia, Vancouver, BC, Canada, [3] School of Earth Sciences, University of Queensland, Brisbane, QLD, Australia, [4] Department of Botany, University of British Columbia, Vancouver, BC, Canada, [5] Canadian Institute for Advanced Research, Toronto, ON, Canada

Within the subarctic climate of Clinton Creek, Yukon, Canada, lies an abandoned and flooded open-pit asbestos mine that harbors rapidly growing microbialites. To understand their formation we completed a metagenomic community profile of the microbialites and their surrounding sediments. Assembled metagenomic data revealed that bacteria within the phylum Proteobacteria numerically dominated this system, although the relative abundances of taxa within the phylum varied among environments. Bacteria belonging to Alphaproteobacteria and Gammaproteobacteria were dominant in the microbialites and sediments, respectively. The microbialites were also home to many other groups associated with microbialite formation including filamentous cyanobacteria and dissimilatory sulfate-reducing Deltaproteobacteria, consistent with the idea of a shared global microbialite microbiome. Other members were present that are typically not associated with microbialites including Gemmatimonadetes and iron-oxidizing Betaproteobacteria, which participate in carbon metabolism and iron cycling. Compared to the sediments, the microbialite microbiome has significantly more genes associated with photosynthetic processes (e.g., photosystem II reaction centers, carotenoid, and chlorophyll biosynthesis) and carbon fixation (e.g., CO dehydrogenase). The Clinton Creek microbialite communities had strikingly similar functional potentials to non-lithifying microbial mats from the Canadian High Arctic and Antarctica, but are functionally distinct, from non-lithifying mats or biofilms from Yellowstone. Clinton Creek microbialites also share metabolic genes ($R^2 < 0.750$) with freshwater microbial mats from Cuatro Ciénegas, Mexico, but are more similar to polar Arctic mats ($R^2 > 0.900$). These metagenomic profiles from an anthropogenic microbialite-forming ecosystem provide context to microbialite formation on a human-relevant timescale.

Keywords: microbialites, non-lithifying microbial mats, metagenomic assembly, carbon sequestration, Gemmatimonadetes, cyanobacteria

OPEN ACCESS

Edited by:
John J. Kelly,
Loyola University Chicago, USA

Reviewed by:
Nico Salmaso,
IASMA Research and Innovation Centre Fondazione Mach-Istituto Agrario di S. Michele all'Adige, Italy
Luisa I. Falcon,
Universidad Nacional Autónoma de México, Mexico
Brendan Paul Burns,
The University of New South Wales, Australia

****Correspondence:***
Curtis A. Suttle,
Department of Earth, Ocean and Atmospheric Sciences, University of British Columbia, 2178-2207 Main Mall, Vancouver, BC V6T 1Z4, Canada
suttle@science.ubc.ca

†Present Address:
Richard Allen White III,
Fundamental and Computational Sciences, Pacific Northwest National Laboratories, Richland, WA, USA

Specialty section:
This article was submitted to Aquatic Microbiology, a section of the journal Frontiers in Microbiology

Received: *12 January 2015*
Accepted: *31 August 2015*
Published: *23 September 2015*

Citation:
White RA III, Power IM, Dipple GM, Southam G and Suttle CA (2015) Metagenomic analysis reveals that modern microbialites and polar microbial mats have similar taxonomic and functional potential. Front. Microbiol. 6:966. doi: 10.3389/fmicb.2015.00966

Introduction

Modern microbialites provide an analog for understanding the structure, composition and function of early microbial communities dating back dating back 3.5 Gya (Grotzinger and Knoll, 1999; Dupraz and Visscher, 2005; Schopf, 2006). Microbialites are microbially lithified organosedimentary structures that manifest the carbonate macrofabric as stromatolites (from the Greek *stromat*; bed-covering, *lithos*; stone, as a layered internal structure with laminated fabrics), and thrombolites (from the Greek *thrombos*, clot; *lithos*, stone as a non-layered, non-laminated structure with clotted fabrics) (Burne and Moore, 1987; Perry et al., 2007; Riding, 2011). Modern microbialites are mainly constructed from calcium carbonate, either as calcite or aragonite), but in rare cases can occur as magnesium carbonate (e.g., hydromagnesite) (Couradeau et al., 2011). Microbialites are globally distributed in diverse environments including marine (Reid et al., 2000; Burns et al., 2004), freshwater (Ferris et al., 1997; Laval et al., 2000; Gischler et al., 2008), hypersaline (Allen et al., 2009; Goh et al., 2009), hot springs (Bosak et al., 2012), and even terrestrial environments, such as landfills (Maliva et al., 2000) and caves (Lundberg and McFarlane, 2011).

Biologically-induced mineralization involves the microbial alteration of water chemistry causing mineral saturation and precipitation (Dupraz et al., 2009). Microbial processes that cycle carbon, particularly within microenvironments, are important for inducing carbonate precipitation under appropriate chemical conditions (e.g., alkaline pH and sufficient cations; Spanos and Koutsoukos, 1998; Dupraz et al., 2009). For instance, cyanobacteria can cause alkalinization through photosynthesis, thereby driving pH to more alkaline conditions that favor carbonate precipitation (Thompson and Ferris, 1990). (Equation 1) $HCO_3^- + H_2O + h\nu \rightarrow CH_2O + OH^- + O_2 \uparrow$. Microbial cell walls and exopolymeric substances (EPS) may provide surfaces for mineral nucleation and aid in concentrating cations (e.g., Ca^{2+}) due to adsorption by negatively charged functional groups (e.g., R-COO^-) (Schultze-Lam et al., 1996). Additionally, heterotrophic bacteria can increase the availability of dissolved inorganic carbon (DIC) for carbonate precipitation through the degradation of organics (Von Knorre and Krumbein, 2000). (Equation 2) $2CHO_2^- + O_2 \rightarrow 2HCO_3^-$. Although aragonite is supersaturated in the Clinton Creek open-pit pond, studies of non-marine environments exhibiting calcifying cyanobacteria show that a 9.5 to 15-fold supersaturation with respect to calcite is required for precipitation to occur (Arp et al., 2001). Such biological activity, especially in microenvironments where carbonate precipitation may be occurring, may increase pH, and/or increase cation and DIC concentrations.

Microbial processes that cycle carbon may also induce carbonate precipitation under certain geochemical conditions (e.g., alkaline pH and sufficient cations; Dupraz et al., 2009). Photosynthesis by cyanobacteria may result in the alkalization of microenvironments by producing hydroxyl anions, causing an increase in pH (Thompson and Ferris, 1990; Ludwig et al., 2005; Tesson et al., 2008); whereas, degradation of organics may increase the concentration of DIC (Slaughter and Hill, 1991; Van Lith et al., 2003).

In the present study we examined the microbial communities associated with microbialites found in a flooded and abandoned open-pit asbestos mine (64°26′42″N, 140°43′25″W) referred to as Clinton Creek, and located in the subarctic, ∼77 km northwest of Dawson City, Yukon, Canada (**Figure 1**), and which was previously studied to elucidate the geology of asbestos deposits (Htoon, 1979) and for its potential for sequestering carbon dioxide in mine wastes (Wilson et al., 2009). The microbialites at Clinton Creek are unusual in that they have estimated accretion rates of up to ∼5 mm per year (Power et al., 2011a), much higher than other modern microbialite-forming systems including Highbourne Cay (∼0.33 mm per year) (Planavsky and Ginsburg, 2009), Shark Bay (0.4 mm per year) (Chivas et al., 1990), and Pavilion Lake (0.05 mm per year) (Brady et al., 2009). Consequently, the Clinton Creek microbialites should be excellent models for understanding the biological processes responsible for microbialites formation.

Studies have examined the diversity of microbialites using both metagenomic and 16S rDNA sequencing. Metagenomic studies have focused mainly on marine systems (Reid et al., 2000; Burns et al., 2004; Papineau et al., 2005; Allen et al., 2009; Goh et al., 2009; Khodadad and Foster, 2012; Mobberley et al., 2013), with Cuatro Ciénegas being the only reported metagenomic investigation of freshwater microbialites (Breitbart et al., 2009). In contrast, 16S rDNA sequencing has been used to examine the diversity of freshwater microbialites in Lake Van (López-García et al., 2005), Pavilion Lake (Russell et al., 2014), Ruidera Pools (Santos et al., 2010), Lake Alchichica (Couradeau et al., 2011), and Cuatro Ciénegas (Centeno et al., 2012). The extent to which microbialite communities are similar or different from those in surrounding sediments and waters remains an unresolved but important question. The microbial communities in the surrounding sediments provide the environmental context needed to better constrain common and unique aspects of microbialite community structure and function. This information may be used to uncover conserved patterns of microbial community assembly and the metabolic pathways mediating microbialite formation under different environmental conditions.

In the present study, we use a metagenomic approach to explore the structure and function of Clinton Creek microbialites in relation to adjacent sediments in order to examine the metabolic drivers of microbialite growth in this freshwater system. We focus on metabolic pathways mediating photosynthetic or heterotrophic carbonate precipitation and the taxonomic distribution of these pathways. We then compare the metagenomic data from Clinton Creek microbialites and sediments to diverse non-lithifying mats, sediments, and microbialites to better define the conserved microbialite community structure and function.

Materials and Methods

Site Description and Water Chemistry

The conditions at the Clinton Creek mine are highly conducive to microbialite formation and are described extensively in

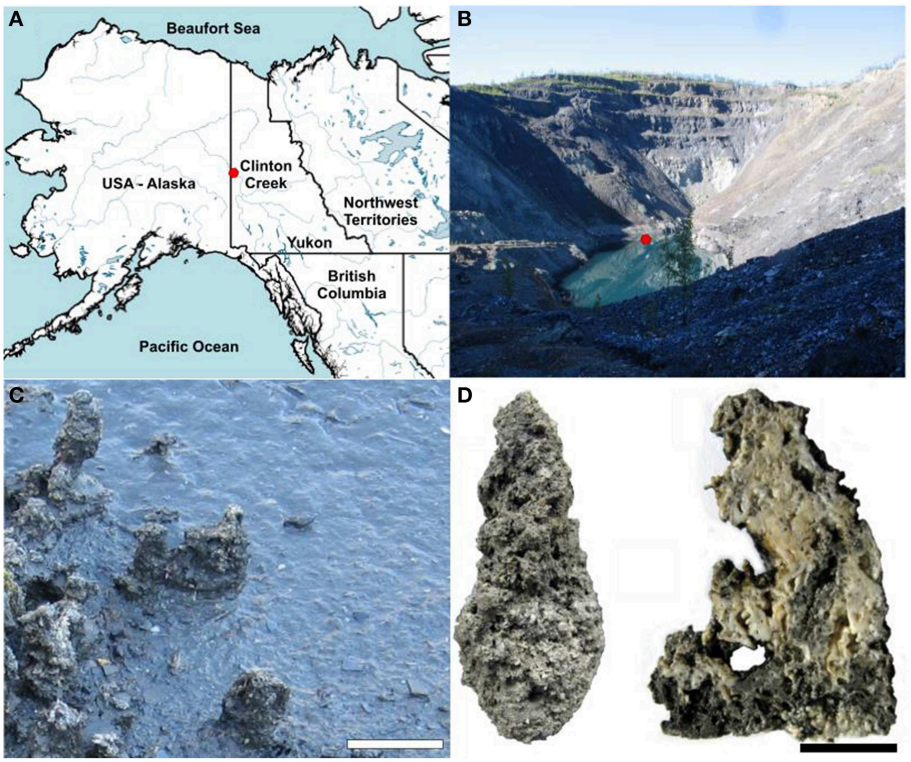

FIGURE 1 | Clinton Creek sample site and examples of microbialite morphology. (A) Map of northwestern North America illustrating the location of Clinton Creek Yukon, Canada. **(B)** Photograph of the Clinton Creek open pit pond, the red dot indicating the sampling location. **(C)** Photograph of the microbialites along the periphery of the open pit pond. Scale bar equals 15 cm. **(D)** Complete microbialite and cross-section of a microbialite. Scale bar represents 5 cm.

Power et al. (2011a), and are summarized briefly below. The photic zone likely occupies the full depth of the open pit pond and there is minimal nutrient input due to the lack of surrounding soil. Sediments are composed of chrysotile, quartz, muscovite, kaolinite, as well as minor amounts of aragonite and trace calcite. The microbialites are columnar, up to 15 cm in height, and are primarily composed of aragonite with spherulitic fabric (**Figure 1D**). The open pit water is subsaline (Na^+ 17.6–35.7 mg L^{-1} and K^+ 2.7–5.2 mg L^{-1}), oligotrophic (undetectable phosphate), alkaline in pH (8.4), possessing a cation concentrations distribution of $Mg^{2+} >> Ca^{2+} >> Na^+ > K^+ > Si^{4+}$, while anions concentrations were $SO_4^{2-} >>$ DIC $> Cl^-$ (**Table 1**). As is common in microbialite forming systems (Dupraz et al., 2009; Lim et al., 2009), the water is oligotrophic with very low iron concentrations and undetectable phosphate which is common in microbialite forming systems (Dupraz et al., 2009; Lim et al., 2009). The water is supersaturated with respect to aragonite (saturation index = 0.6), the dominant mineral forming the microbialites, as well as calcite [$CaCO_3$].

Sampling, DNA Extraction, Purity, and Concentration Measurements

Microbialites and sediment samples were obtained in July 2011. Triplicate sediment and microbialite samples were taken ~10 m apart. Microbialites were ground with mortar and pestle under liquid nitrogen prior to DNA extraction. Community genomic DNA was extracted from triplicate 10 g microbialite and sediment subsamples using a PowerMax soil DNA isolation kit (MoBio Laboratories, Inc., Carlsbad, CA, USA), following the manufacturer's instructions. DNA concentrations were determined using a Nanodrop-3300 (ThermoFisher, Nandrop Wilmington, DE) with PicoGreen® reagent according to the manufacturer's instructions (Invitrogen, Carlsbad, CA). Purity of extracted DNA and samples was determined by absorbance (260/280 and 260/230 ratios) using a Nanodrop-1000 (ThermoFisher, Nandrop Wilmington, DE). Genomic DNA from each replicate was pooled prior to Illumina library construction.

Illumina Hiseq/Miseq Library Construction Quality Control and Quantification

For Illumina library construction, DNA was sheared by ultrasonication (Covaris M220 series, Woburn, MA), and the fragments end-paired, A-tailed (Lucigen NxSeq DNA prep kit, Middleton, WI), and ligated to TruSeq adapters (IDT, Coralville, Iowa); small fragments were removed twice using magnetic beads (Beckman Coulter, Danvers, MA) (White III et al., 2013a,b; White III and Suttle, 2013). No PCR enrichment was used to amplify libraries to avoid PCR duplication bias. Libraries were checked for size and adapter-dimers using a Bioanalyzer HighSens DNAchip (Agilent). Libraries were

TABLE 1 | Clinton Creek water chemistry.

Year	pH	Alkalinity (mg HCO_3^- L^{-1})	$\delta^{13}C$ – DIC ‰ VPDB	Cations (mg L^{-1})							Anions (mg L^{-1})			
				Mg^{2+}	Ca^{2+}	Si^{4+}	Na^{+}	K^{+}	Fe^{3+}	Al^{3+}	Cl^{-}	SO_4^{2-}	NO_3^-	PO_4^{3-}
2004	8.42	177	–	356.1	111.9	0.8	23.9	2.7	0.0	0.0	30.8	1315	–	–
2005	8.36	243	–	350.0	95.7	0.7	35.7	5.2	0.0	0.0	35.6	2378	0.52	–
2007	8.40	231	−7.8	519.7	118.8	–	30.8	5.2	–	–	33.2	1997	–	–
2011	7.90	190	−13.03	276.8	61.6	2.1	17.6	2.7	0.03	0.2	17.5	1600	1.5	–

quantified using Qubit (Invitrogen, Carlsbad, CA), according to the manufacturer's instructions, by qPCR using a microfluidic digital PCR quantified standard curve (White III et al., 2009). The resulting libraries were pooled, and sequenced using both 250 and 100 bp paired-end sequencing on the MiSeq (GenoSeq UCLA Los Angeles, CA) and HiSeq (McGill University/Génome Québec, Montreal, QC) platforms, respectively.

Analysis of Illumina Sequencing Data

Raw Illumina data was screened for PhiX spike-in contaminants sequencing data using Bowtie2 then removed using Picard tools (White III et al., 2013a,b; White III and Suttle, 2013). Reads were quality checked using FastQC, then paired-end reads merged by FLASH and assembled with the Ray assembler (kmer size: 39 and 55) (Boisvert et al., 2010, 2012; White III et al., 2013a,b; White III and Suttle, 2013). The assemblies were selected based on the number of contigs (>100 bp), N50/N90 values, longest contig, and total length (bp) of the assembly (**Table 2**). Based on these analyzes, a kmer size 39 was used for all further analysis (**Table 2**). A kmer size of 55 generally yielded longer but fewer contigs, which would not allow for a comparable differential analysis between microbialites and sediments (**Table 2**). Only contigs with >2x read coverage were used in analysis with average coverage of 3x for both the microbialite and sediment contigs. Nevertheless, only 0.64 and 1.74% of the raw reads from the sediment and microbialite metagenomes, respectively, assembled into contigs, indicating that both environments had complex microbial communities. FragGeneScan was used to predict and translate contig open reading frames (ORFs) (Rho et al., 2010) and ProPas (Wu and Zhu, 2012) was used to calculate predicted protein isoelectric points (pI).

The assemblies were annotated using Metagenomic Rapid Annotations using Subsystems Technology (MG-RAST) (Meyer et al., 2008). MG-RAST analysis of the contigs, used BLAT (BLAST-like Alignment Tool) annotations based on hierarchical classification against M5RNA (MG-RAST ribosomal specific database), SEED subsystems and RefSeq databases with a minimum *e*-value cutoff of 10^{-5}, a minimum percent identity cutoff of 60%, and a minimum alignment length cutoff of 15 base pairs. The SEED, RefSeq and M5RNA (MG-RAST rRNA database) classifications were normalized using relative count abundances for each sample. Principal component analysis (PCA) for the normalized RefSeq classifications (top 25) used R (version 3.0.3) libraries Ecodist (dissimilarity-based functions for ecological analysis), and pvclust (hierarchical clustering with *p*-values via multiscale bootstrap resampling) using ward clustering and Bray-Curtis distance metric at a thousand replicates (Suzuki and Shimodaira, 2006). PCA for the normalized RefSeq classifications was plotted using R library ggplot2 (Wickham, 2009). A dotplot of the normalized RefSeq classifications (top 25), was completed using R libraries Reshape2, using the melt function, then plotted using ggplot2 (Wickham, 2009). The annotations were parsed by custom python scripts and analyzed using statistical analysis of metagenomic profiles (STAMP) (Parks and Beiko, 2010). MG-RAST annotations using SEED subsystems for Clinton Creek microbialite and sediment contigs were loaded into STAMP and compared for metabolic potential using a one sided G-test (w/Yates' + Fisher's), alternative to the chi-squared, with asymptomatic confidence intervals (0.95) using Benjamini-Hochberg FDR procedure (Parks and Beiko, 2010).

In addition to MG-RAST, metabolic pathways were predicted using MetaPathways, a modular pipeline for gene prediction and annotation that uses pathway tools and the MetaCyc database to construct environmental pathway/genome databases (ePGBDs) (Konwar et al., 2013). Metapathways uses the seed-and-extend homology search algorithm LAST (local alignment search tool) for annotations of ORFs with a minimum of 180 bp and minimum alignment length cutoff of 50 (Kiełbasa et al., 2011). Venn diagrams were constructed from predicted MetaCyc pathways based on normalized pathway size and the number of

TABLE 2 | Assembly statistics for Clinton Creek metagenomes.

	Microbialite (*k = 39*)	Microbialite (*k = 55*)	Sediment (*k = 39*)	Sediment (*k = 55*)
No. Contigs >100 bp	109,722	689	59,928	171
Total length (Bp) >100bp	27,180,461	219,687	12,690,391	151,415
Mean >100 bp	247	318	211	885
N50 >100 bp	248	289	200	1307
N90 >100 bp	184	231	160	383
Med Length >100 bp	240	269	186	582
No. Contigs >500 bp	371	46	557	99
Total length (Bp) >500 bp	230,702	37,861	508,559	127,068
Mean >500 bp	621	823	913	1283
N50 >500 bp	588	611	849	1591
Med >500 bp	574	566	608	916
Largest	9491	9752	33,503	5896
Total GC count	16,801,673	135,459	7,329,632	82,490
GC%	61.82	61.66	57.76	54.48

k = kmer size (bp).

ORFs associated with each pathway using R libraries then plotted using ggplot2 (Wickham, 2009).

Comparative Metagenomics

MG-RAST annotations for Clinton Creek microbialite (ID 4532705.3) and sediment (ID 4532704.3) metagenomes were loaded into STAMPS then compared against arctic mats and sediments: Ward Hunt Ice Shelf mat (ID 4532782.3), MarkHam Ice Shelf (ID 4532781.3), and Lost Hammer Sediments (ID 4532786.3), mats from Yellowstone: Octopus Springs Mat (ID 4443749.3), and Mushroom Springs Mat (ID 4443762.3) and Antarctica mats, marine derived lakes, freshwater lakes, and marine; McMurdo ice shelf mat (ID 4532780.3), Marine Lake 1 (ID 4443683), Marine Lake 5 (ID 4443682.3), Marine 8 (ID 4443686.3), Marine 9 (ID 4443687.3), and Ace Lake (ID 4443684.3) using a multiple group ANOVA in STAMP by SEED subsystems (Level III) annotations by post-hoc tests (Tukey-Kramer at 0.95), an effect size (Eta-squared) and multiple test correction using the Benjamini-Hochberg FDR procedure. Clinton Creek microbialites were further examined against polar mats, Cuatro Ciénegas microbialites (4440060.4, 4440067.3) and marine stromatolites from Highbourne Cay (ID 4440061.3) in STAMPs by a one sided G-test (w/Yates' + Fisher's), alternative to the chi-squared, with asymptomatic confidence intervals (0.95) using Benjamini-Hochberg FDR procedure.

Metagenomic Data Depositing

All the data used in this study is freely available and available for public access from the MG-RAST metagenomics analysis server. From MG-RAST, it is listed in the project name Yukon microbialites under the names Clinton Creek microbialite (ID 4532705.3) and sediment contigs (ID 4532704.3).

Results and Discussion

Non-database Based Community Properties

Based on GC content Clinton Creek the microbialite microbial communities are clearly distinct from the sediment microbial communities. The GC content was higher in the microbialites compared to the sediments; whereas, protein isoelectric points (pI) were similar (Figure S1). The GC content was lower in sediments likely due to the higher presence of low GC containing microbes belonging to phyla such as Bacteroides and Firmicutes. The higher GC content in the microbialite data is likely due to the high relative abundance of sequences assigned to anoxic photoheterotrophic Alphaproteobacteria, including Rhodobacterales (59–65% GC content) and Rhodomicrobium (62.2% GC content). GC content across bacterial genomes can be highly variable amongst microbial taxa, although amino-acid usage is typically similar, which is similar to our data on GC and pI content observed in the metagenomes (Lightfield et al., 2011; Figure S1).

Community Composition

The microbial communities within Clinton Creek are distinct from each other (**Figure 2**) and are dominated by differing compositions of Proteobacteria and Cyanobacteria. Proteobacteria comprised >50% of the ORFs and >35% of the 16S sequences recovered from the Clinton Creek sediments and microbialites (**Figure 2**). The microbialite contigs were dominated by anoxic photoheterotrophic Alphaproteobacteria (e.g., Rhodobacterales) (**Figure 2A**). In contrast, sediments contigs had greater abundance nitrogen-fixing Gammaproteobacteria (e.g., *Pseudomonas* spp.) (**Figure 2A**). Alphaproteobacteria are commonly found amongst, and are likely a critical component of, the microbialite-forming microbial consortium due to their role in nitrogen fixation, even in the presence of heterocystous cyanobacteria (Havemann and Foster, 2008). It has been suggested that prior to the evolution of cyanobacteria, anoxic phototrophs like Rhodobacterales could have had a role in the formation of Precambrian stromatolites (Bosak et al., 2007).

Deltaproteobacteria represented ∼10% of the predicted Proteobacterial ORFs (based on RefSeq) from the sediments and microbialites (**Figure 2A**). The microbialite contigs consisted mainly of *Myxococcus* spp. whereas, members of the Desulfuromonadales dominated in the sediments. *Myxococcus* spp. are abundant in a variety of microbialite-forming systems and can mediate precipitate carbonate through the release of ammonium (Jimenez-Lopez et al., 2011). The microbialites and sediments had similar representation from Desulfurovibrionales, Desulfobacterales and Syntrophobacterales, the major orders of dissimilatory sulfate reducers. The dissimilatory sulfate-reducers in the Deltaproteobacteria may be critical drivers of the "the alkalinity engine," thereby inducing carbonate precipitation (Gallagher et al., 2012). Finding the major dissimilatory sulfate-reducing groups of bacteria (Desulfurovibrionales, Desulfobacterales, and Syntrophobacterales) in Clinton Creek microbialites is not surprising; however, their abundances were similar in the sediments, including genes involved in dissimilatory sulfate-reduction. Thus, the sediments and ground water likely generate alkalinity and could also be the source(s) of these dissimilatory sulfate-reducing bacteria in microbialites. For example, sulfate-reducing bacteria may be transported as spores from other environments and then disperse in microbialite cyanobacterial mats.

Cyanobacteria were the fourth most abundant group, comprising 6.1% of the total contigs in the microbialites (**Figure 2A**). The microbialites had 4-fold more protein coding ORFs that were classified as cyanobacteria than the sediments (6.1–1.4%, **Figure 2A**). The cyanobacterial ribosomal sequences were detected in the microbialites only (based on M5RNA database) and from only filamentous cyanobacteria genera, which include Tolypothrix, Leptolyngbya, and unclassified Antarctic cyanobacteria. In contrast, no Cyanobacteria ribosomal sequences (e.g., rDNA) were recovered from the sediments (**Figure 2A**; M5RNA). No Cyanobacteria ribosomal sequences (e.g., rDNA) were detected in the sediments due to very low abundance sediments. Microbialite contigs based on RefSeq classification had higher abundances of filamentous genera including Microcoleus, Lyngbya, Nodularia, and Anabaena, and more unicellular calcifying Synechococcus, than the sediments. The sediments had fewer filamentous cyanobacteria genera as a whole and fewer unicellular cyanobacteria (e.g., Synechococcus)

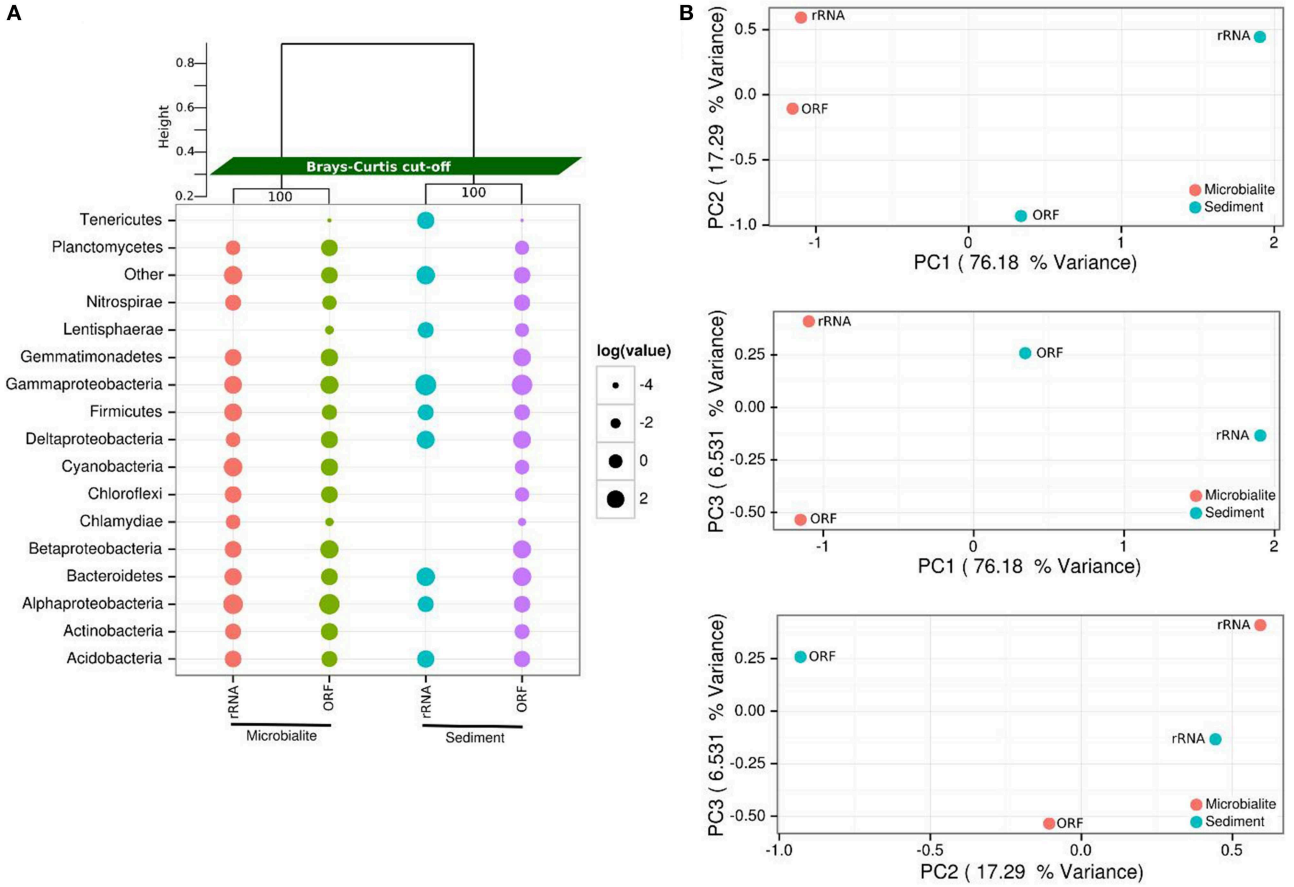

FIGURE 2 | Microbial community structure of Clinton Creek metagenomes. (A) Dot pot of representative taxonomic groups from Clinton Creek sediments and microbialites using RefSeq (protein coding ORFs) and M5RNA (rRNA, MG-RAST rRNA database) in log relative abundances. Samples were clustered (top) by ward clustering matrix using bootstraping of one thousand replications with Bray-Curtis distance cut-offs. "Other" denotes low abundance taxa that were <1% of the total ORF or rRNA, individually, but were all combined here into one point. **(B)** PCAs of top 25 taxonomic groups from Clinton Creek sediments and microbialites by RefSeq (ORFs) and M5RNA (rRNA, MG-RAST rRNA database) classification using ward clustering matrix followed by bootstrapping of one thousand replications with Bray-Curtis distance cut-offs.

contigs. Cyanobacteria likely drive microbialite formation in Clinton Creek by increasing carbon biomass in the form of carbon-rich EPS, which supports the growth of the entire heterotrophic microbial consortium through carbon fixation, which in turn contributes to carbonate precipitation by increasing the saturation index (Dupraz and Visscher, 2005; Braissant et al., 2007; Dupraz et al., 2009; McCutcheon et al., 2014).

The phylum Gemmatimonadetes was present in both the sediments and microbialite contigs, and comprised 7–8% of the protein coding ORFs (**Figure 2A**). To our knowledge, this is the first report of protein sequences from Gemmatimonadetes in microbialites based on metagenomic data, although they were not restricted to that environment. The Gemmatimonadetes contigs annotated mainly as hypothetical proteins; however, positive Gemmatimonadetes annotations included ATPases, Zn-dependent peptidases and glucose/sorbosone dehydrogenase-like genes. Glucose/sorbosone dehydrogenases transform various sugar moieties into vitamins, including L-ascorbic acid (vitamin C), or can make D-glucono-1,5-lactone from D-glucose, which can acidify the extracellular environment, which may lead to dissolution of carbonate by heterotrophic process (Dupraz and Visscher, 2005; Miyazaki et al., 2006; Fender et al., 2012). Although their estimated relative abundance is not high, this could in part be because there are few representative Gemmatimonadetes genomes in databases. Ultimately, whether they are involved in microbialite formation, or are just opportunists, or lead to dissolution, needs to be elucidated.

The microbialite and sediment microbial communities were dominated by bacteria with low abundances of eukaryotes and archaea (**Table 3**). From RefSeq annotations, <1% of microbialite and sediment contigs were of archaeal origin (**Table 3**, RefSeq), and no archaeal ribosomal genes were detected in either the sediment or microbialite contigs (**Table 3**, M5RNA). Clinton Creek microbialites, similar to Highbourne

TABLE 3 | Domain classification of the microbial community in Clinton Creek.

Domains*	Microbialite (RefSeq)	Microbialite (M5RNA)	Sediment (RefSeq)	Sediment (M5RNA)
Bacteria	99.05	73.91	98.22	92.50
Eukaryotes	0.60	25.00	1.16	7.50
Archaea	0.32	0.00	0.45	0.00
Viruses	0.02	0.00	0.13	0.00
Unassigned	0.01	1.09	0.04	0.00

**Based on MG-RAST annotations. RefSeq: Protein coding ORFs. M5RNA: Ribosomal rRNA genes.*

Cay marine microbialites and the freshwater microbialites from Cuatro Ciénegas, had low abundances (<1%) of archaea and eukaryotes (Breitbart et al., 2009; Khodadad and Foster, 2012; Mobberley et al., 2013). Eukaryotes were rare, as they make up <1% of the sediment and microbialite contigs of Clinton Creek (**Table 3**), although common taxa such as diatoms, dinoflagellates, cryptomonads, chlamydomonadales, and fungi were detected. Diatoms and other protists have been observed by microscopy and detected in the metagenomic data from Clinton Creek, but their contribution to the formation of microbialite structures requires further study (Power et al., 2011a). Diatoms may influence carbonate precipitation through photosynthetic alkalinization (Tesson et al., 2008), akin to processes found in cyanobacteria, and/or through the ammonification of amino acids (Castanier et al., 1999).

Clinton Creek microbialites had very low sequence abundance (<0.1%) of metazoans including nematoda, cryptomonads, platyhelminthes, microsporidia, cnidaria (e.g., hydra) and arthropods (e.g., insects). Our sequence data supports prior microscopy data that similarly showed low abundances of metazoans (Power et al., 2011a). With such a low metazoan abundance, the destructive impact of grazing on the Clinton Creek microbialites is presumably very low. Phosphorus was undetectable down to the parts per million detection limit in Clinton Creek (data not shown). It has been suggested that limitation of phosphorus affects metazon growth in microbialites (Elser et al., 2005). Metazoan grazing is the "prime suspect" in the global decline of microbialites as they remove cyanobacterial mats, thereby negatively impacting microbialite formation by removing the main carbon source and structural components (Grotzinger, 1990).

Metabolic Potential

The metabolic potential of the Clinton Creek microbialite metagenome predicts photosynthetic dominance, whereas the sediment metagenomes contained more heterotrophic metabolism (e.g., respiration) (**Figure 3A**). SEED subsystem level I (i.e., highest functional classification group) annotations indicated that carbohydrate metabolism relating to carbon fixation, DNA metabolism and photosynthesis pathways were significantly more abundant in the microbialites than sediments (**Figure 4A**, FDR $p < 0.01$). Lower level SEED subsystem predictions (level III) further revealed a higher abundance of photosynthetic pathways (e.g., photosystem II reaction centers and carotenoids and chlorophyll biosynthesis) in microbialites than sediments (**Figure 3B**, FDR $p < 0.01$). These photosynthetic pathways in microbialites were annotated as filamentous cyanobacteria genera such as Microcoleus, Lyngbya, Nodularia, and Anabaena, which were not found in the sediments.

The metapathway pipeline was used for MetaCyc pathway annotations to complement SEED functional gene annotations. MetaCyc predicted pathways revealed that most pathways were shared between microbialites and sediments (**Figure 4A**). Only 13 pathways were restricted to the sediments and 240 pathways were identified in the microbialites, while 358 pathways were shared (**Figure 4A**). The hundred most abundant shared pathways were housekeeping genes with functions such as protein, nucleic acid, lipid, and carbohydrate biosynthesis and degradation (**Figure 4B**). In the microbialites, MetaCyc annotations predict higher levels of glutamine degradation I, which results in the donation of nitrogen in the form of ammonium, while glutamine biosynthesis appears to be higher in the sediments (**Figure 4B**). Both the sediments and the microbialites are able to recycle ammonium through ammonium assimilation cycle I-II (**Figure 4B**). Ammonium donation provides nitrogen, which feeds the primary photosynthetic production of the filamentous cyanobacterial mats in microbialites, which in turn could lead to further carbonate precipitation.

Isotopic analysis of the carbonate minerals composing the microbialite may indicate a dominant process, e.g., alkalinization by phototrophs vs. increased CO_2 supply via heterotrophic degradation of organic matter. However, microbialites form though complex interactions between the physical and chemical factors with the microbial community. For instance, calcite composing the Pavilion Lake microbialites is enriched in ^{13}C by 2.5 ± 0.5‰ relative to calcite that may precipitate in isotopic equilibrium with lake water DIC, (Brady et al., 2009), indicating that alkalinization driven by cyanobacteria. The biomass-associated aragonite within the Clinton Creek microbialites was modestly enriched in ^{13}C by 0.8‰ relative to aragonite exhibiting no biomass, which is indicative of carbonate precipitation in association with phototrophs, including cyanobacteria (Power et al., 2011a). Electron microscopy of the microbialites confirmed that phototrophs were associated with carbonate that is enriched in 13C (Power et al., 2011a). A greater proportion of heterotrophic activity within the microbialites may explain why microbialite aragonite was isotopically lighter than periphyton found in the open pit. Omelon et al. (2013) hypothesize that microbialites become progressively lithified as the photosynthetically derived carbonate becomes in-filled through subsequent carbonate precipitation by heterotrophic activity. Similarly, Andres et al. (2006) suggest heterotrophs play a more direct role than phototrophs in the lithification stromatolites from Highborne Cay, Bahamas as indicated by isotopically light aragonite (Andres et al., 2006).

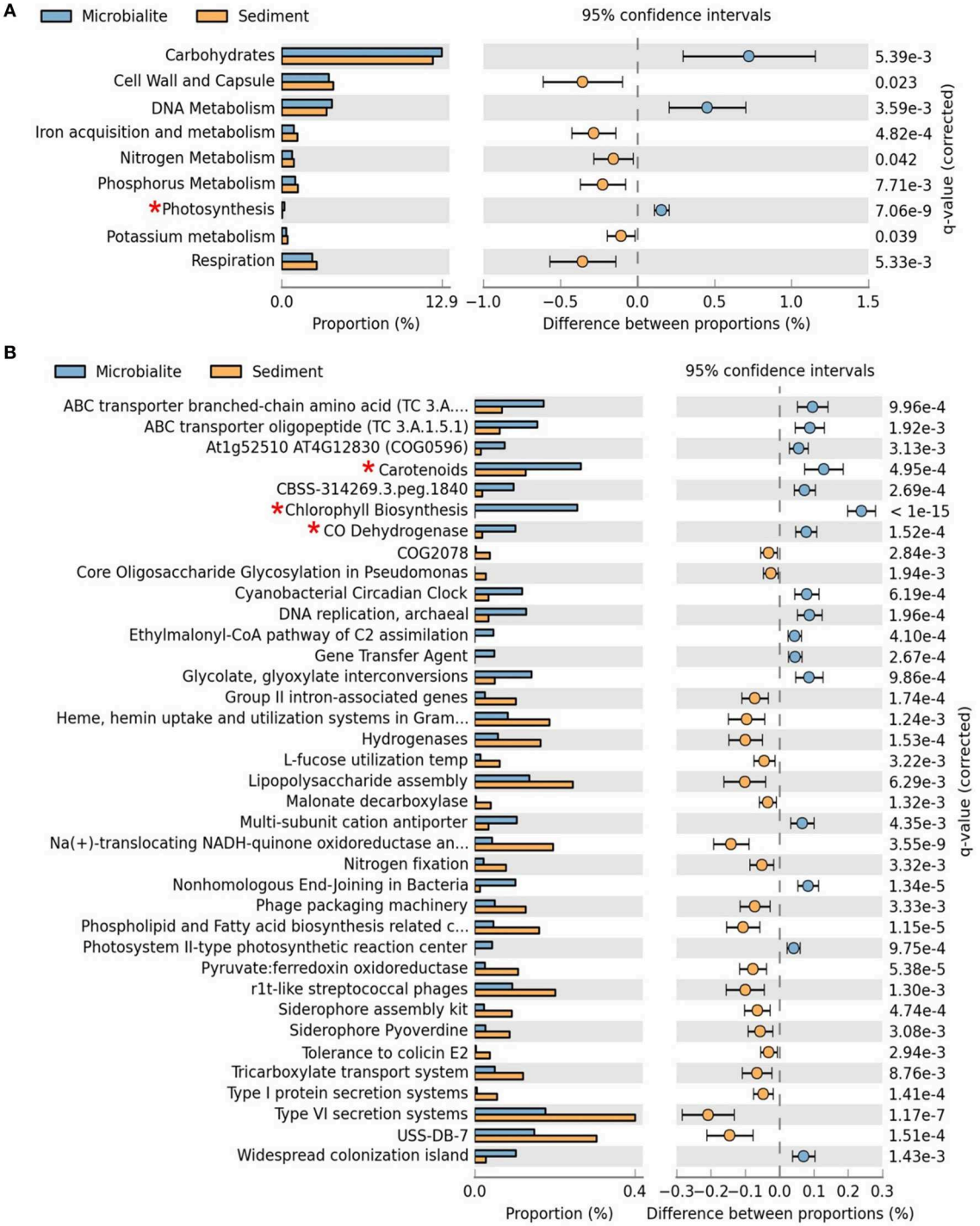

FIGURE 3 | Extended error plots for functional gene annotations for Clinton Creek metagenomes in STAMP using SEED subsystems. (A) SEED subsystem level I (highest level classification in SEED). **(B)** SEED subsystem level III (3rd lowest classification in SEED out of four levels). Extended error plots used a one sided G-test (w/Yates' + Fisher's) with asymptomatic confidence intervals (0.95) using Benjamini-Hochberg FDR procedure. *Red asterisks are significant photosynthetic pathways.

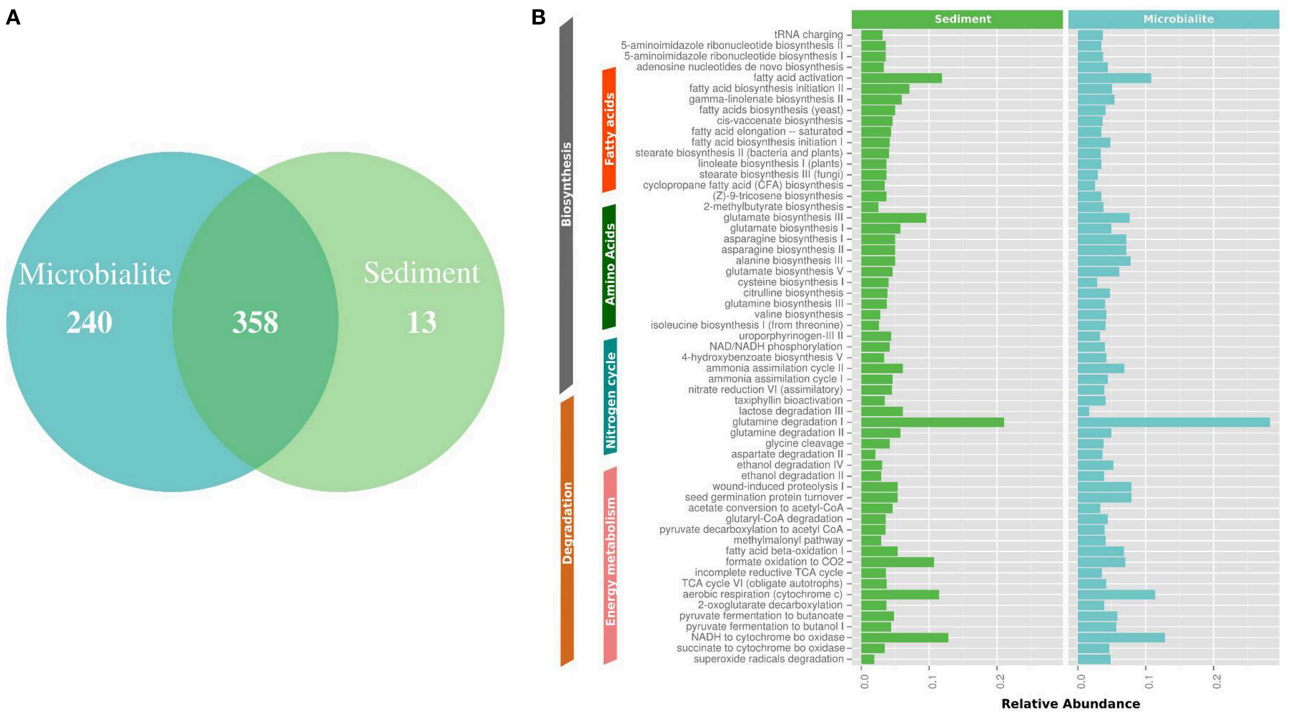

FIGURE 4 | MetaCyc pathway annotations for Clinton Creek metagenomes. (A) Venn diagram of MetaCyc pathways. **(B)** The top 40 shared MetaCyc pathways from Venn diagram.

Comparative Metagenomic Analysis

Clinton Creek microbialite and sediment metagenomes are more functionally related to polar mats than microbialites isolated from marine or tropical ecosystems. Using SEED subsystem level III, PCA indicates better clustering to polar mats and sediments from the Arctic and Antarctica (**Figure 5**). The Clinton Creek samples cluster most closely Markham Ice shelf and Ward Hunt Ice shelf mats isolated from the Canadian High Arctic (**Figure 5**; Varin et al., 2012). Markham mats are functionally the most similar based on strong correlation to Clinton Creek microbialites based on SEED subsystem level III (**Figure 6**, $R^2 = 0.952$). Overall, polar mats (e.g., Markham, Ward Hunt, and McMurdo) had strong correlation of pathways in SEED than other ecosystems (**Figure 6**, $R^2 > 0.900$). Markham mats like Clinton Creek microbialites are dominated by Proteobacteria, and have Gemmatimonadetes present at 3% of the total 16S clones (Bottos et al., 2008). Polar mats, whether on microbialites or on ice shelves, appear to have functional gene similarities; this likely relates to handling shifts in temperature, including temperatures well below freezing (−10°C; Varin et al., 2012).

SEED based functional genes present in Clinton Creek microbialites were also analyzed across both freshwater microbialites from Cuatro Ciénegas and Highbourne Cay stromatolite metagenomes. Clinton Creek microbialites had weak correlations to Pozas Azules II metagenome (**Figure 6**, $R^2 = 0.702$), followed by Rio Mesquites (**Figure 6**, $R^2 = 0.633$), and Highbourne Cay stromatolite (**Figure 6**, $R^2 = 0.018$). Arctic polar mats had stronger correlations for SEED pathways than Cuatro Ciénegas microbialites and Highbourne Cay stromatolite metagenomes. Cuatro Ciénegas microbialites and Highbourne Cay are in tropical climates, which would remove many pathways related to cold-adaptation which are present in Clinton Creek and polar mats (Varin et al., 2012). The Highbourne Cay marine stromatolite had the lowest correlation of SEED functional gene classifications to Clinton Creek microbialites, which further suggests that marine microbialites differ from freshwater microbialites.

Clinton Creek samples were distinct from non-lithifying Octopus and Mushroom spring mats from Yellowstone (**Figure 5**). These data reveal that Clinton Creek microbialites are closely related to polar mats, due possibly to cold-adaptation, and differ greatly from tropical microbialites. This reveals that under the correct chemistry (e.g., alkaline pH, high DIC, and dissolved Ca^{2+} or Mg^{2+}), and with low numbers of metazoans, polar mats on ice shelves could have at least the metabolic potential to make microbialites.

Clinton Creek Geochemistry

The key chemical parameters with regard to $CaCO_3$ precipitation are pH, and concentrations of Ca^{2+} and DIC. These parameters influence the degree of saturation of a solution as given by the Saturation Index (SI), which is defined as $SI = \log(IAP/K_{sp})$, where the IAP is the Ion Activation Product and K_{sp} is the solubility product of a given mineral. Rates of mineral nucleation and precipitation are generally greater with increasing degree of saturation (De Yoreo and Vekilov, 2003). Speciation

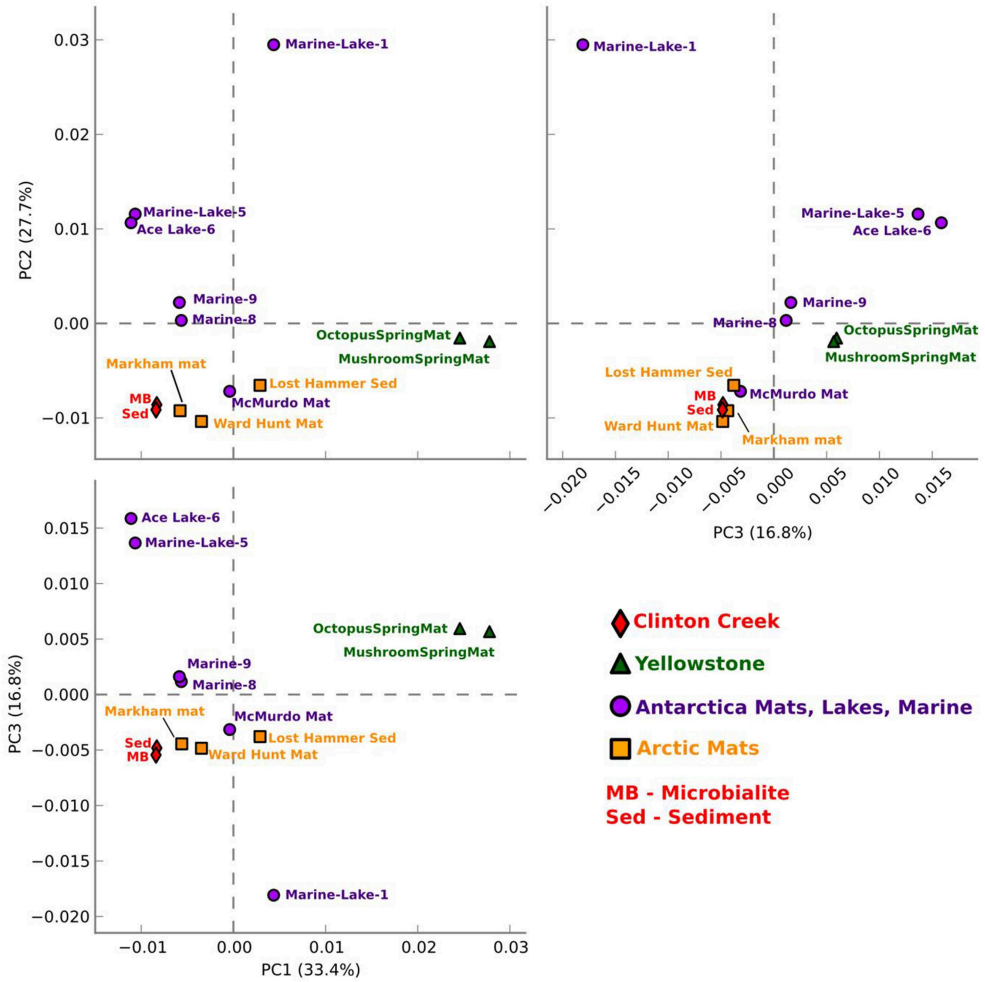

FIGURE 5 | Functional gene comparative PCA plot for Clinton Creek metagenomes. Based on ANOVA for multiple groups using SEED subsystem level III in STAMP.

calculations using PHREEQC (Parkhurst and Appelo, 1999) determined that the average SI for aragonite in the Clinton Creek open pit water is 0.6 vs. 0.72 for calcite of Pavilion Lake (Brady et al., 2009). This may explain the extremely rapid accretion rate in Clinton Creek, which is two orders of magnitude faster than Pavilion Lake microbialites (Brady et al., 2009), and one order faster than Highbourne Cay microbialites (Planavsky and Ginsburg, 2009). Given a similar $CaCO_3$ saturation index as Pavilion Lake, the relatively rapid formation of Clinton Creek microbialites cannot be explained by the bulk chemical parameters of the open pit water. Furthermore, the microbialites and surrounding sediments experience nearly the same environmental conditions (e.g., nutrient availability, bulk water chemistry, and lighting). Consequently, we are able to differentiate between the environmental and microbial controls on carbonate precipitation through a comparative analysis of the microbialites vs. the surrounding sediment using metagenomic analysis. The surrounding sediments do contain some aragonite (Power et al., 2011a); however, it is clear that carbonate precipitation rates are much faster in the microbialites given their greater abundance of aragonite. These finding suggest that microbialite formation in Clinton Creek is indeed driven by the local microbial community. Microbial metabolism is expected to significantly modify the water chemistry in the interstitial waters of the microbialites (Dupraz et al., 2009). On a geologic and even a human timescale, Clinton Creek microbialites are exceedingly young, and it may be that their rapid accretion rates will not extend into the future.

Our data suggest that polar mats have the metabolic potential to make microbialites under the correct chemical conditions. Further work is needed to definitively ascertain specific microbe influence in terms of the speed of microbialite formation. In the future, this may provide an avenue for us to engineer microbial communities to store atmospheric carbon through biolithification, especially given the recent, anthropogenic origin of the Clinton Creek site. Biogenic carbonate deposits are the largest reservoirs of carbon on Earth and could provide a cost-efficient method of carbon sequestration for greenhouse

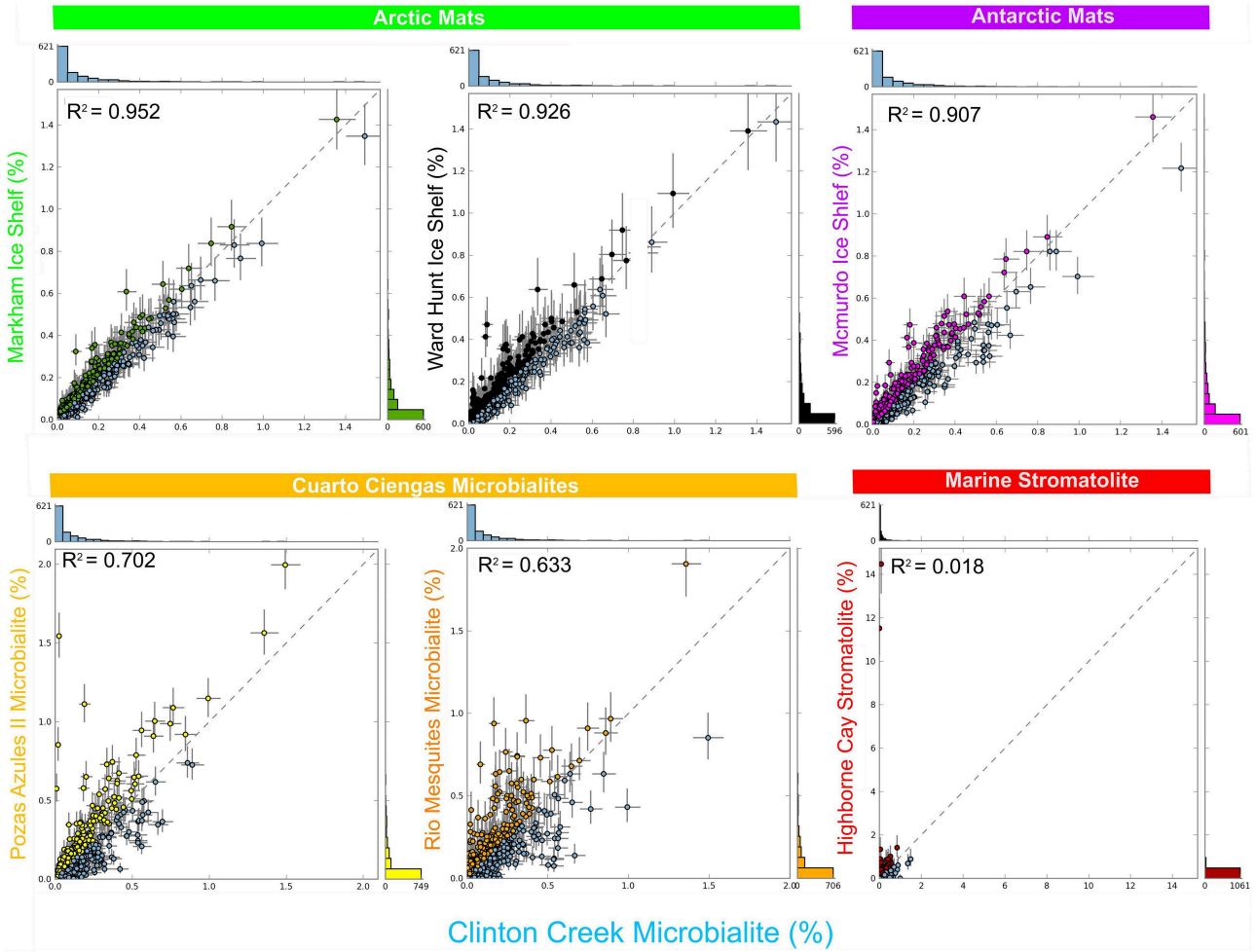

FIGURE 6 | Scatter plots of functional gene annotations using SEED subsystem level III. One sided G-test (w/Yates' + Fisher's) with asymptomatic confidence intervals (0.95) using Benjamini-Hochberg FDR procedure in STAMP. Each dot represents a unique functional classification gene.

gas emissions (Falkowski et al., 2000). Passive carbonation and carbon capture has been documented within the Clinton Creek mine tailings, leading to the proposition that microbially-mediated carbonate precipitation is a means to ameliorate carbon emissions from mining operations (Power et al., 2011a).

Conclusions

The northernmost microbialites known are located at subarctic Clinton Creek (Yukon, Canada). DNA from representative microbialites was extracted and directly sequenced, without bias from DNA amplification, and used to produce the largest set of assembled metagenomic data from a freshwater microbialite-forming ecosystem. The data revealed a high proportion of photosynthetic genes that were absent in the surrounding sediments, implying that microbialite formation is driven by photosynthesis-induced alkalinization, which is supported by 13C isotopic enrichment (Power et al., 2011b). Predicted metabolic pathways overlapped extensively between microbialite and sediment communities, particularly with respect to housekeeping genes; however, they have distinct core communities with microbialites dominated by Alphaproteobacteria (mainly anoxic phototrophs like Rhodobacterales) and sediments dominated by Gammaproteobacteria (mainly heterotrophic nitrogen-fixing *Pseudomonas* spp.).

While Clinton Creek microbialites shared some functional potential with microbialites from Cuatro Ciénegas, they shared far greater relation to Arctic mats (e.g., Markham and Ward Hunt), possibly due to cold-adaptation facilitated by long winters. The shared metabolic potential between Clinton Creek microbialites and polar mats from ice shelves, suggests that under favorable geochemical conditions, (e.g., alkaline pH, high DIC, and dissolved Ca^{2+} or Mg^{2+}), Arctic mats have the metabolic potential to form microbialites.

This study illustrates that cyanobacteria generate alkalinity and support heterotrophic communities, which have the potential to drive the formation of microbialites at Clinton Creek. Together, this suggests that an anthropogenic environment

can foster microbial communities capable of mediating carbonate precipitation, and that these microbes could offer an effective means of carbon sequestration (Power et al., 2011a,b). Microbially-mediated carbonate precipitation is an environmentally safe and novel process that could be harnessed to provide a cost-efficient strategy for the long-term storage of anthropogenic greenhouse gasses (e.g., CO_2).

Acknowledgments

We thank Sugandha Dandekar (Uma) and Hemani Wijesuriya (UCLA Sequencing & Genotyping Core Facility) and Frederick Robidoux (McGill/Genome Quebec) for high quality Illumina sequence data. We also thank Anna Harrison and Jenine McCutcheon for sampling and field logistics. Special thanks to Niels W. Hansen and Kishori M. Konwar for helping in parsing metapathways data outputs. Financial support was provided by Discovery Grants from the Natural Science and Engineering Council of Canada (NSERC) to CS and GD and for equipment grants from the Canadian Foundation for Innovation (CFI) and the British Columbia Knowledge Development Fund (BCKDF). IP was supported by an NSERC Postdoctoral Fellowship.

Supplementary Material

The Supplementary Material for this article can be found online at: http://journal.frontiersin.org/article/10.3389/fmicb.2015.00966

References

Allen, M. A., Goh, F., Burns, B. P., and Neilan, B. A. (2009). Bacterial, archaeal and eukaryotic diversity of smooth and pustular microbial mat communities in the hypersaline lagoon of Shark Bay. *Geobiology* 7, 82–96. doi: 10.1111/j.1472-4669.2008.00187.x

Andres, M. S., Sumner, D. Y., Reid, R. P., and Swart, P. K. (2006). Isotopic fingerprints of microbial respiration in aragonite from Bahamian stromatolites. *Geology* 34, 973–976. doi: 10.1130/G22859A.1

Arp, G., Reimer, A., and Reitner, J. (2001). Photosynthesis-induced biofilm calcification and calcium concentrations in Phanerozoic oceans. *Science* 292, 1701–1704. doi: 10.1126/science.1057204

Boisvert, S., Laviolette, F., and Corbeil, J. (2010). Ray:simultaneous assembly of reads from a mix of high-throughput sequencing technologies. *J. Comput. Biol.* 11, 1519–1533. doi: 10.1089/cmb.2009.0238

Boisvert, S., Raymond, F., Godzaridis, E., Laviolette, F., and Corbeil, J. (2012). Ray Meta: scalable de novo metagenome assembly and profiling. *Genome Biol.* 13:R122. doi: 10.1186/gb-2012-13-12-r122

Bosak, T., Greene, S. E., and Newman, D. K. (2007). A likely role for anoxygenic photosynthetic microbes in the formation of ancient stromatolites. *Proc. Natl. Acad. Sci. U.S.A.* 5, 119–126. doi: 10.1111/j.1472-4669.2007.00104.x

Bosak, T., Liang, B., Wu, T. D., Templer, S. P., Evans, A., Vali, H., et al. (2012). Cyanobacterial diversity and activity in modern conical microbialites. *Geobiology* 10, 384–401. doi: 10.1111/j.1472-4669.2012.00334.x

Bottos, E. M., Vincent, W. F., Greer, C. W., and Whyte, L. G. (2008). Prokaryotic diversity of arctic ice shelf microbial mats. *Environ. Microbiol.* 10, 950–966. doi: 10.1111/j.1462-2920.2007.01516.x

Brady, A. L., Slater, G., Laval, B., and Lim, D. S. (2009). Constraining carbon sources and growth rates of freshwater microbialites in Pavilion Lake using ^{14}C analysis. *Geobiology* 7, 544–555. doi: 10.1111/j.1472-4669.2009.00215.x

Braissant, O., Decho, A. W., Dupraz, C., Glunk, C., Przekop, K. M., and Visscher, P. T. (2007). Exopolymeric substances of sulfate-reducing bacteria: interactions with calcium at alkaline pH and implication for formation of carbonate minerals. *Geobiology* 5, 401–411. doi: 10.1111/j.1472-4669.2007.00117.x

Breitbart, M., Hoare, A., Nitti, A., Siefert, J., Haynes, M., Dinsdale, E., et al. (2009). Metagenomic and stable isotopic analyses of modern freshwater microbialites in Cuatro Ciénegas, Mexico. *Environ. Microbiol.* 11, 16–34. doi: 10.1111/j.1462-2920.2008.01725.x

Burne, R. V., and Moore, L. S. (1987). Microbialites: organosedimentary deposits of benthic microbial communities. *Palaios* 2, 241–254. doi: 10.2307/3514674

Burns, B. P., Goh, F., Allen, M., and Neilan, B. A. (2004). Microbial diversity of extant stromatolites in the hypersaline marine environment of Shark Bay, Australia. *Environ. Microbiol.* 6, 1096–1101. doi: 10.1111/j.1462-2920.2004.00651.x

Castanier, S., Le Metayer-Levrel, G., and Perthuisot, J. P. (1999). Ca-carbonates precipitation and limestone genesis the microbiogeologist point of view. *Sediment. Geol.* 126, 9–23. doi: 10.1016/S0037-0738(99)00028-7

Centeno, C. M., Legendre, P., Beltran, Y., Alcantara-Hernandez, R. J., Lidstrom, U. E., Ashby, M. N., et al. (2012). Microbialite genetic diversity and composition related to environmental variables. *FEMS Microbiol. Ecol.* 82, 724–735. doi: 10.1111/j.1574-6941.2012.01447.x

Chivas, A. R., Torgersen, T., and Polach, H. A. (1990). Growth rates and Holocene development of stromatolites from Shark Bay, Western Australia. *Aust. J. Earth Sci.* 37, 113–121. doi: 10.1080/08120099008727913

Couradeau, E., Benzerara, K., Moreira, D., Gérard, E., Kaźmierczak, J., Tavera, R., et al. (2011). Prokaryotic and eukaryotic community structure in field and cultured microbialites from the alkaline lake Alchichica (Mexico). *PLoS ONE* 6:e28767. doi: 10.1371/journal.pone.0028767

De Yoreo, J. J., and Vekilov, P. G. (2003). "Principles of crystal nucleation and growth," in *Biomineralization,* eds P. M. Dove and J. J. Deyoreo, and S. Weiner (Washington, WA: Mineralogical Soc America), 57–93.

Dupraz, C., Reid, R. P., Braissant, O., Decho, A. W., Norman, R. S., and Visscher, P. T. (2009). Processes of carbonate precipitation in modern microbial mats. *Earth Sci. Rev.* 96, 141–162. doi: 10.1016/j.earscirev.2008.10.005

Dupraz, C., and Visscher, P. T. (2005). Microbial lithification in marine stromatolites and hypersaline mats. *Trends Microbiol.* 13, 429–438 doi: 10.1016/j.tim.2005.07.008

Elser, J. J., Schampel, J. H., Kyle, M., Watts, J., Carson, E. W., Dowling, T. E., et al. (2005). Response of grazing snails to phosphorus enrichment of modern stromatolitic microbial communities. *Freshw. Biol.* 50, 1826–1835. doi: 10.1111/j.1365-2427.2005.01453.x

Falkowski, P., Scholes, R. J., Boyle, E., Canadell, J., Canfield, D., Elser, J., et al. (2000). The global carbon cycle: a test of our knowledge of earth as a system. *Science* 290, 291–296. doi: 10.1126/science.290.5490.291

Fender, J. E., Bender, C. M., Stella, N. A., Lahr, R. M., Kalivoda, E. J., and Shanks, R. M. (2012). *Serratia marcescens* quinoprotein glucose dehydrogenase activity mediates medium acidification and inhibition of prodigiosin production by glucose. *Appl. Environ. Microbiol.* 78, 6225–6235 doi: 10.1128/aem.01778-12

Ferris, F. G., Thompson, J. B., and Beveridge, T. J. (1997). Modern freshwater microbialites from Kelly Lake, British Columbia, Canada. *Palaios* 12, 213–219. doi: 10.2307/3515423

Gallagher, K. L., Kading, T. J., Braissant, O., Dupraz, C., and Visscher, P. T. (2012). Inside the alkalinity engine: the role of electron donors in the organomineralization potential of sulfate-reducing bacteria. *Geobiology* 10, 518–530. doi: 10.1111/j.1472-4669.2012.00342.x

Gischler, E., Gibson, M. A., and Oschmann, W. (2008). Giant Holocene freshwater microbialites, Laguna Bacalar, Quintana Roo, Mexico. *Sedimentology* 55, 1293–1309. doi: 10.1111/j.1365-3091.2007.00946.x

Goh, F., Allen, M. A., Leuko, S., Kawaguchi, T., Decho, A. W., Burns, B. P., et al. (2009). Determining the specific microbial populations and their spatial distribution within the stromatolite ecosystem of Shark Bay. *ISME J.* 3, 383–396. doi: 10.1038/ismej.2008.114

Grotzinger, J. P. (1990). Geochemical model for proterozoic stromatolite decline. *Am. J. Sci.* 290, 80–103.

Grotzinger, J. P., and Knoll, A. H. (1999). Stromatolites in Precambrian carbonates: evolutionary mileposts or environmental dipsticks? *Ann. Rev. Earth Planet. Sci.* 27, 313–358. doi: 10.1146/annurev.earth.27.1.313

Havemann, S. A., and Foster, J. S. (2008). Comparative characterization of the microbial diversities of an artificial microbialite model and a natural stromatolite. *Appl. Environ. Microbiol.* 74, 7410–7421. doi: 10.1128/AEM.01710-08

Htoon, M. (1979). "Geology of the Clinton Creek asbestos deposit, Yukon Territory," in *Department of Earth and Ocean Sciences* (Vancouver: University of British Columbia). Available online at: http://circle.ubc.ca/handle/2429/21374

Jimenez-Lopez, C., Chekroun, K. B., Jroundi, F., Rodríguez-Gallego, M., Arias, J. M., and González-Muñoz, M. T. (2011). *Myxococcus xanthus* colony calcification: A study to better understand the processes involved in the formation of this stromatolite-like structure. *Adv. Strom. Geobiol.* 131, 161–181. doi: 10.1007/978-3-642-10415-2_11

Khodadad, C. L., and Foster, J. S. (2012). Metagenomic and metabolic profiling of nonlithifying and lithifying stromatolitic mats of Highborne Cay, The Bahamas. *PLoS ONE* 7:e38229. doi: 10.1371/journal.pone.0038229

Kiełbasa, S. M., Wan, R., Sato, K., Horton, P., and Frith, M. C. (2011). Adaptive seeds tame genomic sequence comparison. *Genome Res.* 3, 487–493. doi: 10.1101/gr.113985.110

Konwar, K. M., Hanson, N. W., Pagé, A. P., and Hallam, S. J. (2013). MetaPathways: a modular pipeline for constructing pathway/genome databases from environmental sequence information. *BMC Bioinform.* 14:202. doi: 10.1186/1471-2105-14-202

Laval, B., Cady, S. L., Pollack, J. C., McKay, C. P., Bird, J. S., Grotzinger, J. P., et al. (2000). Modern freshwater microbialite analogues for ancient dendritic reef structures. *Nature* 407, 626–629. doi: 10.1038/35036579

Lightfield, J., Fram, N. R., and Ely, B. (2011). Across bacterial phyla, distantly-related genomes with similar genomic GC content have similar patterns of amino acid usage. *PLoS ONE* 6:e17677. doi: 10.1371/journal.pone.0017677

Lim, D. S. S., Laval, B. E., Slater, G., Antoniades, D., Forrest, A. L., Pike, W., et al. (2009). Limnology of Pavilion Lake, B.C., Canada—Characterization of a microbialite forming environment. *Fundam. Appl. Limnol.* 173, 329–351. doi: 10.1127/1863-9135/2009/0173-0329

López-García, P., Kazmierczak, J., Benzerara, K., Kempe, S., Guyot, F., and Moreira, D. (2005). Bacterial diversity and carbonate precipitation in the giant microbialites from the highly alkaline Lake Van, Turkey. *Extremophiles* 9, 263–274. doi: 10.1007/s00792-005-0457-0

Ludwig, R., Al-Horani, F. A., de Beer, D., and Jonkers, H. M. (2005). Photosynthesis-controlled calcification in a hypersaline microbial mat. *Limnol. Oceanogr.* 50, 1836–1843. doi: 10.4319/lo.2005.50.6.1836

Lundberg, J., and McFarlane, D. A. (2011). Subaerial freshwater phosphatic stromatolites in Deer Cave, Sarawak—A unique geobiological cave formation. *Geomorphology* 128, 57–72. doi: 10.1016/j.geomorph.2010.12.022

Maliva, G. R., Missimer, M. T., Leo, C. K., Statom, A. R., Dupraz, C., Lynn, M., et al. (2000). Unusual calcite stromatolites and pisoids from a landfill leachate collection system. *Geology* 28, 931–934. doi: 10.1130/0091-7613(2000)28<931:UCSAPF>2.0.CO;2

McCutcheon, J., Power, I. M., Harrison, A. L., Dipple, G. M., and Southam, G. (2014). A greenhouse-scale photosynthetic microbial bioreactor for carbon sequestration in magnesium carbonate minerals. *Environ. Sci. Technol.* 48, 9142–9151. doi: 10.1021/es500344s

Meyer, F. D., Paarmann, M., D'Souza, R., Olson, E. M., Glass, M., Kubal, T., et al. (2008). The Metagenomics RAST server - A public resource for the automatic phylogenetic and functional analysis of metagenomes. *BMC Bioinformatics* 9:386. doi: 10.1186/1471-2105-9-386

Miyazaki, T., Sugisawa, T., and Hoshino, T. (2006). Pyrroloquinoline quinone-dependent dehydrogenases from Ketogulonicigenium vulgare catalyze the direct conversion of L-sorbosone to L-ascorbic acid. *Appl. Environ. Microbiol.* 72, 1487–1495. doi: 10.1128/AEM.72.2.1487-1495.2006

Mobberley, J. M., Khodadad, C. L., and Foster, J. S. (2013). Metabolic potential of lithifying cyanobacteria-dominated thrombolitic mats. *Photosyn. Res.* 118, 125–140. doi: 10.1007/s11120-013-9890-6

Omelon, C. R., Brady, A. L., Slater, G. F., Laval, B., Lim, D. S. S., and Southam, G. (2013). Microstructure variability in freshwater microbialites, Pavilion Lake, Canada. *Paleogeogr. Paleoclimatol. Paleoecol.* 392, 62–70. doi: 10.1016/j.palaeo.2013.08.017

Papineau, D., Walker, J. J., Mojzsis, S. J., and Pace, N. R. (2005). Composition and structure of microbial communities from stromatolites of Hamelin Pool in Shark Bay, Western Australia. *Appl. Environ. Microbiol.* 71, 4822–4832. doi: 10.1128/AEM.71.8.4822-4832.2005

Parkhurst, D. L., and Appelo, C. A. J. (1999). *User's Guide to PHREEQC (version 2) A Computer Program for Speciation, Batch Reaction, One-dimensional Transport, and Inverse Geochemical Calculations: U.S., Geological Survey Water-Resources Investigations Report*, 99–4259.

Parks, D. H., and Beiko, R. G. (2010). Identifying biologically relevant differences between metagenomic communities. *Bioinformatics* 26, 715–721. doi: 10.1093/bioinformatics/btq041

Perry, R. S., Mcloughlin, N., Lynne, B. Y., Sephton, M. A., Oliver, J. D., Perry, C. C., et al. (2007). Defining biominerals and organominerals: direct and indirect indicators of life. *Sed. Geol.* 201, 157–179. doi: 10.1016/j.sedgeo.2007.05.014

Planavsky, N., and Ginsburg, R. N. (2009). Taphonomy of modern marine Bahamian microbialites. *Palaios* 24, 5–17. doi: 10.2110/palo.2008.p08-001r

Power, I. M., Wilson, S. A., Dipple, G. M., and Southam, G. (2011a). Modern carbonate microbialites from an asbestos open pit pond, Yukon, Canada. *Geobiology* 9, 180–195. doi: 10.1111/j.1472-4669.2010.00265.x

Power, I. M., Wilson, S. A., Small, D. P., Dipple, G. M., Wan, W., and Southam, G. (2011b). Microbially mediated mineral carbonation: roles of phototrophy and heterotrophy. *Environ. Sci. Technol.* 45, 9061–9068. doi: 10.1021/es201648g

Reid, R. P., Visscher, P. T., Decho, A. W., Stolz, J. F., Bebout, B. M., Dupraz, C., et al. (2000). The role of microbes in accretion, lamination and early lithification of modern marine stromatolites. *Nature* 406, 989–999. doi: 10.1038/35023158

Rho, M., Tang, H., and Ye, Y. (2010). FragGeneScan: predicting genes in short and error-prone reads. *Nucleic Acids Res.* 38, e191. doi: 10.1093/nar/gkq747

Riding, R. (2011). "Microbialites, Stromatolites, and Thrombolites," in *Encyclopedia of Geobiology, Encyclopedia of Earth Sciences Series*, eds J. Reitner and V. Thiel (Heidelberg: Springer), 635–654.

Russell, J. A., Brady, A. L., Cardman, Z., Slater, G. F., Lim, D. S. S., and Biddle, J. F. (2014). Prokaryote populations of extant microbialites along a depth gradient in Pavilion Lake, British Columbia, Canada. *Geobiology* 3, 250–264. doi: 10.1111/gbi.12082

Santos, F., Peña, A., Nogales, B., Soria-Soria, E., del Cura, M. A., González-Martín, J. A., et al. (2010). Bacterial diversity in dry modern freshwater stromatolites from Ruidera Pools Natural Park, Spain. *Syst. Appl. Microbiol.* 33, 209–221. doi: 10.1016/j.syapm.2010.02.006

Schopf, J. W. (2006). Fossil evidence of Archean life. *Phil. Trans. R. Soc. B.* 361, 869–885. doi: 10.1098/rstb.2006.1834

Schultze-Lam, S., Fortin, D., Davis, B. S., and Beveridge, T. J. (1996). Mineralization of bacterial surfaces. *Chem. Geol.*, 132, 171–181. doi: 10.1016/S0009-2541(96)00053-8

Slaughter, M., and Hill, R. J. (1991).The influence of organic matter in organogenic dolomitization. *J. Sediment. Petrol.* 61, 296–303. doi: 10.1306/D42676F9-2B26-11D7-8648000102C1865D

Spanos, N., and Koutsoukos, P. G. (1998). Kinetics of precipitation of calcium carbonate in alkaline pH at constant supersaturation. Spontaneous and seeded growth. *J. Phys. Chem. B* 102, 6679–6684. doi: 10.1021/jp981171h

Suzuki, R., and Shimodaira, H. (2006). Pvclust: an R package for assessing the uncertainty in hierarchical clustering. *Bioinformatics* 22, 1540–1542. doi: 10.1093/bioinformatics/btl117

Tesson, B., Gaillard, C., and Martin-Jézéquel, V. (2008). Brucite formation mediated by the diatom Phaeodactylum tricornutum. *Mar. Chem.* 109, 60–76. doi: 10.1016/j.marchem.2007.12.005

Thompson, J. B., and Ferris, F. G. (1990). Cyanobacterial precipitation of gypsum, calcite, and magnesite from natural alkaline lake water. *Geology* 18, 995–998.

Van Lith, Y., Vasconcelos, C., Warthmann, R., and McKenzie, J. A. (2003).Microbial fossilization in carbonate sediments; a result of thebacterial surface involvement in carbonate precipitation. *Sedimentology* 50, 237–245. doi: 10.1046/j.1365-3091.2003.00550.x

Varin, T., Lovejoy, C., Jungblut, A. D., Vincent, W. F., and Corbeil, J. (2012). Metagenomic analysis of stress genes in microbial mat communities from

Antarctica and the High Arctic. *Appl. Environ. Microbiol.* 78, 549–559. doi: 10.1128/AEM.06354-11

Von Knorre, H., and Krumbein, W. E. (2000). "Bacterial calcification," in *Microbial Sediments,* eds R. E. Riding and S.M. Awramik (Berlin: Springer), 25–31.

White, R. A. III., Blainey, P. C., Fan, H. C., and Quake, S. R. (2009). Digital PCR provides sensitive and absolute calibration for high throughput sequencing. *BMC Genomics* 10:116. doi: 10.1186/1471-2164-10-116

White, R. A. III., Grassa, C. J., and Suttle, C. A. (2013a). First draft genome sequence from a member of the genus *Agrococcus*, isolated from modern microbialites. *Genome Announc.* 1, e00391–e00313. doi: 10.1128/genomeA.00391-13

White, R. A. III., Grassa, C. J., and Suttle, C. A. (2013b). Draft genome sequence of *Exiguobacterium pavilionensis* strain RW-2, with wide thermal, salinity, and pH tolerance, isolated from modern freshwater microbialites. *Genome Announc.* 1, e00597–e00513. doi: 10.1128/genomeA.00597-13

White, R. A. III., and Suttle, C. A. (2013). The Draft Genome Sequence of *Sphingomonas paucimobilis* Strain HER1398 (Proteobacteria), Host to the Giant PAU Phage, indicates that it is a member of the genus *Sphingobacterium* (Bacteroidetes). *Genome Announc.* 1, e00598–e00513. doi: 10.1128/genomeA.00598-13

Wickham, H. (2009). *ggplot2: Elegant Graphics for Data Analysis*. New York, NY: Springer.

Wilson, S. A., Dipple, G. M., Power, I. M., Thom, J. M., Anderson, R. G., Raudsepp, M., et al. (2009). Carbon dioxide fixation within mine wastes of ultramafic-hosted ore deposits: examples from the Clinton Creek and Cassiar chrysotile deposits, Canada. *Econ. Geol.* 104, 95–112. doi: 10.2113/gsecongeo.104.1.95

Wu, S., and Zhu, Y. (2012). ProPAS: standalone software to analyze protein properties. *Bioinformation* 8, 167–169. doi: 10.6026/97320630008167

Conflict of Interest Statement: The authors declare that the research was conducted in the absence of any commercial or financial relationships that could be construed as a potential conflict of interest.

frontiers in Microbiology

ORIGINAL RESEARCH
published: 28 January 2016
doi: 10.3389/fmicb.2015.01531

Metagenomic Analysis Suggests Modern Freshwater Microbialites Harbor a Distinct Core Microbial Community

*Richard Allen White III[1†], Amy M. Chan[2], Gregory S. Gavelis[3], Brian S. Leander[3,4], Allyson L. Brady[5], Gregory F. Slater[5], Darlene S. S. Lim[6,7] and Curtis A. Suttle[1,2,4,8]**

[1] Department of Microbiology and Immunology, University of British Columbia, Vancouver, BC, Canada, [2] Department of Earth, Ocean and Atmospheric Sciences, University of British Columbia, Vancouver, BC, Canada, [3] Department of Zoology, University of British Columbia, Vancouver, BC, Canada, [4] Department of Botany, University of British Columbia, Vancouver, BC, Canada, [5] School of Geography and Earth Sciences, McMaster University, Hamilton, ON, Canada, [6] Bay Area Environmental Institute, Petaluma, CA, USA, [7] NASA Ames Research Center, Moffett Field, CA, USA, [8] Canadian Institute for Advanced Research, Toronto, ON, Canada

OPEN ACCESS

Edited by:
John J. Kelly, Loyola University Chicago, USA

Reviewed by:
Zhenfeng Liu, University of Southern California, USA
Anas Ghadouani, The University of Western Australia, Australia

***Correspondence:**
Curtis A. Suttle, Department of Earth, Ocean and Atmospheric Sciences, University of British Columbia, 2020-2207 Main Mall, Vancouver, BC V6T 1Z4, Canada
suttle@science.ubc.ca

†Present address:
Richard Allen White III, Fundamental and Computational Sciences, Pacific Northwest National Laboratories, Richland, WA, USA

Specialty section:
This article was submitted to Aquatic Microbiology, a section of the journal Frontiers in Microbiology

Received: *12 January 2015*
Accepted: *21 December 2015*
Published: *28 January 2016*

Citation:
White RA III, Chan AM, Gavelis GS, Leander BS, Brady AL, Slater GF, Lim DSS and Suttle CA (2016) Metagenomic Analysis Suggests Modern Freshwater Microbialites Harbor a Distinct Core Microbial Community. Front. Microbiol. 6:1531. doi: 10.3389/fmicb.2015.01531

Modern microbialites are complex microbial communities that interface with abiotic factors to form carbonate-rich organosedimentary structures whose ancestors provide the earliest evidence of life. Past studies primarily on marine microbialites have inventoried diverse taxa and metabolic pathways, but it is unclear which of these are members of the microbialite community and which are introduced from adjacent environments. Here we control for these factors by sampling the surrounding water and nearby sediment, in addition to the microbialites and use a metagenomics approach to interrogate the microbial community. Our findings suggest that the Pavilion Lake microbialite community profile, metabolic potential and pathway distributions are distinct from those in the neighboring sediments and water. Based on RefSeq classification, members of the *Proteobacteria* (e.g., alpha and delta classes) were the dominant taxa in the microbialites, and possessed novel functional guilds associated with the metabolism of heavy metals, antibiotic resistance, primary alcohol biosynthesis and urea metabolism; the latter may help drive biomineralization. Urea metabolism within Pavilion Lake microbialites is a feature not previously associated in other microbialites. The microbialite communities were also significantly enriched for cyanobacteria and acidobacteria, which likely play an important role in biomineralization. Additional findings suggest that Pavilion Lake microbialites are under viral selection as genes associated with viral infection (e.g CRISPR-Cas, phage shock and phage excision) are abundant within the microbialite metagenomes. The morphology of Pavilion Lake microbialites changes dramatically with depth; yet, metagenomic data did not vary significantly by morphology or depth, indicating that microbialite morphology is altered by other factors, perhaps transcriptional differences or abiotic conditions. This work provides a comprehensive metagenomic perspective of the interactions and differences between microbialites and their surrounding environment, and reveals the distinct nature of these complex communities.

Keywords: microbialites, Pavilion Lake, metagenomics, thrombolites, metabolic potential

INTRODUCTION

Microbialites are a specialized group of microbial mats that lithify carbonate-rich structures, and include thrombolites that consist of structures with unlaminated clots and stromatolites that have laminated layers (Burne and Moore, 1987; Perry et al., 2007). Fossil evidence points to microbialites being representative of the oldest known persistent ecosystems (Grotzinger and Knoll, 1999; Schopf, 2006). They are an unparalleled system in which to investigate biochemical cycling that may be representative of the earliest known complex microbial communities (Dupraz et al., 2009).

Microbialites are globally distributed, and can be found in marine (Reid et al., 2000; Burns et al., 2004; Khodadad and Foster, 2012; Mobberley et al., 2013), freshwater (Ferris et al., 1997; Laval et al., 2000; Gischler et al., 2008; Breitbart et al., 2009; Couradeau et al., 2011), hypersaline (Allen et al., 2009; Goh et al., 2009), hot spring (Bosak et al., 2012), and remnant mining (Power et al., 2011) environments. To a lesser extent, they have also colonized terrestrial environments, such as landfill soils (Maliva et al., 2000) and caves (Lundberg and McFarlane, 2011). These microbial communities thrive at the intersection of abiotic and biotic factors that promote organosedimentation (Dupraz and Visscher, 2005; Dupraz et al., 2009).

A host of biological factors are favorable to microbialite formation, such as the presence of exopolysaccaride (EPS)-rich cyanobacterial mats, which serve as a location of mineral nucleation and provide a heterotrophic microenvironment favorable for organomineralization via dissimilatory sulfate reduction (Dupraz and Visscher, 2005; Dupraz et al., 2009). Cyanobacterial photosynthetic activity increases pH in the surrounding geochemical environment, promoting precipitation by raising the calcium carbonate saturation index critical to the formation process of microbialites (e.g., Merz, 1992; Dupraz et al., 2009). Microbialites have been purported to form via carbonate precipitation by the benthic community, as well as by trapping detritus from sediment and the overlying water column (Burne and Moore, 1987; Dupraz and Visscher, 2005).

Despite the apparent reliance of microbialites on biotic input from the surrounding environment, there is currently a scarcity of data comparing microbialite communities with those of the sediments or water. Such a comparison allows for the identification of microbialite-specific components that may not be obvious when examining microbialite communities in isolation. Exploring the genetic differences between microbialite communities and those in the surrounding habitats requires identifying the relative abundance of taxa and their metabolic potential. To avoid distorting these ratios, DNA was extracted and unlike in other metagenomic studies of microbialites (Breitbart et al., 2009), sequenced without amplification.

Many studies have focused on examining the abundance and diversity of freshwater microbialites using 16S rDNA sequencing but few metagenomic studies exist. Diversity studies using 16S rDNA amplicons on freshwater microbialites include Lake Van (López-García et al., 2005), Lake Alchichica (Couradeau et al., 2011), Cuatro Ciénegas (Centeno et al., 2012), Pavilion Lake (Chan et al., 2014; Russell et al., 2014), and Ruidera Pools (Santos et al., 2010). While 16S rDNA sequencing is able to obtain the relative abundance of taxa and diversity of taxa; it is unable to capture the metabolic potential or the functional gene abundance of an ecosystem. Metabolic and functional potential obtained by metagenomics allow for functional gene inventories which can be used as databases for further investigations using other omics (e.g., metaproteomics) (Cantarel et al., 2011). Prior metagenomics studies on microbialites have focused primarily on marine environments (Khodadad and Foster, 2012; Mobberley et al., 2013; Ruvindy et al., 2015) with the exception of one tropical freshwater system (Breitbart et al., 2009) and one subarctic abandoned open pit mine (White III et al., 2015). In this study, we sequenced total genomic DNA from cold temperate freshwater microbialites, as well as from the nearby sediment and water, to identify constituent taxa and infer their metabolic functional potential.

Sampling was conducted in Pavilion Lake, in southeastern British Columbia, Canada (50.8°N, 121.7°W). The lake is dimictic, circumneutral (median pH 8.3; mean calcium carbonate, 182 mg L^{-1}), and oligotrophic (mean total phosphorus, 3.3 $\mu g\ L^{-1}$). Further limnological details of Pavilion Lake are given in Lim et al. (2009). The microbialites are primarily calcite thrombolites, covered in a thin (∼5 mm) microbial mat, that change in morphotype with depth; at ∼10 m they resemble shallow domes, at ∼20 m they resemble cabbage heads, at 25 m they consist of conical outcroppings, and at deeper depths they possess mound structures (**Figure 1**; Laval et al., 2000). However, whether morphological changes in the microbialites are associated with changes in community structure or metabolic potential is not well constrained.

Data suggest that photosynthetically induced alkalinization is a major driver of recent carbonate precipitation in shallow Pavilion Lake microbialites (Brady et al., 2010). Two recent 16S studies of Pavilion Lake microbialites indicated that cyanobacteria, including members of the genera *Acaryochloris*, *Leptolyngbya*, *Microcoleus*, and *Pseudanabaena*, are dominant oxygenic photoautotrophic members (Chan et al., 2014; Russell et al., 2014). Moreover, elevated O_2 concentrations, pH and $\delta^{13}C$ carbonate values within surface microbial mats and cyanobacterial rich nodules from microbialites at < 20 m depth indicate photosynthetic influence on carbonate that is being precipitated (Brady et al., 2010, 2014). Whether biomineralization in this system is strictly a photosynthetic process or a mixture of heterotrophic and photosynthetic processes remains unconstrained.

In addition to challenges associated with elucidating the role of bacteria and eukarya in the formation of microbialite structures, the role of viruses in microbialite communities has remained elusive. Viruses are the most prevalent "organisms" on Earth, with an estimated 10^{30} viruses in the ocean (Suttle, 2005). Through cell lysis, they play a role in carbon cycling on a global scale (Suttle, 2005). Metagenomic data for the viral fraction have been published for marine (e.g., Highbourne Cay) and freshwater microbialites (e.g., Cuatro Cienegás) (Desnues et al., 2008). However, because the surrounding water and sediments were not sampled, it is unclear whether the viral taxa were

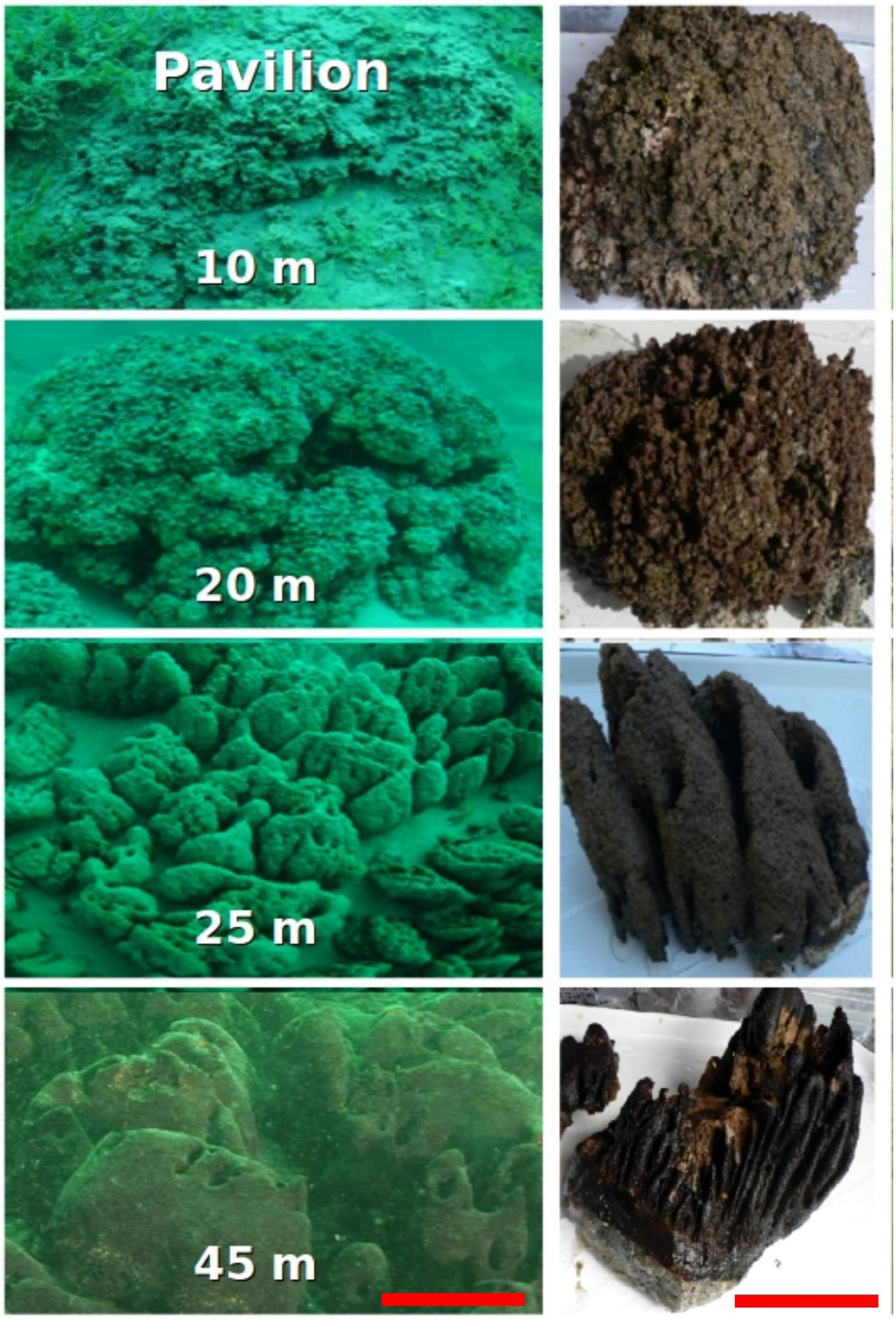

FIGURE 1 | Pavilion Lake microbialite morphology as a function of sampling depth in meters. The scale bar is ~1 m **(left)** and ~15 cm **(right)**.

specifically associated with the microbialites, or were derived from the surrounding environments.

In this contribution, a metagenomic approach was used to uncover the metabolic potential that is specifically associated with microbialites. We examine the novel metabolic potential associated with Pavilion Lake microbialites and investigate whether metabolic potential, not solely taxa, changes as a function of microbialite morphology. We also explore

whether heterotrophic or phototrophic pathways dominate the microbialite functional metabolic potential in association with carbonate precipitation, and examine virus-host whole community interactions. As well, we address the question of whether the microbialite communities are distinct from those found in other microbialite systems and in the adjacent water and sediment.

MATERIALS AND METHODS

Sample Collection

Samples were collected from Pavilion Lake (50.86°N, 121.74°W) during the summers of 2010 and 2011. Triplicate representative microbialites (∼10 kg), were recovered from each collection site (Lim et al., 2011) either by SCUBA divers along a transect [Three Poles (TP) site: 10, 20, 25 m] or by manned DeepWorker submersible (Deep mound site: 45 m; 2010) (Nuytco Research Ltd., North Vancouver, BC, Canada). Diver collected microbialites were placed into separate plastic bags and brought to the surface, whereas DeepWorker samples were collected by a robotic arm and placed into a basket before transport to the surface.

Sediment samples, adjacent to the microbialites (∼20 g of the surface layer; 10, 20, 25 m depths; 2011) were collected into sterile bottles at the same time by divers. At the lake surface, microbialite and sediment samples were immediately placed into insulated containers filled with cold lakewater to maintain *in situ* temperatures until samples were processed. At the field lab, each microbialite was weighed, documented and apportioned for molecular analysis. Replicate sediment samples were pelleted by centrifugation (5000 × *g*). The overlying lakewater was removed and the sediment pellets flash frozen in liquid nitrogen and transported back to the lab in a liquid nitrogen vapor shipper for downstream processing.

Water adjacent to the microbialites (∼100 L) was collected from each depth using a Niskin water sampler (2010) or a diver guided hose at the collection site that was connected to a piston-pump in a boat (2011). Surface water samples (∼1 m depth) were collected using a submersible pump. Each water sample was filtered in series through 120-μm pore-size Nitex® screening to remove large plankton, and 1.2-μm pore-size glass-fiber, followed by 0.45 and 0.22-μm pore-size Durapore polyvinylidene difluoride (PVDF) filters (Millipore, Bedford, MA, USA) (Suttle et al., 1991). Filters were frozen in the field and transported back to the lab in a liquid nitrogen vapor shipper.

DNA Extraction

To sample the microbialite associated microbial communities, a sterile razor blade was used to scrape off 3 to 10 mm (∼5 g) across the surface of three morphologically similar microbialites collected at each depth. DNA was extracted on-site using a PowerMax® Soil DNA Isolation Kit (Mobio, Carlsbad, CA, USA) then flash frozen in liquid nitrogen. Replicate microbialite scrapings were placed into sterile jars and frozen on-site in liquid nitrogen. Frozen samples were transported back to the lab in a liquid nitrogen vapor shipper and stored at −80°C until needed. DNA from frozen samples were extracted using cetyl trimethyl ammonium bromide (CTAB; Untergasser, 2008).

To ascertain the microbial community from the water column (size fraction between 0.2 and 120-μm), DNA was extracted from half of each glass-fiber, 0.45 and 0.22-μm pore-size filter using a PowerWater® DNA Isolation Kit (Mobio, Carlsbad, CA, USA). DNA was extracted from the other half of each filter using the CTAB method (Untergasser, 2008).

Sediment DNA was extracted from triplicate subsamples (∼5 g) using a PowerMax® Soil DNA Isolation Kit (Mobio, Carlsbad, CA, USA). Replicate sediment pellets were also extracted using the CTAB method. Two DNA extraction methods were employed for all samples to minimize extraction biases.

DNA concentrations were determined on-site using a Nanodrop-3300 micro-fluorospectrometer and the Quant-iT™ PicoGreen® dsDNA Assay Kit (ThermoFisher, Wilmington, DE, USA). Nucleic acid quality was determined by absorbance (260/280 and 260/230) using a Nanodrop-1000 (ThermoFisher, Wilmington, DE). CTAB and MoBio DNA extractions were pooled (50:50) by equivalent DNA to reduce extraction bias and then used for library construction.

Metagenomic Library Preparation: 454 FLX Titanium and Illumina HiSeq/MiSeq

Libraries for 454 FLX Titanium sequencing were constructed using random DNA shearing with a Bioruptor (Diagenode Denville, NJ, USA). Fragments were polished and blunt-end ligated (NEBNext DNA Library Prep Kit, New England Biolabs, Ipswich, MA, USA) to in-house Multiplex Identifier barcode oligos (IDT, Coralville, IA, USA), with small fragments removed by magnetic beads (Beckman Coulter, Danvers, MA, USA). The libraries were quantified using a digital PCR quantified standard curve (White III et al., 2009), diluted, and pooled for 454 pyrosequencing with Titanium chemistry (The Centre for Applied Genomics, SickKids Hospital, Toronto, ON, Canada).

For Illumina library construction, DNA was sheared by ultrasonication (Covaris M220 series, Woburn, MA, USA), and the fragments end-paired, A-tailed (NxSeq DNA Sample Prep Kit, Lucigen, Middleton, WI, USA) and ligated to TruSeq adapters (IDT, Coralville, IA, USA); small fragments were removed twice using magnetic beads (Beckman Coulter, Danvers, MA). The resulting libraries were pooled, and sequenced using both 250 bp and 100 bp paired-end sequencing on the MiSeq (UCLA Genotyping & Sequencing Core, Los Angeles, CA, USA) and HiSeq (McGill University and Génome Québec Innovation Centre, Montreal, QC, Canada) platforms, respectively.

Metagenomic Data Assembly and Analysis

The raw sequencing data were processed as follows. For the 454 data, the raw SFF files were converted to FASTQ format and binned by molecular barcode (MID) using a custom Perl script. Barcodes were removed by Tagcleaner (Schmieder et al., 2010) and sequences cleaned for low quality and homopolymers using PRINSEQ (Schmieder and Edwards, 2011). The Illumina data were extracted and demultiplexed using the CASAVA pipeline

v1.8 (Illumina, San Diego, CA, USA), and the PhiX spike-in used for sequencing quality control was screened using Bowtie2 (version 2.1.0; Langmead and Salzberg, 2012) then removed using Picard tools[1] (version 1.90; White III and Suttle, 2013; White III et al., 2013a,b).

The resulting 454 FLX titanium reads, Illumina overlapping merged reads and Illumina non-overlapping reads from replicate libraries were combined and assembled (kmer size: 39) using the Ray DeNovo assembler (Boisvert et al., 2010, 2012). Illumina sequencing compensates for the error-prone homopolymers of 454, while 454 compensates for Illumina's GC bias and substitution errors (Bentley et al., 2008). A hybrid of the two technologies provides a lower chance of obtaining the same sequencing error and results in higher quality assembly at lower cost (Aury et al., 2008). In total, 446 Mbp and 17 Mbp of assembled contigs were obtained from the microbialites and filters (**Table 1**), respectively. Surface (∼1 m) and 10 m water metagenomic reads were pooled at assembly step to yield >15 k contigs for further comparison. Sediment metagenomic data (84 Mbp in total) resulted in a low numerical (<15 k) yield of contigs; hence, the unassembled paired-end reads were extended for overlap and pooled with unextended reads for further analysis (**Table 1**). Metagenomic rapid annotations using MG-RAST were used for contig annotation (Meyer et al., 2008). MG-RAST annotation of the contigs used BLAT (BLAST-like alignment tool) annotations based on hierarchical classification against SEED subsystems[2] and RefSeq databases[3] with a minimum *E*-value cutoff of 10^{-5}, a minimum percent identity cutoff of 60%, and a minimum alignment length cutoff of 50 base pairs.

MetaCyc[4] annotations were provided by MetaPathways, a modular pipeline for gene prediction and annotation that uses pathway tools and the MetaCyc database to construct environmental pathway/genome databases (ePGBDs; Konwar et al., 2013). Metapathways using the LAST (local alignment search tool) for annotations of ORFs with a minimum of 180 bp and minimum alignment length cutoff of 50 bp (Kiełbasa et al., 2011). MetaCyc pathway comparison Venn diagrams were based on normalized pathway size and number of open reading frames (ORFs) associated with each pathway using R, then plotted using ggplot2 (Wickham, 2009).

Statistical analysis was completed using statistical analysis of metagenomic profiles (STAMP) and R (Parks and Beiko, 2010; R Development Core Team, 2015). STAMP and R were used to parse MG-RAST data for RefSeq (class level) and SEED subsystems (level I to function) results. The STAMP ANOVAs (including Principal Component Analysis, PCA) were completed using multiple groups, *post-hoc* tests (Tukey-Kramer at 0.95), an effect size (Eta-squared) and multiple test correction using Benjamini-Hochberg FDR (false discovery rate) procedure. The RefSeq and SEED classifications were normalized for each sample using count-relative abundances and total ORFs obtained per metagenome. PCA for the normalized RefSeq and SEED classifications used R libraries Ecodist (Dissimilarity-based functions for ecological analysis), and pvclust (Hierarchical Clustering with *P*-values via Multiscale Bootstrap Resampling) using ward clustering and the Bray-Curtis distance matrix at a thousand replicates (Suzuki and Shimodaira, 2006). The PCA for the normalized RefSeq and SEED classifications were plotted using R libraries ggplot2 and a dotplot was created using R libraries Reshape2, using the melt function, then plotted using ggplot2 (Wickham, 2009).

Metagenomic Data Depositing

All the data used in this study is freely available from MG-RAST[5]. The data is deposited in the project name Pavilion Lake surrounding environment as PLsfcFil (ID 4532785.3), PL20Fil (ID 4532783.3), PL45Fil (ID 4532784.3), PLMB10 (ID 4532771.3), PLMB20 (ID 4532772.3), PLMB25 (ID 4532774.3), PLMB45 (ID 4532775.3), PL10Sed (ID 4526738.3), PL20Sed (ID 4526739.3), and PL25Sed (ID 4526740.3).

RESULTS AND DISCUSSION

Microbialite Communities Differ from the Surrounding Environment Communities

The microbial community structure and metabolic potential of Pavilion Lake microbialites were statistically different from those in the surrounding environment (e.g., water and sediment metagenomes), based on principle component analyses of RefSeq taxonomic classifications (**Figure 2A**), SEED (**Figure 2C**), and MetaCyc functional gene assignments. STAMP ANOVA of the RefSeq classifications identified thirteen bacterial classes that were significantly enriched in microbialites over the surrounding environment (**Table 2**, $p < 0.01$). ANOVA using STAMP on the highest level classification (level I) in the SEED database indicates that membrane transport, aromatic metabolism, motility, potassium metabolism, cell signaling and virulence genes are significantly enriched in microbialites over the surrounding environment (**Table 3**, $p < 0.05$). MetaCyc functional gene assignments suggest many shared pathways (263) among samples from the water (filters), microbialites and sediments with 246 pathways distinct to Pavilion microbialites (**Figure 2D**). These observations support the idea that microbialite associated microbes are distinct and are not being seeded or introduced (at least not recently), from surrounding environments.

The microbial communities and metabolic potential of the microbialites differed between the sediment and water samples. Compared to the microbialites, the sediment metagenomic data had more sequences assigned to the taxonomic groups *Nitrospirae*, *Betaproteobacteria* and *Spirochaetia*; whereas, metagenomic data from the water had more sequences assigned to *Betaproteobacteria, Bacterioidetes, Verrucomicrobia,* and phototrophic eukaryotes (e.g., *Chlorophyceae*; **Figure 2B**). Although the depth of sequences was not the same across

[1]http://broadinstitute.github.io/picard

[2]http://www.theseed.org

[3]http://www.ncbi.nlm.nih.gov/refseq/

[4]http://metacyc.org/

[5]http://metagenomics.anl.gov/

TABLE 1 | Pavilion Lake metagenome assembly statistics using Ray Meta DeNovo Assembler.

Depth	10 m	20 m	25 m	45 m	Sfc**	20 m	25 m	10 m	20 m	25 m
No. Contig or Read	510415	881449	499134	179215	43909	19977	32086	120680	544185	94150
Total Length (Bp)	115196707	178186326	111159198	41483863	8537385	3836213	5930888	12560841	61059259	10421166
N50 > 500bp	647	752	717	668	649	734	608	(–)	(–)	(–)
Avg > 500bp	721	783	760	736	776	753	644	(–)	(–)	(–)
Med > 500bp	571	633	616	621	524	670	575	(–)	(–)	(–)
Largest (Bp)	3882	6079	2965	1964	7125	4003	1880	190	190	190
G+C%	60.8	57.9	60.1	60.3	47	52.8	52.6	59.6	57.7	52.2

Sediment data were not assembled. Surface water (Sfc) (1 and 10 m samples) of water pooled at the assembly step.
**Not assembled reads only*
***Sfc, surface water filter (~1 to 10 m)*
(–) not available.

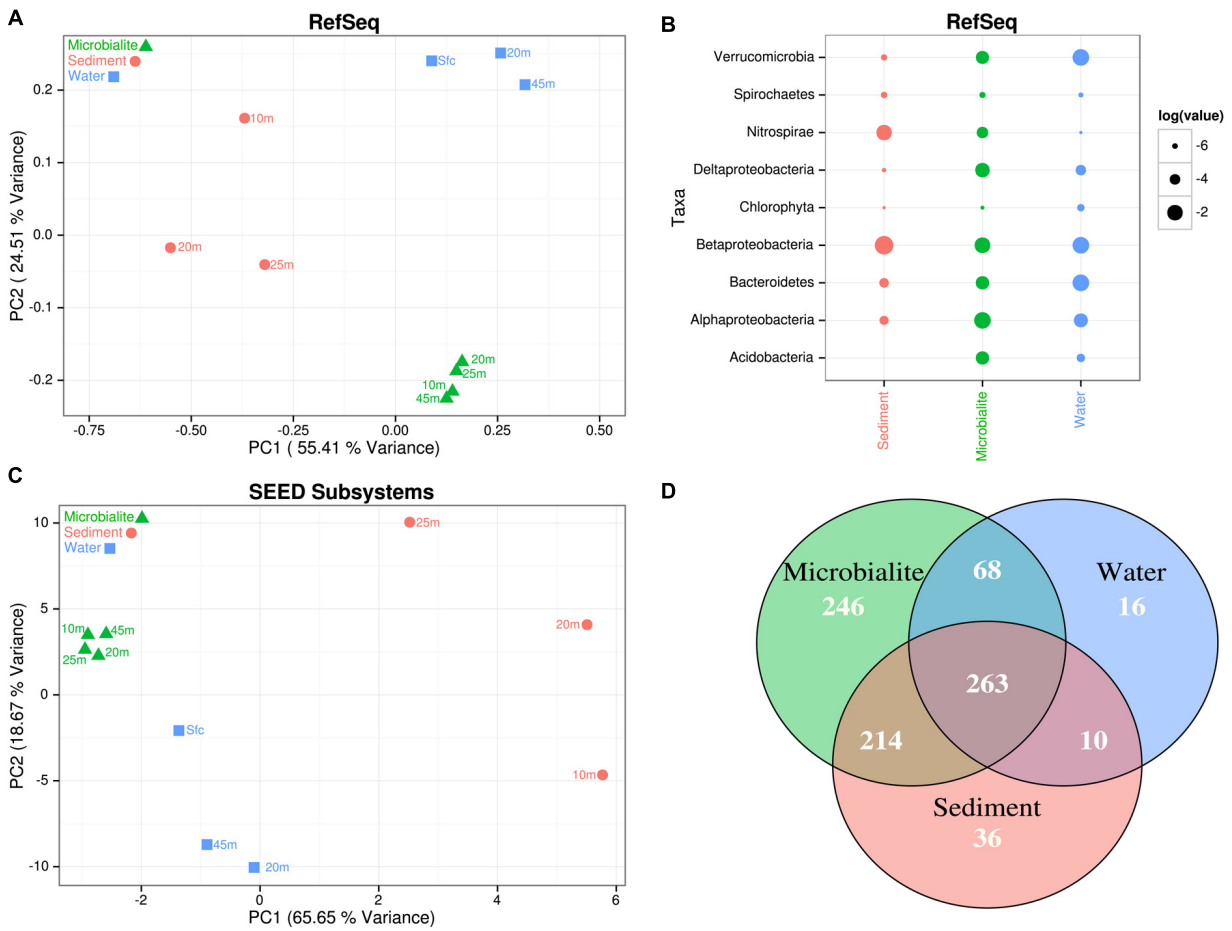

FIGURE 2 | Pavilion Lake microbial community composition and metabolic potential relative to the adjacent sediments and water. (A) PCA plot of the normalized RefSeq classifications. Clustering was done using a ward matrix and Bray-Curtis distance cut-offs, bootstrapped with one thousand replicates. **(B)** Dotplot of the normalized RefSeq class-level in log relative abundances. **(C)** PCA plot of the normalized SEED Subsystems (level II classifications). Clustering was done using a ward matrix and Bray-Curtis distance cut-offs, bootstrapped with one thousand replicates. **(D)** Venn diagram of the MetaCyc pathway abundances for all the microbialite, water and sediment metagenomes normalized by pathway gene abundances and pathway size.

microbialites, sediments and water, it was adequate to clearly show that the microbialite community was distinct from those in the surrounding environments. These findings are consistent with previous works that demonstrate fundamental differences in microbial taxa between microbialite-associated communities and others. Russell et al. (2014) found taxonomically distinct microbial communities in non-lithifying soft-mat biofilms and microbialites in Pavilion Lake. As well, metagenomic

TABLE 2 | Taxonomic classes (RefSeq) that are overrepresented in microbialites relative to the surrounding environment by ANOVA using STAMP.

Bacteria	*p*-value (corr)	Effect size	Fil: Avg Rfreq (%)	Filr: SD (%)	MB: Avg Rfreq. (%)	MB: SD (%)	Sed: Avg Rfreq. (%)	Sed: SD (%)
Acidobacteriia	1.96E-03	0.889	0.314	0.164	0.839	0.139	0	0
Acidobacteria (Unclassified)	8.34E-05	0.972	0.096	0.053	0.849	0.094	0	0
Alphaproteobacteria	4.52E-04	0.947	7.708	0.266	19.768	2.196	2.679	2.008
Chloroflexi (class)	9.30E-05	0.973	0.449	0.142	1.481	0.116	0	0
Deferribacteres (class)	1.13E-03	0.917	0.059	0.014	0.117	0.02	0	0
Deinococci	1.82E-03	0.892	0.335	0.131	0.613	0.081	0	0
Deltaproteobacteria	1.81E-04	0.961	2.151	0.933	7.85	0.448	0.398	0.563
Gemmatimonadetes	1.39E-03	0.904	0.208	0.16	0.797	0.114	0	0
Gloeobacteria	7.68E-05	0.972	0.056	0.038	0.36	0.03	0	0
Ktedonobacteria	1.49E-03	0.9	0.076	0.042	0.31	0.062	0	0
Solibacteres	1.16E-04	0.973	0.386	0.279	3.346	0.331	0	0
Thermomicrobia (class)	1.44E-03	0.905	0.058	0.03	0.481	0.111	0	0
Thermotogae (class)	5.03E-03	0.845	0.044	0.023	0.138	0.006	0.023	0.033

STAMP ANOVA tested significant differences between multiple groups (microbialite, sediments, and filters) using a post-hoc test (Tukey–Kramer at 0.95), an effect size (Eta-squared), a p-value (<0.01) and a multiple-test correction of Benjamini–Hochberg FDR. Results are for RefSeq classifications that significantly differed ($p < 0.01$) for microbialite over the surrounding environments (sediments and filters). Avg Rfreq, Average relative frequency; SD, Standard deviation; p-val corr, p-value ANOVA corrected; Unclass, Unclassified; MB, Microbialite; Sed, Sediment.

Avg Rfreq, Average relative frequency; SD, Standard deviation. P-val corr, p-value ANOVA corrected (By Benjamini–Hochberg FDR); Fil, Filter represents surrounding water; MB, Microbialite; Sed, Sediment.

TABLE 3 | Functional annotations (SEED subsystem level I) that are overrepresented in microbialites relative to the surrounding environment by ANOVA using STAMP.

Seed subsystem	*p*-val (corr)	Effect Size	Fil: Avg Rfeq (%)	Fil: SD (%)	MB: Avg Rfeq (%)	MB: SD (%)	Sed: Avg Rfeq (%)	Sed: SD (%)
Membrane transport	8.12E-03	0.793	1.998	0.157	2.514	0.112	0.941	0.577
Metabolism of aromatics	3.00E-04	0.934	1.27	0.074	1.775	0.111	0.872	0.109
Motility and chemotaxis	3.60E-03	0.649	0.606	0.025	1.063	0.039	0.454	0.356
Potassium metabolism	6.40E-03	0.81	0.182	0.035	0.296	0.013	0.084	0.068
Regulation and cell signaling	1.82E-03	0.874	1.09	0.028	1.506	0.079	0.978	0.133
Virulence, disease, and defense	3.45E-04	0.928	2.069	0.195	2.997	0.057	1.167	0.327

STAMP ANOVA tested significant differences between multiple groups (microbialite, sediments, and filters) using a post hoc test (Tukey–Kramer at 0.95), an effect size (Eta-squared), a p-value (<0.01) and a multiple-test correction of Benjamini–Hochberg FDR. Results are for RefSeq classifications that significantly differed ($p < 0.01$) for microbialite over the surrounding environments (sediments and filters). Avg Rfreq, Average relative frequency; SD, Standard deviation; p-val corr, p-value ANOVA corrected; MB, Microbialite; Sed, Sediment.

Avg Rfreq, Average relative frequency; SD, Standard deviation.

p-val corr, p-value ANOVA corrected (Benjamini-Hochberg FDR).

Fil, Filter represents surrounding water; MB, Microbialite. Sed: Sediment.

analysis of marine microbialites in Highbourne Cay showed distinctly different communities associated with lithifying and non-lithifying microbial mats (Khodadad and Foster, 2012)

Core Microbialite Microbial Community Structure and Metabolic Potential

Microbialite morphology in Pavilion Lake changes predictably with depth, however the metabolic potential and microbial community remains similar. PCA of RefSeq (**Figure 2A**) and SEED (**Figure 2C**) classifications indicate that the microbial community and metabolic potential of microbialite metagenomes cluster closely together, regardless of morphology or depth (**Figure 3D**). Across morphologies, >80% of the MetaCyc pathways predicted by the microbialite metagenomes are shared (596, **Figure 3F**), with few (<30) distinct pathways within a Pavilion Lake microbialite morphotype.

Based on RefSeq taxonomic classification ANOVA using STAMP, the microbialites of Pavilion Lake were dominated by sequences assigned to *Proteobacteria* and *Acidobacteria* (**Figure 2B**). For example, sequences assigned to the classes *Alphaproteobacteria*, *Deltaproteobacteria*, *Acidobacteriia*, and *Gloeobacteria* were significantly more abundant in microbialite metagenomes than in the water or sediment metagenomes (**Table 2**; $p < 0.05$). The dominance of sequences associated with members of the phyla *Proteobacteria* (mainly *Alphaproteobacteria* and *Deltaproteobacteria* classes, **Figure 2B**) is consistent with results from other marine and freshwater microbialite communities (Havemann and Foster, 2008; Breitbart et al., 2009; Goh et al., 2009; Khodadad and Foster, 2012; Mobberley et al., 2013), suggesting that despite geographical and environmental differences, microbialite microbial communities have similar

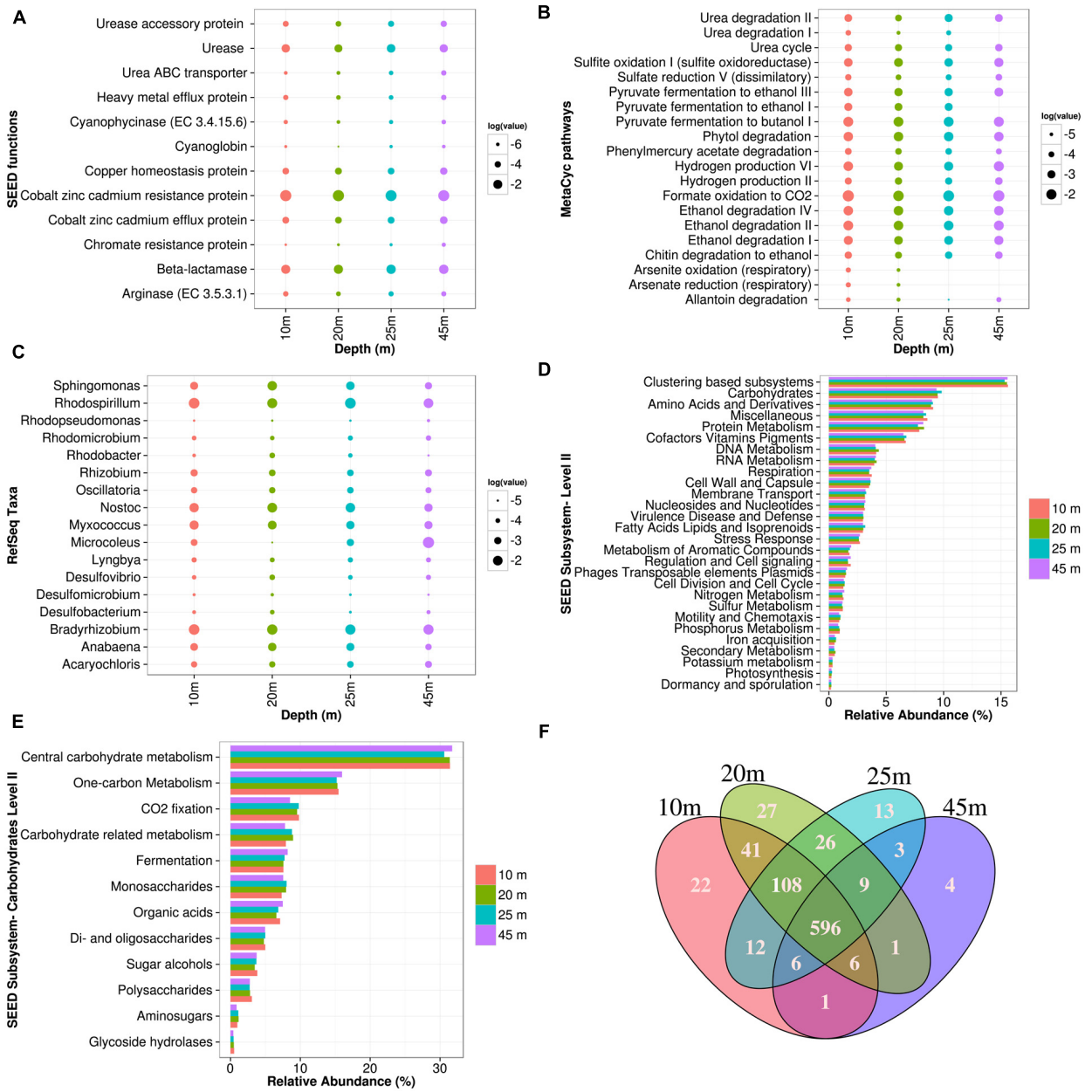

FIGURE 3 | Pavilion Lake microbial community composition and metabolic potential across microbialite morphologies. Microbialite metagenomes are listed as a function of depth in meters. **(A)** Dotplot of the normalized SEED subsystem functions relating to urea metabolism (e.g., urease, ABC transport), heavy metal detoxification (e.g., efflux, resistance), antibiotic resistance (e.g beta-lactamases), and cyanobacteria related functions (e.g., cyanoglobin, cyanophycinase, copper homeostasis) in log relative abundances. **(B)** Dotplot of the normalized MetaCyc pathways relating to urea metabolism, sulfite oxidation, dissimilatory sulfate reduction, heavy metal detoxification (e.g., arsenite/arsenate oxidation/reduction, phenylmercury acetate metabolism), hydrogen production, primary alcohol fermentation/degradation in log relative abundances. **(C)** Dotplot of the normalized RefSeq classifications relating to *Alphaproteobacteria, Deltaproteobacteria*, and filamentous cyanobacterial genera. **(D)** Microbialite metagenome functional annotation ranking using SEED subsystem (level I). **(E)** Microbialite metagenome carbohydrate related SEED subsystem (level II) functional annotations. **(F)** Venn diagram of the MetaCyc pathway abundances for all the microbialite metagenomes normalized by pathway gene abundances and pathway size.

members suggesting a globally shared microbial community structure.

The microbialites had significantly more sequences classified as *Alphaproteobacteria*, both in photoheterotrophic and heterotrophic functional groups, relative to sequences in the neighboring environments (e.g., water and sediment metagenomes) (**Table 2**; $p < 0.05$; **Figure 2B**). Microbialite alphaproteobacterial specific contigs were assigned to genera of photoheterotrophic (e.g., *Rhodobacter, Rhodomicrobium, Rhodopseudomonas,* and *Rhodospirillum*), heterotrophic (e.g.,

Sphingomonas) and nitrogen-fixing (e.g., *Bradyrhizobium*, and *Rhizobium*) bacteria (**Figure 3C**). Alphaproteobacterial based nitrogen fixation complements cyanobacterial nitrogen fixation in microbialites likely because of cyanobacterial diel cycles (Havemann and Foster, 2008). *Alphaproteobacteria* were also found to be the dominant OTU phylotype in Pavilion Lake microbialites in prior pyrosequencing and clone-library amplicon studies (Chan et al., 2014; Russell et al., 2014), consistent with our data on protein-coding gene abundances in the microbialite metagenomes.

Deltaproteobacterial associated sequences within the microbialite metagenomes were assigned to genera of dissimilatory sulfate reducing (e.g., *Desulfobacterium* and *Desulfovibrio*) and heterotrophic (e.g., *Myxococcus*) bacteria (**Figure 3C**). MetaCyc dissimilatory sulfate pathways were abundant across the different microbialite morphologies in Pavilion Lake (**Figure 3B**). Sulfate-reducing deltaproteobacteria are often found where carbonates precipitate, and are important drivers of the "alkalinity engine," by pushing the saturation index via increasing alkalinity (Gallagher et al., 2012). Hydrogen production and formate oxidation to carbon dioxide are predicted by the microbialite metagenomes (**Figure 3B**). Potential electron donors for sulfate reducing deltaproteobacteria in Pavilion Lake microbialites include acetate, lactate, hydrogen, and formate. Whether sulfate reduction helps or hinders carbonate precipitation depends on the electron donor; hydrogen and formate likely promote precipitation, whereas, other organic carbon sources likely lead to dissolution (Gallagher et al., 2012). Future stable isotope probing studies could reveal which compounds are used as electron donors by the sulfate-reducers. *Myxococcus* spp. are abundant in a variety of microbialite-forming systems and can directly precipitate carbonate through the release of ammonium, which can increase alkalinity favoring carbonate precipitation (Ben Chekroun et al., 2004; Jimenez-Lopez et al., 2011). Analysis of the Pavilion Lake microbialite metagenomes supports prior metagenomic and amplicon investigations of microbialites that show members of the *Deltaproteobacteria* include dissimilatory sulfate-reducers (Havemann and Foster, 2008; Breitbart et al., 2009; Goh et al., 2009; Khodadad and Foster, 2012; Mobberley et al., 2013; Wong et al., 2015).

Sequences associated with filamentous cyanobacterial mat-builders from the genera *Anabaena, Lyngbya, Microcoleus, Nostoc, Oscillatoria* and the planktonic *Cyanothece* and *Acrayochoris* were found in all microbialite morphologies (**Figure 3C**). Pathways for synthesis of cyanoglobin and cyanophycin, as well as copper metabolism, were associated with cyanobacterial mat-builders in all microbialites (**Figure 3B**). Cyanoglobin is a peripheral membrane protein that binds oxygen with high affinity, is highly expressed under low oxygen and could be restricted to some strains of *Nostoc* sp. and *Anabaena* sp. (Hill et al., 1996). Cyanophycin is formed in filamentous cyanobacteria in response to low or changing DIC to O_2 ratios (Liang et al., 2014). Copper homeostasis genes were abundant in microbialites, which is common for cyanobacterial derived mats, as copper is essential for growth (Varin et al., 2012) but also toxic at levels $\geq$10 mM (Burnat et al., 2009). The microbialite metagenome indicates that the metabolic potential of filamentous cyanobacterial mats is adaptive to metal homeostasis (e.g., copper), as well as carbon and oxygen limitation (e.g., cyanoglobin and cyanophycin).

Novel Metabolic Potential Within Microbialites

Urealytic metabolism has been hypothesized to be involved in microbialite formation due to its carbonate precipitating effects, but its detection in microbialites has remained elusive (Castanier et al., 1999). MetaCyc and SEED subsystems indicate that urea ABC transporters, arginase and ureases are found in similar abundances across Pavilion Lake microbialites (**Figures 3A,B**), implying the presence of urea metabolism which may be playing a role in precipitation. *Gamma* and *Deltaproteobacteria* specific urease beta subunits and urease accessory proteins (UreD/F) have only been identified in the Pavilion Lake microbialite metagenomes. The linkage of urease related genes to *Proteobacteria* was unexpected due to the strong experimental evidence that *Firmicutes* (mainly *Bacillus* sp.) are the dominant taxa contributing urease related genes (Boquet et al., 1973; Hammes et al., 2003; Lee, 2003; Dick et al., 2006; Dhami et al., 2013).

Antibiotic and heavy-metal resistance pathways associated with *Proteobacteria* were found within the microbialites based on RefSeq classification (**Figures 3A,B**). These included antibiotic resistance pathways such as beta-lactamases (class A) that were assigned to the *Alpha*, *Beta,* and *Gamma* classes of *Proteobacteria* (**Figure 2A**). Genes related to antibiotic resistance could be in response to toxic organic molecules produced by cyanobacterial mats (Neilan et al., 2013). SEED functions and MetaCyc pathways related to heavy-metal detoxification were abundant in microbialites (**Figure 3A**). The occurrence of cobalt–zinc–cadmium resistance proteins, efflux pump proteins, phenylmercury acetate degradation, and chromate resistance was similar across morphologies while arsenite oxidation and arsenate reduction pathways were not found at depths deeper than 25 m (**Figure 3B**). Heavy-metal resistance contigs were taxonomically assigned to *Alpha*, *Beta* and *Gamma* classes of *Proteobacteria*. Pavilion Lake has low levels of zinc (0.01–0.03 mg L^{-1}) and undetectable levels of cobalt, iron, arsenic and cadmium (Lim et al., 2009). Heavy-metal resistance genes may be involved in resistance, homeostasis or sequestration of metals. Antibiotic resistance has also been linked to heavy-metal stress, suggesting that resistance to one can lead to resistance to the other in complex bacterial communities (Nisanian et al., 2014).

Recently published Shark Bay microbialite metagenomes suggest high prevalence of genes associated with heavy-metal resistance including genes for arsenic metabolism (e.g., reductase and resistance genes; Ruvindy et al., 2015). Arsenite oxidation and arsenate reduction genes were also found amongst MetaCyc pathways in only the 10 to 20 m microbialites in Pavilion Lake (**Figure 3B**). Arsenic cycling has been suggested to be a prominent feature in ancient microbial mats over 2.7 billion years old (Sforna et al., 2014). Our data from Pavilion Lake microbialites suggest that heavy-metal resistance could

be a general feature of microbialites globally, which may also provide cross-protection against antibiotics (Nisanian et al., 2014).

The metabolic potential of Pavilion Lake microbialites predict primary alcohol fermentation pathways (e.g., butanol and ethanol biosynthesis) (**Figure 3B**) based on genes that are taxonomically assigned to *Alpha-* and *Beta-proteobacteria*. Pyruvate, phytol, and chitin fermentation appear to be the main predicted pathways for the generation of primary alcohols (e.g., ethanol, butanol). Primary alcohol fermentation has been linked to microbialite dissolution; however, fermentation also provides substrates that fuel dissimilatory sulfate reduction, which can precipitate carbonate (Dupraz and Visscher, 2005; Gallagher et al., 2012) and which could offset carbonate lost by fermentation. Further stable-isotope experiments are needed to confirm the metabolic potential of primary alcohol fermentation predicted by the microbialite metagenomes. Although not previously recognized, members of the *Proteobacteria* appear to be major constituents of Pavilion Lake microbialites, potentially providing important metabolic roles, such as resistance to antibiotics and heavy-metals, and primary alcohol fermentation. Further investigation into the nature of their role in microbialite formation is warranted.

Photosynthetic and Heterotrophic Metabolic Potential Associated with Carbonate Precipitation in Pavilion Lake

The metabolic potential of Pavilion Lake microbialites appears to be dominated by heterotrophy relative to phototrophy. Sequences related to photosynthesis, including those encoding photosystems and electron transport proteins, were ranked 28th out of 29th possible SEED subsystems (**Figure 3D**). In contrast, pathways related to carbohydrate metabolism (carbon-related pathways) were ranked second and accounted for ∼9% of the contigs. Among the carbon-related pathways, ∼45% were related to central (TCA cycle) and one-carbon metabolism (e.g., serine–glyoxlate cycle), while another ∼45% were related to degradation (e.g., fermentation, glycoside hydrolases, and other hydrolytic enzymes; **Figure 3E**). Only ∼10% of the

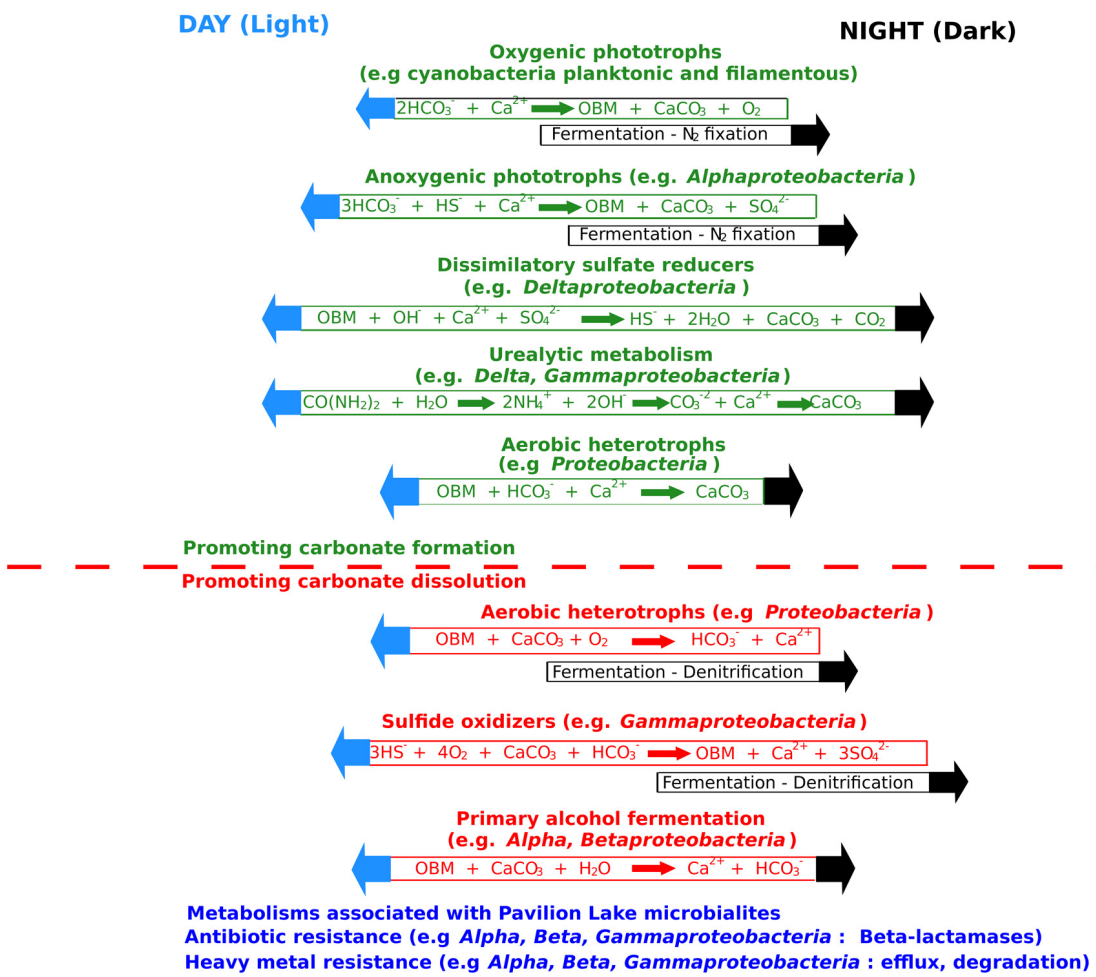

FIGURE 4 | A summary of the factors affecting carbonate precipitation and dissolution as inferred from the Pavilion Lake microbialite metabolic potential and community composition. OBM is organic biomass. Adapted from Dupraz et al. (2009).

microbialite-specific contigs were annotated as carbon-fixation related (e.g., Calvin–Benson cycle) (**Figure 3E**). Stable-isotope studies suggest that photosynthetic processes are linked to carbonate precipitation in shallow (<25 m) microbialites (Brady et al., 2009; Omelon et al., 2013), even though the metabolic potential is dominated by heterotrophic processes. However, Omelon et al. (2013) and Theisen et al. (2015) also suggested that heterotrophs contribute to the lifthification of microbialites in Pavilion Lake by triggering additional carbonate precipitation. Microbialite formation relating to carbonate precipitation in Pavilion Lake is associated with cyanobacterial photosynthesis with contribution from heterotrophic processes such as urealytic metabolism, dissimilatory sulfate reduction and heterotrophic mat degradation (i.e., EPS related carbonate inhibition; **Figure 4**; Dupraz et al., 2009).

Viral Community and Viral Defense

In the cellular fraction from the water, viral sequences represented >1% of reads; whereas, in total DNA extracted from microbialites, viral sequences comprised >0.05% of reads. ANOVA in STAMP based on RefSeq classification confirmed that virus sequences were relatively more abundant in the water than in microbialites or sediments (**Figure 5A**). Specifically, T4-like phage (e.g., *Myoviridae*) and large algal viruses (e.g., *Phycodnaviridae*) dominated the viral sequences in the water and were more abundant than in the microbialites and sediments (**Figure 5A**). The low proportion of viral reads in the microbialite data may be biased by the lack of dsDNA viral genomes in the RefSeq database from microbialites compared to water. Viruses in the water appeared to have higher abundances of proteins related to phage structure (tail fibers), phage replication and phage DNA replication (**Figure 5B**).

An active role for phages in the microbialites is suggested by the higher relative abundances of predicted genes involved with CRISPRs, phage shock and phage excision (**Figure 5B**). CRISPR *cas* genes were associated with the following taxonomic groups: *Chloroflexi* (e.g., *Dehalococcoides*), *Deltaproteobacteria* (e.g., *Myxococcus* and *Desulfuromonadales*), filamentous cyanobacteria (e.g., *Anabaena, Nostoc, Rivularia*) and *Firmicutes* (e.g., *Clostridia*) based on tBLASTx ($1e^{-3}$) analysis. Likewise, more putative genes involved in phage integration and excision occurred in the microbialites than in the nearby environment (**Figure 5B**). Also, CRISPRs were predicted to be associated with key members involved in microbialite formation, such as filamentous cyanobacteria and *Myxococcus* sp., implying that the microbialite community is under continuous selective pressure from viral infection.

It is important to emphasize that the viral DNA was from the cellular fraction (between 0.2 and 120 μm) captured on filters, suggesting that most viral sequences were from infected cells or from viruses attached to particles. It is not uncommon for filters with pore sizes much larger than viruses to contain many viral sequences (Zeigler Allen et al., 2012). The most abundant viral contigs in the water were for T4-like cyanophages and phycodnaviruses (**Figure 5A**). Although gene-specific primers targeted to these groups (Chen and Suttle, 1995; Filée et al., 2005) failed to amplify DNA, it would suggest that the viruses were evolutionarily distinct from the viruses these primers target.

Consistent with reports for other microbialites (Desnues et al., 2008), relatively few viral sequences were

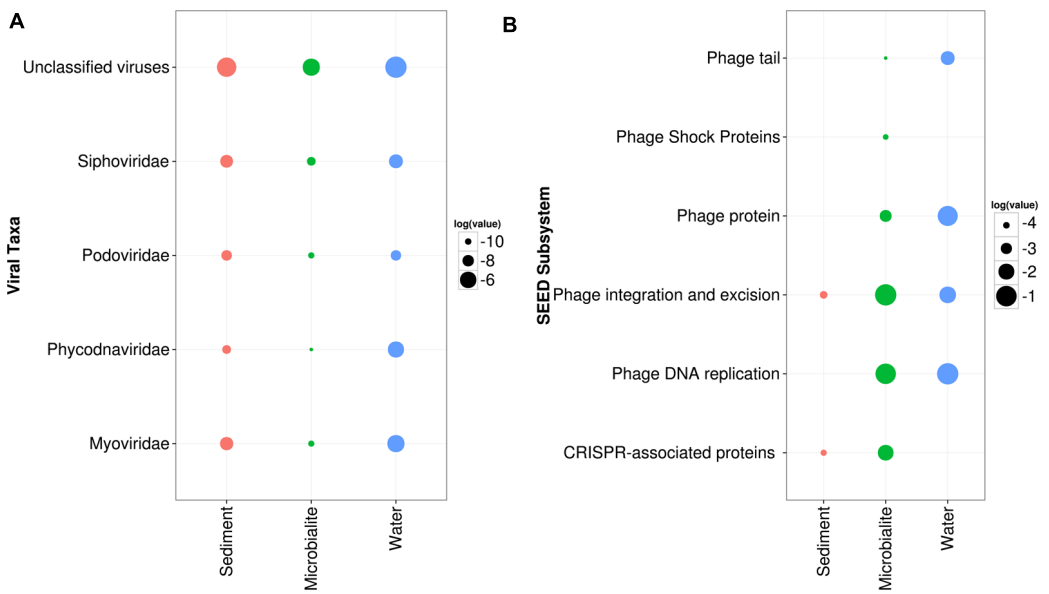

FIGURE 5 | Pavilion Lake viral community composition and metabolic potential. (A) Dotplot of normalized RefSeq viral taxonomic groups in relation to the surrounding environments (e.g., sediments and water) in log relative abundances. **(B)** Dotplot of the normalized SEED subsystem in relation to the surrounding environments (e.g., sediments and water) in log relative abundances.

recovered in this study. Yet, the occurrence of phage integration and CRISPR-*cas* sequences implies that the Pavilion Lake microbialites are under selection from viral infection. It is likely that the relative abundance of viral sequences has been underestimated because of the lack of representative viral sequences from microbialites in databases.

CONCLUSION

This study demonstrates that the microbial community profile and metabolic potential of modern freshwater microbialites in Pavilion Lake are distinct from those in neighboring sediments and water, consistent with previous findings of spatial variation in microbialite systems. These results confirm the notion that the microbialite communities are not being continuously seeded by organisms from the surrounding environment. Our data further suggests a unique microbialite microbial community that encodes a functional guild which is distinctive and likely related to its overall function of carbonate precipitation.

Differences among these metagenomes can be attributed to differing selection pressures among environments, with the microbialite community comprised of taxa essential for microbialite growth, as well as opportunists taking advantage of nutrients and the matrix supplied by filamentous cyanobacterial mats. These findings are consistent with photosynthetic influences on carbonate precipitation by filamentous cyanobacteria, with likely contributions by proteobacteria and acidobacteria.

Pavilion Lake microbialites are enriched for pathways that include heavy-metal and antibiotic resistance, urealytic metabolism as well as primary alcohol fermentation. These pathways are associated with members of the *Proteobacteria*, which are numerically dominant and likely convey resistance to toxins and heavy metals, and may influence carbonate formation through photosynthesis and urea metabolism. This hypothesis is consistent with previous suggestions of heterotrophic contributions to lithification of Pavilion Lake microbialites. Evidence for urealytic metabolism identified here may suggest an important role for this metabolism in carbonate precipitation (Castanier et al., 1999), which has not been reported previously in microbialites.

The prevalence of CRISPR-*cas* systems and phage excision genes imply that the microbialites are under selective pressure from viral infection. In particular, the presence of CRISPRs assigned to taxa that precipitate carbonates (*Cyanobacteria*, *Deltaproteobacteria* and *Firmicutes*) suggest that viruses play an important previously unknown role in the microbialite communities in Pavilion Lake.

FUNDING

Financial support was provided by the MARSLIFE Project (9F052-10-0176) funded by the Canadian Space Agency, the NASA MMAMA program and a Discovery Grant from the Natural Science and Engineering Council of Canada to CAS.

ACKNOWLEDGMENTS

We are grateful to the entire Pavilion Lake Research Project (PLRP) research team, especially Donnie Reid for his exceptional leadership of field logistics and diving operations, as well as the PLRP science divers and the DeepWorker pilots for their help recovering samples from the lake. We also thank Danielle Winget, Kynan Suttle, Jan Finke, Marli Vlok, and Tyler Nelson for assistance with sample processing in the field. Microbialite morphology photographs in **Figure 1** are used with permission and copyrighted by Donnie Reid, Tyler Mackey, Amy M. Chan, Kynan Suttle, and Richard Allen White III. We thank the following individuals and their teams for providing the sequence data: Sugandha Dandekar (Uma) and Hemani Wijesuriya for the MiSeq data (UCLA Genotyping & Sequencing Core), Frederick Robidoux for the HiSeq data (McGill University & Genome Quebec Innovation Centre), and Sergio Pereira for the 454 FLX data (The Centre for Applied Genomics, SickKids Hospital, Toronto). Special thanks to Niels W. Hanson and Kishori M. Konwar for python and R scripts for parsing metapathways data. Also thank you Brendan P. Burns for your excellent comments on draft manuscripts. We are also grateful to Linda and Mickey Macri for hosting the PLRP and MARSLIFE projects and to the Ts'Kw'aylaxw First Nation and British Columbia Parks for their continued support of our research. This is PLRP publication #15-01.

SUPPLEMENTARY MATERIAL

The Supplementary Material for this article can be found online at: http://journal.frontiersin.org/article/10.3389/fmicb.2015.01531

REFERENCES

Allen, M. A., Goh, F., Burns, B. P., and Neilan, B. A. (2009). Bacterial, archaeal and eukaryotic diversity of smooth and pustular microbial mat communities in the hypersaline lagoon of Shark Bay. *Geobiology* 7, 82–96. doi: 10.1111/j.1472-4669.2008.00187.x

Aury, J. M., Cruaud, C., Barbe, V., Rogier, O., Mangenot, S., Samson, G., et al. (2008). High quality draft sequences for prokaryotic genomes using a mix of new sequencing technologies. *BMC Genomics* 9:603. doi: 10.1186/1471-2164-9-603

Ben Chekroun, K., Rodriguez-Navarro, C., Gonzalez-Muñoz, M. T., Arias, J. M., Cultrone, G., and Rodriguez-Gallego, M. (2004). Precipitation and growth morphology of calcium carbonate induced by *Myxococcus xanthus*: implications for regognition of bacterial carbonates. *J. Sedimentary Res.* 74, 868–876. doi: 10.1306/0505047 40868

Bentley, D. R., Balasubramanian, S., Swerdlow, H. P., Smith, G. P., Milton, J., Brown, C. G., et al. (2008). Accurate whole human genome sequencing using reversible terminator chemistry. *Nature* 6, 53–59. doi: 10.1038/nature0 7517

Boisvert, S., Laviolette, F., and Corbeil, J. (2010). Ray: simultaneous assembly of reads from a mix of high-throughput sequencing technologies. *J. Comput. Biol.* 11, 1519–1533. doi: 10.1089/cmb.2009.0238

Boisvert, S., Raymond, F., Godzaridis, E., Laviolette, F., and Corbeil, J. (2012). Ray Meta: scalable de novo metagenome assembly and profiling. *Genome Biol.* 13:R122. doi: 10.1186/gb-2012-13-12-r122

Boquet, E., Boronat, A., and Ramos-Cormenzana, A. (1973). Production of calcite (calcium carbonate) crystals by soil bacteria is a general phenomenon. *Nature* 246, 527–529. doi: 10.1038/246527a0

Bosak, T., Liang, B., Wu, T. D., Templer, S. P., Evans, A., Vali, H., et al. (2012). Cyanobacterial diversity and activity in modern conical microbialites. *Geobiology* 10, 384–401. doi: 10.1111/j.1472-4669.2012.00334.x

Brady, A. L., Laval, B., Lim, D. S. S., and Slater, G. F. (2014). Autotrophic and heterotrophic associated biosignatures in modern freshwater microbialites over seasonal and spatial gradients. *Org. Geochem.* 67, 8–18. doi: 10.1016/j.orggeochem.2013.11.013

Brady, A. L., Slater, G., Laval, B., and Lim, D. S. (2009). Constraining carbon sources and growth rates of freshwater microbialites in Pavilion Lake using 14C analysis. *Geobiology* 7, 544–555.

Brady, A. L., Slater, G. F., Omelon, C. R., Southam, G., Druschel, G., Andersen, D. T., et al. (2010). Photosynthetic isotope biosignatures in laminated micro-stromatolitic and non-laminated nodules associated with modern, freshwater microbialites in Pavilion Lake, B.C. *Chem. Geol.* 274, 56–67. doi: 10.1016/j.chemgeo.2010.03.016

Breitbart, M., Hoare, A., Nitti, A., Siefert, J., Haynes, M., Dinsdale, E., et al. (2009). Metagenomic and stable isotopic analyses of modern freshwater microbialites in Cuatro Cienegas, Mexico. *Environ. Microbiol.* 11, 16–34. doi: 10.1111/j.1462-2920.2008.01725.x

Burnat, M., Diestra, E., Esteve, I., and Solé, A. (2009). In situ determination of the effects of lead and copper on cyanobacterial populations in microcosms. *PLoS ONE* 4:e6204. doi: 10.1371/journal.pone.0006204

Burne, R. V., and Moore, L. S. (1987). Microbialites: organosedimentary deposits of benthic microbial communities. *Palaios* 2, 241–254. doi: 10.2307/3514674

Burns, B. P., Goh, F., Allen, M., and Neilan, B. A. (2004). Microbial diversity of extant stromatolites in the hypersaline marine environment of Shark Bay, Australia. *Environ. Microbiol.* 6, 1096–1101. doi: 10.1111/j.1462-2920.2004.00651.x

Cantarel, B. L., Erickson, A. R., VerBerkmoes, N. C., Erickson, B. K., and Carey, P. A. (2011). Strategies for metagenomic-guided whole-community proteomics of complex microbial environments. *PLoS ONE* 6:e27173. doi: 10.1371/journal.pone.0027173

Castanier, S., Le Metayer-Levrel, G., and Perthuisot, J. P. (1999). Ca-carbonates precipitation and limestone genesis - the microbiogeologist point of view. *Sedim. Geol.* 126, 9–23.

Centeno, C. M., Legendre, P., Beltran, Y., Alcantara-Hernandez, R. J., Lidstrom, U. E., Ashby, M. N., et al. (2012). Microbialite genetic diversity and composition related to environmental variables. *FEMS Microbiol. Ecol.* 82, 724–735. doi: 10.1111/j.1574-6941.2012.01447.x

Chan, O. W., Bugler-Lacap, D. C., Biddle, J. F., Lim, D. S. S., McKay, C. P., and Pointing, S. B. (2014). Phylogenetic diversity of a microbialite reef in a cold alkaline freshwater lake. *Can. J. Microbiol.* 6, 391–398. doi: 10.1139/cjm-2014-0024

Chen, F., and Suttle, C. A. (1995). Amplification of DNA polymerase gene fragments from viruses infecting microalgae. *Appl. Environ. Microbiol.* 61, 1274–1278.

Couradeau, E., Benzerara, K., Moreira, D., Gérard, E., Kaźmierczak, J., Tavera, R., et al. (2011). Prokaryotic and eukaryotic community structure in field and cultured microbialites from the alkaline Lake Alchichica (Mexico). *PLoS ONE* 6:e28767. doi: 10.1371/journal.pone.0028767

Desnues, C., Rodriguez-Brito, B., Rayhawk, S., Kelley, S., Tran, T., Haynes, M., et al. (2008). Biodiversity and biogeography of phages in modern stromatolites and thrombolites. *Nature* 452, 340–343. doi: 10.1038/nature06735

Dhami, N. K., Reddy, M. S., and Mukherjee, A. (2013). Biomineralization of calcium carbonate polymorphs by the bacterial strains isolated from calcareous sites. *J. Microbiol. Biotechnol.* 23, 707–714. doi: 10.4014/jmb.1212.11087

Dick, J., De Windt, W., De Graef, B., Saveyn, H., Van der Meeren, P., De Belie, N., et al. (2006). Bio-deposition of a calcium carbonate layer on degraded limestone by *Bacillus species*. *Biodegradation* 17, 357–367. doi: 10.1007/s10532-005-9006-x

Dupraz, C., Reid, R. P., Braissant, O., Decho, A. W., Norman, R. S., and Visscher, P. T. (2009). Processes of carbonate precipitation in modern microbial mats. *Earth Sci. Rev.* 96, 141–162. doi: 10.1016/j.earscirev.2008.10.005

Dupraz, C., and Visscher, P. T. (2005). Microbial lithification in marine stromatolites and hypersaline mats. *Trends Microbiol.* 13, 429–438. doi: 10.1016/j.tim.2005.07.008

Ferris, F. G., Thompson, J. B., and Beveridge, T. J. (1997). Modern freshwater microbialites from Kelly Lake, British Columbia, Canada. *Palaios* 12, 213–219. doi: 10.2307/3515423

Filée, J., Tétart, F., Suttle, C. A., and Krisch, H. M. (2005). Marine T4-type bacteriophages, a ubiquitous component of the dark matter of the biosphere. *Proc. Natl. Acad. Sci. U.S.A.* 102, 12471–12476. doi: 10.1073/pnas.0503404102

Gallagher, K. L., Kading, T. J., Braissant, O., Dupraz, C., and Visscher, P. T. (2012). Inside the alkalinity engine: the role of electron donors in the organomineralization potential of sulfate-reducing bacteria. *Geobiology* 10, 518–530. doi: 10.1111/j.1472-4669.2012.00342.x

Gischler, E., Gibson, M. A., and Oschmann, W. (2008). Giant holocene freshwater microbialites, laguna bacalar, quintana roo, Mexico. *Sedimentology* 55, 1293–1309. doi: 10.1111/j.1365-3091.2007.00946.x

Goh, F., Allen, M. A., Leuko, S., Kawaguchi, T., Decho, A. W., Burns, B. P., et al. (2009). Determining the specific microbial populations and their spatial distribution within the stromatolite ecosystem of Shark Bay. *ISME J.* 3, 383–396. doi: 10.1038/ismej.2008.114

Grotzinger, J. P., and Knoll, A. H. (1999). Stromatolites in Precambrian carbonates: evolutionary mileposts or environmental dipsticks? *Annu. Rev. Earth Planet Sci.* 27, 313–358. doi: 10.1146/annurev.earth.27.1.313

Hammes, F., Boon, N., de Villiers, J., Verstraete, W., and Siciliano, S. D. (2003). Strain-specific ureolytic microbial calcium carbonate precipitation. *Appl. Environ. Microbiol.* 69, 4901–4909. doi: 10.1128/AEM.69.8.4901-4909.2003

Havemann, S. A., and Foster, J. S. (2008). Comparative characterization of the microbial diversities of an artificial microbialite model and a natural stromatolite. *Appl. Environ. Microbiol.* 74, 7410–7421. doi: 10.1128/AEM.01710-08

Hill, D. R., Belbin, T. J., Thorsteinsson, M. V., Bassam, D., Brass, S., and Ernst, A. (1996). GlbN (cyanoglobin) is a peripheral membrane protein that is restricted to certain *Nostoc* spp. *J. Bacteriol* 178, 6587–6598.

Jimenez-Lopez, C., Chekroun, K. B., Jroundi, F., Rodríguez-Gallego, M., Arias, J. M., and González-Muñoz, M. T. (2011). *Myxococcus xanthus* colony calcification: an study to better understand the processes involved in the formation of this stromatolite-like structure. *Adv. Strom. Geobiol.* 131, 161–181. doi: 10.1007/978-3-642-10415-2_11

Khodadad, C. L., and Foster, J. S. (2012). Metagenomic and metabolic profiling of nonlithifying and lithifying stromatolitic mats of Highborne Cay, The Bahamas. *PLoS ONE* 7:e38229. doi: 10.1371/journal.pone.0038229

Kiełbasa, S. M., Wan, R., Sato, K., Horton, P., and Frith, M. C. (2011). Adaptive seeds tame genomic sequence comparison. *Genome Res.* 3, 487–493. doi: 10.1101/gr.113985.110

Konwar, K. M., Hanson, N. W., Pagé, A. P., and Hallam, S. J. (2013). MetaPathways: a modular pipeline for constructing pathway/genome databases from environmental sequence information. *BMC Bioinform.* 14:202. doi: 10.1186/1471-2105-14-202

Langmead, B., and Salzberg, S. L. (2012). Fast gapped-read alignment with Bowtie 2. *Nat. Methods* 9, 357–359. doi: 10.1038/nmeth.1923

Laval, B., Cady, S. L., Pollack, J. C., McKay, C. P., Bird, J. S., Grotzinger, J. P., et al. (2000). Modern freshwater microbialite analogues for ancient dendritic reef structures. *Nature* 407, 626–629. doi: 10.1038/35036579

Lee, Y. N. (2003). Calcite production by *Bacillus amyloliquefaciens* CMB01. *J. Microbiol.* 41, 345–348.

Liang, B., Wu, T. D., Sun, H. J., Vali, H., Guerquin-Kern, J. L., Wang, C. H., et al. (2014). Cyanophycin mediates the accumulation and storage of fixed carbon in non-heterocystous filamentous cyanobacteria from coniform mats. *PLoS ONE* 9:e88142. doi: 10.1371/journal.pone.0088142

Lim, D. S. S., Brady, A. L., Pavilion Lake Research Project (Plrp) Team, Abercromby, A. F., Andersen, D. T., Andersen, M. et al. (2011). A historical overview of the Pavilion Lake Research Project - Analog science and exploration in an underwater environment. *Geol. Soc. Am. Special Papers* 483, 85–115. doi: 10.1130/2011.2483(07)

Lim, D. S. S., Laval, B. E., Slater, G., Antoniades, D., Forrest, A. L., Pike, W., et al. (2009). Limnology of Pavilion Lake, B.C., Canada - Characterization of a microbialite forming environment. *Fundam. Appl. Limnol.* 173, 329–351. doi: 10.1111/gbi.12121

López-García, P., Kazmierczak, J., Benzerara, K., Kempe, S., Guyot, F., and Moreira, D. (2005). Bacterial diversity and carbonate precipitation in the giant microbialites from the highly alkaline Lake Van, Turkey. *Extremophiles* 9, 263–274. doi: 10.1007/s00792-005-0457-0

Lundberg, J., and McFarlane, D. A. (2011). Subaerial freshwater phosphatic stromatolites in Deer Cave, Sarawak—A unique geobiological cave formation. *Geomorphology* 128, 57–72. doi: 10.1016/j.geomorph.2010.12.022

Maliva, G. R., Missimer, M. T., Leo, C. K., Statom, A. R., Dupraz, C., Lynn, M., et al. (2000). Unusual calcite stromatolites and pisoids from a landfill leachate collection system. *Geology* 28, 931–934. doi: 10.1130/0091-7613(2000)28<931:UCSAPF>2.0.CO;2

Merz, M. U. E. (1992). The biology of carbonate precipitation by cyanobacteria. *Facies* 26, 81–101. doi: 10.1007/BF02539795

Meyer, F. D., Paarmann, M., D'Souza, R., Olson, E. M., Glass, M., Kubal, T., et al. (2008). The Metagenomics RAST server - A public resource for the automatic phylogenetic and functional analysis of metagenomes. *BMC Bioinform.* 9:386. doi: 10.1186/1471-2105-9-386

Mobberley, J. M., Khodadad, C. L., and Foster, J. S. (2013). Metabolic potential of lithifying cyanobacteria-dominated thrombolitic mats. *Photosynth. Res.* 118, 125–140. doi: 10.1007/s11120-013-9890-6

Neilan, B. A., Pearson, L. A., Muenchhoff, J., Moffitt, M. C., and Dittmann, E. (2013). Environmental conditions that influence toxin biosynthesis in cyanobacteria. *Environ. Microbiol.* 5, 1239–1253. doi: 10.1111/j.1462-2920.2012.02729.x

Nisanian, M., Holladay, S. D., Karpuzoglu, E., Kerr, R. P., Williams, S. M., Stabler, L., et al. (2014). Exposure of juvenile Leghorn chickens to lead acetate enhances antibiotic resistance in enteric bacterial flora. *Poult. Sci.* 93, 891–897. doi: 10.3382/ps.2013-03600

Omelon, C. R., Brady, A. L., Slater, G. F., Laval, B., Lim, D. S. S., and Southam, G. (2013). Microstructure variability in freshwater microbialites, Pavilion Lake, Canada. *Palaeogeogr. Palaeoclimatol. Palaeoecol.* 392, 62–70. doi: 10.1016/j.palaeo.2013.08.017

Parks, D. H., and Beiko, R. G. (2010). Identifying biologically relevant differences between metagenomic communities. *Bioinformatics* 26, 715–721. doi: 10.1093/bioinformatics/btq041

Perry, R. S., Mcloughlin, N., Lynne, B. Y., Sephton, M. A., Oliver, J. D., Perry, C. C., et al. (2007). Defining biominerals and organominerals: direct and indirect indicators of life. *Sedim. Geol.* 201, 157–179. doi: 10.1016/j.sedgeo.2007.05.014

Power, I. M., Wilson, S. A., Dipple, G. M., and Southam, G. (2011). Modern carbonate microbialites from an asbestos open pit pond, Yukon, Canada. *Geobiology* 9, 180–195. doi: 10.1111/j.1472-4669.2010.00265.x

R Development Core Team (2015). *R: A Language and Environment for Statistical Computing*. Vienna: The R Foundation for Statistical Computing.

Reid, R. P., Visscher, P. T., Decho, A. W., Stolz, J. F., Bebout, B. M., Dupraz, C., et al. (2000). The role of microbes in accretion, lamination and early lithification of modern marine stromatolites. *Nature* 406, 989–999. doi: 10.1038/35023158

Russell, J. A., Brady, A. L., Cardman, Z., Slater, G. F., Lim, D. S. S., and Biddle, J. F. (2014). Prokaryote populations of extant microbialites along a depth gradient in Pavilion Lake, British Columbia, Canada. *Geobiology* 12, 250–264. doi: 10.1111/gbi.12082

Ruvindy, R., White, R. A. III, Neilan, B. A., and Burns, B. P. (2015). Unravelling core microbial metabolisms in the hypersaline microbial mats of Shark Bay using high-throughput metagenomics. *ISME J Adv.* 29:2015. doi: 10.1038/ismej.2015.87

Santos, F., Peña, A., Nogales, B., Soria-Soria, E., del Cura, M. A., González-Martín, J. A., et al. (2010). Bacterial diversity in dry modern freshwater stromatolites from Ruidera Pools Natural Park. *Spain. Syst. Appl. Microbiol.* 33, 209–221. doi: 10.1016/j.syapm.2010.02.0

Schmieder, R., and Edwards, R. (2011). Quality control and preprocessing of metagenomic datasets. *Bioinformatics* 27, 863–864. doi: 10.1093/bioinformatics/btr026

Schmieder, R., Lim, Y. W., Rohwer, F., and Edwards, R. (2010). TagCleaner: identification and removal of tag sequences from genomic and metagenomic datasets. *BMC Bioinform.* 11:341. doi: 10.1186/1471-2105-11-341

Schopf, J. W. (2006). Fossil evidence of Archean life. *Philos. Trans. R. Soc. Lond. B. Biol. Sci. B* 361, 869–885. doi: 10.1098/rstb.2006.1834

Sforna, M. C., Philippot, P., Somogyi, A., van Zuilen, M. A., Medjoubi, K., Schoepp-Cothenet, B., et al. (2014). Evidence for arsenic metabolism and cycling by microorganisms 2.7 *billion years ago*. *Nat. Geosci.* 7, 811–815. doi: 10.1038/ngeo2276

Suttle, C. A. (2005). Viruses in the Sea. *Nature* 437, 356–361. doi: 10.1038/nature04160

Suttle, C. A., Chan, A. M., and Cottrell, M. T. (1991). Use of ultrafiltration to isolate viruses from seawater which are pathogens of marine phytoplankton. *Appl. Environ. Microbiol.* 57, 721–726.

Suzuki, R., and Shimodaira, H. (2006). Pvclust: an R package for assessing the uncertainty in hierarchical clustering. *Bioinformatics* 22, 1540–1542. doi: 10.1093/bioinformatics/btl117

Theisen, C. H., Sumner, D. Y., Mackey, T. J., Lim, D. S., Brady, A. L., and Slater, G. F. (2015). Carbonate fabrics in the modern microbialites of Pavilion Lake: two suites of microfabrics that reflect variation in microbial community morphology, growth habit, and lithification. *Geobiology* 4, 357–372. doi: 10.1111/gbi.12134

Untergasser, A. (2008). *DNA Miniprep using Ctab Untergasser's Lab*. Available at: http://www.untergasser.de/lab/protocols/miniprep_dna_ctab_v1_0.htm [Accessed July 10, 2010].

Varin, T., Lovejoy, C., Jungblut, A. D., Vincent, W. F., and Corbeil, J. (2012). Metagenomic analysis of stress genes in microbial mat communities from Antarctica and the high Arctic. *Appl. Environ. Microbiol.* 78, 549–559. doi: 10.1128/AEM.06354-11

White, R. A. III, Blainey, P. C., Fan, H. C., and Quake, S. R. (2009). Digital PCR provides sensitive and absolute calibration for high throughput sequencing. *BMC Genomics* 10:116. doi: 10.1186/1471-2164-10-116

White, R. A. III, Grassa, C. J., and Suttle, C. A. (2013a). First draft genome sequence from a member of the genus *Agrococcus*, isolated from modern microbialites. *Genome Announc.* 1:e391–e413. doi: 10.1128/genomeA.00391-13

White, R. A. III, Grassa, C. J., and Suttle, C. A. (2013b). Draft Genome Sequence of *Exiguobacterium pavilionensis* strain RW-2, with wide thermal, salinity, and pH tolerance, isolated from modern freshwater microbialites. *Genome Announc.* 1:e597–e613. doi: 10.1128/genomeA.00597–513

White, R. A. III, Power, I. A., Dipple, G. M., Southern, G., and Suttle, C. A. (2015). Metagenomic analysis reveals that modern microbialites and polar microbial mats have similar taxonomic and functional potential. *Front. Microbiol.* 6:966. doi: 10.3389/fmicb.2015.00966

White, R. A. III, and Suttle, C. A. (2013). The Draft Genome Sequence of Sphingomonas paucimobilis Strain HER1398 (*Proteobacteria*), Host to the Giant PAU Phage, Indicates That It Is a Member of the Genus Sphingobacterium (*Bacteroidetes*). *Genome Announc.* 1:e598–e613. doi: 10.1128/genomeA.00598-13

Wickham, H. (2009). *ggplot2: Elegant Graphics for Data Analysis*. New York, NY: Springer.

Wong, H. L., Smith, D. L., Visscher, P. T., and Burns, B. P. (2015). Niche differentiation of bacterial communities at a millimeter scale in Shark Bay microbial mats. *Sci. Rep.* 5:15607. doi: 10.1038/srep15607

Zeigler Allen, L., Allen, E. E., Badger, J. H., McCrow, J. P., Paulsen, I. T., Elbourne, L. D., et al. (2012). Influence of nutrients and currents on the genomic composition of microbes across an upwelling mosaic. *ISME J.* 6, 1403–1414. doi: 10.1038/ismej.2011.201

Conflict of Interest Statement: The authors declare that the research was conducted in the absence of any commercial or financial relationships that could be construed as a potential conflict of interest.

frontiers in
MICROBIOLOGY

REVIEW ARTICLE
published: 27 May 2014
doi: 10.3389/fmicb.2014.00251

Trait-based approaches for understanding microbial biodiversity and ecosystem functioning

Sascha Krause[1,2]*, Xavier Le Roux[3], Pascal A. Niklaus[4], Peter M. Van Bodegom[5], Jay T. Lennon[6], Stefan Bertilsson[7], Hans-Peter Grossart[8,9], Laurent Philippot[10] and Paul L. E. Bodelier[1]

[1] Department of Microbial Ecology, Netherlands Institute of Ecology (NIOO-KNAW), Wageningen, Netherlands
[2] Department of Chemical Engineering, University of Washington, Seattle, WA, USA
[3] Ecologie Microbienne, CNRS, INRA, Université de Lyon, Université Lyon 1, UMR 5557, USC 1193, Villeurbanne, France
[4] Institute of Evolutionary Biology and Environmental Studies, University of Zurich, Zurich, Switzerland
[5] Subdepartment of Systems Ecology, Department of Ecological Sciences, VU University Amsterdam, Amsterdam, Netherlands
[6] Department of Biology, Indiana University, Bloomington, IN, USA
[7] Limnology and Science for Life Laboratory, Department of Ecology and Genetics, Uppsala University, Uppsala, Sweden
[8] Leibniz-Institute for Freshwater Ecology and Inland Fisheries, Berlin, Germany
[9] Institute for Biochemistry and Biology, Potsdam University, Potsdam, Germany
[10] INRA, UMR 1347 Agroecologie, Dijon, France

Edited by:
Anne Bernhard, Connecticut College, USA

Reviewed by:
Susannah Green Tringe, DOE Joint Genome Institute, USA
Adam Martiny, University of California, USA

***Correspondence:**
Sascha Krause, Department of Chemical Engineering, University of Washington, Seattle, Benjamin Hall IRB, 616NE Northlake Place, WA 98195, USA
e-mail: smb.krause@gmx.com

In ecology, biodiversity-ecosystem functioning (BEF) research has seen a shift in perspective from taxonomy to function in the last two decades, with successful application of trait-based approaches. This shift offers opportunities for a deeper mechanistic understanding of the role of biodiversity in maintaining multiple ecosystem processes and services. In this paper, we highlight studies that have focused on BEF of microbial communities with an emphasis on integrating trait-based approaches to microbial ecology. In doing so, we explore some of the inherent challenges and opportunities of understanding BEF using microbial systems. For example, microbial biologists characterize communities using gene phylogenies that are often unable to resolve functional traits. Additionally, experimental designs of existing microbial BEF studies are often inadequate to unravel BEF relationships. We argue that combining eco-physiological studies with contemporary molecular tools in a trait-based framework can reinforce our ability to link microbial diversity to ecosystem processes. We conclude that such trait-based approaches are a promising framework to increase the understanding of microbial BEF relationships and thus generating systematic principles in microbial ecology and more generally ecology.

Keywords: functional traits, ecosystem function, ecological theory, study designs, microbial diversity

BEF RESEARCH—A BRIEF OVERVIEW

The relationship between biodiversity and ecosystem functioning (BEF) (**Table 1**) is complex and understanding this elusive link is one of the most pressing scientific challenges with major societal implications (Cardinale et al., 2012). However, previous studies established controversial views on BEF relationships, using approaches which experimentally manipulated biodiversity on the one hand and comparative approaches that correlate diversity and ecosystem functioning across treatments or natural gradients on the other hand (Hooper et al., 2005; Balvanera et al., 2006). In essence, comparative studies cannot unequivocally demonstrate causal effects of biodiversity on ecosystem functions, since apparent correlations may arise for many reasons, including the reverse relationship (e.g., ecosystem functions such as productivity altering biodiversity), or unobserved drivers affecting diversity and/or ecosystem functions. In an effort to better understand mechanisms, BEF-research has increasingly moved toward direct manipulation of diversity under otherwise constant environmental conditions, an approach that can attribute observed responses to the direct biodiversity manipulation. It is important to distinguish these two cases. Approaches based on either comparison across environmental gradients/treatments or direct manipulation of biodiversity often led to conflicting results. For example, increasing productivity caused by resource supply often leads to reduced plant diversity, mainly through enhanced competition for light, and hence apparent negative BEF relationships (Abrams, 1995; Hautier et al., 2009), a pattern that has also been reported in microbial systems (Patra et al., 2005). In contrast, diversity manipulations generally reveal positive biodiversity-productivity relationships (Balvanera et al., 2006). These seemingly contradictory results are in fact consistent when accounting for the interplays between site fertility, diversity, and productivity (Schmid, 2002).

Biodiversity effects on ecosystem functioning mainly arise from niche-related mechanisms that shape interactions of the biological units (e.g., OTUs, species, genotypes, ecotypes, functional groups, or phylogenetic groups) that vary genetically and in the expressed functional traits (see **Table 1** for definition). These mechanisms are traditionally classified into three broad groups. First, differentiation in resource niches can lead

to reduced competition, and an increased community niche size (**Table 1**). As a result, the associated capture of limiting resources is more efficient and community or ecosystem-level performance increases (Loreau, 2000). Such "complementarity effects" emerge from competition for resources (Salles et al., 2009), and from differences in niches related to pathogens and predation. When host-specific organisms are involved, an increase in diversity typically positively affects ecosystem function. For instance Zhu et al. (2000) demonstrated that genetically diversified rice crops had 89% greater yield, while a major rice disease had 94% less severe effects on diversified crops compared to rice monoculture controls. A second group of mechanisms is generally summarized under the term "selection effects," represented by the probability that high diversity communities are more likely to contain species with particular traits that translate into above-average performance. Such effects are typically restricted to few species, and occur at the expense of others. Finally, "facilitation effects" occur when certain species modify environmental conditions in a way that is beneficial for other species (Bruno et al., 2003). A typical example is the presence of legumes and their nitrogen-fixing symbionts that lead to a nutrient enrichment of the ecosystem and improved performance of non-fixing plant species and nitrogen-related microbial processes (Spehn et al., 2005; Le Roux et al., 2013).

BEF relationships ultimately arise from functional differences among the biological units of which communities are comprised. For instance, in plant communities, functional diversity was the driving factor explaining plant productivity (Tilman, 1997). In another study Norberg et al. (2001) introduced a framework that suggests a linear relationship between variances in phenotypes within functional groups and responses to environmental changes. A later example focused on the role of functional diversity to explain BEF relationships and whether or not this is linked to phylogenetic diversity (Flynn et al., 2011). However, functional traits and the resulting ecological niches are the determinants of species interactions and consequently ecosystem functioning. Traits refer to the physiology, morphology, or genomic characteristics that affect the fitness or function of an organism. Traits can be used to infer its performance under different environmental conditions (Violle et al., 2007), they can be measured or scaled-up at the community level, and eventually be related to community and ecosystem functioning (Violle et al., 2007; Wallenstein and Hall, 2012).

Meta-analyses clearly demonstrated that the relationship between biodiversity and ecosystem functioning has primarily been studied for higher organisms (Balvanera et al., 2006; Cardinale et al., 2012). A systematic search of published papers which refer to microbial diversity and ecosystem functioning nevertheless shows that the total number of papers is quite similar for plant- and microbe-related studies identifying the analysis of BEF relationships as a key objective (**Figure 1**). However, a closer examination reveals that most microbial BEF studies rely on comparative designs where biodiversity is not directly manipulated (**Figure 1**).

Microbial BEF research is evolving rapidly (Allison and Gessner, 2012; Bouskill et al., 2012) but microbial ecologists often quantify traits at scales ranging from populations (e.g., physiological characteristics of strains) to communities (e.g., functional gene pools or substrate utilization patterns from environmental samples) and rarely consider existing trait-related concepts to evaluate BEF relationships as used in ecology. Trait-based approaches could be particularly useful in microbial ecology by complementing microbial approaches based on taxonomy or functional gene/protein sequence diversity and enhancing our ability to link microbial diversity to the functioning of microbial communities and ecosystems.

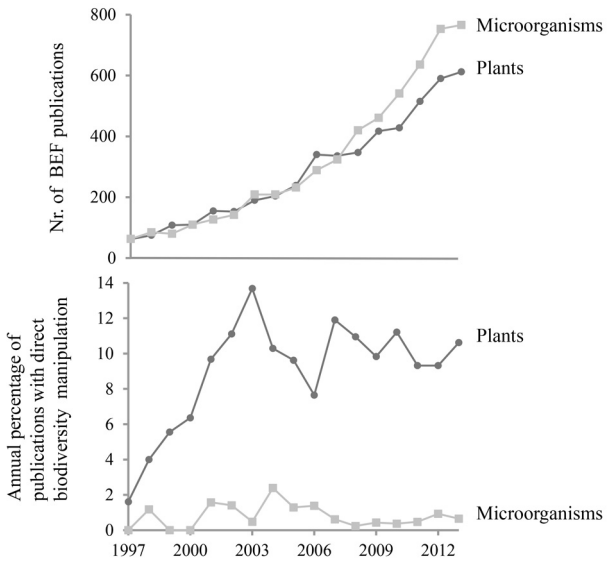

FIGURE 1 | Temporal variations in (top) the number of publications on Biodiversity-Ecosystem Functioning, BEF, relationships in a broad sense for microorganisms as compared to plants, and (bottom) the percentage of publications on microbial BEF or plant BEF where biodiversity was directly manipulated. The search terms used are provided in Supplementary Material 1. At each step of the search profile development, we checked on subsamples that the search hits corresponded to the targeted type of studies. We also checked that a selection of key experiments/papers we knew about were found.

We review microbial studies relating diversity and process rates, focusing more particularly on the application of trait-based approaches, and identify their current progress and pitfalls. We distinguish the application of trait-based approaches for comparative studies across environmental gradients/treatments (**Table 1**), and BEF-studies in which biodiversity is manipulated directly (**Table 2**). We highlight why trait-based approaches could spur significant progress in the understanding of microbial BEF relationships in the future and evaluate how traits can be more directly incorporated into microbial BEF studies. Finally, we discuss the potential and challenges of microbial trait-based approaches to promote the emergence of principles in microbial ecology and BEF relationships in general.

DISTINCTION OF BEF RELATIONSHIPS IN MICROBIAL SYSTEMS

COMPARATIVE INVESTIGATION OF MICROBIAL BEF RELATIONSHIPS

There are many examples where bacterial composition changes along environmental gradients (Hughes Martiny et al., 2006;

Table 1 | Common terms used in BEF and trait-based BEF approaches.

	Definition
Functional traits	Well-defined, measurable properties at the individual level (e.g., organisms, populations) generally used to link performance and contribution to one or several function(s) in any given ecosystem. Thereby, any key property related to physiology, morphology, or genomic information that affects the fitness or function of an organism can be regarded as a functional trait (Violle et al., 2007).
Community trait mean	Mean value calculated for each trait as the mean trait value in a community which can be weighted by the relative abundance of individual taxa in a community (Díaz et al., 2007; Violle et al., 2007)
Gradient analysis	Assessment of functioning, abundances and/or diversity of organisms along an environmental gradient in the field, or in the laboratory along pre-defined treatment gradients (McGill et al., 2006)
Ecosystem functions/functioning	Ecosystem functions in a broad sense can be categorized into functions, e.g., fluxes of energy, nutrients and organic matter; and functioning, e.g., primary production, disturbance resistance, and services like crop yield, wood production, and soil erosion control (Balvanera et al., 2006; Cardinale et al., 2012)
Application	N-dimensional hypervolume with n as the number of dimensions defining the niche, e.g., salinity, temperature, food availability (Begon et al., 2006).

Table 2 | Comparison between trait-based studies that relate microbial biodiversity and ecosystem functioning across environmental gradients/treatments, and those directly manipulating components of diversity.

	Comparative studies	**Manipulated diversity studies**
Level of trait assessment	Functional group/Community	Strain
Trait resolution	Community-mean traits/within community distribution of traits	Taxon-specific traits/multiple traits in individual taxa/tradeoffs among traits
Key eco-physiological techniques	Stable isotope probing; Biolog/Ecoplates; etc.	Metabolic and physiological studies of individual cells and strains
Key -omics techniques	DNA and RNA single gene sequence diversity; environmental (meta-)genomics, transcriptomics, proteomics, and metabolomics	Genomics, transcriptomics, proteomics, and metabolomics on cells and strains
Main scale	The real world (field studies; complex natural communities)	Laboratory (model systems)
Level of understanding	Correlational link between biodiversity and functioning along environmental gradients	Causal/direct/mechanistic link between biodiversity and functioning; complementarity/selection/facilitation effects

Fierer et al., 2007; Van Der Gucht et al., 2007; Attard et al., 2010; Nemergut et al., 2011; Newton et al., 2011; Ghiglione et al., 2012). However, it is often difficult to mechanistically understand the observed correlation between diversity and function in such comparative approaches, because diversity is an observed, dependent variable rather than an applied treatment. Moreover, many environmental parameters can co-vary with diversity, driving observed relationships.

It is particularly difficult to explain such correlations between microbial diversity and ecosystem function in relation to functional diversity. Many bacterial groups are not available in pure culture, which hinders determination of their physiology and consequently assessment of their functional roles in aquatic and terrestrial environments. Recent evidence suggests that a potentially large portion of the microbial diversity detected in gradient studies are not directly contributing to function, being either dead, in a dormant state or present as extracellular DNA (Lennon and Jones, 2011; Blagodatskaya and Kuzyakov, 2013). Although the "dormant diversity" is part of a microbial seed bank from which different traits can be resuscitated (Lennon and Jones, 2011), it can obscure environmental microbial BEF studies. The use of isotope probing (SIP) represents a way to single out taxa that are actively contributing to function while accounting for non-active, members of a community (Bodelier et al., 2013).

It is crucial to relate a particular process to the diversity of the respective, functionally coherent group; such an analysis has the potential for successfully detecting causal links between microbial diversity and ecosystem function. For instance, some studies reported clear relationships between the diversity of soil ammonia- (Webster et al., 2005) or nitrite-oxidizers and nitrification across management practices in relation to the availability of inorganic nitrogen (Attard et al., 2010). The abundance of soil *Nitrobacter*, which are nitrite-oxidizing bacteria with high growth rate/specific activity and low N substrate affinity, increased along a nitrogen gradient (Attard et al., 2010). In contrast, the abundance of *Nitrospira*, which are nitrite-oxidizing bacteria with low growth rate/specific activity and high N substrate affinity tended to decrease along this gradient. While in this case both changes in diversity and functioning of nitrite-oxidizers respond to changes along an environmental gradient, diversity changes are important

in allowing function to increase with increased N availability. Using a number of traits derived from eco-physiological studies with various guilds of nitrifiers, a trait-based modeling framework successfully predicted a number of functions (i.e. ammonia oxidation, N_2O emission) in published datasets in various environmental gradients (Bouskill et al., 2012). Of course, this study heavily relies on the coverage of nitrifier diversity by cultured representatives and associated trait information.

A trait-based perspective can facilitate the handling and interpretation of microbial diversity along environmental gradients by measuring functional traits under the specific conditions a given community is exposed to, i.e. as "realized community mean traits." This differs from "a priori" trait values of organisms measured under standardized conditions, and will in part mirror responses to the specific environment and the specific diversity of the community.

DIRECT MANIPULATION OF DIVERSITY TO STUDY MICROBIAL BEF RELATIONSHIPS

Microbial BEF relationships can also be studied by analyzing the effect of a targeted reduction in microbial biodiversity, e.g., in soil and aquatic microcosms (Le Roux et al., 2011). For instance, reductions in the diversity of pasture soil communities by progressive fumigation or serial dilution had no consistent effect on a range of soil processes (Griffiths et al., 2000, 2004). The removal of diversity for key microbial functional groups such as nitrifiers or denitrifiers provided important information on the extent of functional redundancy within these functional groups (Wertz et al., 2007; Philippot et al., 2013). Reduction of diversity in aquatic microbial communities clearly showed that some metabolic functions (i.e., chitin and cellulose degradation) were controlled by single phylotypes and their traits rather than by richness of the total community (Peter et al., 2011), whereas other functions such as growth were positively correlated to richness. It has to be noted that removal experiments prescribe particular scenarios of diversity loss (e.g., a suspension/dilution approach implies that less abundant species are removed first) which are important for effects on ecosystem functioning (Jones and Lennon, 2010).

An additional step toward understanding the functional role of microbial diversity stems from studies assembling communities through the combination of microbial populations, for example by random selection from a source species pool. This so-called "assemblage approach" has already been used to describe how the diversity of fungal communities influence litter decomposition (Janzen et al., 1995; Cox et al., 2001), the role of mycorrhizal fungal diversity on plant productivity (Van Der Heijden et al., 1998; Jonsson et al., 2001), the role of bacterial diversity on cellulose degradation (Wohl et al., 2004), the role of evenness on the stability of microbial ecosystem functions (Wittebolle et al., 2009), and the role of soil bacterial diversity on mineralization or denitrification (Bell et al., 2005; Salles et al., 2009).

Assemblage experiments offer opportunities to identify mechanisms that may underlie microbial BEF relationships (Le Roux et al., 2011). In particular, functional traits of the assembled strains can be characterized, providing information on whether trait complementarity or selection are major mechanisms for explaining observed BEF relationships (Roscher et al., 2012). For instance, key traits among denitrifying bacteria were linked to the use of different carbon (C) sources that strongly determined the functioning of assembled communities on a mix of C sources (Salles et al., 2009, 2012). The complementarity for traits was a much better predictor of denitrification than taxa richness, the phylogenetic diversity of the communities based on *16S rRNA* gene sequences, or even the diversity assessed by functional gene/protein sequences (Salles et al., 2012). In contrast, antagonistic controlling mechanisms were observed for assembled communities of *Pseudomonas fluorescens*, where inhibition of strains determined the performance of the assembled community (Jousset et al., 2011).

One shortcoming of assemblage experiments is that the assembled, e.g., bacterial communities rarely exceed 100 taxa and hence the diversity is very low compared to the richness observed in most natural communities. Besides, only culturable microorganisms can be used to assemble these communities, even though culture-independent studies suggest the importance of taxa in ecosystem functioning that have not been cultivated (Chen et al., 2008; Mackelprang et al., 2011; Iverson et al., 2012). Nevertheless, studies employing direct manipulation of biodiversity by removal or random assembly of microbial populations remain scarce and represent less than 1% of published microbial studies focusing on the relationship between diversity and ecosystem functioning (**Figure 1**). We believe that an increased effort to couple trait-based approaches and assemblage experiments could be a very powerful strategy to specifically identify and decipher the mechanisms underlying microbial BEF relationships.

TRAIT-BASED APPROACHES TO ADVANCE MICROBIAL BEF STUDIES

INTEGRATING TRAIT-BASED AND PHYLOGENETIC/TAXONOMIC APPROACHES TO UNDERSTAND MICROBIAL BEF

Prior to development and adoption of phylogenetic based tools, bacterial taxonomy was based on phenotypes and physiological characteristics that could only be measured in pure cultures (Staley, 2006). Today, the availability of large databases of marker genes (e.g., the Ribosomal Database Project or Greengenes) has enabled the establishment of a detailed classification scheme for microorganisms that also includes those groups that we have not yet been able to cultivate. However, for studying microbial BEF relationships, a classical taxonomic/phylogenetic approach is hampered by the current species definition (Schleifer, 2009) which can demarcate taxonomic units—which can still be enormously diverse both in functionality and ecology (Staley, 2006; Green et al., 2008). In our opinion, the inherent limitations with regards to the concept of microbial species are not the major issues here, and two other factors are of much more central importance.

To understand BEF relationships it is necessary to study traits at the level of individual cells or organisms (Lavorel et al., 2013). The niches that correspond to traits are hyper-dimensional, and BEF studies call for determining whether niches of functional units overlap. To fully appreciate functional diversity, whether assessed as richness, divergence or dispersion of traits (Hedberg et al., 2013), one has to characterize and account for trade-offs

among the different traits. For example, plant leaf trait trade-offs have been shown to affect litter decomposition and therewith the incidence of wild fires (Brovkin et al., 2012), whereas trade-offs for key traits among bacterial decomposers can restrict the bacterial degradation of recalcitrant carbon to sites with high nitrogen availability (Treseder et al., 2011) and influence how bacteria contend with other abiotic factors such as moisture variability (Lennon et al., 2012). However, characterizing functional trait values and quantifying trade-offs only may lead to spurious correlations and there are only a few examples that demonstrate actual trade-offs supported by plausible physical or chemical mechanisms (e.g., Edwards et al., 2011). Hence, knowledge about trade-offs is indispensable for accurate descriptions of functional BEF relationships and necessitates identification of relevant functional units such as species, ecotypes, or genotypes.

The relevance of trade-offs among microbial traits is recognized (Litchman et al., 2007), but better characterizing trade-offs among microbial traits are likely to be of increasing importance for microbial BEF studies for several reasons. First, they aid in reducing the number of functional dimensions that need to be considered. Second, the co-occurrence of traits and trade-offs help to define microbial strategies beyond the familiar *r* vs. *K* strategies. For example, the life-history scheme designed for plants (Grime, 1977) was used to classify methane-oxidizing bacteria according their competitive ability, ruderal and stress tolerating properties based on culture and environmental traits (Ho et al., 2013). This conceptual approach combines information about phylogeny and function and aggregates traits into community responses, allowing for mixed life strategies and offering more flexibility to accommodate the vast metabolic flexibility of bacteria (**Figure 2**). Though, extrapolation of this conceptual framework to microbial communities deserves experimental validation. There is considerable debate regarding the coherence between phylogeny and the distribution of functional traits (Losos, 2008). If traits are conserved to some degree throughout evolution (trait conservatism), phylogenetic diversity could be a promising proxy for assessing trait diversity. For instance, Cadotte et al. (2008) analyzed 29 studies in which angiosperm biodiversity was manipulated in a systematic way and found that phylogenetic diversity indices explained significantly more variation in

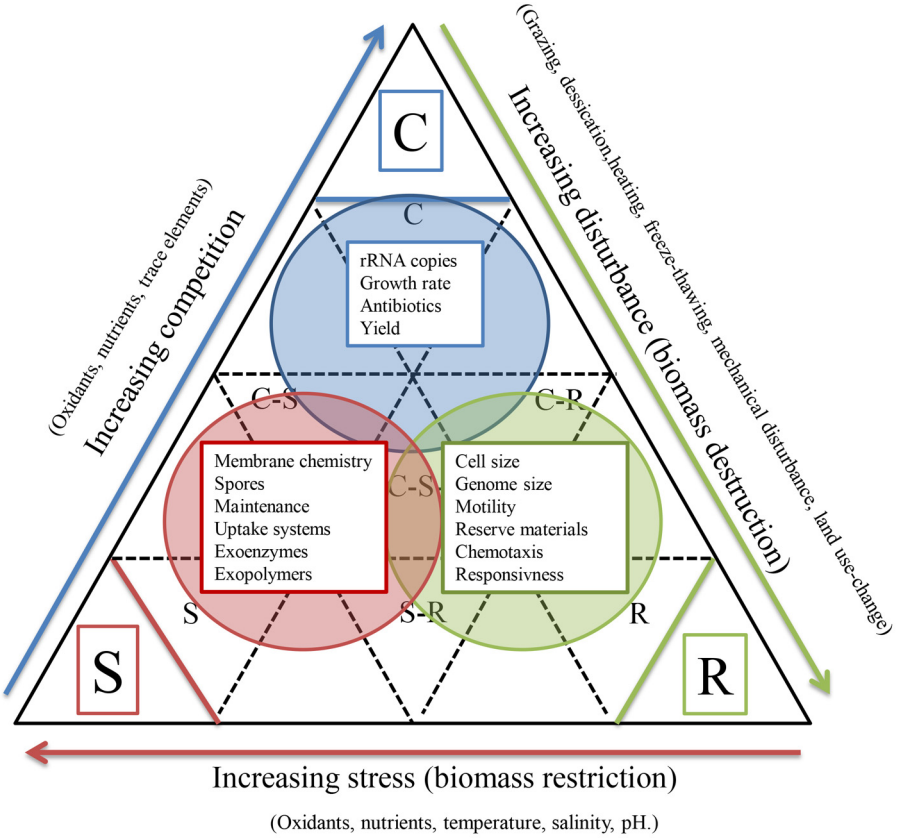

FIGURE 2 | Reflection of microbial traits on the Competitor-Ruderal-Stress tolerator life strategy framework as was proposed for plants (Grime, 1977). The scheme has been adapted for Ho et al. (2013) who used this framework for assigning life-strategies to methane-oxidizing bacteria. The scheme groups subsets of microbial traits which collectively would be of most importance for the respective strategy. The traits collectively accommodate exploring and exploiting habitats, competing with other organisms, tolerating or avoiding surviving stress, and deprivation. This classification is purely qualitative but, for some traits, life-history strategies have been proposed in earlier studies (Fierer et al., 2007; Portillo et al., 2013).

productivity than plant species richness or other diversity measures that were available. Flynn et al. (2011) analyzed data from 29 experiments involving 174 plant species that were present in 1721 combinations and found that functional trait diversity and phylogenetic diversity explained similar amounts of variation in the observed responses. Interestingly, phylogenetic diversity explained variation in data that was not explained by traits, suggesting that it is a surrogate to quantify trait differences along niche axis that are difficult to assess directly (such as pathogen-related niches, or complex hyper-dimensional combinations of single traits assessed).

In microbial ecology, the extent to which functional traits are phylogenetically conserved remains unclear. Considering the rather extensive horizontal gene transfer (Polz et al., 2013) likely compromising a unifying phylogenetic framework, functional diversity measures do not necessarily follow either taxonomy, phylogenetic or apparent evolutionary relationships. For instance, variations in key functional traits of denitrifying bacteria were not well correlated to their (*16S rRNA*-based) phylogenetic relatedness or functional gene/protein sequence relatedness (Jones et al., 2011; Salles et al., 2012). From another perspective, several studies reported broad ecological coherence of high bacterial taxonomic ranks building on *16S rRNA* phylogeny (Fierer et al., 2007; Von Mering et al., 2007; Philippot et al., 2009; Lennon et al., 2012). The question thus remains whether or not one should abandon taxonomy- and phylogeny-based approaches altogether for studies of BEF relationships. If traits are phylogenetically conserved at least for some microbial groups, phylogenetic diversity could serve as proxy for functional diversity. Calculating functional diversity indices generally requires the assessment of traits at the individual or some aggregated taxonomic level, which generally is impossible in microbial studies that do not build assemblage-based designs. Martiny et al. (2012) recently developed a new phylogenetic metric which estimates the clade depth of shared traits between organisms. This approach could be used to translate differences in community composition into consequences for microbial-mediated processes. Another approach models evolutionary dynamics of bacteria to ecologically distinct lineages, so called ecotypes, within natural communities, allowing for a highly resolved ecological classification (Koeppel et al., 2008). Such distinction of microbial taxa based on ecological features would bridge the gap between taxonomy- and trait-based approaches in microbial ecology. We argue that trait-based approaches should build on—not replace—taxonomy-based approaches. The information needed to properly characterize the co-occurrence of traits and trait trade-offs among microorganisms builds on taxonomic ranks, and there is certainly an incentive for more high-throughput surveys of phenotypic characteristics of microbial taxa (Bayjanov et al., 2012). Such approaches could mark the beginning of a deviation from classical phylum-based approaches in microbial BEF studies toward a classification based on functional performance and role in the environment.

TOOLS AVAILABLE TO INTEGRATE TRAITS INTO MICROBIAL BEF STUDIES

Measurements of taxonomic microbial diversity are very challenging since diversity levels are extremely high for most natural microbial systems (Torsvik et al., 2002; Caporaso et al., 2011). To obtain functional diversity measures in microbial BEF studies, the biggest challenges are (i) defining which microbial traits are important with respect to ecosystem functioning or particular ecosystem functions, and (ii) measuring these relevant traits.

For the assemblage studies, microbial ecologists can measure multiple traits for individual microorganisms or populations and quantify tradeoffs between traits. However, defining the types of relevant traits to measure is a challenge, depending on the community functioning under study. On the other hand, traits can be related to shifts in function across environmental gradients or treatments, at the genetic or functional level, or directly at the community scale. However, this is different from analyzing BEF-relationships in the general ecological context, which requires methods capable of quantifying the local functional diversity (i.e., the variation of trait combinations present at the individual level). Community mean traits are not useful for this purpose, since the information about effects of the local trait diversity (i.e., the putative local driver of a BEF-relationship) will be lost by averaging.

The analysis of metabolic processes offers great potential to evaluate aggregated trait values at the community scale. Functional traits can be assessed by high-throughput assays, such as Biolog or Ecoplates. These cultivation-based metabolic assays can be used to characterize the community capacity to oxidize a range of C sources (Garland, 1996) or to measure a functional operating range of soil or aquatic microbial communities (Hallin et al., 2012).

We see some advantage for microbial studies correlating community-mean traits to functional capabilities of the community as a whole, since these are more easily measurable than for higher organisms. Indeed, aggregated trait values would boil down to a metric sizing of "meta-species," which can illuminate responses along environmental gradients and possible effects on ecosystem functioning. A drawback is that the combination of traits of all microbial individuals that compose the community can hardly be characterized.

We can expect that our ability to identify and quantify functional traits of microbial individuals and populations in natural, complex communities will increase in the coming years. Despite the dogma that we cannot study the physiology of ecologically "relevant" microbes from environmental samples owing to the challenges associated with the enrichment and isolation of most taxa, we must recognize that there have already been major advances in cultivation efforts over the past 20 years. *In situ* enrichments (e.g., diffusion chambers and baited beads) and other incubation methods can be used to determine cell-specific metabolic rates, even at extremely low rates (Hoehler and Jorgensen, 2013). Additional physiological features that are tractable today (without isolation) include cell-size related nutrient affinity and nutrient use efficiency (Edwards et al., 2012), and specific substrate use with isotope tracking methods targeting single cells of different size and shape (flow cytometry and stable isotope tracers, microautoradiography, nano-SIMS) (Nielsen et al., 2003; Casey et al., 2007; Behrens et al., 2012; Garcia et al., 2013). In addition, just like in the omics realm, there have been major advances in microscopy and bio-molecular imaging over

the last 20 years (Haagensen et al., 2011), with novel and refined techniques that offer huge opportunities to access key aspects of functional diversity, even within complex microbial communities. For instance, we can now have access to the bulk biochemical composition of cells by RAMAN spectroscopy (Huang et al., 2007), and to their spatial organization (Stiehl-Braun et al., 2011). Sensitive fluorescence-based techniques enable visualization of novel morphological and physiological features (porins, flagella, proteins, and protein-coding genes etc.) and of associations based on syntrophic interactions (Watrous et al., 2013). Hence, even if a proper quantification of the functional diversity of natural, complex communities from multiple trait values of individuals composing these communities remains challenging, a toolkit already exists to help microbial ecologists working in this domain. Finally, the dramatically improved opportunities to reconstruct genomes of so far uncultivated microbial populations and cells by binning of complex metagenomes (Rusch et al., 2010; Iverson et al., 2012) has demonstrated great potential for resolving metabolic and functional traits of uncultured and poorly known representatives in the microbial world (Wrighton et al., 2012). This can even be combined with *in situ* substrate usage of uncultivated microbes (Mayali et al., 2012). Single cell genome sequencing (Stepanauskas, 2012) is another feasible way to elucidate and infer genome encoded traits in uncultured microbial populations that often make up the bulk portion of natural communities and are likely to have a large impact on ecosystem functions.

We believe that microbial ecologist have the ability to provide new insights to trait-based ecology as opposed to just borrowing ideas and approaches from other non-microbial ecologists, fully making use of the particularities of microbial systems and tools. In particular, microbial ecology should play a key role in deciphering the effects of functional diversity and spatial distribution in BEF studies, offering very relevant and manageable models to address this key issue.

CONCLUSION AND PERSPECTIVES

Microbial communities are a key variable in how natural and anthropogenic disturbances, including climate change, will affect ecosystem functioning and hence delivery of services to human societies. The trait-based approach is not the Holy Grail (Lavorel and Garnier, 2002) but a promising framework and discourse for future microbial research. In particular, promising experimental approaches that incorporate functional traits can pave the road to increase the understanding of microbial BEF relationships, and BEF relationships in general.

Microbial ecologists face challenges but also great opportunities in this context. Instead of simply suggesting the need to renew approaches in BEF research using traits, we argue that two main priorities for microbial BEF studies are (i) to reinforce experimentally-sound studies of the role of microbial (trait-based) diversity on ecosystem functioning, and (ii) to promote efforts for measuring and archiving microbial traits in a way suitable for the highly diverse and dynamic microbial communities that make up the biosphere.

The first priority arises from the current paucity of microbial ecology in terms of BEF studies that directly manipulate diversity using a trait-based approach. While assembled communities clearly differ from complex communities from natural environments, this does not diminish the value and potential of such studies to disentangle the possible key mechanisms underlying BEF relationships.

Concerning the second priority, we call for more innovative physiological studies in order to measure traits and their relevant unit (e.g., single strains, population, or community-level). More specifically, by measuring traits in a standardized manner, e.g., incubation condition and media, and by applying analogous tests also to organisms we cannot get in pure culture, we may be able to reveal important trait distributions and generate a microbial trait database similar to, e.g., the TRY global traits initiative for plants (Kattge et al., 2011). Microbial ecologists can also capitalize on novel powerful genome sequencing tools being applied to communities or single uncultured cells, which may serve as a tool for predicting ecosystem function from detected (genomic) traits (Raes et al., 2011; Barberan et al., 2012).

Microbial ecologists can provide new insights and concepts to trait-based BEF studies, according to the particularities of microbial systems and the tools available in microbial ecology. For instance, BEF studies over many microbial generations allow researchers to reveal the effect of eco-evolutionary feedbacks on BEF relationships over reasonable time scales. Also, accounting for spatial and temporal niche variability as well as assessing the role of diversity in multiple related ecosystem functions, microbial trait-based approaches may deliver mechanistic insights in areas practically not feasible in higher organisms, thus providing benefits to ecology as a whole, which is still a major challenge for microbial ecologists (Prosser et al., 2007).

ACKNOWLEDGMENTS

This study was part of the European Science Foundation EUROCORES Programme EuroEEFG and was financially supported by grants from the Netherlands Organization for Scientific Research (NWO) (Grant number 855.01.150) and the German Science Foundation (GR 1540/17-1). Additional financial support was given to Jay T. Lennon by grants from National Science Foundation (DEB 1146149) and the US Department of Agriculture (2013-02775), and to Stefan Bertilsson from the Swedish Research Council. Many thanks to all participants of the ESF EuroEEFG workshop Understanding, managing and protecting microbial communities in aquatic and terrestrial ecosystems: "Exploring the trait-based functional biodiversity approach," held in Wageningen, the Netherlands, 10–13th February, 2013. This publication is publication nr. 5610 of the Netherlands Institute of Ecology.

SUPPLEMENTARY MATERIAL

The Supplementary Material for this article can be found online at: http://www.frontiersin.org/journal/10.3389/fmicb.2014.00251/abstract

REFERENCES

Abrams, P. A. (1995). Monotonic or unimodal diversity-productivity gradients: what does competition theory predict? *Ecology* 76, 2019–2027. doi: 10.2307/1941677

Allison, S. D., and Gessner, M. (2012). A trait-based approach for modelling microbial litter decomposition. *Ecol. Lett.* 15, 1058–1070. doi: 10.1111/j.1461-0248.2012.01807.x

Attard, E., Poly, F., Commeaux, C., Laurent, F., Terada, A., Smets, B. F., et al. (2010). Shifts between *Nitrospira*- and *Nitrobacter*-like nitrite oxidizers underlie the response of soil potential nitrite oxidation to changes in tillage practices. *Environ. Microbiol.* 12, 315–326. doi: 10.1111/j.1462-2920.2009.02070.x

Balvanera, P., Pfisterer, A. B., Buchmann, N., He, J. S., Nakashizuka, T., Raffaelli, D., et al. (2006). Quantifying the evidence for biodiversity effects on ecosystem functioning and services. *Ecol. Lett.* 9, 1146–1156. doi: 10.1111/j.1461-0248.2006.00963.x

Barberan, A., Fernandez-Guerra, A., Bohannan, B. J. M., and Casamayor, E. O. (2012). Exploration of community traits as ecological markers in microbial metagenomes. *Mol. Ecol.* 21, 1909–1917. doi: 10.1111/j.1365-294X.2011.05383.x

Bayjanov, J. R., Molenaar, D., Tzeneva, V., Siezen, R. J., and Van Hijum, S. A. (2012). PhenoLink—a web-tool for linking phenotype to ∼omics data for bacteria: application to gene-trait matching for *Lactobacillus plantarum* strains. *BMC Genomics* 13:170. doi: 10.1186/1471-2164-13-170

Begon, M., Townsend, C. R., and Harper, J. L. (2006). *ECOLOGY: From Individuals to Ecosystems.* Malden: Blackwell Publishing.

Behrens, S., Kappler, A., and Obst, M. (2012). Linking environmental processes to the *in situ* functioning of microorganisms by high-resolution secondary ion mass spectrometry (NanoSIMS) and scanning transmission X-ray microscopy (STXM). *Environ. Microbiol.* 14, 2851–2869. doi: 10.1111/j.1462-2920.2012.02724.x

Bell, T., Newman, J. A., Silverman, B. W., Turner, S. L., and Lilley, A. K. (2005). The contribution of species richness and composition to bacterial services. *Nature* 436, 1157–1160. doi: 10.1038/nature03891

Blagodatskaya, E., and Kuzyakov, Y. (2013). Active microorganisms in soil: critical review of estimation criteria and approaches. *Soil Biol. Biochem.* 67, 192–211. doi: 10.1016/j.soilbio.2013.08.024

Bodelier, P. L. E., Meima-Franke, M., Hordijk, C. A., Steenbergh, A. K., Hefting, M. M., Bodrossy, L., et al. (2013). Microbial minorities modulate methane consumption through niche partitioning. *ISME J.* 7, 2214–2228. doi: 10.1038/ismej.2013.99

Bouskill, N., Tang, J., Riley, W. J., and Brodie, E. L. (2012). Trait-based representation of biological nitrification: model development, testing, and predicted community composition. *Front. Microbiol.* 3:364. doi: 10.3389/fmicb.2012.00364

Brovkin, V., Van Bodegom, P. M., Kleinen, T., Wirth, C., Cornwell, W. K., Cornelissen, J. H. C., et al. (2012). Plant-driven variation in decomposition rates improves projections of global litter stock distribution. *Biogeosciences* 9, 565–576. doi: 10.5194/bg-9-565-2012

Bruno, J. F., Stachowicz, J. J., and Bertness, M. D. (2003). Inclusion of facilitation into ecological theory. *Trends Ecol. Evol.* 18, 119–125. doi: 10.1016/S0169-5347(02)00045-9

Cadotte, M. W., Cardinale, B. J., and Oakley, T. H. (2008). Evolutionary history and the effect of biodiversity on plant productivity. *Proc. Natl. Acad. Sci. U.S.A.* 105, 17012–17017. doi: 10.1073/pnas.0805962105

Caporaso, J. G., Lauber, C. L., Walters, W. A., Berg-Lyons, D., Lozupone, C. A., Turnbaugh, P. J., et al. (2011). Global patterns of 16S rRNA diversity at a depth of millions of sequences per sample. *Proc. Natl. Acad. Sci.* 108, 4516–4522. doi: 10.1073/pnas.1000080107

Cardinale, B. J., Duffy, J. E., Gonzalez, A., Hooper, D. U., Perrings, C., Venail, P., et al. (2012). Biodiversity loss and its impact on humanity. *Nature* 486, 59–67. doi: 10.1038/Nature11148

Casey, J. R., Lomas, M. W., Mandecki, J., and Walker, D. E. (2007). Prochlorococcus contributes to new production in the Sargasso Sea deep chlorophyll maximum. *Geophys. Res. Lett.* 34:L10604. doi: 10.1029/2006GL028725

Chen, Y., Dumont, M. G., Neufeld, J. D., Bodrossy, L., Stralis-Pavese, N., McNamara, N. P., et al. (2008). Revealing the uncultivated majority: combining DNA stable-isotope probing, multiple displacement amplification and metagenomic analyses of uncultivated *Methylocystis* in acidic peatlands. *Environ. Microbiol.* 10, 2609–2622. doi: 10.1111/j.1462-2920.2008.01683.x

Cox, P., Wilkinson, S. P., and Anderson, J. M. (2001). Effects of fungal inocula on the decomposition of lignin and structural polysaccharides in *Pinus sylvestris* litter. *Biol. Fert. Soils* 33, 246–251. doi: 10.1007/s003740000315

Díaz, S., Lavorel, S., De Bello, F., Quétier, F., Grigulis, K., and Robson, T. M. (2007). Incorporating plant functional diversity effects in ecosystem service assessments. *Proc. Natl. Acad. Sci. U.S.A.* 104, 20684–20689. doi: 10.1073/pnas.0704716104

Edwards, K. F., Klausmeier, C. A., and Litchman, E. (2011). Evidence for a three-way trade-off between nitrogen and phosphorus competitive abilities and cell size in phytoplankton. *Ecology* 92, 2085–2095. doi: 10.1890/11-0395.1

Edwards, K. J., Becker, K., and Colwell, F. S. (2012). The deep, dark energy biosphere: intraterrestrial life on earth. *Annu. Rev. Earth Planet. Sci.* 40, 551–568. doi: 10.1146/annurev-earth-042711-105500

Fierer, N., Bradford, M. A., and Jackson, R. B. (2007). Toward an ecological classification of soil bacteria. *Ecology* 88, 1354–1364. doi: 10.1890/05-1839

Flynn, D. F. B., Mirotchnick, N., Jain, M., Palmer, M. I., and Naeem, S. (2011). Functional and phylogenetic diversity as predictors of biodiversity-ecosystem-function relationships. *Ecology* 92, 1573–1581. doi: 10.1890/10-1245.1

Garcia, S. L., McMahon, K. D., Martinez-Garcia, M., Srivastava, A., Sczyrba, A., Stepanauskas, R., et al. (2013). Metabolic potential of a single cell belonging to one of the most abundant lineages in freshwater bacterioplankton. *ISME J.* 7, 137–147. doi: 10.1038/ismej.2012.86

Garland, J. L. (1996). Analytical approaches to the characterization of samples of microbial communities using patterns of potential C source utilization. *Soil Biol. Biochem.* 28, 213–221. doi: 10.1016/0038-0717(95)00112-3

Ghiglione, J. F., Galand, P. E., Pommier, T., Pedros-Alio, C., Maas, E. W., Bakker, K., et al. (2012). Pole-to-pole biogeography of surface and deep marine bacterial communities. *Proc. Natl. Acad. Sci. U.S.A.* 109, 17633–17638. doi: 10.1073/pnas.1208160109

Green, J. L., Bohannan, B. J. M., and Whitaker, R. J. (2008). Microbial biogeography: from taxonomy to traits. *Science* 320, 1039–1043. doi: 10.1126/science.1153475

Griffiths, B. S., Kuan, H. L., Ritz, K., Glover, L. A., McCaig, A. E., and Fenwick, C. (2004). The relationship between microbial community structure and functional stability, tested experimentally in an upland pasture soil. *Microb. Ecol.* 47, 104–113. doi: 10.1007/s00248-002-2043-7

Griffiths, B. S., Ritz, K., Bardgett, R. D., Cook, R., Christensen, S., Ekelund, F., et al. (2000). Ecosystem response of pasture soil communities to fumigation-induced microbial diversity reductions: an examination of the biodiversity-ecosystem function relationship. *Oikos* 90, 279–294. doi: 10.1034/j.1600-0706.2000.900208.x

Grime, J. P. (1977). Evidence for the existence of three primary strategies in plants and its relevance to ecological and evolutionary theory. *Am. Nat.* 111, 1169–1194. doi: 10.2307/2460262

Haagensen, J. A., Regenberg, B., and Sternberg, C. (2011). Advanced microscopy of microbial cells. *Adv. Biochem. Eng. Biotechnol.* 124, 21–54. doi: 10.1007/10_2010_83

Hallin, S., Welsh, A., Stenstrom, J., Hallet, S., Enwall, K., Bru, D., et al., (2012). Soil functional operating range linked to microbial biodiversity and community composition using denitrifiers as model guild. *PLoS ONE* 7:e51962. doi: 10.1371/journal.pone.0051962

Hautier, Y., Niklaus, P. A., and Hector, A. (2009). Competition for light causes plant biodiversity loss after eutrophication. *Science* 324, 636–638. doi: 10.1126/science.1169640

Hedberg, P., Saetre, P., Sundberg, S., Rydin, H., and Kotowski, W. (2013). A functional trait approach to fen restoration analysis. *Appl. Veg. Sci.* 16, 658–666. doi: 10.1111/Avsc.12042

Ho, A., Kerckhof, F.-M., Luke, C., Reim, A., Krause, S., Boon, N., et al., (2013). Conceptualizing functional traits and ecological characteristics of methane-oxidizing bacteria as life strategies. *Environ. Microbiol. Rep.* 5, 335–345. doi: 10.1111/j.1758-2229.2012.00370.x

Hoehler, T. M., and Jorgensen, B. B. (2013). Microbial life under extreme energy limitation. *Nat. Rev. Microbiol.* 11, 83–94. doi: 10.1038/nrmicro2939

Hooper, D. U., Chapin, F. S., Ewel, J. J., Hector, A., Inchausti, P., Lavorel, S., et al. (2005). Effects of biodiversity on ecosystem functioning: a consensus of current knowledge. *Ecol. Monogr.* 75, 3–35. doi: 10.1890/04-0922

Huang, W. E., Stoecker, K., Griffiths, R., Newbold, L., Daims, H., Whiteley, A. S., et al. (2007). Raman-FISH: combining stable-isotope Raman spectroscopy and fluorescence *in situ* hybridization for the single cell analysis of identity and function. *Environ. Microbiol.* 9, 1878–1889. doi: 10.1111/j.1462-2920.2007.01352.x

Hughes Martiny, J. B. H., Bohannan, B. J. M., Brown, J. H., Colwell, R. K., Fuhrman, J. A., Green, J. L., et al. (2006). Microbial biogeography: putting microorganisms on the map. *Nat. Rev. Microbiol.* 4, 102–112. doi: 10.1038/nrmicro1341

Iverson, V., Morris, R. M., Frazar, C. D., Berthiaume, C. T., Morales, R. L., and Armbrust, E. V. (2012). Untangling genomes from metagenomes: revealing an uncultured class of marine euryarchaeota. *Science* 335, 587–590. doi: 10.1126/science.1212665

Janzen, R. A., Dormaar, J. F., and McGill, W. B. (1995). A community-level concept of controls on decomposition processes: decomposition of barley straw by *Phanerochaete chrysosporium* or *Phlebia radiata* in pure or mixed culture. *Soil Biol. Biochem.* 27, 173–179. doi: 10.1016/0038-0717(94)00164-V

Jones, C. M., Welsh, A., Throbäck, I. N., Dörsch, P., Bakken, L. R., and Hallin, S. (2011). Phenotypic and genotypic heterogeneity among closely related soil-borne N_2– and N_2O-producing *Bacillus* isolates harboring the nosZ gene. *FEMS Microbiol. Ecol.* 76, 541–552. doi: 10.1111/j.1574-6941.2011.01071.x

Jones, S. E., and Lennon, J. T. (2010). Dormancy contributes to the maintenance of microbial diversity. *Proc. Natl. Acad. Sci. U.S.A.* 107, 5881–5886. doi: 10.1073/pnas.0912765107

Jonsson, L. M., Nilsson, M.-C., Wardle, D. A., and Zackrisson, O. (2001). Context dependent effects of ectomycorrhizal species richness on tree seedling productivity. *Oikos* 93, 353–364. doi: 10.1034/j.1600-0706.2001.930301.x

Jousset, A., Schmid, B., Scheu, S., and Eisenhauer, N. (2011). Genotypic richness and dissimilarity opposingly affect ecosystem functioning. *Ecol. Lett.* 14, 537–545. doi: 10.1111/j.1461-0248.2011.01613.x

Kattge, J., Díaz, S., Lavorel, S., Prentice, I. C., Leadley, P., Bönisch, G., et al. (2011). TRY—a global database of plant traits. *Glob. Change Biol.* 17, 2905–2935. doi: 10.1111/j.1365-2486.2011.02451.x

Koeppel, A., Perry, E. B., Sikorski, J., Krizanc, D., Warner, A., Ward, D. M., et al. (2008). Identifying the fundamental units of bacterial diversity: a paradigm shift to incorporate ecology into bacterial systematics. *Proc. Natl. Acad. Sci. U.S.A.* 105, 2504–2509. doi: 10.1073/pnas.0712205105

Lavorel, S., and Garnier, E. (2002). Predicting changes in community composition and ecosystem functioning from plant traits: revisiting the Holy Grail. *Funct. Ecol.* 16, 545–556. doi: 10.1046/j.1365-2435.2002.00664.x

Lavorel, S., Storkey, J., Bardgett, R. D., De Bello, F., Berg, M. P., Le Roux, X., et al. (2013). A novel framework for linking functional diversity of plants with other trophic levels for the quantification of ecosystem services. *J. Veg. Sci.* 24, 942–948. doi: 10.1111/Jvs.12083

Lennon, J. T., Aanderud, Z. T., Lehmkuhl, B. K., and Schoolmaster, D. R. Jr. (2012). Mapping the niche space of soil microorganisms using taxonomy and traits. *Ecology* 93, 1867–1879. doi: 10.1890/11-1745.1

Lennon, J. T., and Jones, S. E. (2011). Microbial seed banks: the ecological and evolutionary implications of dormancy. *Nat. Rev. Microbiol.* 119, 119–130. doi: 10.1038/nrmicro2504

Le Roux, X., Recous, S., and Attard, E. (2011). "Soil microbial diversity in grasslands and its importance for grassland functioning and services," in *Grassland Productivity and Ecosystem Services*, eds. G. Lemaire, J. Hodgson, and A. Chabbi (Wallingford: CAB International), 158–165.

Le Roux, X., Schmid, B., Poly, F., Barnard, R. L., Niklaus, P. A., Guillaumaud, N., et al. (2013). Soil environmental conditions and microbial build-up mediate the effect of plant diversity on soil nitrifying and denitrifying enzyme activities in temperate grasslands. *PLoS ONE* 8:e61069. doi: 10.1371/journal.pone.0061069

Litchman, E., Klausmeier, C. A., Schofield, O. M., and Falkowski, P. G. (2007). The role of functional traits and trade-offs in structuring phytoplankton communities: scaling from cellular to ecosystem level. *Ecol. Lett.* 10, 1170–1181. doi: 10.1111/j.1461-0248.2007.01117.x

Loreau, M. (2000). Biodiversity and ecosystem functioning: recent theoretical advances. *Oikos* 91, 3–17. doi: 10.1034/j.1600-0706.2000.910101.x

Losos, J. B. (2008). Phylogenetic niche conservatism, phylogenetic signal and the relationship between phylogenetic relatedness and ecological similarity among species. *Ecol. Lett.* 11, 995–1003. doi: 10.1111/j.1461-0248.2008.01229.x

Mackelprang, R., Waldrop, M. P., Deangelis, K. M., David, M. M., Chavarria, K. L., Blazewicz, S. J., et al. (2011). Metagenomic analysis of a permafrost microbial community reveals a rapid response to thaw. *Nature* 480, 368–371. doi: 10.1038/Nature10576

Martiny, A. C., Treseder, K., and Pusch, G. (2012). Phylogenetic conservatism of functional traits in microorganisms. *ISME J.* 7, 830–838. doi: 10.1038/ismej.2012.160

Mayali, X., Weber, P. K., Brodie, E. L., Mabery, S., Hoeprich, P. D., and Pett-Ridge, J. (2012). High-throughput isotopic analysis of RNA microarrays to quantify microbial resource use. *ISME J.* 6, 1210–1221. doi: 10.1038/ismej.2011.175

McGill, B. J., Enquist, B. J., Weiher, E., and Westoby, M. (2006). Rebuilding community ecology from functional traits. *Trends Ecol. Evol.* 21, 178–185. doi: 10.1016/j.tree.2006.02.002

Nemergut, D. R., Costello, E. K., Hamady, M., Lozupone, C., Jiang, L., Schmidt, S. K., et al. (2011). Global patterns in the biogeography of bacterial taxa. *Environ. Microbiol.* 13, 135–144. doi: 10.1111/j.1462-2920.2010.02315.x

Newton, R. J., Jones, S. E., Eiler, A., McMahon, K. D., and Bertilsson, S. (2011). A guide to the natural history of freshwater lake bacteria. *Microbiol. Mol. Biol. Rev.* 75, 14–49. doi: 10.1128/mmbr.00028-10

Nielsen, J. L., Christensen, D., Kloppenborg, M., and Nielsen, P. H. (2003). Quantification of cell-specific substrate uptake by probe-defined bacteria under *in situ* conditions by microautoradiography and fluorescence *in situ* hybridization. *Environ. Microbiol.* 5, 202–211. doi: 10.1046/j.1462-2920.2003.00402.x

Norberg, J., Swaney, D. P., Dushoff, J., Lin, J., Casagrandi, R., and Levin, S. A. (2001). Phenotypic diversity and ecosystem functioning in changing environments: a theoretical framework. *Proc. Natl. Acad. Sci. U.S.A.* 98, 11376–11381. doi: 10.1073/pnas.171315998

Patra, A. K., Abbadie, L., Clays-Josserand, A., Degrange, V., Grayston, S. J., Loiseau, P., et al. (2005). Effects of grazing on microbial functional groups involved in soil N dynamics. *Ecol. Monogr.* 75, 65–80. doi: 10.1890/03-0837

Peter, H., Beier, S., Bertilsson, S., Lindstrom, E. S., Langenheder, S., and Tranvik, L. J. (2011). Function-specific response to depletion of microbial diversity. *ISME J.* 5, 351–361. doi: 10.1038/ismej.2010.119

Philippot, L., Bru, D., Saby, N. P. A., Cuhel, J., Arrouays, D., Simek, M., et al. (2009). Spatial patterns of bacterial taxa in nature reflect ecological traits of deep branches of the 16S rRNA bacterial tree. *Environ. Microbiol.* 11, 3096–3104. doi: 10.1111/j.1462-2920.2009.02014.x

Philippot, L., Spor, A., Henault, C., Bru, D., Bizouard, F., Jones, C. M., et al. (2013). Loss in microbial diversity affects nitrogen cycling in soil. *ISME J.* 7, 1609–1619. doi: 10.1038/ismej.2013.34

Polz, M. F., Alm, E. J., and Hanage, W. P. (2013). Horizontal gene transfer and the evolution of bacterial and archaeal population structure. *Trends Genet.* 29, 170–175. doi: 10.1016/j.tig.2012.12.006

Portillo, M. C., Leff, J. W., Lauber, C. L., and Fierer, N. (2013). Cell size distributions of soil bacterial and archaeal taxa. *Appl. Environ. Microbiol.* 79, 7610–7617. doi: 10.1128/aem.02710-13

Prosser, J. I., Bohannan, B. J. M., Curtis, T. P., Ellis, R. J., Firestone, M. K., Freckleton, R. P., et al. (2007). The role of ecological theory in microbial ecology. *Nat. Rev. Microbiol.* 5, 384–392. doi: 10.1038/nrmicro1643

Raes, J., Letunic, I., Yamada, T., Jensen, L. J., and Bork, P. (2011). Toward molecular trait-based ecology through integration of biogeochemical, geographical and metagenomic data. *Mol. Syst. Biol.* 7:473. doi: 10.1038/msb.2011.6

Roscher, C., Schumacher, J., Gubsch, M., Lipowsky, A., Weigelt, A., Buchmann, N., et al. (2012). Using plant functional traits to explain diversity–productivity relationships. *PLoS ONE* 7:e36760. doi: 10.1371/journal.pone.0036760

Rusch, D. B., Martiny, A. C., Dupont, C. L., Halpern, A. L., and Venter, J. C. (2010). Characterization of Prochlorococcus clades from iron-depleted oceanic regions. *Proc. Natl. Acad. Sci. U.S.A.* 107, 16184–16189. doi: 10.1073/pnas.1009513107

Salles, J., Le Roux, X., and Poly, F. (2012). Relating phylogenetic and functional diversity among denitrifiers and quantifying their capacity to predict community functioning. *Front. Microbiol.* 3:209. doi: 10.3389/fmicb.2012.00209

Salles, J. F., Poly, F., Schmid, B., and Roux, X. L. (2009). Community niche predicts the functioning of denitrifying bacterial assemblages. *Ecology* 90, 3324–3332. doi: 10.1890/09-0188.1

Schleifer, K. H. (2009). Classification of bacteria and archaea: past, present and future. *Syst. Appl. Microbiol.* 32, 533–542. doi: 10.1016/j.syapm.2009.09.002

Schmid, B. (2002). The species richness productivity controversy. *Trends Ecol. Evol.* 17, 113–114. doi: 10.1016/S0169-5347(01)02422-3

Spehn, E. M., Hector, A., Joshi, J., Scherer-Lorenzen, M., Schmid, B., Bazeley-White, E., et al. (2005). Ecosystem effects of biodiversity manipulations in European grasslands. *Ecol. Monogr.* 75, 37–63. doi: 10.1890/03-4101

Staley, J. T. (2006). The bacterial species dilemma and the genomic-phylogenetic species concept. *Philos. Trans. R. Soc. Lond. B. Biol. Sci.* 361, 1899–1909. doi: 10.1098/rstb.2006.1914

Stepanauskas, R. (2012). Single cell genomics: an individual look at microbes. *Curr.Opin. Microbiol.* 15, 613–620. doi: 10.1016/j.mib.2012.09.001

Stiehl-Braun, P. A., Hartmann, A. A., Kandeler, E., Buchmann, N., and Niklaus, P. A. (2011). Interactive effects of drought and N fertilization on the spatial

distribution of methane assimilation in grassland soils. *Glob. Change Biol.* 17, 2629–2639. doi: 10.1111/j.1365-2486.2011.02410.x

Tilman, D. (1997). The influence of functional diversity and composition on ecosystem processes. *Science* 277, 1300–1302. doi: 10.1126/science.277.5330.1300

Torsvik, V., Ovreas, L., and Thingstad, T. F. (2002). Prokaryotic diversity—Magnitude, dynamics, and controlling factors. *Science* 296, 1064–1066. doi: 10.1126/science.1071698

Treseder, K. K., Kivlin, S. N., and Hawkes, C. V. (2011). Evolutionary trade-offs among decomposers determine responses to nitrogen enrichment. *Ecol. Lett.* 14, 933–938. doi: 10.1111/j.1461-0248.2011.01650.x

Van Der Gucht, K., Cottenie, K., Muylaert, K., Vloemans, N., Cousin, S., Declerck, S., et al. (2007). The power of species sorting: local factors drive bacterial community composition over a wide range of spatial scales. *Proc. Natl. Acad. Sci. U.S.A.* 104, 20404–20409. doi: 10.1073/pnas.0707200104

Van Der Heijden, M. G. A., Klironomos, J. N., Ursic, M., Moutoglis, P., Streitwolf-Engel, R., Boller, T., et al. (1998). Mycorrhizal fungal diversity determines plant biodiversity, ecosystem variability and productivity. *Nature* 396, 69–72. doi: 10.1038/23932

Violle, C., Navas, M. L., Vile, D., Kazakou, E., Fortunel, C., Hummel, I., et al. (2007). Let the concept of trait be functional! *Oikos* 116, 882–892. doi: 10.1111/j.2007.0030-1299.15559.x

Von Mering, C., Hugenholtz, P., Raes, J., Tringe, S. G., Doerks, T., Jensen, L. J., et al. (2007). Quantitative phylogenetic assessment of microbial communities in diverse environments. *Science* 315, 1126–1130. doi: 10.1126/science.1133420

Wallenstein, M. D., and Hall, E. K. (2012). A trait-based framework for predicting when and where microbial adaptation to climate change will affect ecosystem functioning. *Biogeochemistry* 109, 35–47. doi: 10.1007/s10533-011-9641-8

Watrous, J. D., Phelan, V. V., Hsu, C.-C., Moree, W. J., Duggan, B. M., Alexandrov, T., et al. (2013). Microbial metabolic exchange in 3D. *ISME J.* 7, 770–780. doi: 10.1038/ismej.2012.155

Webster, G., Embley, T. M., Freitag, T. E., Smith, Z., and Prosser, J. I. (2005). Links between ammonia oxidizer species composition, functional diversity and nitrification kinetics in grassland soils. *Environ. Microbiol.* 7, 676–684. doi: 10.1111/j.1462-2920.2005.00740.x

Wertz, S., Degrange, V., Prosser, J. I., Poly, F., Commeaux, C., Guillaumaud, N., et al. (2007). Decline of soil microbial diversity does not influence the resistance and resilience of key soil microbial functional groups following a model disturbance. *Environ. Microbiol.* 9, 2211–2219. doi: 10.1111/j.1462-2920.2007.01335.x

Wittebolle, L., Marzorati, M., Clement, L., Balloi, A., Daffonchio, D., Heylen, K., et al. (2009). Initial community evenness favours functionality under selective stress. *Nature* 458, 623–626. doi: 10.1038/nature07840

Wohl, D. L., Arora, S., and Gladstone, J. R. (2004). Functional redundancy supports biodiversity and ecosystem function in a closed and constant environment. *Ecology* 85, 1534–1540. doi: 10.1890/03-3050

Wrighton, K. C., Thomas, B. C., Sharon, I., Miller, C. S., Castelle, C. J., Verberkmoes, N. C., et al. (2012). Fermentation, hydrogen, and sulfur metabolism in multiple uncultivated bacterial phyla. *Science* 337, 1661–1665. doi: 10.1126/science.1224041

Zhu, Y., Chen, H., Fan, J., Wang, Y., Li, Y., Chen, J., et al. (2000). Genetic diversity and disease control in rice. *Nature* 406, 718–722. doi: 10.1038/35021046

Conflict of Interest Statement: The authors declare that the research was conducted in the absence of any commercial or financial relationships that could be construed as a potential conflict of interest.

Received: 31 March 2014; paper pending published: 25 April 2014; accepted: 07 May 2014; published online: 27 May 2014.

Citation: Krause S, Le Roux X, Niklaus PA, Van Bodegom PM, Lennon JT, Bertilsson S, Grossart H-P, Philippot L and Bodelier PLE (2014) Trait-based approaches for understanding microbial biodiversity and ecosystem functioning. Front. Microbiol. ***5****:251. doi: 10.3389/fmicb.2014.00251*

This article was submitted to Aquatic Microbiology, a section of the journal Frontiers in Microbiology.

Advantages of publishing in Frontiers

OPEN ACCESS
Articles are free to read, for greatest visibility

COLLABORATIVE PEER-REVIEW
Designed to be rigorous – yet also collaborative, fair and constructive

FAST PUBLICATION
Average 85 days from submission to publication (across all journals)

COPYRIGHT TO AUTHORS
No limit to article distribution and re-use

TRANSPARENT
Editors and reviewers acknowledged by name on published articles

SUPPORT
By our Swiss-based editorial team

IMPACT METRICS
Advanced metrics track your article's impact

GLOBAL SPREAD
5'100'000+ monthly article views and downloads

LOOP RESEARCH NETWORK
Our network increases readership for your article

Frontiers
EPFL Innovation Park, Building I • 1015 Lausanne • Switzerland
Tel +41 21 510 17 00 • Fax +41 21 510 17 01 • info@frontiersin.org
www.frontiersin.org

Find us on